

---

# COLUMBIA

## ACCIDENT INVESTIGATION BOARD

---



**Note:** Volumes II - VI contain a number of conclusions and recommendations, several of which were adopted by the Board in Volume I. The other conclusions and recommendations drawn in Volumes II - VI do not necessarily reflect the opinion of the Board, but are included for the record. When there is conflict, Volume I takes precedence.

---

REPORT VOLUME III  
OCTOBER 2003

---

## On the Front Cover



*This was the crew patch for STS-107. The central element of the patch was the microgravity symbol,  $\mu\text{g}$ , flowing into the rays of the Astronaut symbol. The orbital inclination was portrayed by the 39-degree angle of the Earth's horizon to the Astronaut symbol. The sunrise was representative of the numerous science experiments that were the dawn of a new era for continued microgravity research on the International Space Station and beyond. The breadth of science conducted on this mission had widespread benefits to life on Earth and the continued exploration of space, illustrated by the Earth and stars. The constellation Columba (the dove) was chosen to symbolize peace on Earth and the Space Shuttle Columbia. In addition, the seven stars represent the STS-107 crew members, as well as honoring the original Mercury 7 astronauts who paved the way to make research in space possible. The Israeli flag represented the first person from that country to fly on the Space Shuttle.*



## On the Back Cover

*This emblem memorializes the three U.S. human space flight accidents – Apollo 1, Challenger, and Columbia. The words across the top translate to: “To The Stars, Despite Adversity – Always Explore”*

The Board would like to acknowledge the hard work and effort of the following individuals in the production of Volumes II – VI.

Maj. Gen. John L. Barry	Executive Director to the Chairman
Dennis R. Jenkins	Investigator and Liaison to the Board
Lt. Col. Donald J. White	Technical Editor
Lt. Col. Patrick A. Goodman	Technical Editor
Joshua M. Limbaugh	Layout Artist
Joseph A. Reid	Graphic Designer
Christine F. Cole	Administrative Assistant
Jana T. Schultz	Administrative Assistant
Lester A. Reingold	Lead Editor
Christopher M. Kirchhoff	Editor
Ariel H. Simon	Assistant Editor
Jennifer L. Bukvics	Lead Project Manager
Donna J. Fudge	Senior Paralegal, Group II Coordinator
Susan M. Plott	Project Supervisor, Group III Coordinator
Ellen M. Tanner	Project Supervisor

Limited First Printing, October 2003, by the  
Columbia Accident Investigation Board

Subsequent Printing and Distribution by the  
National Aeronautics and Space Administration  
and the  
Government Printing Office  
Washington, D.C.

## VOLUME I

PART ONE	THE ACCIDENT
Chapter 1	The Evolution of the Space Shuttle Program
Chapter 2	<i>Columbia's</i> Final Flight
Chapter 3	Accident Analysis
Chapter 4	Other Factors Considered
PART TWO	WHY THE ACCIDENT OCCURRED
Chapter 5	From <i>Challenger</i> to <i>Columbia</i>
Chapter 6	Decision Making at NASA
Chapter 7	The Accident's Organizational Causes
Chapter 8	History as Cause: <i>Columbia</i> and <i>Challenger</i>
PART THREE	A LOOK AHEAD
Chapter 9	Implications for the Future of Human Space Flight
Chapter 10	Other Significant Observations
Chapter 11	Recommendations
PART FOUR	APPENDICES
Appendix A	The Investigation
Appendix B	Board Member Biographies
Appendix C	Board Staff

## VOLUME II

	CAIB TECHNICAL DOCUMENTS CITED IN THE REPORT
	Reader's Guide to Volume II
Appendix D.a	Supplement to the Report
Appendix D.b	Corrections to Volume I of the Report
Appendix D.1	STS-107 Training Investigation
Appendix D.2	Payload Operations Checklist 3
Appendix D.3	Fault Tree Closure Summary
Appendix D.4	Fault Tree Elements – Not Closed
Appendix D.5	Space Weather Conditions
Appendix D.6	Payload and Payload Integration
Appendix D.7	Working Scenario
Appendix D.8	Debris Transport Analysis
Appendix D.9	Data Review and Timeline Reconstruction Report
Appendix D.10	Debris Recovery
Appendix D.11	STS-107 Columbia Reconstruction Report
Appendix D.12	Impact Modeling
Appendix D.13	STS-107 In-Flight Options Assessment
Appendix D.14	Orbiter Major Modification (OMM) Review
Appendix D.15	Maintenance, Material, and Management Inputs
Appendix D.16	Public Safety Analysis
Appendix D.17	MER Manager's Tiger Team Checklist
Appendix D.18	Past Reports Review
Appendix D.19	Qualification and Interpretation of Sensor Data from STS-107
Appendix D.20	Bolt Catcher Debris Analysis

### VOLUME III

#### OTHER TECHNICAL DOCUMENTS

	Reader's Guide to Volume III .....	5
Appendix E.1	CoFR Endorsements .....	7
Appendix E.2	STS-107 Image Analysis Team Final Report .....	27
Appendix E.3	An Assessment of Potential Material Candidates for the "Flight Day 2" Radar Object Observed during the NASA Mission STS-107 .....	139
Appendix E.4	Columbia Early Sighting Assessment Team Final Report .....	171

### VOLUME IV

#### OTHER TECHNICAL DOCUMENTS

	Reader's Guide to Volume IV
Appendix F.1	Water Absorption by Foam
Appendix F.2	Follow the TPS
Appendix F.3	MADS Sensor Data
Appendix F.4	ET Cryoinsulation
Appendix F.5	Space Shuttle STS-107 Columbia Accident Investigation, External Tank Working Group Final Report – Volume 1

### VOLUME V

#### OTHER SIGNIFICANT DOCUMENTS

	Reader's Guide to Volume V
Appendix G.1	Requirements and Procedures for Certification of Flight Readiness
Appendix G.2	Appendix R, Space Shuttle Program Contingency Action Plan
Appendix G.3	CAIB Charter, with Revisions
Appendix G.4	Group 1 Matrix Brief on Maintenance, Material, and Management
Appendix G.5	Vehicle Data Mapping (VDM) Team Final Report, Jun 13, 2003
Appendix G.6	SRB Working Group Presentation to CAIB
Appendix G.7	Starfire Team Final Report, Jun 3, 2003
Appendix G.8	Using the Data and Observations from Flight STS-107... Exec Summary
Appendix G.9	Contracts, Incentives, and Safety/Technical Excellence
Appendix G.10	Detailed Summaries: Rogers Commission Report, ASAP Report, SIAT Report
Appendix G.11	Foam Application and Production Chart
Appendix G.12	Crew Survivability Report
Appendix G.13	Aero/Aerothermal/Thermal/Structures Team Final Report, Aug 6, 2003

### VOLUME VI

#### TRANSCRIPTS OF BOARD PUBLIC HEARINGS

	Reader's Guide to Volume VI	
Appendix H.1	March 6, 2003	Houston, Texas
Appendix H.2	March 17, 2003	Houston, Texas
Appendix H.3	March 18, 2003	Houston, Texas
Appendix H.4	March 25, 2003	Cape Canaveral, Florida
Appendix H.5	March 26, 2003	Cape Canaveral, Florida
Appendix H.6	April 7, 2003	Houston, Texas
Appendix H.7	April 8, 2003	Houston, Texas
Appendix H.8	April 23, 2003	Houston, Texas
Appendix H.9	May 6, 2003	Houston, Texas
Appendix H.10	June 12, 2003	Washington, DC



# Reader's Guide to Volume III

Volume III of the Report contains other technical documents produced by NASA and other organizations, which were provided to the Columbia Accident Investigation Board in support of its inquiry into the February 1, 2003 destruction of the Space Shuttle *Columbia*. The documents are compiled in the interest of establishing a complete record, but they do not necessarily represent the views of the Board. Volume I contains the Board's findings, analysis, and recommendations. The documents in Volume III are also contained in their original color format on the DVD disc in the back of Volume II.

**THIS PAGE INTENTIONALLY LEFT BLANK**



# Volume III

## Appendix E.1

### CoFR Endorsements

This Appendix contains copies of STS-107 CoFR Endorsements and signature delegation authority letters.

THIS PAGE INTENTIONALLY LEFT BLANK



STS- 107 CoFR ENDORSEMENT		
ELEMENT	SERIAL NUMBER	PAYLOAD
ORBITER	OV-102	SPACEHAB RDM FREESTAR
ET	ET-93	SIMPLEX RAMBO
RSRM	RSRM-88	
SSME	2055, 2053, 2049	
SRB	BI-116	

Projects having exceptions to this CoFR document are as follows (see Exception Log for details):

001 Orbiter

**STS- 107 CoFR ENDORSEMENT**

The Flight Preparation Process Plans documented in NSTS 08117, Requirements and Procedures for Certification of Flight Readiness, have been satisfied. Required products and other responsibilities for each project (NSTS 08117, Section 8) have been or will be produced or completed.

- a. Certified flight hardware elements have been delivered to the SFOC at the Kennedy Space Center.
- b. Required hardware element processing specifications and requirements have been delivered to the SFOC.
- c. All identified "out-of-family" events that occurred after delivery of hardware for launch processing/ assembly/testing have been resolved.
- d. For "out-of-family" conditions detected during manufacturing, testing, or post-mission tear down and analysis, notification to the Space Shuttle Program has been made, and corrective action, if any, identified.
- e. The as-built flight element configuration satisfies the released requirements and engineering, based on data compiled and reviewed by SFOC.
- f. For the Space Shuttle Main Engine Project: Certified main engine controller software has been delivered for this mission.

CONTRACTOR			NASA	
SSME (8.5.3.1, 8.5.3.2, Apx. C)	PROGRAM MANAGER, ROCKETDYNE <i>J. J. Paulsen</i> J. J. PAULSEN	DATE 1/9/03	MANAGER, SSME PROJECT, MSFC <i>G. D. Rufson</i> G. D. RUFSON	DATE 1/9/03
ET (8.5.4.1, 8.5.4.2, Apx. D)	PROGRAM MANAGER, LMSS <i>R. W. Wetmore</i> R. W. WETMORE	DATE 1/9/03	MANAGER, ET PROJECT, MSFC <i>J. W. Smelser</i> J. W. SMELSER	DATE 1/9/03
RSRM (8.5.5.1, 8.5.5.2, Apx. E)	PROGRAM MANAGER, THICKOL <i>E. C. Ralston</i> E. C. RALSTON	DATE 1/9/03	MANAGER, RSRM PROJECT, MSFC <i>J. A. Singer</i> J. A. SINGER	DATE 1/9/03
CONCURRENCE				
MSFC SHUTTLE PROJECTS	NA		MANAGER, MSFC SHUTTLE PROJECTS <i>A. A. McCool</i> A. A. MCCOOL	DATE 1/9/03

**STS- 107 CoFR ENDORSEMENT**

The Flight Preparation Process Plans documented in NSTS 08117, Requirements and Procedures for Certification of Flight Readiness, have been satisfied. Required products and other responsibilities for each organization (NSTS 08117, Section 8) have been or will be produced or completed.

- a. For Payload Processing: Flight and ground requirements, payload logistics, and configuration requirements provided by the flight projects, have been maintained, performed, or are planned to be performed per approved TOPs.
- b. For EVA project: Audit, insight, and surveillance of SFOC activities have been completed or are planned for completion, and all discrepancies have been resolved. Oversight functions have been conducted in conjunction with Hamilton Sundstrand.

**NASA**


<b>FLIGHT CREW OPERATIONS</b> (8.5.11.1, 8.5.11.2, Apx. K)	<b>DIRECTOR, FLIGHT CREW OPERATIONS</b> <i>Robert D. Cabana</i> R. D. CABANA		<b>DATE</b> 1-9-03
<b>FERRY OPERATIONS</b> (8.5.16.1, 8.5.16.2, Apx. P)	<b>FERRY OPERATIONS MANAGER</b> D. L. McCORMACK		<b>DATE</b>
<b>SPACE AND LIFE SCIENCES</b> (8.5.15.1, 8.5.15.2, Apx. O)	<b>DIRECTOR, SPACE AND LIFE SCIENCES</b> <i>James R. Davis</i> J. R. DAVIS		<b>DATE</b> 9/2/03
<b>SPACE SHUTTLE SR&amp;QA</b> (8.5.17.1, 8.5.17.2, Apx. Q)	<b>MANAGER, SPACE SHUTTLE SR&amp;QA</b> <i>Mark D. Erminger</i> M. D. ERMINGER		<b>DATE</b> 1/9/03
	<b>CONTRACTOR</b>		<b>NASA</b>
<b>PAYLOAD PROCESSING</b> (8.5.10.1, 8.5.10.2, Apx. J)	<b>PROGRAM MANAGER, CAPPS BOEING, KSC</b> <i>J. W. Elbon</i> J. W. ELBON	<b>DATE</b> 1-9-03	<b>DIRECTOR OF ISS/PAYLOAD PROCESSING</b> <i>J. J. Talone, Jr.</i> J. J. TALONE, JR.
<b>EVA</b> (8.5.2.1, 8.5.2.2, Apx. B)	<b>PROGRAM MANAGER, HAMILTON SUNDSTRAND</b> <i>Charles Seaback</i> C. SEABACK	<b>DATE</b> 1-9-03	<b>MANAGER, EVA PROJECT OFFICE</b> <i>G. A. Flynt</i> G. A. FLYNT

### STS- 107 CoFR ENDORSEMENT

The Flight Preparation Process Plans documented in NSTS 08117, Requirements and Procedures for Certification of Flight Readiness, have been satisfied. Required products and other responsibilities for each organization (NSTS 08117, Section 8) have been or will be produced or completed.

- a. For Payload Processing: Flight and ground requirements, payload logistics, and configuration requirements provided by the flight projects, have been maintained, performed, or are planned to be performed per approved TOPs.
- b. For EVA project: Audit, insight, and surveillance of SFOC activities have been completed or are planned for completion, and all discrepancies have been resolved. Oversight functions have been conducted in conjunction with Hamilton Sundstrand.

#### NASA

<b>FLIGHT CREW OPERATIONS</b> (8.5.11.1, 8.5.11.2, Apx. K)	DIRECTOR, FLIGHT CREW OPERATIONS  R. D. CABANA		DATE
<b>FERRY OPERATIONS</b> (8.5.10.1, 8.5.10.2, Apx. P)	FERRY OPERATIONS MANAGER  D. L. MCCORMACK		DATE 1/8/03
<b>SPACE AND LIFE SCIENCES</b> (8.5.15.1, 8.5.15.2, Apx. Q)	DIRECTOR, SPACE AND LIFE SCIENCES  J. R. DAVIS		DATE
<b>SPACE SHUTTLE SR&amp;QA</b> (8.5.17.1, 8.5.17.2, Apx. O)	MANAGER, SPACE SHUTTLE SR&QA  M. D. ERMINGER		DATE
	<b>CONTRACTOR</b>		<b>NASA</b>
<b>PAYLOAD PROCESSING</b> (8.5.10.1, 8.5.10.2, Apx. J)	PROGRAM MANAGER, CAPPS BOEING, KSC  J. W. ELBON	DATE	DIRECTOR OF ISS/PAYLOAD PROCESSING  J. J. TALONE, JR.
<b>EVA</b> (8.5.2.1, 8.5.2.2, Apx. B)	PROGRAM MANAGER, HAMILTON SUNDSTRAND  C. SEABACK	DATE	MANAGER, EVA PROJECT OFFICE  G. A. FLYNT

**STS- 107 CoFR ENDORSEMENT**

The Flight Preparation Process Plans documented in NSTS 08117, Requirements and Procedures for Certification of Flight Readiness, have been satisfied. Required products and other responsibilities (shared or independent) for each organization (NSTS 08117, Section 8) have been or will be produced or completed.

- a. The following NASA organizations have completed or plan to complete audit, insight, and surveillance of contractor activities, and have resolved all discrepancies.

**NASA**

CUSTOMER AND FLIGHT INTEGRATION (8.5.14.1, 8.5.14.2, Apx. N)	MANAGER, SPACE SHUTTLE CUSTOMER AND FLIGHT INTEGRATION	DATE
	M. A. BREKKE	
KSC INTEGRATION (8.5.12.1, 8.5.12.2, Apx. L)	MANAGER, SPACE SHUTTLE KSC INTEGRATION <i>R. L. Segert</i> R. L. SEGERT	DATE 1/9/03
SHUTTLE PROCESSING (8.5.8.1, 8.5.8.2, Apx. H)	DIRECTOR OF SHUTTLE PROCESSING, KSC <i>M. E. Wetmore</i> M. E. WETMORE	DATE 1-9-03
MISSION OPERATIONS (8.5.7.1, 8.5.7.2, Apx. G)	DIRECTOR, MISSION OPERATIONS <i>J. C. Harpold</i> J. C. HARPOLD	DATE 1/9/03
SRB (8.5.6.1, 8.5.6.2, Apx. F)	MANAGER, SRB PROJECT, MSFC <i>A. A. McCool</i> A. A. MCCOOL	DATE 1/9/03
SSP S&MA	MANAGER, SSP S&MA <i>W. J. Harris</i> W. J. HARRIS	DATE 1/9/03
SYSTEMS INTEGRATION (8.5.13.1, 8.5.13.2, Apx. M)	MANAGER, SPACE SHUTTLE SYSTEMS INTEGRATION <i>L. D. Austin</i> L. D. AUSTIN	DATE 1/9/03
VEHICLE ENGINEERING (8.5.1.1, 8.5.1.2, Apx. A)	MANAGER, SPACE SHUTTLE VEHICLE ENGINEERING <i>R. R. Roe</i> R. R. ROE	DATE 1/9/03

## STS- 107 CoFR ENDORSEMENT

The Flight Preparation Process Plans documented in NSTS 08117, Requirements and Procedures for Certification of Flight Readiness, have been satisfied. Required products and other responsibilities (shared or independent) for each organization (NSTS 08117, Section 8) have been or will be produced or completed.

- a. The following NASA organizations have completed or plan to complete audit, insight, and surveillance of contractor activities, and have resolved all discrepancies.

### NASA

CUSTOMER AND FLIGHT INTEGRATION (8.5.14.1, 8.5.14.2, Apx. N)	MANAGER, SPACE SHUTTLE CUSTOMER AND FLIGHT INTEGRATION	DATE
	<i>N. A. Brekke</i> N. A. BREKKE	1/9/03
KSC INTEGRATION (8.5.12.1, 8.5.12.2, Apx. L)	MANAGER, SPACE SHUTTLE KSC INTEGRATION  R. L. SEBERT	DATE
SHUTTLE PROCESSING (8.5.8.1, 8.5.8.2, Apx. H)	DIRECTOR OF SHUTTLE PROCESSING, KSC  N. E. WETMORE	DATE
MISSION OPERATIONS (8.5.7.1, 8.5.7.2, Apx. G)	DIRECTOR, MISSION OPERATIONS  J. C. HARPOLD	DATE
SRB (8.5.6.1, 8.5.6.2, Apx. F)	MANAGER, SRB PROJECT, MSFC  A. A. MCCOOL	DATE
SSP S&MA	MANAGER, SSP S&MA  W. J. HARRIS	DATE
SYSTEMS INTEGRATION (8.5.13.1, 8.5.13.2, Apx. M)	MANAGER, SPACE SHUTTLE SYSTEMS INTEGRATION  L. D. AUSTIN	DATE
VEHICLE ENGINEERING (8.5.1.1, 8.5.1.2, Apx. A)	MANAGER, SPACE SHUTTLE VEHICLE ENGINEERING  R. R. ROE	DATE

**STS- 107 CoFR ENDORSEMENT**

The Space Shuttle Flight Preparation Process Plans (shared or independent) documented in NSTS 08117, Requirements and Procedures for Certification of Flight Readiness, have been satisfied. Required products and other responsibilities (shared or independent) for the SFOC (NSTS 08117, Section 8) have been or will be produced or completed.

- a. All out-of-family conditions have been identified and resolved with the NASA.
- b. The SSV has been processed in accordance with requirements and policies baselined by the SSP.

**UNITED SPACE ALLIANCE**

SFOC SQ&MA CONCURRENCE	VICE PRESIDENT, SAFETY, QUALITY AND MISSION ASSURANCE, SFOC  <i>R. C. Beagley</i> R. C. BEAGLEY Pending Bistarone letter	DATE  1/9/03
SFOC (8.5.18.1, 8.5.18.2, App. R)	SSP, PROGRAM MANAGER, SFOC  <i>H. L. De Castro</i> H. L. DeCASTRO	DATE  1/9/03

Boeing endorses that the requirements for CoFR documented in SSP 50108 and the Boeing Flight CoFR Implementation Plan have been satisfied in accordance with the Boeing specific responsibilities for this flight. Any issues that have arisen since the Stage Operations Readiness Review (SORR) have been resolved or have been presented at the Flight Readiness Review. This certification is subject to clause H.43 of NAS 15-10000 (for ISS Missions).

**BOEING**

ISS PRIME CONCURRENCE	VICE PRESIDENT AND PROGRAM MANAGER, ISS, BOEING  N/A	DATE
-----------------------	--	------

**STS- 107 CoFR ENDORSEMENT**

**NASA SSP READINESS**

The preparation of all Space Shuttle Program and Project organizations for this mission has been reviewed. All required processes, products, and responsibilities are complete or will be completed prior to launch. Deviations, exceptions or waivers have been reviewed and will be dispositioned by the Prelaunch MMT Review for this mission. The Space Shuttle Program is ready to proceed with the conduct of this mission.

*L. J. HAN*  
MANAGER, SPACE SHUTTLE  
PROGRAM INTEGRATION

9 Jan 03  
DATE

*L. J. HAN*  
MANAGER, LAUNCH INTEGRATION

9 Jan 03  
DATE

*R. D. DITTEMORE*  
MANAGER, SPACE SHUTTLE PROGRAM

9 Jan 03  
DATE

**NASA ISS PROGRAM READINESS**

All necessary activities required to support the flight, stage and increment have been accomplished or are planned. All deviations, waivers, and exceptions have been reviewed and satisfactorily dispositioned. The International Space Station Program is ready to proceed with launch and on-orbit operations. Any issues that have arisen since the SORR have been resolved or have been presented at the Flight Readiness Review (for ISS Missions).

N/A  
MANAGER, INTERNATIONAL SPACE  
STATION PROGRAM

DATE

**CONCURRENCE**

I concur that the Space Shuttle Program and the International Space Station Program (for ISS Missions) are ready to proceed with this mission.

*M. C. ...*  
DEPUTY ASSOCIATE ADMINISTRATOR FOR  
INTERNATIONAL SPACE STATION AND  
SPACE SHUTTLE PROGRAMS

9 Jan 2003  
DATE



<b>STS- 107 CoFR ENDORSEMENT</b>	
<b>CONCURRENCE</b>	
<p>As a member of the FRR Board, I concur that, pending completion of planned work, the Space Shuttle Program and International Space Station Program (for ISS Missions) are ready to execute this mission.</p>	
<p><u>J. D. HOWELL</u> DIRECTOR, JOHNSON SPACE CENTER</p>	<p><u>1/5/03</u> DATE</p>
<p><u>R. D. BRIDGES</u> DIRECTOR, KENNEDY SPACE CENTER</p>	<p><u>1/9/03</u> DATE</p>
<p><u>A. C. STEPHENSON</u> DIRECTOR, MARSHALL SPACE FLIGHT CENTER</p>	<p><u>1/9/03</u> DATE</p>
<p><u>W. W. FARSONS</u> DIRECTOR, STENNIS SPACE CENTER</p>	<p><u>1/9/03</u> DATE</p>
<p>As a member of the FRR Board, I concur that, pending completion of planned work, the Prime Mission is ready to execute this mission (for non-ISS missions).</p>	
<p><u>M. E. KICZA</u> ASSOCIATE ADMINISTRATOR FOR PRIME MISSION</p>	<p><u>1/09/2003</u> DATE</p>
<p>NASA S&amp;MA has reviewed the status of preparations for this mission and has performed an independent assessment of the readiness of the Space Shuttle Program for the conduct of this mission, and the readiness of the International Space Station for launch and on-orbit operations (for ISS missions). We are in concurrence with proceeding with this mission.</p>	
<p><u>B. D. CONNOR</u> ASSOCIATE ADMINISTRATOR, SAFETY AND MISSION ASSURANCE</p>	<p><u>1/9/03</u> DATE</p>
<b>APPROVAL</b>	
<p>The FRR Board has conducted a comprehensive assessment of the readiness of all flight and ground systems and supporting personnel. For ISS missions, the FRR Board has also conducted a comprehensive assessment of the readiness of the Launch Package/Cargo Element (LP/CE), ground hardware/software support facilities and personnel to support the flight, stage and increment including the readiness of the on-orbit stage to accept the LP/CE and return items. The Certificate of Flight Readiness has been endorsed by each program element. I have concluded, with the concurrence of the FRR Board, that pending completion of planned work, the Space Shuttle Program is ready to execute this mission and the International Space Station Program is ready for launch and on-orbit operations (for ISS missions).</p>	
<p><u>William R. ...</u> ASSOCIATE ADMINISTRATOR, OFFICE OF SPACE FLIGHT (CHAIR, FRR BOARD)</p>	<p><u>January 9, 2003</u> DATE</p>

National Aeronautics and  
Space Administration  
Lyndon B. Johnson Space Center  
2101 NASA Road 1  
Houston, Texas 77058-3696



January 7, 2003

Reply to Attn of: SA-03-001

TO: John F. Kennedy Space Center  
Attn: MK/Manager, Launch Integration

FROM: SA/Director, Space and Life Sciences

SUBJECT: Certificate of Flight Readiness (CoFR) Signature Authority

I authorize SA/Sam Pool and SD/Craig Fischer to have full signature authority to sign the Space and Life Sciences Flight Readiness Review of CoFR statement for STS-107 and subsequent flights.

A handwritten signature in cursive script, appearing to read "Jeff R. Davis, M.D.".

Jeffrey R. Davis, M.D.

cc:  
SA/J. Davis  
SA/S. Pool  
SD/C. Fischer

AK91-T012-JWE-M03002  
7 January 2003



**MEMORANDUM**

**Subject: DELEGATION OF AUTHORITY FOR STS-107 CoFR**  
**To: MK / Manager Launch Integration**

As my representative, Mr. James H. Chilton is delegated signature authority for the CoFR for STS-107 and for subsequent flight CoFR signature requirements when he attends as a representative of this office.

Please advise this office if additional information is required. Thank you.

A handwritten signature in black ink, appearing to read 'John W. Elbon, III'.

John W. Elbon, III  
Vice President - Program Manager  
Checkout, Assembly & Payload Processing Services

pb

National Aeronautics and  
Space Administration  
Lyndon B. Johnson Space Center  
2101 NASA Road 1  
Houston, Texas 77058-3696



January 9, 2003

REC'D 10 487 27 DA8-03-004

TO: MK/Manager, Launch Integration  
FROM: DA/Director, Mission Operations  
SUBJECT: Certificate of Flight Readiness (CoFR) Signature Authority

This is to inform you that N. Wayne Hale's signature for CoFR signature authority has been revoked and the following individuals are delegated signature authority for any applicable Level I Certificate of Flight Readiness requiring Mission Operations Directorate endorsement.

DA8/J. Milton Heflin	(281) 483-5428	Fax: (281) 483-3304
DA8/Robert E. Castle	(281) 483-0780	Fax: (281) 483-3304
DA8/Phillip L. Engelau	(281) 483-4416	Fax: (281) 483-3304

A handwritten signature in black ink, appearing to read "Jon C. Harpold".

Jon C. Harpold

cc:  
AB/B. R. Stone  
AC/S. H. Garman  
CA/R. D. Cabana  
DA8/S. J. Elsner  
DA8/J. M. Heflin  
DA8/R. E. Castle  
DA8/P. L. Engelau  
DA8/N. W. Hale  
DF/R. N. Fitts  
DL/L. J. Uljohn  
DM/R. C. Epps  
DO/L. D. Davis  
DT/P. J. Beauregard  
DV/J. Knight  
DX/R. D. Dell'Osso  
EA/F. J. Benz  
MA/R. D. Dittmore  
QA/W. H. Gerstenmaier  
SA/D. R. Williams

National Aeronautics and  
Space Administration  
George C. Marshall Space Flight Center  
Marshall Space Flight Center, AL 35812



Reply to Attn of MP01

OCT 15 2001

TO: Kennedy Space Center  
Attn: MK/James D. Halsell

FROM: MP01/A. A. McCool

SUBJECT: Designation of MSFC Representatives to Space  
Shuttle Readiness Reviews

The enclosed matrix is updated, designating individuals authorized to represent their respective organizations at the various readiness reviews.

*A. A. McCool*  
A. A. McCool  
Manager, Space Shuttle Projects Office

Enclosure

cc:  
MP01/Mr. Clever  
MP21/Mr. Hopson  
MP31/Mr. Smelser  
MP41/Mr. Martin  
MP51/Mr. Rudolphi  
MP71/Ms. Martin  
JSC/MA/Mr. Dittmore

*Mission Success Starts with Safety*

**MSFC SHUTTLE PROJECTS REPRESENTATIVES TO SPACE SHUTTLE READINESS  
REVIEWS**

<u>OFFICE</u>	<u>ET/SRB MATE</u>	<u>ORBITER ROLLOUT</u>	<u>ERB</u>	<u>L-1 &amp; 2 MMT</u>
SPACE SHUTTLE PROJ. MGR	A. A. MCCOOL W. W. CLEVER* J. A. SINGER*	A. A. MCCOOL W. W. CLEVER* J. A. SINGER*	A. A. MCCOOL W. W. CLEVER* J. A. SINGER*	A. A. MCCOOL W. W. CLEVER* J. A. SINGER*
ET PROJECT MGR, MSFC	J. W. SMELSER T. F. GREENWOOD* N. OTTE*	N/A	J. W. SMELSER T. F. GREENWOOD* N. OTTE*	J. W. SMELSER T. F. GREENWOOD* N. OTTE*
SRB PROJECT MGR, MSFC	D. M. MARTIN J. L. LUSK*	N/A	D. M. MARTIN J. L. LUSK*	D. M. MARTIN J. L. LUSK*
RSRM PROJECT MGR, MSFC	M. U. RUDOLPHI R. K. BURT* S. F. CASH*	N/A	M. U. RUDOLPHI R. K. BURT* S. F. CASH*	M. U. RUDOLPHI R. K. BURT* S. F. CASH*
SSME PROJECT MGR, MSFC	N/A	G. D. HOPSON A. E. GOLDMAN* A. L. WORLUND*	G. D. HOPSON A. E. GOLDMAN* A. L. WORLUND*	G. D. HOPSON A. E. GOLDMAN* A. L. WORLUND*

\* ALTERNATE REPRESENTATIVE

ENCLOSURE (REVISED 10/18/01)

National Aeronautics and  
Space Administration  
Lyndon B. Johnson Space Center  
2101 NASA Road 1  
Houston, Texas 77058-3696



Reply to AIB of: MS2-00-057

SEP 20 2000

TO: John F. Kennedy Space Center  
Attn: MK/Manager, Launch Integration Office

FROM: MS/Manager, Space Shuttle Systems Integration

SUBJECT: Delegation of Authority for Certificate of Flight Readiness (CoFR)

As my representative, Mr. Rodney O. Wallace is delegated signature authority for the CoFR for STS-92 and for subsequent flight CoFR signature requirements when he attends as representative of this office.

  
Lambert D. Austin, Jr.

cc:  
MA/R. D. Dittmore  
MA2/W. H. Gerstenmaier  
MS/D. S. Noah  
MS2/R. O. Wallace

National Aeronautics and  
Space Administration  
Headquarters  
Washington, DC 20546-0001



January 8, 2003

Reply to Airmail:

U

TO: MK/Manager, Launch Integration  
FROM: U/Associate Administrator for Biological and Physical Research  
SUBJECT: Delegation of Authority

Due to other exigencies, I will not be attending the STS-107 Flight Readiness Review. Mr. Richard Zwierko, of my senior staff, is delegated the authority to sign the Certificate of Flight Readiness, on behalf of Code U. Should you have any questions, I can be reached at (202) 358-0215.

A handwritten signature in cursive script that reads "Mary E. Kicza".

Mary E. Kicza

cc:  
M/Mr. Readdy  
KSC/MK/Ginny Kinslow



National Aeronautics and  
Space Administration  
Lyndon B. Johnson Space Center  
2101 NASA Road 1  
Houston, Texas 77058-3696



December 16, 2002

Reply to AIB of: MA-02-082

TO: Distribution  
FROM: MA/Manager, Space Shuttle Program  
SUBJECT: STS-107 Launch Integration

We all join in congratulating the Space Shuttle Program Manager for Launch Integration, Col. Jim Halsell, on his new assignment as commander of the STS-120 mission, the capstone mission of the International Space Station (ISS) assembly effort. With the successful completion of STS-120, ISS core assembly will be complete. This mission is especially significant in that it represents the culmination of the challenges overcome and the amazing successes recorded in establishing this great international orbiting laboratory.

Col. Halsell will be shifting focus and momentum immediately in order to begin preparations for STS-120. Consequently, effective January 8, 2003, Ms. Linda Ham will assume all launch integration duties relating to STS-107 and subsequent flights until a successor to Col. Halsell is named and in place.

On behalf of the entire Space Shuttle Program, we extend our personal thanks and gratitude to Col. Halsell for his untiring efforts, leadership, and service.

A handwritten signature in black ink, appearing to read "R. Dittmore".

Ronald D. Dittmore

cc:  
See List

**THIS PAGE INTENTIONALLY LEFT BLANK**



# Volume III

## Appendix E.2

### STS-107 Image Analysis Team Final Report

This Appendix contains NSTS-37384, STS-107 Image Analysis Team Final Report in support of the *Columbia Accident Investigation*, 30 June 2003.

**THIS PAGE INTENTIONALLY LEFT BLANK**



NSTS-37384



**STS-107 Image Analysis Team**  
**Final Report**  
**in support of the**  
***Columbia* Accident Investigation**

**June 30, 2003**

Submitted by

Dr. Gregory J. Byrne, NASA  
Team Lead

Dr. Cynthia A. Evans, Lockheed  
Martin, Co-Team Lead

This information is being distributed to aid in the investigation of the Columbia mishap and should only be distributed to personnel who are actively involved in this investigation. 1

## CONTENTS

<b>1.0 EXECUTIVE SUMMARY .....</b>	<b>7</b>
<b>2.0 INTRODUCTION.....</b>	<b>9</b>
<b>3.0 PURPOSE &amp; SCOPE .....</b>	<b>10</b>
<b>4.0 LAUNCH ANALYSES .....</b>	<b>11</b>
<b>4.1 Launch Data Sources.....</b>	<b>11</b>
4.1.1 Launch Film and Video .....	11
4.1.2 Shuttle Reference Data .....	13
4.1.3 Star Data.....	14
<b>4.2 Launch Imagery Analyses: Methods.....</b>	<b>14</b>
4.2.1 Obtain Best Quality Imagery (Film and Video) .....	14
4.2.2 Launch Video and Film Screening .....	15
4.2.3 Image Enhancement and Analysis Techniques.....	16
4.2.4 Determination of the Highest Fidelity Camera Timing Data.....	19
<b>4.3 Launch Imagery Analyses: Primary Results.....</b>	<b>20</b>
4.3.1 Analyses Performed during the STS-107 Mission.....	20
4.3.1.1 Initial Findings .....	20
4.3.1.2 Reporting.....	21
4.3.1.3 Other Action Taken during Mission .....	21
4.3.2 Post-Accident Launch Analyses .....	21
4.3.2.1 Debris Event Timeline .....	21
4.3.2.2 Debris Source.....	28
4.3.2.3 Debris Size.....	30
4.3.2.4 Debris Rotation/Tumbling .....	32
4.3.2.5 Debris Trajectory, Impact Location, Angle, and Velocity Analysis.....	33
4.3.2.6 Post Impact Damage Assessment and Debris Analysis.....	37
<b>4.4 Other Launch Analyses .....</b>	<b>40</b>
4.4.1 Bright Spot near Bipod 9 Seconds Prior to Debris Strike.....	40
4.4.2 STS-107 Launch Radar Analysis.....	41
4.4.3 Navy Airship Analysis.....	42
4.4.4 Debris Seen Exiting SRB Exhaust Plume.....	43
4.4.5 Analysis of ET Bipod Ramp Foam on STS-112, 50, 32, 7.....	43
4.4.5.1 STS-112 (CFVR-112-01, Cameras E-207, E-212, E-220, E-222) .....	43
4.4.5.2 STS-50 .....	44
4.4.5.3 STS-32 .....	46
4.4.5.4 STS-7 .....	46
4.4.6 Post-landing Walk-around Videos.....	47

This information is being distributed to aid in the investigation of the Columbia mishap and should only be distributed to personnel who are actively involved in this investigation. 2

<b>5.0</b>	<b>ON-ORBIT ANALYSES .....</b>	<b>48</b>
<b>5.1</b>	<b>On-orbit Imagery Data Sources .....</b>	<b>48</b>
<b>5.2</b>	<b>Process/Methods for Analysis .....</b>	<b>48</b>
<b>5.3</b>	<b>On-orbit Analyses .....</b>	<b>48</b>
5.3.1	Downlinked Video of the External Tank .....	49
5.3.2	Upper Wing Survey Analysis .....	50
5.3.2.1	Air Force Maui Optical and Supercomputing Site (AMOS) Photos .....	50
5.3.2.2	Analysis of Israeli News Account of Damage of the Orbiter Wing .....	51
5.3.2.3	Dark Spot on Orbiter Left Wing .....	51
5.3.2.4	Discolorations on Orbiter Left Wing .....	52
5.3.3	Debris Observed on Orbit (Downlinked Imagery) .....	55
5.3.3.1	Orbit 3 Debris .....	55
5.3.3.2	Orbit 5 Debris .....	56
5.3.4	Insulation on Ku-band Antenna .....	56
<b>6.0</b>	<b>RE-ENTRY ANALYSES .....</b>	<b>57</b>
<b>6.1</b>	<b>Re-entry Data Sources .....</b>	<b>58</b>
6.1.1	Re-entry Imagery .....	58
6.1.2	Observer Positions .....	58
6.1.3	Orbiter Position vs. Time .....	58
6.1.4	Nominal Re-entries from Previous Missions .....	59
6.1.5	Celestial References .....	59
<b>6.2</b>	<b>Re-entry Processes/Methods .....</b>	<b>59</b>
6.2.1	Processing of Submissions .....	59
6.2.2	Video Processes .....	59
6.2.2.1	Duplication for Screening .....	59
6.2.2.2	Time Synchronization .....	60
6.2.2.3	Digitization of Video Clips .....	60
6.2.2.4	Calibration of Focal Lengths .....	61
6.2.2.5	Other Video Camera Calibrations .....	63
6.2.2.6	Motion of Debris Relative to Orbiter .....	63
6.2.2.7	Relative Light Intensity of Orbiter and Debris .....	65
6.2.2.8	Methods for Debris Mass Estimates .....	66
6.2.2.9	Methods to Identify Debris Composition .....	66
6.2.3	Still Image Processes .....	67
6.2.3.1	Digital Conversion .....	67
6.2.3.2	Image Quality .....	67
6.2.3.3	Assigning Timing in a Long-exposure Photograph .....	68
6.2.3.4	Potential for Spectral Information in Still Photography .....	68
<b>6.3</b>	<b>Re-entry Analyses: Primary Results .....</b>	<b>69</b>
6.3.1	Re-entry Video Screening and Data Base .....	69

This information is being distributed to aid in the investigation of the Columbia mishap and should only be distributed to personnel who are actively involved in this investigation. 3

6.3.2	Entry Debris Timeline and Debris Event Descriptions.....	69
6.3.3	Nominal Re-entry Characterization .....	75
6.3.4	Relative Motion .....	78
6.3.5	Debris Mass .....	81
6.3.6	Characterization of the Flash .....	84
<b>6.4</b>	<b>Other Re-entry Analyses .....</b>	<b>86</b>
6.4.1	Star Fire Imagery Analysis .....	86
6.4.2	The Near Earth Asteroid Tracking Program on Mount Palomar .....	86
6.4.3	Special Still Imagery Analyses of Alleged “Lightning” Image.....	86
6.4.4	Tile Number Enhancement .....	86
6.4.5	Special Analysis of Video from The Colony, TX.....	86
6.4.6	Video Sequence Compilation .....	87
6.4.7	Videos Showing Columbia’s Break-up Over Texas.....	87
<b>7.0</b>	<b>LESSONS LEARNED AND RECOMMENDATIONS.....</b>	<b>88</b>
7.1	Launch Imagery - Ground .....	88
7.2	Launch Imagery - Onboard .....	90
7.3	Entry Imagery .....	91
7.4	Analysis Resources and Protocols .....	92
<b>8.0</b>	<b>STS-107 INVESTIGATION IMAGE ANALYSIS TEAM .....</b>	<b>94</b>
8.1	Image Analysis Sub-teams .....	94
8.2	Individual Team Contributors.....	95
8.3	Selected Biographies for Key Contributors.....	98
<b>9.0</b>	<b>ACRONYMS .....</b>	<b>106</b>
<b>10.0</b>	<b>REFERENCES.....</b>	<b>107</b>
<b>11.0</b>	<b>APPENDICES .....</b>	<b>108</b>

This information is being distributed to aid in the investigation of the Columbia mishap and should only be distributed to personnel who are actively involved in this investigation. 4



## FIGURES AND TABLES

Table 4.1.1 Launch cameras that viewed the debris event at 82 seconds MET .....	11
Figure 4.1.1a Map showing the camera locations used to image the debris strike.....	12
Figure 4.1.1b Frames from ET-208, E-212 and ET-204 cameras .....	13
Figure 4.2.3 Scaling when reference object is aligned with measurement object.....	17
Figure 4.3.2.1a ET-208 View of the debris near point of origin .....	22
Figure 4.3.2.1b ET-208 View of the debris at 016:15:40:21.858 UTC.....	23
Figure 4.3.2.1c ET-208 Composite with debris trajectory.....	24
Figure 4.3.2.1d Debris object in full illumination (E-212, Frame 4914).....	25
Figure 4.3.2.1e Composite image showing the debris trajectory.....	26
Figure 4.3.2.1f Debris impact cloud seen on E-212 (Frame 4924).....	27
Figure 4.3.2.2a Enhanced images of the ET forward bipod ramp area .....	29
Figure 4.3.2.2b 3-D model of the debris trajectory.....	29
Table 4.3.2.3 Apparent debris size by E-212 frame number .....	30
Figure 4.3.2.3 Debris size measurement methodology.....	32
Figure 4.3.2.4 Color ratio analysis of debris from E-212 frames .....	33
Figure 4.3.2.5a Debris trajectories derived by separate independent analyses.....	34
Figure 4.3.2.5b Debris trajectory analysis — impact area on Orbiter left wing.....	35
Table 4.3.2.5 Summary of debris velocities, impact angles, and strike location.....	37
Figure 4.3.2.6a Comparison of images from before and after the debris impact .....	38
Figure 4.3.2.6b Post-impact debris fragments (E-212 frame 4927) .....	39
Figure 4.3.2.6c Post-impact debris size measurements .....	39
Figure 4.4.1 Comparison of bright spot near bipod on STS-58 and STS-107.....	40
Figure 4.4.2 Patrick AFB 0.14 radar boresite view .....	41
Figure 4.4.3 U.S. Navy airship location and image.....	42
Figure 4.4.5.1 STS-112 debris trajectory and umbilical well image .....	44
Figure 4.4.5.2a STS-50 ET damage recorded on umbilical well camera .....	45
Figure 4.4.5.2b Detailed view of wing tile damage, STS-50.....	45
Figure 4.4.5.3 Image from STS-32 on-board umbilical well camera .....	46
Figure 4.4.5.4 Image from STS-7 on-board umbilical well camera .....	47
Figure 5.3.1 View from the STS-107 downlink video of the External Tank.....	49
Figure 5.3.2.1 AMOS image of Columbia (taken January 28, 2003).....	50
Figure 5.3.2.3a Dark spot seen on Columbia’s left wing.....	51
Figure 5.3.2.3b Payload bay door latches/rollers superimposed on Orbiter left wing.....	52
Figure 5.3.2.4a On-orbit and pre-launch views of left wing discolorations .....	53
Figure 5.3.2.4b No detectable changes on left wing RCC panels, T-seals.....	54
Figure 5.3.2.4c Discolorations on Columbia’s left wing .....	55
Figure 6.1 Example of full frame grab of a typical re-entry video .....	58
Figure 6.2.3.1 Example of one of the best still photographs of re-entry .....	67
Figure 6.2.3.3 Long-exposure still image with Orbiter trail and celestial features .....	68
Table 6.3.2 Re-entry debris timeline revision 7.....	72

This information is being distributed to aid in the investigation of the Columbia mishap and should only be distributed to personnel who are actively involved in this investigation. 5

Figure 6.3.2a Map summarizing locations of observed debris events..... 73  
Figure 6.3.2b Detailed map of the Western U.S. re-entry debris event locations ..... 74  
Figure 6.3.2c Detailed map of the Texas re-entry debris event locations..... 75  
Table 6.3.3 Nominal entry videos screened to compare with STS-107 videos ..... 76  
Figure 6.3.3a Video image of normal Shuttle re-entry, STS-109..... 77  
Figure 6.3.3b Video image of normal Shuttle re-entry, STS-109..... 77  
Figure 6.3.3.c Summary of Events not seen in Nominal Re-entry Video ..... 78  
Figure 6.3.4.a Debris 6 position relative to Orbiter measured from three videos..... 79  
Figure 6.3.4b Debris 14 position relative to Orbiter measured from four videos..... 80  
Table 6.3.4 Calculated separation times and ballistic coefficients ..... 81  
Figure 6.3.5a Debris 6 intensity versus time..... 82  
Figure 6.3.5b Field-by-field Debris 6/Shuttle intensity ratio versus times..... 83  
Table 6.3.5 Estimated masses for Debris events 6, 14, 1 and 2..... 83  
Figure 6.3.6a Frame grabs from the Sparks, NV video ..... 84  
Figure 6.3.6b Preliminary Orbiter light curve from the Springville, CA video..... 85

This information is being distributed to aid in the investigation of the Columbia mishap and should only be distributed to personnel who are actively involved in this investigation. 6

## 1.0 Executive Summary

This report documents the results of the STS-107 Image Analysis Team, formed to assess and analyze all available STS-107 mission imagery from ascent, orbit, and entry. The Team objective was to provide insight into the condition of the Orbiter and the events leading to its breakup through imagery processing and analysis.

One of the primary investigation tasks was to analyze the launch imagery to characterize the debris that impacted the Orbiter during launch at approximately 82 seconds Mission Elapsed Time (MET). The film and video imagery used in this work was derived from NASA and Air Force equipment used for launch monitoring. The analysis of the launch imagery produced the following conclusions:

- The visual evidence implicated the External Tank -Y bipod ramp as the source of the debris.
- One large piece of debris impacted the underside of the left wing. There was no conclusive evidence of other impacts.
- The size of the debris was approximately (24" +/- 3") x (15" +/- 3").
- There was no visible evidence of damage to the left wing.
- The debris was observed to tumble, with an estimated rotation rate on the order of 18 cycles/second.
- Impact was on the underside of the left wing leading edge, in the area of RCC panels 5-9, with most likely impact in the area of panels 6-8.
- Calculations of the debris velocity at impact ranged from 625 ft/sec to 840 ft/sec depending on the various methods and assumptions used, with the most probable velocity estimated to be approximately 700 ft/sec.
- Within the post-impact debris cloud were distinct but unidentifiable objects. The sizes of two of the objects were measurable, estimated to be 12"x11" and 7"x7", respectively.

From analysis of the imagery acquired on-orbit, there was no visual indication of damage or anomalies to the Orbiter during the orbit phase of the mission.

Another primary task for the Image Analysis Team was analysis of the re-entry imagery of the Orbiter to identify, timeline, and characterize the observed anomalies and debris-shedding events during entry. Most of the imagery was obtained from the public using consumer-grade equipment. From analysis of the entry imagery, the following conclusions were reached:

- 24 anomalous events were observed in the imagery along the Orbiter's re-entry track between California and New Mexico. Events over Texas are still being characterized.
- The anomalies noted included debris-shedding events, large flashes or flares, and non-uniformities in the Orbiter's plasma trail.
- Debris motions relative to the Orbiter were measured from which debris ballistic coefficients were determined.

This information is being distributed to aid in the investigation of the Columbia mishap and should only be distributed to personnel who are actively involved in this investigation. 7

- Mass estimates of the shedding debris were determined from the imagery. The estimates ranged from ~ 0.2-8 lbs for small debris events, to 20-500 lbs for the largest debris events, with the most probable masses for those large events in the 100-200 lb range.

This information is being distributed to aid in the investigation of the Columbia mishap and should only be distributed to personnel who are actively involved in this investigation. 8

## 2.0 Introduction

In response to the Shuttle Columbia accident, the Image Analysis Team was activated in accordance with JSC-14273, "Space Shuttle Program Contingency Action Plan for Johnson Space Center". The Team was responsible for assessing and analyzing all available visual imagery from ascent, orbit, and entry to provide insight into the condition of the Orbiter and the events leading to its breakup. Of particular interest during ascent was analysis of the debris impact event at approximately 82 seconds Mission Elapsed Time (MET), and during entry, analysis of the debris-shedding events emanating from the Orbiter. The Team reported its findings directly to the Orbiter Vehicle Engineering Working Group (OVEWG).

The primary sources of imagery for the ascent analysis included launch film and video from tracking cameras located around the launch complex. On-orbit imagery was either downlinked during the mission or recovered from the Orbiter debris on the ground. Entry analysis was accomplished primarily with video and still photos submitted to NASA by the public after the accident.

The image processing and analysis tasks for this investigation were numerous and diverse, many involving low quality imagery. In some cases the analyses required problem solving for which there were no established methods, such as characterizing the entry debris events from consumer-grade videos. To address these challenges, a wide variety of resources and expertise was called upon from various centers within NASA, as well as from industry and organizations outside of NASA. A complete listing of Image Analysis Team contributing organizations and personnel is provided in Section 8.

This information is being distributed to aid in the investigation of the Columbia mishap and should only be distributed to personnel who are actively involved in this investigation. 9

### 3.0 Purpose & Scope

This report documents the processes and findings of the Image Analysis Team based upon analysis of STS-107 imagery from launch, orbit, and entry. The main body of the report presents a summary of the analysis techniques and primary results. These summarized results represent the consensus of the Image Analysis Team, and are in some cases compilations of independent analyses by multiple contributors within the Team. Additional details of all the individual analyses are attached as appendices and are referenced in the report.

The primary findings from analysis of STS-107 launch imagery are summarized in Section 4. The launch analysis centered on characterizing the impact parameters for the debris strike event at approximately 82 seconds MET. Other launch-related analyses included in this report were in support of requests from the Columbia Accident Investigation Board (CAIB). Analyses from imagery acquired from orbit are summarized in Section 5, and the entry analyses are found in Section 6. Section 7 provides lessons learned and recommendations for enhancements of NASA's capabilities for imagery acquisition and imagery analysis to support human space flight missions. Finally, Chapter 8 lists the contributors to the Image Analysis Team.

This information is being distributed to aid in the investigation of the Columbia mishap and should only be distributed to personnel who are actively involved in this investigation. 10

## 4.0 Launch Analyses

This section provides a summary of the data sources, analytical methods, and major findings from analyses of the STS-107 launch imagery, taken January 16, 2003. All mission elapsed times are referenced to the liftoff time 2003:016:15:39 UTC.

### 4.1 Launch Data Sources

#### 4.1.1 Launch Film and Video

Film and video cameras around the launch complex provided the primary data for observing events during the STS-107 launch, including the debris that impacted the left wing at approximately 82 seconds after lift-off. Detailed descriptions of all of the standard launch pad and range cameras that were used to image the launch of STS-107 are summarized in Appendix 4.1.1.

The primary cameras providing views of the debris event at 82 sec MET were mounted to long-range tracking telescopes and are listed in Table 4.1.1. The locations of these cameras with respect to the launch pads at Cape Canaveral are shown in Figure 4.1.1a. The launch site coordinates for the cameras that imaged the debris event seen at 82 sec MET were extracted from the National Space Transportation System (NSTS) 08244 Space Shuttle Program Launch and Landing Photographic Engineering Evaluation document, Revision B, 1997 and are presented in Appendix 4.1.1.

Camera	Type	Focal Length	Frame Rate	Shutter speed	Location
ET-208	Video MII	200 inches	30 frames (60 fields)/sec	Estimated to be between 1/250 and 1/500 seconds	Outlying Cocoa Beach/DOAMS
E-208	35 mm Film	400 inches	48 frames/sec	TBD	Co-located with ET-208
E-212	35 mm Film	400 inches	64 frames/sec	1/136 seconds	Outlying UCS-23/ATOTS
ET-204	Video MII	120 inches	30 frames (60 fields)/ sec	TBD	Outlying Patrick AFB/PIGOR
E-204	35 mm Film	360 inches	64 frames/sec	TBD	Co-located with ET-204

**Table 4.1.1 Launch cameras that viewed the debris event at 82 seconds MET**

This information is being distributed to aid in the investigation of the Columbia mishap and should only be distributed to personnel who are actively involved in this investigation. 11

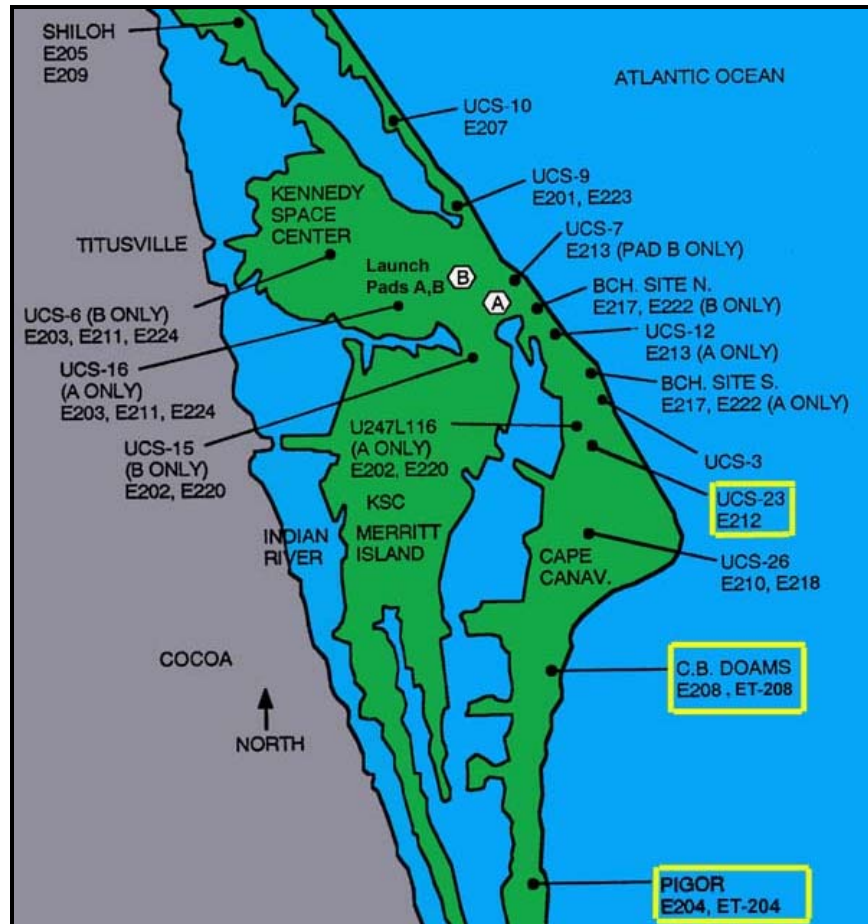


Figure 4.1.1a Map showing the location of the cameras used to image the debris strike

The video cameras provided standard National Television Standards/System Committee (NTSC) format video of the launch. The video was recorded on M-II format videotape with the timing information recorded in the audio channel. The video imagery was transmitted to Marshall Space Flight Center (MSFC) and Johnson Space Center (JSC) via satellite replays within hours of the launch for rapid analysis. In order to obtain best quality video for analysis during the investigation, the original M-II tapes were duplicated and distributed to the team. DPS Reality was used for digital frame grabs and resampling from the video to provide 640 by 480 pixel images for each frame. The Mitchell 35 mm film cameras provided higher resolution imagery of the launch sequence with finer time resolution. The films were processed by Continental Labs under contract to Kennedy Space Center (KSC) and distributed to the teams at KSC, MSFC and JSC. Details about the video and film reproduction are included in the Methods section (Section 4.2).

The ET-208 video camera provided the best view of the underside of the left wing and the debris strike area (Figure 4.1.1b). However, the moment of impact was not recorded due to insufficient time resolution of the imagery, limited by the camera frame rate. The

This information is being distributed to aid in the investigation of the Columbia mishap and should only be distributed to personnel who are actively involved in this investigation. 12



time of impact is constrained by the video fields immediately before and after the impact. A 35 mm film camera, E-208, was co-located with video camera ET-208 and would have provided the highest resolution view of the debris impact area. However, the E-208 imagery was out of focus due to problems with the camera optics. Efforts were made to de-blur the E-208 imagery, but were unsuccessful (see Section 4.1.3 Star Data). Therefore the E-208 camera images were not useful for analysis of the debris strike.



**Figure 4.1.1b Frames from ET-208, E-212 and ET-204 cameras showing the respective views**

The 35 mm film camera E-212 imaged the top side of the Orbiter's left wing, and provided the best high-resolution view of the debris before it disappeared behind the left wing prior to impact. The E-212 views show the debris as it is first seen originating from the vicinity of the External Tank (ET)/Orbiter -Y bipod attach area, and show the post-impact debris cloud and debris fragments.

Two other launch cameras provided faint views of the 82 sec MET debris, ET-204 video and E-204 film, located well south of ET-208/E-208 and much further away from the Orbiter. Because of their further distance, imagery from ET-204/E-204 was of much poorer resolution than the imagery from ET-208. Also, the ET-204/E-204 cameras provided a view similar in perspective to the 208 cameras — no additional areas of the Orbiter could be seen. The ET-204/E-204 cameras did contain images of the debris at slightly different times than the other cameras; some analysts found this useful. However, other analysts felt that the debris was so poorly defined in the ET-204/E-204 camera views that it might add too much error into the analyses. For these reasons, the ET-204/E-204 cameras added little to most analyses of the debris strike.

#### **4.1.2 Shuttle Reference Data**

The following sources for Shuttle ascent trajectory and structural dimension information were used in making the image analysis measurements:

- STS-107 Ascent Trajectory from the JSC Ascent/Descent Dynamics Branch

This information is being distributed to aid in the investigation of the Columbia mishap and should only be distributed to personnel who are actively involved in this investigation. 13

- Computer Aided Design (CAD) Models compatible with the Shuttle Master Dimensions Book MD-V70, supplied by the JSC Aerospace and Flight Mechanics Division/EG.
- On-line Shuttle Reference Manual at <http://spaceflight.nasa.gov/shuttle/reference/shutref/index.html>.

### 4.1.3 Star Data

In an effort to de-blur the E-208 film and enhance the E-212 film, imagery of several stars was acquired with the respective cameras. The imagery was collected at KSC using the launch configuration of the cameras, and the film and video were processed according to launch imagery protocols. The purpose was to use the star images to determine the point spread function of the cameras for de-blurring algorithms to be applied to the out-of-focus E-208 imagery, and also to enhance the E-212 views. The primary result was a determination that the E-208 camera optics were significantly compromised. Details of the star imagery and recommendations resulting from these data are discussed in Appendix 4.1.3.

## 4.2 Launch Imagery Analyses: Methods

The methods and procedures for analyzing the launch imagery, including the reproduction of the imagery to obtain the highest quality for analysis, protocols for documenting anomalies during the imagery screening, and specific methods for digital enhancements of the imagery are summarized in this section.

Initial analyses of the launch imagery, including a description of the debris that impacted the left wing, were performed immediately after launch and reported in the STS-107 Launch +4 Report (See Section 4.3.1). These initial results provided the basis for subsequent analyses of the debris event after the Columbia accident. Additional image analysis methods evolved throughout the investigation. New findings and hypotheses drove requirements for increasingly sophisticated image enhancements. This section describes key elements of the image enhancement and analysis approaches.

### 4.2.1 Obtain Best Quality Imagery (Film and Video)

The investigation tasks required that the team use the highest quality imagery, thereby allowing detection and enhancement of details defined by the limits of resolution of the imagery.

#### Film Reproduction

During the STS-107 mission, standard procedures for film distribution were followed: after the launch, engineering launch film prints were provided to other centers by KSC for analysis. These film duplicates were second-generation positive copies made directly from the original negative films (Kodak 250 daylight film). However, these engineering copies were used extensively during the mission for screening and analysis and had been distorted by heat from projectors and scratched by extensive handling. Additional third

This information is being distributed to aid in the investigation of the Columbia mishap and should only be distributed to personnel who are actively involved in this investigation. 14

generation copies of key films such as E-208 and E-212 were also used for early analyses. Important segments of the films were scanned at the JSC Digital Imaging Lab using a Kodak scanner to produce digital imagery for analysis.

The image analysis team had concerns about the potential loss of detail on the third generation imagery. The most detailed analysis of the debris strike to the left wing required the highest quality imagery to be copied directly from the original camera E-208 and E-212 launch films. To accomplish this, the original E-208 and E-212 film negatives were hand-carried to Kodak facilities in Rochester, New York for scanning in a clean room environment. Kodak scanned the E-208 and E-212 frames using two different digital scanning systems (Spirit Data Cine 2K film scanner providing 10 bit, 2048 x 1556 pixel images, and Genesis 4K scanner providing 12 bit, 4096 x 3112 pixel images). A total of three scans at a range of exposure stops (-1, normal, and +1) were performed. The Genesis digital scans (files) were printed directly back to film providing positive engineering prints for the different analysis groups. The digital scans were made available to the investigators via an ftp computer site. This scanning process eliminated the slight data loss inherent in making contact prints from the original film with minimum degradation to the original film.

#### Video Reproduction

During the mission, the original ET-208 video was recorded on an M-II recorder. KSC screened the original ET-208 video one day after launch to verify that there was no loss of quality on the copies of the tape and transmitted the video via satellite to JSC and MSFC. The satellite-routed ET-208 video was used by JSC and MSFC during the remainder of the STS-107 flight for the analysis of the debris strike to the Orbiter left wing. Inherent in the satellite transmission was a slight reduction in the quality and resolution of the video available at JSC and MSFC for analysis. During the investigation, KSC copied the M-II tape to a state-of-the-art digital Betacam (Digi-beta) format tape in order to capture the best quality ET-208 camera video of the debris strike to the left wing. These first generation Digi-beta clones from the original Digi-beta tape and DVCAM format copies were provided to the various analysis groups.

#### **4.2.2 Launch Video and Film Screening**

Video and film screening is the initial step for all subsequent image analyses. For each mission all launch imagery is screened in parallel by the KSC, MSFC, JSC and System Integration image analysis groups. Each of the image analysis groups thoroughly review the launch videos and films within the first few days of launch. All anomalies are visually described and documented in a mission-specific screening database, and significant events are illustrated, reported to other teams and the Mission Evaluation Room (MER), and posted to the Image Science and Analysis web page ([references/shuttleweb/mission\\_support/missions.html](http://references/shuttleweb/mission_support/missions.html)). Following the STS-107 accident, the image analysis groups re-screened the STS-107 launch films and video using their traditional equipment and procedures in order to document any additional events that could possibly provide information of value to the investigation. KSC was the lead center for the re-screening of the launch imagery. KSC also re-screened the STS-107

This information is being distributed to aid in the investigation of the Columbia mishap and should only be distributed to personnel who are actively involved in this investigation. 15

pre-launch imagery data, including all Operation Television and Infrared videos from ET loading (T-6 hours through launch.). Any additional observations were added to the launch film screening data sheets; however, no significant new observations were reported by any of the analysis groups.

### 4.2.3 Image Enhancement and Analysis Techniques

#### Enhancement

A number of different techniques were employed to bring out additional detail in both the film and the video imagery. Most of the analyses of the launch imagery involved digital enhancements, including intensity contrast stretching and sharpening. For specific tasks, more sophisticated image enhancements were applied to the launch imagery. Image enhancement and analysis techniques included:

- Spatial filtering aided in removing noise and sharpening the detail in the images (examples include median filters, Gaussian blur filters, unsharp mask).
- Frequency domain methods were used to design deconvolution filters for reducing focus and motion blur, thus reducing image noise, and sharpening the image.
- Standard contrast stretching was used to make low contrast areas more readily visible for analysis.
- Image stabilization and registration methods were used to remove camera motion when analyzing the motion of debris in digital movies or for performing frame averages.
- Frame averaging from stabilized image sequences was used to reduce noise and enhance subtle details that could not be seen in a single image.
- Color analysis of the debris in the Red, Green, and Blue (RGB) bands, including band ratioing.
- Analysis of the data in color spaces other than RGB was also employed. Images were converted to the L\*a\*b color mode, which separates luminosity information in the 'L' channel from color information in the 'a' and 'b' channels, so that sharpening of the luminosity does not enhance noise patterns in the color channels.
- Intensity profiles across the debris were used to help determine debris sizes and distinguish the true extent of the debris from focus and atmospheric blurring of the edges.
- Image differencing from consecutive frames/fields as well as differencing consecutive frames/fields from an average image were used to help determine debris location and size.

Measurements of the debris sizes, impact velocity, impact location, and impact angle were all made from the launch imagery. To obtain the best quantitative results from the imagery, the Image Analysis Team focused on image scaling, edge detection, centroid measurement, motion blur correction, and the use of CAD models, as addressed below.

This information is being distributed to aid in the investigation of the Columbia mishap and should only be distributed to personnel who are actively involved in this investigation. 16

Scaling

Scales were computed to relate measurements made on the imagery (in pixels) to actual real-world distances in object space. Scaling can be accomplished in several ways. One method is to simply use a known object in the field of view that is at approximately the same distance from the camera and has approximately the same orientation as the object to be measured. This method works well when the camera focal length and the distance from the camera to the object are large (as is the case in all of the cameras used in the STS-107 debris analyses). Note that this method assumes that the rays of the perspective projection are essentially parallel. For the long camera-to-object distances and lens focal lengths used in the STS-107 analyses, this assumption is reasonable; it simplifies the scale derivations. Figure 4.2.3 illustrates this concept with the scale given simply as  $D/d$ , which is the length of a reference object divided by its projection onto the camera's image plane. An example of this scaling method uses the Shuttle Solid Rocket Booster (SRB) as the reference object as seen in camera E-212. The scale at the distance of the SRB and in a plane oriented along the length of the SRB is given by:

Scale = SRB distance (in inches)/ Number of pixels subtended by the SRB on the image.  
For E-212, frame 4914, the scale is 1,790 inches/1000 pixels = 1.8 inches/pixel

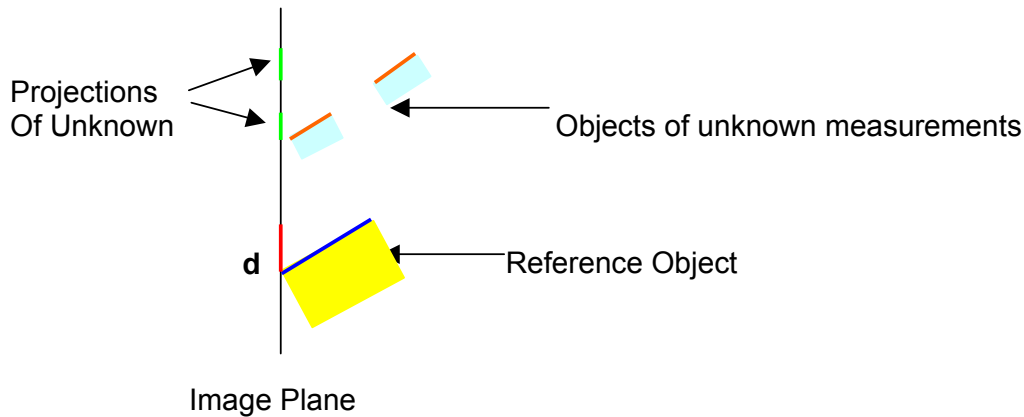


**Figure 4.2.3 Scaling when reference object is aligned with measurement object.  $D$  is the length of a reference object with known dimensions and  $d$  is the length of the projection of the reference object onto the camera's image plane.**

If the orientation of the object to be measured is assumed to be parallel to the camera's image plane and there is no reference object that is parallel to the image plane to use for scaling, then the following methods can be used to determine the scale in the image plane at the distance of the object:

This information is being distributed to aid in the investigation of the Columbia mishap and should only be distributed to personnel who are actively involved in this investigation. 17

- Use a reference object at approximately the same distance as the object to be measured and with a known angle to the camera's image plane. The image plane scale would be:  $(D/d) \cdot \cos(\theta)$ .

Where:

D = length of the reference object (in object space coordinates such as inches.)

d = the length of the projection of the reference object onto the camera's image plane (in pixels).

$\theta$  = the angle of the reference object to the image plane.

- Use the camera's angular field of view, the number of pixels across the image corresponding to the entire camera field of view, and the distance from the camera to the object. The camera field of view and the number of pixels across the image can be determined for either the horizontal or vertical dimensions, but the scale should be the same in both dimensions. The formula for determining the image plane scale is:

$$\text{Scale} = (2 \cdot R \cdot \tan(\theta/2)) / d$$

Where:

R = Distance from the camera to the object

$\theta$  = Camera angular field of view (can be derived from the camera focal length)

d = The total number of pixels across the image.

- Use a circular reference object at approximately the same distance as the object to be measured. The longest dimension of the reference object will always be its diameter regardless of its orientation relative to the image plane. The image plane scale would then be the diameter of the reference object divided by the number of pixels subtended by that object on the image.

All of these techniques were employed in the STS-107 image analyses.

#### Edge Detection

To measure the extent of an object seen on an image, the boundary of that object must be defined. The most difficult part of establishing boundaries is accurately defining the object's edges in the image because the edges always contain some amount of blur due to imperfect focus, atmospheric distortions, camera motion, and insufficient resolution to detect a sharp boundary. Many methods exist for detecting edges; most are based on some type of spatial gradient filtering. A method known as the full-width at half-maximum to measure the edges of the debris was utilized in the STS-107 image analyses. See section 4.3.2.3 for more details on this technique.

#### Finding Object Centroids

Once the boundary around an object has been determined, either by manual definition or automated edge detection, image analysis algorithms are used to automatically determine the area, perimeter, and centroid of the defined object. The center of an object can also be selected manually, but automated techniques help to obtain subpixel accuracy and are

This information is being distributed to aid in the investigation of the Columbia mishap and should only be distributed to personnel who are actively involved in this investigation. 18

objective and consistent. Finding the centroids of an irregularly shaped object was particularly important for determining the best estimate for the positions of the debris that impacted the Shuttle's left wing at 82 seconds. To find the debris centroids on the image, an ellipse was fit to the object. The center of the ellipse defined the debris centroid. Because the debris had a generally elliptical shape, this method was considered adequate for determining the center of the debris. These centroid locations were then used for trajectory and velocity analyses.

#### Motion Blur Correction

When examining imagery of high-speed events such as the 82-second debris-shedding event, it is necessary to correct or at least account for blurring of the fast moving object. Motion blur is especially important when the velocity of the object being imaged is significant compared to the time that the camera shutter is open. In the case of the debris seen at 82 seconds, the velocity at impact was on the order of 700 ft/second while the shutter on camera E-212 was open for 1/136 second. If the debris motion were entirely parallel to the image plane, the motion blur of the debris would be more than 5 feet. Because the orientation of the Orbiter and the debris trajectory were mostly out of the E-212 image plane by approximately 65 degrees, the effect of motion on the image was greatly reduced, but still significant. Definition of motion blur was an important consideration for the debris size measurements.

#### Combining CADs and Imagery

CAD (Computer Aided Design) models of the Shuttle were used in concert with the imagery to determine the three-dimensional trajectory of the debris. The CAD-to-image overlay methods involve precisely registering a CAD model of an object to the imagery of that same object. In the case of the STS-107 analysis, the imagery from cameras E-212 and ET-208 were digitally overlaid on a Shuttle CAD model using CAD software such as IDEAS or Pro-E. In general, most of the alignment of the CAD model to the imagery was done using known parameters such as the camera's field of view, position, and pointing angles as well as the distance to the Shuttle based on the known ascent trajectory. In theory, if the camera parameters and Shuttle trajectory are perfectly known then the model should align perfectly with the imagery. In practice, the fit is less than perfect due to slight errors in the CAD models and atmospheric and lens distortions in the imagery. Minor position adjustments to refine the alignment of the CAD to the imagery are then made manually. After the CAD and imagery are aligned, line-of-sight vectors from the cameras to the frame-by-frame positions of the debris along its trajectory were computed. The vectors formed surfaces, one for each camera. The intersection of the two surfaces formed a 3D spatial curve defining the trajectory of the debris.

#### **4.2.4 Determination of the Highest Fidelity Camera Timing Data**

Accurate and precise timing data on the film and video were important for all analyses of the launch imagery. Detailed comparisons between different imagery sources and between different analysis groups revealed timing inconsistencies introduced by the video cloning and transmittal processes. Considerable effort was invested in understanding the timing mechanisms on both the film and the video cameras, and the timing offsets

This information is being distributed to aid in the investigation of the Columbia mishap and should only be distributed to personnel who are actively involved in this investigation. 19

introduced by reproduction of the launch video due to the timing data recorded into the audio channel. Data about the respective camera timing parameters are provided in Appendix 4.2.4.

### **4.3 Launch Imagery Analyses: Primary Results**

This section contains an overview of the analyses performed on the launch imagery. The analyses focused on fully characterizing the debris that impacted the left wing at approximately 82 seconds MET. Early work performed immediately after launch and throughout the STS-107 mission is summarized in Section 4.3.1, and the analyses performed after the accident are presented in Section 4.3.2.

#### **4.3.1 Analyses Performed during the STS-107 Mission**

The KSC, MSFC, JSC and Systems Integration imagery screening groups submitted initial launch video screening reports the day after the launch of STS-107 describing the debris impact to the Orbiter left wing at approximately 81.86 seconds MET. Due to a problem with receiving and transmitting the second video replays, the review of the long range tracking camera videos was delayed until the day after launch. In the next few days, the film imagery was reviewed and each group provided additional screening reports based on the findings from the launch films. Appendix 4.3.1 contains the Intercenter Launch +4 day Screening Report.

##### **4.3.1.1 Initial Findings**

The key findings reported in the Launch +4 day Screening Report include a description of the debris anomaly. The source was determined to be from an area near the ET/Orbiter -Y bipod. The report documents four distinct objects — the initial analyses could not discern whether the objects originated as separate pieces or were derived from a single piece that breaks apart. The physical description and motion of all four pieces are qualitatively described, including the impact under the leading edge of the left wing by the largest piece of debris. The report also references comparison views of the impact area immediately before and after the event for indications of damage to the wing. Because of the poor resolution of the imagery, the initial analyses could reach no conclusions about the extent of any damage that may have occurred from the debris strike event.

The early pre-accident screening reports stated that evidence of a smaller, second debris impact to the Orbiter left wing also occurred. During the post-accident investigation, subsequent detailed analysis using “best quality” enhanced imagery showed that only one debris object definitely struck the wing and that there was no visual evidence of a second impact to the wing. What appeared to be a faint cloud indicating a second debris strike on the pre-accident imagery was later determined to be several smaller pieces of debris that had passed under the wing with no apparent vehicle contact.

This information is being distributed to aid in the investigation of the Columbia mishap and should 20  
only be distributed to personnel who are actively involved in this investigation.



#### 4.3.1.2 Reporting

- The Intercenter Launch +4 Day Screening Report was not received by the Shuttle Program management and engineers until approximately launch + 8 days due to an unknown computer error at KSC.
- The JSC video and film screening reports documenting the debris strike were delivered to the Shuttle MER (Mission Evaluation Room) on schedule prior to the delivery of the Launch +4 day Intercenter report.
- The daily video and film screening reports from JSC, KSC, and MSFC were also sent to a wide distribution that included key personnel at all levels of the Shuttle program management and engineering at each of the three NASA centers.
- For Shuttle Program reference, the preliminary information and imagery of the STS-107 debris impact to the left wing were placed on the web sites at the three NASA centers prior to the re-entry of Columbia. The web-based products included:
  - Preliminary measurement of the debris size on STS-107.
  - ‘Before’ and ‘After’ views of the debris impact showing no visible damage to the vehicle.
  - Debris trajectory plot of the debris seen on ET-208 and E-212 imagery
  - CAD images overlaid to ET-208 and E-212.
  - Views of the STS-112 and STS-50 damage caused by missing Thermal Protection System (TPS) from the ET/Orbiter -Y bipod ramp and measurement of debris size seen on STS-112.

#### 4.3.1.3 Other Action Taken during Mission

- JSC and KSC imagery analysts supported a Shuttle engineering teleconference on “Preliminary Debris Transport Assessment of Debris Impacting Orbiter Lower Surface in the STS-107 Mission” prior to landing day (1/22/03).
- The Intercenter Photo Working Group (IPWG) chairman made a request for additional on-orbit photographic coverage of the Orbiter prior to landing (this was not approved).

#### 4.3.2 Post-Accident Launch Analyses

This section summarizes the major findings from detailed analyses of the launch imagery after the Columbia accident occurred on February 1, 2003. It includes a description of the imagery that documents the debris that struck the left wing, and quantitative characterization of the debris using the imagery as the primary data source. Details of the analyses are presented in Appendices that are referenced in the report.

##### 4.3.2.1 Debris Event Timeline

The debris that struck the Orbiter during ascent was first seen near the ET/Orbiter -Y bipod attach area at approximately 81.7 seconds MET, and it impacted the left wing at approximately 81.86 seconds MET (016:15:40:21.86 Universal Time Code or UTC).

This information is being distributed to aid in the investigation of the Columbia mishap and should only be distributed to personnel who are actively involved in this investigation. 21

The debris was visible in the launch imagery for a period of approximately 0.16 seconds. Descriptions of the debris event as viewed from the two primary cameras, ET-208 and E-212 are given below. A detailed discussion of the determination of the debris impact time is provided in Appendix 4.3.2A. Note that the times on the imagery are given in UTC.

#### Camera ET-208

A single piece of light-colored debris was first seen on ET-208 imagery near the ET/Orbiter -Y bipod attach area at 016:15:40:21.674 UTC. Figure 4.3.2.1a is a good view of the debris after it becomes more clearly visible. The debris traveled outboard in a -Y direction (Orbiter structural coordinate system) before falling aft. Figure 4.3.2.1b shows the debris just after it struck the wing (the moment of impact was between video images). The location of the debris was mapped from frame to frame to build a trajectory from the approximate source to impact as viewed by Camera ET-208, shown in Figure 4.3.2.1c.

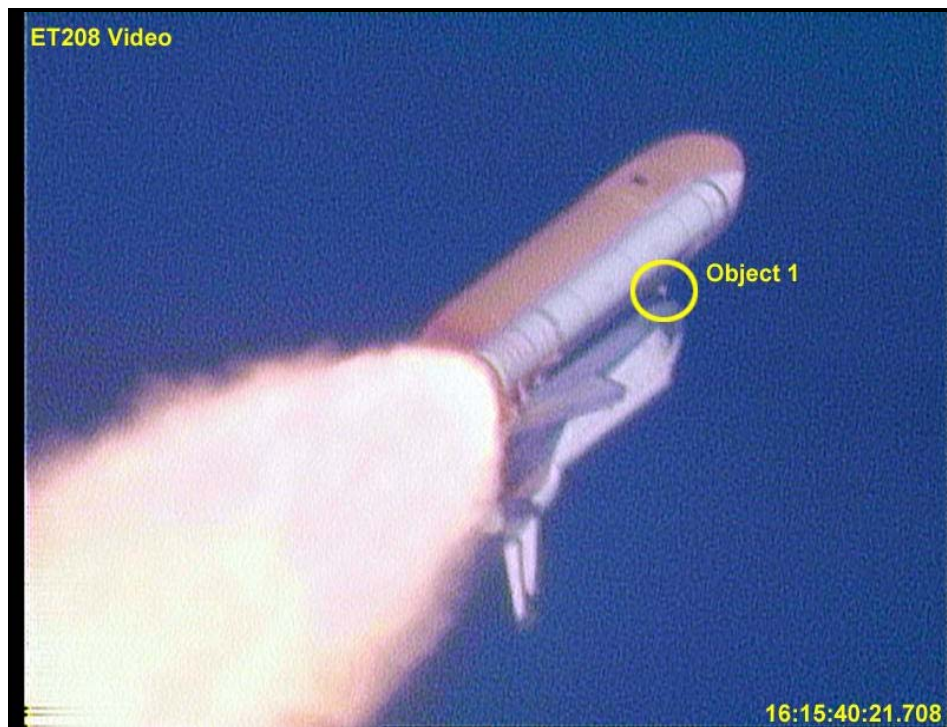


Figure 4.3.2.1a ET-208 View of the debris near point of origin

This information is being distributed to aid in the investigation of the Columbia mishap and should only be distributed to personnel who are actively involved in this investigation. 22



Figure 4.3.2.1b ET-208 View of the debris at 016:15:40:21.858 UTC just after impact with the underside of the leading edge of left wing

This information is being distributed to aid in the investigation of the Columbia mishap and should only be distributed to personnel who are actively involved in this investigation. 23

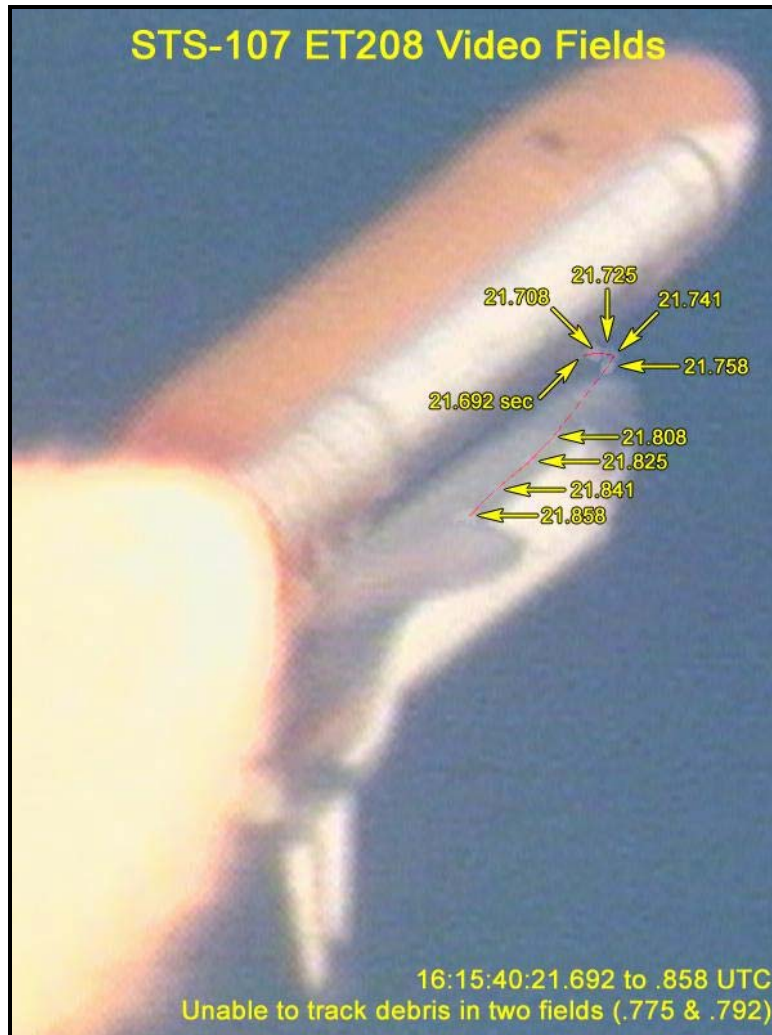


Figure 4.3.2.1c ET-208 Composite with trajectory of debris (times are in seconds after 16:15:40 UTC)

#### Camera E-212

A single, large piece of light-colored debris was first seen near the ET/Orbiter -Y bipod attach area from Camera E-212 at 016:15:40:21.691 UTC. Figure 4.3.2.1d is a view of this debris (Object 1) after it had moved into sunlight. Object 1 appeared to move in a -Y direction before falling aft and striking the wing. Its location was also mapped frame to frame to build a trajectory of the debris as viewed by Camera E-212. Figure 4.3.2.1e is a composite image that shows the debris position as it fell aft over the time span of camera frames 4913 through 4922. From this perspective, the wing obscured the view of Object 1 prior to impact.

At least two other smaller pieces of debris in the vicinity of Object 1 were also visible from E-212 during this timeframe. It is possible that these pieces broke off from Object 1 along the upper portion of its trajectory; however, this interpretation from the imagery is inconclusive. The imagery data are also insufficient to determine the exact number of

This information is being distributed to aid in the investigation of the Columbia mishap and should only be distributed to personnel who are actively involved in this investigation. 24

smaller debris pieces or their sizes. Therefore, the debris characteristics noted refer to Object 1 throughout the remainder of this section.

Only Object 1 was confirmed to impact the left wing. There is no conclusive evidence of more than one debris impact to the Orbiter. A large, light-colored cloud, which emanated from the underside of the left wing due to debris impact (Figure 4.3.2.1f), was first observed at 016:15:40:21.863 UTC. Within the post-impact cloud, at least two large pieces of debris were observed and measured (see Section 4.3.2.6). There is no conclusive visual evidence of post-impact debris flowing over the top of the wing.

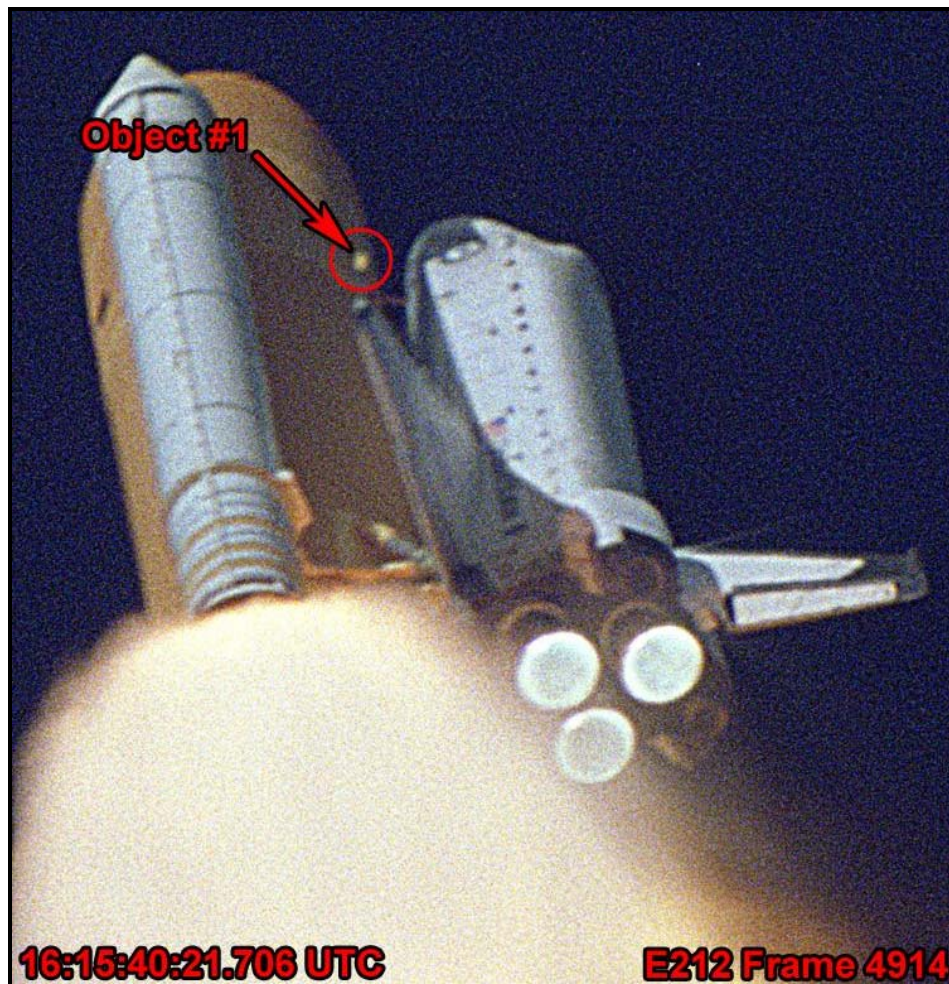


Figure 4.3.2.1d Debris object in full illumination (E-212, Frame 4914)

This information is being distributed to aid in the investigation of the Columbia mishap and should only be distributed to personnel who are actively involved in this investigation. 25

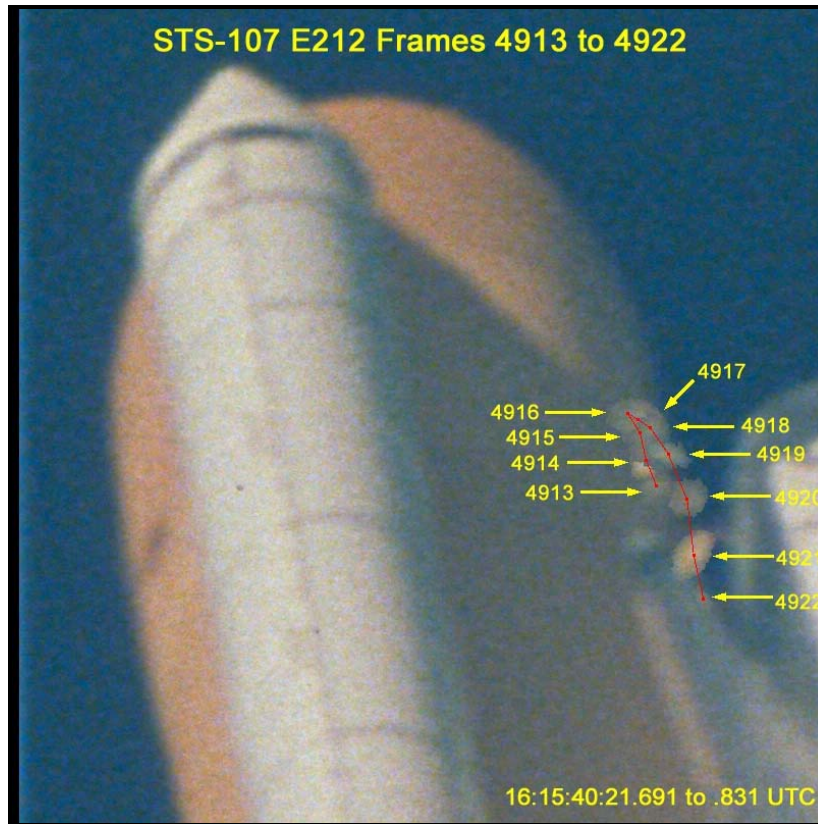


Figure 4.3.2.1e Composite image showing the trajectory of the major piece of debris (Object 1) mapped from camera E-212, frames 4913 through 4922.

This information is being distributed to aid in the investigation of the Columbia mishap and should only be distributed to personnel who are actively involved in this investigation. 26

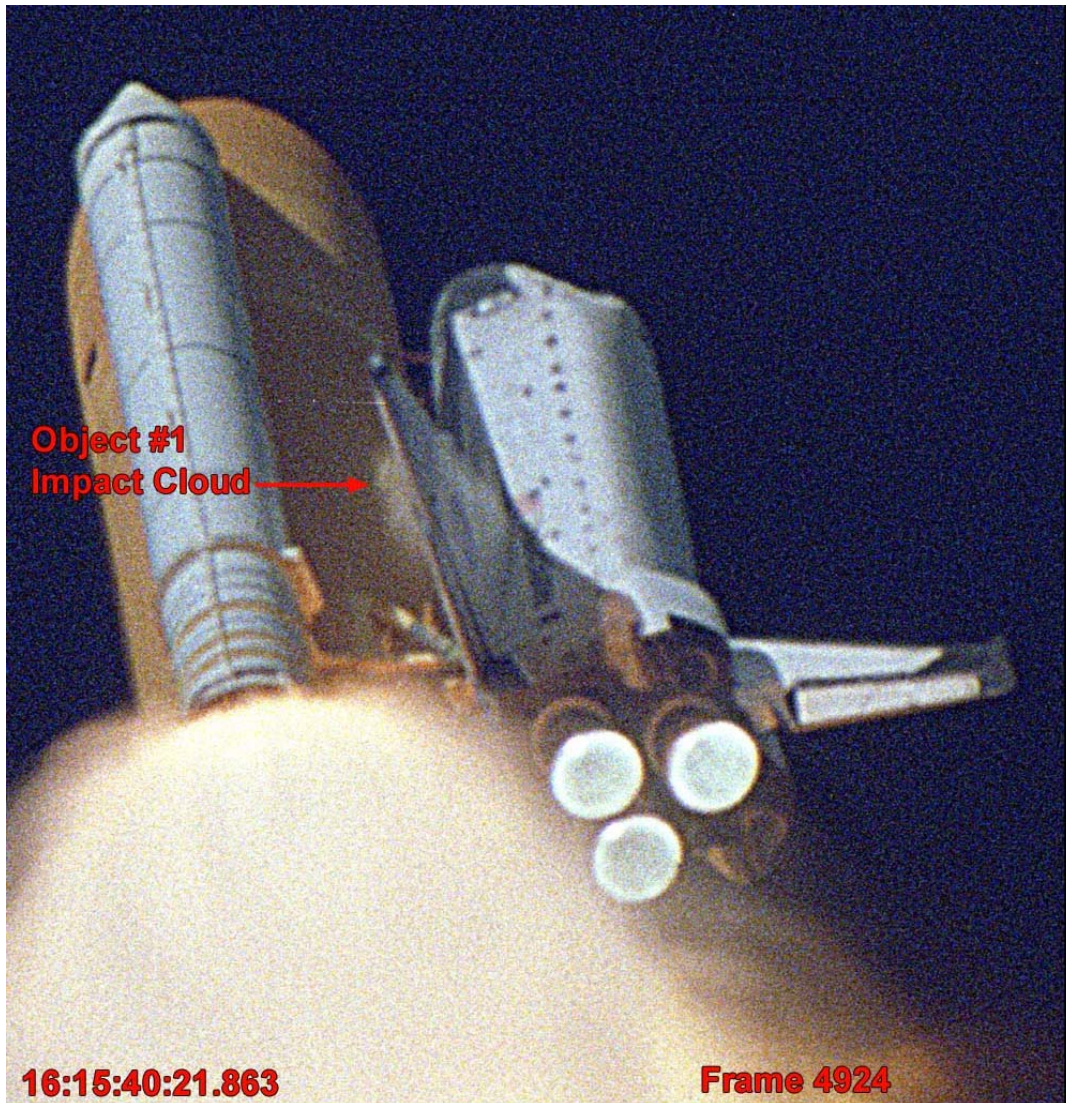


Figure 4.3.2.1f Debris impact cloud seen on E-212 (Frame 4924)

More images of the debris from camera ET-208 and E-212 views are provided at the Image Science and Analysis web site,

[references/shuttleweb/mission\\_support/sts-107/contingency/launch/107\\_launch.html](http://references/shuttleweb/mission_support/sts-107/contingency/launch/107_launch.html)

Including:

- Comparison views of ET-208 and E-212
- Frame by frame debris impact sequences for both ET-208 and E-212
- High resolution Quick Time movies of the ET-208 and E-212 camera views
- Camera ET-208 difference movie highlighting the debris

This information is being distributed to aid in the investigation of the Columbia mishap and should only be distributed to personnel who are actively involved in this investigation. 27

#### 4.3.2.2 Debris Source

Based on the imagery from cameras ET-208 and E-212, there was strong evidence that the debris that struck the wing at 82 seconds MET originated from the ET/Orbiter -Y bipod attach area.

Figure 4.3.2.2a shows the results of a detailed analysis using imagery from Camera E-212 immediately before and after the debris-shedding event. Twenty-one frames before and nineteen frames after the debris event were averaged to lessen image noise and bring out detail, creating before and after images for comparison. Note that there is a clear change in brightness in the area of the left bipod ramp after the debris event. This indicates a significant physical change, leading to the assumption that the change was the result of the shedding of foam from the bipod ramp. When the before and after images are aligned (registered on top of one another) and flickered back and forth, the area of change is very noticeable to the human eye. While this [“flicker”](#) image also shows that the two averaged images have a slightly different viewing perspective caused by the orbiter moving down range, there is no significant change in the sun angle or in the shadows falling on the tank. This means that the change in appearance of the bipod cannot be explained by changes in lighting. The ramp area has a definite scar that appeared after the debris-shedding event.

The dimensions of the area of change seen in the region of the ET bipod ramp were as large as 35 inches by 20 inches when measured approximately in the Orbiter’s XY plane, and as small as 20 inches by 8 inches when measured in a plane parallel to the camera’s image plane. These dimensions provide upper and lower bounds on the area of change. Because the orientation of the area of change is unknown from this single camera view, only this range of sizes can be determined. See Appendix 4.3.2B for a detailed description of this analysis.

Further evidence that the source of the debris was the bipod ramp area is illustrated in Figure 4.3.2.2b. The upper portion of the debris trajectory is shown, based upon a dual-camera analysis using the imagery from E-212 and ET-208 (see Section 4.3.2.5 for detail on the trajectory analysis). The origin of the debris trajectory is shown to map directly to the area of the bipod ramp.

This information is being distributed to aid in the investigation of the Columbia mishap and should only be distributed to personnel who are actively involved in this investigation. 28



JSC Image Analysis -- STS-107 E212 view bipod area enhancement

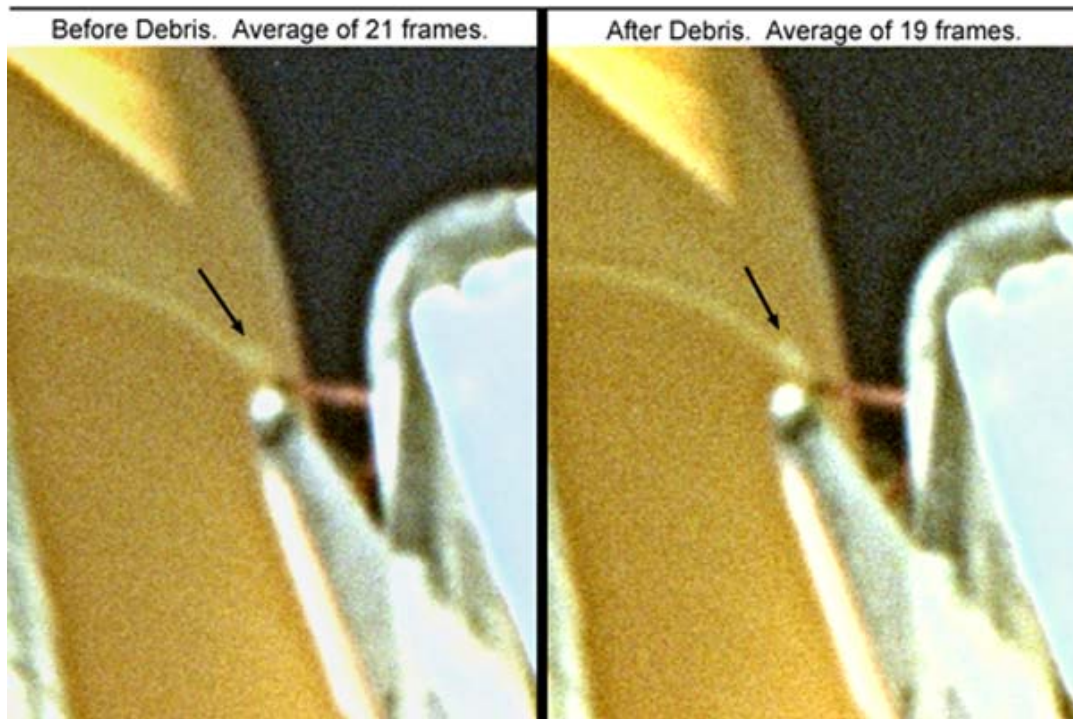


Figure 4.3.2.2a Enhanced images of the ET forward bipod ramp area before and after the debris shedding event

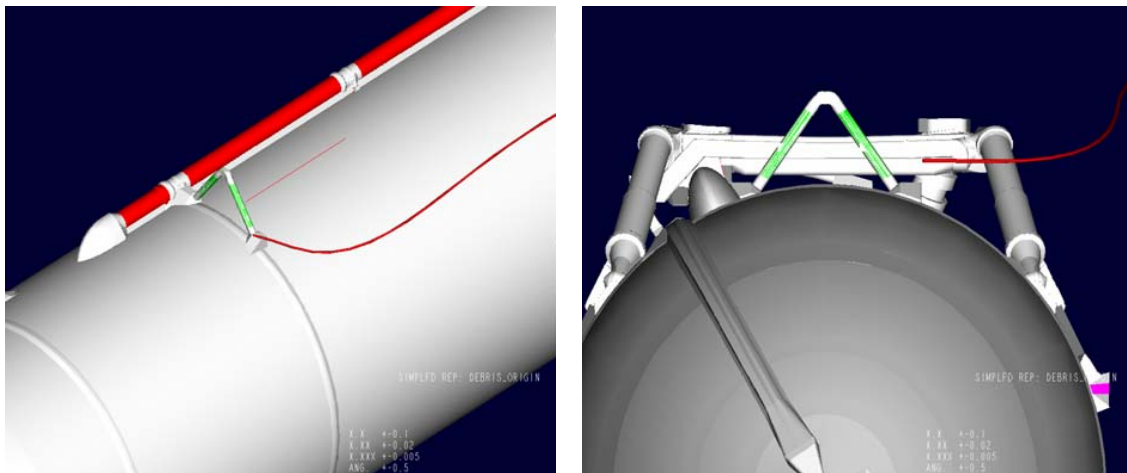


Figure 4.3.2.2b 3-D model of the debris trajectory (red curve) relative to the external tank, based upon ET-208 and E-212 camera imagery

This information is being distributed to aid in the investigation of the Columbia mishap and should only be distributed to personnel who are actively involved in this investigation. 29

### 4.3.2.3 Debris Size

The E-212 film camera provided the best view of the debris for size measurements. The debris size was estimated to be 24 inches x 15 inches (length x width), with an uncertainty of +/-3 inches in each dimension. The third dimension, depth, was indeterminate from the imagery alone. A simple transport analysis based upon the imagery was used to derive the depth, estimated to be 5 +/- 1 inch. However, the estimated depth of the debris has been refined by more detailed transport analysis by the JSC engineering community.

Although the shape of the debris could not be determined, from the imagery it was “plate-like” in appearance (length > width >>depth). The debris perspective relative to the camera line of sight varied from frame-to-frame as it tumbled (see Section 4.3.2.4). Therefore, the apparent size of the debris also varied from frame-to-frame. The apparent debris size measured from each frame is displayed in Table 4.3.2.3. The measurements for Dimension 1 refer to the apparent length of the debris in each frame, and Dimension 2 refers to the apparent width. Note that these dimensions represent an Image Analysis Team consensus. Size measurements from independent analyses within the team (see Appendix 4.3.2F) were generally in good agreement with the dimensions presented in Table 4.3.2.3.

<b>Frame from E-212</b>	<b>Dimension 1 (inches)</b>	<b>Dimension 2 (inches)</b>
<b>4913</b>	<b>21 +/- 4</b>	<b>20 +/-3</b>
<b>4914</b>	<b>19 +/- 3</b>	<b>19 +/-3</b>
<b>4915</b>	<b>16 +/-3</b>	<b>15 +/-3</b>
<b>4916</b>	<b>24 +/-3</b>	<b>16 +/-3</b>
<b>4917</b>	<b>35 +/-3</b>	<b>23 +/-3</b>
<b>4918</b>	<b>33 +/-4</b>	<b>23 +/-3</b>
<b>4919</b>	<b>26 +/-2</b>	<b>16 +/-3</b>
<b>4920</b>	<b>27 +/-4</b>	<b>24 +/-3</b>
<b>4921</b>	<b>30 +/-4</b>	<b>19 +/-3</b>

**Table 4.3.2.3 Apparent debris size by E-212 frame number**

The following assumptions were employed in the final determination of the actual debris size from the frame-to-frame apparent sizes:

- The translational motion blurring was considered to be insignificant in frames 4913-4916, but in later frames 4919-21 the apparent dimensions may have been enlarged by approximately 1 to 8 inches due to motion blur.
- Frames 4917 and 4918 were excluded because the debris was ill-defined. Interpretation of the imagery suggests that the debris might have been breaking up or magnified from optical distortion.

This information is being distributed to aid in the investigation of the Columbia mishap and should only be distributed to personnel who are actively involved in this investigation. 30

- Frame 4916 appeared to provide the best representation of the actual debris shape, and provided an approximate minimum length of 24 inches for the long dimension and minimum width of 16 inches. As additional compensation for motion blur, the width measurement was biased downward to 15 inches because the motion of the debris during that frame appeared to be mostly in the direction of the debris width.

Taking the various debris perspectives into account, the apparent debris sizes from the other frames are not inconsistent with this choice of actual debris dimensions. A more detailed discussion of the methodology, assumptions, and limitations for the debris size measurements is presented in Appendix 4.3.2C. It is also noted that the estimated debris dimensions are within the limits of the debris source measurements discussed in Section 4.3.2.2.

To measure the apparent size of the debris in each frame, a method was used to account for the blurring of the edges due to factors such as focus and atmospheric blurring, as illustrated in Figure 4.3.2.3. The measurement of the debris on each film frame was made using multiple profiles, or transects, running across the debris. The profiles began in a background area clearly outside the debris, extending through the debris, and ending outside the debris area. The average intensity values of the pixels in the profile were determined both in the areas outside the debris and in the area of the peak intensity within the debris area. An image analysis method known as the full-width at half-maximum technique was applied to determine the edges of the debris. This technique uses the locations of the pixels that corresponded to the midpoints between the average intensity maximum and the average background outside the debris.

The uncertainty in the debris size measurements of approximately +/- 3 inches was derived from a +/- 2-pixel uncertainty in locating the debris borders at half-maximum values.

This information is being distributed to aid in the investigation of the Columbia mishap and should only be distributed to personnel who are actively involved in this investigation. 31

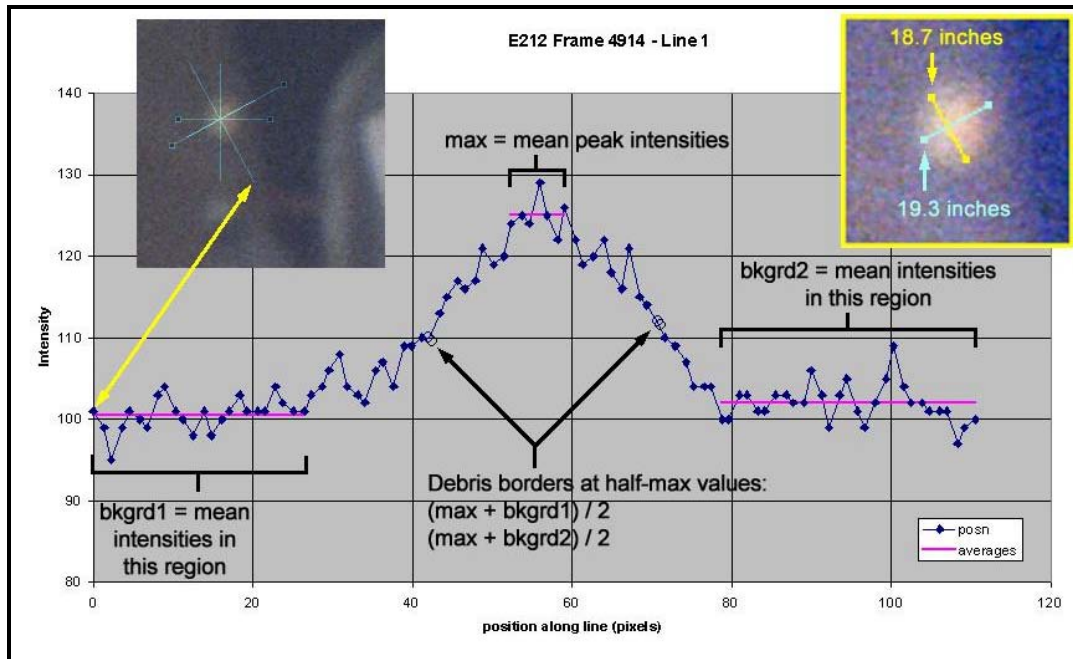


Figure 4.3.2.3 Debris size measurement methodology full width at half maximum intensity profile. The curve represents the image intensity values for a transect across the debris in one frame 4914, illustrated in the upper left image.

#### 4.3.2.4 Debris Rotation/Tumbling

The motion of the debris as seen from camera E-212 clearly exhibits some type of rotation or tumbling. A method was developed for estimating the debris rotation rate using the debris color variations. This analysis was based on the fact that the debris object was observed to exhibit a color variation as it moved along its trajectory. One explanation for this color variation is that the sides of the debris were different colors. This is consistent with insulating foam from the ET, which has an orange surface while the underlying foam is off-white. As the debris tumbled, it would alternately expose the orange colored and off-white surfaces to the camera line-of-sight.

To begin the analysis, the red, green, and blue color channels of the debris were recorded for each frame on E-212 in which the debris was observed prior to impact. Ratios of the green to blue and red to blue were then calculated and plotted as a function of time (see Figure 4.3.2.4). The use of color ratios reduces the effect of variations in illumination and makes the analysis more sensitive to color change. The plot shows a definite sinusoidal pattern with a frequency of approximately 18 Hz. Details of this analysis are given in Appendix 4.3.2D. In the absence of any other data for measuring rotation, the best estimate of the debris rotation rate based upon the imagery is approximately 18 Hz.

This information is being distributed to aid in the investigation of the Columbia mishap and should only be distributed to personnel who are actively involved in this investigation. 32

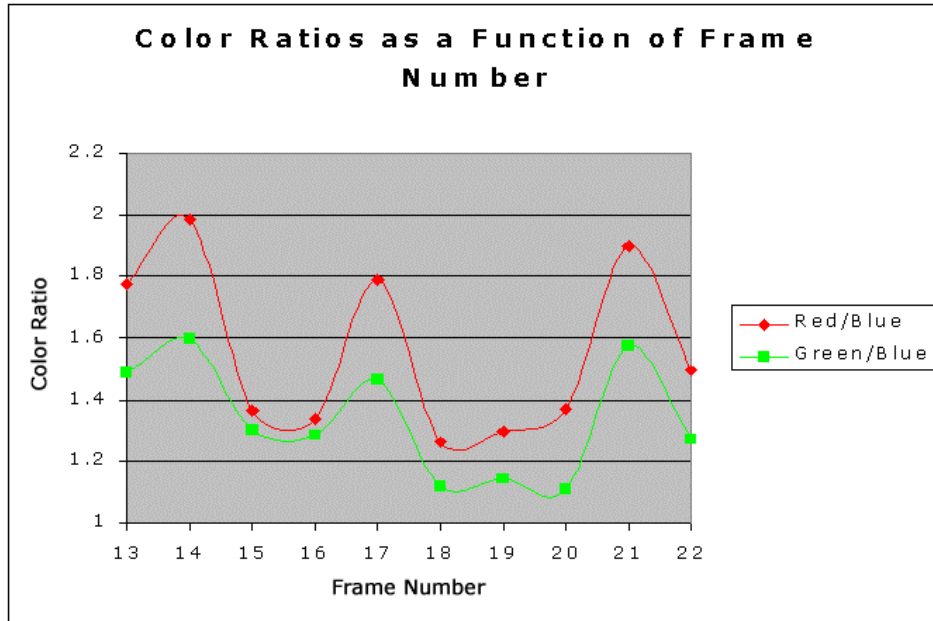


Figure 4.3.2.4 Color ratio analysis of debris from E-212 frames

#### 4.3.2.5 Debris Trajectory, Impact Location, Impact Angle, and Velocity Analysis

##### Trajectory

Imagery from cameras ET-208 and E-212 was used to obtain the trajectory of the debris from the time it was first seen in the vicinity of the ET/Orbiter -Y bipod attach area until it impacted the wing. ET-208 provided views of the entire debris trajectory. The wing obscured the E-212 camera view of the debris impact. Debris trajectories were obtained using two different techniques. One technique involved overlaying CAD models of the Shuttle with images from ET-208 and E-212 and then determining the 3D debris trajectory by combining the two camera views. The CAD-to-image overlay method involved precisely registering a CAD model of the Shuttle to the imagery. Line-of-sight vectors from the cameras to the frame-by-frame positions of the debris along its trajectory were then computed. The vectors formed surfaces, one for each camera, and the intersection of these two surfaces formed a 3D spatial curve defining the trajectory of the debris. The trajectory in the CAD model is graphically represented by a tube, whose radius defines the uncertainty in the trajectory. Results are sensitive to both the registration of the CAD models with the imagery and the interpretation of the frame-to-frame debris location. The results of the primary trajectory analyses are displayed in Figure 4.3.2.5a. Note that each “tube” represents a possible trajectory from the origin of the debris near the ET/Orbiter -Y bipod attach area and extending towards the Orbiter’s left wing. Each of these trajectory “tubes” is derived from an independent 3D CAD-based analysis employing different CAD software and based on independent debris selection of debris positions from the launch imagery.

This information is being distributed to aid in the investigation of the Columbia mishap and should only be distributed to personnel who are actively involved in this investigation. 33

The other technique for determining the debris trajectory was to use the intersection of the line-of-sight vectors from the camera to the debris in two separate camera views to derive a triangulated 3D position of the debris in each frame. This was a more classical photogrammetric approach, which relied on the debris being visible in both cameras at the same time in each frame along the trajectory.

The accuracy of the trajectory results were affected by:

- not seeing the debris on E-212 as it passed behind the wing just prior to impact;
- uncertainty in timing offsets between E-212 and ET-208. This was less of a concern for the CAD surface intersection methods, but a major issue for the methods that relied on intersecting vectors from multiple cameras extending from each camera to the debris at discrete points in time.

Details of all trajectory analyses are given in Appendix 4.3.2F.

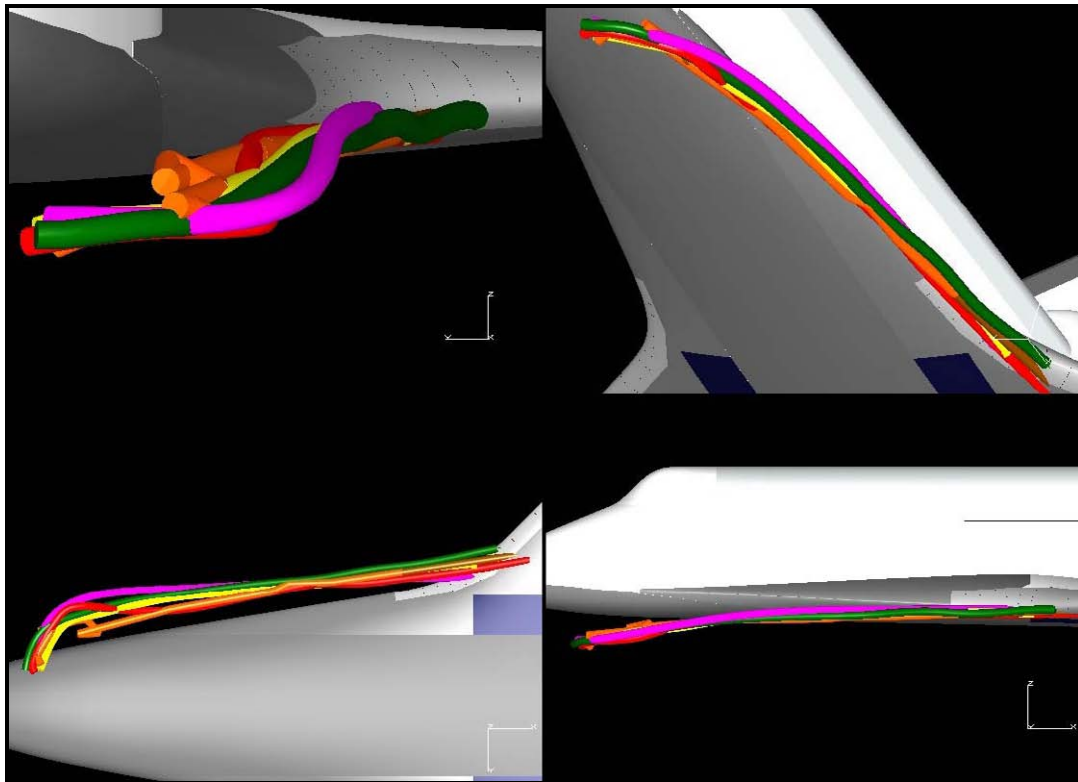


**Figure 4.3.2.5a Debris trajectories derived by separate independent analyses.**

Impact Location

The debris impact location based upon the trajectory analyses ranged from Reinforced Carbon-Carbon (RCC) panels 6 to 8. Given the large debris size and uncertainty in trajectory “tubes” of about 1 foot radius, panels 5 or 9 may have also been at least partially impacted. While the modeled trajectories do not preclude partial impact to tile

This information is being distributed to aid in the investigation of the Columbia mishap and should only be distributed to personnel who are actively involved in this investigation. 34

acreage aft of the leading edge panels, no damage to the tiles was observed in the imagery (see Section 4.3.2.7). Figure 4.3.2.5b shows the impact area on the Orbiter left wing as predicted by one example trajectory analysis.

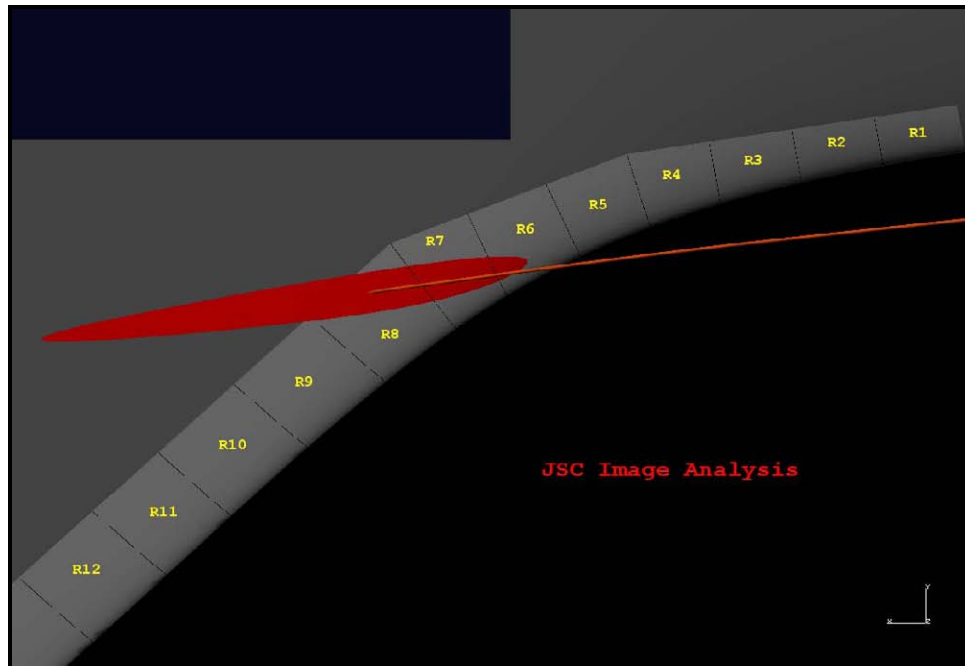


**Figure 4.3.2.5b Debris trajectory analysis — impact area on Orbiter left wing. A 1-foot-radius, trajectory tube projected onto the left wing, showing probable impact to the panel 6, 7, 8 area.**

### Impact Angle

At the point of impact, the 3D trajectory analyses indicate that the debris motion was predominantly in the +X direction relative to the Orbiter coordinate system, with a slight outboard and upward motion. The trajectory angles ranged from approximately 0 to 12 degrees in the XY plane (outboard direction) and 0 to 5 degrees in the XZ plane (upward direction), relative to the Orbiter coordinate system. The local impact angle on the left wing is uniquely defined by the geometry of the surface at the impact location. The orientation of the debris at impact was indeterminate from the imagery.

Based on the camera E-212 imagery, there is no conclusive evidence of debris traveling over the top of the wing. This implies that the impact was most likely entirely below and aft of the stagnation point of the wing leading edge. Although no debris was observed passing over the top of the wing during extensive reviews of the available launch imagery, subtle color changes on the top of the wing were detected in the E-212 film at approximately the time of the debris impact (see Appendix 4.3.2E). Because these color changes are near the noise limit in the imagery and no debris was actually observed coming over the top of the wing, no firm conclusions can be reached from this colorimetric analysis.

This information is being distributed to aid in the investigation of the Columbia mishap and should only be distributed to personnel who are actively involved in this investigation. 35

### Impact Velocity

Several independent measurements from the imagery were made of the debris velocity along its trajectory and at the moment of impact. Two basic approaches were used:

1. A multi-camera approach employing the 3D debris coordinate positions derived from the trajectory analysis. This method provided estimates for the three components, X, Y, and Z of the velocity vector.
2. Single camera approaches employing the assumption that, after initial breakaway and movement away from the ET, the debris motion was all in the X direction. These methods provided a verification of the 3D methods since they required fewer assumptions and were not sensitive to time offsets between cameras.

The impact velocity computed from all independent analyses (both the 3D trajectory approach and single camera methods) ranged between 625 ft/sec and 840 ft/sec. Detailed descriptions of the methodologies used in the individual analyses to compute the debris velocity are contained in Appendix 4.3.2F.

The wide variation in the debris velocity measurements is attributed to the following factors:

1. The velocity measurements are highly dependent on the inferred debris locations from the imagery. The ET-208 resolution, in particular, was insufficient to provide unambiguous debris locations in all video fields. This resulted in significant differences from one analysis to another in defining the debris points, which in turn, affected the velocity calculations. A sensitivity analysis was performed on a single camera, 2<sup>nd</sup> order polynomial fit solution by randomly varying the image X,Y coordinates of the debris in each ET-208 field: variation by as little as two image pixels caused the range of measured velocities to vary between 540 ft/sec and 800 ft/sec.
2. The numerical methods used to determine the velocity also significantly affected the result. Most of the velocity calculations used a curve fit to the debris distance vs. time. Different orders of curve fits to the data yielded different resulting velocities. In general, higher order polynomial least-squares fits yielded the highest calculated impact velocities. Given the known physics of the debris motion, the favored curve fitting method was one with an increasing slope, which yielded increasing velocities with time. The selection of the order of the polynomial is somewhat subjective and can only provide a rough model of the true physics of the debris motion. Another method used was to simply calculate the difference between adjacent debris positions and divide by their time differences. This method also had its limitations since it is greatly influenced by small errors in the debris positions, much more than the curve fitting methods.
3. The accuracy of the velocity calculations was fundamentally limited by lack of resolution in the imagery, both spatial and temporal. The poor temporal resolution in particular, limited by the camera frame rates, contributed much of the wide range of velocity measurements from one analysis to another.

This information is being distributed to aid in the investigation of the Columbia mishap and should only be distributed to personnel who are actively involved in this investigation. 36



4. The calculated velocities using multi-camera methods can be drastically affected by the derived time offset between cameras, and are in general very sensitive to small errors in the offset.
5. Single camera methods use fewer position points than the multi-camera methods, and hence are more sensitive to inferred positions of each of those points.

The debris velocities, impact angles, and impact locations determined by the various analyses are summarized in Table 4.3.2.5.

Team	Total Debris Velocity at Impact in ft/sec	Impact Angle in XY plane in degrees	Impact Angle in XZ plane in degrees	RCC Panel Strike location
JSC – SX <sup>1</sup>	638	9.6	1	6 to 8
JSC – ES <sup>1</sup>	700	2.5 <sup>8</sup>	2.5 <sup>8</sup>	5 to 7
JSC – EG <sup>1</sup>	730	8.3	1.8	8 to 9
KSC <sup>1</sup>	725 <sup>3</sup>	8.5 <sup>4</sup>	1	7 to 8
MSFC <sup>1</sup>	841	10.6 <sup>5</sup>	2.7	8 to 9
JSC-SX <sup>2</sup>	670	NA	NA	NA
LM – M&DS <sup>7</sup>	625	NA	NA	8
NIMA <sup>6</sup>	700	NA	NA	NA
Averages	704	8	2	5 to 9

<sup>1</sup> 3D CAD-based method

<sup>2</sup> Single Camera-based method

<sup>3</sup> Average based on reported range of 650 to 800 ft/sec.

<sup>4</sup> Average based on reported range from 6 to 11 degrees.

<sup>5</sup> Average based on reported range from 9.4 to 11.8 degrees.

<sup>6</sup> Combined single camera views but did not use 3D CAD-based method

<sup>7</sup> Used single camera views for velocity and combined two camera views for trajectory.

<sup>8</sup> Average based on reported range from 0 to 5 degrees.

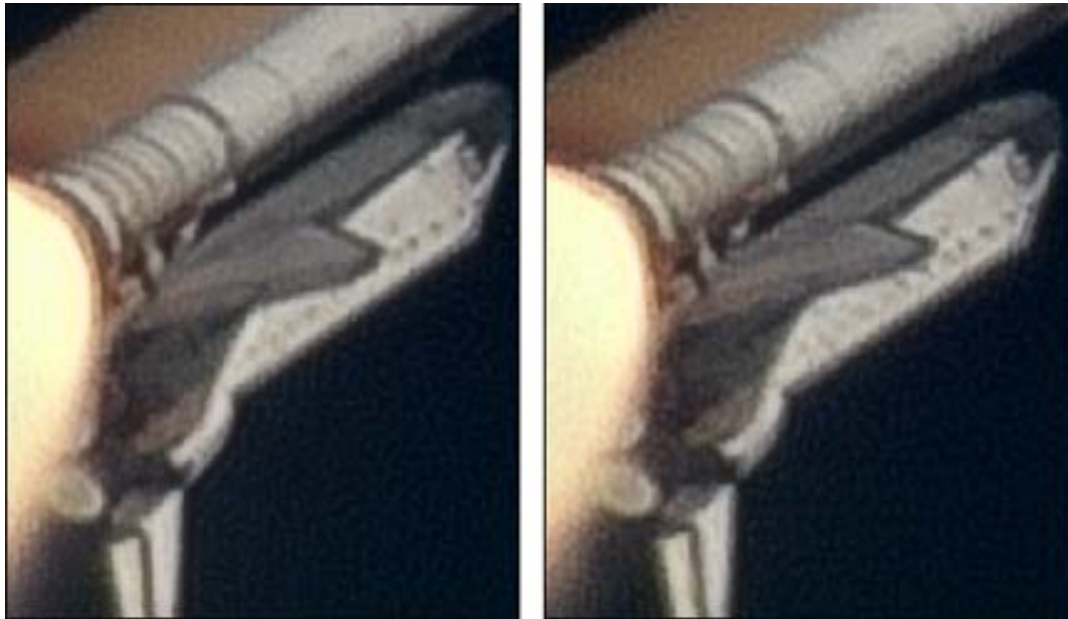
**Table 4.3.2.5 Summary of calculated debris velocities, impact angles, and strike location**

#### 4.3.2.6 Post Impact Damage Assessment and Debris Analysis

No visible damage to the left wing was detected in the imagery from camera ET-208, which was determined to be the camera with the best view of the debris impact. Figure 4.3.2.6a shows frame-averaged image enhancements of the underside of the left wing from before and after the impact event. There is no conclusive, detectable change in the impact area. In the “before” image, a relatively bright area on the wing is observed just aft of the leading edge, which is attributed to an area of lighter-colored tile acreage, as verified in the Orbiter close-out photos. The “after” image shows a slight brightening to this area, but in the noise level of the image. The brightening may be attributed to a lighting effect caused by slight changes in the Orbiter orientation, or is simply an artifact of the image processing.

A constraint to this analysis is the low resolution of the ET-208 imagery; a damage area smaller than an area of approximately 2 feet by 1 foot (in Orbiter X and Y respectively) would be undetectable in the imagery.

This information is being distributed to aid in the investigation of the Columbia mishap and should only be distributed to personnel who are actively involved in this investigation. 37



**Pre-impact: 30-frame average**

**Post-impact: 21-frame average**

**Figure 4.3.2.6a Comparison of images from before and after the debris impact**

Imagery of the post-impact debris cloud shows at least two distinct, sizeable objects emanating from the location of the debris impact on the wing (Figure 4.3.2.6b, from E-212). Identification of these objects is not possible from the imagery, but they are presumed to be remnant fragments of the debris that struck the wing. The objects are visible in only two image frames and are badly motion-blurred. Compensating for the motion blur, the estimated sizes of these objects are 12 inches by 11 inches, and 7 inches by 7 inches, respectively (Figure 4.3.2.6c). See Appendix 4.3.2G for details of these post-impact debris size measurements. Note that these dimensions are based on an estimated velocity of approximately 900 ft/sec, which is used to compensate for the motion blur. No other distinct particles were observed in the post-impact debris cloud.

This information is being distributed to aid in the investigation of the Columbia mishap and should only be distributed to personnel who are actively involved in this investigation. 38

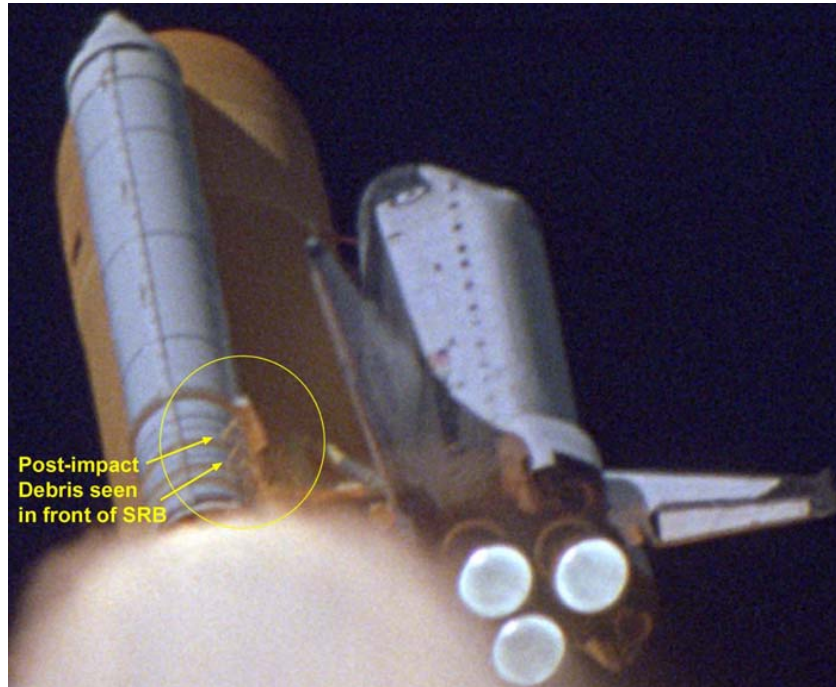


Figure 4.3.2.6b Post-impact debris fragments (E-212 frame 4927)

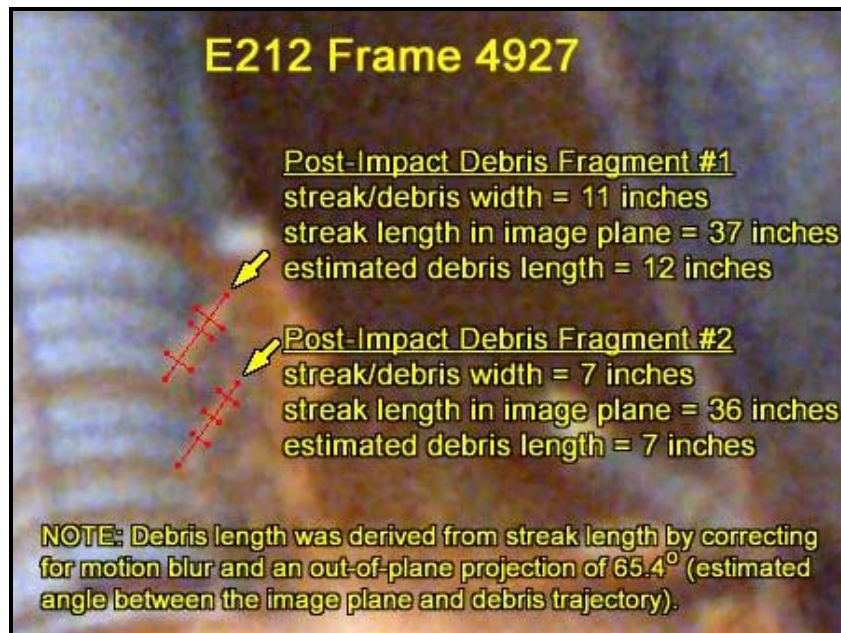


Figure 4.3.2.6c Post-impact debris size measurements

This information is being distributed to aid in the investigation of the Columbia mishap and should only be distributed to personnel who are actively involved in this investigation. 39

#### 4.4 Other Launch Analyses

In addition to the analyses of the ascent debris strike, the Image Analysis Team fielded several related requests for analyses of launch imagery. The results of those analyses are summarized in this section.

##### 4.4.1 Bright Spot near Bipod 9 Seconds Prior to Debris Strike

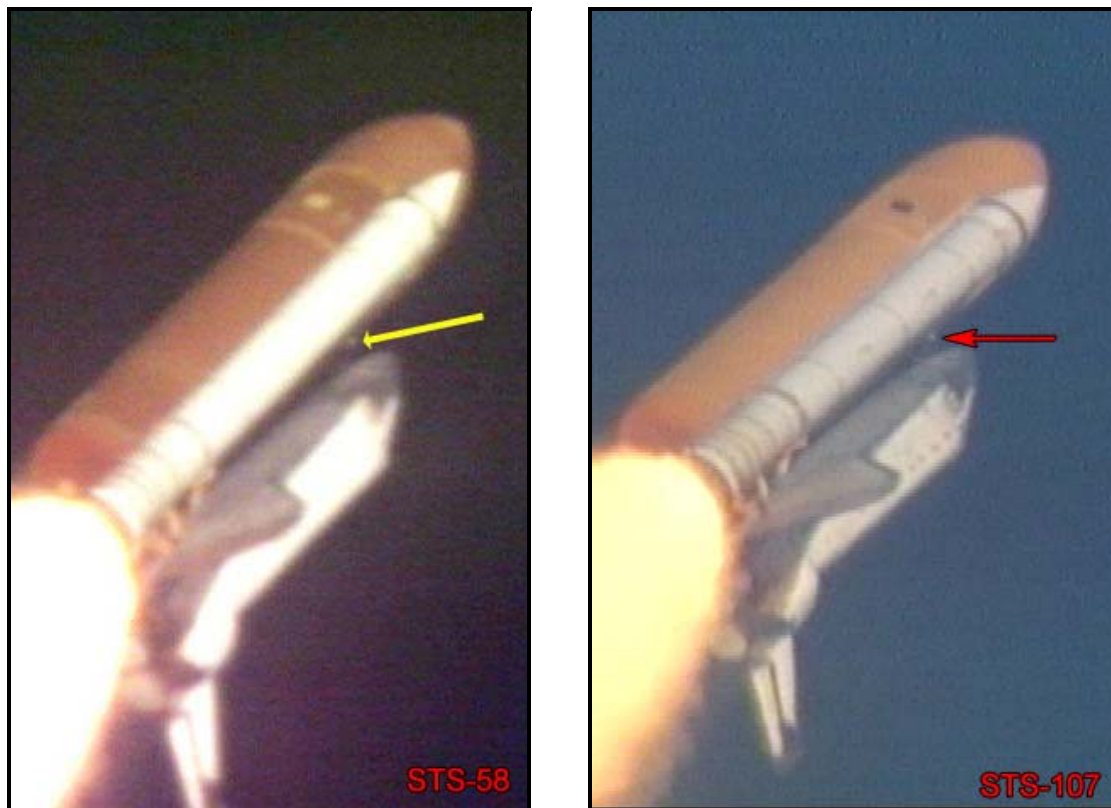


Figure 4.4.1 Comparison of bright spot near bipod on STS-58 and STS-107

A bright spot was seen near the ET/Orbiter -Y bipod attach area on the STS-107 camera ET-208 video approximately nine seconds prior to the debris strike to the Orbiter left wing (Figure 4.4.1). There was a concern that this white area may be related to the debris that struck the left wing — it is very close to where the debris appeared to originate. The white-colored mark is visible for about two seconds prior to fading away. It is most apparent on either side of some horizontal video noise that runs across the frame. As part of this analysis, the STS-58 ET-208 video was reviewed due to its similarity in lighting conditions at launch. Figure 4.4.1 is a comparison of the STS-58 and STS-107 ET-208 views. A similar bright spot was also seen near the ET/Orbiter -Y bipod attach area on the STS-58 video. Because of the similarity of the lighting and the appearance of similar

This information is being distributed to aid in the investigation of the Columbia mishap and should only be distributed to personnel who are actively involved in this investigation. 40

bright spots near the bipod on both launches, it was concluded that this was most likely a lighting effect unrelated to the debris-shedding event.

#### 4.4.2 STS-107 Launch Radar Analysis

The Eastern Range (ER) land-based C-band radar and metrics optics systems tracked the STS-107 launch and ascent to provide real-time data for Range Safety and for post-flight analysis. Optical systems imagery was recorded on video cassettes and film. Radars 19.14, 0.14, and 28.14 recorded both metric data and full range video. Systems Analysis Department, Computer Sciences Raytheon (CSR) personnel (in support of the US Air Force 45<sup>th</sup> Space Wing) at Patrick Air Force Base (AFB), Florida examined the data to identify debris. CSR reported that none of the radars detected debris prior to SRB separation. However, following SRB separation, 21 debris items were detected on Radar 0.14 and 6 debris items were detected on Radar 28.14 between T+150 and T+230 seconds after liftoff. The radar signal was reported to be too weak to allow the CSR analysts to determine the shape, size, or rigidity of the debris. Additionally, the CSR analysts were unable to make any correlations between the individual radars. CSR concluded that the STS-107 radar analysis results are consistent with the debris analysis from previous Space Shuttle launches. The full CSR report on the analysis of this optical and radar data collected during launch is provided in the Computer Sciences Raytheon, Systems Analysis Department, Instrumentation Systems Analysis Special Report, CDR A205, 14, February 2003.

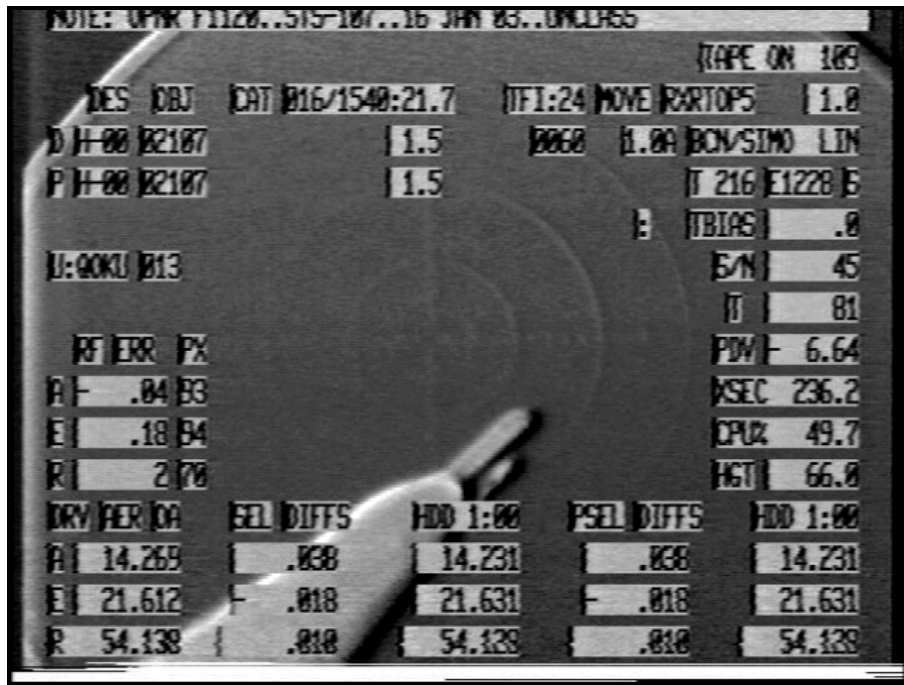


Figure 4.4.2 Patrick AFB 0.14 radar boresite view taken at the time of debris strike event approximately 81 seconds after launch.

This information is being distributed to aid in the investigation of the Columbia mishap and should only be distributed to personnel who are actively involved in this investigation. 41

The radar data was classified and not available to the NASA Image Analysis Team. However, six optical videos (bore-sighted with the radar) were screened by Image Analysis Team members at KSC and JSC. The detail visible on the Air Force metric optics video is significantly less than can be seen on the NASA long range tracking imagery (Figure 4.4.2). No anomalous events were noted during the screening of the STS-107 launch metrics video that was bore-sighted with the radar tracker. The only event seen on a CSC digital video file was a piece of debris exiting the SRB plume at 17 seconds MET.

#### 4.4.3 Navy Airship Analysis

Optical video of the STS-107 launch was acquired by the U.S. Navy "WESCAM". The view was taken from an Airship 70 NM at sea off the coast of Florida and transmitted to the Whale Search Operations Center Ground Site by wireless data link. The Shuttle is extremely small in the U.S. Navy WESCAM view, at the end of a long engine exhaust trail (Figure 4.4.3). The U.S. Navy identified one area of possible debris emanating from the exhaust trail far aft of the launch vehicle.

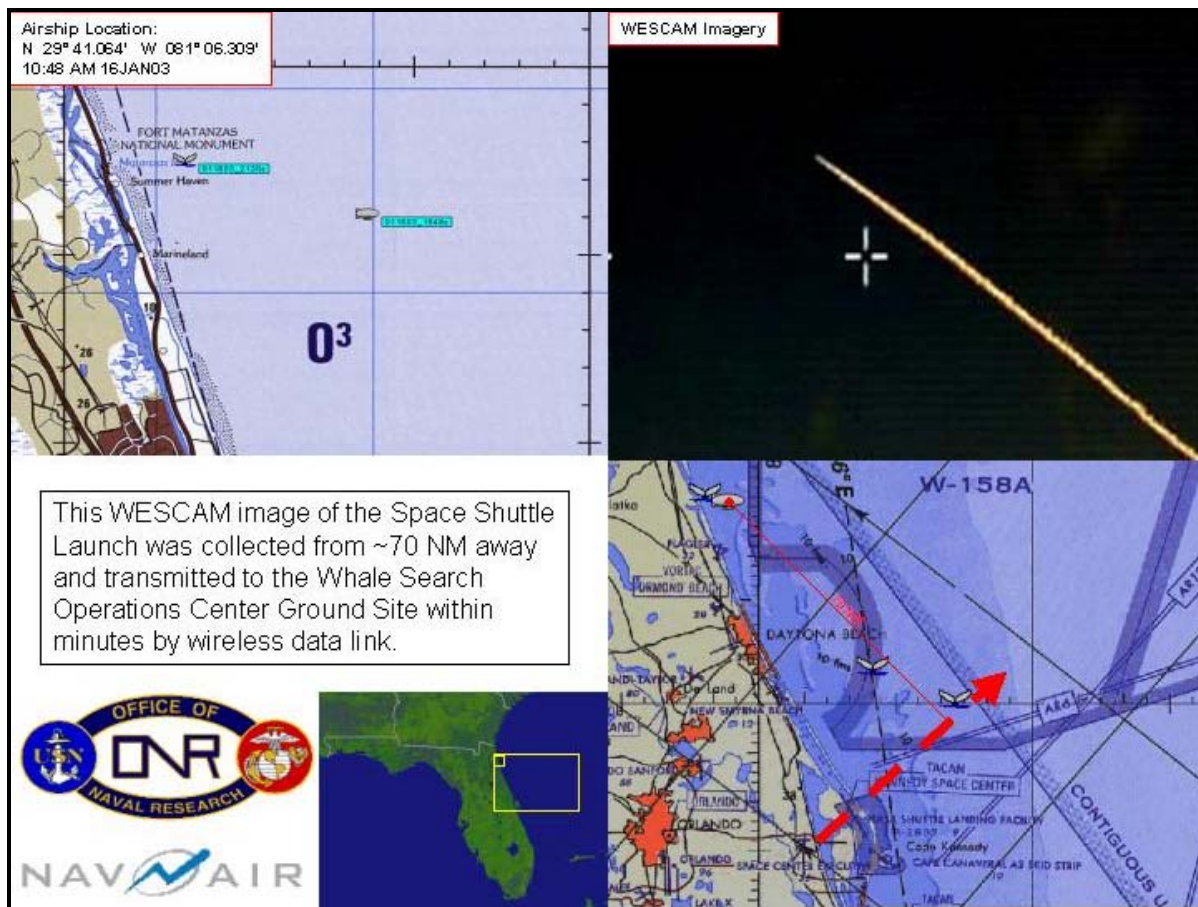


**Figure 4.4.3 U.S. Navy airship location and image**

This information is being distributed to aid in the investigation of the Columbia mishap and should only be distributed to personnel who are actively involved in this investigation. 42

#### 4.4.4 Debris Seen Exiting SRB Exhaust Plume

From the KTV4A and an HDTV (High Definition Television) view, the Image Analysis Team observed a piece of debris exiting the SRB exhaust plume approximately two seconds prior to the debris strike to the left wing. However, no debris was seen coming from the forward end of the ET or the left wing area. Also, no debris was seen two seconds prior to the wing strike event on the primary ET-208 and E-212 views of the impact. If debris from the forward end of the vehicle had been present two seconds prior to the impact it should have been detected on the camera ET-208 and E-212 views. Therefore, it was concluded that the two events were most likely unrelated.

#### 4.4.5 Analysis of ET Bipod Ramp Foam on STS-112, 50, 32, 7

The launch films and videos from missions STS-112, STS-50, STS-32, and STS-7 were reviewed to compare the size and trajectory of foam debris with that seen on the STS-107 imagery. Although this task is not complete, the preliminary analyses are presented in this section.

##### 4.4.5.1 STS-112 (CFVR-112-01, Cameras E-207, E-212, E-220, E-222)

During the STS-112 launch, a single piece of light-colored debris was seen to impact the ET Attach (ETA) ring near the Integrated Electronic Assembly (IEA) box on the Left SRB (LSRB) at approximately 33 seconds MET (19:46:24.690 UTC) on the long range tracking camera films. After impact the debris broke into multiple pieces and fell aft along the LSRB exhaust plume. Camera E-207 recorded a large spray of debris falling aft along the LSRB aft skirt that correlates to this event (19:46:24.727 UTC). The debris was first visible aft of the ET Intertank one tenth of a second prior to the debris impact with the ETA ring (19:46:24.590 UTC). The debris trajectory is tracked on Figure 4.4.5.1.

When the ET imagery from the on-board umbilical well camera was examined after landing, it revealed that a large portion of the ramp adjacent to the ET/Orbiter -Y bipod attach was missing and bipod substrate material was visible. The damaged area was measured on the film to be approximately 6 x 12 inches (Figure 4.4.5.1).

This information is being distributed to aid in the investigation of the Columbia mishap and should only be distributed to personnel who are actively involved in this investigation. 43

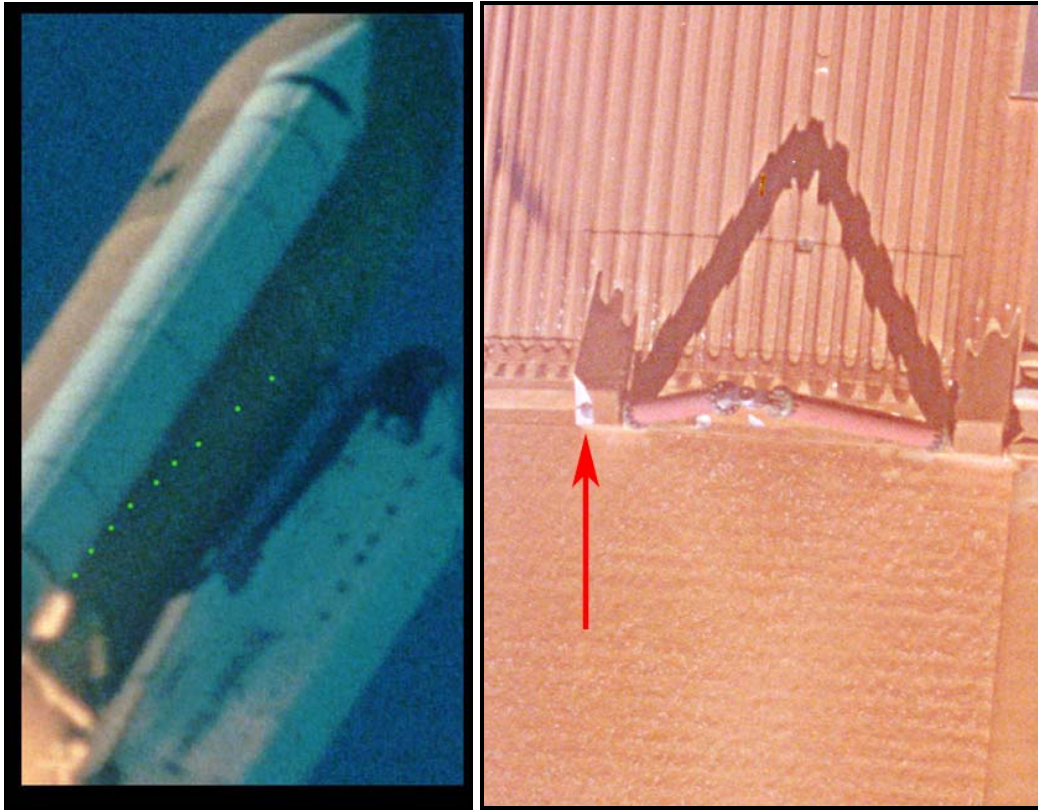


**Figure 4.4.5.1 STS-112 debris trajectory and umbilical well image of damage near ET bipod ramp**

During the post-flight SRB inspection, evidence of a debris impact on the LSRB ETA ring near the IEA box was found. This location coincided with the reported event documented in the high-speed tracking films. The impact site was reported to be approximately 4 inches in diameter and 3 inches in depth.

Future work on this task includes a trajectory analysis of the STS-112 debris path from the forward end of the ET to the LSRB ETA ring to compare with the STS-107 debris trajectory.

#### **4.4.5.2 STS-50**

Examination of the STS-50 umbilical well imagery revealed that approximately 60 percent of the ramp adjacent to the ET/Orbiter -Y bipod attach was missing (Figure 4.4.5.2a). The damage area was of sufficient depth that a portion of the bipod spindle housing appeared to be exposed. A portion of the intertank acreage foam at the leading edge of the ramp was also missing. The damage site measured approximately 26x10 inches. Because clouds and haze obscured the STS-50 long range launch tracking camera views, no debris events were recorded on the STS-50 launch imagery that correlated to the damaged ET/Orbiter -Y bipod ramp.

This information is being distributed to aid in the investigation of the Columbia mishap and should only be distributed to personnel who are actively involved in this investigation. 44



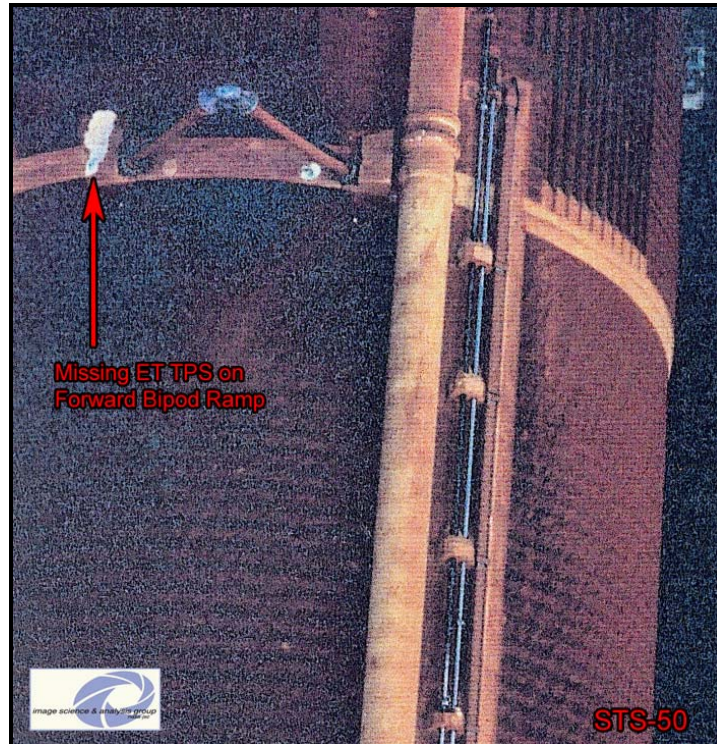


Figure 4.4.5.2a STS-50 ET damage recorded on umbilical well camera

During the post-landing Orbiter inspection, KSC reported that a 9 x 4.5 x 0.5 inch damage site was found on the Orbiter lower left wing surface tiles (outboard of the left umbilical well) that may have been caused by the loss of the ET foam (Figure 4.4.5.2.b).



Figure 4.4.5.2b Detailed view of wing tile damage, STS-50

This information is being distributed to aid in the investigation of the Columbia mishap and should only be distributed to personnel who are actively involved in this investigation. 45

#### 4.4.5.3 STS-32

During the STS-32 launch, the launch tracking cameras KTV-5 and E-207 documented a large piece of debris near the SRB exhaust plume at approximately 83.9 seconds MET. The source of this debris was not imaged, however the time of this event was similar to the time of the STS-107 debris strike. After landing, the STS-32 on-board umbilical well camera film revealed five large divots on the External Tank intertank TPS just forward and between the ET/Orbiter-Y and +Y bipod attach ramps (Figure 4.4.5.3).

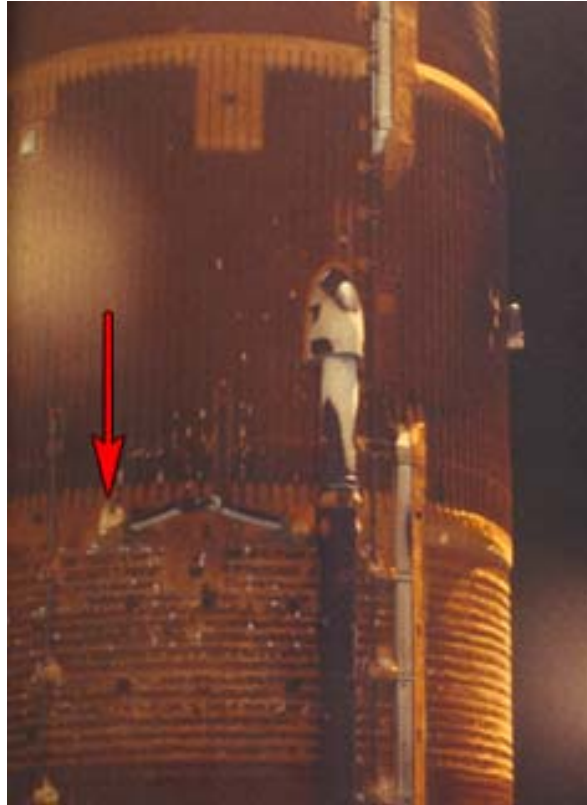


Figure 4.4.5.3 Image from STS-32 on-board umbilical well camera film showing damage to ET intertank TPS

#### 4.4.5.4 STS-7

A portion of the STS-7 ET/Orbiter-Y bipod attach ramp was observed to be missing on the on-board umbilical well camera films (Figure 4.4.5.4). The damaged area was estimated to be approximately 18 x 12 inches in size using the umbilical photography. The bipod spindle was not exposed. It is not known if any launch debris was seen on STS-7 that was correlated to the missing bipod ramp.

This information is being distributed to aid in the investigation of the Columbia mishap and should only be distributed to personnel who are actively involved in this investigation. 46



**Figure 4.4.5.4 Image from STS-7 On-board Umbilical Well Camera Film Showing Damage to ET -Y Bipod Ramp**

#### **4.4.6 Post-landing Walk-around Videos**

Previous mission, post-landing walk-around videos were screened for examples of damage sites to the T-seals and RCC panels on the leading edge of the Orbiter wings. Damage sites on the wing leading edge were found on several previous mission views that were white in color and provided strong contrast with the surrounding wing material. The conclusion, based on the appearance of the damage sites on the wing leading edge on previous missions, was that if STS-107 had received damage on the wing leading edge of resolvable size in the imagery (approximately 1' by 2'), there may have been enough contrast in the launch imagery to detect the change on successive frames before and after the impact.

This information is being distributed to aid in the investigation of the Columbia mishap and should only be distributed to personnel who are actively involved in this investigation. 47

## 5.0 On-orbit Analyses

The Image Analysis Team screened all imagery downlinked during the STS-107 mission and recovered on the ground. A few pieces of debris near the Orbiter were observed in the downlinked video taken during orbit. The debris were analyzed, and interpreted to be pieces of ice. Imagery taken from the Orbiter viewed the top of the wing and the RCC panels (above the stagnation point) except for areas of the wing that were either outside of the field-of-view or obscured. The team detected no visible damage or anomalies on the left wing from any of the STS-107 on-orbit camera imagery.

### 5.1 On-orbit Imagery Data Sources

The data sources for on-orbit imagery were:

- Video downlink from the Orbiter Payload Bay cameras
- Video downlink from in-cabin camcorders
- Electronic still imagery from the in-cabin Kodak DCS-760 digital cameras
- On-board film recovered from the East Texas debris field, including experiment and Earth Observations imagery
- Closeout imagery from pre-launch imagery surveys of the Orbiter

### 5.2 Process/Methods for Analysis

Many of the same methods that were employed for the launch imagery analyses were also used for the on-orbit analysis. Most of the analyses involved enhancements of the on-orbit imagery for comparison with pre-flight closeout photography. Image enhancement methods included simple intensity contrast stretching and sharpening using unsharp masking. More sophisticated image enhancements were generally not required for the on-orbit imagery. The imagery was of sufficient quality to make adequate comparisons with the closeout photography to assess if any damage or anomalies were visible.

### 5.3 On-orbit Analyses

Several analyses of on-orbit imagery were conducted as part of the STS-107 mishap investigation. Shuttle crew members commonly observe pieces of debris in the vicinity of the Orbiter after the Payload Bay Doors open, and the STS-107 crew documented a few such pieces of debris on the first day of the mission. Also, although much of the left wing was outside the camera viewing fields, the Image Analysis Team examined all potentially anomalous aspects of Columbia's left wing. Finally, downlinked imagery of the ET was reviewed. Summaries of significant analyses are presented below.

This information is being distributed to aid in the investigation of the Columbia mishap and should only be distributed to personnel who are actively involved in this investigation. 48

### 5.3.1 Downlinked Video of the External Tank

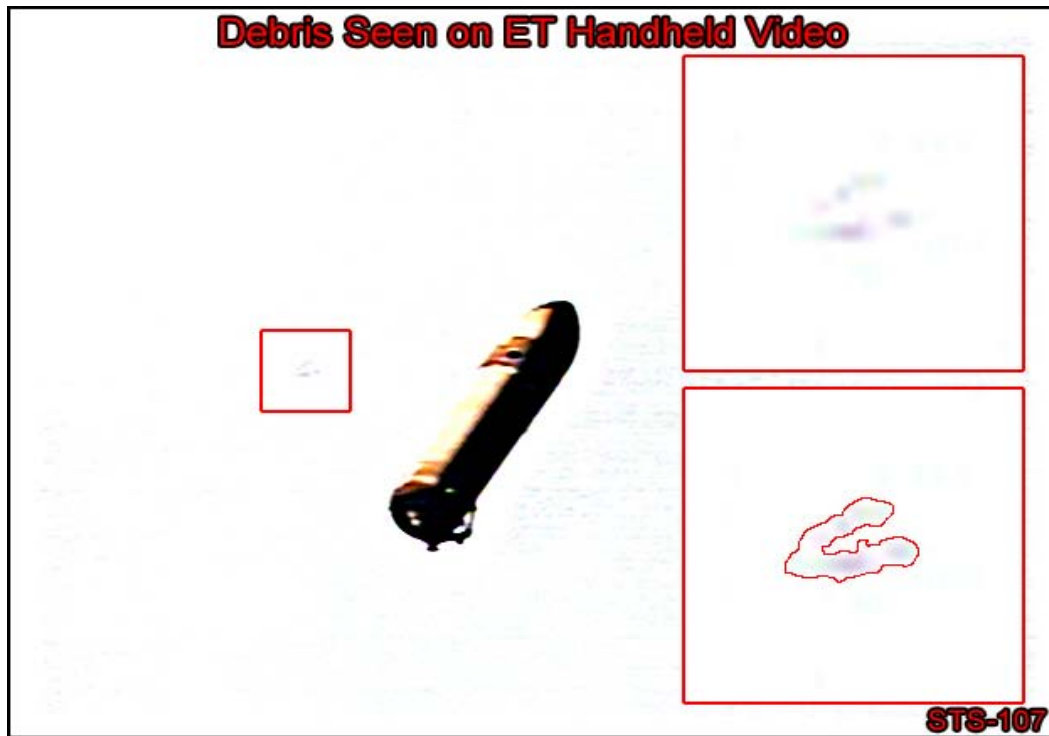


**Figure 5.3.1 View from the STS-107 downlink video of the External Tank and the debris, including an enhancement of the debris on the right side of the frame.**

The STS-107 crew acquired and downlinked video of the STS-107 ET after separation (Figure 5.3.1). This video shows three objects floating through the view, one appearing larger than the others. The ET downlink video of the debris objects was enhanced by the Image Analysis Team and reviewed with Space Shuttle Program engineers in an attempt to determine if the debris was identifiable hardware from the launch vehicle. A full report of this analysis is available in Appendix 5.3.1.

The debris tumbled as it moved from the bottom of the video view upwards in the view past the ET. It was variably white-colored and dark, depending on the lighting and shadows. The shape of the debris in the imagery was also variable (linear, irregular, “c” shaped), and its texture did not appear to be smooth or machined. The size of the object could not be determined because the distance of the debris from the camera was not known. The debris appeared similar to the ice debris from the orifice of the 17 inch Liquid Hydrogen (LH<sub>2</sub>) umbilical disconnect that has been observed on previous mission ET imagery. Engineering Directorate personnel were able to eliminate some of the possible hardware candidates for the debris based on appearance and other known engineering data. Although the team could not unequivocally eliminate all possible hardware fragments to explain the debris (hardware fragment from the wing, landing gear door, or the forward External Tank), the debris was determined NOT to be hardware from

This information is being distributed to aid in the investigation of the Columbia mishap and should only be distributed to personnel who are actively involved in this investigation. 49

either the SRBs or the ET/Orbiter umbilicals. Therefore, it was concluded that the debris seen on the STS-107 ET downlink video was most likely ice from the LH<sub>2</sub> umbilical.

### 5.3.2 Upper Wing Survey Analysis

#### 5.3.2.1 Air Force Maui Optical and Supercomputing Site (AMOS) Photographs

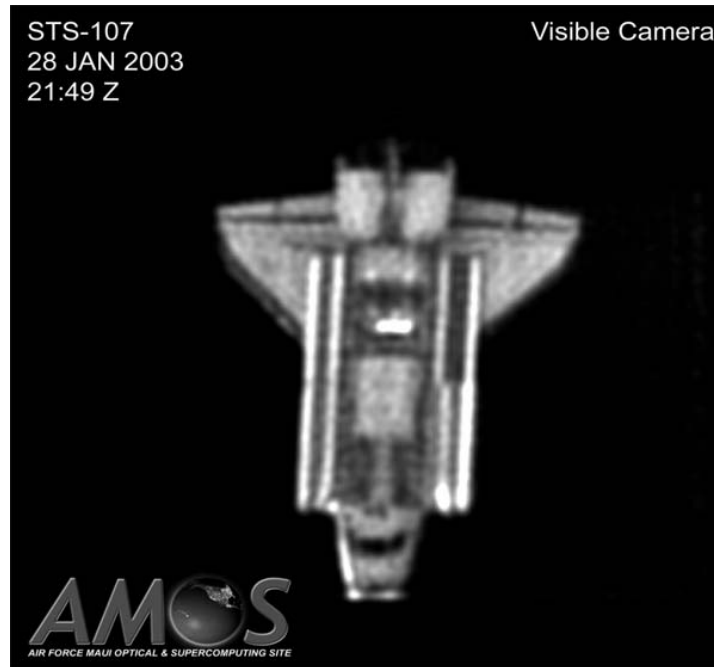


Figure 5.3.2.1 AMOS image of Columbia (taken January 28, 2003)

The Air Force Maui Optical and Supercomputing Site (AMOS) acquired photographs of Columbia while on-orbit during the STS-107 mission (Figure 5.3.2.1). The pictures were taken at approximately 21:49 UTC on January 28, 2003. All of the AMOS views are grainy and only major features of the Orbiter upper (+Z) surface are visible.

The AMOS views were enhanced to increase the contrast and interpretability of the imagery. The left wing from the area of RCC panel 7 outboard to the wing tip is visible. The team investigated a light-toned area near the leading edge of the left wing adjacent to the payload bay door. By comparing several different AMOS views with changing sun angles, it was concluded that the light-toned band is probably a lighting effect and does not represent damage to the left wing. Appendix 5.3.2 contains three AMOS views showing the variation in lighting on the Orbiter, an AMOS image registered to a pre-launch photograph, and a more detailed description of the analysis.

This information is being distributed to aid in the investigation of the Columbia mishap and should only be distributed to personnel who are actively involved in this investigation. 50

### 5.3.2.2 Analysis of Israeli News Account of Damage of the Orbiter Wing

The Image Analysis Team investigated stories about a video showing damage to the top of the wing that was downlinked during a conversation between Ariel Sharon and crewmember Ilan Ramon. An Israeli newspaper article included an image of purported damage to the wing. The image was real, from downlink video from STS-107; however, it was actually a view of the forward bulkhead of the Shuttle's payload bay and not the wing. From image analysis, it was confirmed that the “damage” was a normal seam in thermal blankets combined with some shadow effects.

### 5.3.2.3 Dark Spot on Orbiter Left Wing

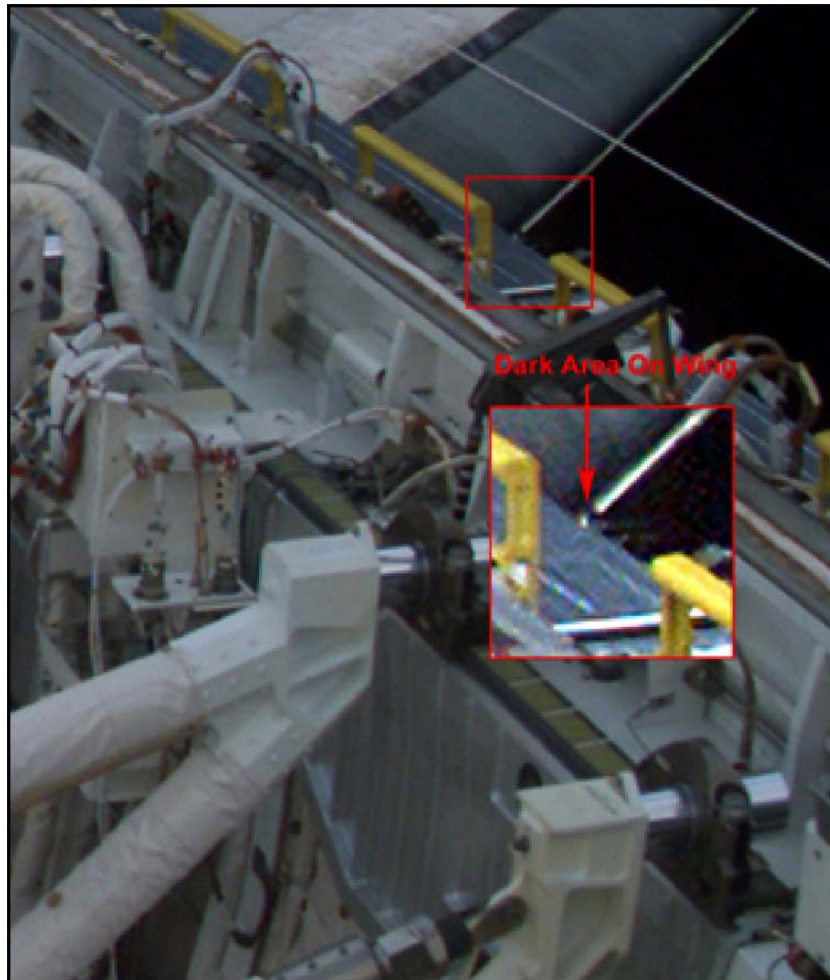


Figure 5.3.2.3a Dark spot seen on Columbia's left wing

Video and Electronic Still Camera (ESC) images taken during the STS-107 mission showed a dark feature on the STS-107 Orbiter left wing. See Figure 5.3.2.3a. Using imagery analysis and through consultations with engineering personnel, it was concluded

This information is being distributed to aid in the investigation of the Columbia mishap and should only be distributed to personnel who are actively involved in this investigation. 51

that the dark feature was a portion of the payload bay latch mechanism, which extends to the side of the latch and partially obscures the leading edge of the wing in the view. The latches and rollers were identified and labeled as seen in Figure 5.3.2.3b. The same feature was observed in a previous mission image (STS-68) when the Shuttle was in a similar orientation and with a similar view and lighting of the left wing.



Figure 5.3.2.3b Payload bay door latches/rollers superimposed on Orbiter left wing

#### 5.3.2.4 Discolorations on Orbiter Left Wing

Discolorations were noted on the upper surface of the Orbiter left wing on the on-orbit imagery. Specifically, discolorations were observed on the tiled surface of the upper surface of the wing, the thermal blanket between the NASA insignia and the tiled area of the wing, the RCC panels from panel 12 and outboard to the wing tip, the RCC carrier panels, and the outboard elevon. The discolorations were compared to imagery of the wing taken at KSC prior to launch and were found to be unchanged between the pre-launch and on-orbit imagery (other changes seen on the Orbiter left wing compared to the pre-launch photography were due to lighting, shadowing, and resolution). The discolorations were attributed by engineering personnel to be normal out-gassing from the Room Temperature Vulcanizing (RTV) adhesive applied to the RCC and tile installations and refurbishments that have accumulated over previous missions.

This information is being distributed to aid in the investigation of the Columbia mishap and should only be distributed to personnel who are actively involved in this investigation. 52



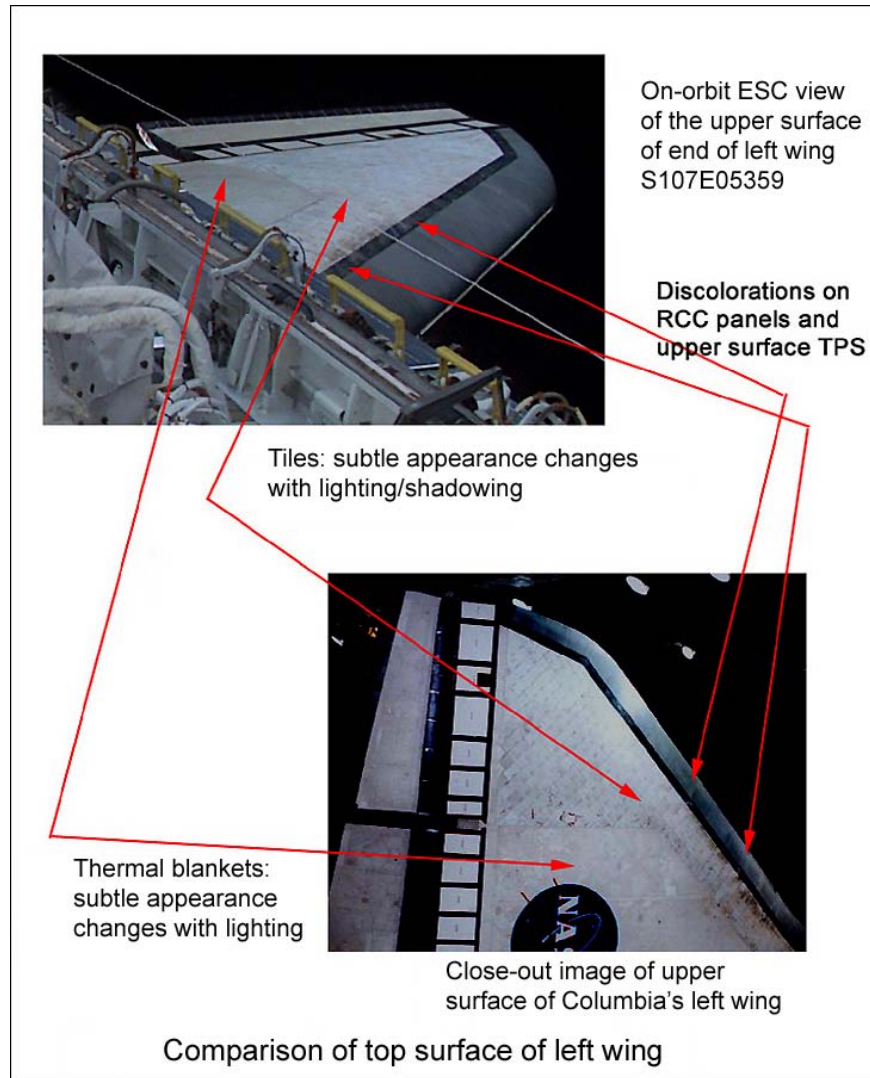


Figure 5.3.2.4a On-orbit and pre-launch views of left wing discolorations

Visual comparisons of the on-orbit and pre-launch views of the Orbiter left wing showed that there were no changes in the discoloration patterns on tile surfaces, thermal panels, RCC panels and the RCC carrier panels other than slight changes due to lighting. See Figure 5.3.2.4a.

This information is being distributed to aid in the investigation of the Columbia mishap and should only be distributed to personnel who are actively involved in this investigation. 53

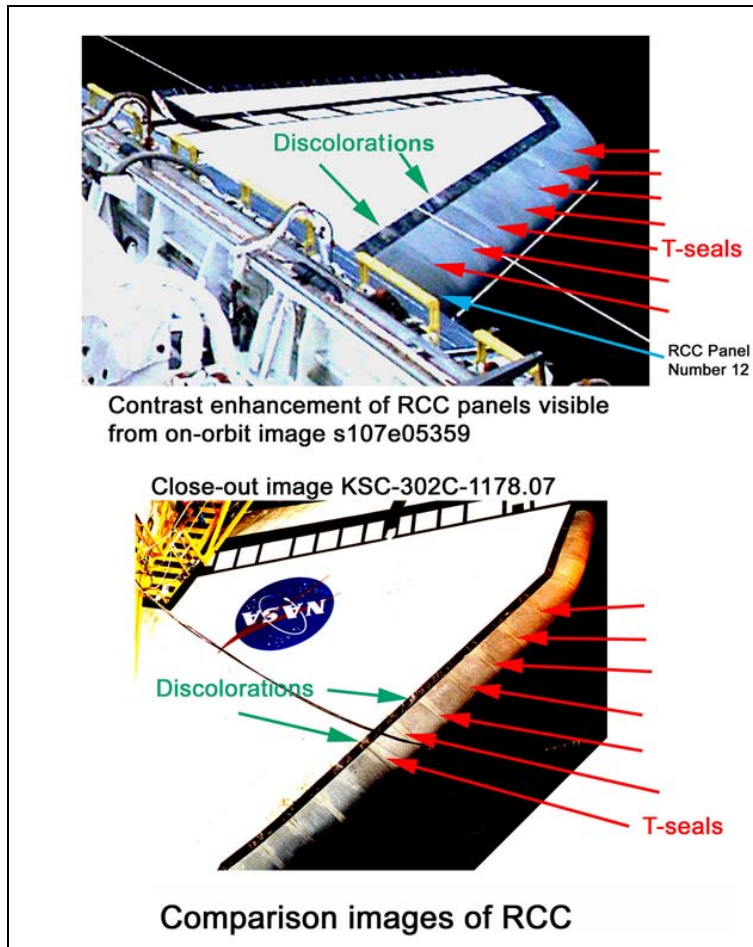
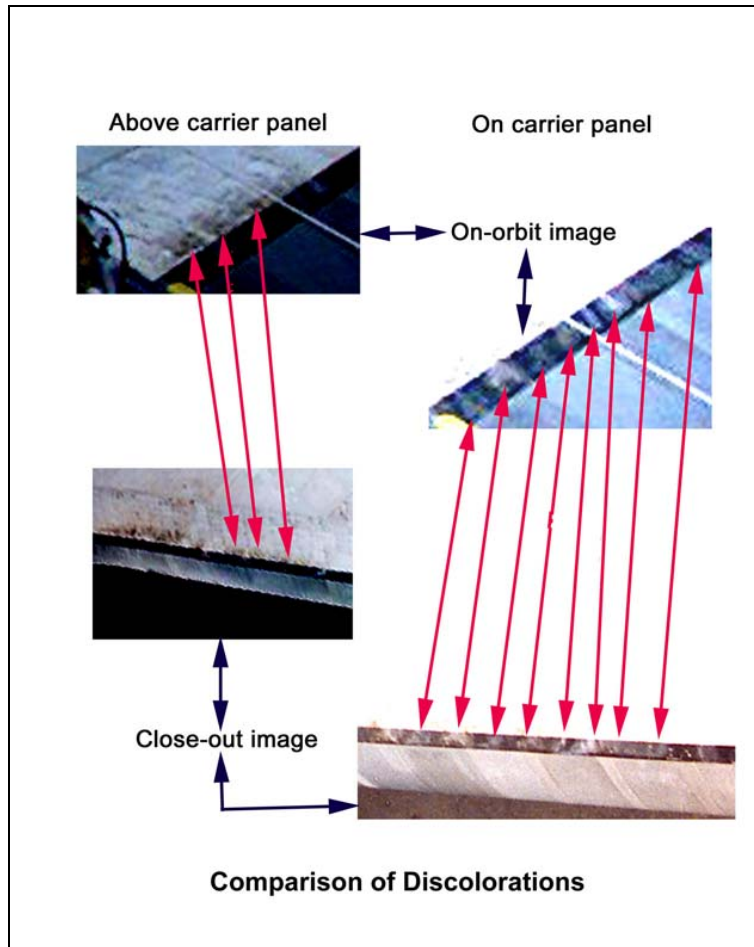


Figure 5.3.2.4b No detectable changes on left wing RCC panels, T-seals

Figure 5.3.2.4b contains both on-orbit and pre-launch close-out images that were enhanced to bring out detail on the RCC panels and T-seals on the left wing leading edge. Different shades of gray are visible on the RCC panels on the comparison views that were attributed by engineering personnel to be a pre-launch condition caused by aging of the panels and recent refurbishments of some of the panels. The lighter-colored vertical stripes separating the RCC panels are T-seals used to join the RCC panels. Discolorations of the RCC panels were not confirmed when comparing the on-orbit imagery to the pre-launch close-out photography (red-colored arrows on Figure 5.3.2.4b). However, the discolorations of the RCC carrier panels just aft of the RCC panels are easily seen on both the on-orbit image and the close-out photograph (green-colored arrows on Figure 5.3.2.4b).

This information is being distributed to aid in the investigation of the Columbia mishap and should only be distributed to personnel who are actively involved in this investigation. 54



**Figure 5.3.2.4c Discolorations on Columbia’s left wing carrier panels and adjacent tile surfaces**

Figure 5.3.2.4c contains enhanced, comparison views of the left wing leading edge that show the same discolorations on the carrier panels and on the tile surfaces adjacent to the carrier panels on both the pre-launch view and on the on-orbit view. Engineering personnel reported that the discolorations result from previous mission out-gassing, especially in the RTV adhesive and waterproofing substances.

### **5.3.3 Debris Observed on Orbit (Downlinked Imagery)**

#### **5.3.3.1 Orbit 3 Debris**

Payload Bay Camera A recorded video containing a 36-second view of a piece of unidentified debris on day 1, orbit 3 (downlink time was 18:59:44:00 - 19:00:20:00). The debris was white-colored, bright and reflective, and tumbled as it traveled away from the vertical stabilizer. It was a rectangular-shaped, flat, “plate-like” object with a thin edge. Because the debris did not pass in front of any of the Orbiter structure, the size of the object could not be determined. Similar appearing debris has been seen and documented

This information is being distributed to aid in the investigation of the Columbia mishap and should only be distributed to personnel who are actively involved in this investigation. 55

on previous mission payload bay camera views. KSC payload bay close-out engineers reported that it is possible that the debris was a piece of blanket material from inside the payload bay or from the SpaceHab module.

#### **5.3.3.2 Orbit 5 Debris**

Downlinked video obtained from a Shuttle payload bay camera during orbit 5 showed a bright circular shaped object moving in a generally vertical direction in the image and apparently away from the Orbiter. During the time that the debris was observed the primary debris appeared to eject a small piece of debris. The Image Analysis Team performed an extensive analysis of this object and concluded that the debris was probably ice that dislodged from within the payload bay. Appendix 5.3.3 contains the details of the analysis. No other Orbiter hardware was in the field of view for reference, so scaling the object was impossible, and no size or velocity measurements could be made.

#### **5.3.4 Insulation on Ku-band Antenna**

The Image Analysis Team attempted to verify whether or not the thermal blankets on the Ku-band antenna dish were in place during the mission to address a concern that a detached thermal blanket could have been the object seen by radar on flight day 2. Due to the poor quality of the available imagery, it could not be conclusively determined if the insulation was still in place, but the imagery analyses indicated that it probably was.

This information is being distributed to aid in the investigation of the Columbia mishap and should only be distributed to personnel who are actively involved in this investigation. 56

## 6.0 Re-Entry Analyses

Immediately after the accident, NASA was inundated with information from the public on their observations of re-entry. Information submitted included verbal descriptions of observations, digital files of still images and video, videotapes, and still photographs (prints, slides, and negatives). The Image Analysis Team reviewed and prioritized all the re-entry information, identified the pieces most likely to contribute to the investigation, and then conducted the primary analyses. The analyses included extracting any quantitative data and converting it to a form that would provide insights into problems occurring during re-entry. The primary useful data sources that emerged were a small subset of 25 key video tapes showing debris coming off the Orbiter as it entered over the western United States. Twenty-four anomalous events were documented as the Orbiter passed from California to Texas. Detailed analysis of late breakup events over Texas is still in work and will be reported separately.

Throughout the process, close cooperation was required with personnel from JSC-Mission Operations Directorate (Flight Design and Dynamics, and Systems Divisions) and the Early Sightings Assessment Team. In addition, team members with the appropriate knowledge base for gleaning technical information from the non-technical data sources joined the team, including JSC-Orbital Debris, KSC-Applied Physics Lab, MSFC-Space Environments, and ARC-Reacting Flow Environments Branch.

Three main efforts for analyzing re-entry imagery emerged during the investigation and were handled by three matrixed groups within the Image Analysis Team. The first effort from the Timeline Group focused on creating a database of imagery information and connecting the information to absolute time references. The resulting “Debris Event Timeline” product was integrated into the Orbiter Vehicle Engineering Working Group (OVEWG) configuration controlled “Data Review & Timeline”. Also from the timeline activity, key cameras were identified and acquired from the public for calibration of field-of-view, point spread function, signal response, noise characteristics, and other parameters relevant to subsequent analyses. A second group, the Debris Motion Tracking Group, performed detailed video analysis to characterize the relative motion of the key debris events compared to the motion of the Orbiter. This relative motion data was provided to the Early Sightings Assessment Team who applied it to determine ballistic numbers, and identify possible areas in the western United States where debris might be found on the ground. The third group, the Luminosity Working Group, measured the luminous intensities of the Orbiter and debris in the videos, and developed models of the physics of debris re-entry that could be used to estimate the masses for the debris. The mass estimates were provided to various teams for use in developing the consolidated re-entry scenario.

This information is being distributed to aid in the investigation of the Columbia mishap and should only be distributed to personnel who are actively involved in this investigation. 57

## 6.1 Re-entry Data Sources

### 6.1.1 Re-entry Imagery

The majority of re-entry imagery was video collected by the public (non-professional videographers) on consumer-grade equipment (Figure 6.1). This imagery was sent to NASA and screened and analyzed by the Image Analysis Team. These data had several limitations: settings used on the cameras were often not optimal for imaging a re-entry, and amateur videographers had difficulty finding the Orbiter, had trouble keeping the camera steady and tracking its movement, zoomed in and out, and made other changes that significantly compromised the quality of the information for analysis. Most of the imagery sent to NASA had also been copied in ways that further degraded its quality. Still photo imagery represented long exposures. Photographers that did not control the shutter remotely introduced patterns in the imagery from camera motion that looked intriguing to non-technical viewers, but actually contained little information about re-entry anomalies. A number of studies had to be made to explain imagery that appeared at first to be important, but actually contained image artifacts rather than useful information.

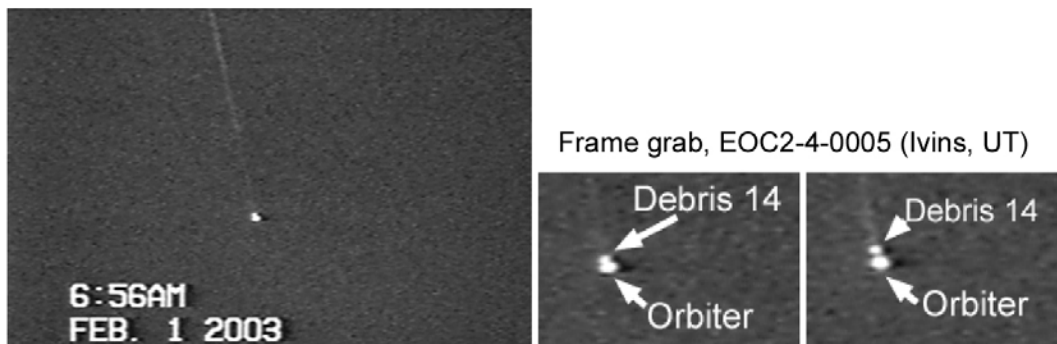


Figure 6.1 Example of full frame grab of a typical re-entry video, and an enhancement showing the separation of debris 14 at 13:55:58 UTC.

### 6.1.2 Observer Positions

Observers were contacted to determine approximate locations for screening of imagery. For the analytically important videos, they were contacted to determine their precise locations when capturing the imagery (Global Positioning System (GPS) coordinates or street addresses), and to document as much as they could recall about the camera settings they used to record the re-entry.

### 6.1.3 Orbiter Position vs. Time

The validated Orbiter GPS trajectory for Columbia's re-entry over the western U.S. was obtained from the JSC-Ascent/Descent Dynamics Branch. These data were provided at a 10-Hertz frequency sampling from a piecewise-linear interpolation of the actual intermittently sampled data. The 10 Hz sampled data covered only the times between

This information is being distributed to aid in the investigation of the Columbia mishap and should only be distributed to personnel who are actively involved in this investigation. 58

UTC 13:53:00.00 and 13:58:00.00 on February 1, 2003. A projected trajectory generated by the Ascent/Descent Branch was used for times after 13:58 UTC.

#### **6.1.4 Nominal Re-entries from Previous Missions**

Videos and still images of re-entries from previous missions were obtained for comparative analysis. In several cases the videographers of analytically important videos also provided video of previous re-entries.

#### **6.1.5 Celestial References**

Several software packages were used to identify and correlate celestial fields seen in the videos. A commercial program, TOPO USA, converted observer locations (street addresses) to latitudes and longitudes and altitude. These data were input into celestial reference programs. Skywatch is a Java-based celestial acquisition program developed by the Flight Design and Dynamics Division, and was used for initial time synchronization. Supersighter is a celestial acquisition program certified for operational use in the Mission Control Center for the STS and International Space Station (ISS) Programs. Sky, a commercial program, was used to determine identities and magnitudes of celestial objects seen in the videos.

### **6.2 Re-entry Processes/Methods**

#### **6.2.1 Processing of Submissions**

Most imagery submitted by the public was delivered to the Emergency Operations Center (EOC). The Early Sightings Assessment Team (ESAT) pre-screened the submissions and then hand-carried items to the Mission Video Lab (videos) or Digital Imaging Lab (for still images). The ESAT Final Report contains details of the process.

#### **6.2.2 Video Processes**

##### **6.2.2.1 Duplication for Screening**

The Mission Video lab duplicated the tapes received each day and delivered copies to the Image Analysis Team, Early Sightings Assessment Team, and other NASA Centers. The Image Analysis team received this screening tape in D2 digital format. All videos that were digitally acquired were also delivered to us in DVCam format. The Mission Video Lab maintains tape duplication and archive records.

##### Video quality

The D2 copy of the original submission was of sufficient quality for the timelining group and relative motion analysis. The luminosity team required best quality duplication from original material. Original tapes were obtained from the submitters for all analytically important videos in order to make the best possible quantitative measurements. These tapes were duplicated to DVCam format under our supervision to insure that the

This information is being distributed to aid in the investigation of the Columbia mishap and should only be distributed to personnel who are actively involved in this investigation. 59

duplicating system configuration maintained the best quality. Then the DVCam was cloned, and the clone used for JSC analysis. The DVCam clone was also converted to Digital8 format for use by MSFC team members. Details of tape duplication and video quality are tracked in the “Entry Video and Still Database” (<http://vdas-huey.jsc.nasa.gov/Contingency/107/web/>) and in the document Appendix 6.2A.

### 6.2.2.2 Time Synchronization

#### Time code standardization

In order to maintain a standard time code that would be accurate within 1/60<sup>th</sup> of a second on repeat viewings, a digital copy of each D2 with the SMPTE (Society of Motion Picture and Television Engineers) time code standard embedded into the video image was made and used for timing video events.

#### Relating SMPTE time to UTC time

A variety of techniques were used to get the best possible timing of events in videos with little or no time information. Military-provided videos included verified embedded UTC timing. Whenever possible, times for the events were based upon passage of the Orbiter envelope near celestial objects recorded in the videos. Longer-duration videos were used as a unified time check between the celestial time-referenced events early in the sequence and later in the sequence. Key overlapping events were then cross-referenced from UTC-embedded or celestially synchronized videos with other videos that did not have a time reference. Uncertainties for each time the debris was first observed were determined based on the estimated accuracy of the time synchronization. As ballistic modeling was completed for events seen in multiple videos, improved estimates of debris separation time were used to improve the accuracy of the time synchronization for videos with overlapping events.

During the screening and timing process, the “Entry Video and Still Database” (<http://vdas-huey.jsc.nasa.gov/Contingency/107/web/>) was expanded to track and display the most current metadata, including time synchronization, screen captures, and other information.

### 6.2.2.3 Digitization of Video Clips

Events from previously screened videos that were given high priority for analysis were captured from the Sony D2 format master tapes or from DVCam copies of the submitted tapes. Although these digital movies were captured from duplicate generation tapes having relatively high background noise, they were adequate for motion analysis of the larger, brighter debris events.

Single debris events were captured as separate short movie clips using DPS Reality software with image dimensions 720 horizontal by 486 vertical samples.

This information is being distributed to aid in the investigation of the Columbia mishap and should only be distributed to personnel who are actively involved in this investigation. 60



### De-interlacing

All the consumer cameras employed a standard NTSC video format, which groups two interlaced video fields to make a single video frame. Each field consists of a set of alternate (odd or even numbered) horizontal video lines separated in time by 1/59.97 seconds. By default, the frame capture process combines successive pairs of these odd and even fields into full size frames which must then be separated out, or de-interlaced, for proper analysis. The default 720 x 486 size movies were de-interlaced into field movies sized 720 x 243 using the Video Investigator software developed by Cognitech, Inc.

### Restoration of Aspect Ratio

The capture and de-interlacing process created images which were geometrically distorted, or stretched, in the horizontal direction relative to the vertical direction in two ways. First, the initial 720 x 486 frame size stretches the image horizontally by a factor of 1.1 relative to the vertical. This distortion factor was confirmed with test imagery prior to analysis. Second, the de-interlacing reduces the vertical dimension by a factor of 2. Restoration of the proper aspect ratio was accomplished in one step by resizing the vertical dimension by a factor of 2.2, (from 243 to 533). The resizing was done using a cubic spline interpolation in Video Investigator. The movies were also converted from color to monochrome to conserve hard disk space.

### Intensity measurements

A modified digitization method was used for intensity measurements. DVCam tapes were captured using DPS Reality Software. When images were captured in digital form, meaningful signal above the arbitrary 100 IRE level was truncated (IRE is a scale defined by the Institute of Radio Engineers to measure the amplitude of a video signal; an IRE unit is equal to 1/140 volts). To prevent this truncation, the “digital proc amp” level control in DPS reality was used to bring the video peak to peak signal within the dynamic range of the capture system and eliminate inadvertent clipping. The signal was then converted back to its original levels as part of the intensity measurement analysis.

#### **6.2.2.4 Calibration of Focal Lengths**

From early screening and preliminary identification of key imagery in February 2003, 17 video and 8 still cameras were procured from the public for calibration. One important input needed for the motion analysis was the focal length setting of the lens or, as an equivalent, a value for the Horizontal Field of View (HFOV) for each observation. This input was crucial because the larger the focal length (smaller the HFOV) used by the observer, the more the lens will have magnified the distance between the debris and the Shuttle. See Appendix 6.2B for a table of calculated fields-of-view for the various videos.

All the cameras used to capture video for this analysis had variable focal length zoom lenses and many observers zoomed in and out numerous times. Some observers made statements that they were at the maximum magnification or fully zoomed during certain events. If software magnification (digital zoom) was not enabled for these videos, then

This information is being distributed to aid in the investigation of the Columbia mishap and should only be distributed to personnel who are actively involved in this investigation. 61

the focal length and HFOV was either based on the camera specifications from the manufacturer or was determined empirically by the Image Analysis Team once the actual camera was received. For all other videos, a focal length had to be determined based on additional information in the image.

In most of the videos, the only objects in view are the Shuttle, the luminous trail behind it and occasional debris events. Both the debris and the Shuttle are too small to be resolved in detail and appear only as points or spots. The sizes of these points depend on several things: the resolving power of the lens, the apparent brightness of the objects (which was not constant), and the exposure and gain settings of the camera (some of which were automatically set and variable). So for these reasons, spot size could not be used reliably to measure changes in focal length.

There were, however, circumstances that allowed calibration of the HFOV. One observer remembered his zoom setting and calibrated his camera's HFOV the next day using the diameter of the full moon. Two videos had stars or a planet in view near the time of a debris event, and some observers enabled a digital zoom setting in their cameras which magnified the imagery beyond the optical zoom limit at the time of observations.

#### Use of Stars and Planets

In some key videos, a debris event was observed soon before or after the appearance of the star or planet and with no apparent change in zoom. These observations allowed the image motion of the Shuttle to be measured relative to a fixed point in the sky, and through this, the field of view could be determined.

Initially, a method was developed to compare the angular separation between the Shuttle and the star (based on Orbiter positional data) with the separation measured in image pixels. However, because the Shuttle was moving so rapidly across the sky, (about one degree per second for some observers) this method required a very accurate knowledge of the absolute time that events were recorded onto tape. A small error in timing the video had a drastic effect on the angle-to-pixel comparison, and timing uncertainty was estimated to be at least 1 or 2 seconds.

Our other method for deriving field-of-view relied less on the absolute timing of events, and more on the relative timing of the Shuttle motion. This method simply used the position of the Shuttle at two different times and compared the change in its image position relative to the fixed sky object (in pixels) with its change in angular position in the sky. This relative change in angular position of the Shuttle is much less affected by timing uncertainty than is the absolute position, so it provided a more reliable estimate of the field-of-view.

#### Maximum Optical Zoom Calibrations

Cameras purchased from the public were received at Johnson Space Center and quick measurements were made with each to calibrate the HFOV at the maximum optical zoom setting (maximum focal length). These quick measures were done using rulers observed through the eyepiece of each camera and served as temporary initial values for the

This information is being distributed to aid in the investigation of the Columbia mishap and should only be distributed to personnel who are actively involved in this investigation. 62

analysis until more thorough calibrations were conducted by Neptec, Inc. Field-of-view calibrations at multiple camera settings were performed by Neptec, and are summarized in Appendix 6.2A.

#### Digital Zoom Estimations

Some observers enabled a camera setting called digital zoom, which magnifies the image beyond the optical zoom limit. The magnification is applied within the camera using software to “blow up” a centralized sub-region of the image. It becomes noticeable as a change in the pixelation or granularity of the image. The granularity increases because the image is being generated from a smaller and smaller number of pixels on the imaging chip. Images of the Shuttle re-entry in digital zoom are easy to identify because of the highly amplified noise in the dark background sky. This noise is not generated optically, but is a random fluctuation generated while the image is captured, but before the digital zoom software acts on the image. Because it is not an optical signal, it will not change character during optical zooming, but it will change during digital zooming. So, measuring a change in the background noise characteristics can provide a measure of the amount of digital zoom applied by the software. A technique was developed to use measurements of background noise and maximum focal length to estimate the degree of digital zoom and accurately calibrate the effective focal length (or horizontal field of view) used during the videos. Estimations of the amount of digital zoom based on background noise characteristics were made for observations from Flagstaff, AZ, Mount Hamilton, CA, and St. George, UT. Details of the new technique are documented in Appendix 6.2B.

#### **6.2.2.5 Other Video Camera Calibrations**

Additional camera calibrations were conducted to support the measurements of signal intensity. The gamma curve was determined empirically for the black to peak white region (0 to 100 IRE units). In addition, the linearity of the signal above peak white was determined. Both tests were performed using a gamma gray scale chart. Saturation response and point spread function were measured using an artificial variable star source comprised of a collimator, pinhole, rotating neutral density filter and a stable light source. By recording the response to the artificial star, an empirical correction for the response of each camera could be made so that stellar photometry techniques could also be employed in measuring the intensity of the debris recorded in the videos. A minimum illumination test was performed by testing the light received (at the camera location) with a light meter and then recording the corresponding video output of the camera. Minimum illumination is considered the first light level that can be distinguished above the noise floor.

#### **6.2.2.6 Motion of Debris Relative to Orbiter**

##### Tracking of Orbiter and Debris

In order to calculate ballistic coefficients for individual debris objects, the Image Analysis Team tracked the relative position for each named debris object in the debris timeline relative to the Orbiter in priority video imagery. De-interlaced digital field

This information is being distributed to aid in the investigation of the Columbia mishap and should only be distributed to personnel who are actively involved in this investigation. 63

movies of the debris were imported into a tracking program called ISee (developed by Inovision, Inc.). The software facilitated automatic tracking of the Orbiter and any bright stars or planets using a centroid algorithm, or “p-node” that was applied within a customized multiple p-node routine, or “network”. The network contained a number of parameters, which had to be adjusted for each debris movie based on aspects like the brightness, contrast, and the presence of text within the field.

One important parameter was a threshold value used for binarizing the grayscale values, reducing the fields down to two values, black and white. This threshold was set to a high enough grayscale value so that the luminous trail behind the Orbiter would not seriously affect the shape of the Orbiter outline and centroid.

The automatic tracking network worked extremely well for objects that remained consistently bright or were saturated, and it produced centroid positions with a sub-pixel precision better than 0.1 pixel. The debris pieces, however, were often too dim or fluctuated in brightness too greatly for the automatic tracking to work effectively. Therefore the dim debris pieces were tracked manually using the same Isee software in an interactive mode. Sub-pixel precision of 0.25 to 0.5 pixels was obtainable in this interactive mode.

#### Assumptions about Debris Trajectory

It was necessary to make some assumptions about the motion of the debris shed during re-entry in order to determine its distance from the Orbiter using only a single camera view. Two independent groups worked with the video tracking data to determine the relative motion of the debris and these groups used different assumptions and scaling methods. The JSC Image Analysis Group (JSC-SX) assumed that, relative to the Orbiter’s forward motion, the luminous debris pieces traveled along the trajectory path but behind the Orbiter. The debris still had forward motion relative to the ground, but relative to the Orbiter, the motion was exactly opposite the Orbiter velocity vector. The Flight Design and Dynamics Group (JSC-DM44) assumed the debris fell behind the Orbiter but could have fallen anywhere in a plane perpendicular to the ground that also contains the Orbiter trajectory path. The first assumption places a greater constraint on the debris motion, allowing for a very simple and straightforward photogrammetric solution to the one-camera problem. The second assumption places looser constraints on the debris motion, which, in turn, requires greater knowledge about the camera’s orientation (including camera roll) relative to the horizon and requires the curvature of the earth be taken into account in order to derive the plane containing the debris. There was generally good agreement between relative motion solutions between the two groups, except for debris events that were observed from southwestern Utah. It is assumed those differences result from the viewing geometry of the observers (the Orbiter passed almost directly overhead).

#### Image to Object Scale

Positional GPS data for the orbiter was combined with the observer locations, camera field-of-view calibrations and the time-sequenced video tracking data to precisely define the geometry for each observation. Understanding this geometry made it possible to

This information is being distributed to aid in the investigation of the Columbia mishap and should 64  
only be distributed to personnel who are actively involved in this investigation.

directly calculate the relative feet of separation between the debris and the orbiter by applying the law of sines and law of cosines for triangular relationships. Once the debris distance was calculated, a scale factor, in feet-per-pixel, was then calculated as a final step. Because the orbiter was moving very fast, the perspective geometry of the observations changed quickly, and so this calculation was made separately for every video field that contained both the debris and the orbiter. The calculation was applied as an Excel spreadsheet program. The generalized solution for calculating the debris separation as a function of time without a fixed sky reference is provided in detail in Appendix 6.2A.

#### **6.2.2.7 Relative Light Intensity of Orbiter and Debris**

Determining relative light intensities of the debris and the Orbiter in each video was a complex task. Video data of the Orbiter were often saturated in intensity, videos may have been acquired in different camcorder modes (e.g. night shot), and the camcorder operators frequently used both optical and digital zoom features of their camcorders, making direct comparisons difficult. Two methods of measuring the intensities were developed. Methods were validated using consumer-grade videos of stars of known intensities. Depending on the characteristics of a particular event and video, one or both methods were applied.

##### Photometry method

The first method was based on a circular aperture photometry technique that is normally conducted on saturated video images of meteor showers. The automated software that does the measurements from Digital 8 tapes was modified for application to Columbia re-entry videos. Empirical calibrations of the cameras were used to model the photometric response of each camera. Saturation of the camera detectors clips the signal above the maximum intensity. A double Moffit fit is used to estimate the intensity of the signal above the saturation threshold. Calibration is needed to determine the response of each camera to signals brighter than the saturation threshold. This method requires a calibration tape taken under similar conditions to the original video, and a sufficient duration of record to get a good signal. These methods are described in more detail in Appendix 6.2A.

##### Video engineering method

The second method is based on understanding the electronic signal response of the camera and the algorithms used to record and display that signal. Equations were developed to relate the observed signal to the actual intensity of the event recorded. The intensity of the signal is integrated across the frame for an irregular area around the “blob” of light that is the Orbiter or debris. This method can be done on single frames, and can compensate for low levels of signal clipping, but cannot compensate for high degrees of saturation of the video. These methods are described in more detail in Appendix 6.2A.

This information is being distributed to aid in the investigation of the Columbia mishap and should only be distributed to personnel who are actively involved in this investigation. 65

#### **6.2.2.8 Methods for Debris Mass Estimates**

Prior to the Columbia investigation, there was not an established method for characterizing the Orbiter's re-entry radiative signature, including the re-entry debris events seen on the publicly acquired videos. Despite this challenge, several models were developed to use the relative intensities of the visual signature of the debris as recorded in the videos to estimate the debris mass. All the models assumed that the visible light was produced by the change in kinetic energy as the debris moved through the upper atmosphere and decelerated. If the debris is treated as a non-ablative object, the kinetic energy from deceleration is "dumped" into the atmosphere, causing the atmospheric molecules to become excited and emit light with no mass loss of the debris. A simple non-ablative approach established the upper bound for debris mass. A modified non-ablative approach, modeled on an object of known shape and orientation for the debris that would give the maximum possible brightness per unit mass, established an absolute lower bound for debris mass.

A total ablative approach (assuming the debris completely ablates) was also considered as a model for estimating mass. However, light curves for the debris events do not support the use of a total ablative approach. Instead, a moderate ablative approach was applied to estimate debris mass by using the trajectory and deceleration of the debris and the observed light curve to estimate an ablation rate. Whenever the debris is visible in the videos for long enough to measure intensity curves to provide a good ablation estimate, the moderate ablative methods were applied, providing our best estimate for debris mass. The methods are described in detail in Appendix 6.2A. A final report from the Luminosity Working Group will include additional debris mass estimates and other debris characterization.

#### **6.2.2.9 Methods to Identify Debris Composition**

If different Orbiter materials have different spectral signatures in the re-entry environment, it may be possible to determine the composition of the debris material by examining signal intensities in the red, green, and blue channels of video and still imagery. This is also a complex task and the challenges include acquiring spectral data from the imagery, acquiring the spectral sensitivity data from the individual cameras, and determining if the debris itself is the source of the luminosity or whether the source is the associated shock wave. Arcjet testing at Ames will determine if luminosity characteristics depend on material characteristics. If luminosity characteristics do not depend on material characteristics, the material composition cannot be determined from the data available. Additional information on the potential for spectral information in the publicly acquired videos can be found in Appendix 6.2A. The results of this testing and additional information on debris composition will be included in the "Luminosity Working Group Columbia Re-entry Debris Characteristics Final Report".

This information is being distributed to aid in the investigation of the Columbia mishap and should only be distributed to personnel who are actively involved in this investigation. 66

## 6.2.3 Still Image Processes

### 6.2.3.1 Digital Conversion

Still imagery received by NASA in any form (digital, print, negative, slide) was quickly scanned into electronic form for rapid screening and distribution. Metadata associated with each image, including camera characteristics and observer location were compiled in the “Entry Video and Still Database” (<http://vdas-huey.jsc.nasa.gov/Contingency/107/web/>). A subset of approximately 25 of the available 1500 still images in the database (all long exposures) could be timelined on the basis of stars or simultaneous video acquisitions (Figure 6.2.3.1). These images covered the time period of debris events observed in videos, and were of sufficient quality to contain possible analytical information. Debris events were not visible in any of the photographs, but a few did show plasma anomalies and the flash corresponding to observations from the videos.



Figure 6.2.3.1 Example of one of the best still photographs of re-entry taken from Owens Valley, CA

### 6.2.3.2 Image Quality

For the analytically significant still images, best image quality was assured by acquiring the original digital file or film. Film images were over-scanned so that all information was available in digital form down to the grain size of the film. Digital images were acquired in the original form from the camera or users archive. Cameras were calibrated for pixel defects, focal length, and signal response. Spectral response calibrations were delayed until it could be determined from arcjet testing whether spectral analysis of imagery could provide information on debris composition.

This information is being distributed to aid in the investigation of the Columbia mishap and should only be distributed to personnel who are actively involved in this investigation. 67

### 6.2.3.3 Assigning Timing in a Long-exposure Photograph

Still imagery was acquired using long exposures (15 to 45 seconds), so each image represents a summative record of the brightness of the Orbiter, the trail behind it and any anomalous events. Starfield and observer position were used to identify the time of passage of the Orbiter at different points in the photograph (Figure 6.2.3.3).

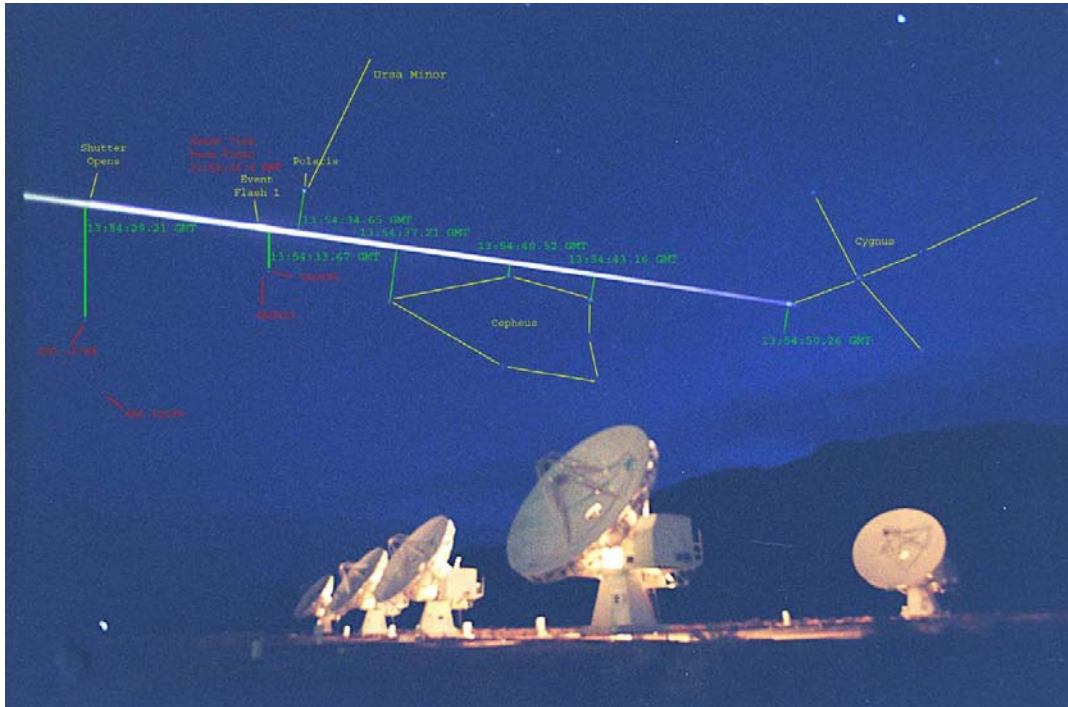


Figure 6.2.3.3 Long-exposure still image with Orbiter trail and celestial features, allowing for timing of features in the image

### 6.2.3.4 Potential for Spectral Information in Still Photography

A preliminary assessment of the digital photographs most likely to contain information identified differences in the color signature of the Orbiter and its luminous trail. If different debris materials are determined to give different spectral signatures on re-entry, a handful of photographs can be analyzed to determine if they can confirm material composition for events they record. Digital photographs have more color information than the videography and could yet prove to contain valuable information. However, to date, we have not characterized re-entry anomalies using the still photographs.

This information is being distributed to aid in the investigation of the Columbia mishap and should only be distributed to personnel who are actively involved in this investigation. 68



## 6.3 Re-entry Analyses: Primary Results

### 6.3.1 Re-entry Video Screening and Data Base

A total of 150 videos and over 1500 still images were sent to NASA. A few submitters provided both video and still imagery acquired simultaneously. Other submitters supplied information on previous nominal re-entries. The Image Analysis Team screened video and still images, created a searchable database for imagery, and added metadata through the screening and cataloging process. The metadata records include cross-referenced EOC and NASA-JSC numbers, media type, contact information about the observer, observer location, camera type and setting information, any comments supplied by the observer, detailed screening notes, frame captures, timing data, light curves for selected frames, and other cross-referenced media such as original tape or copies, or other imagery acquired by the same observer. The STS-107 Entry Video and Still Database can be accessed at <http://vdas-huey.jsc.nasa.gov/Contingency/107/web/>.

### 6.3.2 Entry Debris Timeline and Debris Event Descriptions

A total of 23 videos submitted by the public and two videos from military sources (one from Kirtland AFB, NM and one from an Apache FLIR near Fort Hood, TX) contained records of anomalous events on re-entry that could be correlated to absolute time. From this information, an imagery time line was established which was integrated into the OVEWG configuration controlled "Data Review & Timeline". A total of 24 anomalous visual events were detected between California and New Mexico, and another 10 events were identified from Texas videos (Figure 6.3.2a). NASA did not receive good quality video that covers Eastern Arizona and New Mexico, and no video at all that covers Eastern New Mexico to Central Texas (Figures 6.3.2b and c). Because of the gap in video coverage, it was impossible to link the Western and Eastern segments of the entry debris timeline into a single unified timeline. Also, all of the videos contain short periods when the Orbiter is out of the camera's field of view, obscured by clouds, or is out of focus. As a result, there is a high probability that additional events occurred which are not visible on the available videos.

The anomalies in the timeline include debris shedding events, large flashes, flares, and non-uniformities in the Orbiter's plasma trail. The times recorded in the timeline represent the earliest moment in time when the team could distinguish an event outside the Orbiter plasma envelope. These debris times do not represent the actual time when debris physically separated from Columbia because the Orbiter is not visible in the luminous envelope. However, the STS-107 Early Sighting Assessment Team estimated the actual debris separation times based on ballistic calculations derived from the videos (Table 6.3.4 and ESAT Final Report).

Table 6.3.2 presents Version 7 of the re-entry debris timeline. A complete and updated copy of the "Entry Debris Events Timeline" can be found at [references/shuttleweb/mission\\_support/sts-107/contingency/entry/reports/107\\_reports.html](http://references/shuttleweb/mission_support/sts-107/contingency/entry/reports/107_reports.html). Figures

This information is being distributed to aid in the investigation of the Columbia mishap and should only be distributed to personnel who are actively involved in this investigation. 69

6.3.2a, b & c present maps that show where the debris events occurred along the re-entry trajectory, as well as the locations of the observers.

<b>Western Debris Events</b>			
<b>Event</b>	<b>GMT</b>	<b>EOC Video Number</b>	<b>Description</b>
Debris 1	13:53:46 (+/- 1 sec)	EOC2-4-0056 EOC2-4-0064 EOC2-4-0201 Plasma Anomaly seen in EOC2-4-0136	Seen just aft of Orbiter envelope, one second after a plasma anomaly which consisted of a noticeably luminescent section of the plasma trail.
Debris 2	13:53:48 (+/- 2 sec)	EOC2-4-0056 EOC2-4-0064 EOC2-4-0201	Seen just aft of Orbiter envelope.
Debris 3	13:53:56 (+/- 2 sec)	EOC2-4-0055 Δ EOC2-4-0056 Plasma Anomaly seen in EOC2-4-0064 EOC2-4-0136	Seen just aft of Orbiter envelope followed one second later by a plasma anomaly which consisted of a noticeably luminescent section of the plasma trail.
Debris 4	13:54:02 (+/- 2 sec)	EOC2-4-0055 Δ EOC2-4-0056	Seen just aft of Orbiter envelope.
Debris 5	13:54:09 (+/- 2 sec)	EOC2-4-0055 EOC2-4-0056	Seen just aft of Orbiter envelope at the head of a plasma anomaly.
Flash 1	13:54:33.6 (+/- 0.3 sec)	EOC2-4-0009-B EOC2-4-0055 Δ EOC2-4-0034 EOC2-4-0066 EOC2-4-0070	Orbiter envelope suddenly brightened (duration 0.3 sec), leaving noticeably luminescent signature in plasma trail.
Debris 6	13:54:36 (+/- 1 sec)	EOC2-4-0009-B EOC2-4-0055 Δ EOC2-4-0030 EOC2-4-0066 EOC2-4-0070	Very bright debris seen just aft of Orbiter envelope.
Debris 7	13:55:05 (+/- 1 sec)	EOC2-4-0030	Seen just aft of Orbiter envelope.
Debris 7A	13:55:18 (+/- 1 sec)	EOC2-4-0161	Seen just aft of Orbiter envelope.

This information is being distributed to aid in the investigation of the Columbia mishap and should only be distributed to personnel who are actively involved in this investigation. 70

Debris Shower A	13:55:23 to 13:55:27 (+/- 1 sec)	Saw Debris EOC2-4-0098 EOC2-4-0161 EOC2-4-0005 EOC2-4-0030 Saw Shower EOC2-4-0017 EOC2-4-0021 EOC2-4-0028	Seen just aft of Orbiter envelope. Over the course of these four seconds a luminescent section of plasma trail is observed which appears to contain a shower of indefinite particles and multiple, larger discrete debris that includes Debris 8, 9 and 10.
Debris 8	13:55:23 (+/- 2 sec)	EOC2-4-0030 EOC2-4-0098 EOC2-4-0161	Seen aft of Orbiter envelope inside the aforementioned Debris Shower A.
Debris 9	13:55:26 (+/- 2 sec)	EOC2-4-0005 EOC2-4-0098	Seen aft of Orbiter envelope inside the aforementioned Debris Shower A.
Debris 10	13:55:27 (+/- 2 sec)	EOC2-4-0005	Seen aft of Orbiter envelope inside the aforementioned Debris Shower A.
Debris 11	13:55:37 (+/- 2 sec)	EOC2-4-0050 EOC2-4-0098	Appears at the head of a secondary parallel plasma trail well aft of Orbiter envelope. A second piece of debris is also seen in the secondary plasma trail.
Debris 11A	13:55:39 (+/- 1 sec)	EOC2-4-0098	Seen just aft of Orbiter envelope.
Debris 11B	13:55:40 (+/- 2 sec)	EOC2-4-0098	Seen at head of a parallel plasma trail aft of the Orbiter envelope.
Debris 11C	13:55:44 (+/- 2 sec)	Sees debris and parallel trail: EOC2-4-0098 Sees parallel plasma trail only: EOC2-4-0028 EOC2-4-0050	Seen at head of a parallel plasma trail well aft of the Orbiter envelope.
Debris 12	13:55:45 (+/- 1 sec)	EOC2-4-0028 EOC2-4-0050 EOC2-4-0098	Seen aft of Orbiter envelope followed by secondary plasma trails.
Debris 13	13:55:56 (+/- 2 sec)	EOC2-4-0005 EOC2-4-0017 EOC2-4-0021 EOC2-4-0161	Seen well aft of Orbiter envelope with momentary brightening of plasma trail adjacent to debris.
Debris 14	13:55:58 (+/- 1 sec)	EOC2-4-0005 EOC2-4-0017 EOC2-4-0021 EOC2-4-0028 EOC2-4-0030	Very bright debris just aft of Orbiter envelope.
Debris 15	13:56:10 (+/- 2 sec)	EOC2-4-0017	Seen just aft of Orbiter envelope.
Debris 16	13:57:24 (+/- 5 sec)	EOC2-4-0148-2	Very faint debris just aft of Orbiter.
Flare 1	13:57:54.5 (+/- 1 sec)	EOC2-4-0148-4	Asymmetrical brightening of Orbiter shape.
Flare 2	13:58:00.5 (+/- 1 sec)	EOC2-4-0148-4	Asymmetrical brightening of Orbiter shape.

This information is being distributed to aid in the investigation of the Columbia mishap and should only be distributed to personnel who are actively involved in this investigation. 71

The Photo/TV Analysis Team currently does not have any good quality video that covers Eastern Arizona to Central Texas (no video is available that covers Eastern New Mexico to Central Texas), making it impossible to link the Western and Eastern segments into a single unified timeline.

<b>Eastern Debris Events</b>			
<b>Event</b>	<b>GMT</b>	<b>EOC Video Number</b>	<b>Description</b>
Debris "A"	13:59:47 (+/-1 sec)	EOC2-4-0018 EOC2-4-0024 EOC2-4-0209-B EOC2-4-0221-3 EOC2-4-0221-4	Large debris seen falling rapidly away from the Orbiter envelope.
Debris "B"	14:00:02 (+/- 1 sec)	EOC2-4-0024	Debris first seen well aft of Orbiter envelope.
Debris "C"	14:00:03 (+/- 1 sec)	EOC2-4-0024	Debris first seen aft of Orbiter envelope.
Late Flash 1	14:00:05.7 (+/- 0.5)	EOC2-4-0018 EOC2-4-0024 EOC2-4-0209-B EOC2-4-0221-3 EOC2-4-0221-4	Sudden brightening of the Orbiter envelope.
Late Flash 2	14:00:06.7 (+/- 0.5)	EOC2-4-0018 EOC2-4-0024 EOC2-4-0209-B EOC2-4-0221-3 EOC2-4-0221-4	Sudden brightening of the Orbiter envelope, followed by a shower of debris seen aft of the Orbiter envelop during the next 4 seconds (shower seen only in EOC2-4-0221-4).
Debris "D"	14:00:10 (+/- 2 sec)	EOC2-4-0018 EOC2-4-0209-B EOC2-4-0221-3 EOC2-4-0221-4	Debris first seen slightly aft of Orbiter envelope and begins generating its own trail.
Debris "E"	14:00:11 (+/- 2 sec)	EOC2-4-0209-B EOC2-4-0221-3 EOC2-4-0221-4	Debris first seen aft of Debris "D"
Debris "F"	14:00:12 (+/- 2 sec)	EOC2-4-0209-B EOC2-4-0221-4	Debris first seen aft of Orbiter envelope, which for a short time begins generating its own trail.
Debris Shower	14:00:15 (+/- 2 sec)	EOC2-4-0209-B EOC2-4-0221-4	Multiple debris seen immediately aft of the Orbiter envelope over the next 2 seconds.
Catastrophic Event	14:00:18.3 (+/- 0.5 sec)	MIT-DVCAM-0001 EOC2-4-018 EOC2-4-0024 EOC2-4-0209-B EOC2-4-0221-3 EOC2-4-0221-4	Catastrophic Event of an unknown nature (formally referred to as "Main Body Breakup) consisting of a sudden brightening of the Orbiter Envelope followed by a definitive change in the character of the trail.  Numerous debris seen aft of Orbiter envelope over the next 10 seconds, followed by disintegration of the main Orbiter envelope into multiple pieces.

**Table 6.3.2 Re-entry debris timeline revision 7**

This information is being distributed to aid in the investigation of the Columbia mishap and should only be distributed to personnel who are actively involved in this investigation. 72

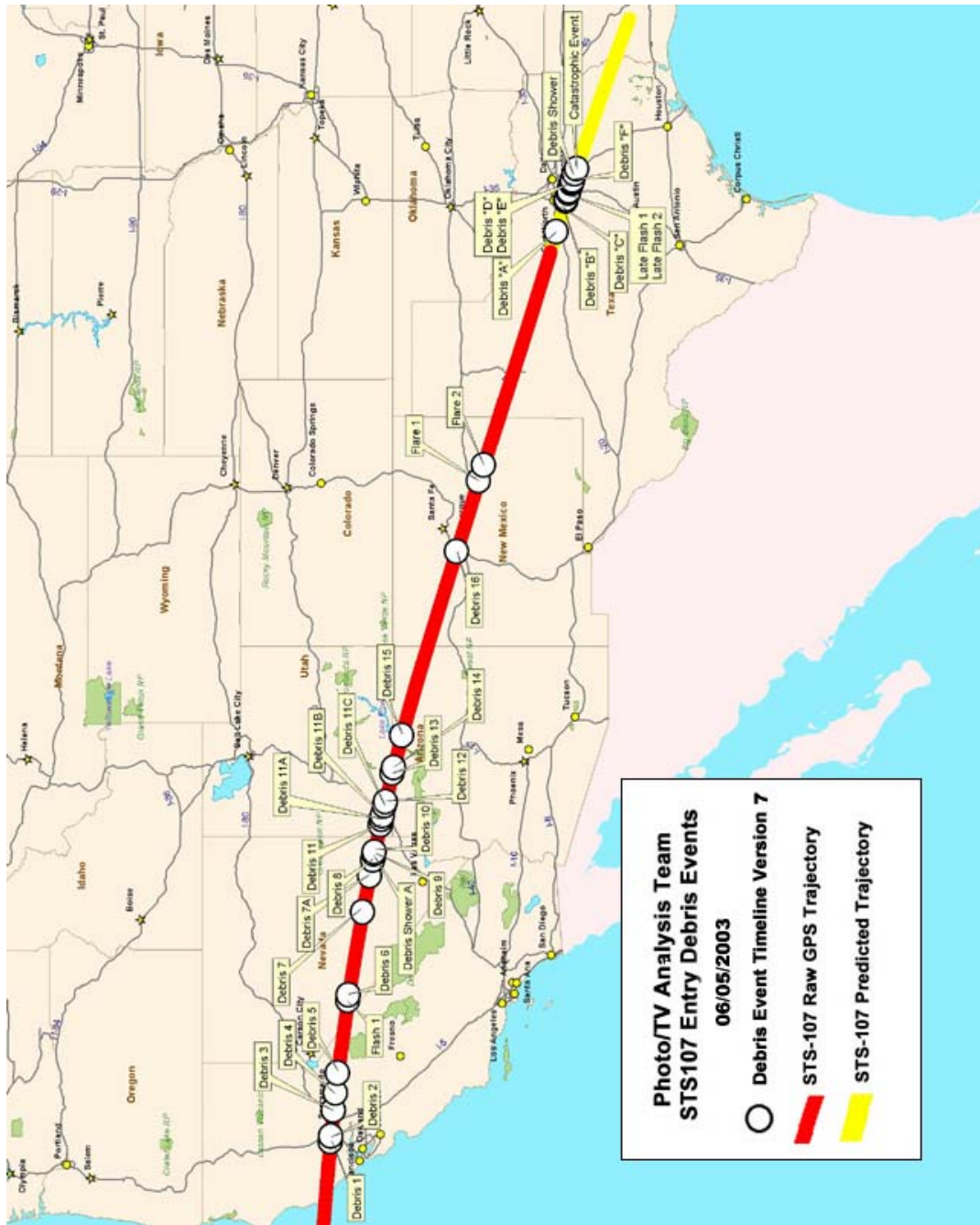


Figure 6.3.2a Map summarizing locations of observed debris events during STS-107 re-entry. Details for each event are found in Table 6.3.2.

This information is being distributed to aid in the investigation of the Columbia mishap and should only be distributed to personnel who are actively involved in this investigation. 73

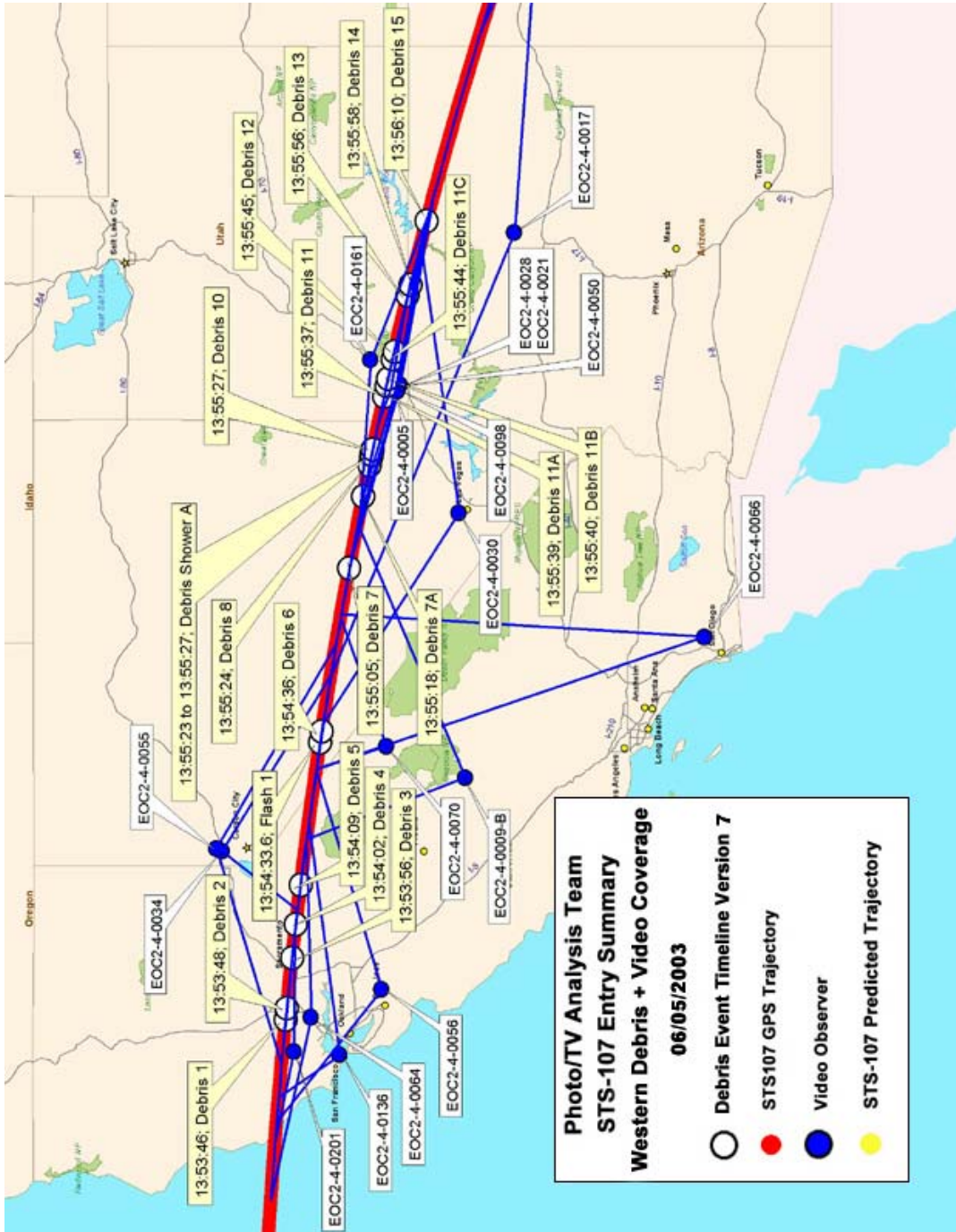
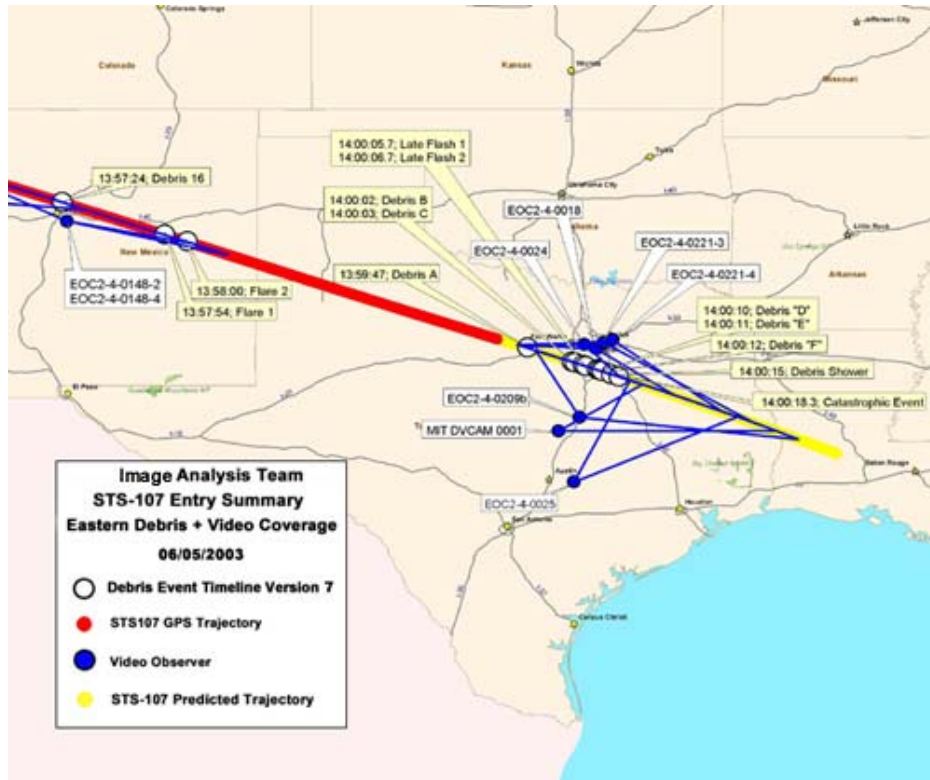


Figure 6.3.2b Detailed map of the Western U.S. re-entry debris event locations. The blue dots and connecting lines are the observer positions (identified by video number) and their relative fields-of-view captured by their videos.

This information is being distributed to aid in the investigation of the Columbia mishap and should only be distributed to personnel who are actively involved in this investigation. 74



**Figure 6.3.2c Detailed map of the Texas re-entry debris event locations. The blue dots and connecting lines are the observer positions (identified by video number) and their relative fields-of-view captured by their videos.**

### 6.3.3 Nominal Re-entry Characterization

Comparison of the Columbia re-entry videos with nominal entry videos from previous missions confirmed that the observed STS-107 events were anomalous. To better characterize the appearance of a normal Shuttle re-entry, videos were collected from the public of previous Shuttle entries. Seven videos were screened in detail (five of them were previous Columbia re-entries) to establish baseline characteristics of nominal Shuttle entry for comparison with and in contrast to the entry events of STS-107 seen in public video (Table 6.3.3). Analyses of these nominal re-entry videos indicate that the vehicle is not visible, rather, it is hidden from view by a bright “plasma” envelope. The vehicle’s plasma envelope appears normally as a bright oval, slightly tapered at its aft end, and predominately white with at times a slight blue or pink hue (Figure 6.3.3a). The plasma trail is normally a white glow with little apparent structure, and has uniform texture, uniform thickness, and uniform luminosity.

This information is being distributed to aid in the investigation of the Columbia mishap and should only be distributed to personnel who are actively involved in this investigation. 75

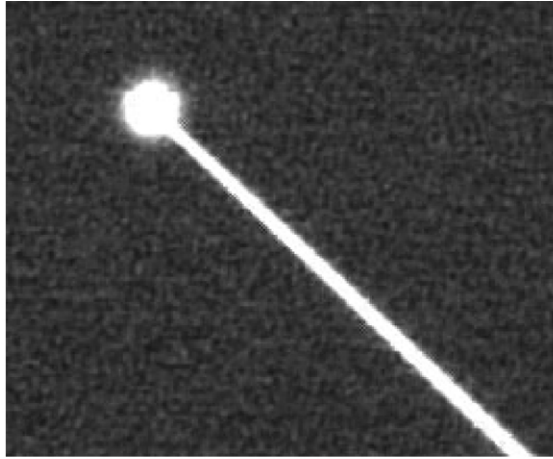
<b>Mission</b>	<b>Date</b>	<b>Vehicle</b>	<b>Video Duration (Min: Sec)</b>	<b>Viewer Location</b>	<b>Viewer's Local Time (approx.)</b>	<b>Vehicle Location</b>	<b>RCS Firings during Video Coverage</b>
STS-62	Mar. 1994	Columbia	1:34	Campbell, CA	04:50 PST	CA/NV	9
STS-73	Nov. 1995	Columbia	2:07	Campbell, CA	03:25 PST	CA/NV	13
STS-77	May 1996	Endeavor	2:49	Campbell, CA	03:50 PDT	CA/NV	25
STS-78	July 1996	Columbia	2:28	Twain Harte, CA	05:15 PDT	CA/NV	21
STS-82	Feb. 1997	Discovery	2:48	Houston, TX	02:15 CST	TX/LA	77
STS-93	July 1999	Columbia	1:46	Houston, TX	22:05 CDT	TX/LA	7
STS-109	Mar. 2002	Columbia	2:46	San Angelo, TX	03:15 CDT	NM/TX	8

**Table 6.3.3 Nominal entry videos screened to compare with STS-107 videos**

Multiple Reaction Control System/Subsystem (RCS) thruster firings occurred over the duration of each video (160 firings from 7 mission videos). The RCS firings were not visible in the videos; no flashes were seen coincident with any of the RCS firings. During wide-angle camera views, short segments of dissipated or “quenched” plasma trail were sometimes seen well aft of the vehicle (Figure 6.6.3b). The dissipated segments appear to correlate in time with the longer-duration RCS firings (in excess of one second). No noticeably over-luminous portions of the plasma trail were ever observed as a result of RCS firings.

This information is being distributed to aid in the investigation of the Columbia mishap and should only be distributed to personnel who are actively involved in this investigation. 76





**STS-109 Entry viewed from San Angelo, TX**

Image used eoc2-4-0209\_20505520.jpg

**Figure 6.3.3a** Video image of normal Shuttle re-entry, STS-109

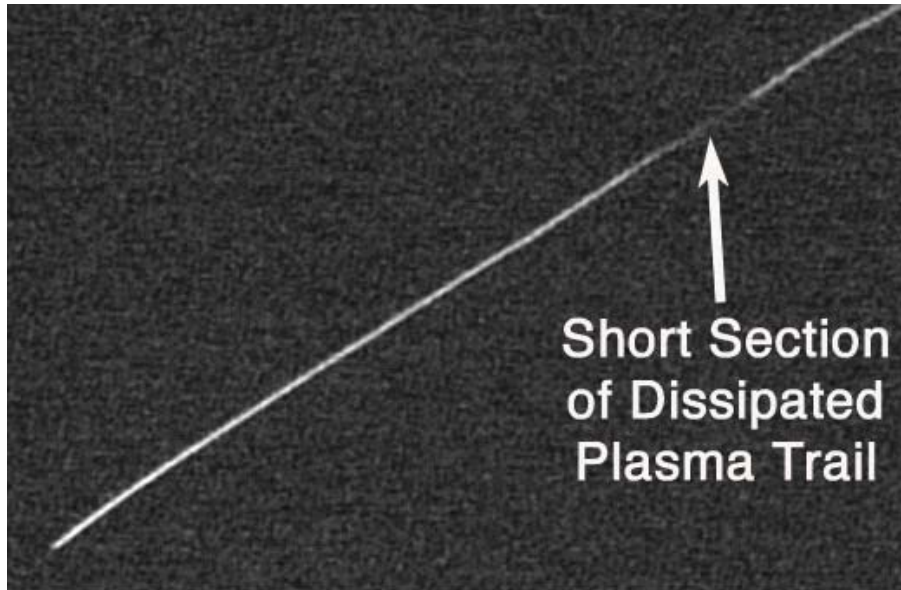


**Figure 6.3.3b** Video image of normal Shuttle re-entry, STS-109. Taken from San Angelo, TX, showing dissipated plasma trail after RCS firing.

Other characteristics of nominal re-entries include the observations that no debris-like events are observed at any time, and no “Flashes” or “Flares” are observed at any time. In fact, no non-uniformities of the plasma trail are observed (other than the RCS quenching effect). Figure 6.3.3c summarizes these differences.

This information is being distributed to aid in the investigation of the Columbia mishap and should only be distributed to personnel who are actively involved in this investigation. 77

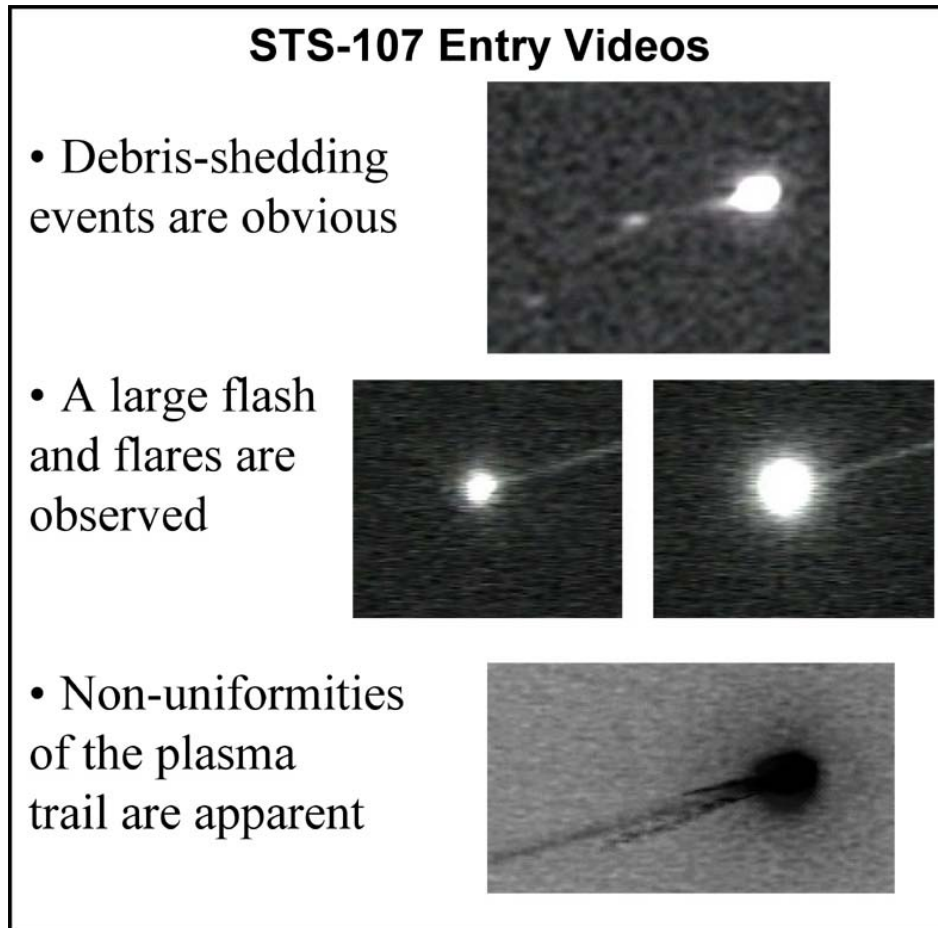


Figure 6.3.3.c Summary of Events not seen in Nominal Re-entry Video

#### 6.3.4 Relative Motion

Debris positions relative to the Orbiter were tracked for 11 different debris events over the western U.S., some in multiple videos (e.g., Debris 6 and 14, shown in Figure 6.3.4a and b respectively). Our tracking data were passed to JSC Flight Dynamics personnel in support of the Early Sightings Assessment Team. These data were used to calculate debris separation times and ballistic coefficients; the results are summarized in Table 6.3.4, which was jointly produced by the Image Analysis Team and Early Sightings Assessment Team. These data are integrated into the OVEWG configuration controlled “Data Review & Timeline”.

All of our current relative motion tracking reports are hosted on the Image Analysis STS-107 Investigation website at [references/shuttleweb/mission\\_support/sts-107/contingency/entry/107\\_entry.html](http://references/shuttleweb/mission_support/sts-107/contingency/entry/107_entry.html). Figures 6.3.4a and b show the position (in feet) of the respective debris objects (6 and 14) relative to the Orbiter. These data were fit to a ballistic model, which relates the ballistic trajectory of the debris to the known ballistic trajectory of the Orbiter. There are two parameters in this fit, the time of separation of

This information is being distributed to aid in the investigation of the Columbia mishap and should only be distributed to personnel who are actively involved in this investigation. 78

the debris, and the ballistic coefficient of the debris (which is directly related to its deceleration). The debris decelerations were then used by the Image Analysis Team's Luminosity Working Group to calculate debris mass. While Figure 6.3.4a shows very good agreement in the relative motion for Debris 6 for the three separate videos analyzed for this event, there was some disagreement for the motion of Debris 14 (Figure 6.3.4b) for the four videos analyzed for this event. Possible explanations for the Debris 14 discrepancy include the following: errors in the in the assumed focal lengths (fields-of-view) for some observers; errors in the precise timing of the videos; significant motion of the debris out of the Orbiter trajectory path causing an unmeasured component of its motion to be missed by observers in Utah. The last explanation is based on the fact that observers from Utah were directly under the Columbia flight path and were looking eastward, so if the debris dropped enough in altitude, it might appear to move away more slowly relative to observations from Flagstaff. Details about the relative motion analyses including determination of the camera fields-of-view are discussed in Section 6.2, Methods.

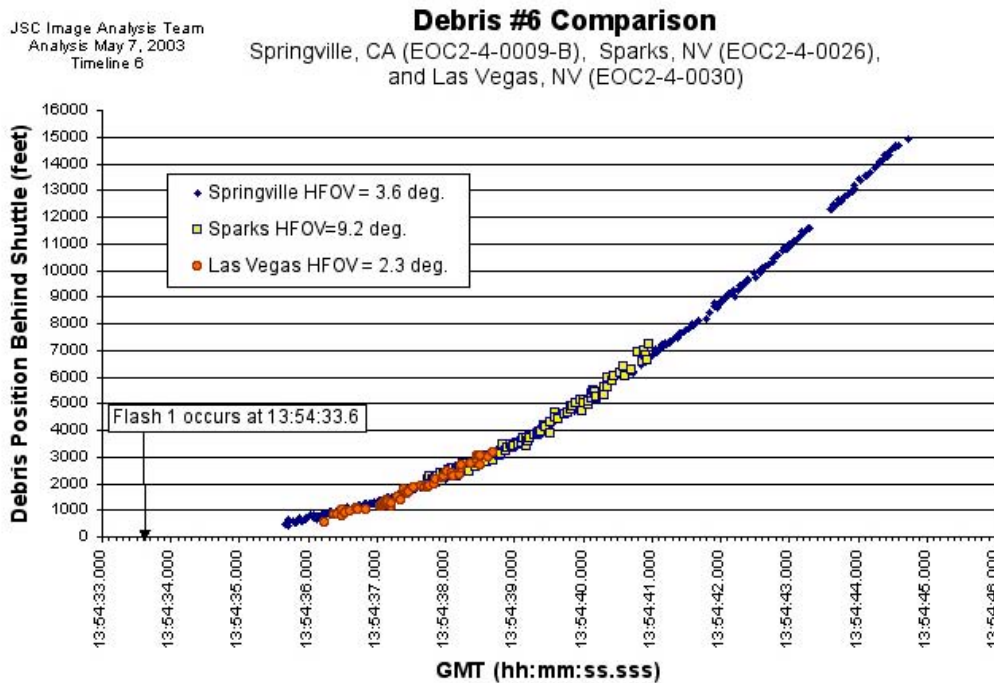


**Figure 6.3.4.a Debris 6 position relative to Orbiter as measured from three videos, identified by their EOC number.**

This information is being distributed to aid in the investigation of the Columbia mishap and should only be distributed to personnel who are actively involved in this investigation. 79

Photo/TV Analysis Team  
May 6, 2003  
Timeline 6

**Comparison of Debris 14 Analyses  
between St. George(2-4-0021, 2-4-0028) Mins (2-4-0005)  
Flagstaff (2-4-0017) and Las Vegas (2-4-0030)**

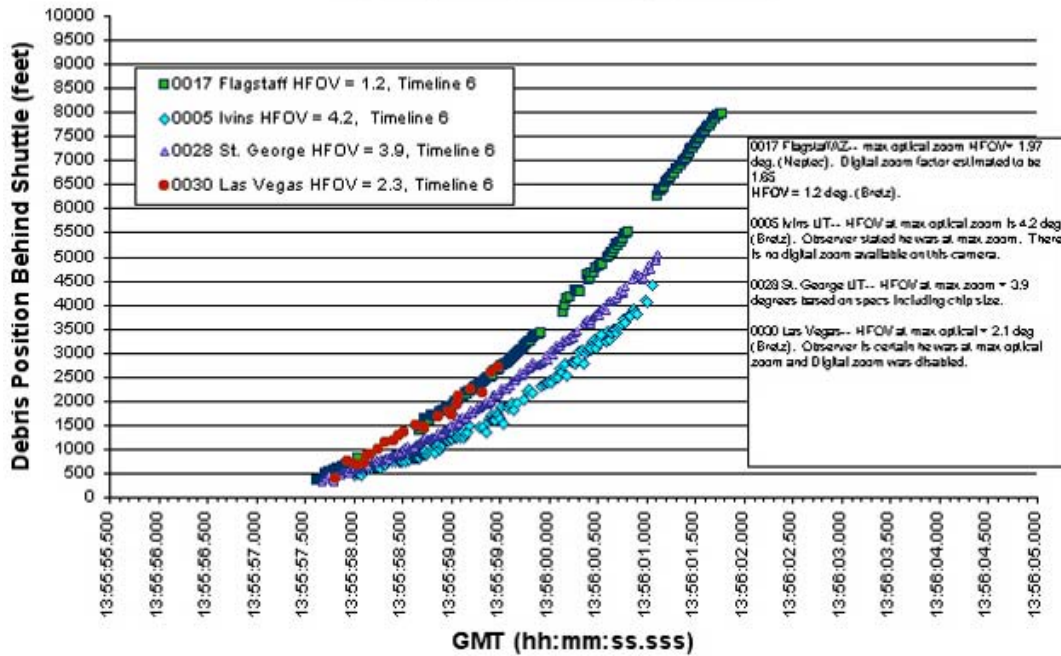


Figure 6.3.4b Debris 14 position relative to Orbiter, measured from four videos, identified by their EOC number.

This information is being distributed to aid in the investigation of the Columbia mishap and should only be distributed to personnel who are actively involved in this investigation. 80

Debris #	Videos Analyzed	JSC DM44 Best Estimate of Separation Time (GMT)	JSC DM44 Ballistic Coefficient with Range (Pounds/square foot)
1	EOC2-4-0056 Lick, Mt. Hamilton, CA EOC2-4-0064 Fairfield, CA	13:53:44.80	1.1 (0.6 – 1.6)
2	EOC2-4-0056 Lick, Mt. Hamilton, CA EOC2-4-0064 Fairfield, CA	13:53:46.50	1.3 (0.7 – 1.9)
3	EOC2-4-0056 Lick, Mt. Hamilton, CA EOC2-4-0026 Sparks, NV	13:53:56.10	0.55 (0.1 – 1.0)
4	EOC2-4-0056 Lick, Mt. Hamilton, CA	13:54:02.90	0.9 (0.3 – 1.5)
5	EOC2-4-0055 Sparks, NV	13:54:08.80	0.01 (0.00 – 0.5)
6	EOC2-4-0026 Sparks, NV EOC2-4-0009-B Springville, CA EOC2-4-0030 Las Vegas, NV	13:54:34.20	3.5 (3.0 – 4.0)
7	EOC2-4-0030 Las Vegas, NV	13:55:04.10	1.1 (0.5 – 1.7)
8	EOC2-4-0030 Las Vegas, NV	13:55:20.80	3.4 (2.6 – 4.0)
13	EOC2-4-0017 Flagstaff, AZ EOC2-4-0005 Ivins, UT	13:55:53.80	0.65 (0.2 – 1.1)
14	EOC2-4-0017 Flagstaff, AZ EOC2-4-0005 Ivins, UT EOC2-4-0021 St. George, UT EOC2-4-0028 St. George, UT EOC2-4-0030 Las Vegas, NV	13:55:56.70	1.7 (1.0 – 2.4)
15	EOC2-4-0017 Flagstaff, AZ	13:56:09.50	1.4 (0.8 – 2.0)
16	EOC2-4-0148 Kirtland AFB	13:57:23.90	0.3 (0.1 – 1.0)

**Table 6.3.4 Calculated separation times and ballistic coefficients for early debris events 1 through 16.**

### 6.3.5 Debris Mass

Relative motion analyses and mass estimates for Debris 6 became a priority early in the investigation. Debris 6 was the largest, western-most significant event, it was recorded on several videos, it was associated with a large Flash (allowing for time synchronization between videos), and one video from Sparks NV contained celestial features that allowed absolute timing. Later, Debris 14 was analyzed as another large and significant western event. The much smaller Debris events 1 and 2 were also analyzed because they represented our earliest visual indication of debris shedding from the Orbiter.

Debris mass estimates were based on relative luminosity measurements of the debris and the Orbiter in the videos and their calculated rates of deceleration. Establishing a method for accurately measuring luminosity values from the videos and determining the luminosity ratios associated with the debris events and Orbiter became one of the most complex tasks for the Image Analysis Team. Luminosity values were validated using two approaches independently developed at JSC and MSFC.

Luminosity ratios for debris events 6, 14, 1, and 2 were measured from the videos. The first application of these ratios was to establish upper and lower limits on the mass estimates for each debris. In order to determine those absolute mass bounds for the

This information is being distributed to aid in the investigation of the Columbia mishap and should only be distributed to personnel who are actively involved in this investigation. 81

debris events, the luminosity ratio was used in different mass estimation methods based on extent of debris ablation. Current calculations use non-ablative approaches to provide the upper and lower bounds for debris mass calculations — the debris light curves indicate that the debris events did not experience total ablation. Those mass estimates, with associated uncertainties range from ~ 0.2-8 lbs for small events such as debris events 1 and 2, up to 20-500 lbs for the largest events (6 and 14).

However, light curves for the Orbiter and debris events (e.g., Figure 6.3.5a and b) indicate that the debris experienced moderate amounts of ablation. This assumption is consistent with observations of ablation on pieces of debris recovered in the East Texas debris field. Hence, the approach modeled on moderately ablating debris provides mass estimates of 87 kg (190 lb) for Debris 6, 55 kg (120 lb) for Debris 14, 0.2 kg (0.44 lb) for Debris 1, and 0.3 kg (0.66 lb) for Debris 2.

The methods, calculations and a fuller description of the assumptions for the mass estimates are provided in Appendix 6.2A. Table 6.3.5 provides our current estimates of debris masses. A complete and updated copy of the “Entry Debris Characterization” table can also be found at [references/shuttleweb/mission\\_support/sts-107/contingency/entry/107\\_entry.html](http://references/shuttleweb/mission_support/sts-107/contingency/entry/107_entry.html).

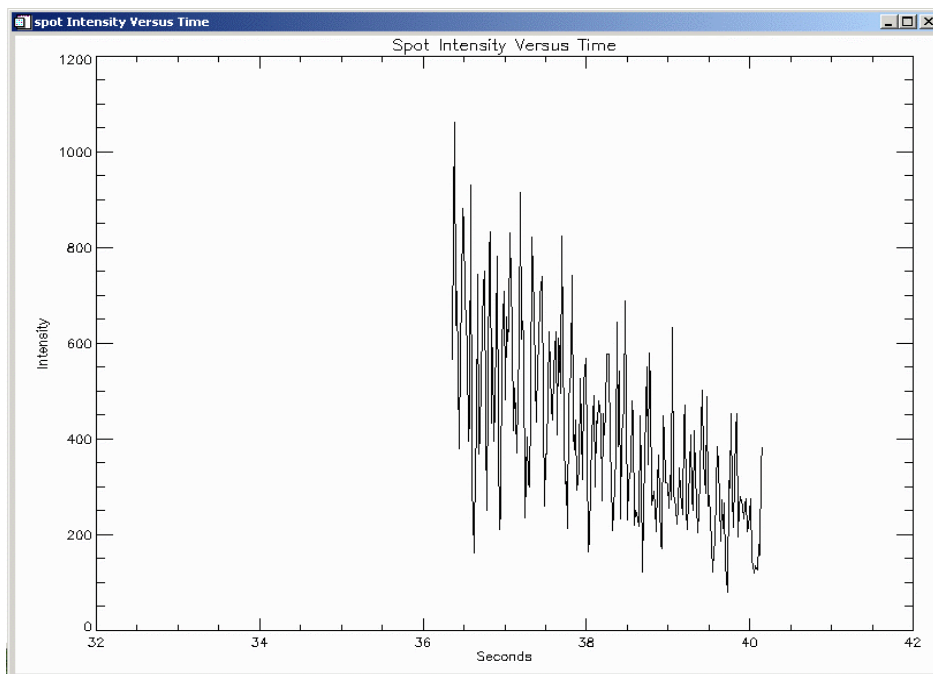


**Figure 6.3.5a Debris 6 intensity versus time (seconds after 13:54:00 UTC). The debris intensity decreased over the measurement interval. The light curve suggests that the debris was ablating by approximately 2% per second.**

This information is being distributed to aid in the investigation of the Columbia mishap and should only be distributed to personnel who are actively involved in this investigation. 82

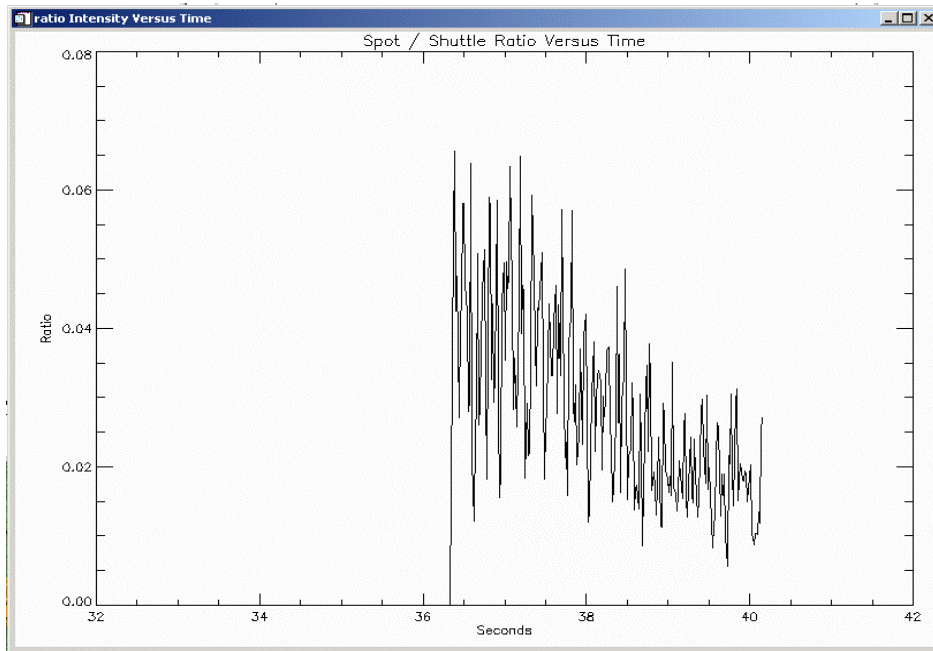


**Figure 6.3.5b Field-by-field Debris 6/Shuttle intensity ratio versus times (seconds after 13:54:00 UTC)**

Debris Event and Observer Location	Intensity Ratio at Time of Separation (Debris/Orbiter)	Upper Bound Non-Ablative Mass Estimate, kg (lb)	Moderate Ablative Mass Estimate		Lower Bound Non-Ablative Mass Estimate*, kg (lb)
			Ablation Rate	Mass kg (lb)	
Debris 6 Springville, CA	0.04 - 0.063	144 – 225 (316 – 495)	2% / sec	86.5 (190)	4.68 – 7.37 (10.3 – 16.2)
Debris 14** St. George, UT	0.135	250 (550)	9% / sec	55 (121)	7.7 (17)
Debris 1 Fairfield, CA	0.0016 – 0.0026	1 – 3 (2 – 7)	27% / sec	0.2 (0.44)	0.057 – 0.092 (0.12 – 0.2)
Debris 2 Fairfield, CA	0.0027	2 - 4 (4 - 8)	27% / sec	0.3 (0.66)	0.11 (0.24)

\*For a flat plate disk falling face front onto the velocity vector.

\*\*Debris Event is lit partially by sunlight.

Mass estimates for debris based upon various models. We consider the moderate ablation method, with ablation rates estimated from light curves, as the best estimate of debris mass.

**Table 6.3.5 Estimated masses for Debris events 6, 14, 1 and 2**

The Orbiter’s attitude at the stage of re-entry in association with the possibility of sizable debris events like Debris 6 and 14 requires further analysis by other teams. If the mass estimates are realistic, they suggest new strategies for interpreting the other data from the last few minutes of Columbia’s re-entry.

This information is being distributed to aid in the investigation of the Columbia mishap and should only be distributed to personnel who are actively involved in this investigation. 83

### 6.3.6 Characterization of the Flash

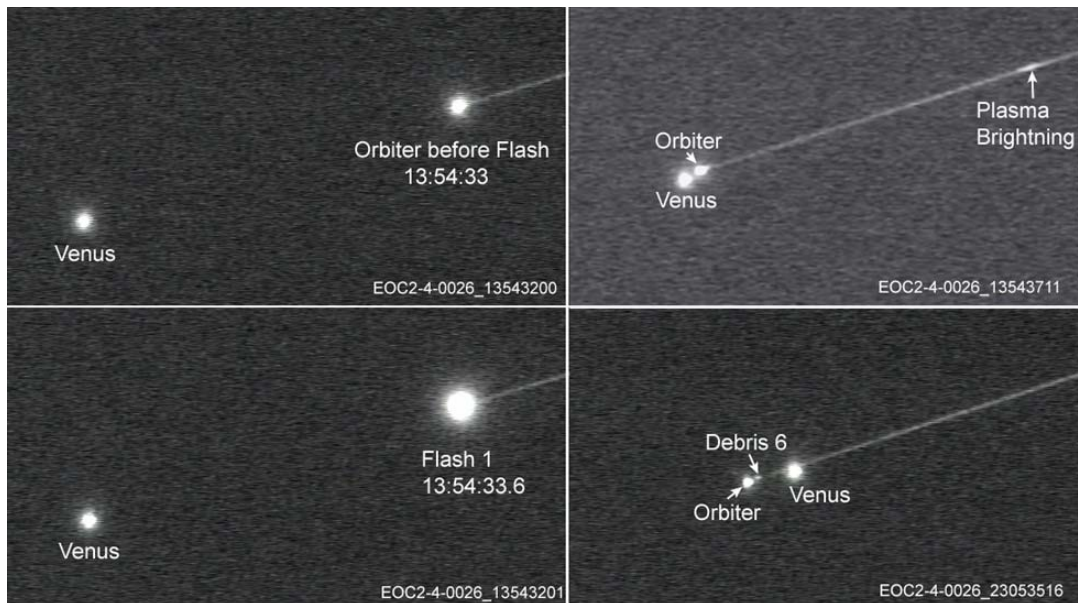


**Figure 6.3.6a** Frame grabs from the Sparks, NV video illustrating the Flash 1 event and the separation of Debris 6 from the luminous envelope of the Orbiter as it crosses Venus

Flash 1 was an intense over-brightening of the luminous envelope of Columbia (see the debris events timeline Table 6.3.2). The event, which lasted .3 sec, consisted of an initial brightening, followed by peak brightening .067 sec later. Immediately following the Flash, a luminous blob in the plasma trail was left in the Orbiter's wake (Figure 6.3.6a). Debris 6 was observed emerging from the plasma envelope 2 seconds after the flash. However, relative motion data calculated from the videos indicate that the Flash 1, which occurred at 13:54:33.6 (+/- .3 sec) UTC, was concurrent with the calculated separation of Debris 6 from the Orbiter at 13:54:33.86. Further, the light curves from the videos show that the Orbiter signature remains brighter than pre-Flash levels until after Debris 6 is observed to separate from the Orbiter's luminous envelope, suggesting an additional light source contributed to the Orbiter's intensity value (Figure 6.3.6b). Although two RCS firings were coincident with the Flash 1 event (R3R and R2R firings were initiated at 13:54:33.537 and 13:54:33.617, respectively), and the duration of the RCS firings and the Flash were roughly the same (.3 sec), our review of comparative nominal re-entry videos allowed us to rule out the possibility that the Flash event was a normal event, such as an RCS firing (see Section 6.3.3).

This information is being distributed to aid in the investigation of the Columbia mishap and should only be distributed to personnel who are actively involved in this investigation. 84



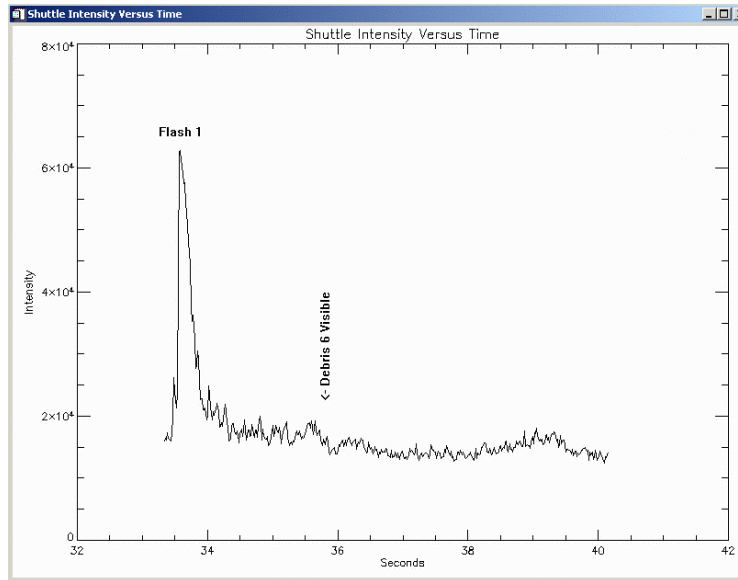


**Figure 6.3.6b Preliminary Orbiter light curve from the Springville, CA video. The Orbiter signature remains bright after the flash, until Debris 6 is observed to separate from the Orbiter.**

Physical interpretations of the relationship between the Flash and Debris 6 are being evaluated, but we believed that Flash 1, and the subsequent shedding of Debris 6 was a major structural event on the Orbiter, and the RCS firings were a response to events on the Orbiter. One model for the Flash optical signature assumes that when Debris 6 separated from the Orbiter it also released a mass of small material (possibly TPS or blanket particulate, each particle less than 2 mm diameter), which decelerated rapidly. The rapid deceleration and large interaction of the particles with the atmosphere would increase the brightness in the chemiluminescent “plasma” trail, causing light to be emitted for a short time and resulting in the Flash.

Although the characteristics of such particles may never be known, if the small objects are assumed to be spheres that ablated as they decelerated, a total predicted mass for the material would be on the order of 40 kg. The methods are described in detail in Appendix 6.2A.

Other explanations consider the possibility that the flash results from atomized droplets of molten aluminum, or other liquids. These ideas will be explored more fully in future work.

This information is being distributed to aid in the investigation of the Columbia mishap and should only be distributed to personnel who are actively involved in this investigation. 85

## **6.4 Other Re-entry Analyses**

### **6.4.1 Star Fire Imagery Analysis**

A unique set of re-entry videos was obtained through telescopes at the Starfire Optical Range, in Albuquerque, New Mexico. Image Analysis Team members participated on the Starfire Analysis Team. The work of that team will be reported separately as the “Starfire Team Final Report”.

### **6.4.2 The Near Earth Asteroid Tracking Program on Mount Palomar**

A California citizen provided a 60-second-exposure telescope image of the Columbia re-entry taken from Mount Palomar. After examining the image, it was determined that the long exposure and low spatial resolution of the image limited its ability to provide information on debris shedding or other re-entry anomalies.

### **6.4.3 Special Still Imagery Analyses of Alleged “Lightning” Image**

A still image taken from California was submitted to NASA by a member of the public. A superficial look at the image suggested that it might record an anomalous re-entry event that was claimed to be lightning striking the Orbiter. Our analysis suggested that the pattern was due to camera vibrations during a long-exposure. A separate upper atmospheric scientific team also investigated the image. The results of those analyses are being reported separately.

### **6.4.4 Tile Number Enhancement**

A tile that was recovered on the ground in Lufkin, TX had numbers that were impossible to read. The Image Analysis Team received a digital photograph taken of the tile. Image enhancements and noise reduction were performed to bring out information on the number that was not readily visible to the eye. Based on this information, the tile could be located to a location on the Orbiter.

### **6.4.5 Special Analysis of Video from The Colony, TX**

A view of the Orbiter in one of the publicly acquired videos caused speculation from within NASA and the general public that video EOC2-4-0012 taken over Texas showed Orbiter detail. The Image Analysis Team conducted a detailed analysis of the imagery and cameras, and analysts at Aerospace were involved as an independent validation. It was concluded that given the spatial resolution of the camera, it would be impossible for the image to show Orbiter detail. The observed pattern was actually an artifact created by a combination of the following factors: the camera was out of focus, the object was too bright for the camera causing pixel saturation and blooming, a diffraction pattern from the triangular shape of the camera aperture produced the observed geometry, and the camera’s internal digital magnification increased the effects. To put all speculation to

This information is being distributed to aid in the investigation of the Columbia mishap and should only be distributed to personnel who are actively involved in this investigation. 86

rest, the effect was also simulated using the same camera model. The full report of this analysis can be obtained at [shuttleweb/mission\\_support/sts-107/contingency/other/Aero.pdf](http://shuttleweb/mission_support/sts-107/contingency/other/Aero.pdf).

#### **6.4.6 Video Sequence Compilation**

At the request of the OVEWG and CAIB, broadcast-quality compilations of the re-entry video sequence were produced to accompany the written timeline of events. They were produced by the Image Analysis Team with support from JSC Public Affairs. NASA public affairs sought permissions from the videographers and the compilation was shown to Congress and in CAIB public hearings. The final version produced, "Photo/TV Analysis Team – Entry Debris Events Version 7" master is archived by the Imagery Services Branch (Video), Information Systems Directorate.

#### **6.4.7 Videos Showing Columbia's Break-up Over Texas**

As of the date of this report, support for additional analyses of videos showing Columbia's break-up over Texas has been requested. These analyses will not be included in this report.

This information is being distributed to aid in the investigation of the Columbia mishap and should only be distributed to personnel who are actively involved in this investigation. 87

## 7.0 Lessons Learned and Recommendations

The investigation following the STS-107 accident demonstrated the importance of imagery to observe, document, and analyze key elements of a Shuttle mission and off-nominal events. The investigation also demonstrated that existing imagery resources are inadequate in every phase of flight - launch, orbit, and entry. In the wake of this investigation, the Image Analysis Team recommends upgrades and improvements to the imaging capabilities for all phases of Shuttle flights and the analytical capabilities to interpret that imagery. The recommendations address lessons learned specifically from STS-107 and from the limitations of the Shuttle imaging capabilities that have been encountered over the course of the Shuttle Program.

After the Shuttle Challenger accident in 1986, the Shuttle Program implemented significant improvements to the Shuttle imaging and image analysis capabilities, including greatly expanded camera coverage for launches and the establishment of imagery review and analysis facilities at the NASA centers. Since the post-Challenger return to flight, the Shuttle imagery capabilities have weakened considerably. For example, camera coverage for launch and landing has been significantly reduced and camera systems are outdated or in need of upgrades. In the post-Columbia era, a continuous improvement in imaging capabilities is needed to fully support Shuttle missions with imagery analysis and to avoid a repeat of post-Challenger decay of Shuttle imaging capabilities.

This report contains recommendations for the launch and entry phases of flight. For the orbit phase, the Shuttle Program has begun to establish the capability for comprehensive on-orbit imagery inspection of the Orbiter. At the time of this writing, the Image Analysis Team is engaged in the definition of the on-orbit capability, which is beyond the scope of this document.

### 7.1 Launch Imagery - Ground

Both during the STS-107 mission and post-accident, the image analyses of the debris-impact event during ascent were severely hindered by limitations of the launch imagery. The need for the most sophisticated and detailed analyses underscored other limitations of the launch imagery. Key limitations included insufficient spatial and temporal resolution of the imagery, indeterminate variations in the timing data for the film and video, and late access to reproductions of the best quality imagery. Recommendations are given below for improvements to the launch camera hardware, coverage, and imagery reproduction and distribution.

#### Launch Camera Upgrades

- Increase the frame rates of all 35 mm film trackers to at least 100 frames per second. The current frame rates for the tracking cameras provide inadequate temporal resolution for analyzing high-speed, transient events during ascent, such as debris shedding.

This information is being distributed to aid in the investigation of the Columbia mishap and should only be distributed to personnel who are actively involved in this investigation. 88

- Replace all video cameras with HDTV or high-speed digital cameras. The current NTSC-format video cameras provide insufficient spatial and temporal resolution for detailed analysis.
- Increase the focal lengths for selected long-range tracking cameras. Current focal lengths for some tracking cameras provide inadequate spatial resolution for assessing vehicle details during ascent.
- Upgrade the timing data on all tracking film cameras to digital timing. Current IRIG timing must be manually decoded. This can introduce error and is a slow process.
- Time-sync selected launch cameras. Currently, the launch cameras are not synchronized, resulting in indeterminate timing offsets from one camera to another, hampering image analyses that employ multi-camera solutions.
- Improve launch pad lighting for night launches. Currently, prior to SRB ignition on night launches, critical areas of the launch vehicle are in darkness resulting in severely underexposed imagery of those areas.
- Implement auto-tracking on selected long-range tracking cameras. The current manual tracking for some cameras is often inadequate, causing loss of image coverage.
- Modernize the Operational TV system. The cameras are old, and some are black and white. Higher resolution technology is available.
- Evaluate new camera locations east of the launch site (via aircraft/ships). Currently, camera coverage east of the launch site is unavailable and it would provide additional data for triangulation and new views of the vehicle.
- Evaluate reinstating cameras deleted in the FY95 Program Requirements Definition scrub. The numbers of launch-site cameras were greatly decreased in this cost-savings scrub, which adversely reduced the launch imagery coverage.

#### Camera Maintenance

- Revise camera maintenance protocols to ensure consistent focus and exposure. Currently, out-of-focus imagery for the launch cameras is a common problem. Technologies for improved image focus should be investigated.
- Establish routine optical calibrations for all tracking camera systems. Currently, the camera systems are uncalibrated for removing distortions in the optics, hindering detailed image analyses.

This information is being distributed to aid in the investigation of the Columbia mishap and should only be distributed to personnel who are actively involved in this investigation. 89

- Establish protocols for routine camera inspections to detect and repair optical problems. The loss of critical launch imagery due to camera optics problems, such as with E-208 during STS-107, is unacceptable.

#### Data Handling and Distribution

- Provide consistent, stabilized timing on the launch + 5 hours video tracking camera replays. Currently, the timing data for these replays are often missing or inaccurate.
- Improve the timeliness for distributing the launch +5 hours video tracking camera replays. On STS-107, the replays were not received outside of KSC until the day after the launch.
- Replace analog video recorders with digital recording for the video data. The current analog recording results in loss of data, degrading the image resolution and timing accuracy.
- Improve the timeliness for distributing the highest quality imagery for analysis. On STS-107, a great deal of time was spent analyzing and re-analyzing imagery each time a better copy of the imagery (i.e., closer to the original) was obtained. The processes for acquiring the best quality imagery, developed on STS-107 and documented in this report, should be implemented on a routine basis.

#### Other Recommendations

- Provide more complete, higher resolution closeout photography of the entire vehicle prior to launch. The current coverage and quality of the pre-mission closeout imagery is often inadequate for detailed comparison with on-orbit imagery of the vehicle.
- Add requirements that specify a minimum, critical subset of launch camera systems that must be operational prior to launch. Currently, the minimum imagery capability required to support launch is undefined.

### **7.2 Launch Imagery - Onboard**

The primary imagery for post-launch evaluation of the ET is acquired onboard by the umbilical well film cameras and by the crews (video and photography) after ET separation. The STS-107 ET video imagery was downlinked by the crew early in the mission, but the umbilical well images and crew photography of the ET were unrecovered after the accident. This resulted in the loss of critical data for the accident investigation to assess the condition of the ET foam insulation. The recommendations below are made to improve the onboard imaging capabilities for assessments of the conditions of the ET and Orbiter during ascent.

This information is being distributed to aid in the investigation of the Columbia mishap and should only be distributed to personnel who are actively involved in this investigation. 90

- Provide at least one digital video, digital still, or digital motion camera in an Orbiter umbilical well, with downlink capability for the umbilical well imagery early in the mission. Currently, the umbilical well imagery is all film, which is unavailable for screening and analysis until processed post-landing.
- Provide crew-handheld, high-resolution digital video and still cameras for ET imaging. Institute a crew procedure to expedite downlink of the imagery early in the mission. Currently, the crew film photography of the ET is unavailable for analysis until post-landing. Video cameras with higher resolution than those currently flown are available.
- Install digital, down-linkable video cameras on the SRBs and the ET to provide views of critical areas of the Orbiter and ET during ascent on every mission. Onboard imaging assets are currently not employed. These onboard assets are needed to improve overall imagery coverage during ascent and to extend coverage beyond the range of the launch-site cameras.

### 7.3 Entry Imagery

Analyses of the Columbia debris-shedding events during STS-107 re-entry were severely hindered by the poor quality of the imagery available for analysis. Analyses were also hindered by the general lack of information on the optical signatures, visual and spectral, of nominal Shuttle re-entries for comparison with the anomalies observed in the STS-107 re-entry imagery. As a result of the STS-107 experience, the Image Analysis Team recommends that the Shuttle Program develop the capability to image Shuttle re-entries with scientific instrumentation. Analysis techniques, such as those reported in Section 6 of this document, also need further development to provide a better understanding of the visual characteristics of Shuttle re-entries and the physical nature of the optical radiation. Specific recommendations are given below for the systematic acquisition of imagery for future Shuttle re-entries and imagery analysis. Also, recommendations are provided for improved imagery coverage for the primary landing sites.

#### Re-Entry Imagery Acquisition

- Deploy ground-based scientific instrumentation near ground-track locations for imaging Shuttle re-entries. This instrumentation should be selected to have the spatial resolution, spectral response, and timing accuracy needed for identification and analyses of off-nominal events. Make use of outside agency resources for observations when applicable. It is unacceptable to rely solely on the general public with consumer grade equipment to provide critical imagery of Shuttle re-entries, as was the case for STS-107.
- Investigate the use of airborne observations of Shuttle re-entries. Aircraft equipped with imaging sensors operating above the cloud level have successfully imaged spacecraft re-entries, and would provide valuable data for understanding the optical signatures of Shuttle re-entry.

This information is being distributed to aid in the investigation of the Columbia mishap and should only be distributed to personnel who are actively involved in this investigation. 91

- Investigate the use of re-entry imagery acquired from the crew cabin through the Shuttle windows. In-situ observations of the Orbiter's plasma environment would provide a valuable perspective for comparison with ground- or airborne-based imagery of re-entry.

#### Re-Entry Analysis

- Research the nature of the optical radiation generated during Shuttle re-entries. The Shuttle's optical signature via interaction with the upper atmosphere has not been researched in detail, which is necessary to detect and characterize off-nominal conditions. The research initiated by the STS-107 investigation, reported in Section 6 of this document, should continue and be expanded to develop imaging techniques for assessing Orbiter health during entry.
- Conduct spectral analysis from the arcjet testing of Orbiter materials and compare with imagery from Shuttle re-entries. In addition to the basic research noted above, the arcjet laboratory studies address the fundamental lack of knowledge of the optical characteristics of Shuttle re-entry.
- Adopt the video reproduction methods developed during the STS-107 investigation as the protocol for video imagery duplication. Image Analysis Team re-entry analyses were compromised early in the investigation by not having access to the highest quality imagery for analysis.

#### Landing Site Imagery

- Evaluate reinstating landing-site cameras deleted in the FY95 Program Requirements Definition scrub, in particular, for Dryden and White Sands. For trans-Atlantic landing sites, provide a minimum set of video tracking and landing cameras. The numbers of landing-site cameras were greatly decreased in this cost-savings scrub, which adversely reduced the imagery coverage for landing.

### **7.4 Analysis Resources and Protocols**

The Image Analysis Team recommends continuous upgrades to existing image analysis facilities to handle the anticipated larger volume of mission imagery and associated analyses, such as from on-orbit inspections, and to facilitate the steady improvements in the state-of-the-art analysis hardware and software. Of greatest importance is the capability to quickly ingest, manipulate, duplicate, and distribute best digital formats of all imagery. Upgrades for server systems to accommodate the new imagery and database requirements, software for data analysis, and display and reproduction to facilitate communications are important components of the analysis facilities. Together, these upgrades will enhance the quality of imagery analysis products and reduce the turn-around time for delivery. Other recommendations include the following:

This information is being distributed to aid in the investigation of the Columbia mishap and should only be distributed to personnel who are actively involved in this investigation. 92



- Utilize the NASA Intercenter Photographic and Television Analysis Contingency Action Plan (NSTS 08218). The Program decision to not implement NSTS 08218 following the accident led to duplication of work, confusion on tasks to be performed, and miscommunication within the image analysis community and with external organizations. Ultimately, the Team reported to Orbiter Vehicle Engineering Working Group, however, NSTS 08218 specified direct reporting to Space Shuttle Program management.
- Maintain a pool of contingency image analysts. The STS-107 investigation demonstrated the need to maintain a complement of imagery specialists that can be quickly matrixed to support a large number of unplanned image analysis tasks. For example, the JSC Earth Observations image specialists were immediately assimilated into the STS-107 Image Analysis Team, and were crucial to the quick response to the many varied image analyses.
- Establish and maintain a state-of-the-art imagery analysis database for Shuttle engineering performance assessments, anomaly and contingency support, quick reference, and comparisons across missions. The need for this type of database was clearly demonstrated throughout the STS-107 investigation, a massive undertaking for analyses of imagery from all phases of the mission with cross-references to previous missions. The database, once developed, would be an invaluable and long overdue resource for cataloging and archiving imagery and supporting data for observed events, nominal and anomalous, for all phases of flight.

This information is being distributed to aid in the investigation of the Columbia mishap and should only be distributed to personnel who are actively involved in this investigation. 93

## 8.0 STS-107 Investigation Image Analysis Team

This section provides an overview of the structure and personnel of the STS-107 Image Analysis Team. The launch and entry analyses were highly disparate in terms of the imagery to work with and analysis processes and objectives. Therefore the Image Analysis Team was broadly partitioned into two major sub-teams, launch and entry, each with a unique set of expertise for the analysis tasks at hand. Groups from multiple NASA centers and organizations outside of NASA contributed to the Team effort; a short description of their roles is provided in Section 8.1. Individual contributors are listed in Section 8.2, with biographies of key contributors provided in Section 8.3.

### 8.1 Image Analysis Sub-teams

#### Launch and On-orbit Analysis Sub-team

- **JSC-SX – Image Science and Analysis Group** – Performed full characterization of the launch debris event including a complete frame-by-frame description of the debris shedding, calculation of debris size, trajectory, impact velocity, impact angle, and impact location on the Orbiter’s left wing. In addition, JSC-SX, compiled and evaluated the debris characterization results obtained by the other Image Analysis team members. JSC-SX also performed a thorough review of all on-orbit imagery of the Orbiter’s left wing and debris seen in downlinked imagery.
- **JSC-ES – Structural Engineering Division** – Performed trajectory, impact velocity, impact angle, and impact location for the launch debris event.
- **JSC-EG – Aeroscience and Flight Mechanics Division** – Supplied key reference data such as the Shuttle CAD models and performed trajectory, impact velocity, impact angle, and impact location for launch debris event.
- **MSFC – Engineering Photographic Analysis Team** – Provided image analysis of the primary STS-107 launch events with an emphasis on the debris event. A complete frame-by-frame description of the debris shedding event as well as analyses for the debris size, trajectory, impact velocity, impact angle, and impact location were performed.
- **KSC – Ice/Debris and Image Analysis Team** – Performed a detailed re-screening of all STS-107 launch video and film cameras. Also provided analysis of the debris seen at 82 seconds MET. A complete frame-by-frame description of the debris shedding event as well as analyses for the debris size, trajectory, impact velocity, impact angle, and impact location were performed.
- **LaRC – NASA Langley Research Center** performed image enhancements on the launch video and film.
- **National Imagery and Mapping Agency (NIMA)** – At the request of NASA, NIMA provided specific analyses of the debris seen at 82 seconds MET. NIMA analyses focused primarily on the debris velocity, rotation rate, and whether any debris was detected coming over the top of the wing after the main debris impact.
- **Lockheed Martin Management and Data Systems (LM–M&DS) and Advanced Technology Center** – At the request of NASA, industry experts in

This information is being distributed to aid in the investigation of the Columbia mishap and should only be distributed to personnel who are actively involved in this investigation. 94

image analysis were brought in to help with the investigation. Lockheed Martin analyses for the STS-107 investigation focused on image deblurring and sharpening as well as determining the 82 second MET debris size, velocity and trajectory.

#### Entry Analysis Sub-team

- **JSC-SX – Human Exploration Science Office** – Three groups from within SX collaborated to support the re-entry image analysis. The Image Science and Analysis Group, the Earth Observations group, and the Orbital Debris group all worked together to coordinate and perform all phases of the re-entry analysis, including the imagery screening, cataloging and timelining, debris relative motion analyses and debris luminosity characterization and mass estimates.
- **JSC-DM – Flight Design and Dynamics Branch, Mission Operations Directorate** – Members from JSC-DM performed relative motion analyses in conjunction with JSC-SX in order to derive ballistic coefficients, and reviewed re-entry videos as part of the timelining team.
- **MSFC Space Environments Team** – Contributed to the Luminosity Working Group analysis. They applied their techniques for analyzing videos of meteorites to the STS-107 re-entry videos to facilitate the calculation of mass estimates for the re-entry debris events.
- **KSC Applied Physics Lab** – Participated in the Luminosity Working Group to help define the physics equations for interpreting the light curves of the debris events and calculate mass estimates for events.
- **AMES Reacting Flow Environments Lab** – Participated in the Luminosity Working Group to coordinate the arcjet testing to determine whether the debris spectral signatures could be interpreted, and helped to frame the lower bound conditions for a non-ablating object.
- **Neptec** – Characterized key optical properties of the cameras used by the public to capture imagery of the entry that was later used for analysis. This effort was made possible by a team effort that consisted of a group of 2 engineers, 1 physicist and 1 technologist. The team gained its experience in the characterization of optical systems through the operational support of their Space Vision System and Laser Camera System.

## **8.2 Individual Team Contributors (Biographies for key contributors are given in Section 8.3)**

### Image Analysis Team Contributors - Launch and Orbit Analyses

Greg Byrne/JSC/SX  
Mike Snyder/JSC/Lockheed Martin/SX  
Jon Disler/JSC/Lockheed Martin/SX  
Cynthia Evans/JSC/Lockheed Martin/SX  
David Bretz/JSC/Hernandez/SX  
Fred Martin/JSC/EG

This information is being distributed to aid in the investigation of the Columbia mishap and should only be distributed to personnel who are actively involved in this investigation. 95

Joe Gessler/JSC/ES  
Robert Page/KSC  
Armando Oliu/KSC  
Robbie Robinson/KSC/Johnson Controls  
Tom Rieckhoff/MSFC  
Michael O'Farrell/MSFC  
Ivar Svendson/NIMA  
Jim Salacain/NIMA/Spatial Analytics  
Dwight Divine/Lockheed Martin Management & Data Systems  
Eamon Barrett/Lockheed Martin Management & Data Systems  
Marv Klein/Lockheed Martin Management & Data Systems  
Lorelei Lohrli-Kirk/Boeing  
Travis Bailey/JSC/Lockheed Martin/EA  
Joe Caruana/JSC/Lockheed Martin/SX  
Ken Castleman/ADIR/SX  
Fred Clark/JSC/Lockheed Martin/EA  
Chris Cloudt/JSC/Hernandez/SX  
Michael Cohen/Lockheed Martin Management & Data Systems  
Richard Coles/JSC/Lockheed Martin/EV  
Dean Coleman/JSC/Lockheed Martin/EA  
Kevin Crosby/JSC/Lockheed Martin/SX  
Don Curry/JSC/ES  
Horacio de la Fuente/JSC/ES  
Jim Dragg/JSC/LZ Tech/SX  
Curt Erck/JSC/Lockheed Martin/EA  
Mansour Falou/JSC/Lockheed Martin/EA  
Steve Frick/JSC/CB  
Jeff Froemming/JSC/Lockheed Martin/EA  
Ray Gomez/JSC/EG  
Susan Gomez/JSC/ES  
Brad Henry/JSC/Lockheed Martin/EA  
James Heydorn/JSC/Lockheed Martin/SX  
William Kleinfelder/KSC  
John Lane/KSC/ASRC Aerospace  
Brad Lawrence/KSC/USA  
Brett McRay/JSC/Lockheed Martin/SX  
Erica Miles/JSC/Lockheed Martin/SX  
Teresa Morris/JSC/Lockheed Martin/SX  
Eric Nielsen/JSC/Hernandez/SX  
Carlos Ortiz/Boeing  
Ed Oshel/JSC/Hernandez/SX  
Philip Peterson/Boeing  
Michelle Phlegley/KSC/USA  
Mark Pritt/Lockheed Martin Management & Data Systems  
Jerry Posey/JSC/Lockheed Martin/EA  
Brian Rochon/JSC/Lockheed Martin/EA

This information is being distributed to aid in the investigation of the Columbia mishap and should only be distributed to personnel who are actively involved in this investigation. 96

Rob Scharf/JSC/Lockheed Martin/SX  
Leslie Upchurch/JSC/Lockheed Martin/SX  
Benjamin Quasius/JSC/ES  
Rich Ulrich/JSC/Lockheed Martin/EA  
Glenn Woodell/LaRC  
Tom Scully/Lockheed Martin Management & Data Systems  
David A. Bennett/Lockheed Martin Advanced Technology Center  
Dr. Don Flagg/Lockheed Martin Advanced Technology Center  
Constantine Orogo/Lockheed Martin Advanced Technology Center  
Paul Payton/Lockheed Martin Advanced Technology Center  
Dr. Bob Remington/Lockheed Martin Advanced Technology Center  
Dr. Gary Mastin/Lockheed Martin Management & Data Systems  
Sean Hatch/Lockheed Martin Management & Data Systems  
Doug Rohr/Lockheed Martin Management & Data Systems  
Dave Goodwin/Lockheed Martin Management & Data Systems  
Dr. Bryan Stossel/Lockheed Martin Management & Data Systems  
Dr. David Tyler/Lockheed Martin Management & Data Systems  
Rod Pickens/Lockheed Martin Management & Data Systems  
Dr. Randy Thompson/Lockheed Martin Management & Data Systems

Image Analysis Team Contributors – Entry Analyses

Greg Byrne/JSC/SX  
Cynthia Evans/JSC/Lockheed Martin/SX  
David Bretz/JSC/Hernandez/SX  
Donn Liddle/JSC/Lockheed Martin/SX  
Julie Robinson/JSC/Lockheed Martin/SX  
Kandy Jarvis/JSC/Lockheed Martin/SX  
Kira Jorgensen/JSC/SX  
Nicole Stott/JSC/CB  
Doug Holland/JSC/EV  
Bob Youngquist/KSC Applied Physics Lab  
Phil Metzger/KSC Applied Physics Lab  
George Raiche/ARC Reacting Flow Environments  
Bill Cooke/MSFC Space Environments Team  
Rob Suggs/MSFC Space Environments Team  
Wes Swift/MSFC Space Environments Team  
Jeff Anderson/MSFC Space Environments Team  
Heather Lewis/MSFC Space Environments Team  
Kevin Crosby/JSC/Lockheed Martin/SX  
James Heydorn/JSC/Lockheed Martin/SX  
Amanda Johnson/JSC/Lockheed Martin/SX  
Brett McRay/JSC/Lockheed Martin/SX  
Teresa Morris/JSC/Lockheed Martin/SX  
Eric Nielsen/JSC/Hernandez/SX  
Ed Oshel/JSC/Hernandez/SX

This information is being distributed to aid in the investigation of the Columbia mishap and should only be distributed to personnel who are actively involved in this investigation. 97

Rob Scharf/JSC/Lockheed Martin/SX  
Mike Snyder/JSC/Lockheed Martin/SX  
Alan Spraggins/JSC/Hernandez/SX  
Leslie Upchurch/JSC/Lockheed Martin/SX  
Justin Wilkinson/JSC/Lockheed Martin/SX  
Kim Willis/JSC/Lockheed Martin/SX  
Glynda Robbins/Lockheed Martin/  
Prem Saganti/JSC/Lockheed Martin/SX  
Tracy Thumm/JSC/Lockheed Martin/SX  
Mark Matney/JSC/Lockheed Martin/SX  
Barbara Nowakowski/LZ Tech/JSC/SX  
Jim Dragg/JSC/LZ Tech/SX  
Steve Frick/JSC/CB  
John Gowan/JSC/DM4  
Mark Abadie/JSC/DM4  
Ryan Proud/JSC/DM4  
Chris Edelen/JSC/DM4  
Dennis Bentley/JSC/DM4  
Tom Schmidt/JSC/DM4  
Ron Spencer/JSC/DM4  
Jenney Gruber/JSC/DM3  
Jeff Kling/JSC/DF5  
Kevin McCluney/JSC/DF5  
Ken Smith/JSC/DF5  
Dana Jake/JSC/DF5  
Ovideo Oliveras/JSC/Lockheed Martin/ER  
Chris Bennett/Neptec  
Jean-Sebastien Valois/Neptec  
Doug Aikman/Neptec  
Adam DesLauriers/Neptec  
Dewey Houck/Boeing/Autometrics

### 8.3 Selected Biographies for Key Contributors

#### Johnson Space Center

**Dr. Gregory Byrne** served as the NASA lead of the Image Analysis Team for the STS-107 investigation. He is currently the Assistant Manager of the Space and Life Sciences Directorate (SLSD) Human Exploration Science Office and manager of the Earth and Image Sciences Laboratory within that office. He has 12 years of NASA experience, beginning in the Mission Operations Directorate at JSC, where he was certified as a Space Shuttle flight instructor of astronaut crews. He joined the SLSD in 1996 as a senior scientist in the Earth and Image Sciences. He earned a B.S. in Physics from Syracuse University and a Ph.D. in Space Physics and Astronomy from Rice University in 1985. His doctoral work at Rice centered on atmospheric processes. He joined the Space Physics group at the University of Houston (U of H) in 1986 as a Research

This information is being distributed to aid in the investigation of the Columbia mishap and should only be distributed to personnel who are actively involved in this investigation. 98

Associate and then as an Assistant Professor researching the upper atmosphere. He continues his affiliation with U of H as an adjunct assistant professor.

**Dr. Cynthia Evans** served as co-lead of the Image Analysis Team for the STS-107 investigation. Her current position is Manager and Research Scientist for Lockheed Martin Space Operations' Image Analysis Section at the NASA Johnson Space Center. Evans has more than 20 years professional experience in the Earth sciences and remote sensing. Her tenure at the NASA Johnson Space Center includes direct planning and operational Earth observations support to more than 100 Shuttle, Mir and ISS missions. She received her Ph.D. in Earth Sciences from Scripps Institute of Oceanography, U.C. San Diego, and a B.S. in Geology from University of Rochester. Before coming to NASA, Evans was an Assistant Professor in the Colgate University Geology Department, and a Visiting Professor at Columbia University's Lamont-Doherty Earth Observatory.

**Michael Snyder** was team lead for the launch imagery analyses for the STS-107 Image Analysis Team. He is a Staff Research Scientist with Lockheed Martin Space Operations. Mr. Snyder has over 19 years of professional experience in the fields of image analysis and remote sensing. He is the Lockheed Martin project manager for the Image Science and Analysis group; a position he has held for the past 3 years. Mike holds an M.S. degree in Geography from the University of Illinois and a B.S. degree in Geography from the University of Texas at Austin.

**Jon Disler** is JSC's liaison with the Intercenter Photo Working Group. He is a Staff Research Scientist with Lockheed Martin Space Operations. Mr. Disler has more than 34 years experience in remote sensing and image analysis. He has supported remote sensing and imagery analysis for NASA in the LACIE/Agristars and STS Earth Observations, and JSC's Shuttle image science group since 1986. He leads JSC's STS launch and landing image analysis effort. He received his B.S. in Biology from Roanoke College.

**Donn Liddle**, Senior Research Engineer, Lockheed Martin Space Operations. For the STS-107 investigation, he was the Team lead for the re-entry video timelining, and the Image Analysis lead for imagery and photogrammetry recommendations for return-to-flight activities. Mr. Liddle is a photogrammetric engineer with more than 10 years professional experience in photogrammetry and digital image analysis. Mr. Liddle received his B.S. and M.S. in Survey and Photogrammetric Engineering, and has completed post-graduate work in Digital Photogrammetry. Since joining Lockheed Martin in 1997 he has designed and implemented photogrammetry analyses for several STS, ISS and HST surveys.

**Dr. Julie Robinson**, was the re-entry timelining co-lead and instrumental in facilitating analyses of re-entry imagery of the Columbia accident. She is a Senior Scientist for Lockheed Martin Space Operations, NASA Johnson Space Center. Dr. Robinson received her Ph.D. in Ecology, Evolution, and Conservation Biology, University of Nevada, Reno; a B.S. in Biology and a B.S. in Chemistry, Utah State University, Logan, Utah. She is part of an interdisciplinary team of scientists that work on remote sensing of Earth from human spaceflights, including astronaut training, data distribution, and

This information is being distributed to aid in the investigation of the Columbia mishap and should only be distributed to personnel who are actively involved in this investigation. 99

research collaborations. She is the Project Lead for using Landsat-7 data to develop global maps of coral reef areas for distribution in the third world, participates in scientific collaborations involving coral reef remote sensing in French Polynesia, and classification of coastal land use in Thailand. She also managed the implementation of Web-based database searching, browsing, and distribution of the nearly 400,000 photographs taken by astronauts.

**Dr. Kira Jorgensen** was the co-lead for the STS-107 Luminosity Working Group. She aided in the development and then processing of the JSC method for determining the ratio of intensities used to obtain an estimate of mass for the debris events. In addition, she will assist in the analysis of the spectral characteristics of the re-entry, if future testing warrants the procedure. Dr. Jorgensen currently holds a post-doctorate position through the National Research Council (NRC) in the Orbital Debris Program Office (SX2) at Johnson Space Center. Her main area of research uses remote reflectance spectra to obtain physical properties of orbiting objects, specifically orbital debris. She works closely with scientists at the Air Force Maui Optical and Supercomputing (AMOS) site where most of the observations for the project are taken. In addition to her spectral project, she assists the orbital debris group in obtaining and reducing optical observations of the LEO and GEO debris environment.

**Nicole Stott**, NASA Astronaut (Mission Specialist). Ms. Stott was team lead for the Image Analysis Team's Luminosity Working Group, and provided interfaces with several other STS-107 investigation teams. She received her M.S. in Engineering Management, University of Central Florida, and a B.S. in Aeronautical Engineering, Embry-Riddle Aeronautical University. Ms. Stott began her career as a structural design engineer with Pratt and Whitney Government Engines, then worked with the Advanced Engines Group performing structural analyses of advanced jet engine component designs. She joined NASA in 1988 at the Kennedy Space Center (KSC), Florida as an Operations Engineer in the Orbiter Processing Facility (OPF). She worked with the Director of Shuttle Processing as part of a two-person team tasked with assessing the overall efficiency of Shuttle processing flows, identifying and implementing process improvements, and implementing tools for measuring the effectiveness of improvements. She was the NASA KSC Lead for a joint Ames/KSC software project to develop intelligent scheduling tools. During her time at KSC, Ms. Stott also held a variety of positions within NASA Shuttle Processing, including Vehicle Operations Engineer; NASA Convoy Commander; Shuttle Flow Director for Endeavour; and Orbiter Project Engineer for Columbia. During her last two years at KSC, she was a member of the Space Station Hardware Integration Office where she served as the NASA Project Lead for the ISS truss elements under construction at the Boeing Space Station facility. In 1998, she joined the Johnson Space Center (JSC) team as a member of the NASA Aircraft Operations Division., where she served as a Flight Simulation Engineer (FSE) on the Shuttle Training Aircraft (STA) before joining the Astronaut Office.

**S. Douglas Holland** (MSEE, BSEE), NASA / EV2. Currently detailed to NASA / SX as member of the Luminosity Working Group (LWG). Prior to joining the LWG served 16 years at NASA / JSC as Project Engineer for the following systems: a) Shuttle Digital

This information is being distributed to aid in the investigation of the Columbia mishap and should only be distributed to personnel who are actively involved in this investigation. 100



Television (DTV), b) Shuttle Sequential Still Video (SSV), c) Shuttle High Definition Television (HDTV) DTO, d) X-38 Imaging Systems, e) Shuttle and Station M-JPEG Compression Encoder, f) Shuttle Hercules Payload, g) Electronic X-Ray Camera (EXC), h) Shuttle Electronic Still Camera (ESC) DTO, and i) Shuttle Camcorder DTO. Served 107 Image Analysis Team / LWG in developing methods of obtaining quantitative intensity characteristics of debris events from consumer camcorders. Prior to coming to NASA, employed by commercial companies including: Sony Electronics International (5 years), AT&T, and General Instruments. Master of Science thesis, 'Video Compression for Space Based Applications'. Multiple publications including: IGARSS, NASA Tech Briefs, International Journal of Remote Sensing, NASA Spinoffs, TV Technology.

**David R. Bretz** was team lead for the STS-107 Image Analysis Team for re-entry debris relative motion analysis, and the Image Analysis team interface with the Early Sightings and Assessment Team. He also performed stabilization and enhancement of launch film showing change to the External Tank bipod ramp area. He is currently a Senior Scientist with Hernandez Engineering, in JSC Image Science & Analysis Group, and the lead image analyst for activities in support of Hubble Space Telescope Servicing Missions including 2D motion analysis and 3D measurements of solar arrays, photographic surveys of the damage to the insulation blankets and study of orbital debris strikes to the exterior surfaces. Bretz received special recognition for assisting local law enforcement by enhancing video images of suspected criminals. He has a M.S. in Imaging Science from Rochester Institute of Technology.

**Fred W. Martin** has 23 years of experience in the Engineering Directorate at the Johnson Space Center in aerodynamics, aerothermodynamics, and computational fluid dynamics. He has had unique experience in solving fluid mechanics related problems on the Space Shuttle; including Orbiter transonic ascent venting problems and main engine feed line disconnect valve issues. Following the Challenger accident, he led a multi-center NASA/contractor team that created the Space Shuttle ascent vehicle CFD capability that was used to refine the vehicle's transonic aerodynamic loads. He has also had considerable experience in visualizing engineering data, from animating the STS-5 windward surface entry temperatures, comparing the Space Shuttle ascent pressure measurements to wind tunnel and flight data, and comparing the X-38 flight imaged streamlines to wind tunnel data and numerical predictions.

**Joe Gessler**, JSC ES5 (Mech Design & Analysis). Aerospace Engineer in the Structural Engineering Division at the NASA/Johnson Space Center for the past three years, specializes in the area of structural analysis. Over the course of several weeks, Joe mapped the ascent debris' 3-D trajectory. In addition, he estimated the possible impact areas and impact angles with respect to both the orbiter's orthogonal planes and the local impact area.

#### Kennedy Space Center

**Armando Oliu**, Lead of the NASA Ice/Debris Team; which includes leading the Space Shuttle Final Inspection Team and the KSC Image Analysis Team. Mr. Oliu received his

This information is being distributed to aid in the investigation of the Columbia mishap and should only be distributed to personnel who are actively involved in this investigation. 101

B.S. in Mechanical Engineering from the University of Miami, FL. He has been involved with Flight Hardware processing since joining NASA in 1988, and currently serves as Co-Lead of the KSC Image Analysis Team for the STS-107 Investigation.

**John Lane** received his B.S. and M.S. in Physics from Florida Atlantic University where his thesis research involved measurement of electronic transport properties of organic semiconductors. His Ph.D. dissertation research at the University of Central Florida involved hydro meteorological instrumentation, modeling, and analysis, in support of the NASA Tropical Rainfall Measurement Mission (TRMM). Dr. Lane is presently an Applications Scientist for ASRC Aerospace at Kennedy Space Center, FL where he specializes in mathematical and numerical modeling and simulation of a variety of problems such as: analysis of magnetic force fields of air core solenoids; 3D image processing algorithms for precision position measurement; and development of instrumentation and analysis techniques for measurement of rainfall and hail size distributions.

**Charles G. (Robbie) Robinson** is the Photo Instrumentation Planner for Johnson Controls at KSC, providing visual services at CCAFS and KSC since 1992. His positions over the years as Quality Assurance and Safety Manager; Maintenance Manager; Production Manager; and now in his current position gives him a broad understanding of contract requirements. His former management of Still and Motion Picture Laboratories; Film and Video Production; Metric Instrumentation; Optics; and Camera Operations make him uniquely qualified as Space Shuttle Photo Instrumentation Planner. His leadership, management and keen attention to detail led the company's support through 17 Space Shuttle launch cycles - with excellent results. He has over 33 years total in providing audiovisual support, including 23 years in the Air Force.

**Robert Youngquist** heads the Applied Physics Laboratory in the Spaceport Engineering and Technology Directorate at the Kennedy Space Center. During most of his 15 years at KSC he has been active in resolving a wide variety of Shuttle ground processing issues. His primary background is optics--his Ph.D. thesis was in the development of fiber optic components--but he has developed Shuttle hardware utilizing most of the electromagnetic spectra as well as ultrasonics, novel sensor designs, fluid dynamics, and other fields. His primary role in the 107 Image Analysis Team investigation was to develop the nonablative models whereby the mass and effective area of debris could be determined from luminosity and trajectory data. He also developed a possible model to explain the flash events and developed a method to obtain debris deceleration data from trajectory data supplied to the team.

#### Marshall Space Flight Center

**Tom Rieckhoff** has served as the Engineering Photographic Analysis Team Lead, responsible for photographic review and analytical support to the MSFC Shuttle Projects for the past 15 years. He graduated from the University of South Florida with a degree in Motion Picture Film Production in 1973. He worked in the Marshall Space Flight Center Photographic Laboratory as a motion picture cameraman, film editor and Director.

This information is being distributed to aid in the investigation of the Columbia mishap and should only be distributed to personnel who are actively involved in this investigation. 102

**Dr. Michael O'Farrell** graduated from Auburn University in 1982 with Ph.D. in Mathematics. His current position is a Senior Engineering Specialist for United Space Alliance at MSFC. His primary activities at USA include engineering evaluation of ground-based and on-board camera film and video for launch of the Space Shuttle vehicle and image analyses for specialized propulsion related tests. Dr. O'Farrell has held a wide range of positions Rockwell International Space Systems Division (statistical analyst for the NASA Space Shuttle Problem Assessment Center) and Boeing North American (Senior Engineering Specialist). His work includes flow modeling of vortex induced vibrations, construction of optimal Space Shuttle ascent trajectories, determination of the effectiveness of turbulence models to estimate convective heating in space vehicle base flow recirculation regions, performing acoustic environment analyses during liftoff conditions for the proposed Liquid Flyback Booster (LFBB) and investigating the re-entry aeroheating environments for a modified Space Shuttle vehicle. He authored several technical aerospace engineering related works, including the "Handbook of High Frequency Flow/Structural Interactions in Dense Subsonic Fluids".

**Bill Cooke**, Computer Sciences Corporation contractor supporting MSFC Space Environments Team - In the decade since receiving his PhD in astronomy, Dr. Cooke has become one of NASA's experts on meteoroids and their effects on spacecraft, especially in the area of meteor shower forecasting. As a member of the Luminosity Working Group, he provides expertise in meteor physics, especially with regard to ablative processes, and in astrometry, determining which (if any) stars ought to be visible in the various videos analyzed by the group.

**Wesley R. Swift** earned his MS (physics) at the University of Alabama in Huntsville and was employed by the Optical Aeronomy Laboratory (OAL) at UAH from 1986 to 2001. NASA/OAL projects include the ISUS, a balloon instrument, the ISO, which flew on ATLAS I, and the UVI on the POLAR satellite. He is presently employed by Raytheon and is located at MSFC/ED44 in the Space Environments group. His duties include the adaptation of multisatellite data archives and space science models for space weather engineering applications. He participated in the 2001 and 2002 Leonid Global Video Meteor campaigns and has developed calibration methods and software to significantly improve meteor photometry. He is the recipient of a 2002 NASA Technology Achievement Award, the 2003 Raytheon Peer Award and numerous group achievement awards. As a member of the Luminosity Working Group, he adapted his meteor photometry method to obtain valuable information regarding the intensity ratios of the debris objects with respect to the orbiter.

#### Ames Research Center

**George A. Raiche** has been a Research Scientist in the Reacting Flow Environments Branch at NASA's Ames Research Center for six years. His Ph.D. is in physical chemistry and spectroscopy, and he has published over 15 technical papers on the topics of spectroscopy of high-temperature gases, hypersonic facility instrumentation, and optical diagnostics. He is group leader for ARC's Arcjet Characterization Group, which develops spectroscopic techniques for measuring arcjet test environments. His role in the

This information is being distributed to aid in the investigation of the Columbia mishap and should only be distributed to personnel who are actively involved in this investigation. 103

Image Analysis Team investigation has been to provide expertise on the physics and chemistry of shock-induced luminosity phenomena. He is also principal investigator for the arcjet testing described in Luminosity Working Group report.

#### NIMA

**Ivar Svendsen** was an Imagery Analyst for 28 years most recently in the NIMA Missiles and Space Issues Branch. During his career Mr. Svendsen had participated in a temporary reassignment to NASA to participate in the first launches of the Space Transport System, and, as NIMA's space systems expert, Mr. Svendsen was eager and able to lend his experience and support to all of the Hubble Space Telescope servicing missions. At the time of his sudden death on May 20, Mr. Svendsen was an active leader of NIMA's efforts to support the NASA Columbia accident investigation.

**James Salacain** is president of Spatial Analytics, Inc., an imaging and visualization-consulting firm and serves as the chief system engineer for the National Imagery and Mapping Agency (NIMA) Image Quality and Utility Program. He has a B.S in Photographic Science and Instrumentation and an M.S. in Imaging Science, both from the Rochester Institute of Technology. Mr. Salacain was employed as an Image Scientist by Eastman Kodak Co. for 15 years and was responsible for performing image quality optimization and image chain analysis for a wide variety of imaging systems and imaging technologies.

#### Lockheed Martin

**Dwight Divine, III**, Chief Scientist, Imagery & Geospatial Solutions, M&DS, Lockheed Martin. Mr. Divine coordinated Lockheed Martin Management & data Systems' STS-107 analyses. He has worked for over 35 years in the fields of optics, data estimation and prediction, and image and signal processing. He joined IBM's T .J. Watson Research Center in New York to work on solid-state laser development (GaAs lasers) after graduating from the University of Florida with a BSEE in 1964. He worked on the development of the laser video disc (including initial development of CD sound and data storage formats and techniques) from 1976 through 1982. From 1982 through 1985, Mr. Divine helped develop, model, and test the estimation and prediction approach used in the Global Positioning System (GPS). He has been working in the field of image processing for classified applications since 1989. Mr. Divine has authored eight patents in varying fields and a number of papers, articles, and presentations.

**Dr. Marvin Kleine** is the Chief Scientist for Lockheed Martin Management & Data Systems ISR Systems. He received his Ph.D. in Physics from Arizona State University in 1994. Dr. Kleine's technical strengths are in the areas of SAR and optical signal processing, ground processing architectures, molecular spectroscopy, hyperspectral imaging, data compression, radiation transfer modeling, and electromagnetic scattering. For the past 22 years, Dr. Kleine has been responsible for the management, development, and insertion of new technology to strategically place Lockheed Martin ISR Systems for the next generation of remote sensing systems.

This information is being distributed to aid in the investigation of the Columbia mishap and should only be distributed to personnel who are actively involved in this investigation. 104

**Dr. Eamon B. Barrett**, Image Scientist, Lockheed Martin Advanced Technology Center (LM/ATC); Modeling, Simulation and Information Sciences Dept., Sunnyvale, CA. Dr. Barrett received a Ph.D. in Mathematics from Stanford University in 1968. He has over 40 years of experience conducting and directing R&D projects in applied physics, imagery science, automated change detection and cartography. Dr. Barrett joined Lockheed in 1986 as a research scientist. His previous positions include: President, Smart Systems Technology Inc., 1980-1985; Director, Intelligent Systems Program, National Science Foundation, 1977-1980; Senior Imagery Scientist, ESL Inc., 1971-1977; Associate Professor in Operations Research, Naval Postgraduate School, 1966-1971. Since 1960 he has authored more than 50 technical publications in physics, mathematics and image science.

#### Boeing

**Lorelei Lohrli-Kirk**, Boeing Senior Engineer. Bachelor of Science in Aerospace Engineering, Master of Science in Systems Architecture and Engineering. Lohrli-Kirk has supported the Space Shuttle Program for 16 years in several disciplines including: integrated vehicle guidance, navigation and control; liftoff and ascent trajectory analysis; liftoff sub-system performance and design; and photographic evaluation and analysis. She provided Boeing System Integration support for the STS-107 Mishap Investigation.

#### Neptec

**Jean-Sebastien Valois**, Operations Analyst: BSc Mech Eng, Ecole Polytechnique de Montreal, MS Elect Eng, McGill University, Montreal.

**Chris Bennett**, Operations Engineer: B.S. Mech Eng, University of Virginia, M.S. for Neptec, Inc.

This information is being distributed to aid in the investigation of the Columbia mishap and should only be distributed to personnel who are actively involved in this investigation. 105

## 9.0 Acronyms

AFB	Air Force Base
AMOS	Air Force Maui Optical and Supercomputing Site
AZ	Arizona
CA	California
CAD	Computer Aided Design
CAIB	Columbia Accident Investigation Board
CSR	Computer Sciences Raytheon
EOC	Emergency Operations Center
ER	Eastern Range
ESAT	Early Sighting Assessment Team
ESC	Electronic Still Camera
ET	External Tank
ETA	ET Attach
GPS	Global Positioning System
HDTV	High Definition Television
HFOV	Horizontal Field of View
IEA	Integrated Electronic Assembly
IRE	Institute of Radio Engineers
ISS	International Space Station
JSC	Johnson Space Center
KSC	Kennedy Space Center
LH <sub>2</sub>	Liquid Hydrogen
LSRB	Left Solid Rocket Booster
LWG	Luminosity Working Group
MER	Mission Evaluation Room
MET	Mission Elapsed Time
MSFC	Marshall Space Flight Center
NASA	National Aeronautics and Space Administration
NSTS	National Space Transportation System
NTSC	National Television Standards/System Committee
OVEWG	Orbiter Vehicle Engineering Working Group
RCC	Reinforced Carbon Carbon
RCS	Reaction Control System/Subsystem
RTV	Room Temperature Vulcanizing
SMPTE	Society of Motion Picture and Television Engineers
SRB	Solid Rocket Booster
STS	Space Transportation System
TPS	Thermal Protection System
UT	Utah
UTC	Universal Time Code

This information is being distributed to aid in the investigation of the Columbia mishap and should only be distributed to personnel who are actively involved in this investigation. 106

## 10.0 References

Computer Sciences Raytheon, Systems Analysis Department, Instrumentation Systems Analysis Special Report, CDR A205, 14, February 2003

“Entry Debris Characterization” [references/shuttleweb/mission\\_support/sts-107/contingency/entry/107\\_entry.html](references/shuttleweb/mission_support/sts-107/contingency/entry/107_entry.html)

“Entry Debris Events Timeline”  
[references\shuttleweb\mission\\_support\sts-107\contingency\entry\107\\_reports.html](references\shuttleweb\mission_support\sts-107\contingency\entry\107_reports.html)

“Entry Video and Still Database”  
<http://vdas-huey.jsc.nasa.gov/Contingency/107/web/>

Image Analysis STS-107 Investigation website at  
[references/shuttleweb/mission\\_support/sts-107/contingency/entry/107\\_entry.html](references/shuttleweb/mission_support/sts-107/contingency/entry/107_entry.html)

Image Science and Analysis web page  
[references/shuttleweb/mission\\_support/missions.html](references/shuttleweb/mission_support/missions.html)

Image Science and Analysis web site  
[references/shuttleweb/mission\\_support/sts-107/contingency/launch/107\\_launch.html](references/shuttleweb/mission_support/sts-107/contingency/launch/107_launch.html)

JSC-14273, Space Shuttle Program Contingency Action Plan for Johnson Space Center

NSTS 08244 Space Shuttle Program Launch and Landing Photographic Engineering Evaluation document, Revision B, 1997

Shuttle Reference Manual at  
<http://spaceflight.nasa.gov/shuttle/reference/shutref/index.html>

Video from The Colony, TX  
[shuttleweb/mission\\_support/sts-107/contingency/other/Aero.pdf](shuttleweb/mission_support/sts-107/contingency/other/Aero.pdf)

Columbia Earth Sighting Assessment Team Final Report, 13 June 2003.

Starfire Team Final Report

This information is being distributed to aid in the investigation of the Columbia mishap and should only be distributed to personnel who are actively involved in this investigation. 107

## 11.0 Appendices

### Appendix 4.1.1

[Launch Camera Tracking Site Locations](#)  
[KSC Launch Camera Documentation](#)

### Appendix 4.1.3

[E208 and E212 Tracking Camera Star Shots for Image Enhancement](#)

### Appendix 4.2.4

[Camera Timing](#)

### Appendix 4.3.1

[STS-107 Launch+4 Day Consolidated Film/Video Report KSC, JSC, MSFC and Program Integration Film/Video Analysis Teams](#)

### Appendix 4.3.2A

[Debris Impact Timing](#)

### Appendix 4.3.2B

[E212 Bipod Area Enhancements](#)

### Appendix 4.3.2C

[Debris Size Measurement Issues](#)

### Appendix 4.3.2D

[Verification of Color Analysis Repeatability for Estimating Debris Rotation Rate](#)

### Appendix 4.3.2E

[Examination E212 Frames During Debris Impact](#)

### Appendix 4.3.2F STS-107 Mishap Investigation Sub-team Reports

[NASA-JSC/SX – Debris Trajectory, impact location, velocity, and impact angle](#)

[NASA-JSC/ES – Debris Trajectory, impact location, velocity, and impact angle](#)

[NASA-JSC/EG – Debris Trajectory, impact location, velocity, and impact angle](#)

[NASA-KSC – Debris Trajectory, impact location, velocity, impact angle, and size](#)

[NASA-MSFC – Debris Trajectory, impact location, velocity, impact angle, and size](#)

[NASA-JSC/SX – Single Camera Velocity](#)

[Lockheed Martin Management and Data Systems – Debris Velocity](#)

[Lockheed Martin Management and Data Systems – Trajectory](#)

[National Imagery and Mapping Agency – Debris Velocity](#)

### Appendix 4.3.2G

[Post-Impact Debris Size Estimates](#)

This information is being distributed to aid in the investigation of the Columbia mishap and should only be distributed to personnel who are actively involved in this investigation. 108



Appendix 5.3.1  
[ET Downlink Video Analysis](#)

Appendix 5.3.2  
[Air Force Maui Optical and Supercomputing Site \(AMOS\) STS-107 Photographs](#)

Appendix 5.3.3  
[Analysis of STS-107 On-Orbit Debris – Orbit 5](#)

Appendix 6.2A  
[Luminosity Working Group Columbia Re-entry Debris Characteristics Preliminary Report – May 6, 2003](#)  
[Luminosity Working Group Columbia Re-entry Debris Characteristics Interim Report – June 6, 2003](#)

Appendix 6.2B  
[Video Scale and Zoom Determination](#)

This information is being distributed to aid in the investigation of the Columbia mishap and should only be distributed to personnel who are actively involved in this investigation. 109

**THIS PAGE INTENTIONALLY LEFT BLANK**



# Volume III

## Appendix E.3

### An Assessment of Potential Material Candidates for the "Flight Day 2" Radar Object Observed during the NASA Mission STS-107

This Appendix contains the Air force Research Laboratory Technical Note, AFRL-SNS-2003-001, An Assessment of Potential Material Candidates for the "Flight Day 2" Radar Object Observed During the NASA STS-107 (*Columbia*), Final Summary Report, 20 July 2003.



Air Force Research Laboratory  
Technical Note  
AFRL-SNS-2003-001

An Assessment of Potential Material Candidates  
for the "Flight Day 2" Radar Object Observed  
During the NASA Mission STS-107 (Columbia)

Final Summary Report

20 July 2003

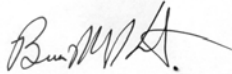
Brian M. Kent, Ph.D., Kueichien C. Hill, Ph.D.,  
and Capt. John Gulick, USAF  
Sensors Directorate  
Air Force Research Laboratory  
2591 K St  
Wright-Patterson Air Force Base, Ohio  
45433-7602  
(937)-255-9181  
[brian.kent@wpafb.af.mil](mailto:brian.kent@wpafb.af.mil)

Tri Van  
Mission Research Corporation  
2975 Research Blvd  
Beavercreek, OH 45430

**Report Documentation Page**

This report describes the results of an investigative analysis performed by the Air Force Research Laboratory Sensors Directorate at the specific request of the Defense Columbia Investigation Support Team (DCIST) who was supporting the Columbia Accident Investigation Board (CAIB). The work was performed during the period February 20, 2003 through 20 July 2003. An interim release of measurement findings was provided the CAIB on 24 April 2003, and the information was released in public testimony to the CAIB on May 6, 2003 at the Hilton Hotel, Houston, Texas. The overall assessment and conclusions of this report are consistent with the CAIB 6 May 2003 testimony, with one notable exception discussed in Section VI.

This report has been reviewed by the AFRL/SN "Flight Day Two" DCIST appointed assessment team, and is hereby released to the CAIB and DCIST for final disposition.



Brian M Kent, Ph.D.  
Research Fellow, Sensors Directorate  
Air Force Research Laboratory

### Acknowledgements

The author wishes to recognize the many collaborators and co-workers on this project, without whose help this task would not have been successfully completed. First, I would like to thank AFRL co-workers Mr. Dan Turner and Mr. William Brandewie. Mr. Turner skillfully scheduled all radar signature testing of the various radar objects in AFRL's advanced compact range, and wrote up many of the test reports. Mr. Bill Brandewie is commended for his role in arranging the shipping, receiving, and disposition of the many NASA parts tested throughout this project, including flight qualified assets that needed extremely careful handling and shipping. AFRL Co-workers Dr. Kueichien C. Hill and Captain John Gulick are credited for their in-depth assessment of the UHF RCS of the Tee-Seal, and are the primary authors of Appendix I. Next, the author recognizes the efforts of Mission Research Corporation employees Mr. Bill Forster, Mr. Christopher Clark, Mr. Frank Fails, and Mr. Travis Mensen. These collaborative on-site contractors supported over 1,000 hours of range testing during the months of March through May of 2003, and their crucial data was the key in narrowing the mystery of the flight day two object. Mr. William Griffin of MRC is credited with the creation of the geometry files through laser collections for the Tee-seal 21 RCS calculations. Next, the author wishes to recognize Mr. Robert Morris and Mr. Taft Devere of US STRATCOM, Peterson AFB, CO, who thoroughly assessed the "area-to-mass" ballistic coefficients for the flight day 2 assessment. Last, I am deeply indebted to Mr. Steve Rickman, NASA's Chief of the Thermal Design Branch, Johnson Space Center. Mr. Rickman tirelessly educated me about the composition and location of the myriad of materials on the Shuttle, obtained representative samples of each, and greatly assisted in coordinating NASA's support of radar signature testing. This assignment would not have been accomplished without your collective assistance, and I am professionally indebted to all of you for your tireless help and support.

Finally, I wish to recognize working members of the Columbia Accident Investigation Board who moved mountains and enabled unparalleled access to the NASA Orbiter flight worthy materials, as well as access to the debris recovery hanger at Kennedy Space Center. The author specifically recognizes USAF officers Lt Colonel Pat Goodman and 1Lt Steve Clark. Finally, I would like to add my thanks for the time, attention, and commitment of Major General John Barry who provided our team with everything we needed to successfully complete this assignment. On behalf of all members of the technical community involved with this effort, we salute the professionalism and commitment of the CAIB board members who have dedicated their time and talents to identify the root causes of this most unfortunate national tragedy.

Brian M. Kent  
11 June 03

**Table of Contents**

Title Page .....	1
Report Documentation Page .....	2
Acknowledgements.....	3
Table of Contents.....	4
I - Introduction and Background on the STS-107 (Columbia) “Flight Day 2” Object.....	5
II - Measured Radar and Ballistic Properties of the “Flight Day 2” Object.....	8
III - Brief Description of STS-107 External Orbiter Materials...	10
IV - “Flight Day 2” Candidate Elimination Process.....	15
V - Best Assessment of the Flight Day 2 Object Composition...	22
VI - Summary and Conclusions.....	30
VII - References.....	30
Appendix I – Radar Cross-Section Predictions of the Left Wing Reinforced Carbon-Carbon Tee-Seals #6 through #11 on the Space Shuttle Columbia.....	31

## **Section I - Introduction and Background on the STS-107 (Columbia) “Flight Day 2” Object**

On February 1, 2003, The National Aeronautics and Space Administration (NASA) Manned Mission STS-107 (Columbia) tragically ended when the Orbiter broke up upon reentering the atmosphere, killing the entire crew. The Columbia Accident Investigation Board (CAIB) was established to launch and execute a thorough and exhaustive investigation to establish the likely root cause of the accident, and to make recommendations to prevent a reoccurrence in the future.

Within a few days of the accident, NASA requested the United States Air Force (US STRATCOM) to carefully review the automated track records from the US space tracking network during the period the Columbia was in orbit on mission STS-107. US STRATCOM operates a very sophisticated network of radar systems to track nearly every know piece of space debris and satellite in orbit around the earth. Most objects tracked include known artificial satellites as well as various pieces of debris leftover from nearly 50 years of launching objects from earth into space. These radar systems have the necessary angular coverage and sensitivity to track even small objects in orbit around the earth. The CAIB wanted to know if this network detected and tracked any unusual radar events related to the STS-107 mission.

Within a few weeks of being tasked, an exhaustive analysis by US STRATCOM reported back that a new space object designated “2003-003B” was detected in orbit on January 17<sup>th</sup>, 18<sup>th</sup>, and 19<sup>th</sup>, 2003. The object had confirmed tracks by the PAVE PAWS UHF Phased array tracking radar at Beale Air Force on January 17<sup>th</sup>, as well as the Cape Cod PAVE PAWS UHF Phased array radar on the January 17<sup>th</sup>, 18<sup>th</sup>, and 19<sup>th</sup>. In addition, other fragmentary VHF radar track files were recovered from Eglin AFB, Florida and the Kwajelien Atoll “Altair” radar. The collective tracking information from these radars was used by US STRATCOM to re-construct the orbit of object “2003-003B”. When the orbit was traced backward in time from its measured orbital parameters, the resultant object orbit merged precisely with the orbit of STS-107 in the mid- to late-afternoon of STS-107 flight day 2 on 17 January 2003. Figure 1 shows the tracked orbit of object “2003-003B” and where in time it appears to originate from the Shuttle.

Though the part was never visually “observed departing the Shuttle”, the radar data unequivocally shows the object originated from the Shuttle on the 17<sup>th</sup> of January, and departed the Shuttle at a very low exit velocity of under 1 meter per second. In addition, the radars tracked the object until it reentered the atmosphere approximately 60 hours after it originated from the Shuttle and the object was subsequently destroyed on re-entry. In order to simplify nomenclature, from this point forward, the author will refer to object “2003-003B” simply as the “flight day 2 object”, or FD2 for short.



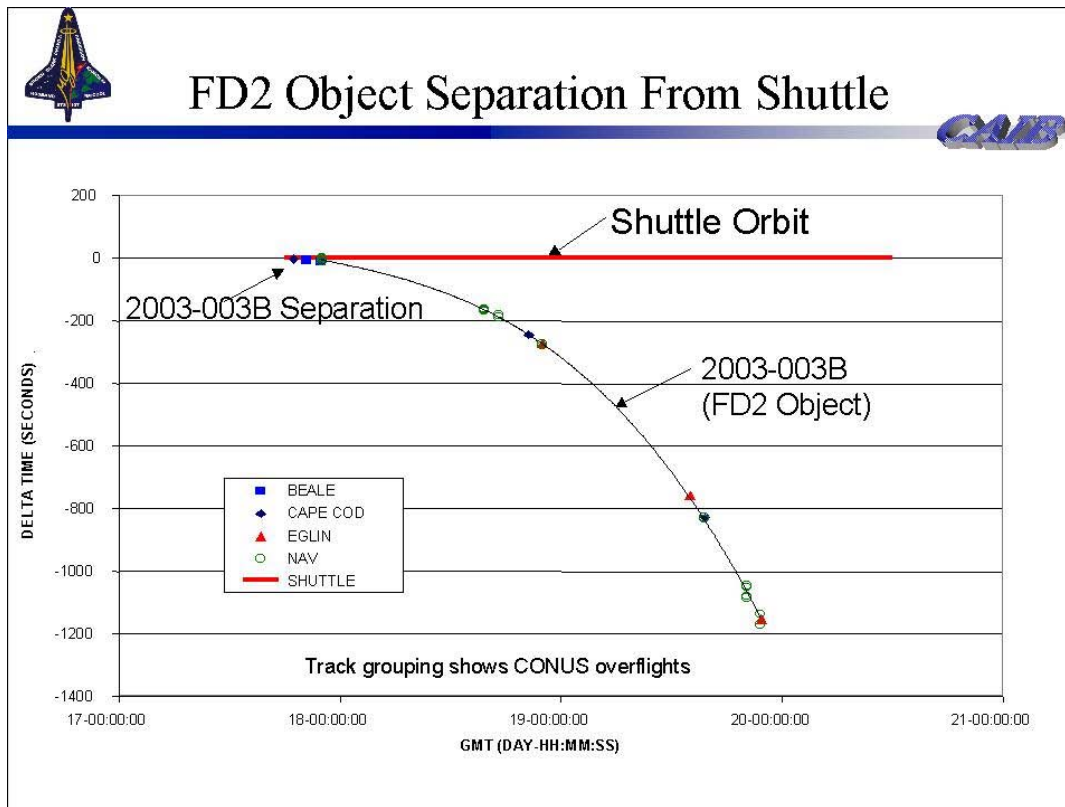


Figure 1 – Flight Day 2 (FD2) Object Orbit Relative to Shuttle

Many questions obviously arose after this discovery. How did the FD2 object come to separate from the Columbia in the first place? Did some “on-orbit” hypervelocity event dislodge a piece of material, or did the piece dislodge after some earlier event as the Orbiter was propelled into orbit? Was it possible to identify the make-up of the FD2 piece?

Although these questions are all related to the FD2 piece, this report solely concentrates on the third question, namely would it be possible to identify the origin and nature of the FD2 piece. The other aspects of what could have caused the FD2 piece to depart the Shuttle in the first place is the subject of an entire separate investigative team lead by NASA-JSC, and will not be discussed further. However, I will point out that the Orbiter made 2 minor and benign attitude changes using the 25 lb vernier jets on flight day 2. The Orbiter, oriented in a bay-to-earth, tail on velocity vector orientation, maneuvered to a biased starboard wing on velocity attitude at mission elapsed time (MET) 23 hours and 7 minutes and returned to the bay-to-earth, tail on velocity vector attitude at MET 23 hours and 42 minutes. There were no other maneuvers performed in approximately sixteen hours prior to this maneuver nor were there any additional maneuvers performed until approximately one day after. While it cannot be confirmed, it is possible that this maneuver imparted the departure velocity to the FD2 object.

This document may only be publicly released by the authority of the Columbia Accident Investigation Board

From this point forward, this report will concentrate on establishing a methodology for identifying candidates for the FD2 object, and to use engineering tests and data to reduce the potential candidates for the FD2 object to the smallest number feasible based on observed on orbit data as well as follow-on ground test data.

## Section II - Measured Radar and Ballistic Properties of the “Flight Day 2” Object

Since the FD2 object burned up upon re-entering the atmosphere, it obviously could not be physically recovered. Without physical evidence, unequivocally identifying the FD2 object appears initially to be an intractable problem. However, the CAIB suggested that any information provided that *eliminated* potential material candidates was nearly as valuable as knowing precisely what the object was. Based on this direction, the team devised a methodology for eliminating candidates from consideration. The basis for eliminating candidates relied very much on knowing certain physical properties of the FD2 object, and measuring those properties for various candidate materials to methodically eliminate possibilities. Before describing this process, however, we need to know precisely what is known, with high certainty, about the FD2 object.

As mentioned earlier, US STRATCOM radars were able to track the FD2 object on three separate days from 17-19 January 2003 (Figure 1) and in the process were able to measure a physical property of the object called the “radar signature” or “radar cross section (RCS)”. The RCS of an object is a property that relates how much incident radar energy is reflected from an object or target. The RCS is a complex function that depends on the SIZE, SHAPE, and MATERIAL COMPOSITION of the object in question, as well as the operating FREQUENCY of the radar and the ANGLE or orientation of the object relative to the observing radar. RCS is usually expressed in either square meters (m<sup>2</sup>) or in decibels per square meter (dBsm), and is represented by the Greek lower case letter sigma ( $\sigma$ ). The relationship between RCS in dBsm and RCS in m<sup>2</sup> are shown in Equation 1 below.

$$RCS(dBsm) = 10\text{Log}\{(\sigma)m^2\} \quad (1)$$

The radar frequency is a known quantity, as both the Beale and Cape Cod PAVE PAWS radar systems operate at a frequency of 433 Megahertz (MHz). For those who think in radar “wavelengths” instead of frequency, this represents a radar wavelength of 69.28 cm (27.28 in). The FD2 object appeared to tumble in space, resulting in a time varying RCS value whose rotation rate gradually increased over the three days it was tracked on orbit prior to re-entering the atmosphere. On-orbit RCS data from the 17<sup>th</sup> – 19<sup>th</sup> of January showed the unknown object’s RCS varied between –1.0 and –20 dBsm with a confidence level of +/-1.3 dB. The object appeared to be initially tumbling approximately once a minute on the 17<sup>th</sup>, increasing to once every 3 seconds by January 19<sup>th</sup>. It is thought aerodynamic drag caused the object to increase its tumble rate with time, and this increased tumble phenomena was extensively studied and reported by another investigative team from Lincoln Laboratory and will not be discussed further here. The main point to understand is that the object’s RCS variation (a measured physical property) at the radar frequency of 433 MHz is known over a tumble period, and this important physical property is essential to screen potential candidates for the flight day 2 object.

In addition to the RCS information, the various US STRATCOM space tracking radars also provided another very important piece of information. From the orbital decay parameters measured from the FD2 trajectory, US STRATCOM was able to quantify the object's "ballistic coefficient" or "B-Term" for short. The B-Term is a physical property related to the object's area to mass ratio, and is expressed in metric units as meters squared per kilogram or  $m^2/kg$ . In the case of the FD2 object, US STRATCOM calculated the FD2 object's B-Term as  $0.1 m^2/kg$  +/- 15%.

Therefore, there were now two physical quantities known for the FD2 object; its RCS at the UHF frequency of 433 MHz was known to lie between  $-1.0$  and  $-20$  dBsm and its B-term was known to be  $0.1 m^2/kg$ . Armed with this information, a joint team drawn from NASA-JSC, US STRATCOM, and the Air Force Research Laboratory (AFRL) was formed. NASA-JSC identified potential Shuttle Orbiter material candidates to examine. US STRATCOM evaluated those candidates by calculating the B-term for each candidate, and AFRL's Sensor's Directorate measured, in a controlled ground test environment, the RCS of the various candidate objects. In parallel, another small team performed a computational UHF RCS assessment of various reinforced carbon-carbon tee-seals and tee-seal fragments, in order to narrow down possible variants of tee-seal fragments. It was hoped that the information gleaned from these tests could provide insight into the nature of the FD2 object.

### Section III - Brief Description of STS-107 External Orbiter Materials

If one agrees with the scenario that the FD2 object originated from the Orbiter, it is possible to quickly identify candidate Orbiter materials to study. Since we have no insight at this point on the origin of the material, the process of elimination begins with all known and reasonable Orbiter candidate materials. For those not intimately familiar with the composition of the Shuttle Orbiter, this section will briefly list the materials one finds on the exterior surface of the Shuttle, as well as materials that could originate from the payload bay while on orbit.

In the most general sense, the Shuttle Orbiter consists of two general classes of materials. The first class is the "Thermal Protection System or "TPS". These materials compose the largest share of the exterior of the Orbiter, and are responsible for protecting the Orbiter during the searing heat of re-entry. The second class of materials makes up the "Thermal Control System" or "TCS" materials. These materials protect elements of the payload bay, payload bay interior, and various experiments that may be present in the Orbiter payload bay while on orbit. Since the Orbiter essentially goes through an entire day/night cycle in a roughly 90 minute period, the TPS and TCS materials must survive the several hundred degree change in temperature in space from full sun to full shadow.

First, let's describe the Thermal Protection System or TPS materials. Figure 2 below shows a schematic of the materials composing the TPS system. Clearly from Figure 2, the silica-based tiles make up a large majority of the Shuttle exterior real estate. The Shuttle tiles come in a variety of densities, 9 lb/ft<sup>2</sup>, 12 lb/ft<sup>2</sup>, and 22 lb/ft<sup>2</sup>, respectively. These are referred to as LI900, FRCI 12, and LI2200. Additionally, there are a very small number of 8 lb/ft<sup>2</sup> tiles (AETB 8) on the base heat shield near the main engines. With the exception of the Reinforced Carbon-Carbon (RCC) edges, the tiles cover most of the lower half of the delta wing structure. Since the Shuttle re-enters the atmosphere at high angles of attack, the majority of the upper surface of the Orbiter sees far lower temperatures than the lower tiles and leading RCC edges. In these areas, blanket insulations such as Advanced Flexible Reusable Surface Insulation (AFRSI) and Flexible Reusable Surface Insulation (FRSI) are used. Closeout of the RCC panel attach regions is accomplished using "carrier panels". There is a row of "carrier panels" just beyond the RCC edges on both the top side and bottom side of the edges. These are referred to as "upper carrier panels" and "lower carrier panels". Carrier panels consist of either 3 or 4 high density LI2200 tiles bonded onto Nomex felt, and subsequently, aluminum structure using Room Temperature Vulcanizing (RTV) adhesive. Each carrier panel, in turn, is bolted onto the Orbiter using two attach bolts. A "horse collar" seal, comprised of Inconel over Nextel fabric, is used to preclude the flow of hot gases into the wing leading edge cavity.

This document may only be publicly released by the authority of the Columbia Accident Investigation Board

### Thermal Protection System Constituent Materials

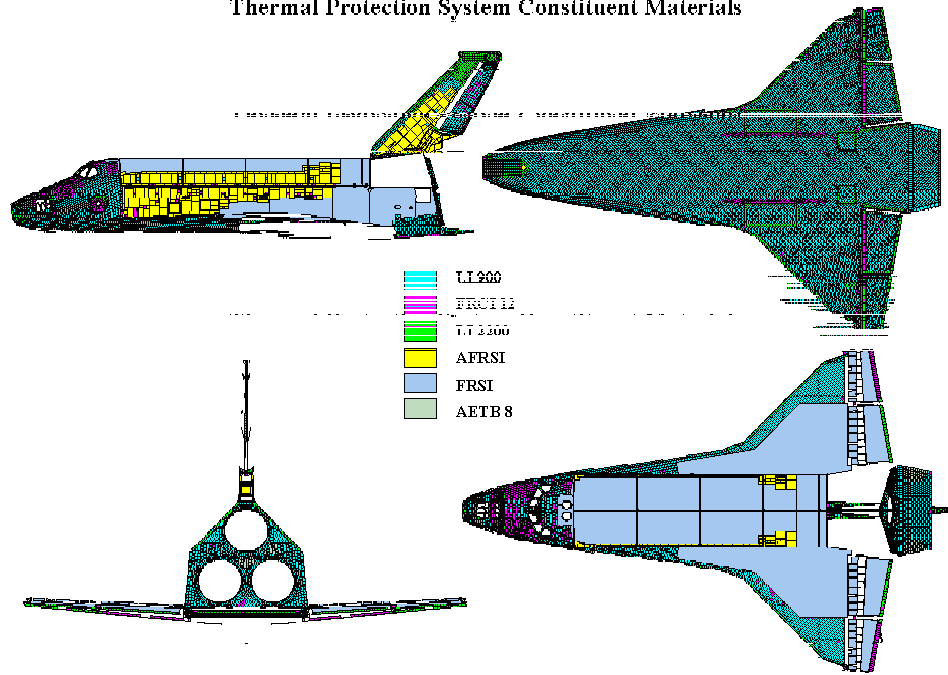


Figure 2 – Thermal Protection System on the Orbiter Exterior

### Thermal Protection System Materials Tested

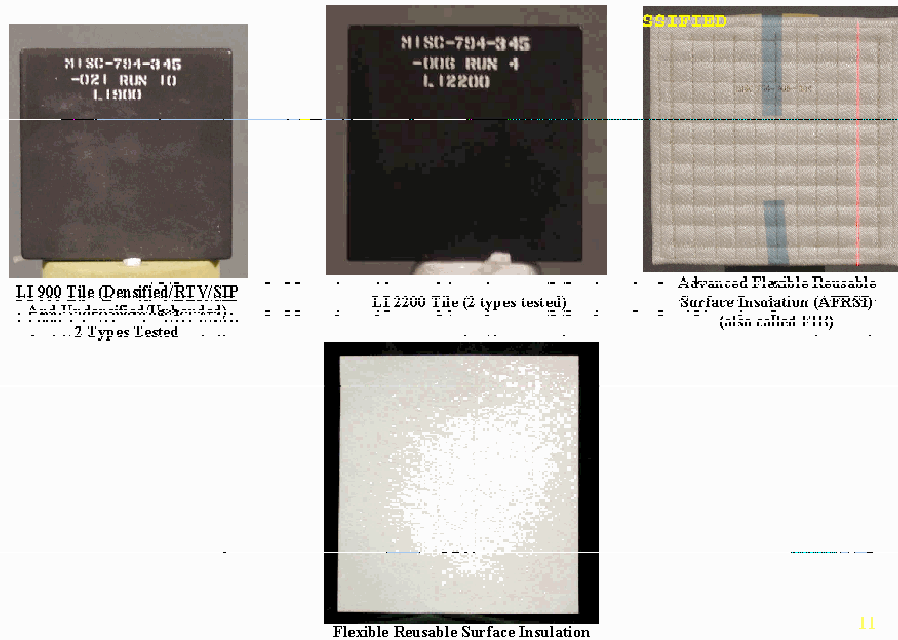


Figure 3 – Shuttle TPS Materials LI900, LI2200, AFRSI, and FRSI

This document may only be publicly released by the authority of the Columbia Accident Investigation Board

**Carrier Panel and Horse Collar**

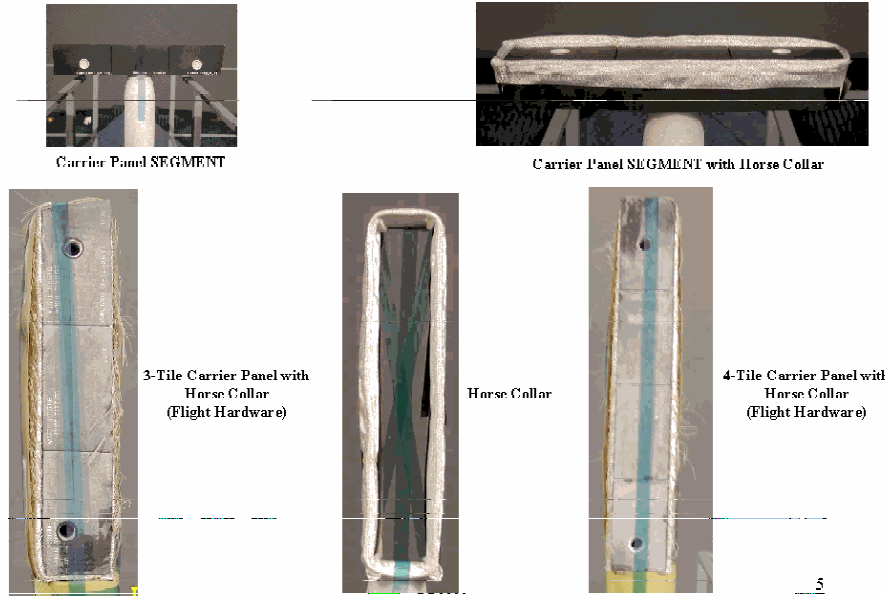


Figure 4 – Shuttle TPS Materials Including a Lower Carrier Panel, Horse Collar, and Carrier Panel with Horse Collar

The reinforced carbon-carbon (RCC) materials consist primarily of leading edge panels with Tee-Seals between adjacent RCC panels. Figure 5 below shows an entire RCC panel with the Tee-Seal clearly visible on the end. The rightmost picture of Figure 5 is the tee seal alone without any edge attached. The center picture is called the Incoflex spanner beam insulation piece, though NASA engineers commonly call it the “ear muff” seal. This insulation is typical of that found in the wing leading edge cavity and is used to protect the structure from high temperatures during reentry. Taken together, Figures 3,4, and 5 comprise the suite of materials of the TPS system.

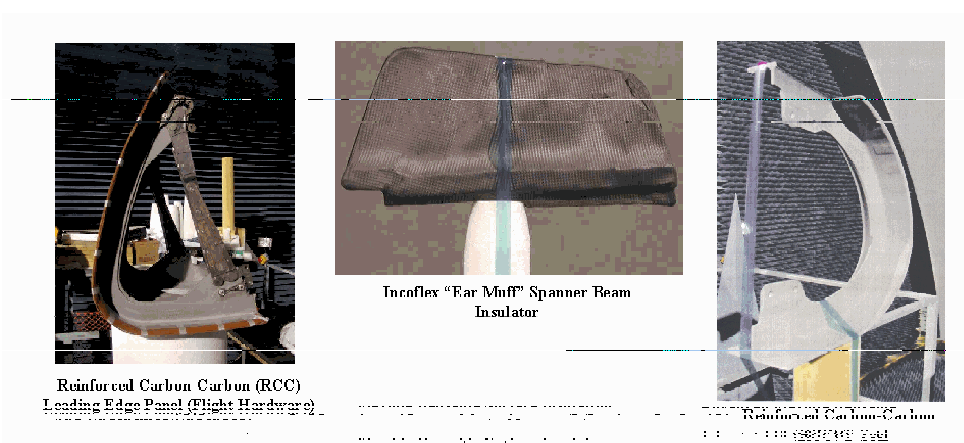


Figure 5 – Elements of the Reinforced Carbon Carbon (RCC) Leading Edge Thermal Protection System (TPS)

This document may only be publicly released by the authority of the Columbia Accident Investigation Board

Next is the Thermal Control System (TCS) materials. These materials are altogether different from the TPS materials, and primarily reside in the payload bay of the Orbiter. Most are highly reflective (silver or white) and lightweight, as they are not exposed to re-entry heating since the payload bay door is closed during re-entry. Figure 6 depicts samples of multi-layer insulations used on STS 107 payloads in the cargo bay.

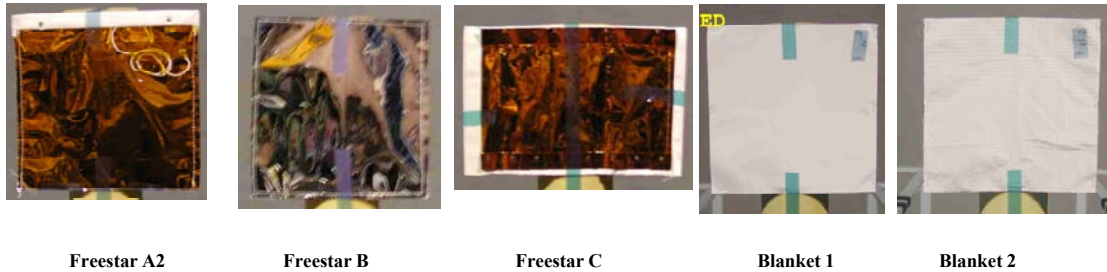


Figure 6 – Samples of the Orbiter TCS Materials

The “Freestar” samples are all lightweight highly conductive thermal blankets, while the rightmost two are beta cloth covered thermal blankets. Although not shown, we also examined TCS components consisting of plain beta cloth with and without its ground wire quilting. Orbiter TCS materials are shown in Figure 7, which also includes a common tool, used to snap the thermal blankets in place or to one another. Looking at these materials, one quickly comes to the realization that most look very much like a metal conducting plate from a radar signature standpoint. This meant the blankets were relatively easy to evaluate in the laboratory.

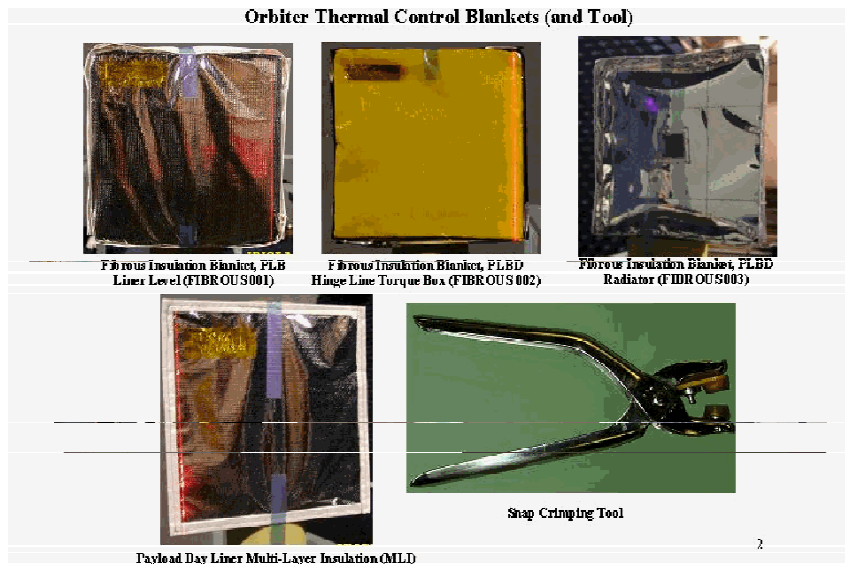


Figure 7 – Orbiter TCS samples including metalized insulation blankets and a typical “crimping” tool



In all, NASA ultimately identified 31 distinct material samples to assess their potential to match the known characteristics of the FD2 object. In addition, several specialized items were postulated as possibilities for the FD2 object, including various tools that could conceivably have been left in or “lost” in Columbia’s payload bay during one of its normal pre-flight maintenance period. Although NASA attempted an in-depth 2-year audit of missing tools in any facility used by Columbia up to its final STS-107 mission, the handful of tools that came up as “unaccounted for” were not likely matches for the physical and radar characteristics of the FD2 object, and therefore were not pursued further by this team. [Note that there was no evidence provided to the WPAFB FD2 team that any of these lost tools were likely in the Columbia payload bay, though it is impossible to totally discount the possibility that some tool or part was left in the payload bay unknown to all.] Having identified candidates, the next step was devising a scheme for assessing the potential FD2 candidates.

## Section IV - “Flight Day 2” Candidate Elimination Process

Having exhaustively examined the exterior of the Shuttle Orbiter and payload bay in depth, NASA-JSC identified 31 different potential candidate materials and/or exterior parts to assess for potential as the FD2 object. The next step was to come up with a systematic method for examining these candidates in the context of the known physical properties of the FD2 object. It is emphasized that the nature of the physical information available about the FD2 object requires that exclusionary logic must be applied to eliminate potential candidates.

The process for excluding potential FD2 candidates involved three separate test conditions:

(1) The measured Circular Polarization (CP) UHF RCS of the candidate object had to equal or exceed  $-1$  dBsm over some angular coverage of target orientations, within the stated measured on-orbit uncertainty of  $\pm 1.3$  dB at the measured frequency of 433 MHz. Note that the uncertainty values were obtained based on a fairly extensive set of on-orbit RCS calibration measurements performed by both the Beale AFB and Cape Cod PAVE PAWS radar. In addition, common sense dictates that the maximum value of RCS needs to occur over a fairly broad set of angles relative to the target orientation, since the FD2 part tumbled in space and therefore presented a somewhat random orientation relative to the radar. Fortunately, since the radar wavelength is fairly long (27.28 inches), and since many of the parts examined are shorter than the radar wavelength, their scattering behavior exhibits the large angular coverage that makes the alignment between the tumbling FD2 piece and the radar line of sight less problematic.

(2) The calculated ballistic coefficient or “B-term”, based strictly on the geometry and aeronautical drag coefficients of the candidate parts, must fall within 15% of the measured FD2 value of  $0.1 \text{ m}^2/\text{kg}$ .

(3) The candidate part is not refuted by the forensic evidence recovered from the Columbia debris field. For instance, if an item appears in the debris, it can’t possibly be the FD2 object, since the FD2 object burned up on re-entry. Another example may be a part that might match the B-term and RCS data, but which mechanically is excluded from having come off the Orbiter for other reasons.

Therefore the approach taken for each candidate material was to perform the requisite RCS test and/or B-Term analysis to assess the viability of the candidate in question. Early on in this process, the B-Term analysis and RCS testing occurred in parallel, meaning US STRATCOM and AFRL conducted their analysis nearly simultaneously in time, in order to produce the results as quickly as possible. As both organizations refined their approaches, and as new material candidates emerged, the team shifted to a “serial” test hypothesis approach, meaning we would evaluate potential candidates for “B-term” compliance first, and then perform the more expensive and

extensive UHF RCS tests on the successful B-term candidates only, rather than perform RCS tests on every piece imaginable. This “serial” approach helped reduce the needed UHF RCS test time to down-select candidates from potentially many thousands of test hours to about a thousand test hours. In addition, this assessment approach freed up AFRL RCS range time that NASA requested for higher frequency RCS testing needed by the CAIB and DCIST for other purposes. Specifically, NASA requested extensive AFRL RCS measurement support for L-Band (1.2-1.4 GHz), S-band (2.7-2.9 GHz), and C-Band (5.6-5.7 GHz) to assess the Shuttle ascent debris shedding analysis (C-Band) as well as the NASA Early Sighting and Assessment team (ESAT) at L and S bands. Both of these efforts were focused on debris recovery efforts. None of the L, S, and C band RCS data and information was necessary or relevant to the FD2 assessment, and won’t be reported here as it has been extensively documented in other NASA technical reports related to the Columbia investigation. [1,2]

At this point, a brief “top level” technical description of the specific technical down selection approaches is in order. Let’s begin with the B-Term analysis performed by Mr. Robert Morris and Taft Devere of US STRATCOM. Given the plotted trajectory of the FD2 piece, and information on the state of the atmosphere at about the time of the FD2 event, Mr. Morris and analysts from US STRATCOM oriented the candidate parts in one of two orientations hereafter referred to as pure “spin” and “tumble”. The “spin” axis refers to rotation about the shortest axis (dimension) through the part’s center of mass, while the “tumble” referred to rotation about the longest axis (dimension) through the part’s center of mass. For example, if the part was an ordinary writing “pencil”, pure “spin” would refer to rotation of the pencil about an axis along the length of the pencil including the center pencil lead, while pure “tumble” would refer to rotation of the pencil “end over end” point to eraser. Naturally, a part tumbling in space would likely consist of some element of both rotational planes, so any number of states between pure “spin” and pure “tumble” are possible. However, for simplicity US STRATCOM concentrated on the pure “spin” and pure “tumble” cases as bounding the possible complex tumble state in space.

Once the part geometry is known, and its center of aerodynamic mass is identified based on the part geometry, a very complex model of the atmosphere is used to estimate the density of the very sparse atmosphere encountered by the part as it proceeds in low earth orbit. It is a highly sophisticated computational model, which has been used for many years by US STRATCOM to predict orbital dynamics of satellites and debris in low earth orbit. Using this model to help establish estimates for the coefficient of drag, the candidate part’s B-term or area/mass ratio is computed for the spin and tumble orientation. (In some candidate cases, B-term calculations are only done in the tumble orientation, since the spin axis is very short and is very unlikely to occur. For instance, the B-term of flat square pieces were only calculated in the tumble axis.)

The second down selection criteria is the UHF RCS test properties. Numerically modeling the UHF RCS for a complex body with non-metallic properties is an extremely difficult RCS computational problem. In fact, in the area of computational electromagnetics, it is the most complex problem being studied by electromagnetic

specialists today. Though it is possible to get reasonably accurate RCS predictions for simple flat conducting shapes (like flat metallic plates) or for simple bodies of revolutions (like spheres or cylinders), more complex parts like RCC edges, spanner beam insulation pieces, and RCC Tee-seal represent a far more difficult RCS prediction problem. Though attempts to model a few isolated cases with RCS predictions were reasonably successful (See for instance the Tee-seal RCS calculations in Appendix I), the team decided that the most accurate and fastest way to complete the RCS assessments for the myriad of other complex parts were through direct RCS measurements performed in a very controlled ground based RCS measurement environment. Fortunately, the Air Force Research Laboratory in Dayton Ohio had precisely the facility needed to perform the required UHF RCS measurements, namely the Advanced Compact RCS range or ACR.

The AFRL ACR is a large laboratory room of lined with radar absorbing or “anechoic” material. The large anechoic main chamber room is 65 ft wide, 45 ft high, and 96 feet long. The room is dominated by a “dual reflector” compact range reflector system, shown below in Figure 8. Only the main reflector is shown in the large chamber, as the feed antennas and sub-reflector are located in a smaller anechoic room below the main chamber. Much like the optics in a telescope, the dual reflector system converts the spherical wave originating from the feed antenna into what is called a “plane wave” in radar terminology. A “plane wave” is an electromagnetic wave whose amplitude and phase properties are nearly constant in a plane sliced perpendicular to the direction of propagation. As a result, the advanced compact range very accurately simulates the very large separation that normally occurs between the source radar and the target under test. In technical terms, we say that the compact range simulates the “far field” conditions from an electromagnetics standpoint. Since the FD2 object was 300-1200 km away from the radars at points through its orbit, the FD2 was considered to be in the “far field” of the earth based radars. Therefore, the ACR accurately simulates these conditions.



Figure 8 – The AFRL Advanced Compact RCS Measurement Range (ACR)  
(This test facility is located at Wright-Patterson AFB, Ohio)

In order to support the targets under test, AFRL uses very low radar cross section mounting structure. This consists of a tilted metallic wing-like structure referred to as a target support “pylon”. Since most of the pieces in this assessment were fairly light (the largest was well under 20 kilograms, and some as light as 0.5 kg), we use a lightweight foam cylinder to support the test objects. Figure 9 shows one of the very lightweight space thermal blankets held in place for RCS testing. Note that the tiny RCS contribution due to the mounts can be coherently subtracted out of the RCS test so that they do not contribute measurably to indoor RCS measurement uncertainty. The steel platform that surrounds the sample in Figure 9 is the target placement work platform, which is



Figure 9 –Thermal Blanket on Low RCS Support at the AFRL Compact Range.

removed from the facility during the actual RCS measurement. The sample, as mounted in the range, can be seen in Figure 10 below. For scale purposes, the sample in Figure 10 is roughly 30 cm (12 inches) on a side. The reflector is 19 m forward, and its dimensions are roughly 14 m x 14 m.



Figure 10 – ML-004 TPS Blanket in the AFRL ACR for UHF RCS Testing

There is one other aspect of the radar testing worth mentioning. The earth based radar systems transmit an electrical field whose orientation constantly revolves with time perpendicular to the axis of propagation. This is technically referred to as “circular polarization”, and used by space based and weather radars because of its superior ability to penetrate clouds and rain. Although RCS is not a function of weather and rain, it is a function of the orientation of the electric field. In the AFRL ACR, we measured the two linear polarizations, horizontal (or HH) and vertical (or VV). We then combined these results mathematically respectively to re-create the equivalent on-orbit circular

polarization (CP) results. (The PAVE PAWS results previously mentioned in earlier sections report CP RCS results.) The “linear to CP” conversion routine was tested theoretically and experimentally with a known 12 inch by 12 inch flat metallic plate, and is shown in Figure 11. The green trace shows the UHF RCS for HH polarization, the red trace for VV polarization, and the blue trace show the results for circular polarization.

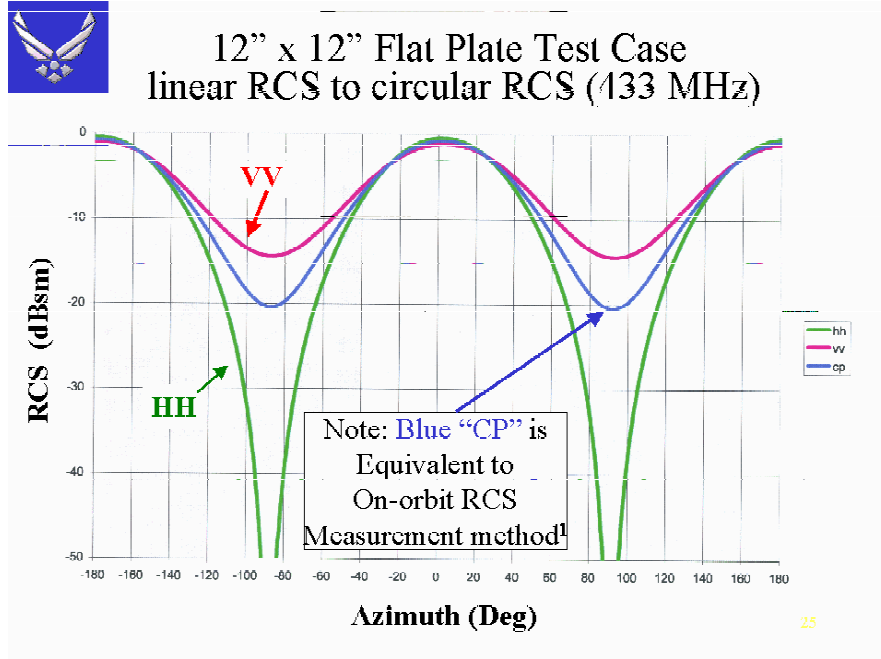


Figure 11 – Linear and Circular Polarization UHF RCS Results for a Simple 12” by 12” Flat Metallic Plate

This leads me to the final comment about this section. Of the 31 items identified by NASA for consideration in the FD2 identification process, some of these items had very simple geometries and others had very complex geometries. In the simple cases, notably the flat plate-like samples, we only needed to mount the test article once and rotate the object 360 degree off a single axis. We chose orientations we were reasonably certain would present the minimum and maximum RCS to the direction of the radar. For the complex targets like the carrier panels, spanner beam insulation pieces, and RCC tee seal and edge samples, we mounted the device in up to three different “near orthogonal” orientations. (Because of the complex shapes, precise 3 axis orthogonal mounts were impractical and unnecessary). We chose the three axes to present the minimum and maximum RCS in the various rotational planes. When you added the multiple configuration mounts to the 31 materials considered, we reported over 40 different target mount results. Therefore, the reader should not get confused when more RCS “results” are reported than candidate materials, since several candidates were measured in several orientations.

Before we move into the final down selection process, it would be appropriate to use some of the actual UHF RCS measurements to illustrate our down selection process

This document may only be publicly released by the authority of the Columbia Accident Investigation Board

in detail. Figure 12 shows the measured linear and CP UHF RCS results for the AFRSI example. The sample plot shows the item tested photographically, the actual linear and circular RCS data, and a square “box” that represents the range of the on-orbit RCS measurements of the FD2 object. Remember, in this data display, the RCS in blue must exceed or “break” the top of the observed on-orbit RCS limits to be a viable candidate. RCS values that are several decibels below the peak are not viable candidates for the FD2 object. Since this is a decibel scale, it is clear that the RCS of AFRSI is 2 or more orders of magnitude too small. This object would be quickly rejected as a potential candidate for the FD2 object based solely on the RCS data. If we perform the same measurement of one of the payload bay TCS blankets, namely MLI-004, the UHF RCS results are shown in Figure 13. Based solely on RCS test results alone, one would have to consider the MLI-004 a very viable candidate for the FD2 piece.

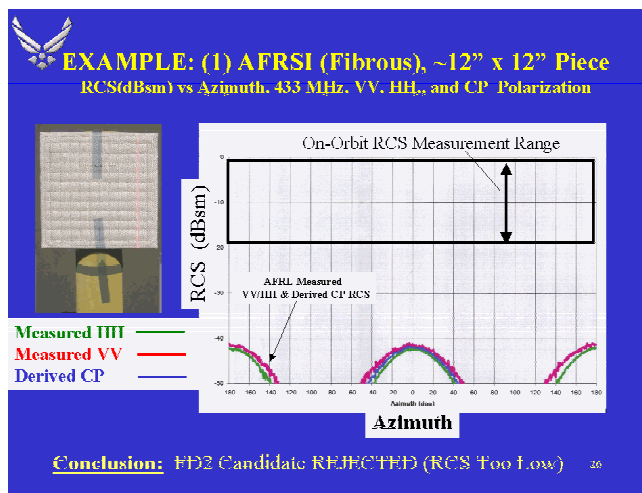


Figure 12 – AFRSI CP UHF RCS Measurement of a 12” by 12” Sample

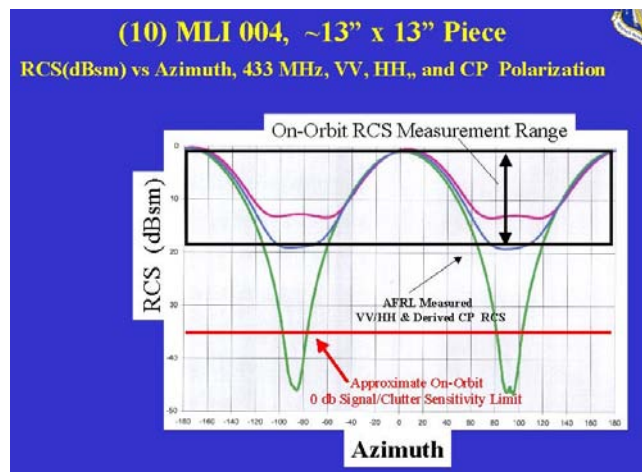


Figure 13 – MLI-004 TPS UHF RCS Measurement of a 13” by 13” Sample

Looking at the results of Figures 12 and 13 the RCS test and elimination process looks fairly straightforward. When we combine our knowledge of the ballistic coefficient or “B-term” for these cases, the situation becomes much clearer. A “B-term” analysis shows the MLI-004 (and other similar thermal blankets of the TPS system) are a factor of 7 or more too light to exhibit the B-term properties of the FD2 object. The MLI-004 object above, for instance, was rejected as a FD2 candidate based on the exclusionary B-term analysis. The AFRSI blanket failed both the “B-term” test, and the RCS test, and therefore was also rejected as the FD2 candidate. In a similar fashion, the team methodically proceeded through all the configurations and materials NASA identified as potential candidates.



### Section V - Best Assessment of the Flight Day 2 Object Composition

Since the nature of this report is to produce an overall description and working summary of the results, the readers will be spared a detailed description of every B-term calculation and UHF RCS measurement performed under this study. The interested reader can refer to our originally reported UHF RCS results on the CAIB web site at [WWW.CAIB.us](http://WWW.CAIB.us), under May 6, 2003 public hearing, to see a complete summary of the UHF test results produced under this effort. At this point, it would be advantageous to create a table summarizing all of the materials screened, and then present relevant RCS and ballistic coefficient data for only those items that survived the dual screening criteria.

Table 1 shows the complete list of candidate materials evaluated by the FD2 assessment process. Glancing over the table, it is evident the RCS tests eliminated 14 of the tested components, while the B-term analysis eliminated 18 candidates. The thermal protective materials making up the TPS system are generally lightweight and are very inefficient scattering devices. Most of the results exhibited exceptionally low RCS, especially the Shuttle thermal tiles, FRSI, and AFRSI materials. Looking over many of the Thermal Control System (TCS) samples, many of them exhibited good RCS levels at UHF frequencies. This should be no surprise since most of the TCS systems consist of metalized Mylar or Kapton, so many of these samples scattered similar to the 12” by 12” flat plate test case presented earlier. However, these classes of objects are very lightweight, so their area to mass “B-term” calculations were far above the observed on-orbit quantity of 0.1 m<sup>2</sup>/kg. Figure 14 shows representative values for the area-to mass for some of the components listed in Table 1 as “excluded” under the B-term analysis. Specifically, it is seen that the TCS samples are generally too light to meet the observed B-term value for the FD2 object.

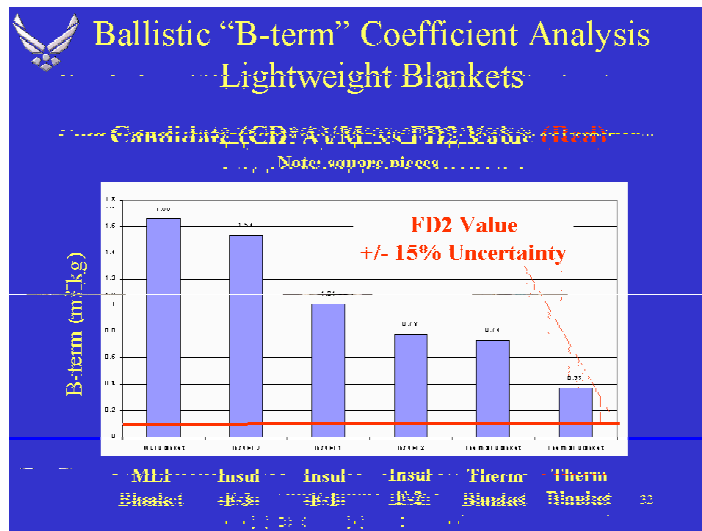


Figure 14 – B-term Calculation for 6 of the TCS Samples  
Note that other TCS samples behaved similarly.

Table I - Summary of Ballistic and UHF RCS Results for FD2 Candidate assessments

Test Article	UHF RCS Results	Ballistic “B-term” Results	FD2 Candidate Conclusion	Comments
AFRSI	Excluded	Excluded	Excluded	12” x 12” sample
FRSI	Excluded	Excluded	Excluded	
HRSI LI900	Excluded	Excluded	Excluded	9 lb/ft <sup>3</sup> Shuttle tile
Dense HRSI LI900	Excluded	Excluded	Excluded	9 lb/ft <sup>3</sup> tile densified
HRSI LI2200	Excluded	Not Excluded	Excluded	22 lb/ft <sup>3</sup> Shuttle tile
Fib 001 TPS Blanket	Not Excluded	Excluded	Excluded	
Fib 002 TPS Hinge	Not Excluded	Excluded	Excluded	
Fib 003 TPS Radiator	Not Excluded	Excluded	Excluded	
Beta Cloth, no thread	Excluded	Excluded	Excluded	
Beta Cloth, metal thread	Excluded	Excluded	Excluded	
MLI004 Cargo liner	Not Excluded	Excluded	Excluded	
Freestar panel “A”	Not Excluded	Excluded	Excluded	
Freestar panel “B”	Not Excluded	Excluded	Excluded	
Freestar panel “C”	Not Excluded	Excluded	Excluded	
Freestar panel “Logo”	Excluded	Excluded	Excluded	
TPS Ins. Blanket 1	Not Excluded	Excluded	Excluded	
TPS Ins. Blanket 2	Not Excluded	Excluded	Excluded	
Lower Carrier Panel seg	Excluded	Not Excluded	Excluded	<b>Without</b> horse collar
Lower carrier panel seg	Excluded	Not Excluded	Excluded	<b>With</b> horse collar
Upper Carrier Panel	Excluded	Not Excluded	Excluded	
RCC Flight Edge Panel	Not Excluded	Excluded	Excluded	All bolts & tee seal
“Ear Muff” TPS Seal	Not Excluded	Not Excluded	Not Excluded	“Spanner beam insulator”
4-Tile lower carrier panel	Excluded	Not Excluded	Excluded	“Flight hardware”
3-Tile lower Carrier Panel	Excluded	Not Excluded	Excluded	“Flight hardware”
RCC Tee Seal (whole, #6-11)	Not Excluded	Excluded	Excluded	
TPS Crimping tool	(Not tested)	Excluded	Excluded	Similar for other tools
<b>These Samples below are representative “Acreage” RCC fragments taken from recovered “right side” pieces</b>				<sup>1</sup> <b>Note:</b> RCC acreage pieces must be on the order of 0.33” thick to meet B-term. These occur only in RCC panel areas 8,9,10. See text for complete description
RCC Fragment #51311	Not Excluded	Not excluded <sup>1</sup>	Not excluded <sup>1</sup>	RCC Fragment with lip
RCC Flat acreage #2018	Not Excluded	Not excluded <sup>1</sup>	Not excluded <sup>1</sup>	Locally flat
RCC Fragment #37736	Not Excluded	Not excluded <sup>1</sup>	Not excluded <sup>1</sup>	Large curvature, no lip
Tee Seal Fragment #51313	Excluded	Not excluded	Excluded	~34”, no flange or apex

Used together, the RCS and B-Term exclusionary tests eliminated all but 4 items making up 2 different classes of materials. Let’s examine each of the candidates that survived the exclusionary tests in detail.

We wish to begin with the “Ear Muff” spanner beam insulation piece. Made of “Inconel”, a nickel alloy, with internal Cerachrome batting, the purpose of this piece is to protect the interior aluminum spar from the heat reradiated from the RCC edges into the

*interior cavity* of the Shuttle edge. The principle threat is the reradiated IR from the RCC could damage the aluminum spar of the Shuttle if this piece were not present. However, for this piece to come out in orbit, several things would have to happen first. (1) A sufficiently large breach in the RCC would be required so as to allow this piece the opportunity to float out while on orbit. (2) The "ear muff" would have to break free of its four fasteners. This is where the third criteria discussed in Section IV comes into play. There is no forensic evidence to indicate the RCC edge and spanner piece were absent upon re-entry. In fact, forensic evidence indicates most of the RCC edge was originally in place, and chemical analysis performed on some of the recovered debris fragments in the vicinity of left wing RCC panel 8 and 9 show Inconel metal was deposited onto the recovered left wing RCC debris fragments. This reasonably excludes the possibility that the spanner beam insulator was absent, meaning it could not have been the FD2 object.

NASA engineers diligently brainstormed and thought of every lost tool or device that potentially could have been left in the Columbia's payload bay. After all, previous missions had released small, unexpected items from the payload bay into space. Scouring tool records and receipts, over a two year period, the NASA FD2 team assembled a list of about 10 tools/objects that "could have" been left in the payload bay at some time in the past. These included lost screwdrivers, sockets, and hex head Allen wrenches. Using our RCS expertise and the sizes of the tools, we quickly rejected them out of hand because their sizes were not consistent with the sizes necessary to produce the -1 dBsm circular polarization RCS peak observed on orbit. The AFRL team found no postulated tool or device other than those found in Table 1 that could have met the dual criteria for the FD2 object.

As of the CAIB public hearing of May 6, 2003, based on the measured UHF RCS data *available at that time*, AFRL/SN believed the Tee-seals could not be eliminated as a potential candidate for the flight day two object. However, we acknowledged at the hearing that there was a measurement inconsistency between the station 21 43" Tee-seal measured UHF RCS data results and the 35" measured Tee-seal fragment 51313. The former RCS results seemed to indicate the Tee-seal *was* a candidate for the FD2 object, while the latter UHF measurements seem to indicate it *was not* a candidate for the FD2 object because its UHF RCS values were too low. We testified that a more detailed study of the Tee-seal was warranted because we had only a approximate idea what length of tee seal fragment was needed to reach the requisite UHF RCS values for the FD2 object.

AFRL/SN rigorously followed up our 6 May 2003 testimony and the measurement discrepancy with a thorough study of the RCS characteristics of Tee-Seals #6 though #11 on the left side. Using the Boeing CARLOS moment method code, we systematically "cut up" a tee seal geometry in an incremental fashion and recomputed its RCS for tee-seal #9 starting with the region beyond the flange and adding one inch at a time until the entire tee seal was re-created. The results of this assessment were the following: (1) In no case, at 433 MHz, was the peak RCS of a partial Tee-seal as large as the RCS of a whole tee seal. (2) Although the Tee-seal 21 had a predicted CP RCS close to the -1 dBsm +/-1.3 dB peak value within the limit of the on-orbit measurement uncertainty, Tee seal 21 was only provided as a notional case, and is not of real interest in

the current accident scenario. The Tee-seals #6 through #11 were of most interest. (3) No combinations of angles and Tee-seal piece sizes for Tee-seals #6 through #11 produced a Tee-seal candidate whose RCS met the  $-1$  dBsm maximum within the  $\pm 1.3$  dB on-orbit uncertainty.

The Tee-Seal #9 is shown in Figure 15 as it is incrementally “cut up” on the computer, and Figure 15 also shows the global maximum RCS calculated by Carlos for nearly  $4\pi$  steradian coverage. This analysis, along with the correction of the original RCC Station 21 Tee-Seal RCS data from the 6 May 03 testimony now *eliminates the Tee-Seal as a possible candidate for the FD2 object*.

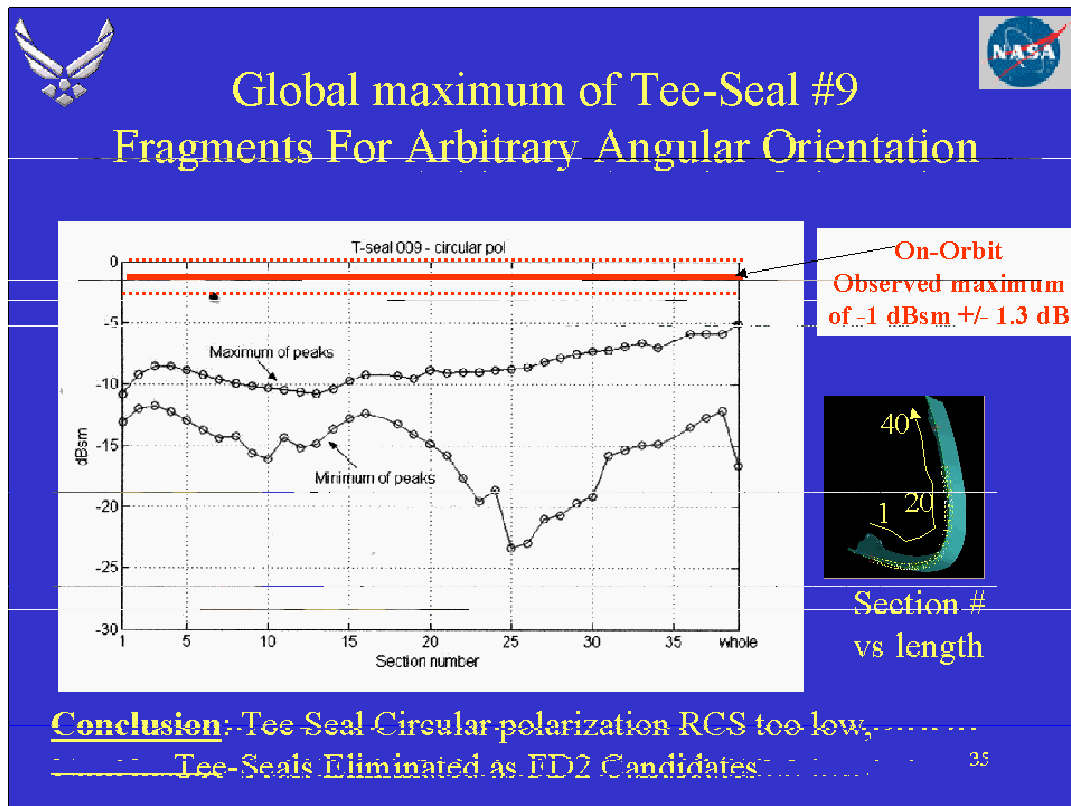


Figure 15 - Global RCS maximum and minimum of peaks of Tee-seal 009 versus incremental length. The highest possible RCS occurs for the whole Tee-seal.

To ascertain the validity of the RCS predictions, AFRL/SN laser scanned the tee-seal #21 provided by NASA-JSC and compared linear RCS measurements to CARLOS predictions. Initially, the prediction and measurement comparisons were off by 3-4 dB. We therefore re-examined all measured RCS data relative to the station 21 tee seal and tee-seal fragment 51313. We found that *for this set of files only* we had used the wrong theoretical calibration file in the creation of our original measured UHF RCS data for the Station 21 tee-seal. This produced RCS data that was about 3-4 dB higher than originally

reported. Once we made the correction for the station 21 Tee-seal RCS results, we found that the resultant measurements and predictions were in outstanding agreement, giving our team confidence that the tool was working properly. A sample of the comparisons between theory and measurements of Tee-Seal #21 is shown in Figure 16 below. Note that Figure 16 shows the two linear polarization components. The circular polarization would lie somewhat between the two curves, clearly lower than the on-orbit circular polarized RCS maximum of  $-1 \text{ dBsm} \pm 1.3 \text{ dB}$ .

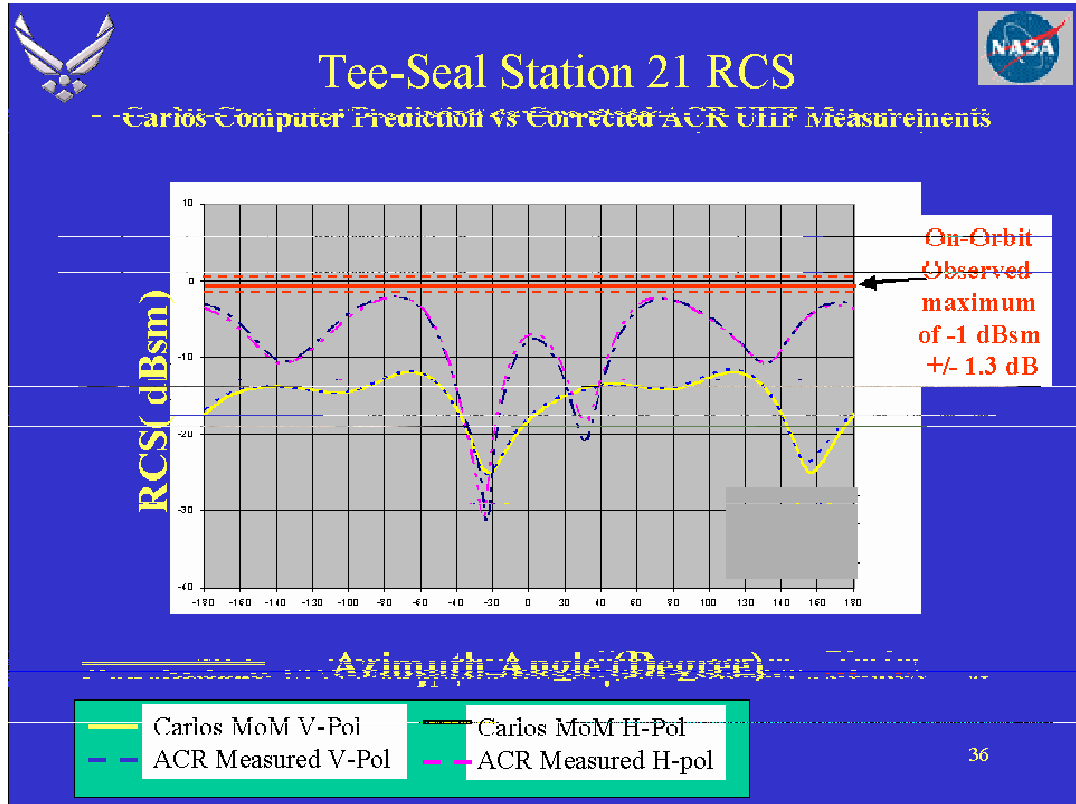


Figure 16 – Predicted CARLOS 3D RCS Vs AFRL/SN ACR UHF RCS Measurements at Linear VV and HH Polarizations. Note Tee Seal 21 is now below on-orbit observed maximum RCS for the FD2 Object. (From Appendix I)

We also thoroughly explored the resultant variations due to the unknown relative phase between HH and VV polarization in the prediction of the CP polarization. However, we also know we are interested in exploring the peak values of observed RCS, and that the peak observed RCS in CP could never exceed the highest linear polarization RCS data point, per the linear to CP polarization conversion equation in Appendix 1, equation 1. Once we understood that the CARLOS predictions and laboratory measurements assumed different phase reference points, the differences are easily explained.

This document may only be publicly released by the authority of the Columbia Accident Investigation Board

The overall conclusion of the detailed tee-seal RCS study is that, within on-orbit measurement uncertainties, AFRL/SN now believes the tee seal (#6,7,8,9, 10, or 11) are **no longer viable candidates for the FD2 object** based on our extensive evaluation of both whole tee-seals as well as fragmentary tee seal predictions.

Having provided background on what we could “eliminate” let’s now shift towards FD2 candidates we *cannot eliminate*. These include mainly fragments of leading edge RCC panels that might have been created in the event the RCC edge was struck in flight. Our team measured an entire RCC edge (although it was rejected as the FD2 object based on ballistic characteristics), and then measured 4 selected pieces of RCC debris recovered from Columbia’s *right wing*. Several relatively small pieces of RCC were found to provide sufficient signature to meet the UHF RCS criteria. However, forensic evidence rejects the idea that an entire leading edge wing segment departed the Shuttle on FD2, so we must consider more realistic cases. At this point, it became clear to us that if part of the RCC TPS system did separate from the Shuttle on FD2, it represented a serious issue regarding re-entry.

Since cutting up flight RCC hardware was prohibitively expensive, we requested permission to visit the Kennedy Space Center (KSC) Columbia debris recovery hangar to examine and select RCC fragments from the recovered *right wing* of the Orbiter that would be representative of RCC fragments that may have originated in flight on the *left wing*. We selected four RCC “fragments” from the Panel 8-9 area of the Orbiter’s right side, and brought these samples back to WPAFB for additional compact range testing. Some of the RCC samples were relatively flat, others had lips or edges to them (sometimes called “webs”), while others had large curvature. However, the physical area of the RCC fragments chosen ran from ~90-140 square inches in physical size. In addition, we borrowed a recovered Station 9 Tee-Seal fragment approximately 35 inches in length, the largest recovered Tee-Seal piece found on the right side in the area of panels 8, 9, and 10. A picture of these debris fragments is shown in Figure 17 below.



Figure 17 – RCC Fragments 51313 (Tee-Seal), 51311, 2018, and 37736 Recovered from Columbia’s *right wing*

This document may only be publicly released by the authority of the Columbia Accident Investigation Board

Fragment 51313 did not meet the on-orbit RCS values, which is consistent with the RCS computational analysis performed on a 35 inch piece of RCC tee-seal shown in Figures 15. Between the measured results (as corrected) for the station 21 Tee-seal and the fragment 51313, the Tee-seals were ultimately eliminated as candidates for the FD2 parts.

Subsequent RCS testing of the other RCC debris fragments showed their UHF RCS was consistent with on-orbit measurements, showing that fragments of RCC “acreage” could not be rejected as a class as the FD2 object. Figure 18 shows the RCS test results, while Figure 19 shows the B-term ballistic analysis.

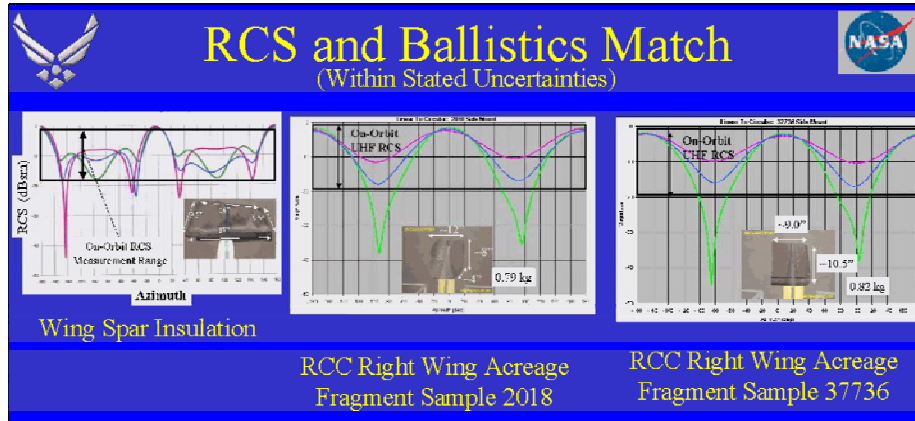


Figure 18- UHF RCS Test Results for RCC Acreage Pieces

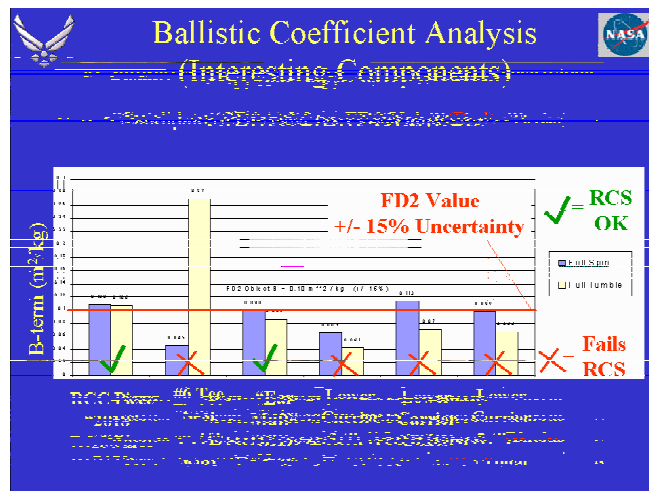


Figure 19- B-Term Analyses Results for RCC Tee seal and acreage pieces

Looking at the analysis of Figure 19, the RCC acreage piece “2018” fits very nicely with the observed on-orbit B-term data. Interestingly enough, the piece *only* fits the B-term if it is on the order of 0.33” thick. The RCC panels in the vicinity of the so-called “shock-shock” region of the wing are, in fact, 0.33” thick in the lower panel acreage regions. Most of the RCC on the Shuttle is only 0.25” thick, and this value is too

This document may only be publicly released by the authority of the Columbia Accident Investigation Board

low to meet the B-term. So the analysis indicates that RCC panels originating in the areas of panels 8,9, or 10 could meet these criteria. The other components shown in Figure 19 were rejected based on their RCS test data.

What can we conclude from the data and analysis performed to date? Clearly, RCC panel acreage satisfies both the B-term and UHF RCS criteria. Such a panel would have to be minimally 90-100 square inches in size, though larger sizes of 120-140 inches square clearly meet the criteria as well. Since the wavelength of the UHF radar is 27.28", pieces with local curvature or a lip will still scatter similar to the values shown above. After a review of the corrected Tee-seal #21 data, as well as an extensive computational examination of RCC Tee-seal scattering described in Appendix I, no Tee-Seal from Seal #6 through seal #11, whether whole or in a fragment, met the UHF RCS maximum, and are hereby eliminated as a possibility for the FD2 object.



## Section VI - Summary

In summary, the FD2 candidate list has been substantially reduced to the most probable candidate. This candidate is a class that includes a fragment of RCC panel acreage (0.33" thick) on the order of 90-140 square inches. All other candidates evaluated from the list of exterior Orbiter TPS or TCS materials failed to meet one or both of the RCS or B-term physically observed data. One candidate ("Ear muff seal") is not supported by the forensic debris evidence, and was rejected by that consideration.

Does this mean we can say with certainty the FD2 object was an RCC fragment? No, this cannot be said with absolute certainty, because the FD2 object burned up and was not recovered. Does this mean that something else could have been the FD2 object? We concede this is a distinct possibility, although we as a team evaluated every candidate NASA has provided us, and to our knowledge the candidate list is exhausted at this time. Certainly if a new candidate emerges even after this report is written, AFRL and US STRATCOM could still evaluate that candidate and a potential FD2 object. But as of the date of this report, the only candidate we have to offer for the FD2 piece from a list of materials that are routinely present on the Orbiter is an RCC panel fragment originating in the region of #8, 9, or 10.

What can be said is that *if* the FD2 piece was a small acreage piece of RCC, that scenario is consistent with other aspects of the overall CAIB investigation. In addition, *if* the FD2 object was an RCC fragment of the size indicated (90-140 square inches) this missing piece would represent a serious breach in the RCC Thermal Protection System, and could well explain the remaining events that occurred on re-entry.

## Section VII - References

[1] Hill, Paul s., Spencer, Ron, Edelen, Chris, Proud, Ryan W., Mrozinski, Richard B, Graybeal, Sarah R., Mendeck, Gavin F, Hartman, Scott, Herron, Mellisa, **Columbian Early Sighting and Assessment Team (ESAT) Final Report**, 13 June 2003, NASA-Johnson Space Center Mission Operations Directorate

[2] Cook, Chuck, Beauchamp, Karen, VonNiederhausern, **Bolt Catcher Debris Analysis for Shuttle STS-107**, Technical Note 25 June 2003

**THIS PAGE INTENTIONALLY LEFT BLANK**



# Volume III

## Appendix E.4

### Columbia Early Sighting Assessment Team Final Report

This Appendix contains NSTS-60507 *Columbia Early Sighting Assessment Team Final Report*, 13 June 2003.

### 10.3. DOD - JSC Actions

#### DOD Data Priorities

- 1) Process all data from 1340Z -1400Z for high-energy events (include any luminosity and spectral analysis which may indicate size, mass and constituents). Key events to focus on:
  - Discrete debris shedding times.
  - Times associated with off-nominal tlm signatures.
  - Times indicated as off-nominal in infrasonic data (infrasonic data collection in work separately)
  - Bolide detonation reported from Oceanside, CA 1300-1410Z
- 2) Process all data from Beale Pave Paws
- 3) Confirm any and all imagery from 1 Feb 1340-1400Z has been identified, processed and received
- 4) All data from de-orbit burn through break-up
- 5) Process the object that has been correlated back to Columbia approx 24 hrs after launch
- 6) Provide trajectory data to all other national agency/organizations so they can check for data
- 7) Confirm any and all imagery from Ascent-2 Feb, 1340Z has been identified, processed and received
- 8) Any "unexpected events" DOD might identify throughout duration of mission via own analysis

Closed	Priority	Actionee	Request
	1	DOD	Detailed data from NAVSPASUR re AZ, NM fence detects. In work. Expected 2/28.
	1	DOD	Pam Clark, Army Research Lab pclark@arl.army.mil 410-203-2133, 301-394-3447 Apparently passed on classified information to Dave Hess regarding infrasonic data recorded by a military sensor which shows an event over Arizona. It mentions that this was recorded by White Sands. Suggests they have time, range, altitude. Please follow up May be rolled into the action below.
	1	DOD	Coordinate with Fusion Analysis Cell on infrasonic data and other sensor data for: entry day bolide reports, other infrasonic event correlation to Shuttle timeline and ground track.
	6	JSC	In a separate run of the ephemerides, add the following locations: Alice Springs, 23.5 deg S X 134 deg E; Longreach, 22 deg S X 144 deg E; and Laverton, 28.66 deg S X 122.5 deg E. If they show possible acquisitions, especially for the entry ephemeris, then NASA should pursue getting the data from Australia. DM has it and will add it to the hopper.
	6	DOD	Can you reach into civilian intelligence databases for assets which may have been tasked to regions Columbia overflow in the event they captured images? Optical assets over the Middle East come to mind if there are any, since we flew over and I'd expect it to be a hot intel area now. In work.
2/7/2003	9	DOD	DOD approved Kirtland photo for released. NASA released it.
2/8/2003	1	JSC	DM/Greg Oliver sent Columbia GPS data to Simpson.
2/8/2003	1	DOD	DOD confirmed no other fences similar to NAVSPASUR.
2/8/2003	9	DOD, JSC	Confirmed JSC Orbital Debris Program will request data through the NASA and DOD POCs. Normal working relationships permitted to continue with POCs in the loop.

<b>Closed</b>	<b>Priority</b>	<b>Actionee</b>	<b>Request</b>
2/9/2003	1	DOD	Ames is offering help with photo/video analysis. They suggested that DOD may have spectral data from entry that would help them estimate size, material and mass of the debris. Ring a bell, and if so, are you expecting data back? I'll forward Ames contact info to you for security clearance verification on any classified (including the data you brought last week).
2/9/2003	9	JSC	Updated NASA data request priorities.
2/10/2003	1	DOD	DM/Greg Oliver is interested in getting help from Dick Stearns. Mr. Stearns has been notified.
2/12/2003	5	JSC	Provide DOD with the following for FD2 radar analysis: <ul style="list-style-type: none"> <li>- Precision ephemeris on the Shuttle for day 17</li> <li>- The density (gm/cm**3) of heat tiles, carbon-carbon leading edge, spacecraft aluminum, and tool steel</li> <li>- A summary chart of the accelerometer events for all of day 17</li> </ul> Density data e-mailed 2/12/03. Full flight ephemeris e-mailed 2/12/2003. DF6/Sarafin and Allega working accel tlm.
2/12/2003	5	JSC	ES3/Steve Rickman sent material descriptions and densities for external components, specifically various TPS materials.
2/12/2003	6	JSC	Entire ephemeris (on orbit and entry) for STS-107 through the SAT ACQ program using every sensor that they have in their database with an elevation angle of -5 degrees E-mailed 2/12/2003 by DM/Leleux.
2/12/2003	6	JSC	Ephemeris for the entire flight. At this time vectors every 6 hours in the ECI format would suffice. In work. E-mailed M50 2/12/2003 by DM/Leleux
2/14/2003	1	DOD	E-mailed unclass DOD data estimating possible Orbiter debris shedding events and impact locations.
2/14/2003	3	DOD	Confirm Maui and Kirtland do not have any other images, classified or unclass, which would help evaluate both leading edges and the bottom surface of the orbiter, whether in orbit ops or during entry. Confirmed no other entry images 2/11/2003. Confirmed no other orbit ops images exist 2/14/2003 via JSC call to Maui.
2/14/2003	5	JSC/DOD	Telecon with Bob Morris re other thermal insulation on the exterior and PLB.
2/17/2003	8	DOD	Approve normal working interface between individual below and JSC Engineering to discuss and obtain any available information concerning the properties of Kapton (polyimide) insulated wire in high/extreme heat conditions. This may help in precluding duplicate testing already performed by the DoD or guide us better in developing our own test to characterize the data seen on STS-107.  George A. Slenski AFRL/MLSA 2179 12th Street, B652 Rm 25 WPAFB, OH 45433-7718 Phone: 937-656-9147 e-mail: george.slenski@wpafb.af.mil
2/18/2003	1	DOD	Provide any DOD ascent video for NASA review and analysis. DCIST approved Patrick AFB provide their asc video to NASA.
2/18/2003	3	DOD	Provide Kirtland camera location and pointing information in support of entry photo. Also provide Kirtland POC to discuss engineering analysis.

<b>Closed</b>	<b>Priority</b>	<b>Actionee</b>	<b>Request</b>
2/19/2003	3	DOD	Post-process AMOS imagery for: indications of upper surface leading edge damage; missing thermal insulation in the payload bay, including but not limited to the SpaceHab trunnions.
2/19/2003	8	DOD	Provide OAFS/VTS data per GSFC- Ted Sobchak/ND, (301) 286-7813 Approved 2/13/03. In work.
2/21/2003	4	DOD	Confirmed no ship based or AWACS radar data taken during entry.
2/21/2003	5	DOD, JSC	It was reported to JSC-SX/Nick Johnson from DOD that an object was tracked separating from the orbiter at 5 m/s, 17 Jan, 1600Z (STS-107 flight day 2). JSC is pulling timeline data for water dumps, which may account for this. We will also evaluate accelerometer data much more closely on this day. We had already decided to screen all accelerometer data for the full mission. No water dumps. Manual fuel cell purge initiated 1625Z. Accelerometer data tracked in another action.
2/21/2003	8	DOD	Confirmed no tracks objects approached within 5 km of Columbia throughout orbit ops.
2/24/2003	1	JSC	Debris sighting data on timeline. In work. Sent ground track with rev 12.1 but no sightings on 2/12/2003. 1 <sup>st</sup> 6 discrete shedding times to ship 2/13. Remainder expected 2/20.
2/27/2003	1	DOD	On a similar note, we're hearing from NOAA that there is some DOD site on the west coast with infrasonic capability similar to what NOAA is sending us from Boulder, CO. He suggests that the west coast data could show us good data over the Pacific. DOD request went to AFTAC for this data. JSC requested direct support to NOAA-LANL review in Colorado. Message 2/18/2003: The "Center for Monitoring Research at the Defense Threat Reduction Agency in Arlington, VA" has apparently "forbidden" DOE to get involved in the investigation. Various data is being withheld from LANL, including Air Force Technical Applications Center data. DOD data analysis in work.
2/27/2003	2	DOD	Confirm Vandenburg and/or any other DOD tracking did not track Columbia. Provide raw tracking radar data for debris searches. 84 <sup>th</sup> RADES has all DOD ATC radar.
2/27/2003	5	DOD	Based on the possible FD2 debris strike, focus radar searches to obtain skin paints before 17 Jan 1600Z, any time after, and as late as possible before deorbit. No data.

## 10. Appendices

### 10.1. Team Members and Contributors

<b>Early Sighting Assessment Team Members</b>	
<b>Hill, Paul</b> - Flight Director	ESAT Lead - DA8
<b>Koerner, Cathy</b> - Flight Director	Co-Lead - DA8
<b>Oliver, Greg</b>	Management Coordination (DM4)
<b>Anthony, Col Jack</b>	DCIST POC to NASA
Bryant, Jeralynn	Admin support-DA8
Shaw, Jackie	Admin support-DA8
Moore, Patti	DB Tracking-DA8
Spohr, Rob	DB Tracking-DA8
<b>Conover, Sharon</b>	Sighting Reports - OA/MA
<b>Craig Schafer</b>	Sighting Reports, DB Tracking - OZ4/SAIC
<b>Beck, Kelly</b> - Flight Director	Sighting Reports-DA8
<b>Ceccacci, Tony</b> Flight Director	Sighting Reports-DA8
<b>Curry, John</b> - Flight Director	Sighting Reports-DA8
<b>Knight, Norm</b> - Flight Director	Sighting Reports-DA8
<b>Lunney, Bryan</b> - Flight Director	Sighting Reports-DA8
<b>Abadie, Marc J.</b>	Ballistics (Co-lead) (DM4)
<b>Gowan, John W.</b>	Ballistics (Co-lead) (DM4)
Conte, Barbara A. (DM44 Lead)	Ballistics, Group Lead (DM4)
<b>Mrozinski, Richard (Rich) B.</b>	Footprints (Lead) (DM4)
<b>Graybeal, Sarah R.</b>	Footprints (DM4)
Kadwa, Binaifer (Bini) K. (Co-Op)	Footprints (DM4)
<b>Mendeck, Gavin F.</b>	Footprints (DM4)
Chi, George	Footprints/Groundtrack QA (DM4)
Rask, John (Doug) D.	Ground tracks/Timelines (DM4)
<b>Hartman, Scott A.</b>	RAT (Radar Analysis Team) (lead) (DM4)
<b>Herron, Marissa S.</b>	RAT (b/u lead) (DM4)
<b>Evans, Michael</b>	RAT (DM2)
<b>Brogan, Jonathan</b>	RAT (DM3)
<b>Zaczek, Mario</b>	RAT (DM3)
<b>Braun, Angela N.</b>	RAT (DM4)
<b>Cutri-Kohart, Rebecca M.</b>	RAT (DM4)
<b>Shaver, Matthew (Matt) D.</b>	RAT (USA Navigation)

<b>Early Sighting Assessment Team Members</b>	
<b>Spencer, James R. (Ron)</b>	Sighting - Video Screening (Lead) (DM4)
<b>Edelen, James C. (Chris)</b>	Sighting - Video Screening (DM4)
<b>Proud, Ryan W.</b>	Sighting - Video Screening (DM4)
Bentley, Dennis L.	Sighting Team Support (DM4)
Branham, Doug	Sighting Team Support - DF
<b>Campa, Todd</b>	Sighting Team Support - DF
Hendrickson, Larry A.	Sighting Team Support (DM4)
Horlacher, Gary	Sighting Team Support - DF
<b>Jarvis, Bobby</b>	Sighting Team Support - DF
Schmidt, Tom	Sighting Team Support (DM4)
Schottel, Matthew L. (Matt)	Sighting Team Support (DM4)
<b>Lawson, Keith</b>	Infrasonics, Seismic, Pointing-DO
<b>Dworak, Natalie</b>	Infrasonics, Pointing-DO
Watts, Karen	Pointing-DO
<b>Johnson, Nick</b>	Orbital Debris-SX
Stansbery, Eugene	Orbital Debris-SX

Individuals in bold invested considerable time to support ESAT



<b>Early Sighting Assessment Team Contributors</b>	
Silvestri, Ray (DM42 Lead)	Footprints Group Lead - (DM4)
Carman, Gilbert	BET vector Transformations (DM4)
Pogue, Glenn	BET/GPS Vector Transformations (DM4)
Blanton, Mark	Pointing-DO
Hemingson, Greg "Ernie"	Pointing-DO
McKinley, David	Pointing-DO
Stocco, Marcos	Pointing-DO
Kling, Jeff	Shuttle Systems, MMACS-DF
Lenort, Dean	Shuttle Systems, PROP - DF
Marasia, Amy	Shuttle Systems, PROP - DF
McCluney, Kevin	Shuttle Systems, MMACS-DF
Cerimele, Chris	Management (EG)
Stuart, Phil	Aero Ballistics (EG3)
Rochelle, Bill	Aero Heating Analysis (EA/LMCO)
Smith, Reis	Aero Heating Analysis (EA)
Dobarco-Otero, Jose	Aero Heating Analysis (EA/LMCO)
Bryant, Lee	Backward Propagation (EG5)
Sostaric, Ron	Ballistics (EG)
Tigges, Mike	Footprints (EG)
Broome, Joey	Mapping (EG5)
<b>Gaffney, Bob</b>	EOC - JA
<b>Perrin, Dennis</b>	EOC - JA
<b>Roeh, Bill</b>	EOC - JA
Curry, Don	Radar Test Support - JSC-ES
<b>Rickman, Steve</b>	Radar Test Support - ES
Schomburg, Calvin	Radar Test Support - JSC-EA
Austin, Larry	Radar Test Support - KSC
Banks, Marvin E.	Radar Test Support - KSC
Chambers, Tony	Radar Test Support - KSC
Henn, Becky	Radar Test Support - KSC
Stoner, Mike	Radar Test Support - KSC
<b>Bower, Dan</b>	Radar Assessment Team - NTSB
<b>Brazy, Doug</b>	Radar Assessment Team - NTSB
<b>Crider, Dennis</b>	Radar Assessment Team - NTSB

<b>Early Sighting Assessment Team Contributors</b>	
<b>Duhham, Scott</b>	Radar Assessment Team - NTSB
Fox, Todd	Radar Assessment Team - NTSB
Gregor, Joe	Radar Assessment Team - NTSB
Grossi, Dennis	Radar Assessment Team - NTSB
<b>Kakar, Abdullah</b>	Radar Assessment Team - NTSB
<b>Kolly, Joe</b>	Radar Assessment Team - NTSB
O'Callaghan, John	Radar Assessment Team - NTSB
<b>Park, Alice</b>	Radar Assessment Team - NTSB
Pereira, Charley	Radar Assessment Team - NTSB
Beaulieu, Steve	Radar Assessment Team - FAA
Olsen, Mark	Radar Assessment Team - FAA
Clark, Chris	Radar Tests - AFRL, WPAFB, OH
Fails, Frank	Radar Tests - AFRL, WPAFB, OH
Forster, William	Radar Tests - AFRL, WPAFB, OH
<b>Kent, Brian</b>	Radar Tests - AFRL, WPAFB, OH
Turner, Dan	Radar Tests - AFRL, WPAFB, OH
<b>Ailor, William</b>	Aerospace Ballistics Management
Hallman, Wayne	Aerospace Corp. Ballistics Lead
Moody, Douglas	Aerospace Corp. Ballistics
Patera, Russell	Aerospace Corp. Ballistics
Rudy, Donald	Aerospace Corp. Video Analysis
<b>Stern, Richard</b>	Aerospace Corp. Ballistics
Bellue, Dan	SMG - Atmospheres (ZS8)
Garner, Tim	SMG - Atmospheres (ZS8)
Lafosse, Richard	SMG - Atmospheres (ZS8)
Oram, Tim	SMG - Atmospheres (ZS8)
Rotzoll, Doris	SMG - Atmospheres (ZS8)
Chimes, Patrick	Image process - GP
<b>Fennelly, Jason</b>	Video processing - GA
Gross, Debbie	Image process - GP
White, Maura	Still image processing - GA
Zarella, Susan	Video processing - GA

<b>DCIST Support</b>	
Maj Gen Hamel	DCIST CHIEF
Col Roberts	DCIST DEPUTY
Lt Col John Amrine	14AF Spt
Maj Brian Renga	14AF Spt
Capt Kevin D. Brooks	14AF Spt
SSgt Tom Dickerson	14AF Spt
Mr Jim Gin	14AF Spt
Lt Col Cyndie Visel	STRATWEST/J33
Maj Paul Pease	STRATWEST/J33
Roger Simpson	NASA LNO to USSTRAT
Stan Newberry	NASA LNO to AFSPC
Lt Col John Kress	AFSPC/XOCS
Maj Eric Olson	AFSPC/XOCS
Gary W. Dahlen	AEROSPACE
Marc Dinnerstein	AEROSPACE
Ruth Matias	AEROSPACE
Eric Urig	AEROSPACE
Doug Vier	AEROSPACE
Col Kenneth Schroer	AFSPC/JA
Maj Robert Ramey	AFSPC/JA
Lt Col Mary Ensminger	AFSPC/FM
Lt Col Andy Roake	AFSPC/PA
DR Finkleman	NORTHCOM/AN
Col Linda Marchione	STRATCOM/J33
Lt Col Rod Burnett	STRATCOM/J33
Maj Jeff Lamb	STRATCOM/J33
Capt Aaron Spaans	STRATCOM/J33
Capt James Taylor	STRATCOM/PA
Julie Holland	STRATCOM/PA

<b>DCIST Support</b>	
Maj John Paradis	STRATCOM/PA
Capt Brett Ashworth	STRATCOM/PA
MSgt Planki	STRATCOM/FM
Capt Mary McLendon	NNSOC
Dr Paul Schumacher	NNSOC
Jon Boers	NNSOC
Larry Gallop	NNSOC
CDR Mark Sanford	NNSOC
Col Pierson	ARSPACE
Matt Scott	ARSPACE
Jay Donnelly	ARSPACE
Dave Svetz	NRO
Lt Col Gene Brown	NRO
Frank Giegerich	NRO
Eleanor Padgett	NSA/DEFSMAC
Jack Bobela	NSA/DEFSMAC
Mr Christian Chatfield	DCI Rep
Mr Joseph Convery	DIA Rep
Maj Jeff Wohlford	CMOC/J3S
MSgt Tom Dickerson	SPACEAF
Maj Bob Rochester	1 SPCS
Robin Thurston	1 SPCS
Chris Irrgang	1 SPCS
Bill Barker	1 SPCS
Steve Casali	1 SPCS
Todd Bunker	1 SPCS
Bill Schick	1 SPCS
Lt Col Bob Gibson	2SWS
6SWS: Bernadette VanBurskirk	21 SW
Norm Davis	21 SW

<b>DCIST Support</b>	
Mike Ayres	21 SW
7SWS: Chet Burress	21 SW
Lt Col Cynthia Grey	45 SW
Maj John Talarico	50 SW
Capt Chris Collins	50 SW
MGen Paul D. Nielsen	AIR FORCE RESEARCH LAB (AFRL)
Col Mark D. Stephen	AIR FORCE RESEARCH LAB (AFRL)
Lt Col Mike Caylor	AIR FORCE RESEARCH LAB (AFRL)
Lt Col Jeff McCann	AFRL/AMOS
Tom Glesny/Dan Diehl	AFRL/AMOS
LtCol Joseph Pugliese	AFRL/STARFIRE
Mr Patrick Serna	AFRL/ RF TW/AR
Herbert (John) Mucks	AFRL/IFEA
Jay Jesse	AFRL/IFEA
Robert Morris	AFRL/VSV
Col Neil R. Wyse	45TH WEATHER SQUADRON
Lt Col Harms	45TH WEATHER SQUADRON
Mr. Bill Roeder	45TH WEATHER SQUADRON
Maj Robert Hauser	AFWA
Capt Herb Keyser	AFWA
Lt Col Rick Rehs	84th RADES
Lanny Clelland	84th RADES
Lt Steve Cruz	84th RADES
TSgt Kevin Powell	84th RADES
Kirk Sharp (NASA POC to 84 RADES)	84th RADES
MSgt John Muir	AFTAC
Alt: Paula Patterson	AFTAC
TSgt Kenneth B. Edgcombe	AFTAC

<b>DCIST Support</b>	
INFRASONIC POCS AND DATA	
Stephen Tenney	Army Research Lab (ARL)
Pam Clark	Army Research Lab (ARL)
Dr Doug Drob	Navy Research Lab (NRL)
Mr. Patrick Wakefield	OUUSD (AT&L)/NCB
Dr. Stephen Mangino	OUUSD (AT&L)/NCB
Bob North	CMR
Dr Xiaoping Yang	CMR
Dr Joydeep Bhattacharyya	CMR
Dr Hans Israelsson	CMR
Mr. Michael Skov	CMR
Dr Bob Woodward	CMR
Dr Rob Gibson	BBN Inc
Dr David Norris	BBN Inc
Dr Gene Herrin	SMU
Chris Hayward	SMU
Alfred J. Bedard, Jr	NOAA/ETO
Dr. Rod Whitaker	LANL
Dr Doug Revelle	LANL
Dr Milton Garces	University of Hawaii
Dr Hank Bass	University of Mississippi
Dr Michael Hedlin	UC at San Diego
Dr Gerald D'Spain	UC at San Diego
Dave Derosher	AEROSPACE
Larry L. Benson	National Air Intelligence Center (NAIC)
Korin Elder	National Air Intelligence Center (NAIC)
TSGT Par Soulati	National Air Intelligence Center (NAIC)
Mr. Randall Bostick (Infrasonic POC)	National Air Intelligence Center (NAIC)

<b>DCIST Support</b>	
Lt Col Dale Smith	Aerospace Fusion Center (AFC)
Peter Soller	Aerospace Fusion Center (AFC)
Todd Beltracci	Aerospace Fusion Center (AFC)
Steve Hammes	Aerospace Fusion Center (AFC)
Maj Anthony Cruciani	Aerospace Research Center (ARC)(Los Angeles)
Col TS Kelso, PhD	Air Force Space Analysis Center (ASAC)
Bob Morris	Air Force Space Analysis Center (ASAC)
Taft Devere	Air Force Space Analysis Center (ASAC)
Nancy Ericson	Air Force Space Analysis Center (ASAC)
Bruce Bowman	Air Force Space Analysis Center (ASAC)

## 10.2. Entry Debris Events Timeline, Version 6 - 05/27/03

### Photo/TV Analysis Team STS-107 Investigation

#### Entry Debris Events Timeline

Photo/TV Analysis Team  
Version 6 - 05/27/03

**This revision slightly modifies the times of debris events 7, 8, and 15 based on a resynchronization of four videos based on ballistic calculations.**

#### Data Summary

The Photo Analysis Team has screened over 140 videos received from the public. Approximately 25 contain good records of debris emanating from the Orbiter plasma envelope. Our emphasis has been on obtaining the most accurate GMT's possible for the debris observations. This report documents the 28 Western-most events identified to date. In addition, the four Eastern-most events for which GMT's have been determined are also listed. The Photo/TV Analysis Team currently does not have any good quality video that covers Eastern Arizona to Central Texas and no video at all that covers Eastern New Mexico to Central Texas. This makes it impossible to link the Western and Eastern segments into a single unified timeline. Finally, all of the videos contain short periods when the Orbiter is out of the camera's field of view, obscured by clouds, or is out of focus. As a result, it is possible that additional events may have occurred which to date have not been seen on available videos.

#### Event Timing

The GMT's for the Western-most seven events (Debris 1-6 and Flash 1) were based upon passage of the Orbiter envelope near celestial objects recorded in three separate videos (EOC2-4-0055, 0034, 0064). The times for Debris 7A and 9 - 14 were based upon passage of the Orbiter envelope near celestial objects recorded in two separate videos (EOC2-4-0098, 0161). Video EOC2-4-0030 overlaps the time period from Debris 6 through Debris 14, providing a unified time check between the former celestial time-referenced events (Debris 1-6 and Flash 1) and latter celestial time-referenced events (Debris 7A, 9 - 15). Key overlapping events were then cross-referenced with other videos that did not have a time reference, in order to compute GMT's for Debris 16.

The time for Debris 7, 8 and 15 were computed by synchronizing the videos in which they were seen to other synchronized videos based on the time of separation of the debris from the vehicle based on ballistic calculations made from these videos.

The GMT's for Flares 1 and 2, which occurred over Eastern Arizona and New Mexico, were based on a verified GMT embedded in the telescope video in which they are seen (EOC2-4-0148-4).

GMT's for the Eastern-most 4 events are based on a GPS time synchronization contained in a video provided by a military source. We then cross-referenced events seen in the military imagery with videos that did not have a time reference. The accuracy of the GPS reference has been verified to be correct.



## Notes

*Each event time, reported below, represents the earliest moment in time when we can distinguish an event outside the Orbiter plasma envelope. Debris times do not represent the point in time when debris physically separated from Columbia, because the Orbiter is not visible within the plasma envelope. A report entitled "STS-107 Early Debris Ballistics Results;" produced by the Early Sighting Assessment Team (EAST) lists the computed separation time from the vehicle of some of the debris events based on ballistic calculations from these entry videos (contact Marc Abadie @ 281-244-5434 or John Gowan @ 281-483-1923 for more information).*

Plasma anomalies (sudden widening and/or brightening in the plasma trail) have been added to the description because after screening a number of videos there is strong evidence to show that when a plasma anomaly is seen, a debris event has almost always occurred.

<b>Western Debris Events</b>			
<b>Event</b>	<b>GMT</b>	<b>EOC Video Number</b>	<b>Description</b>
<u>Debris 1</u>	13:53:46 (+/- 1 sec)	EOC2-4-0056 <u>EOC2-4-0064</u> EOC2-4-0201 Plasma Anomaly seen in EOC2-4-0136	Seen just aft of Orbiter envelope, one second after a plasma anomaly which consisted of a noticeably luminescent section of the plasma trail.
<u>Debris 2</u>	13:53:48 (+/- 2 sec)	EOC2-4-0056 <u>EOC2-4-0064</u> EOC2-4-0201	Seen just aft of Orbiter envelope.
<u>Debris 3</u>	13:53:56 (+/- 2 sec)	EOC2-4-0055 Δ <u>EOC2-4-0056</u> Plasma Anomaly seen in <u>EOC2-4-0064</u> EOC2-4-0136	Seen just aft of Orbiter envelope followed one second later by a plasma anomaly which consisted of a noticeably luminescent section of the plasma trail.
<u>Debris 4</u>	13:54:02 (+/- 2 sec)	EOC2-4-0055 Δ <u>EOC2-4-0056</u>	Seen just aft of Orbiter envelope.
<u>Debris 5</u>	13:54:09 (+/- 2 sec)	EOC2-4-0055 <u>EOC2-4-0056</u>	Seen just aft of Orbiter envelope at the head of a plasma anomaly.
<u>Flash 1</u>	13:54:33.6 (+/- 0.3 sec)	EOC2-4-0009-B EOC2-4-0055 Δ <u>EOC2-4-0034</u> EOC2-4-0066 EOC2-4-0070	Orbiter envelope suddenly brightened (duration 0.3 sec), leaving noticeably luminescent signature in plasma trail.
<u>Debris 6</u>	13:54:36 (+/- 1 sec)	EOC2-4-0009-B EOC2-4-0055 Δ <u>EOC2-4-0030</u> EOC2-4-0066 EOC2-4-0070	Very bright debris seen just aft of Orbiter envelope.
<u>Debris 7</u>	<b>13:55:05 (+/- 1 sec)</b>	<u>EOC2-4-0030</u>	Seen just aft of Orbiter envelope.
<u>Debris 7A</u>	13:55:18 (+/- 1 sec)	EOC2-4-0161	Seen just aft of Orbiter envelope.
Debris Shower A	13:55:23 to 13:55:27 (+/- 1 sec)	Saw Debris EOC2-4-0098 EOC2-4-0161 <u>EOC2-4-0005</u> EOC2-4-0030 Saw Shower <u>EOC2-4-0017</u> <u>EOC2-4-0021</u> <u>EOC2-4-0028</u>	Seen just aft of Orbiter envelope. Over the course of these four seconds a luminescent section of plasma trail is observed which appears to contain a shower of indefinite particles and multiple, larger discrete debris that includes Debris 8, 9 and 10.

D EOC2-4-0055 Replaces a lower quality VHS copy EOC2-4-0026.

<b>Western Debris Events (continued)</b>			
<b>Event</b>	<b>GMT</b>	<b>EOC Video Number</b>	<b>Description</b>
Debris 8	<b>13:55:23 (+/- 2 sec)</b>	EOC2-4-0030 EOC2-4-0098 EOC2-4-0161	Seen aft of Orbiter envelope inside the aforementioned Debris Shower A.
<u>Debris 9</u>	13:55:26 (+/- 2 sec)	<u>EOC2-4-0005</u> EOC2-4-0098	Seen aft of Orbiter envelope inside the aforementioned Debris Shower A.
<u>Debris 10</u>	13:55:27 (+/- 2 sec)	<u>EOC2-4-0005</u>	Seen aft of Orbiter envelope inside the aforementioned Debris Shower A.
<u>Debris 11</u>	13:55:37 (+/- 2 sec)	<u>EOC2-4-0050</u> EOC2-4-0098	Appears at the head of a secondary parallel plasma trail well aft of Orbiter envelope. A second piece of debris is also seen in the secondary plasma trail.
Debris 11A	13:55:39 (+/- 1 sec)	EOC2-4-0098	Seen just aft of Orbiter envelope.
Debris 11B	13:55:40 (+/- 2 sec)	EOC2-4-0098	Seen at head of a parallel plasma trail aft of the Orbiter envelope.
Debris 11C	13:55:44 (+/- 2 sec)	Sees debris and parallel trail: EOC2-4-0098 Sees parallel plasma trail only: EOC2-4-0028, EOC2-4-0050	Seen at head of a parallel plasma trail well aft of the Orbiter envelope.
<u>Debris 12</u>	13:55:45 (+/- 1 sec)	<u>EOC2-4-0028</u> <u>EOC2-4-0050</u> EOC2-4-0098	Seen aft of Orbiter envelope followed by secondary plasma trails.
<u>Debris 13</u>	13:55:56 (+/- 2 sec)	<u>EOC2-4-0005</u> <u>EOC2-4-0017</u> <u>EOC2-4-0021</u> EOC2-4-0161	Seen well aft of Orbiter envelope with momentary brightening of plasma trail adjacent to debris.
<u>Debris 14</u>	13:55:58 (+/- 1 sec)	<u>EOC2-4-0005</u> <u>EOC2-4-0017</u> <u>EOC2-4-0021</u> <u>EOC2-4-0028</u> <u>EOC2-4-0030</u>	Very bright debris just aft of Orbiter envelope.
Debris 15	<b>13:56:10 (+/- 2 sec)</b>	<u>EOC2-4-0017</u>	Seen just aft of Orbiter envelope.
<u>Debris 16</u>	13:57:24 (+/- 5 sec)	<u>EOC2-4-0148-2</u>	Very faint debris just aft of Orbiter.
<u>Flare 1</u>	13:57:54.5 (+/- 1 sec)	<u>EOC2-4-0148-4</u>	Asymmetrical brightening of Orbiter shape.
<u>Flare 2</u>	13:58:00.5 (+/- 1 sec)	<u>EOC2-4-0148-4</u>	Asymmetrical brightening of Orbiter shape.

The Photo/TV Analysis Team currently does not have any good quality video that covers Eastern Arizona to Central Texas (no video is available that covers Eastern New Mexico to Central Texas), making it impossible to link the Western and Eastern segments into a single unified timeline.

<b>Eastern Debris Events</b>			
<b>Event</b>	<b>GMT</b>	<b>EOC Video Number</b>	<b>Description</b>
<u>Debris "A"</u>	14:00:04 (+/-2 sec)	<u>EOC2-4-0024</u> <u>EOC2-4-0018</u> <u>EOC2-4-0118</u>	Large debris seen falling rapidly away from the Orbiter envelope.
<u>Debris "B"</u>	14:00:19 (+/-2 sec)	<u>EOC2-4-0024</u> <u>EOC2-4-0118</u>	Time is for debris first seen well aft of Orbiter envelope.
<u>Debris "C"</u>	14:00:20 (+/-2 sec)	<u>EOC2-4-0024</u> <u>EOC2-4-0118</u>	Time is for debris first seen aft of Orbiter envelope.
<u>Main Body Breakup</u>	14:00:23 (+/-2 sec)	<u>EOC2-4-0024</u> <u>EOC2-4-0018</u>	Onset of the main body breakup.

These times represent a consensus among photo team members from SX, DM, DF and Boeing.

The following list of viewer's locations is provided to correct inaccurate information displayed on some publicly released maps.

\*Viewer locations are rounded and only displayed to two decimal places to protect the individual privacy of the viewer.

<i>STS-107 View Location Data</i>					
<b>EOC</b>	<b>Location</b>	<b>North Latitude* (degrees)</b>	<b>West Longitude* (degrees)</b>	<b>First View of Vehicle (GMT)</b>	<b>Last view of vehicle (GMT)</b>
<b>EOC2-4-0064</b>	<b>Fairfield, CA</b>	<b>38.28</b>	<b>122.01</b>	<b>13:53:15</b>	<b>13:54:17</b>
<b>EOC2-4-0056</b>	<b>Mt. Hamilton, CA</b>	<b>37.34</b>	<b>121.64</b>	<b>13:53:28</b>	<b>13:54:29</b>
<b>EOC2-4-0034</b>	<b>Reno, NV</b>	<b>39.47</b>	<b>119.79</b>	<b>13:54:04</b>	<b>13:54:45</b>
<b>EOC2-4-0055 (Replaces a lower quality VHS copy EOC2-4-0026)</b>	<b>Sparks, NV</b>	<b>39.54</b>	<b>119.76</b>	<b>13:53:38</b>	<b>13:54:51</b>
<b>EOC2-4-0009-B</b>	<b>Springville, CA</b>	<b>36.22</b>	<b>118.81</b>	<b>13:54:17</b>	<b>13:55:13</b>
<b>EOC2-4-0030</b>	<b>Las Vegas, NV</b>	<b>36.31</b>	<b>115.27</b>	<b>13:54:37</b>	<b>13:56:06</b>
<b>EOC2-4-0017</b>	<b>North of Flagstaff, AZ</b>	<b>35.57</b>	<b>111.53</b>	<b>13:54:45</b>	<b>13:57:30</b>
<b>EOC2-4-0005</b>	<b>Ivins, UT</b>	<b>37.17</b>	<b>113.66</b>	<b>13:55:18</b>	<b>13:56:10</b>
<b>EOC2-4-0028</b>	<b>St. George, UT</b>	<b>37.10</b>	<b>113.57</b>	<b>13:55:05</b>	<b>13:56:02</b>
<b>EOC2-4-0021</b>	<b>St. George, UT</b>	<b>37.10</b>	<b>113.56</b>	<b>13:55:13</b>	<b>13:56:16</b>
<b>EOC2-4-0050</b>	<b>St. George, UT</b>	<b>37.22</b>	<b>113.62</b>	<b>13:55:31</b>	<b>13:55:55</b>
<b>EOC2-4-0098</b>	<b>Santa Clara, UT</b>	<b>37.13</b>	<b>113.65</b>	<b>13:55:10</b>	<b>13:56:10</b>
<b>EOC2-4-0161</b>	<b>Kolob Arch, UT</b>	<b>37.49</b>	<b>113.23</b>	<b>13:55:14</b>	<b>13:56:11</b>
<b>EOC2-4-0136</b>	<b>Mill Valley, CA</b>	<b>37.90</b>	<b>122.51</b>	<b>13:55:33</b>	<b>13:54:19</b>

<b>STS-107 View Location Data (continued)</b>					
<b>EOC</b>	<b>Location</b>	<b>North Latitude* (degrees)</b>	<b>West Longitude* (degrees)</b>	<b>First View of Vehicle (GMT)</b>	<b>Last view of vehicle (GMT)</b>
EOC2-4-0070	Bishop, CA	37.28	118.39	13:54:12	13:55:03
EOC2-4-0066	Ramona, CA	33.03	116.93	13:54:29	13:54:56
EOC2-4-0201	St. Helena, CA	38.51	122.47	13:53:25	13:54:01
EOC2-4-0148-2	Kirtland AFB, NM	34.97	106.46	13:56:48	13:58:12
EOC2-4-0148-4	Kirtland AFB, NM	34.97	106.46	13:56:49	13:58:01
EOC2-4-0024	Arlington, TX	32.74	97.11	14:00:00	14:00:35
EOC2-4-0118	Arlington, TX	32.63	97.11	14:00:04	14:00:21
EOC2-4-0018	Duncanville, TX	32.67	96.90	13:59:59	14:00:53
EOC2-4-0025	Camp Swift, TX	30.26	97.30	14:00:21	14:01:01
MIT DVCAM 0001	Fort Hood, TX	31.18	97.58	14:00:26	14:01:19

**Note:** This list does not include all 140+ videos that have been submitted to date by the public. Although all videos received to date have been screened by the NASA Entry Screening Team; this list shows the most useful of the videos that have been assembled to document STS-107 entry debris events as fully as possible.

# Columbia

## Early Sighting Assessment Team

### Final Report



13 June 3 2003

DA8/Paul S. Hill  
DM4/Ron Spencer, Chris Edelen, Ryan W. Proud  
DM4/Marc Abadie, John Gowan  
DM4/Richard B. Mrozinski, Sarah R. Graybeal, Gavin F. Mendeck  
DM4/Scott Harman, Marissa Herron  
OZ4/Craig Schafer

National Aeronautics and Space Administration  
Johnson Space Center  
Mission Operations Directorate



This information is being distributed to aid in the investigation of the *Columbia* mishap and should only be distributed to personnel who are actively involved in this investigation.

Columbia  
Early Sighting Assessment Team  
Final Report

13 June 2003

Prepared By

/S/

---

Paul S. Hill  
Team Leader



This information is being distributed to aid in the investigation of the *Columbia* mishap and should only be distributed to personnel who are actively involved in this investigation.



## Table of Contents

1. Executive Summary
2. Early Sightings Assessment Team Overview
  - 2.1. Early Sightings Assessment Team Summary
  - 2.2. Early Sightings Assessment Team Lessons Learned
3. Debris Sighting Report Evaluation
  - 3.1. Types of reports and priorities
  - 3.2. Process for handling videos
  - 3.3. Debris Sighting Report Evaluation Lessons Learned
4. Debris Trajectory Analysis
  - 4.1. Debris Sighting Timeline
    - 4.1.1. Debris Sighting Timeline Summary and Methodology
    - 4.1.2. Detailed Time Sequencing
  - 4.2. Relative Motion and Ballistics
    - 4.2.1. Relative Motion and Ballistics Summary and Methodology
    - 4.2.2. Detailed Relative Motion and Ballistic Analysis
  - 4.3. Trajectory and Footprints
    - 4.3.1. Trajectory and Footprints Summary and Methodology
    - 4.3.2. Primary Debris Footprint
    - 4.3.3. Generic Pre-Breakup Debris Swath
    - 4.3.4. Pre-Breakup Shedding Debris Footprints
    - 4.3.5. Estimated Separation Time for Littlefield Tile
  - 4.4. Debris Trajectory Analysis Lessons Learned
5. Radar Search Areas
  - 5.1. Radar Analysis Team Summary
  - 5.2. Radar Database and Search Method
  - 5.3. California Fence Search
  - 5.4. Radar Based Search Boxes
  - 5.5. Radar Test Implications for Radar Based Search Boxes
  - 5.6. Radar Search Areas Lessons Learned
6. Witness Reports
  - 6.1. Witness Report Summary
  - 6.2. Credible Sightings
  - 6.3. Witness Reports Lessons Learned

7. DOD Data
  - 7.1 Remote sensors during entry
  - 7.2 Imagery: AMOS, Kirtland
  - 7.3 FD2 Radar Data
  - 7.4 Radar Tests
  - 7.5 Miscellaneous Other DOD Data
  - 7.6 DOD Data Lessons Learned
  
8. Other Sensor Data
  - 8.1 Infrasonic
  - 8.2 Seismic
  - 8.3 Other Sensor Data Lessons Learned
  
9. References
  
10. Appendices
  - 10.1 Team Members and Contributors
  - 10.2 Entry Debris Events Timeline, Version 6 - 05/27/03
  - 10.3 DOD - JSC Actions

The following appendices are under separate cover:

- 10.4 STS-107 Early Entry Debris Sighting Timeline; May 2003
- 10.5 STS-107 ESAT Final Report Relative Motion and Ballistics Analysis; May 20, 2003
- 10.6 STS-107 Columbia Accident Debris Footprint Boundary Estimates; May 24, 2003
- 10.7 JSC Radar Assessment Team Final Report; May 23, 2003
- 10.8 Results of Search for Observed Debris Landing Events, and EOC Hotline and Database Lessons Learned for STS-107 Accident Investigation
- 10.9 Infrasonic Data: Report to the Department of Defense on Infrasonic Re-Entry Signals from the Space Shuttle Columbia (STS-107) (Revision 3.0)
- 10.10 Seismic Data: Analysis of Sonic Booms from the Reentry of the Space Shuttle Columbia over California and Nevada

## 1. Executive Summary

The Early Sightings Assessment Team (ESAT) was formed two days after the Space Shuttle Columbia accident on February 1, 2003. The ESAT had two primary goals:

- Sift through and characterize the witness reports during entry.
- Obtain and analyze all available data to better characterize the pre-breakup debris and ground impact areas. This included providing the NASA interface to the DOD through the DOD Columbia Investigation Support Team (DCIST).

Video supplied by the general public showed 20 distinct debris shedding events and three flashes/flares during Columbia's entry over the CONUS. Analysis of these videos and corresponding air traffic control radar produced 20 pre-breakup search areas extending from the California-Nevada border through West Texas. These search areas ranged in size from 1 to 1,700 square miles.

In an effort to characterize various orbiter materials and their ability to be detected by available radar, tests were performed by AFRL, Wright-Patterson AFB, OH. A complement of materials and components from inside the payload bay and on the exterior of the Orbiter were tested. These tests characterized both the material radar cross-sections and the detection ranges for the radars that tracked during ascent, orbit operations and entry.

Final analysis concluded there are no reliable indications of off-nominal events in any DOD, DOE, NOAA, and USGS remote sensor data during ascent or pre-breakup during entry, including debris shedding. The only anomalous event detected by remote sensors during the mission was a series of DOD radar tracks indicating an object originating from the Orbiter on flight day 2. A subset of the radar tests and related analyses were designed to identify this object. Conclusions are deferred to the tiger team specifically formed under the OVE Working Group to study the Flight Day 2 event.

## 2. Early Sightings Assessment Team Overview

### 2.1. Early Sightings Assessment Team Summary

The Early Sightings Assessment Team (ESAT) was formed 2 days after the Space Shuttle Columbia accident on February 1, 2003. The ESAT had two primary goals:

- Sift through and characterize the witness reports during entry.
- Obtain and analyze all available data to better characterize the pre-breakup debris and ground impact areas. This included providing the NASA interface to the DOD through the DOD Columbia Investigation Support Team (DCIST).

Of the 17,400 public phone, e-mail, and mail reports received from February 1 through April 4, more than 2,900 were witness reports during entry, prior to the vehicle breakup. Over 700 of the reports included photographs or video of Columbia during entry. It was quickly discovered that public imagery provided a near complete record of Columbia's entry over the United States and that the video showed debris being shed from the Orbiter. Final analysis showed 20 distinct debris shedding events and three flashes/flares during entry over the CONUS. To facilitate the trajectory analysis, these witness reports were prioritized in order to process entry imagery with precise observer location and time calibration first, with an emphasis on video.

The ESAT set up a process to time synchronize all video, determine the exact debris shedding time, measure relative motion, determine ballistic properties of the debris, and perform trajectory analysis to predict the potential ground impact areas or footprints. Key videos were hand carried through the JSC system, expedited through the Photo Assessment Team, and put into ballistic and trajectory analysis as quickly as possible. The Aerospace Corporation independently performed the ballistic and trajectory analysis for Debris 1, 2, 6, and 14 for the purpose of process verification.

Figures 2-1 and 2-2 summarize the debris shedding events and flashes/flares observed in public video. These are shown on the entry ground track and include each photographer's location and approximate field of view recorded in video. Times listed in the figures for each event indicate the earliest each is seen in video. Exact debris shedding times were calculated based on detailed relative motion analysis as explained in detail in Section 4.2. Figure 2-3 shows the predicted ground impact areas for each debris shedding event.

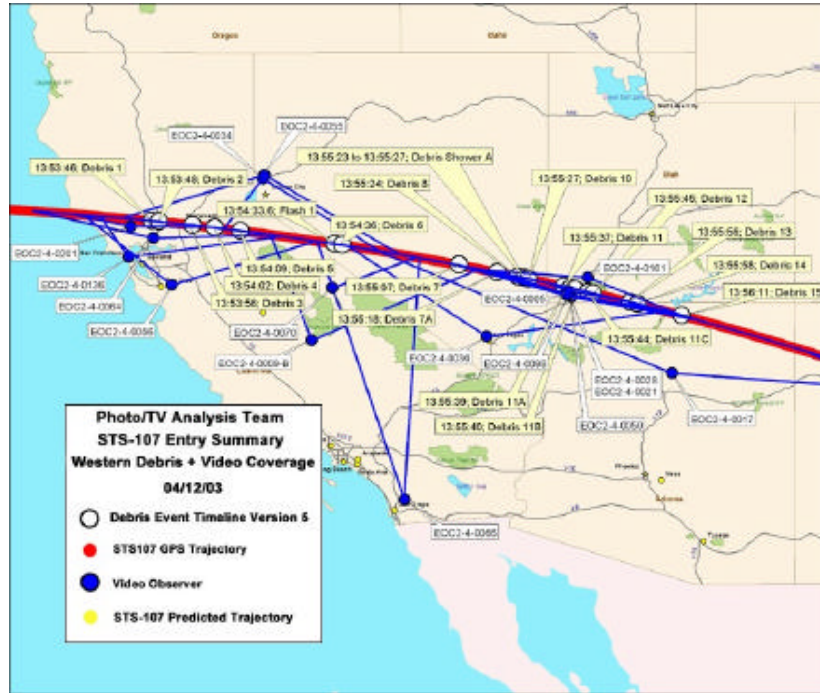


Figure 2-1: Public Video Coverage of the Western United States STS-107 Entry Trajectory [21]

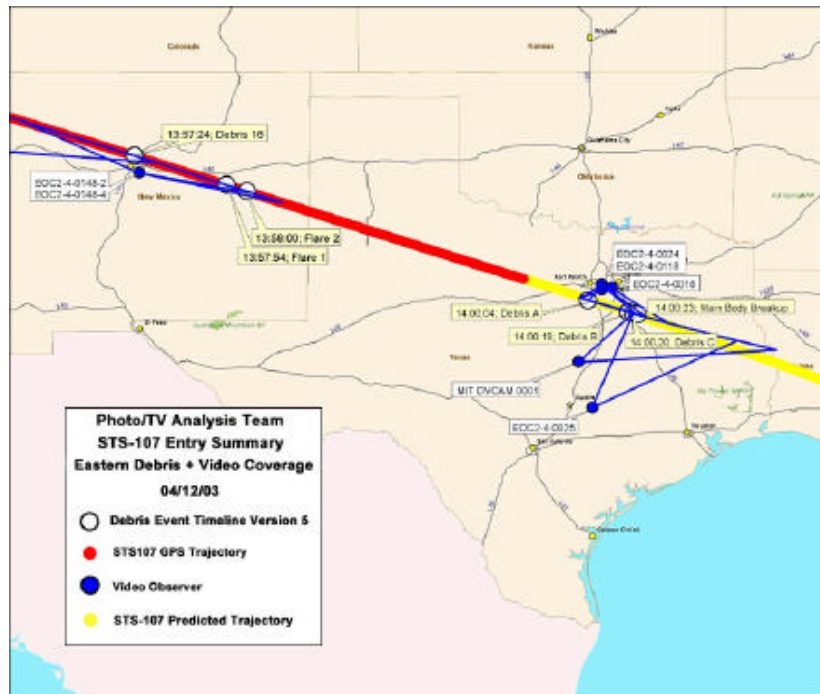


Figure 2-2: Public Video Coverage of the Central United States STS-107 Entry Trajectory [21]

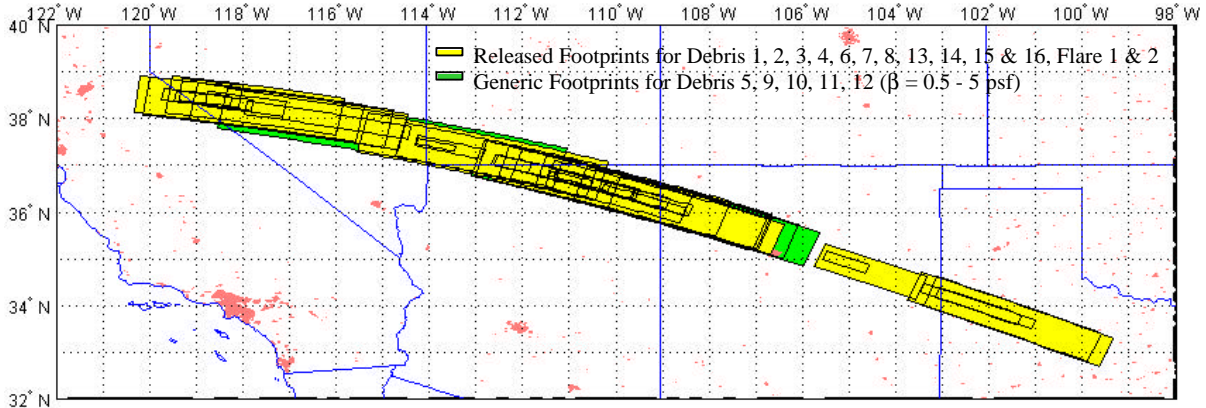


Figure 2-3: Combined Ground Impact Footprints  
of Observed Debris 1 Through 16 and Assumed Debris at Flare 1 & 2  
Constant Ballistic Coefficients, 0-0.15 L/D,  $C_d$  1.0 [24]

Similar footprints were generated for 35,000 and 80,000 ft altitude for use in searching recorded FAA and DOD air traffic control radar in close partnership with the NTSB and FAA. The Radar Analysis Team searched through more than 2 million individual radar returns generated between 1330 and 1500Z on February 1, 2003. Footprints for all debris observed in video were searched by analysts at JSC and the NTSB for indications of any uncorrelated radar threads falling through the air space. A generic debris swath extending from California through break-up in Texas was also searched for radar threads in long range radar.

The combination of trajectory analysis and radar searches led to 20 pre-breakup search areas extending from the California-Nevada border through West Texas. The search areas were prioritized by overall confidence based on the trajectory analysis, radar data quality, and in one case a supporting witness account. The search areas ranged in size from as low as 1 - 11 square miles for the radar based areas, to 300 - 1700 square miles for trajectory-only based areas. All areas were typically in high desert or mountainous terrain. Although ground searches of several of the smaller areas did not produce any Columbia debris, the "Littlefield Tile" (KSC Database object #14768) was determined to have been shed from the Orbiter in the approximate time of Flare 1 through Flare-2 seen in public video.

Results from a series of radar tests by the Air Force Research Laboratory at Wright-Patterson AFB, OH show that the various Orbiter external materials have low maximum detection ranges for the air traffic control radars. Although the larger, leading edge components have much higher radar detection ranges, ballistic analysis and telemetry analysis suggest the long stream of debris observed in video is comprised of smaller objects, not a series of large, near intact, leading edge components. Thus, confidence was reduced that the radar threads used as the basis for search boxes are Columbia debris. This leaves the much larger trajectory based areas as best predictions for pre-breakup debris.

Emphasis was then given to the areas in which the highest probability regions of multiple early debris shedding footprints overlap as shown in Figure 2-4. The darkest regions in the plot indicate the most overlap.

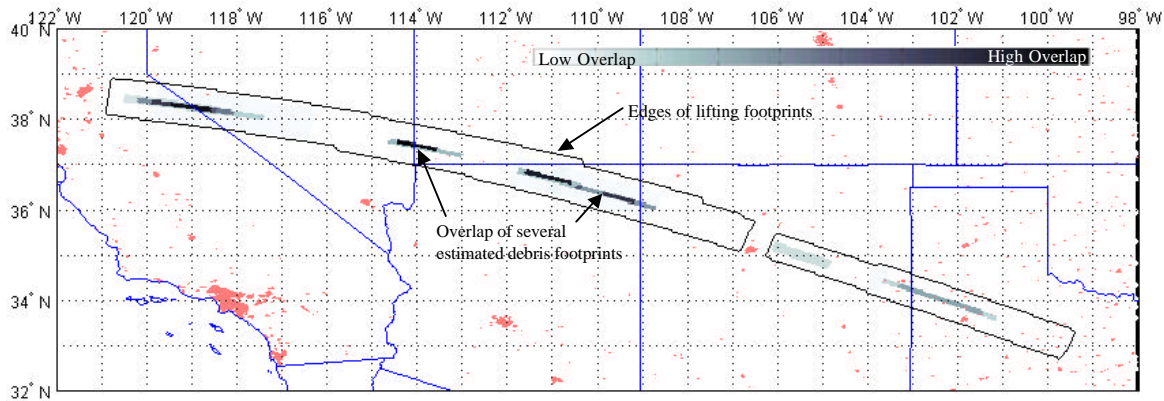


Figure 2-4: Combined Overlapping Ground Impact Footprints of Observed Debris 1 Through 16 [24]

Table 2-1 lists the ten high confidence ballistics and radar based search areas in priority order. The full list is shown in Section 5.

JSC/NTSB Priority	Box	Location Description	# radar hits	# radar antennas	Box Area Sq. NM / Acres (size of Non-lifting areas reflects ONLY the PRIMARY NL areas)	Inside any Lifting or Non Lifting (Ballistic) Footprint? Y/N (see separate Lookup Table)	Thread ID	Comment
1	8	west of Elgin, NV	11	1 (QAS)	1.68 / 1424	Y (Lifting 01 thru 06)	QAS-11-114.77	Delamar Lake, NV witness
2	7-1	Near Pioche, and Caliente, NV	75	1 (CDC)	4.25 / 3602	Y (Non lifting 02 thru 04, and Lifting 01,05,06)	CDC-075-114.4689	Well outside non-lifting, but in Debris-6 lifting foot print.
3	3	Near Floydada, TX	10	2 (QXS,LBB - ASR)	169.02 / 143251	Y (Lifting 16, non-lifting for Flare 1 and Flare2)	LBB-ASR-18-101.3186	Tile found 40 NM west of box
4	7-2	Near Pioche, and Caliente, NV	75	1(CDC)	11.03 / 9384	Y (Lifting 01 thru 06)	CDC-075-114.4690	Well outside non-lifting, but in Debris-6 lifting foot print.
5	6-south	Dixie Natl Forest - Zion Natl Park, UT	18	2 (QXP, CDC)	1.42 / 1203	Y (Lifting 02 thru 07)	QXP-18-113.1506	In/near Debris-6 dense overlap
6	6-north	Dixie Natl Forest - Zion Natl Park, UT	18	2 (QXP, CDC)	1.58 / 1339	Y (Lifting 02 thru 07)	QXP-18-113.1505	In/near Debris-6 dense overlap
7	Dense overlap non-lifting debris 04 thru 06	Near St. George Utah	N/A	N/A	Approx 300 Sq. NM	N/A	N/A	Best relmo cues and ballistics. Considered 1 of 2 most significant events in video. Most dense overlap area.
8	Dense Overlap non-lifting 07 thru 14	NE Arizona, Navajo Indian Reservation	N/A	N/A	approx 1162 Sq. NM	N/A	N/A	Measured relmo, but not as good as Debris-6. Considered 2 of 2 most significant events in video. 2nd most dense overlap area.
9	7-3	Near Pioche, and Caliente, NV	75	1 (CDC)	9.19 / 7789	Y (Lifting 01 thru 06)	CDC-075-114.4691	Outside non-lifting, but in Debris-6 lifting foot print.
10	Dense overlap - non-lifting Debris 01 thru 04	CA/NV Border	N/A	N/A	approx 775 Sq. NM	N/A	N/A	Measured relmo, but not as good as Debris-14. 3rd most dense overlap area.

Table 2-1: High Confidence Western Search Box Priorities [25]

AFRL performed additional radar tests on materials and components inside the payload bay and on the exterior of the Orbiter. This was done in order to fully characterize the radar cross-sections for correlation with the C-band radars which track during ascent and two deep space tracking radars. The C-band radar tests were added to investigate the ability to track debris during ascent, with a primary goal of quantifying the likelihood of discriminating Shuttle debris in the ascent plume and the ability to track the most likely Shuttle debris with the C-bands in general. The deep space tracking radar tests were used to evaluate radar data from an object tracked by Air Force Space Command during the mission that was shown to have originated at the Orbiter on Flight Day 2. Detailed discussion of the evaluations of the Flight Day 2 object are deferred to the tiger team formed under the OVE WG to study this data.

In the first 2 weeks of the investigation, there were preliminary indications in various unclassified and classified sensors of some anomalous events during entry. There were similar preliminary indications of anomalous events during ascent. After additional analysis, however, there are no reliable indications in any DOD remote sensor data of anomalous events during ascent or pre-breakup during entry, including debris shedding.

Columbia was imaged during 3 days of STS-107 orbit operations by the Air Force Maui Optical & Supercomputing (AMOS) site and during entry by employees of the Starfire Optical Range at Kirtland AFB, NM. The AMOS and Kirtland images are the only DOD images taken of Columbia during STS-107 from any source, unclassified or classified. The AMOS images are predominantly of the upper surfaces with payload bay doors open, obscuring a significant portion of the wings, and showing no discernible damage. Detailed discussion of the Kirtland images are deferred to the tiger team formed under the OVE WG to study them.

DOD, DOE, and NOAA infrasound researchers collaborated to study infrasonic signals recorded during STS-107 entry. Similarly, the USGS studied seismic data recorded throughout the southwest CONUS during entry. Although signals associated with the Orbiter are found in both sets of data, analysis to date does not provide any data that can be positively identified as off-nominal, such as debris shedding, high energy release, ground impact, etc.

Analysis of luminosity data, embedded in public imagery, was initiated in an effort to extract an estimate of the size and mass of specific debris material. Ames Research Center has developed a series of tests to explore this possibility, but at the time of this writing, these tests had not yet begun, but the confidence that this will yield significant data is considered low. Also investigated early on was the use of spectral data for constituent determination, but this is not expected to be pursued based on the relatively poor quality video data.

The top level interfaces and data paths within the JSC team are shown in Figure 2-5 below. Not depicted are the interfaces to the various non-NASA groups.



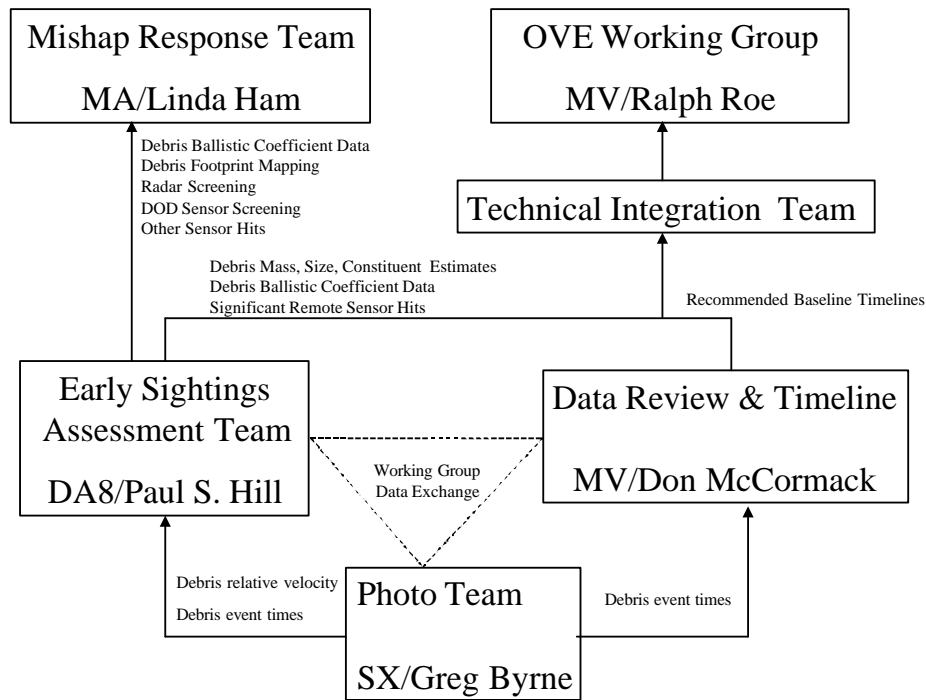


Figure 2-5: ESAT Interfaces

## **2.2. Early Sightings Assessment Team Lessons Learned**

### **2.2.1 Debris Sighting Report Evaluation Lessons Learned**

- 1) The public report form should be standardized and ready for use in any future incident to maintain uniformity of collected information. This form should include key interview questions, detailed locations, contact information and zip codes.
- 2) All phone interviews (and any public reports) should be entered directly into an electronic form as the interview takes place to facilitate immediate accessibility by all investigation teams. These should include fields to distinguish reports of human remains, debris, and visual sightings. Additionally, the database should have a search function for the various types of input fields.
- 3) Eyewitness reports should be treated as a 'case file' rather than as separate reports. This would allow the team to add to an existing report and note when video or other media was received without logging repeated calls from the same witness as separate reports.
- 4) A single point of contact should be used for responding to EOC reports whenever possible due to sensitivity among some of the public to being contacted repeatedly for the same EOC report.
- 5) Various products referencing EOC reports should be built using the EOC reference number not the public caller's name.
- 6) Record exact location, weight, dimensions, and a digital still of all debris as it is recovered and input it into a single database daily. This would allow the use of some back-propagation techniques to better define the debris field, identify debris separation times, and confirm validity of objects as debris. Additionally, it should be noted how the location was determined (GPS coordinates, map location, street address, etc.)

### **2.2.2 Debris Trajectory Analysis Lessons Learned**

- 1) Observer provided information on location, camera specifications, zoom settings, and time synchronization was invaluable as the debris analysis progressed.
- 2) The combination of automation and parallel processes for calculating a relative range for each time step in video ensured both a quick and accurate answer and is highly recommended to anyone performing a similar analysis in the future.
- 3) The Debris Footprint Team generated the method to shape a debris footprint between the heel and toe specifically for this accident to aid the Search and Recovery Team in avoiding unnecessary search areas, and will be used in all future debris footprint predictions.

- 4) In this incident, the first debris footprint predictions were not available until 4 hours after the accident. To improve the possibility of crew rescue, either:
  - a “running” debris footprint should be designed for future STS missions such that as soon as telemetry is lost, a debris footprint and estimated crew module impact point are available, or
  - a footprint prediction team should be available during entry.
- 5) An upper bound on ballistic coefficient was not known for an Orbiter on entry; the Debris Footprint Team now has a maximum ballistic coefficient to use in any future Orbiter-only debris field analysis, based on the Columbia observed value of 220 psf.

### **2.2.3 Radar Search Areas Lessons Learned**

- 1) Focus energy looking for localized “blob” tracks, vice linear radar tracks.
- 2) Focus the search for tracks closer to the groundtrack within the non-lifting footprint.
- 3) Integrate eye-witness reports into radar search as early as possible.
- 4) Station NASA Radar Analysis Team representative at the field operations center for debris searches to help coordinate search box data and act as primary liaison between the RAT and MIT/Search Coordinators.
- 5) Conduct daily telecons with NTSB/FAA/RADES to discuss radar tracks, search boxes, etc.

### **2.2.4 Witness Reports Lessons Learned**

NASA should consider developing a method of educating the public on how best to record future reentries so that, if such a mishap ever occurs again, the video would more easily facilitate post-flight analysis. This would include all important imagery characteristics and supporting data which are key to the analysis.

### **2.2.5 DOD Data Lessons Learned**

- 1) A single DOD POC, located at the NASA center conducting the investigation, is essential to effectively exchanging data and requesting additional support.
- 2) Generic DOD tracking capability and the resulting routine taskings on Shuttle flights should be reviewed and updated as required for all phases of flight.
- 3) Generic DOD imaging/sensor capability and the resulting routine and contingency taskings on Shuttle flights should be reviewed and updated as required for all phases of flight.

- 4) NASA and the USAF should study the use of Orbiter-specific material maps to facilitate AMOS' thermal mapping of all Orbiters during orbit operations.

#### **2.2.6 Other Sensor Data Lessons Learned**

- 1) The state of the art for infrasonic and seismic data does not support their use for monitoring Orbiter entry.
- 2) The state of the art for infrasonic and seismic data does not provide significant engineering value for Columbia's post-incident investigation.

### 3. Debris Sighting Report Evaluation

#### 3.1. Types of reports and priorities

The Emergency Operations Center (EOC) at JSC received 17,400 public phone, e-mail, and mail reports from February 1 through April 4, with approximately 50 percent of them received in the first week. These reports ranged from people who saw or heard something, to condolences, offers to help, photographs and video of Columbia in flight, or some part of the sky after Columbia had flown past.

Of the total reports received, more than 2,900 were witness reports during entry, over 700 of which included photographs or video. As it became clear that public imagery provided a near complete record of Columbia's entry over the United States, the highest priorities were placed on identifying credible imagery of Columbia in flight and debris on the ground. The ESAT then focused exclusively on imagery and witness reports of debris in the sky, while reports of debris on the ground were forwarded to the MIT. [6]

All witness reports were sorted geographically with an emphasis on the western most reports. These were then judged for credibility by comparing the time of the observation and location of the observer to the known entry ground track and an estimated debris swath from California through Texas. (Refer to section 5 for a description of the trajectory analysis and debris swaths.) Reports that were considerably before or after entry and from areas which could not have observed entry were easily eliminated from consideration. This includes reports of observations hours or days before entry or from hours after entry. Similarly, witness reports from areas like Jacksonville, Florida could obviously be eliminated since Columbia could not have been observed there from entry interface through break up. The less credible reports were not discarded, but they were moved to low confidence files for follow up later, if necessary.

Of the remaining reports, highest priority was given to reports with photographs and video and with witness descriptions of debris falling near the ground. The ESAT made direct contact with the witness for each of these reports in order to further screen the less credible reports. Extreme examples of the less credible reports would be video from parking lot security cameras after sunrise that show views of parked cars or traffic on a city street, or offers to explain premonitions from days or weeks before the flight which foretold the accident.

It quickly became clear that some of the public imagery showed debris being shed from Columbia. With this discovery, the witness descriptions of small objects appearing to separate from the Orbiter became much less important, and the strong emphasis was given to finding all video and key still photographs. Further, many of the photographers had measured their positions with GPS receivers and/or provided the address of their viewing location. The observer position data enabled JSC to establish accurate relative geometry to the Orbiter, since we had GPS and tracking radar-based Orbiter state vectors. Several of the videos also had clear celestial references, which combined with the observer's location, gave JSC a means to establish absolute time for the video. (Refer to section 4 for more detail on time synchronizing video.)

As a minimum, the ESAT concluded early on that exact times could be determined for the debris shedding captured in time-correlated video. In a best case, the goal was to use the time and geometry to measure ballistic properties of each discrete piece of debris in video. If ballistic properties could be accurately determined, this would lead to predicted areas the debris would fall through at altitude and predicted ground impact areas or footprints. This, in turn, would enable JSC to calculate pre-breakup debris footprints with a goal of locating early debris. There was also a low probability objective of using luminosity and spectral data in the imagery to estimate mass and constituents of the specific debris. (Refer to section 5 for more detail on trajectory analysis.)

Ultimately, witness report priorities were processed as follows, with the highest priority first: entry imagery with precise observer location and time calibration, with an emphasis on video; remaining entry imagery with an emphasis on video; witness reports of debris falling near the ground. As the analysis progressed, these priorities updated to emphasize videos which included: knowledge of field of view, length of debris observation at a constant zoom setting, potential significance of debris, accuracy of time sync for video, accuracy of observer location information, and multiple views of the same debris event. Knowledge of the field of view was important for scaling of the motion of the debris relative to the Shuttle. Brighter and longer duration debris observations were suggestive of a relatively higher ballistic coefficient than other debris observations. Westernmost debris or debris with a unique characteristic such as a flash were also higher priority. Multiple views for debris events such as debris 6 and 14 allowed for cross checking of field of view and time sync estimates.

This led to a prioritized video “hot list” of the most promising witness reports. The videos on this list were given highest priority when routing through JSC for analysis. The final Hot List is shown in Table 3-1.

Priority	Event	Tape #	Time Debris First Observed Aft of Vehicle		FOV info	Observer Location	Event Description	Observed duration
			GMT	Tape Time (TCR)				
1	Debris 6	EOC2-4-0026 Sparks, NV	13:54:38	23:05:35.16	Venus in FOV during events	Lat: 39.5409 Lon: -119.7682 Alt: 4444 ft	Flash, plasma brightening, bright debris	6 sec
	Debris 6	EOC2-4-0009B, Springville, CA	13:54:36	19:50:35.17	Plasma trail brightening visible during event	Lat: 36.2264 Lon: -118.8052 Alt: 2230 ft	Flash, plasma brightening, bright debris	12.2 sec
	Debris 6	EOC2-4-0030, Las Vegas	13:54:38	01:11:06.28	Plasma trail brightening visible during event	Lat: 36.3099 Lon: -115.2744 Alt: 2513 ft	plasma brightening, bright debris	2.4 sec
2	Debris 14	EOC2-4-0017, N. of Flagstaff	13:55:56.4	01:05:40.23	Observer reports ~80% zoom	Lat: 35.5745 Lon: -111.5294 Alt: 5600 ft	very bright debris, subsequent breakoff of secondary debris from primary debris	5.4 sec
	Debris 14	EOC2-4-0005, Ivins, UT	13:55:58.1	20:04:07.11	Observer reports max zoom	Lat: 37.1681 Lon: -113.6575 Alt: 3080 ft	Very bright debris	4 sec
	Debris 14	EOC2-4-0028, St. George, UT	13:55:57.7	04:34:03.26		Lat: 37.1048 Lon: -113.5721 Alt: 2713 ft		3.6 sec
	Debris 14	EOC2-4-0030, Las Vegas	13:55:58.0	01:12:28.20	zoomed in and out since debris 9 observation	Lat: 36.3099 Lon: -115.2744 Alt: 2513 ft		1.1 sec
3	Debris 1	EOC2-4-0056, Lick Observatory	13:53:46	07:57:13.03	Observer reports max zoom	Lat: 37.3416 Lon: -121.6430 Alt: 4232 ft	Westernmost debris to date	2.5+ sec
	Debris 1	EOC2-4-0064, Fairfield, CA	13:53:46	00:50:59.17	Vega in view later in video	Lat: 38.2804 Lon: -122.0065 Alt: 69 ft	NOTE: Appears to have occasional missing frames.	0.8+ sec
4	Debris 16	EOC2-4-0148-2, Kirtland AFB	13:57:24	23:11:54.24	5 deg FOV	Lat: 34.9646 Lon: -106.4636 Alt: 6155 ft	Easternmost early debris event, very faint	0.9 sec
5	Debris 2	EOC2-4-0056, Lick Observatory	13:53:48	07:57:14.26	Observer reports max zoom	Lat: 37.3416 Lon: -121.6430 Alt: 4232 ft		2.8 sec
	Debris 2	EOC2-4-0064, Fairfield, CA	13:53:48	00:51:01.12	Vega in view later in video	Lat: 38.2804 Lon: -122.0065 Alt: 69 ft	NOTE: Appears to have occasional missing frames.	0.8+ sec
6	Debris 3	EOC2-4-0026 Sparks, NV	13:53:58	23:04:55.08	celestial object in FOV shortly after event	Lat: 39.5409 Lon: -119.7682 Alt: 4444 ft	Debris possibly reacquired at 13:54:03 after zoom-out	2.7 sec
	Debris 3	EOC2-4-0056, Lick Observatory	13:53:56	07:57:23.04	Observer reports max zoom	Lat: 37.3416 Lon: -121.6430 Alt: 4232 ft		2.9 sec
7	Debris 4	EOC2-4-0056, Lick Observatory	13:54:03	07:57:30.17	Observer reports max zoom	Lat: 37.3416 Lon: -121.6430 Alt: 4232 ft		1.4 sec
8	Debris 13	EOC2-4-0005, Ivins, UT	13:55:56.1	20:04:05.12	same FOV as debris 14	Lat: 37.1681 Lon: -113.6575 Alt: 3080 ft	Debris 13 breaks up at the end	0.8 sec
	Debris 13	EOC2-4-0017, N. of Flagstaff	13:55:55.6	01:05:39.29	same FOV as debris 14	Lat: 35.5745 Lon: -111.5294 Alt: 5600 ft		0.7 sec
	Debris 13	EOC2-4-0021	13:55:56.2	03:06:43.27		Lat: 37.0952 Lon: -113.5561 Alt:		0.6 sec
9	Debris 8 (9?)	EOC2-4-0030, Las Vegas	13:55:22.0	01:11:52.20	zoom in and out since debris 6 & 7, observer reports max optical zoom	Lat: 36.3099 Lon: -115.2744 Alt: 2513 ft		3.7 sec
	Debris 9	EOC2-4-0005	13:55:26.2	20:03:40.00	observer reports max zoom, pre-event plasma trail brightening. Possibly same FOV as debris 14.	Lat: 37.1681 Lon: -113.6575 Alt: 3080 ft	Overtaken by debris 10 later	5.0 sec
	Debris 9	EOC2-4-0098 Santa Clara, UT	13:55:27.6	17:35:48.04		Lat: 37.1327 Lon: -113.6470 Alt: 2846 ft		2.4 sec
10	Debris 10	EOC2-4-0005	13:55:26.8	20:03:40.18	observer reports max zoom, pre-event plasma trail brightening. Possibly same FOV as debris 14.	Lat: 37.1681 Lon: -113.6575 Alt: 3080 ft	Overtakes debris 9	3.2 sec

Table 3-1: Video Hot List [17]

Priority	Event	Tape #	Time Debris First Observed Aft of Vehicle		FOV info	Observer Location	Event Description	Observed duration
			GMT	Tape Time (TCR)				
11	Debris 11C	EOC2-4-0098 Santa Clara, UT	13:55:44.4	17:36:04.27	probably same FOV as debris 9	Lat: 37.1327 Lon: -113.6470 Alt: 2846 ft	Measure head of secondary plasma trail, since debris view is intermittent	4.6 sec
	Debris 11C	EOC2-4-0028, St. George, UT	13:55:45.2	04:33:51.10	same FOV as debris 14	Lat: 37.1048 Lon: -113.5721 Alt: 2713 ft	debris not visible, measure head of secondary plasma trail	
	Debris 11C	EOC2-4-0050, St. George, UT	13:55:45.5	07:33:18.27		Lat: 37.2195 Lon: -113.6218 Alt: 3940 ft	debris not visible, measure head of secondary plasma trail	
12	Debris 7	EOC2-4-0030, Las Vegas	13:55:04.9	01:11:35.19	same FOV as debris 6	Lat: 36.3099 Lon: -115.2744 Alt: 2513 ft	Debris 7 splits midway through pass	2.3 sec
13	Debris 5	EOC2-4-0026 Sparks, NV	13:54:09	23:05:06.24	Antares and Venus in FOV after event, prior to change in zoom setting	Lat: 39.5409 Lon: -119.7682 Alt: 4444 ft		1.3 sec
14	Debris 12	EOC2-4-0028, St. George, UT	13:55:45.3	04:33:51.13	same apparent FOV as in debris 14	Lat: 37.1048 Lon: -113.5721 Alt: 2713 ft		1.5 sec
	Debris 12	EOC2-4-0098 Santa Clara, UT	13:55:45.4	17:36:05.28	probably same FOV as debris 9	Lat: 37.1327 Lon: -113.6470 Alt: 2846 ft		1.4 sec
	Debris 12	EOC2-4-0050, St. George, UT	13:55:46.0	07:33:19.12	same FOV as debris 11C	Lat: 37.2195 Lon: -113.6218 Alt: 3940 ft		0.5+ sec
15	Debris 15	EOC2-4-0017, N. of Flagstaff	13:56:10.1	01:05:54.15	zoom change between debris 14 and debris 15	Lat: 35.5745 Lon: -111.5294 Alt: 5600 ft	Easternmost debris of continuous western U.S. coverage	2.2 sec
16	Debris 11	EOC2-4-0050, St. George, UT	13:55:37.2	07:33:10.20		Lat: 37.2195 Lon: -113.6218 Alt: 3940 ft		
	Debris 11	EOC2-4-0098	13:55:37.2	17:35:57.21	probably same FOV as debris 9	Lat: 37.1327 Lon: -113.6470 Alt: 2846 ft		0.9 sec
17	Debris 7A	EOC2-4-0161	13:55:18.1	23:57:24.08	zooming during 1st 0.2 sec	Lat: 37.4875 Lon: -113.2250 Alt:		0.9+ sec
18	Debris 11B	EOC2-4-0098 Santa Clara, UT	13:55:40.1	17:36:00.17		Lat: 37.1327 Lon: -113.6470 Alt: 2846 ft		0.5 sec
19	Debris 11A	EOC2-4-0098 Santa Clara, UT	13:55:39.3	17:35:59.24		Lat: 37.1327 Lon: -113.6470 Alt: 2846 ft		

Table 3-1: Video Hot List, continued [17]



### 3.2. Process for handling videos

There were many organizations involved in receiving, distributing, processing, and evaluating imagery, and still more who were users of any usable data from the images. As already described, this imagery followed several routes getting to JSC, some of which were to individual's personal e-mail accounts or through regular mail. As the report priorities and Hot List were developed, the volume of reports flowing in made it apparent we also needed a standard procedure for each piece of the process to efficiently route the video to facilitate immediate analysis, as well as to ensure no images went overlooked. This procedure follows:

#### Information Handling/Processing

General: Always include EOC tracking number(s) if available in any correspondence.

##### Telephone Calls

1. EOC takes call, records pertinent information onto Information Sheet, assigns EOC tracking number, enters info into data base
2. For debris on the ground, EOC forwards Information Sheet to the MER and faxes to Barksdale, Lufkin, and FEMA regions.
3. For sightings, EOC forwards two copies of Information Sheet to Early Sighting Assessment Team (ESAT).
4. For human remains, EOC immediately faxes Information Sheet to FBI Lufkin with follow-up phone call. Then EOC faxes to B.L. FEMA regions.

##### E-mail ([Columbiaimages.nasa.gov](mailto:Columbiaimages.nasa.gov))

1. Electronic media should be e-mailed to [Columbiaimages.nasa.gov](mailto:Columbiaimages.nasa.gov)
2. If e-mail is received in personal e-mail account that did not come from [Columbiaimages.nasa.gov](mailto:Columbiaimages.nasa.gov), forward to that address. Include EOC tracking number or cross-references, if available.
3. EOC Information Systems Directorate (ISD) personnel screen e-mail in the [Columbiaimages.nasa.gov](mailto:Columbiaimages.nasa.gov) account, move to appropriate folder, and assign an EOC tracking number.
4. For electronic images, Bldg 8 (e.g., Maura White) scans the e-mail folders and posts images to website, includes information in body of e-mail in caption. (Currently don't have EOC number on the Bldg 8 website - in work by Pat Chimes, Maura White, etc.)
5. ISD EOC rep will be in EOC to follow-up with individuals who have e-mailed that they have video or images but have not yet sent them in. The ISD EOC rep will ask the individual to reference the EOC tracking number on the information they supply.

Hard Copy (tapes, cards, CDs, etc.)

*EOC Operations*

1. Hard copy material should be mailed (preferably FED EX or similar carrier which tracks items) to Columbia MIT/JA17, 2101 NASA Rd 1, Houston, TX 77058
  - For sightings, include “Attention: Paul Hill” on outside of envelope and EOC tracking number inside envelope.
2. When the EOC receives mail, the EOC screens out sympathy cards, condolences, etc.
3. EOC rep completes an Information Sheet for each hard copy media and assign a 2-4-xxxx EOC tracking number.
4. The EOC rep contacts the ESAT (x34013) for media that contains video or images, and notifies them they have material to be picked up. The material will be labeled with the 2-4-xxxx EOC tracking number and will be accompanied by three copies of the Information Sheet (one copy inside the envelope with the media for Building 8 and two copies for the ESAT).
5. The ESAT rep signs for each piece of media removed from the EOC.

*ESAT Transfer Operations*

6. The ESAT rep logs the tracking numbers of received media onto a blank Transfer Log, compares the received media to the “Hot List,” and annotates any “Hot items” on the Transfer Log with an asterisk. The ESAT rep also writes a brief summary of each item to expedite screening media in building 8 (EOC number, Name of sender, City and State, type of media, and brief description, e.g., video with clock sync).
7. The ESAT rep carries the received media with the blank Transfer Log and summary sheet to the Building 8 Help Desk and informs the Help Desk that they have media to be transferred.
8. The Help Desk calls the Building 8 point of contact (different people for video versus still images - generally, Jason Fennelly for videos, Cara Johnston/Maura White for still images). The POC then meets the ESAT rep at the front desk.
9. For videos:
  - a. The Building 8 video POC plays each video for the ESAT rep to confirm “Hot items.” “Hot Items” are marked with an asterisk on the Transfer Log.
  - b. If required, the ESAT rep will update the Information Sheet describing the video/images and the summary sheet.
  - c. For video of human remains, contact CB/Andy Thomas for further directions (i.e., do not follow process below).
  - d. The Building 8 Video POC signs for each piece of media on the Transfer Log and photo copies the Transfer Log (so they know which are “Hot Items”).
  - e. The Building 8 video POC copies the video and retains the original media, following their standard process for logging and archiving the information.
    - (1) For sightings, one high quality (D2) copy for the Imagery personnel and two VHS copies for the ESAT rep are made. Note: the ESAT copies will contain multiple “cuts” so they will not be provided immediately - expect to return for pickup at a later time.
    - (2) For debris on the ground, one VHS copy is made for the MER.

- f. The Building 8 Video POC will distribute their log of EOC received items on a daily basis via e-mail including DL ESAT on the distribution list.
10. For still images:
  - a. The Building 8 Still Images POC signs for each piece of media on the Transfer Log.
  - b. The Building 8 Still Images POC retains the original media, following their standard process for logging and archiving the information.
  - c. For CD's, the Building 8 POC provides one copy to the ESAT rep.
    - (1) For sightings, copy is for the ESAT.
    - (2) For debris on the ground, the ESAT rep delivers the copy to the MER Manager.
  - d. The Building 8 Still Images POC posts the images on the Imagery web site.

*ESAT Follow-up Operations*

11. The ESAT rep updates the "Hot List" indicating which media are being processed by Building 8.
12. The ESAT rep attempts to cross-reference any applicable EOC tracking numbers from phone calls or e-mails and notes these EOC tracking numbers on the Information Sheet that was provided by the EOC with the hard copy media. A copy of this updated Information Sheet will be returned to the EOC to update the database.
13. The ESAT rep notifies the Imagery, FDO, and MMACS personnel when "Hot Items" are being processed by Building 8.
14. When VHS or CD copies are received, the ESAT rep notifies FDO and MMACS personnel that a quick-look copy is available. Any media removed from the CSR must be logged out on the posted Hard Copy Media Sign-Out Sheet.

### 3.3. Debris Sighting Report Evaluation Lessons Learned

- 1) The public report form should be standardized and ready for use in any future incident to maintain uniformity of collected information. This form should include key interview questions, detailed locations, contact information, and zip codes.
- 2) All phone interviews (and any public reports) should be entered directly into an electronic form as the interview takes place to facilitate immediate accessibility by all investigation teams. These should include fields to distinguish reports of human remains, debris, and visual sightings. Additionally, the database should have a search function for the various types of input fields.
- 3) Eyewitness reports should be treated as a 'case file,' rather than as separate reports. This would allow the team to add to an existing report and note when video or other media was received without logging repeated calls from the same witness as separate reports.
- 4) A single point of contact should be used for responding to EOC reports whenever possible due to sensitivity among some of the public to being contacted repeatedly for the same EOC report.
- 5) Various products referencing EOC reports should be built using the EOC reference number not the public caller's name.
- 6) Record exact location, weight, dimensions, and a digital still of all debris as it is recovered and input it into a single database daily. This would allow the use of some back-propagation techniques to better define the debris field, identify debris separation times, and confirm validity of objects as debris. Additionally, it should be noted how the location was determined (GPS coordinates, map location, street address, etc.)

## 4. Debris Trajectory Analysis

### 4.1. Debris Sighting Timeline

Unless otherwise footnoted, Section 4.1 is referenced to [22], Spencer, J.R.; JSC-DM; STS-107 Early Entry Debris Sighting Timeline; May 2003. This is included in its entirety in Appendix 10.4.

#### 4.1.1. Debris Sighting Timeline Summary and Methodology

The Early Sighting Assessment Team worked in conjunction with the Photo/TV Analysis Team to screen over 140 public videos of the STS-107 entry. Of these, 19 videos show a total of twenty debris shedding events and three flares, or flashes, as the vehicle flew from California to New Mexico. Videos had poor timing information, so synching the videos to true GMT had to be done by timing any celestial observations and comparing times across videos for common debris/flash event observations. One video had set internal GMT, which was verified as correct. Another video was time synched by the observer's reported calibration to true GMT from WWV (a National Institute of Standards and Technology radio station which broadcasts time and frequency information).

The blue dots in Figures 4-1 and 4-2 represent videographer locations and the blue lines represent video coverage of the Shuttle filmed by that videographer. Although there is overlapping video coverage from just off the California coast to Eastern New Mexico, all of the videos contain short periods when the Shuttle is out of the camera field of view (FOV), out of focus, or obscured by clouds. Therefore, additional off-nominal events may have occurred during this timeframe which were not observed.

There was a lack of good quality video coverage from Eastern New Mexico to the Dallas/Fort Worth Area. The only available video in this region was recorded from Lubbock looking east, and briefly shows the orbiter possibly at the start of the breakup sequence just prior to disappearing over the horizon. Videos from the Dallas/Fort Worth area were not reviewed by the Early Sighting Assessment Team, but were screened by the Photo/TV Analysis Team alone.

Times listed in these figures indicate when the debris was first observed aft of the vehicle and is not the time the debris was shed from the vehicle. These are listed in tabular form with more detail in Appendix 10.2: Entry Debris Events Timeline, Version 6 - 05/27/03.

Twenty distinct debris shedding events and three Shuttle plasma envelope flashes or flares were filmed as the Shuttle flew from California to Eastern New Mexico during STS-107. Many of these events were seen in multiple videos, in one case as many as seven videos recorded the same event.

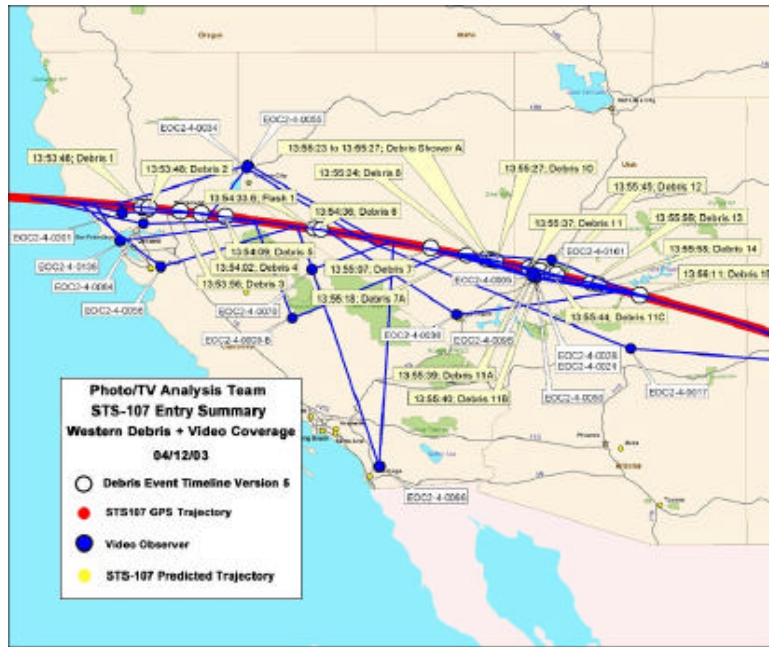


Figure 4-1: Public Video Coverage of the Western United States STS-107 Entry Trajectory [21]

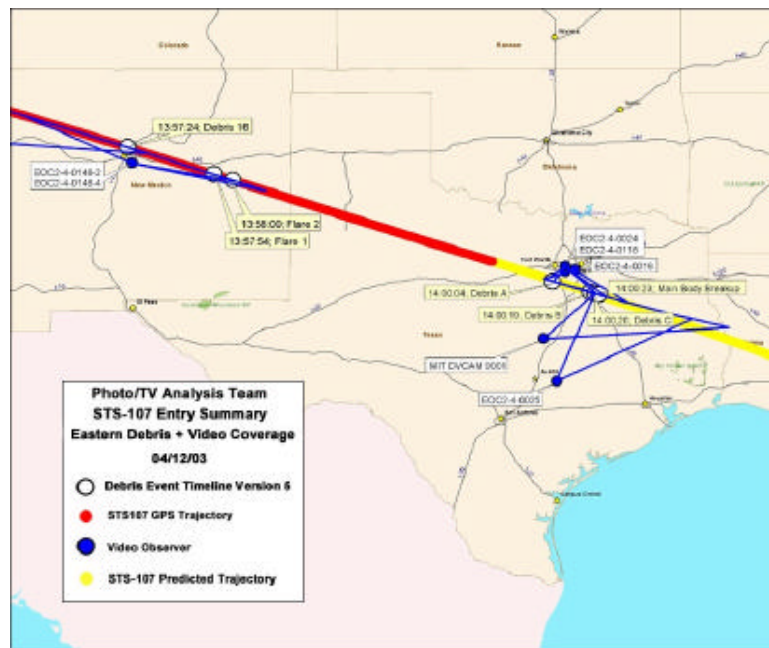


Figure 4-2: Public Video Coverage of the Central United States STS-107 Entry Trajectory [21]



Figure 4-3: STS-107 Early Debris Shedding Events [21]

STS-107 videos were screened for off-nominal events. Observed off-nominal events include debris shedding, bright segments of the plasma trail, flares and flashes in the Shuttle plasma envelope, forks in the plasma trail emanating from the Shuttle plasma envelope, and parallel plasma trails. Entry videos from previous flights were also screened to characterize nominal events such as RCS firings. In none of the previous entry videos were any of the anomalous events described above seen. Examples are shown in Figure 4-4.

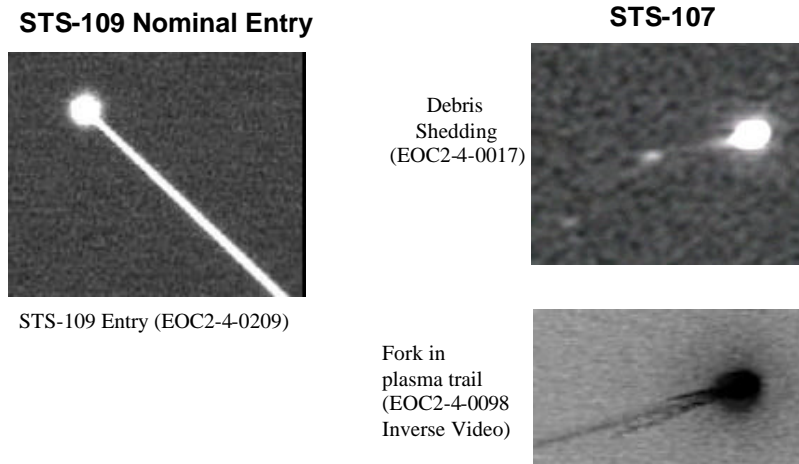


Figure 4-4: Example of Nominal Entry vs. STS-107 Entry

In no video was the Shuttle structure directly discernible. In nearly all the videos, it was displayed as a saturated bright plasma disc. In the Kirtland AFB telescope videos, the plasma

envelop of the orbiter has a shape similar to the orbiter but actual orbiter structure is most likely not seen.

Videos varied greatly in quality, and were initially screened to determine whether they contained footage of the STS-107 entry and if so, for evidence of off-nominal events. Skywatch was used to determine what portion of the STS-107 trajectory, if any, each viewer could have possibly seen. (Skywatch is a JAVA-based celestial acquisitions program developed by the NASA/JSC Flight Design and Dynamics Division.)

In order to use Skywatch, the observer's position and the Shuttle's trajectory had to be known. The as-flown STS-107 GPS trajectory was the source of Shuttle position data. In a few cases, observer-provided GPS coordinates were utilized in Skywatch, but in most cases, this data had to be determined from the viewer's location description, or from video landmarks. Commercially available mapping programs TOPO USA and MapQuest were used to determine/verify latitude, longitude, and altitude locations. Once the observer's location was known, Skywatch was used to determine the viewing arc and maximum elevation angle for the STS-107 flyover.

Nearly all of the videotapes had missing or inaccurate time information. One of the biggest challenges was to accurately time synchronize each videotape. The first step in this process was done by using Skywatch to determine the time of maximum elevation from each viewer's perspective. This time was then applied to the video at the point that depicted the apparent max elevation, assuming that the camera was level. Since the camera was nearly always handheld, this assumption was known to be subject to some error, therefore the accuracy of this initial time sync was only valid to a few seconds.

Refined time synchronization was then done based on celestial references, observer WWV time sync, asset internal GMT, camcorder clock drift measurement, and event correlation across tapes. (WWV is a radio station that broadcasts time, including UT1 corrections, 24 hours a day, 7 days a week.)

Figure 4-5 is a summary of the multiple videos linked to provide times for the entire debris timeline. Some of these debris events were seen in videos not shown above. In those cases, the videos were not useful in providing timing information for the debris event but may be useful for further analysis of the event.



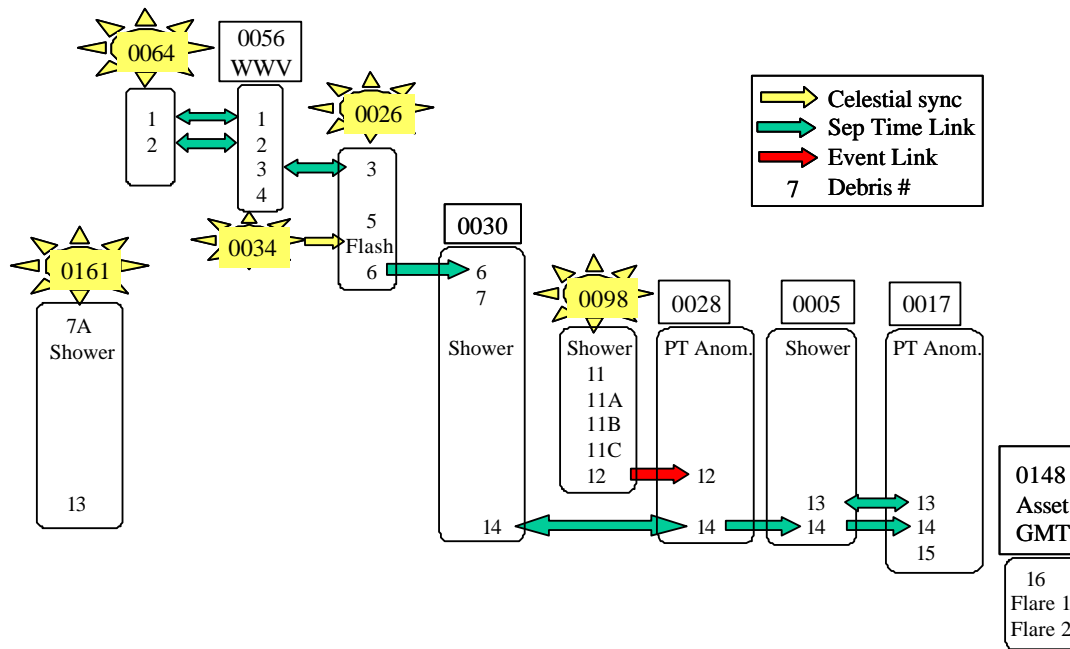


Figure 4-5: STS-107 Early Debris Shedding Events

Synchronizing the videos based on the time of closest approach (TCA) of the Shuttle passage near a celestial body is the most accurate method of time synchronization. Skywatch was used to identify candidate celestial objects seen in the videos based on proximity to the Shuttle’s trajectory from the viewer’s perspective and a rough TCA (within a few seconds). Positive identification of candidate celestial objects was done by selecting the highest magnitude object in the correct proximity to the Shuttle within the expected time range. Personnel from the NASA/JSC Shuttle Flight Planning and Pointing Group then provided the TCA of the Shuttle with respect to that celestial body from their Supersighter program. (Supersighter is a celestial acquisitions program certified for operational use in the Mission Control Center.)

These TCA’s were accurate to 0.1 seconds. One video, EOC2-4-0161, had footage of Venus and the Shuttle but Venus was not in the field of view during TCA, due to zoom in. Several images before and after Venus TCA were used to generate a curve fit of the Shuttle passage near Venus. The image frame that would have depicted the TCA of the Shuttle to Venus on this videotape was then calculated from the curve fit and synced to the actual TCA from this viewer’s perspective.

<b>Tape Reference</b>	<b>Observer Location</b>	<b>Celestial Reference</b>
EOC2-4-0026/0055	Sparks, NV	Venus eclipse (Antares, Gienah also seen)
EOC2-4-0034	Reno, NV	Venus TCA
EOC2-4-0064	Fairfield, CA	Vega TCA
EOC2-4-0136	Mill Valley, CA	Vega TCA
EOC2-4-0098	Santa Clara, UT	Tania Australis TCA
EOC2-4-0161	Kolob Arch, UT	Venus TCA curve fit (Venus not in FOV at TCA)

Table 4-1: Public Video Tapes of Columbia with Celestial References

Even though only a small percentage of the videos that saw debris were able to be celestially referenced, these few videos did have observations of over 70% of the off-nominal events. These videos served as the starting point for the time sequencing of all the videos depicting the STS-107 entry between California and Arizona and eventually time synching debris 1 through 15.

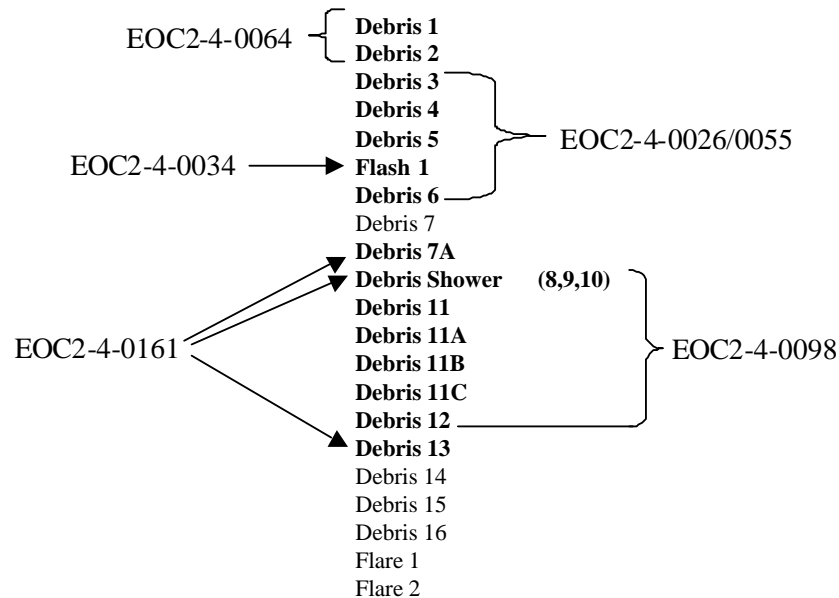


Figure 4-6: Debris Events Observed on Public Video Tapes with Celestial References

EOC2-4-0026/0055 was the most accurate celestial sync of all the videos because it actually captured the Shuttle eclipsing Venus, instead of just a close approach. Also the observer's location was well known since the observer provided his GPS coordinates. Altitude of the observer's location was then determined by referencing his latitude and longitude in TopoUSA. From Supersighter, NASA/JSC personnel determined the time of Venus eclipse to be 13:54:38.3 GMT. The margin of error for this time sync was less than 0.1 seconds. Two additional celestial references were available in this video, the stars Antares and Gienah, but were not needed due to the more accurate Shuttle eclipse of Venus. (This video has two EOC numbers: EOC2-4-0026

is a VHS copy but was the original video reviewed. EOC2-4-0055 is reported to be the original but is not an improvement in quality.)



Figure 4-7: Shuttle Eclipse of Venus as Seen in EOC2-4-0026/0055 from Sparks, Nevada

Some videos without celestial syncs were able to be time synchronized very accurately due to event correlation with videos with celestial syncs. Flash 1 and the Debris 12 brightening well aft of Shuttle are considered such marker events. These had duration of 0.1 sec or less and were seen on multiple videos, including some with celestial syncs.

Other videos without accurate time syncs were synchronized based on matching debris separation times with those of celestially synced videos. Also, in some cases, multiple videos with accurate time syncs contained footage of the same debris object. When possible, separation times for these events were compared between the videos and showed agreement within 0.2 seconds. All separation times were computed by the relative motion team by calculating the ballistic number of the debris and propagating its relative motion back to an origin at the Shuttle.

Debris Event	Tape of Debris Event with Celestial Reference	Tape with Same Debris Event, Time Synchronized/Correlated to Tape with Celestial Reference
Debris 1	EOC2-4-0064	EOC2-4-0056
Debris 2	EOC2-4-0064	EOC2-4-0056
Debris 3	EOC2-4-0026/0055	EOC2-4-0056
Debris 6	EOC2-4-0026/0055	EOC2-4-0030
Debris 14		EOC2-4-0005, EOC2-4-0017, EOC2-4-0028, EOC2-4-0030

Table 4-2: Public Video Tapes which Were Time Synchronized via Overlapping Coverage

Debris 14 was not depicted on a video that had a celestial time sync, but an accurate time sync was able to be performed for one of the tapes which depicted debris 14 via the debris 12 brightening event.

#### 4.1.2. Detailed Time Sequencing

EOC2-4-0056 provided a link between the celestially synced EOC2-4-0064 which had footage of debris 1 and 2 and the celestially synced EOC2-4-0026/0055 which had footage of debris 3-6 plus the flash. The videographer of EOC2-4-0056 reported a WWV sync of his tape. A coarse verification of this was done by the NASA/JSC Flight Design and Dynamics Division using Skywatch. Even though EOC2-4-0056 did not depict any celestial objects, the observer took a time-elapsd still photo simultaneous with his video which did depict several celestial objects. This is due to the greater light gathering capability of a still camera with the shutter held open versus a camcorder. The Aerospace Corporation was able to time sync the video based on changes in the plasma trail in the time-elapsd still photo to within 0.25 seconds of the observer's reported WWV sync.

The relative motion team calculated the separation times for debris 1 and 2 using EOC2-4-0064 and EOC2-4-0056. The separation times for these debris agreed between the 2 videos to within 0.2 seconds. Similar analysis was done for debris 3 using videos EOC2-4-0056 and EOC2-4-0026. Debris 3 separation times agreed within 0.1 seconds. Therefore EOC2-4-0056 showed good agreement with both EOC2-4-0064 and EOC2-4-0026, providing an overlapping link between those two celestially synced videotapes.

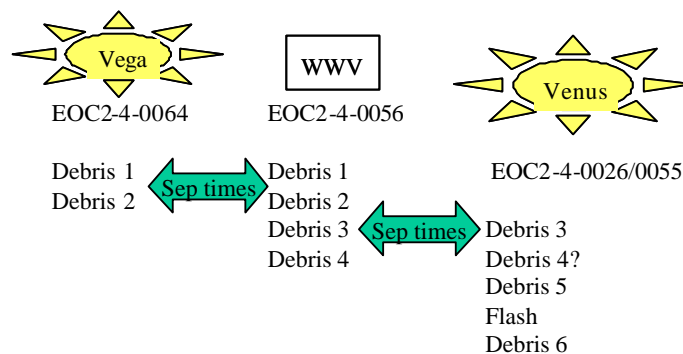


Figure 4-8: Overlapping Debris Observations with EOC2-4-0064 and EOC2-4-0026/0055

The Flash was observed on five videotapes. Four of these observed a brief brightening of the plasma trail, followed by debris 6 emerging from the Shuttle plasma envelope shortly after the flash. EOC2-4-0034 was too noisy to observe any debris (i.e., the brightness of random static, or noise, was the same or greater magnitude as that expected for the debris). Also, it was determined from the STS-107 RCS firing history that aft RCS jets R2R and R3R fired for a total of 0.26 seconds at the same time as the flash was observed. This duration matches the duration of the flash to within 0.04 seconds. However, based on analysis of previous nominal entry overflights, RCS firings do not result in a flash of the Shuttle plasma envelope or a brightening of the plasma trail. It is impossible to determine if the RCS firings contributed to the cause, or are an effect of this event. Therefore, it is concluded that the flash is an off-nominal event which may or may not be related to the RCS jet firing. The previous RCS firing occurred at GMT 13:51:45, which was prior to any video coverage of the STS-107 entry. Later RCS firings, at

13:56:17 and 13:56:53, did occur during video coverage but no unusual signature was seen. However, any flashing may have been difficult to detect since it was daylight by then and all events were more difficult to discern.

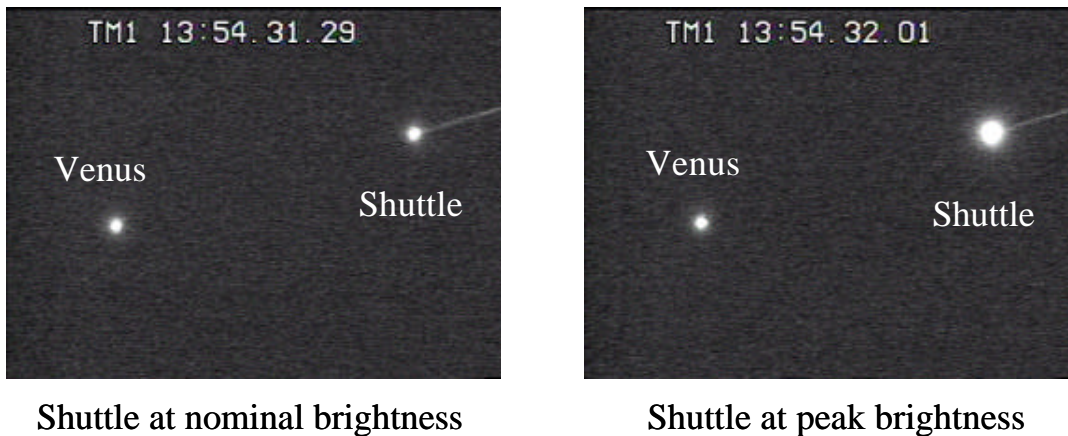


Figure 4-9: Flash 1 as Seen in EOC2-4-0026/0055

Two of the tapes showing the flash had celestial syncs (EOC2-4-0026/0055, EOC2-4-0034). The peak brightening of the flash lasted for only 0.1 seconds and occurred at GMT 13:54:33.6 in both EOC2-4-0026/0055 and EOC2-4-0034, which were celestially synced. EOC2-4-0009B, EOC2-4-0066, and EOC2-4-0070 were then time synced based on the above peak flash time.

Debris 6 was visible for 12 seconds in EOC2-4-0009B, which was the longest duration that any debris was seen in any video.

Note that even though four of the videos observed debris 6, the difference between the time of first observance of debris 6 emerging from the Shuttle plasma envelop varied by as much as 2.2 seconds. This can be explained by differences in field-of-view, viewer look angle to the Shuttle, and camera capability. In each of these cases, the debris may have had to travel a different distance away from the Shuttle before it could be distinguished as a separate object.

The relative motion team determined that debris 6 was shed immediately after the flash.

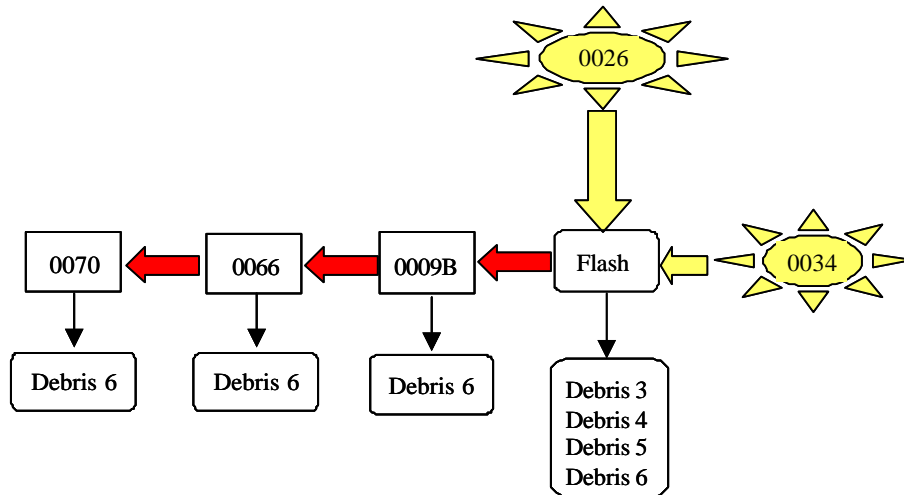


Figure 4-10: Overlapping Observations of Flash 1 and Debris 6

Debris 12 brightened significantly for 1/30th of a second (one frame) in three videotapes (EOC2-4-0028, 0050, 0098), as it was well aft of the Shuttle plasma envelope. EOC2-4-0098 was celestially synced based on a visible TCA with the star Tania Australis; therefore, the time of this brightening event was known to be GMT 13:55:46.5. EOC2-4-0028 and EOC2-4-0050 were then time synchronized to this time for the debris 12 brightening. EOC2-4-0028 contained footage of debris 14, an event that was not on a celestially synced video, thereby providing an accurate time source for this debris event.

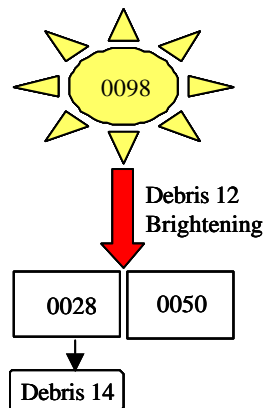


Figure 4-11: Debris 12 Brightening and Time Synchronization of Debris 14

Only one video, EOC2-4-0030, provided overlap between the California/Reno area observations and the Utah/Arizona observations of the STS-107 entry. EOC2-4-0030 starts with observations of debris 6 as the observer reported turning on his video camera shortly after seeing the Shuttle flash and ends with debris 14. No valid time sync information was reported by the observer, so the video was initially time synced to the apparent maximum elevation with the time from Skywatch. This time sync proved that the initial debris depicted on the tape was debris 6 and

the final debris on the tape was debris 14. Since the separation time for debris 6 was known based on relative motion analysis of EOC2-4-0026, the time sync for EOC2-4-0030 was updated to match the debris 6 separation time. The separation time for debris 14 was also known due to relative motion analysis of EOC2-4-0028 (which was linked to celestially synced EOC2-4-0098 through the debris 12 brightening). The separation time for debris 14 in EOC2-4-0030 matched the separation time of debris 14 in EOC2-4-0028 to within 0.1 seconds, therefore linking the Venus eclipse time sync of EOC2-4-0026/0055 to the Tania Australis TCA time sync of EOC2-4-0098.

EOC2-4-0030 was the only videotape that showed footage of debris 7. By linking this tape to EOC2-4-0026 and indirectly to EOC2-4-0098, the time of this debris event was now known.

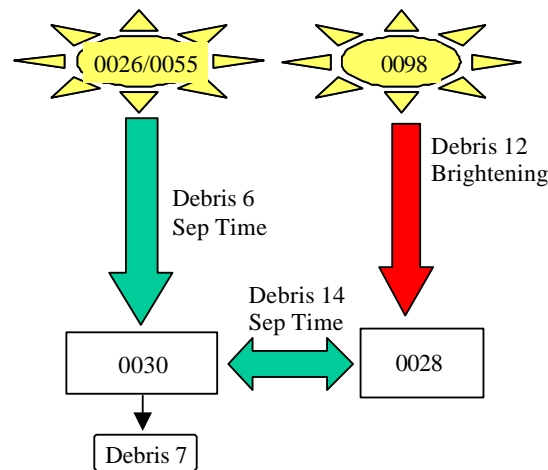


Figure 4-12: EOC2-4-0030 Links Second Two Celestially Referenced Segments

Five videos show debris 14: EOC2-4-0005, EOC2-4-0017, EOC2-4-0021, EOC2-4-0028, and EOC2-4-0030. EOC2-4-0028 and EOC2-4-0030 have accurate time syncs based on the debris 12 brightening and debris 6 separation times, respectively. Based on relative motion analysis of EOC2-4-0028 and EOC2-4-0030, the debris 14 separation time is 13:55:56.7. This time was then used to update the time syncs of EOC2-4-0005 (second half) and EOC2-4-0017. EOC2-4-0005 has a break in the continuous footage in the middle of its track of the STS-107 entry, so only the footage after the break in coverage could be updated with this timing information. Relative motion analysis of EOC2-4-0021 debris 14 could not be done due to changes in zoom during the event. The time syncs for EOC2-4-0017 and EOC2-4-0005 (second half) were confirmed with agreement of debris 13 separation times within 0.1 seconds.

EOC2-4-0017 was originally time synced based on measuring camcorder clock drift at 7 days and 14 days after the STS-107 entry to correct the camcorder clock time imbedded in the video. Camcorder clock drift relative to true GMT was assumed to be linear over this time period but based on different battery uses between the two measurements, may not be. Time syncing EOC2-4-0017 based on the more accurate debris 14 separation time resulted in a 1.2 second shift earlier. Based on engineering judgment, this seemed to be a reasonable refinement of the time sync given the known rough assumptions of the camcorder clock drift.

EOC2-4-0017 was the only videotape which contained footage of debris 15, so the time for this event was now known.

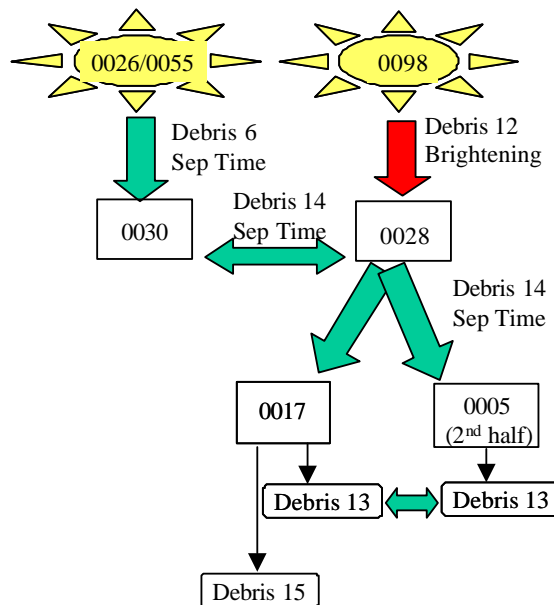


Figure 4-13: Additional Videos Time Synchronized to Establish Debris 15 Separation Time

A debris shower and/or a plasma trail anomaly is visible in seven videos at approximately GMT 13:55:22: EOC2-4-0005, EOC2-4-0017, EOC2-4-0021, EOC2-4-0028, EOC2-4-0030, EOC2-4-0098, and EOC2-4-0161. In the poorer quality videos of this event, only a brief brightening of the plasma trail is seen - approximately 0.5 seconds duration. However, four of the videos - EOC2-4-0005, 0030, 0098 and 0161 - show distinct debris trailing the orbiter from immediately prior to the plasma trail anomaly to 5 seconds after the event. Many pieces are seen briefly flickering aft of the vehicle in and out of the plasma trail on these videos at this time with only two pieces distinctly trackable for more than 0.25 seconds as they trail aft of the vehicle in any one video. EOC2-4-0030 only shows debris 8, at GMT 13:55:22.0, and the plasma trail anomaly. EOC2-4-0098 shows debris 8 at 13:55:24.1, has a zoom-out occur, and acquires another debris object at 13:55:27.2 well aft of the Shuttle plasma envelope with a parallel plasma trail emanating from the Shuttle plasma envelope. Due to the zoom-out, it is unknown whether the debris evident after zoom-out is debris 8 re-acquired, or is a new debris object, debris 9. EOC2-4-0005 clearly shows a shower of debris at GMT 13:55:26.2 with one piece, debris 9, trackable for 5 seconds before it fades from view. Also, the time sync of EOC2-4-0005 (first half) is not nearly as accurate as most of the other videos. This video was synced based on a possible common image of debris 9 as it trailed aft in EOC2-4-0098 and EOC2-4-0005. However, debris 9 did not have any marker events such as the brightening seen in debris 12. Therefore, EOC2-4-0005 could be off in its time sync.

EOC2-4-0161 shows several pieces of debris briefly before they fade from view, but does not show any in continuous track for greater than 0.25 second during this time. Therefore, it is



impossible to correlate any of these debris observations to any single debris shown in any of the other videos.

EOC2-4-0005 did show unique behavior between debris 9 and 10. Debris 10 is observed emerging from the Shuttle plasma envelope 0.6 seconds after debris 9. However, debris 10 quickly decelerates and is overtaken by debris 9. This is the only video evidence of any piece of debris overtaking another piece.

Videos from Kirtland AFB provided the only coverage over most of New Mexico. The observer was viewing the STS-107 entry through daylight by this time, so debris events were more difficult to detect. However, by using inverse video, debris 16 was discernible on EOC2-4-0148-2. This video had imbedded azimuth, elevation, and GMT, which were verified using Skywatch. EOC2-4-0148-4 was a more close-up view from the same telescope mount as EOC2-4-0148-2. This videotape showed two brightening events, or “flares,” of the Shuttle plasma envelope at 13:57:54.5 and 13:58:00.5. The Shuttle plasma envelop was at the edge of the field of view at this time, so it was not known whether debris was ejected during these flare events.

## 4.2. Relative Motion and Ballistics

Unless otherwise footnoted, Section 4.2 is referenced to [23], Abadie, M.; JSC-DM; STS-107 ESAT Final Report Relative Motion and Ballistics Analysis; May 20, 2003. This is included in its entirety in Appendix 10.5.

### 4.2.1. Relative Motion and Ballistics Summary and Methodology

Twenty debris objects were viewed in the “early sightings” videos sent to NASA by the general public as the Shuttle passed over the western United States during STS-107 entry. Eleven of the objects viewed in these videos have been fully analyzed for relative motion and ballistics. The objective of the analysis was to determine the ballistic coefficient and separation time of “early sightings” debris pieces from the video footage of each debris shedding event. With ballistic coefficients ranging from 0.1 psf to 4.0 psf, these estimates were then handed off to the JSC-DM Entry Analysis Group for footprint determination as described in Section 4.3.

This analysis was a team effort across JSC, including JSC-DM Flight Design and Dynamics Division, JSC-SX Image Science and Analysis Group, and JSC-EG Aeroscience and Flight Mechanics Division. JSC-SX provided imaging expertise along with scaling and relative motion estimates. JSC-EG provided help in reviewing the analysis methods and simulation tools. JSC-DM focused on the relative motion calculations, separation time estimates, and ballistics estimates. The NASA JSC organizations involved in this effort (DM, EG, and SX) worked cooperatively to obtain a final result, but in certain areas, multiple organizations performed the same tasks using different methods in order to further ensure accuracy.

To verify the results generated by the NASA JSC community, an independent assessment was performed by the Aerospace Corporation, who had previous experience with predicting debris ballistic coefficients from the video footage of the MIR re-entry. The Aerospace Corporation provided an independent assessment for Debris events 1, 2, 6, and 14. They were given access to the videos and any comments provided by the videographers, along with camera specifications or other information derived from tests with the actual cameras. All other information (scaling data, pixel data, etc) was derived independently.

JSC-SX and JSC-DM relative motion calculations agree in most instances. Due to differing assumptions in the calculations, cases where the observer is near the trajectory plane result in larger differences than those where the observer’s line-of-sight is nearly perpendicular to the Shuttle trajectory. These differences are well understood and described in more detail later in this section. JSC-EG and JSC-DM show good agreement in simulated relative motion curves. The independent assessment performed by the Aerospace Corporation corroborates the results and conclusions found by NASA-JSC. Overall, the relative motion methodology and results are believed to be accurate due to the agreement in results between all the participating teams and between the different videos that observe the same debris piece.

Table 4-3 below summarizes ballistics for all the “early sighting” debris objects analyzed. Separation time estimates and ranges are listed along with ballistic coefficient estimates and

ranges. These times vary from those displayed in the original timeline. Originally, the separation times were determined by the Debris Timeline Team to be the first GMT the debris object is visible in the video footage. Typically, the debris object becomes visible slightly later than the actual separation time.

Debris 6 reveals the highest ballistic coefficient, estimated at 3.5 psf with an error bar extending as high as 4.0 psf. The lowest ballistic coefficient is estimated at 0.3 psf for Debris 16 with error bar extending as low as 0.1 psf. The density used to simulate the relative motion is listed with each debris object. Finally, all debris objects that were not analyzed are marked as such, and the video footage gathered for these objects is listed.

Debris #	Best Estimate of Separation Time (GMT)	Separation Time Range (GMT)	Best Estimate of Ballistic Coefficient (psf)	Ballistic Coefficient Range (psf)	Density at Altitude (slug/ft <sup>3</sup> )
1	13:53:44.80	13:53:44.20 - 13:53:45.40	1.1	0.6 - 1.6	1.18041358E-07
2	13:53:46.50	13:53:45.90 - 13:53:47.10	1.3	0.7 - 1.9	1.19096239E-07
3	13:53:56.10	13:53:55.60 - 13:53:56.60	0.55	0.1 - 1.0	1.21767023E-07
4	13:54:02.90	13:54:02.30 - 13:54:03.50	0.9	0.3 - 1.5	1.25415914E-07
5	Was not analyzed. 1 video : Sparks 0026				
6	13:54:34.20	13:54:33.70 - 13:54:34.70	3.5	3.0 - 4.0	1.40823380E-07
7	13:55:04.10	13:55:03.60 - 13:55:04.60	1.1	0.5 - 1.7	1.54495779E-07
7a	Was not analyzed. 1 video : Kolob Arch 0161				
8	13:55:20.80	13:55:20.20 - 13:55:21.40	3.4	2.6 - 4.0	1.64515972E-07
9	Was not analyzed. 1 video : Ivins 0005				
10	Was not analyzed. 1 video : Ivins 0005				
11	Was not analyzed. 1 video : St. George 0050				
11a	Was not analyzed. 1 video : Santa Clara 0090				
11b	Was not analyzed. 1 video : Santa Clara 0090				
11c	Was not analyzed. 1 video : Santa Clara 0090				
12	Was not analyzed. 1 video : St. George 0028				
13	13:55:53.80	13:55:53.30 - 13:55:54.30	0.65	0.2 - 1.1	1.83054334E-07
14	13:55:56.70	13:55:56.20 - 13:55:57.20	1.7	1.0 - 2.4	1.85877832E-07
15	13:56:09.50	13:56:09.00 - 13:56:10.00	1.4	0.8 - 2.0	1.98522953E-07
16	13:57:23.90	13:57:23.20 - 13:57:24.20	0.3	0.1 - 1.0	2.18514602E-07

Table 4-3: STS-107 Early Debris Ballistics Results

For most debris events, multiple videos observe the event and can therefore be used to verify the accuracy of the relative motion calculations. Some videos that observe debris events are not analyzed for relative motion due to camera zooming or insufficient data. For each video, several inputs are provided by JSC-SX. The JSC-SX team tracks the debris and Orbiter positions in the video, and provides these pixel locations for all frames where both the debris and Orbiter are visible. The video scaling information, which consists of either the focal length or the horizontal field-of-view (HFOV), is also provided by JSC-SX. Once the relative motion / ballistics analysis is complete for a given case, the estimated ballistic coefficient and separation time are passed on to the debris footprint team. In order to perform their calculations, the luminosity team is also given the ballistics results and relative motion raw data.

To automate the detailed process of analytically calculating the relative range between the Orbiter and the debris piece, a relative motion tool was developed to take the video tracking and scaling data and output the relative motion for that video. For each frame of interest, the distance (in pixels) between the Orbiter and debris in the image plane are converted to an actual distance (in feet) in the trajectory plane. One of the assumptions of the analysis is that the debris remains in the trajectory plane during the time region of interest, usually only several seconds in duration. Also during this short time period, the debris is assumed to have zero lift and the ballistic coefficient is assumed to be constant. The error associated with these assumptions is deemed to be relatively small, and the assumption that the debris piece remains in the trajectory plane is considered to be the best assumption that could be made to calculate the relative motion explicitly.

Adjustments to the relative motion calculations include accounting for the off-set of the Orbiter from the principal point (image center) and accounting for camera rotation effects. Once all the relative motion curves for a debris piece are generated, the curves are compared with simulated relative motion data for a constant ballistic coefficient. The ET-SRB simulation, an official range safety external tank (ET) debris footprint tool, models the ballistic trajectory of the debris piece given the initial state vector from the Orbiter best-estimated-trajectory (BET) data. A post processor script then compares the simulated debris trajectory with the actual Orbiter trajectory to calculate a relative motion curve. The video relative motion curve is co-plotted with a set of constant beta, simulated relative motion curves for a given separation time. If none of the constant beta curves match the video relative motion data, then the separation time is adjusted until the closest match is achieved.

Another approach to this analysis would utilize several videos together to triangulate a relative motion solution for a single object. However, this option was not used because several sets of data are erroneous due to zooming or HFOV error. The team felt a more accurate estimation of separation time and ballistic coefficient for each debris object could be made by analyzing each video independently.

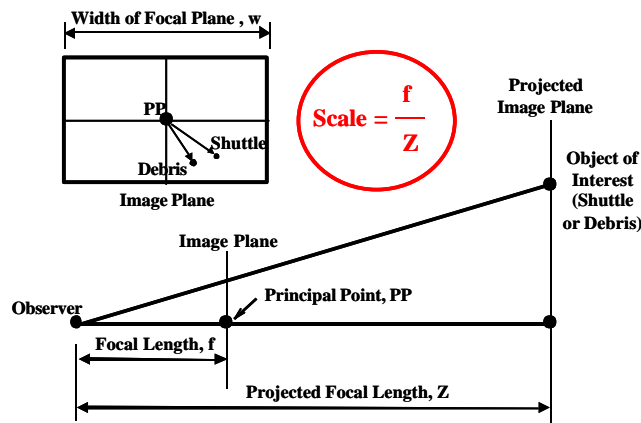


Figure 4-14: Relative Motion Geometry

In the upper left-hand corner of the figure above is an example of the debris and Shuttle positions in the image plane. The actual objects are being projected onto the image plane, which is defined by the focal length (i.e., distance from the observer) and horizontal field-of-view, both of which are a function of the camera specifications and zoom setting. The locations of objects in the image plane correspond directly to their appearance on the screen. The tracking data, which is one of the inputs into the relative motion tool, consists of the location of the debris and Shuttle in the image plane for each frame where the debris is visible. The tracking data is manipulated to calculate the distance (in pixels) from the Shuttle to the debris in the image plane. Another plane, parallel to the image plane, is set at a distance from the observer so that it passes through the location of the Shuttle. Distances (in feet) in this displaced (or projected) image plane are related to distances (in pixels) in the true image plane through a scale factor. Since the two image planes form similar triangles, the scale factor is simply the ratio of the true focal length,  $f$ , to the projected focal length,  $Z$ . If the trajectory plane was also parallel to the image plane, then the calculated separation distances in the projected image plane would be the actual, true distances between the Orbiter and the debris. In reality, however, the trajectory plane is never parallel to the image plane, so further calculations are necessary.

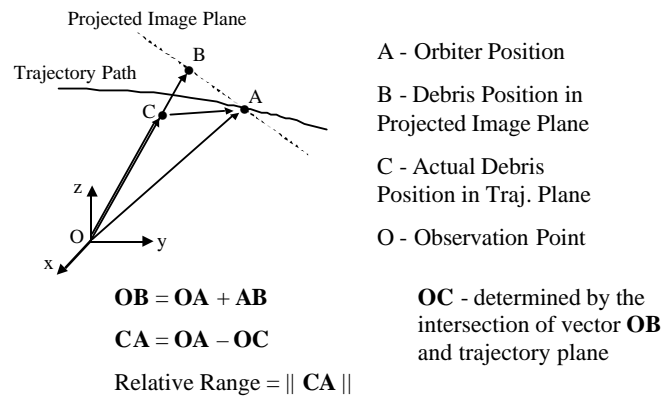


Figure 4-15: Relative Motion Geometry

The dashed line in the figure above represents the projected image plane described earlier. Point A is the actual position of the Orbiter and point C is the actual position of the debris piece, which is assumed to remain in the trajectory plane. Point B represents the point where the projection of the debris piece intersects the image plane. In other words, point B is the debris location as seen on the video, without accounting for the viewing geometry. Point O represents the observer's location. The vector from point O to point A is determined based on the trajectory data, and the vector from point A to point B is calculated using the measured distances on the screen (in pixels) and the scale factor shown on the previous figure. Vector OB is calculated by adding vectors OA and AB. The vector from point O to point C is determined by finding the point of intersection between vector OB and the trajectory plane. The vector from point C to point A is then calculated by subtracting vector OC from vector OA, and the magnitude of vector CA is equal to the relative range from the Orbiter to the debris.

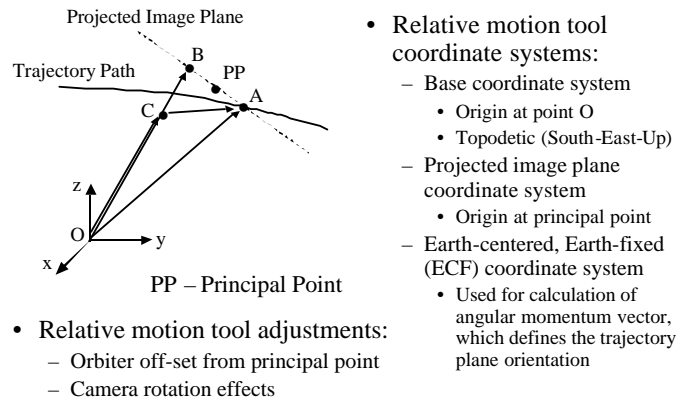


Figure 4-16: Relative Motion Geometry

All vector operations mentioned are calculated in the base coordinate system, located at the observation point. Coordinate systems are also established at the Earth's center and at the projected image plane principal point. Coordinate transformations are then derived to transform vectors in the projected image plane coordinate system and the Earth-centered, Earth-fixed coordinate system to the base coordinate system. The orientation of the trajectory plane is defined by the angular momentum vector of the Orbiter at the time of the given frame. The angular momentum vector is calculated in the Earth-centered, Earth-fixed coordinate system and then transformed to the base coordinate system, which is a topodetic (South-East-Up) coordinate system. The trajectory data is also manipulated to calculate the range, azimuth, and elevation from the observer to the Orbiter.

Since the Orbiter location is not coincident with the principal point (PP), the orientation of vector OA is adjusted to determine the projected image plane orientation, which is needed to perform the necessary coordinate transformation. This adjustment is performed by a series of intermediate coordinate transformations utilizing the scaled tracking data in the projected image plane. The camera rotation effects also needed to be taken into account since the methodology described earlier assumes zero camera rotation. To visualize the effects of the camera rotation on the desired solution, consider what happens to vector OB as the camera rotates from 0 deg to 360 deg. As the camera rotates a full 360 deg, the orientation of vector OB rotates around to form a cone that intersects the trajectory plane at a series of points instead of one exact location. To calculate the camera rotation angle for a given frame, the plasma trail orientation in the video is compared with the trajectory data and then adjusted by iterating on the rotation angle until its orientation matches the trajectory. The solution of the camera rotation angle iteration is then applied to the relative motion calculations to nullify the effects associated with the rotation.

Ranges on separation time and ballistic coefficient have been determined for each debris object. These ranges are derived through an error analysis that takes into consideration all significant error sources. As it turns out, the same error sources applied to separation time also apply to ballistic coefficient. Most of these are independent of which video or debris object is being analyzed and are assigned a constant value for each case. However, a few of the error values are debris/video specific. Conservatism is used throughout the error analysis because small

increases in separation time and ballistic coefficient ranges have little impact on the overall footprint area when these estimates are used as initial conditions for footprint analysis. Once the contribution from each error source is estimated, the errors are stacked in a worst-on-worst fashion. Worst-on-worst analysis was chosen over a RMS calculation for the added conservatism. There are six significant error sources: time synchronization, horizontal field-of-view, beta curve fit method, relative motion calculations, video tracking, and simulation errors.

Time synchronization error is a measure of how well the actual GMT is known for each video. By the end of the analysis, most times were synchronized through celestial references, either directly or indirectly. However, a conservative estimate for error is used. An error of  $\pm 0.2$  seconds is applied to separation time, and an error of  $\pm 0.05$  psf is applied to ballistic coefficient for time synchronization error. While many of the cases truly have less than 0.2 seconds of error because the celestial references are quite accurate, 0.2 is still used for conservatism.

Horizontal field-of-view (HFOV) error is a measure of how well the zoom for a particular camera is known. In most cases, HFOV estimates were done by the Image Science and Analysis Group (JSC-SX). HFOV is known quite well for some video data, while others rely on the observers' estimates of zoom. In some cases, the camera zoom is in the digital zoom region. This region of zoom provides a noise characteristic that can be measured in order to obtain a HFOV estimate. Other cases of footage have camera zoom in the optical zoom region. Without specific zoom information, the actual camera zoom cannot be determined. In cases where zoom was not well defined, a relative motion calculation is performed with multiple HFOV's. For these situations, the error is then included in the beta curve fit error calculation as will be discussed next. Fortunately, changes in HFOV affect separation time estimates very little. For this reason this error source is neglected for separation time estimates. However, HFOV errors certainly impact ballistic coefficient estimates. HFOV error for the ballistic coefficients is assessed on a case-by-case basis, and values range from as little as  $\pm 0.05$  psf to as large as  $\pm 0.2$  psf.

Errors in the beta curve fit method are a measure of how well separation time and ballistic coefficient can be estimated by fitting the ET-SRB generated relative motion curves with the relative motion curves derived from video data. This method is quite accurate because small changes in separation time and ballistic coefficient (on the order of 0.1 sec and 0.1 psf, respectively) are noticeable in the curve fitting. However, errors creep into the beta curve fit method when the relative motion data is dispersed, either because the observer is close to the trajectory plane or because the relative motion data from several videos has less than perfect agreement. This error source applies to both separation time and ballistic coefficient estimates, and the magnitude is determined on a case-by-case basis. The magnitude of this error source can range from 0.1 seconds to 0.2 seconds for separation time and from 0.1 psf to 0.3 psf for ballistic coefficient.

Errors in the relative motion calculations measure the combined accuracy in the components of this calculation. Early in the development of the relative motion tool, assumptions were used to simplify the calculations. Eventually, the calculations were refined, and the simplifications were extracted. For instance, original calculations were made assuming the Earth is a perfect sphere

until the proper coordinate transformations were developed to incorporate the 1960 Fischer Ellipsoid model. To account for this error source, a value of 0.05 seconds and 0.05 psf is included in the error ranges for separation time and ballistic coefficient, respectively.

Additionally, there are small errors associated with tracking the debris and Shuttle from the video footage. The Image Science and Analysis Group uses a tool called ISEE to obtain pixel location as a function of time for objects in a video. This tool approximates the location of the “light source” on the screen. Due to distortion, the pixel data will have errors on the order of a few pixels. The errors in separation time and ballistic coefficient estimates associated with these tracking errors are estimated at less than 0.05 seconds and 0.05 psf, respectively.

Finally, the ET-SRB simulation contains slight errors in the calculations of the relative motion curves. Since these curves are used to estimate the separation time and ballistic coefficient, this error must be accounted for in the estimates. Aerospace Corporation and the Aerospace and Flight Mechanics Division at JSC (JSC-EG) used independent simulations to derive these curves. The good agreement between the simulations justifies a rather low error range for this error source. Separation time error due to this source is less than 0.05 seconds. Ballistic coefficient error due to this source is less than 0.1 psf. Table 4-4 summarize the error components for debris 6 as an example.

Error in Separation Time (sec) : 0.45		Error in Ballistic Coefficient (psf) : 0.55	
Error Source	Error (plus/minus seconds)	Error Source	Error (plus/minus psf)
Beta Curve Fit Method *	0.1	Beta Curve Fit Method *	0.1
Time Synchronization	0.2	Time Synchronization	0.05
FOV	0	FOV *	0.2
Relative Motion Calculations	0.05	Relative Motion Calculations	0.05
Tracking	0.05	Tracking	0.05
Simulation Errors	0.05	Simulation Errors	0.1

Table 4-4: Example Error Calculation for Debris 6

As mentioned above, relative motion between the debris and Columbia has been calculated independently by JSC-DM, JSC-SX, and Aerospace Corporation. The calculation methods differ in the assumptions that were made. There is simply not enough information available to solve this relative motion problem in three dimensional space with video information from one camera, so some simplifying assumption is required. JSC-SX and the Aerospace Corporation assume the debris object remains in the Shuttle trajectory path. JSC-DM assumes the debris object remains in the Shuttle trajectory plane, allowing vertical motion in the plane. Both methods neglect motion out of the trajectory plane. The only force with a component acting outside of the trajectory plane is lift. Neglecting debris motion out of the trajectory plane is a good assumption because debris objects tend to tumble, canceling out lift in any one direction, and because the video observations are only on the order of a few seconds typically.

The difference in assumptions do significantly impact the data; however, these impacts are well understood. JSC-SX and the Aerospace Corporation both project the debris object into the trajectory path. This method works well unless the observer happens to be very close to the



trajectory plane. When this is the case, projecting the debris object introduces some error in the calculation of relative range between the debris and the Shuttle if it is true that the debris has fallen out of the trajectory path. Assuming the debris is falling vertically out of the trajectory path, two possible cases can result. First, if the Shuttle is moving towards the observer, projecting the debris into the trajectory path results in a larger relative range. Unfortunately, none of these cases were analyzed. Alternatively, if the Shuttle is moving away from the observer, projecting the debris into the trajectory path results in a smaller relative range. Ivins 0005 Debris 14 and St. George 0028 Debris 14 illustrate this scenario. This will be discussed in detail subsequently.

The table below lists relative azimuth between the Orbiter trajectory and the line-of-sight of the observer for several Debris 14 videos. A range of azimuths are listed for each video. This range corresponds to the beginning and end of video footage. In other words, Ivins 0005 has a relative azimuth of 7 deg when video footage is acquired, and this decreases to 6 deg when video footage is lost. Note that Flagstaff 0017 is the only case listed where the azimuth increases over the time span. This is because Flagstaff is the only case where the Shuttle is moving toward the observer.

Debris	Video	Relative Azimuth between Orbiter Trajectory and Line- of-sight (degrees)
14	Ivins 0005	7 - 6
	Flagstaff 0017	52 - 61
	St. George 0028	10 - 8
	Las Vegas 0030	32 - 30

Table 4-5: Relative Azimuth Example for Debris 14 Videos

The point here is to illustrate that the cases with a large relative azimuth, Flagstaff 0017 and Las Vegas 0030, are the same cases that demonstrate good agreement using both relative motion assumptions of JSC-DM and JSC-SX/Aerospace Corporation. This result is further illustrated in figure 4-18. The cases with small relative azimuth are scenarios where the observer is close to the Shuttle ground track. Ivins 0005 and St. George 0028 both have small relative azimuths, and thus, do not agree as well between the different teams (figure 4-18).

All teams show very good agreement in the relative motion for Debris 6 as shown in Figure 4-17 below. (These plots are described in detail in Section 4.2.2.) JSC-SX analyzed all three videos: Sparks 0026, Springville 0009B, and Vegas 0030. The differences in the assumptions for the relative motion calculations should not affect the data for Debris 6 because all three observers are not close to the trajectory plane; therefore, the relative azimuths between the Shuttle trajectory and line-of-sight should be large. Aerospace Corporation did not analyze Vegas 0030.

Debris 6 Comparison (JSC-DM, JSC-SX, Aerospace Corporation)

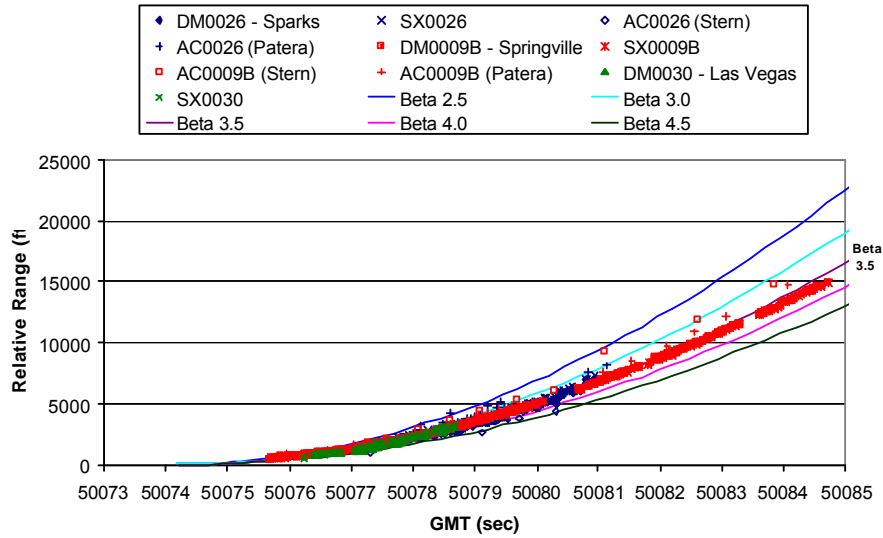


Figure 4-17: Debris 6 Relative Motion Comparison

Variations in Debris 14 data are present due to the different assumptions in the relative motion calculation methods and differences in HFOV estimation for the videos. JSC-DM and JSC-SX Vegas 0030 data matches well. This is expected since the relative azimuth between the Shuttle trajectory and the line-of-sight is 32 deg - 30 deg (table 4-5). JSC-DM and JSC-SX Flagstaff 0017 matches well. Once again the relative azimuth is large (52 deg - 61 deg), so this good comparison is expected.

Debris 14 Comparison (JSC-DM, JSC-SX, Aerospace Corporation)

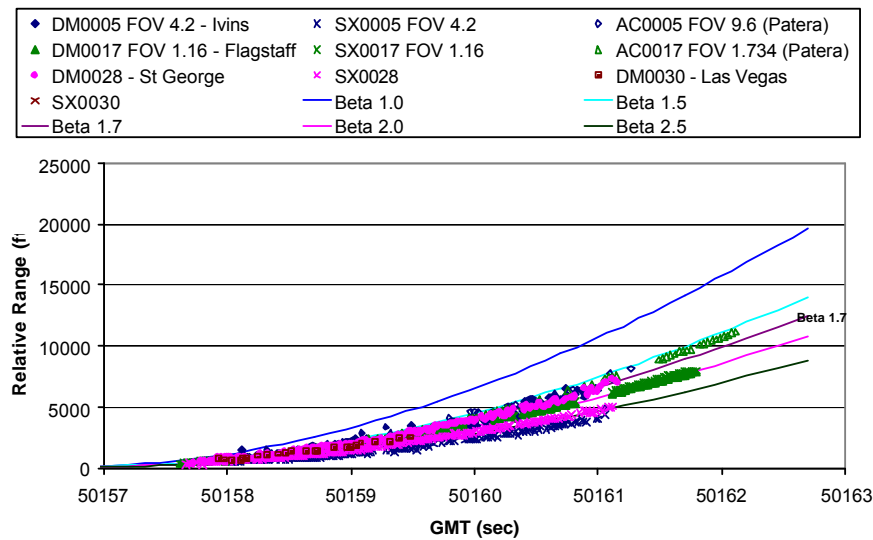


Figure 4-18: Debris 14 Relative Motion Comparison

The comparison between JSC-DM and JSC-SX for Ivins 0005 and St. George 0028 tells a different story. The JSC-SX data indicates a smaller relative range between the debris and the Shuttle for both cases as compared to the JSC-DM data. As discussed above, the difference in assumptions explains this discrepancy. JSC-SX is projecting the debris into the trajectory path; whereas, JSC-DM is accounting for vertical motion of the debris in the trajectory plane. Also, as expected, JSC-DM data for Ivins 0005 and St. George 0028 is more dispersed than the other data sets. This is due to the Line-Plane intersection error present when the observer is close to the trajectory plane as discussed earlier.

The Aerospace Corporation analyzed two of these videos for Debris 14, Ivins 0005 and Flagstaff 0017. Since Aerospace Corporation uses the same assumption as JSC-SX, one would expect the data for both videos to indicate smaller relative range values than the JSC-DM, but this is not the case. The cause is the difference in horizontal field-of-view (HFOV) estimation. JSC-DM uses a HFOV for Ivins 0005 of 4.2 deg; whereas, Aerospace Corporation uses a HFOV of 9.6 deg. JSC-DM uses a HFOV for Flagstaff 0017 of 1.16 deg; whereas, Aerospace Corporation uses 1.734 deg. The larger HFOV estimates Aerospace Corporation uses represent a higher zoom, which results in a larger relative range, as the figure illustrates.

Overall, the agreement between all the teams is quite good, considering the independent efforts and possible error sources. As illustrated, this amount of dispersion in the data still has little effect in the ballistic coefficient estimate - approximately 1 psf.

All teams show good agreement for Debris 1 relative motion. JSC-DM and JSC-SX data matches well for the Lick Observatory 0056 and Fairfield 0064 data sets. Good agreement for both Lick Observatory 0056 and Fairfield 0064 is expected because the observer is well outside of the Shuttle trajectory plane and the relative azimuth is large. Aerospace Corporation estimated one HFOV for Lick Observatory, 3.037 deg, and the data agrees well with the JSC data sets.

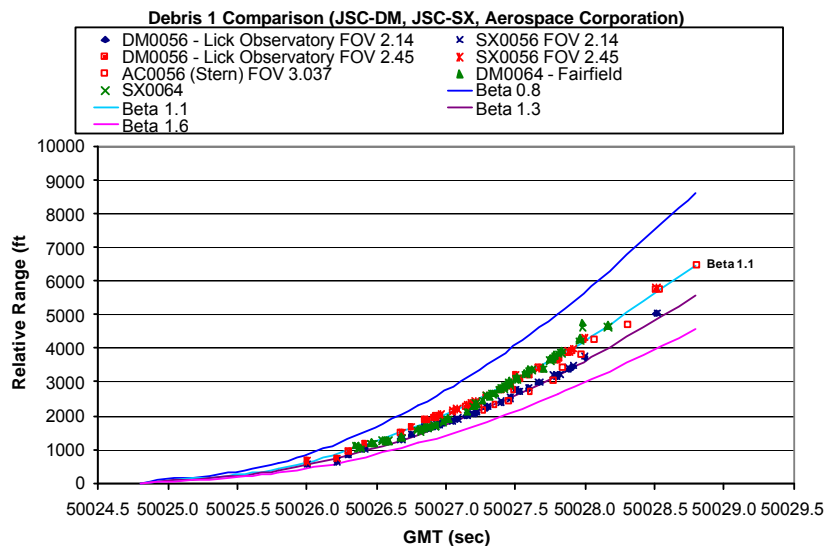


Figure 4-19: Debris 1 Relative Motion Comparison

#### 4.2.2. Detailed Relative Motion and Ballistic Analysis

Relative motion and ballistics data have been organized into several plots, one for each debris object. In each figure, relative range between the Shuttle and the debris object is plotted as a function of GMT in seconds, where 0 seconds corresponds to 12:00 AM February 1, 2003 GMT. Two types of curves are plotted: video data points and simulated beta curves. First, the data points are determined by the relative motion calculations based on pixel data gathered from the videos. The method used in these calculations has been discussed in the methodology section of this report. For each debris, data points are plotted for all videos containing footage usable for relative motion. Second, relative motion curves generated by the ET-SRB simulation and illustrated on the plots as solid lines, are plotted for a range of constant ballistic coefficients. The simulation requires density inputs for each debris, so a constant density corresponding to the estimated separation time for the debris is taken from the flight-derived atmospheric data, which was supplied by the Integrated Entry Environment (IEE) Team.

The simulated curves are compared to the relative motion data points to determine ballistic coefficient and separation time estimates. Typically, simulations are run every 0.1 seconds for separation time and every 0.1 psf for ballistic coefficient. This curve fit method reveals the separation time and ballistic coefficient with a good amount of certainty, as discussed in the Error Analysis portion of this report. The separation time, ballistic coefficient, and error ranges for each are listed on each figure.

Debris 1

The plot below shows the generated relative motion curves for two videos that observe Debris 1. An exact horizontal field-of-view (HFOV) could not be determined for the first video, which filmed from the Lick Observatory in California. As a result, a HFOV range from 2.14 deg to 2.45 deg is applied to the relative motion analysis for this particular video. The HFOV range is based on comments and zoom setting estimations provided by the camera owner. The second video, filmed from Fairfield, CA, provides additional confirmation of the relative motion derived from the Lick Observatory video. The Fairfield relative motion curve is derived based on a HFOV of 5.25 deg and matches well with the relative motion curve for Lick Observatory with a 2.45 deg HFOV. Since the Fairfield relative motion agrees with the Lick Observatory data for the higher HFOV, the estimated ballistic coefficient of 1.1 psf is based on the Lick Observatory 2.45 deg HFOV curve. The estimated separation time is 13:53:44.80 GMT. The error bars for this debris piece are +/- 0.5 psf for ballistic coefficient and +/- 0.60 sec for separation time.

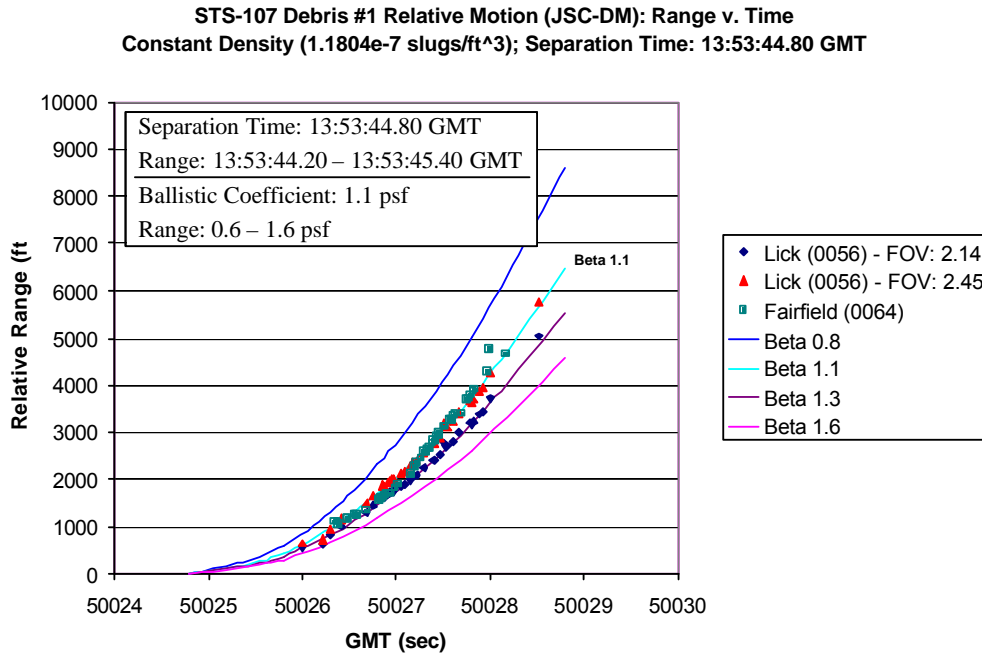
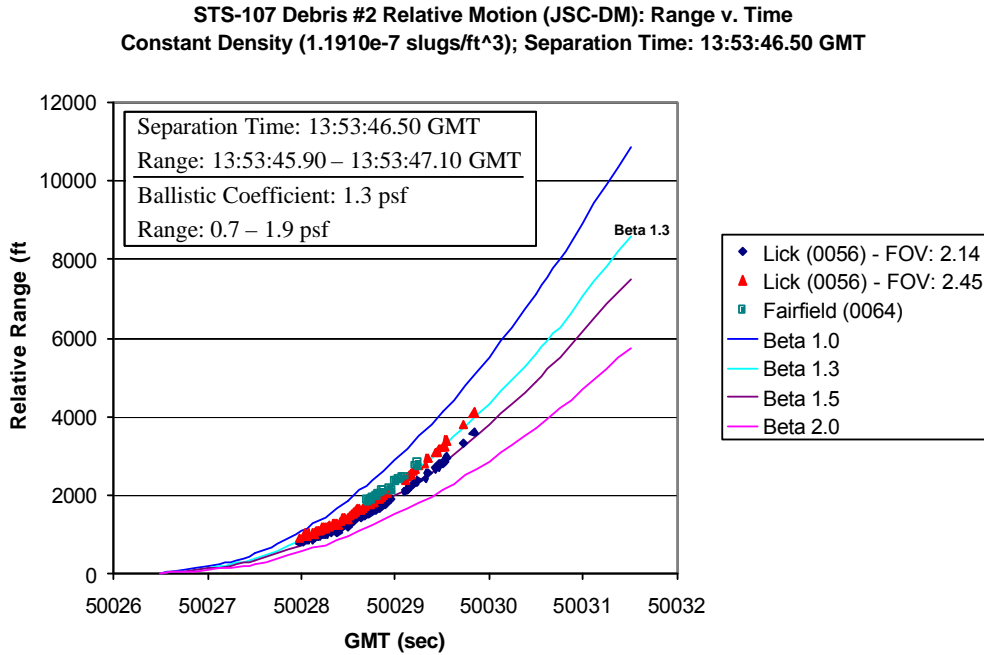


Figure 4-20: Debris 1 vs. Columbia Relative Motion

Debris 2

The same videos and HFOV ranges for Debris 1 are also present for Debris 2. The Fairfield data again suggests that a HFOV of 2.45 deg for the Lick Observatory video is more accurate due to the similarity of the relative motion curves between the two videos at the higher HFOV. Using the Lick Observatory relative motion data with a HFOV of 2.45 deg as the best estimate for ballistic computations, a separation time of 13:53:46.50 GMT and a ballistic coefficient of 1.3 psf are estimated for this debris piece. The estimated error bars for Debris 2 are +/- 0.6 psf for the ballistic coefficient and +/- 0.6 sec for the separation time.



Debris 3

Two observers capture Debris 3 video footage usable for relative motion calculations: one at Lick Observatory and one in Sparks, NV. Yet again, as in Debris 1 and Debris 2, the Lick Observatory 0056 data cannot be narrowed down to one HFOV, so a range has been used, 2.14 deg - 2.45 deg. As in the plots for Debris 1 and Debris 2, the data seems to indicate a better match with a HFOV of 2.45 deg. A low ballistic coefficient of 0.55 psf with the range 0.1 - 1.0 psf is determined for Debris 3. The estimated separation time is 13:53:56.10 GMT with the range 13:53:55.60 - 13:53:56.60 GMT.

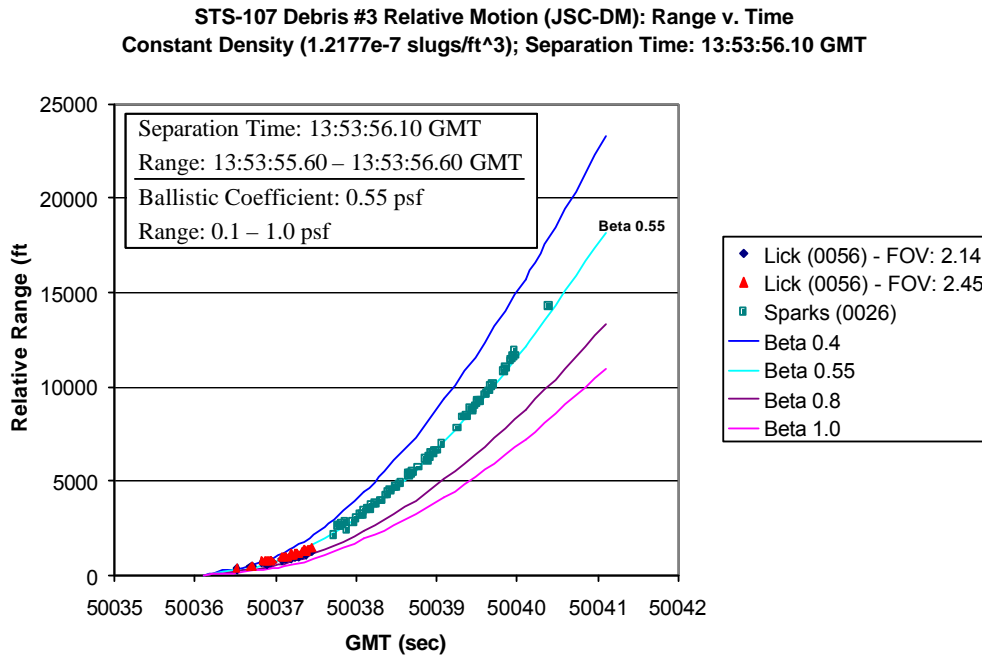
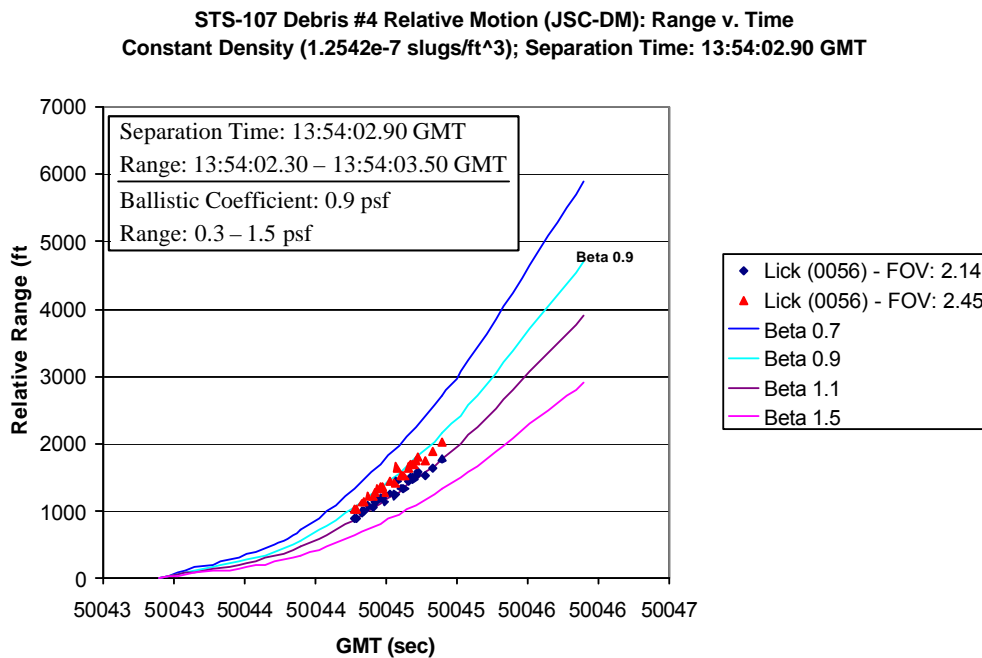


Figure 4-22: Debris 3 vs. Columbia Relative Motion

Debris 4

Only one observer (Lick Observatory 0056) views Debris 4. Once again, relative motion is calculated for both HFOV 2.14 deg and 2.45 deg. However, this time there is no other video data that can help select one HFOV over the other. Here other debris information is used to determine the best ballistic coefficient estimate. Since the relative motion data for Debris 1, 2, and 3 all point to Lick Observatory 0056 with HFOV 2.45 deg as the better HFOV, an assumption is made that the HFOV does not change for Debris 4. Thus, the ballistic coefficient estimate is 0.9 psf with the range 0.3 - 1.5 psf. The separation time is estimated to be 13:54:02.90 GMT with the range 13:54:02.30 - 13:54:03.50 GMT.



Debris 6

Debris 6 was the first “early sighting” debris object to be analyzed because several characteristics of this debris event reduced the complexity of the analysis. Foremost, the Sparks, NV 0026 video for this debris event contains an excellent celestial reference. As the debris separates from the Shuttle, not only does Venus enter the field-of-view, but the Orbiter passes directly through Venus from the observing perspective. This convenient event helps provide a very accurate time synchronization and aids in the determination of scaling information for the video. Debris 6 looked promising because it was also viewed for the longest period of time. An observer in Springville, CA 0009B captures close to ten seconds of footage usable for relative motion calculations. Typically, only 2-3 seconds of usable footage was collected by the



observers. And finally, Debris 6 appears bright in the video footage, which increases the accuracy of tracking (pixel) data for the debris.

Three videos contain adequate data for relative motion calculations: Sparks, NV 0026; Springville, CA 0009B; and Las Vegas, NV 0030. Horizontal field-of-view (HFOV) for Sparks is well known due to the celestial reference. The Springville timing is well known, but the HFOV is uncertain because the camera is zoomed somewhere in the optical region. The Image Science and Analysis group (JSC-SX) estimated HFOV for Springville at 3.6 deg because this HFOV forces Springville relative motion to match the Sparks relative motion. Unfortunately, this approach makes the Springville data mostly obsolete, for no new estimates will result from Springville that could not be derived from Sparks. Consequently, while this HFOV for Springville was used, a rather large error bar has been applied to HFOV error source in ballistic coefficient estimates to account for the HFOV uncertainty. Las Vegas separation time and HFOV are uncertain for Debris 6. Thus, the relative motion has been shifted to match Sparks. This also renders Las Vegas obsolete for estimates; however, Las Vegas views several other debris objects. Using the information gained from this shift for Debris 6 provides additional information for other debris.

As listed for Debris 6, a separation time of 13:54:34.20 GMT and ballistic coefficient of 3.5 psf fit the data the best. The error ranges on these estimates are as follows: 13:54:33.70 - 13:54:34.70 GMT and 3.0 - 4.0 psf. Debris 6 has the highest ballistic coefficient of all debris objects analyzed.

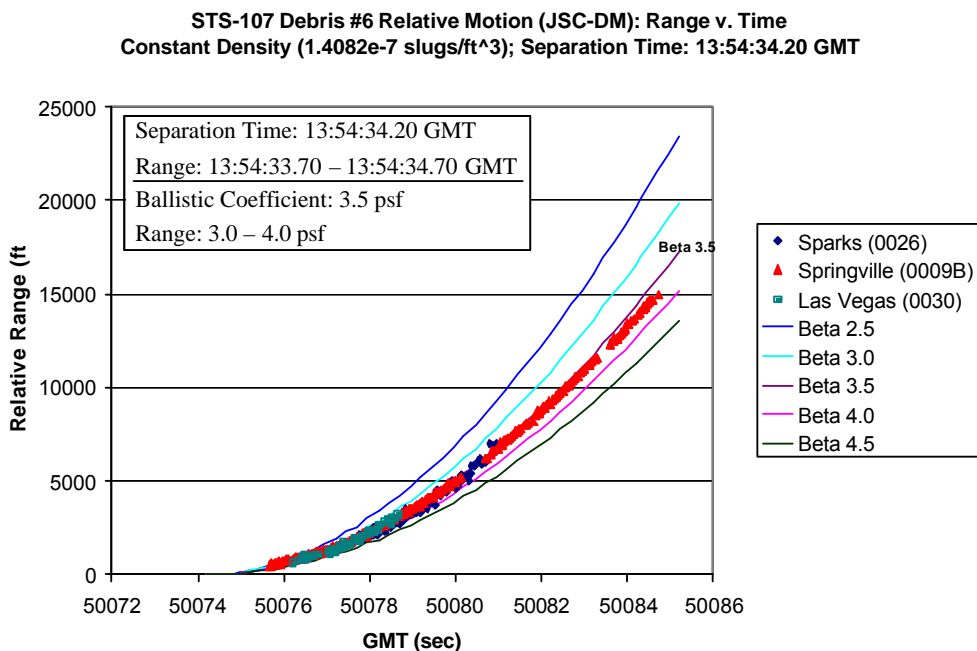
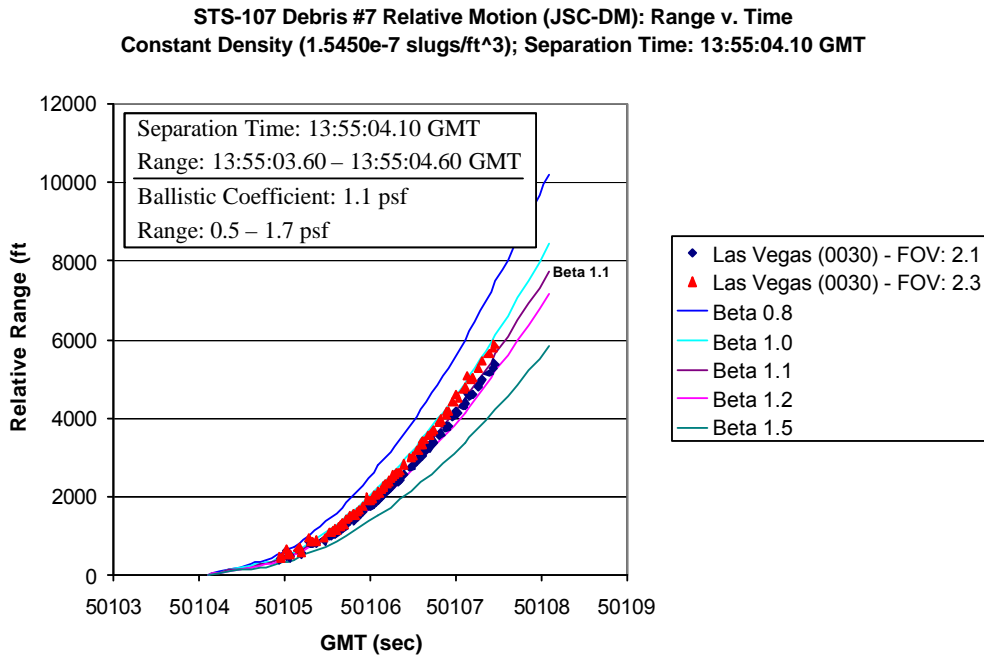


Figure 4-24: Debris 6 vs. Columbia Relative Motion

Debris 7

One observer in Las Vegas, NV views Debris 7. A HFOV range is used: 2.1 deg - 2.3 deg. Since no available information indicates which HFOV is more likely, the ballistic coefficient is estimated using the middle of the HFOV range. However, the error bar on the ballistic coefficient accounts for all possible HFOV's. The estimated ballistic coefficient is 1.1 psf with the range 0.5 - 1.7 psf. The estimated separation time is 13:55:04.10 GMT with the range 13:55:03.60 - 13:55:04.60 GMT.



Debris 8

One observer located in Las Vegas captures video footage suitable for relative motion calculations for Debris 8. This video appears to zoom in from the time Debris 7 is viewed to the time Debris 8 appears. This information indicates that the observer is probably at the maximum optical zoom during Debris 8 footage, corresponding to a HFOV of 2.1 deg. The ballistic coefficient for Debris 8 is surprising because it rivals Debris 6 for the largest beta estimate. The ballistic coefficient for Debris 8 is estimated at 3.4 psf with the range 2.6 - 4.0 psf. The separation time is estimated at 13:55:20.80 GMT with the range 13:55:20.20 - 13:55:21.40 GMT.

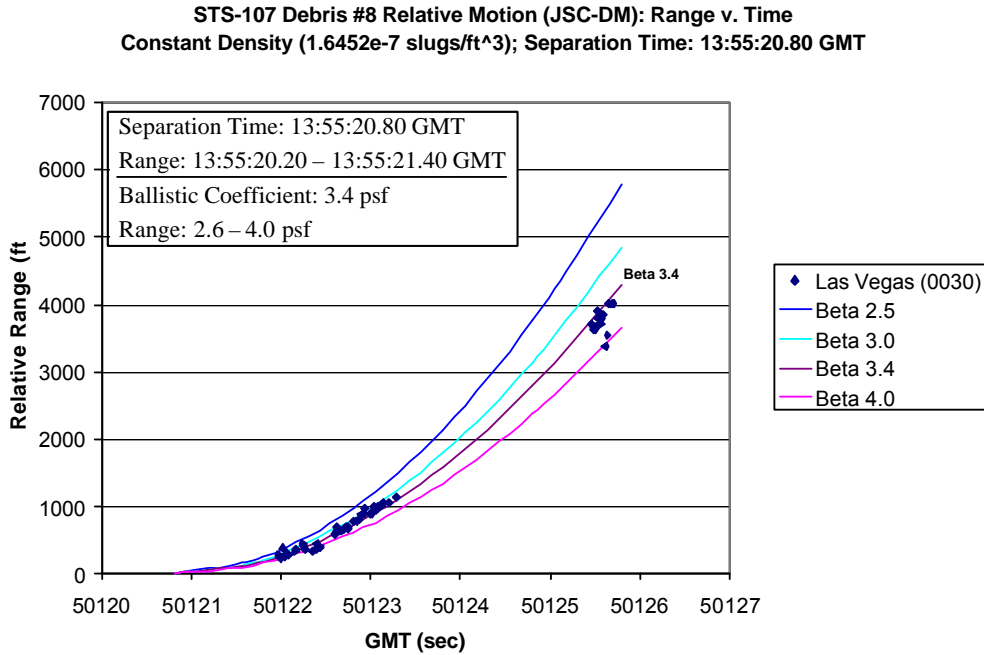


Figure 4-26: Debris 8 vs. Columbia Relative Motion

Debris 13

One of the significant aspects of analyzing Debris 13 is the confirmation of the time sync applied to the Debris 14 videos. The two videos that observe Debris 13 are Ivins and Flagstaff, both of which also observe Debris 14. The time biases that were applied to these two videos for Debris 14 could not be confirmed without the Debris 13 relative motion. As shown in the plot below, the two relative motion curves match very well, thereby significantly increasing the level of confidence in the time syncs. Similarly to Debris 14, the Ivins data for Debris 13 is more noisy than the other relative motion curves analyzed. Again, this is due to the viewing geometry, and one of the beta curves plotted above fits the data quite well. The estimated ballistic coefficient for Debris 13 is 0.65 psf with an error bar of +/- 0.45 psf, and the separation time is estimated at 13:55:53.80 GMT with an error bar of +/- 0.5 sec.

**STS-107 Debris #13 Relative Motion (JSC-DM): Range v. Time**  
Constant Density (1.8305e-7 slug/ft<sup>3</sup>); Separation Time: 13:55:53.80 GMT

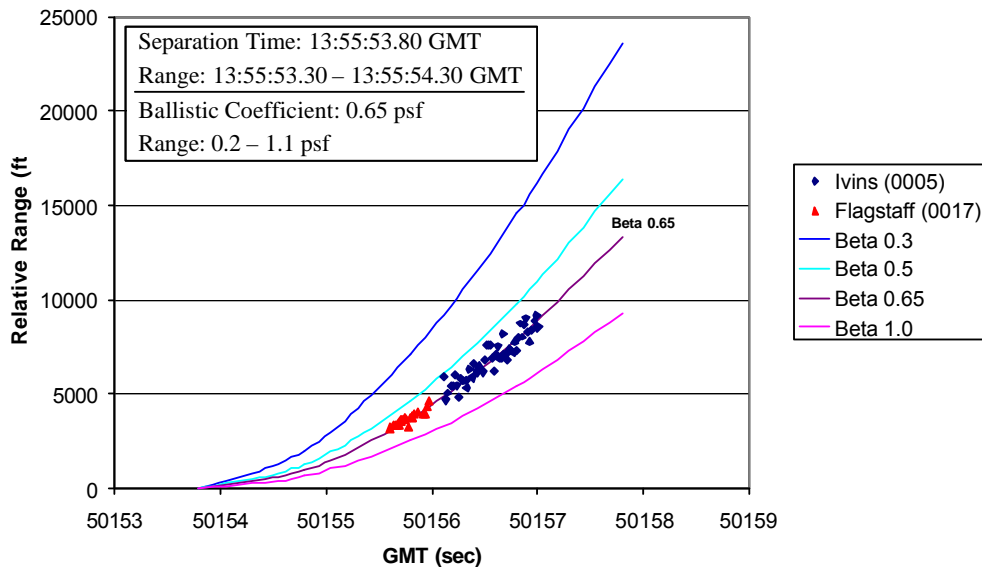


Figure 4-27: Debris 13 vs. Columbia Relative Motion

Debris 14

Debris 14 has the largest amount of relative motion data of all the debris pieces, and along with Debris 6, it was initially considered to be one of the most promising debris pieces. The relative motion curves plotted below are derived from the following videos: St. George, UT (0028), Flagstaff, AZ, Las Vegas, NV, and Ivins, UT. Relative motion was also completed for another video, St. George, UT (0021), but this relative motion curve was thrown out since there is significant zooming taking place during the region of interest. Since the time synchronization of the St. George, UT (0028) video is considered to be the most reliable time sync, the other video time syncs are biased in order to match all the separation times. The only exception is the Las Vegas video time sync, which is set based on Debris 6 relative motion. The Debris 14 relative

motion for Las Vegas confirms the time synch applied for Debris 6. Once the appropriate time biases are applied, the relative motion curves for all four videos match fairly well with each other. With the exception of Las Vegas, the duration of the tracking data is rather large for each of the videos. The relative motion data for Ivins, UT is slightly more noisy than the other relative motion curves, but a curve fit of the Ivins data matches very well with the other Debris 14 videos. The noisiness of the Ivins data is due to the close proximity of the observer location to the Shuttle trajectory plane. As described earlier, the relative motion tool calculates the intersection between a line (vector OB) and a plane (trajectory plane). When the observation point is close to the trajectory plane, a small shift to the line (vector OB) results in a larger shift to the line-plane intersection point, thereby amplifying any errors in the tracking data.

The estimated ballistic coefficient for Debris 14 is mostly based on the St. George, UT (0028) relative motion curve since it has the most reliable time sync and scaling information. The other videos all agree to within +/- 0.2 psf on the ballistic coefficient, and this range is incorporated in the error bar applied to this debris piece. The estimated ballistic coefficient is 1.7 psf with a beta range of 1.0 to 2.4 psf. The separation time is estimated to be 13:55:56.70 GMT with a +/- 0.5 sec error bar.

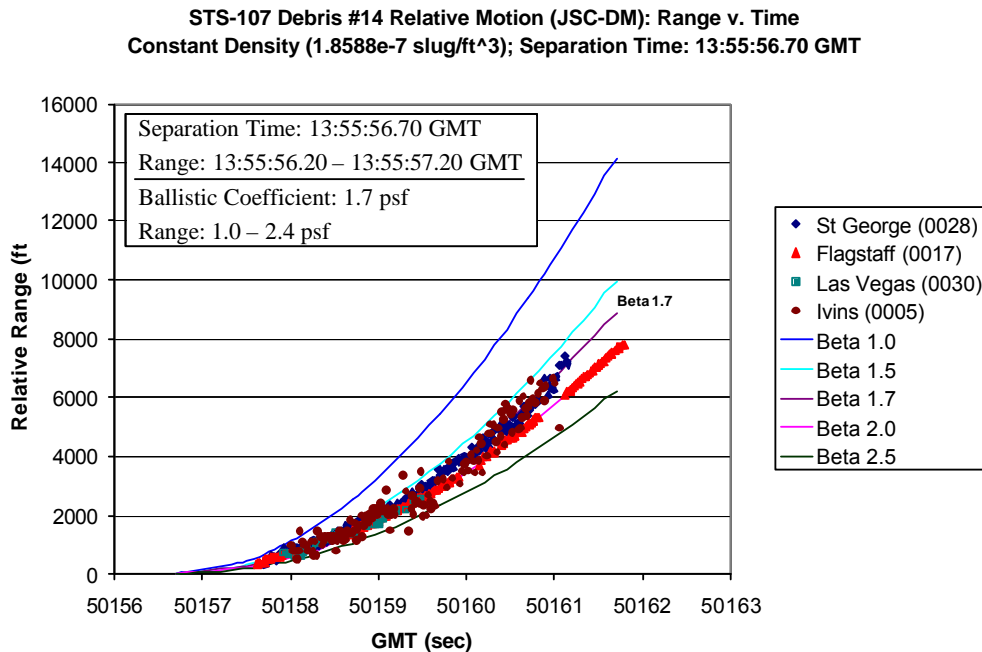


Figure 4-28: Debris 14 vs. Columbia Relative Motion

Debris 16

A video from Kirtland AFB in New Mexico is the only video to observe Debris 16. The amount of relative motion data for this video is quite limited. The debris piece is extremely faint in the video and is therefore very difficult to extract from the video noise. As a result, the chance for inaccurate tracking data is significantly higher, and the error bars are adjusted accordingly. Since this particular video was filmed using a telescope mount, the camera rotation effects are neglected and a high level of confidence is placed on the HFOV estimations. A ballistic coefficient of 0.3 psf is estimated for Debris 16, which is the smallest ballistic coefficient of all of the debris pieces analyzed. The separation time is estimated to be 13:57:23.90 GMT with an error bar of +0.3, -0.7 sec. The error bar on the positive side is limited to +0.3 sec because the beginning of the relative motion data is soon after the estimated separation time. The range for ballistic coefficient is 0.1 to 1.0 psf. The +0.7 psf error bar on beta reflects the low level of confidence in the tracking data.

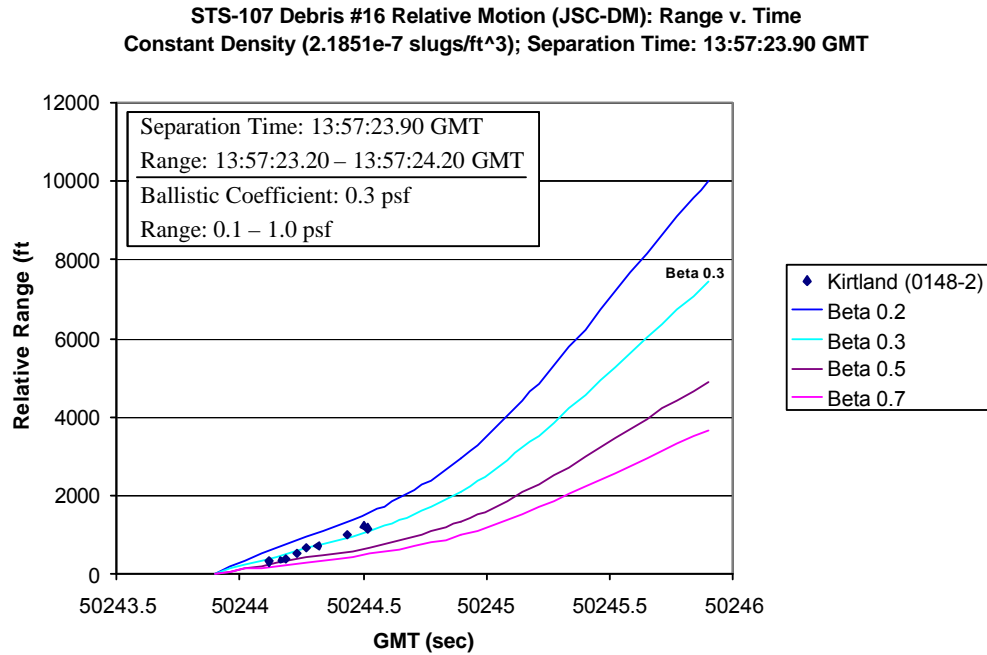


Figure 4-29: Debris 16 vs. Columbia Relative Motion

### 4.3. Trajectory and Footprints

Unless otherwise footnoted, Section 4.3 is referenced to [24], Mrozinski, R. B.; JSC-DM; STS-107 Columbia Accident Debris Footprint Boundary Estimates; June 3, 2003. This is included in its entirety in Appendix 10.6.

#### 4.3.1. Trajectory and Footprints Summary and Methodology

The Flight Design and Dynamics Division (JSC-DM) within JSC's Mission Operations Directorate (MOD) estimated debris footprint boundaries for:

- 1) The primary debris field resulting from Columbia's catastrophic breakup, for which found debris strongly validates the results,
- 2) The debris impact areas for debris observed in video to have separated from Columbia prior to the catastrophic breakup, and
- 3) A general swath that would contain all debris that could have separated from Columbia, whether or not it was seen on video.

Additionally, JSC-DM estimated the separation time of the tile found in Littlefield, Texas (KSC Database object number 14768). This work started on February 01, 2003 and continued through June 03, 2003.

The bulk of the content of this section is devoted to footprint boundary estimates for three categories:

- 1) The Texas/Louisiana debris field resulting from the primary, catastrophic breakup
- 2) A generic debris swath along the entire STS-107 entry trajectory predicting all possible impact locations for pre-breakup debris in the United States for any possible debris characteristics, and
- 3) Specific debris footprint boundaries for debris observed to have separated from the orbiter prior to catastrophic breakup.

JSC MOD-DM has been updating debris footprint boundary estimation methodology since 1998, primarily in support of the X-38/CRV program, and in preparation for the eventual disposal of the International Space Station. Several papers document this evolving methodology and its application to various projects [26], [27], [28].

The X-38/CRV vehicle would dispose of its Deorbit Propulsion Stage (DPS) just prior to entry interface. The DPS would trail the crewed Entry Vehicle on entry, and it would breakup and scatter debris into the ocean, while the Entry Vehicle would use its lifting capabilities to move further downrange to a runway landing. Since the placement of the DPS debris footprint must be entirely over water, and since this requirement severely reduces the available landing locations around the globe, JSC's footprint boundary estimation methodology had to adjust to produce a conservative, but not overly conservative, result. This was very important, because as the DPS footprint grows larger, the number of acceptable landing site locations decreases quickly.

JSC MOD-DM has presented the methods and assumptions used in this investigation to several NASA peer-reviews and in international and U. S. forums for feedback, and continuously refined the methodology presented here.

Air Traffic Control (ATC) radar data, and debris found thus far, both strongly support the STS-107 primary footprint boundary results.

A 3 degree-of-freedom simulation predicts the boundaries of the debris footprints. The simulation in this case is called the Simulation and Optimization of Rocket Trajectories [29].

The simulation uses a fourth-order Runge-Kutta method to integrate the equations of motion. MOD-DM assumed that integration method effects on the footprints were minimal, and did not investigate integration methods further.

This work modeled Earth as an oblate spheroid, as set by the equatorial and polar radii (20,925,741.47 ft and 20,855,591.47 ft, respectively). The model assumes that the polar axis is an axial axis of symmetry, and is the planet's rotational axis with an Earth rotation rate of  $7.292115146 \times 10^{-5}$  deg/sec. The gravitational model consisted of the central gravitational force (planet gravitational constant of  $1.40764685328 \times 10^{16}$  ft<sup>3</sup>/sec<sup>2</sup>), adjusted via the first three oblate zonal harmonic coefficients (J<sub>2</sub>, J<sub>3</sub>, and J<sub>4</sub> with unitless values of  $1.0826271 \times 10^{-3}$ ,  $-2.5358868 \times 10^{-6}$ , and  $-1.6246180 \times 10^{-6}$  respectively). JSC-DM assumed that planet and gravity model effects on the footprints were minimal, and did not investigate these further.

The simulation assumes an instantaneous breakup, not a multi-stage breakup as occurs in reality, because the breakup is simply too chaotic to predict any breakup sequence. Due to the chaotic nature of a breakup, and due to non-linearities in the large number of variables involved, especially in atmospheric effects, a parametric approach is ruled out in favor of a Monte Carlo approach. This study uses a sample size of 500, and by using the maximum and minimum ranges and crossranges flown in the simulation, arrives at footprint boundaries that bound 99% of the debris pieces with 95% confidence, given our assumptions [31].

Experience with the methods used here demonstrates that winds have significant impact on the width of the footprint (more pronounced near the heel, or least-range-flown part of the footprint), but negligible impact on the footprint's toe, or most-range-flown point [26]. Thus, the Monte Carlo method used here uses the GRAM-99 atmospheric density and wind database models for dispersions. GRAM models localized winds, density, density variations and shears, and solar activity effects, all in a Monte Carlo environment. (GRAM localizes density perturbations and winds, such that they are specific to the latitudinal and longitudinal position, as well as altitude, month, etc.) This study used GRAM with an entry date of February 01, 2003, and the actual solar activity values for mean solar 10.7 cm radio noise flux and geomagnetic index on February 01 (values of  $164.0$  Janskys  $\times 10^{-4}$  and  $2.58$ , respectively) [33]. This methodology utilized the 1999 GRAM model for uncertainties (rpscale = 1.0, or  $3\sigma$ ), applied about a "mean" day-of-entry atmosphere as provided by the DAO (rev D) [32], [34].

JSC-DM did not model explosions for two reasons: 1) there is no evidence thus far of any imparted velocities to debris (debris found thus far does not support an explosion, nor is there



any video evidence of an explosion), and 2) any explosion would have been nearly impossible to model with any certainty without performing a detailed blast analysis.

Initial conditions for the primary breakup are from one of these sources: they are the last BET vector, or the last GPS vector, or they are taken along a 220 psf ballistic trajectory initiated at one of these two vectors. The Debris Footprint Team selected a 220 psf trajectory as it will bound in altitude the entire debris field. The simulation sheds debris off this 220 psf trajectory to define the “feather” shape of the debris footprint as shown later. The team selected 220 psf as it was the maximum ballistic coefficient object observed in the debris field.

The initial condition vector for a piece of pre-breakup shed debris is the orbiter BET vector at the time that the Relative Motion Team computed for that piece of debris to have separated from the orbiter.

Note that the simulation terminates when the altitude relative to the oblate spheroid model is zero. This is not when the local topographical altitude is zero. Thus, the footprint boundaries are conservative when the local topography is above zero feet in elevation.

The assumption of constant mass and aerodynamics is erroneous in reality due to the possible ablation and separation of debris pieces through their entry. However, in modeling the heel of the primary debris footprint, and in modeling the post-breakup shedding debris, the ballistic coefficients used (0.5 psf and 20 psf) are intended to represent an equivalent average value, rather than the actual indeterminable values. In the cases where a ballistic coefficient is observed (the toe of the primary debris footprint, and the footprints for all pre-breakup shed debris), it is impossible to model the ballistic coefficient variation with time without knowing the actual mass, area, and drag characteristics of the object, and without knowing of ablation and interaction with other debris; thus one is forced to a constant  $\beta$  assumption even with an observed  $\beta$ . Furthermore, it has been shown for satellite reentries, that variations in drag coefficient do not affect the overall footprint estimates [35].

Note that for a ballistic (non-lifting) trajectory, designating values of  $m$ ,  $S$ , and  $C_d$  is arbitrary, since when the lift is zero it is only the ballistic coefficient that dictates the trajectory of the object. However, when modeling a lifting coefficient, the values are no longer arbitrary. The hypersonic through to subsonic drag coefficient for any debris object is estimated to be approximately 0.5 - 1.5; thus a value of 1.0 is chosen.

The maximum L/D ratio found in the Debris Footprint Team’s research of past studies found a maximum L/D of 0.15 in Soyuz launch vehicle studies [27], [36]. Although debris pieces generally can exhibit higher L/D values, they were unlikely to hold the lift vector in a constant orientation as modeled here. The 0.15 value is a reduced L/D that applies when constant bank angles are used [37]. Since the team assumed that the pieces of debris will neither trim at a stable orientation, nor tumble at a high enough rate to generate substantial lift, and since the methodology is conservative in uniformly dispersing L/D, the methodology is able to assume a L/D in the range of 0.0 - 0.15, for all debris.

For the primary debris footprint, the team bounded the lower end of  $\beta$  at 0.5 psf, rather arbitrarily, assuming that the bulk of the debris will be higher than 0.5 psf. In selecting the low end for the primary debris field, the team felt 0.5 psf to be adequately conservative since any identifiable pieces of less than this value would have the lowest capability of all the pieces to cause damage. The team bounded the upper end at 220 psf, as that was the maximum ballistic coefficient observed. The simulations model post-breakup shedding debris at 0.5 psf and 20 psf. 20 psf is the maximum ballistic coefficient modeled in post-breakup shedding, because it maximizes the width of the footprint (increasing  $\beta$  increases width until around 20 - 30 psf), without overextending the toe of the footprint, e.g., increasing this quantity to 30 psf would not significantly widen the footprint, but would significantly extend the length, which is not supported in the debris located thus far.

For pre-breakup shedding debris whose relative motion and ballistic coefficient was analyzed from video, the methodology uses the resulting ballistic coefficient. Otherwise, the methodology uses a range of 0.5 - 5.0 psf to conservatively bound the results of the debris analyzed by the relative motion and ballistics experts, i.e., the methodology assumed that the non-analyzed debris would be similar to the analyzed debris.

The following data were calculated for each debris item based on public video as described in Section 4.2: the best estimated separation time, the separation time range (accounting for the error range), the best estimate of ballistic coefficient, the ballistic coefficient range (accounting for errors), and the constant atmospheric density value used in the ballistic coefficient calculation (which comes from the DAO day-of-entry atmosphere model). These are listed in Table 4-3 in Section 4.2.

### 4.3.2. Primary Debris Footprint

The Debris Footprint Team received a call to come in at 1030 (central time) on the day of the accident, and presented at 1200 central the first prediction of a debris line and an intact crew module impact location. The initial condition was the closest pre-entry predicted trajectory point (at 13:59:23.96 GMT) to the GMT that remained frozen on the screens in Mission Control (13:59:22 GMT). The team assumed that breakup occurred at that time, and that the intact crew module became a free-flying object at this time (because no better data was available). The United Space Alliance provided quick estimates of crew module size and mass: 30000 lb crew and contents; 17.75 ft diameter area ( $\beta = 121.2$  psf) [39]. A ballistic trajectory predicted an intact crew module impact location of 31.02 N, 93.58 W.

The team estimated the debris line by assuming a ballistic coefficient range of 0.5 - 116 psf, as in previous analyses [26], [27], [28], based on historical studies. Because the first debris line was due at the Mishap Investigation Team at 1200, no time was available to perform a Monte Carlo analysis, so the Debris Footprint Team simulated two ballistic trajectories (0.5 and 116 psf) through a 1976 Standard Atmosphere, without winds, to arrive at a zero-width debris line. Monte Carlo methods would be needed to arrive at a predicted width, but would take several hours to prepare and run, thus the team was released for this day.

The next primary debris footprint release was on February 04. This release added the 1999 Global Reference Atmosphere Model (density, wind speed, and wind direction) for February 01 along the orbiter trajectory. JSC-DM selected a sample size of 500, as done in previous studies [26], [27], [28]. The Debris Footprint Team had also now identified an actual piece of hardware that could have a ballistic coefficient higher than 116 psf, thus the upper limit of ballistic coefficient increased to this value (Reaction Control System jet nozzle  $\beta = 180$  psf).

The next primary debris footprint release was on February 07. The primary difference was an update the initial condition, now at 13:59:30.4 GMT [40]. Since this time was 6.5 seconds later than the original last-known-position time, the results showed a significant shift in the debris footprint boundaries due to the banking and lifting toward the north for those 6.5 seconds. Also, the Debris Footprint Team had now received information that a 220 psf object was observed in the debris field, thus the methodology updated to a maximum ballistic coefficient of 220 psf (SSME powerhead).

The next primary debris footprint release was on February 14. The Debris Footprint Team corrected a minor simulation error, incorporated a somewhat later (0.04 sec) GPS vector [41], and completely abandoned the 180 psf upper limit on ballistic coefficient in favor of the 220 psf observed value.

The next primary debris footprint release was on April 10, and included several major modeling improvements. The biggest improvement was transitioning from the GRAM-99 atmosphere model for density, wind speed, and wind direction, to rev C of a day-of-entry model provided by the DAO, and including recommended 10% uncertainties about the DAO mean for density, wind speed, and wind direction [42].

The next major change was moving to two initial condition vectors, which the Debris Footprint Team believes bounds the time at which the orbiter became ballistic (lost lift). The first time (13:59:37.00 GMT) is the last vector in the BET version 4 [43]. The final time (14:00:02.12 GMT) is the final GPS downlisted vector during the 32 seconds of additional data following the original loss of signal [44]. The reason for looking at two vectors was to capture the complete sweep in the debris centerline as in the final stages before catastrophic breakup the vehicle was banking toward the north. If the vehicle began losing debris, but still continued to bank and pull lift toward the north, some debris could lie on a centerline south of the centerline generated at the catastrophic breakup point. Thus, the team transitioned to two breakup times and added centerlines to the resulting footprints. There is no GPS data in between these two selected times, and the team strongly believes the vehicle was lifting at the first time and not lifting at the second time; thus the methodology has the shortest possible range of times during which the vehicle became ballistic.

The final major change was simulating shedding debris post-breakup. The simulations did this by shedding debris off of two 220 psf ballistic trajectories starting from each of the two state vectors (BET and GPS) selected above, in 30 second intervals. The 220 psf trajectory will bound all debris in the debris field and will produce upper limits in width of the footprint. As the post-breakup shedding times become closer and closer to the ground, the footprint width begins to shrink, thus forming the “feather” shape.

The current primary debris footprint release incorporates the latest and final DAO day-of-entry atmosphere model. DAO did not provide uncertainties information, other than to use the GRAM model’s uncertainties. Reference 34 states to use the GRAM model with  $rpscale = 1.0$  (3 sigma dispersions).

Figure 4-30 shows the overlaid historical progression of the primary debris footprint boundary predictions. Each box of text highlights the primary differences from the previous footprint prediction.

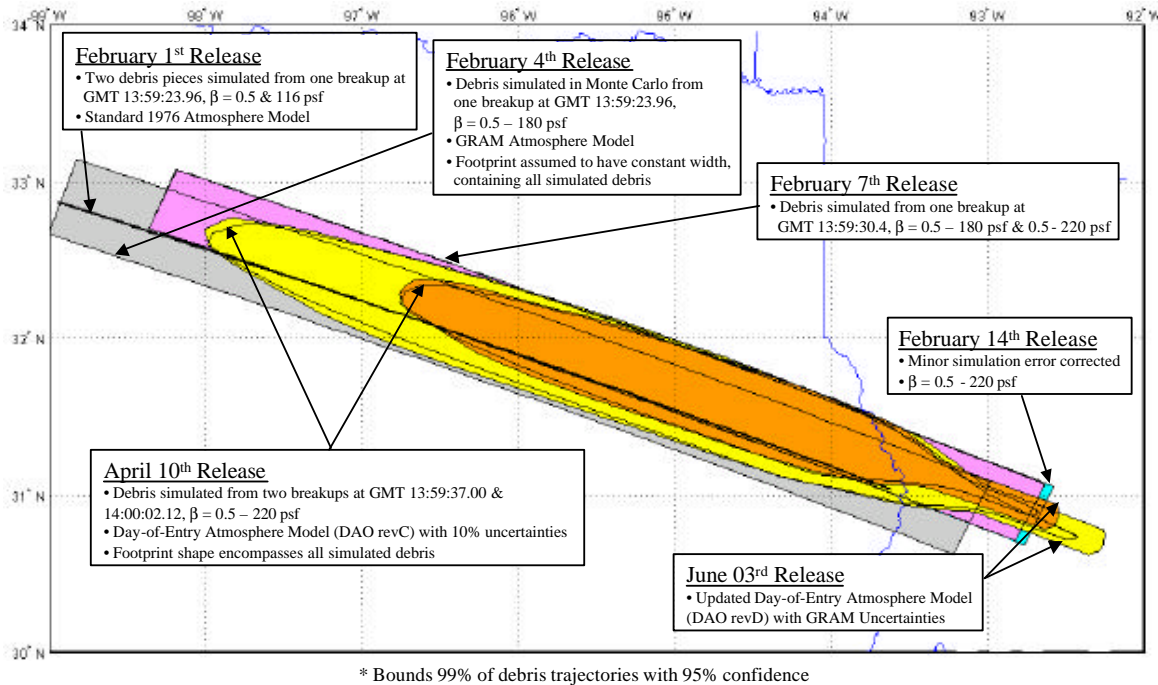


Figure 4-30: Overlaid History of Estimated Columbia Primary Debris Fields

The methodology forms the primary debris footprint by combining four “sub” classes of debris footprints. The Debris Footprint Team begins with shaping the heel of the footprint. The entire ability to shape the footprint revolves around the premise that the maximum ballistic coefficient that can sustain lift is 20 psf. Simulations demonstrate that lifting trajectories produce an increasing footprint width as ballistic coefficient is increased from 20 psf to 30 psf, where the width peaks, then begins to decrease with further increases in ballistic coefficient. The simulations use 20 psf to achieve the maximum width (most conservative) rather than 30 psf because the 30 psf results would artificially extend the footprint boundary too far into Louisiana, which is not supported by found debris or radar data. Thus, the team converged on 20 psf as the appropriate value above which the simulations do not model L/D.

The methodology uniformly distributes a full range of L/D of 0.0 - 0.15 for the ballistic coefficients shown, up to the maximum 20 psf.

Figure 4-31 shows the results of the heel-shaping Monte Carlo runs. The impact points are simulated impact points, and are not representative of actual debris or the actual debris distribution within the debris footprint. Note that to arrive at an actual debris distribution, one would have to know three things:

- 1) A histogram of ballistic coefficients vs. quantity. At some point, if ballistic coefficients are tabulated for ALL Columbia debris, this histogram could be generated. Until then, one could only assume a histogram. The Debris Footprint Team believes that the majority of debris is in the 0.5 - 20 psf range, followed by 20 - 40 psf, 40 - 60 psf, with a minimal amount of debris above 60 psf.

- 2) A histogram of separation altitude vs. ballistic coefficient. In general, the Debris Footprint Team believes that lower ballistic coefficient objects will tend to separate from their parent objects earlier than higher ballistic coefficient objects. Again, one can only make assumptions about this behavior.
- 3) A histogram of L/D vs. ballistic coefficient. In general, the Debris Footprint Team believes that only low ballistic coefficient objects are capable of sustained L/D (in magnitude and direction), and that the L/D capability drops off very sharply as ballistic coefficient increases. However, one can only make assumptions about the exact nature of this curve.

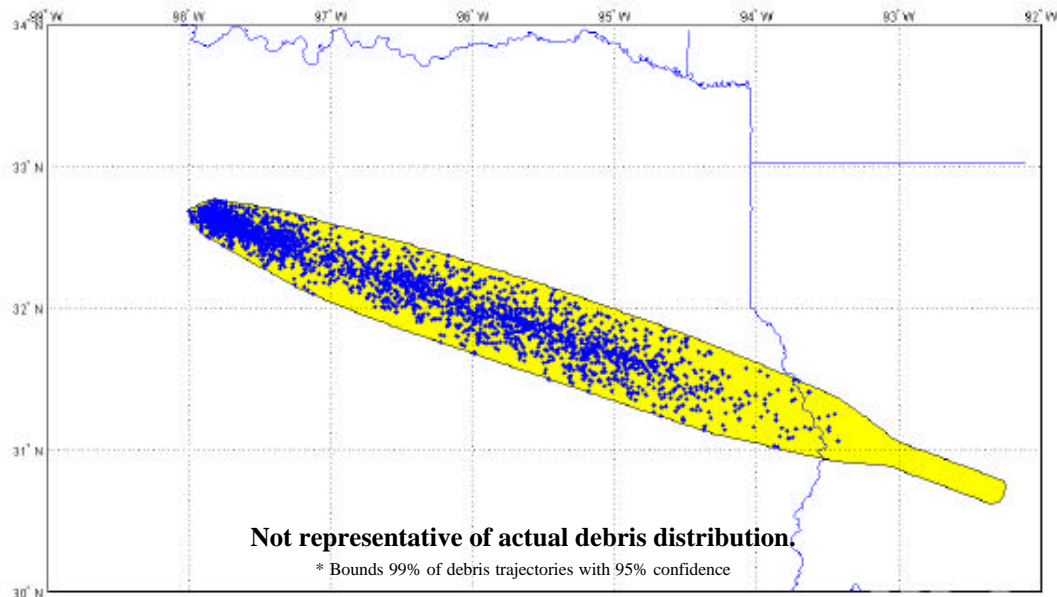


Figure 4-31: Heel Shaping Results of Estimated Columbia Primary Debris Field  
Ballistic Coefficients Between 0.5 psf & 20 psf, L/D 0-0.15,  $C_d$  1.0  
Propagated from Orbiter State at GMT 13:59:37.00

The methodology continues with finding the toe of the footprint. In Figure 4-32, the Debris Footprint Team simulates no L/D for ballistic coefficients from 10 psf up to 220 psf.

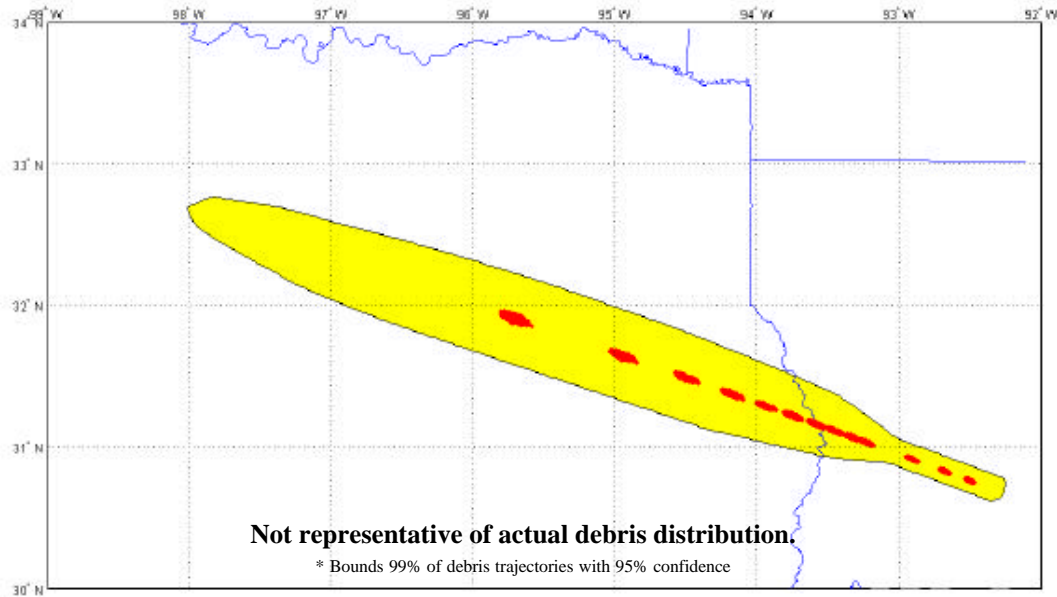


Figure 4-32: Toe Shaping Results of Estimated Columbia Primary Debris Field  
Ballistic Coefficients Between 10 & 220 psf,  $L/D = 0$ ,  $C_d 1.0$   
Propagated from Orbiter State at GMT 13:59:37.00

The methodology continues with defining the shape of the footprint between the heel and the toe. Here the Debris Footprint Team uniformly distributes a full range of  $L/D$  of 0.0 - 0.15 for 1.5 and 20 psf ballistic coefficients, for IC's every 15 seconds along the 220 psf ballistic trajectories. The footprint is shaped by shedding lifting objects every 15 seconds from the highest-altitude trajectory possible, as defined by a ballistic 220 psf (observed) trajectory from the last BET or GPS vector. These are shown below in Figure 4-33, with the 1.5 psf simulation on the left, 20 psf simulation on the right. The impact points are simulated impact points, and are not representative of actual debris or the actual debris distribution within the debris footprint.

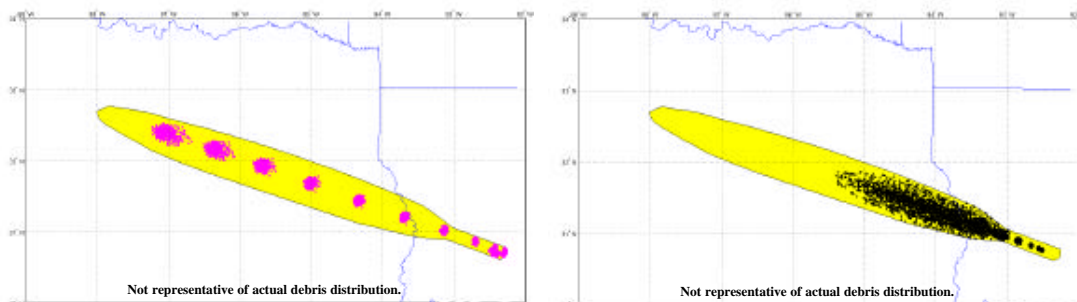


Figure 4-33:  
Post-Breakup Shed Debris Shaping Results of Estimated Columbia Primary Debris Field,  
Ballistic Coefficient of 1.5 and 20 psf,  $L/D 0-0.15$ ,  $C_d 1.0$   
Propagated from Various States Along a Simulated 220 psf Trajectory

The primary debris footprint is shaped by combining the “sub” footprints from Figures 4-31 through 4-33. This is shown below in Figure 4-34.

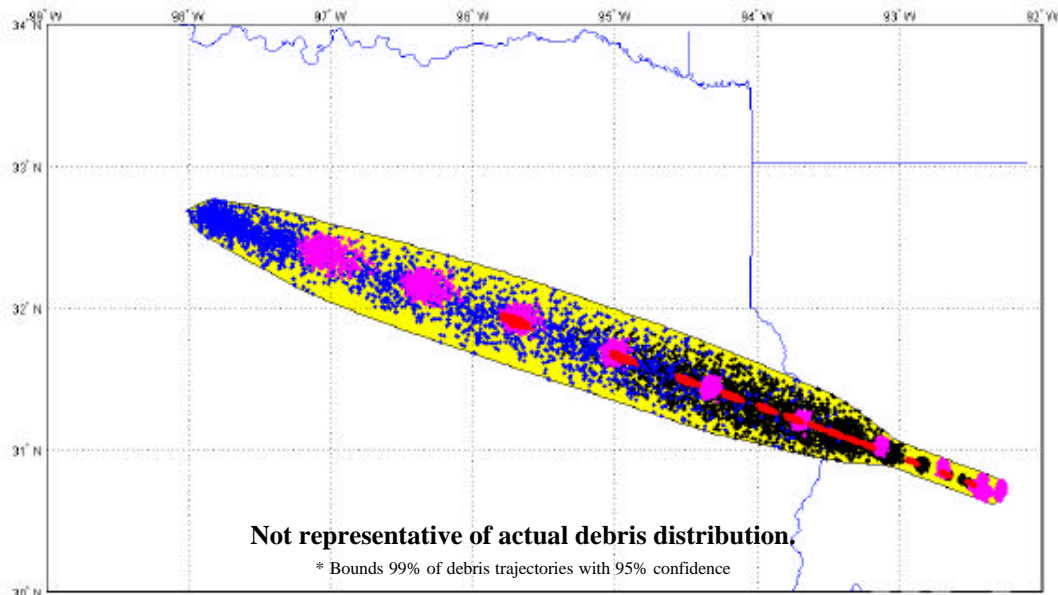


Figure 4-34: Shaping Results of Estimated Columbia Primary Debris Field  
Propagated from Orbiter State at GMT 13:59:37.00

The final primary debris footprint was derived based on this shaping technique and initial conditions that the Debris Footprint Team believes to bound the time during which the orbiter became a ballistic object. Figure 4-35 shows this footprint.



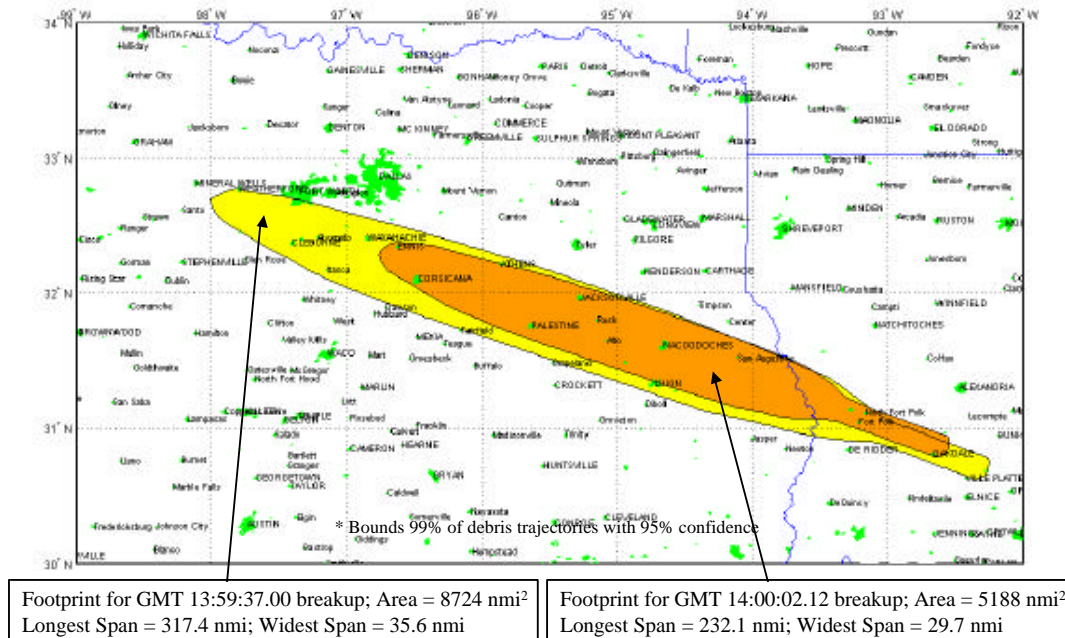


Figure 4-35: Estimated Columbia Primary Debris Fields

Figure 4-36 shows the centerlines of the two predicted primary debris footprints, their relationship to each other and to the “NASA 2/20” (Feb 20) line, as fit to significant debris items found [45]. Figure 4-37 shows the centerlines of the two predicted primary debris footprints and their relationship to the found locations of the three SSME powerheads.

The 13:59:37.00 and 14:00:02.12 centerlines vary in distance from 2.5 - 3.0 nm from each other. The 14:00:02.12 footprint is smaller and shifted north of the 13:59:37.00 footprint. The smaller footprint is due to lower and steeper conditions at 14:00:02.12 as compared to 13:59:37.00 GMT. The northern shift of the 14:00:02.12 footprint relative to the 13:59:37.00 footprint is due to banking lift between these two times.

Excellent agreement is seen between the 14:00:02.12 simulated centerline and the NASA 2/20 curve fit through found debris.

Excellent agreement is seen between the two centerlines and the debris listed in the May 29, 2003 SRIL [46]. The Debris Footprint Team uses the SRIL rather than any of the other debris databases available, based on the belief that investigators have scrutinized the SRIL debris more than the other general debris, and that this scrutiny led to fewer errors in the latitude and longitude coordinates that are common in the other debris databases thus far. (Although the team has spotted some SRIL data that is questionable.) All three Space Shuttle Main Engine (SSME) powerheads landed between the two centerlines, within 3 nm of each other (2 nm in crossrange), and each within 1.0 nm from a centerline (extremely high-β objects should land on the centerline) [47], [48], [49].

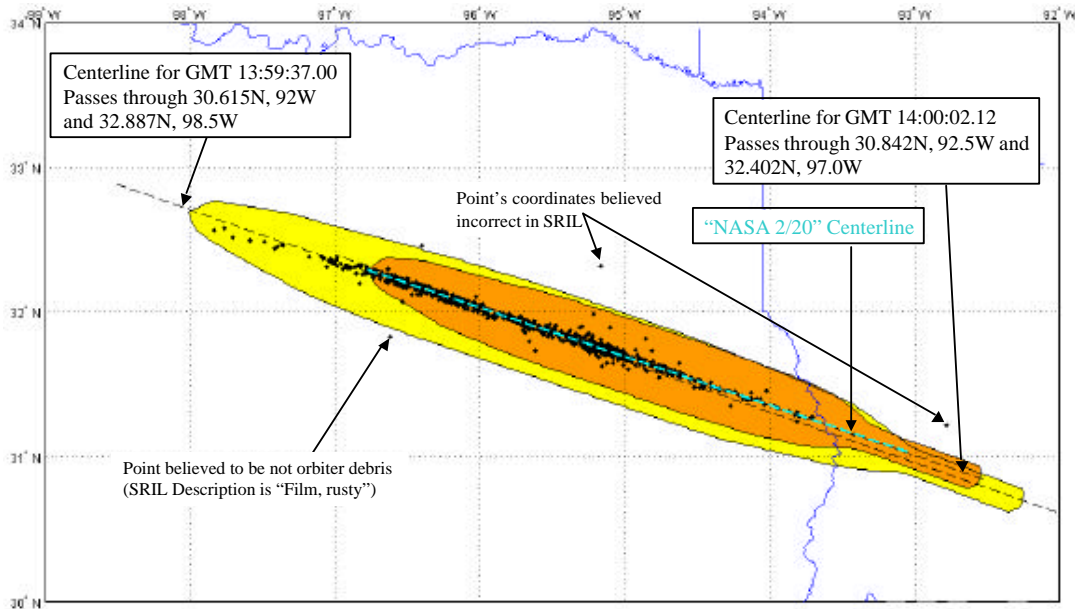


Figure 4-36: Estimated Columbia Primary Debris Fields and Centerlines Points from Significant Recovered Items List (SRIL 5/29/03 [46])

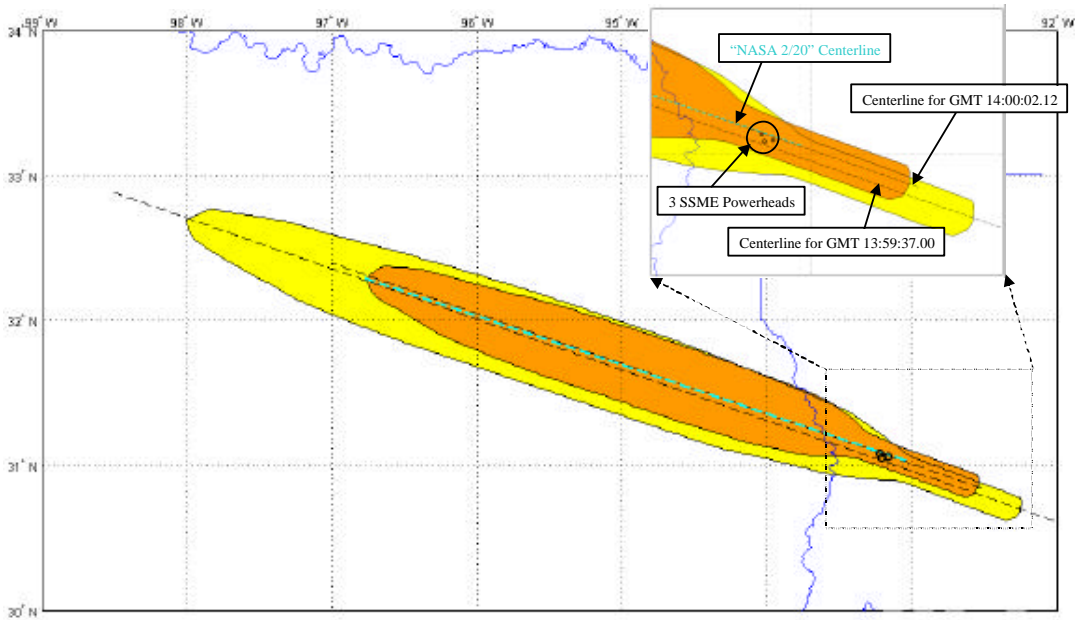


Figure 4-37: Estimated Columbia Primary Debris Fields and Centerlines

Another excellent way to validate the predicted primary debris footprint boundaries is to compare them to Air Traffic Control (ATC) radar hits during the timeframe of the accident. The next five figures coplot ATC radar data with the predicted primary debris footprint boundaries.

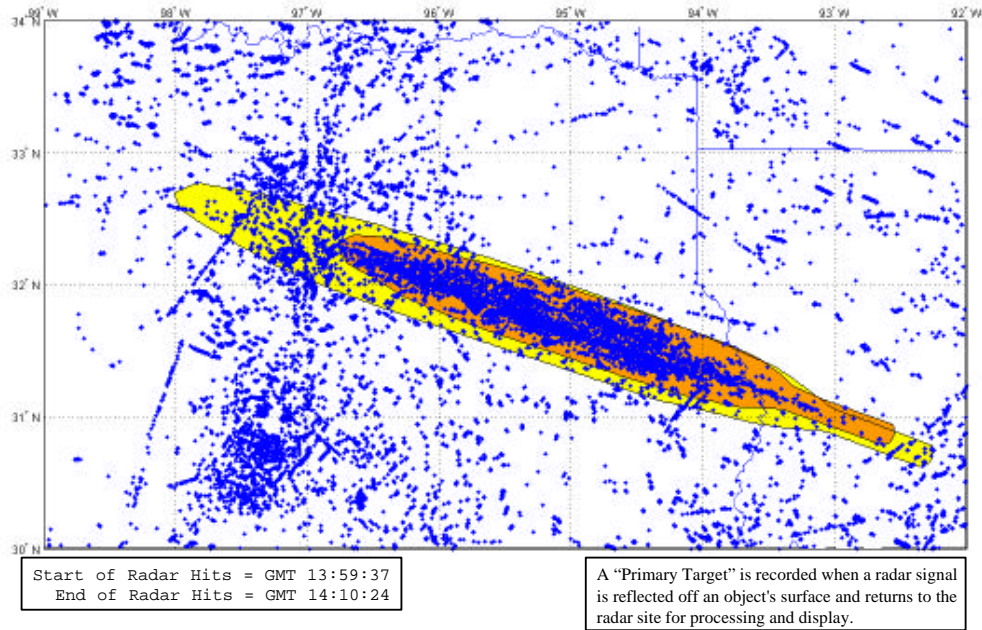


Figure 4-38: Estimated Columbia Primary Debris Fields and "Primary Targets" from Available ATC Radars, 13:59:37 - 14:10:24Z

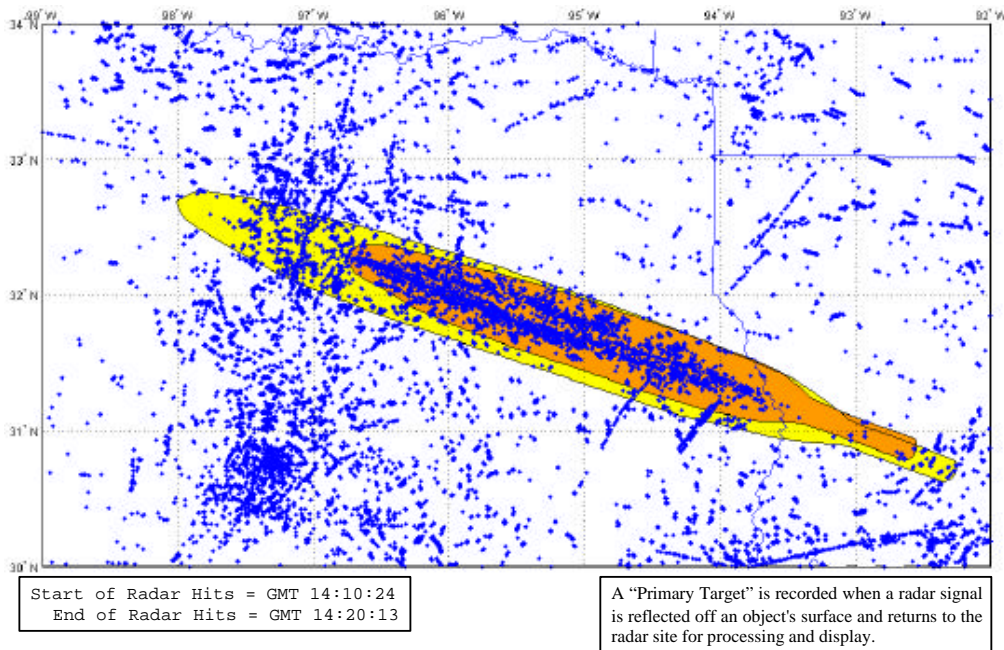


Figure 4-39: Estimated Columbia Primary Debris Fields and "Primary Targets" from Available ATC Radars, 14:10:24 - 14:20:13Z

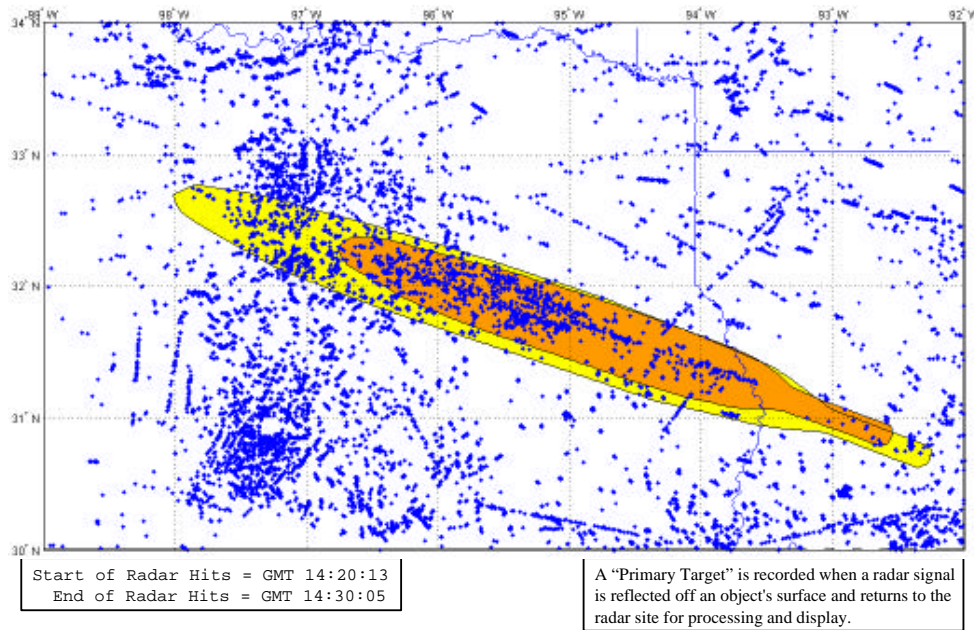


Figure 4-40: Estimated Columbia Primary Debris Fields and "Primary Targets" from Available ATC Radars, 14:20:13 - 14:30:05Z

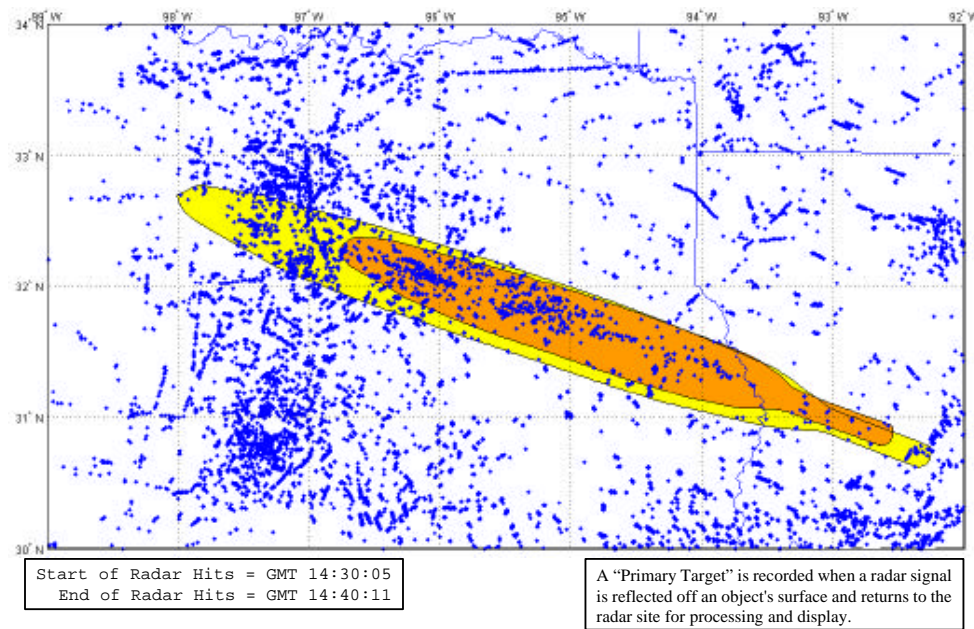


Figure 4-41: Estimated Columbia Primary Debris Fields and "Primary Targets" from Available ATC Radars, 14:30:05 - 14:40:11Z

Figure 4-42 superimposes all ATC radar hits for the period of time approximately starting at the time of the accident and extending for 40 minutes. This is a composite plot of the previous four figures. A clear clustering of radar hits is seen to fit extremely well in the 14:00:02.12 GMT debris footprint boundary.

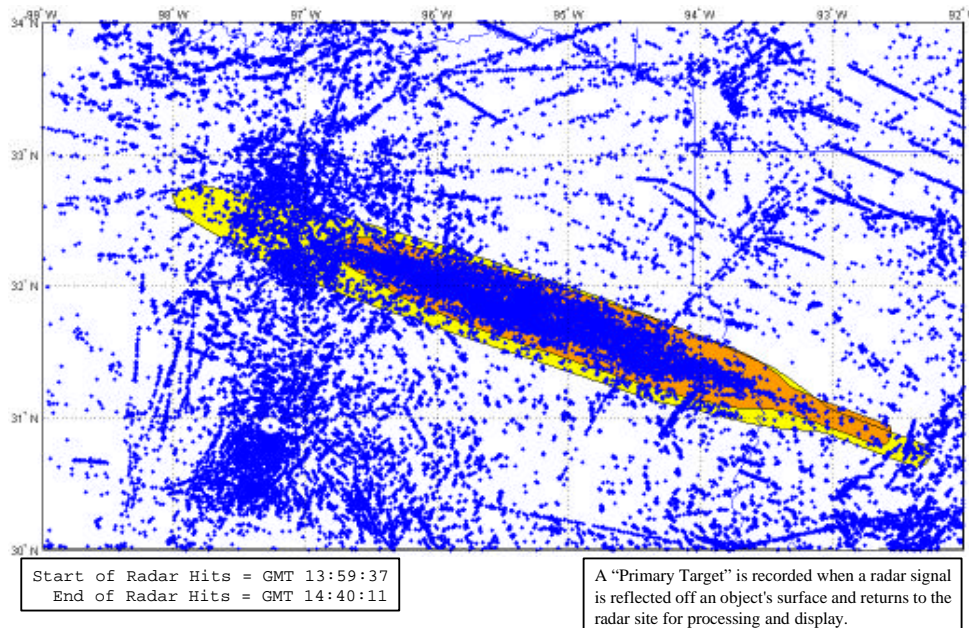


Figure 4-42: Estimated Columbia Primary Debris Fields and “Primary Targets” from Available ATC Radars, 13:59:37 - 14:40:11

### 4.3.3. Generic Pre-Breakup Debris Swath

In the days immediately after the accident, the Emergency Operations Center (EOC) fielded hundreds of calls each day from people believing they found Columbia debris, from all over the United States, and some from outside the continental United States. It was necessary to very quickly determine all possible locations in the United States where it was physically possible for debris to have fallen, in order to assist the EOC in focusing on realistic areas and ignoring impossible areas. For example, on the day of delivery of the debris swath, some reports from Phoenix that had previously held a high priority immediately moved to low priority. The EOC needed this information a week before the relative motion and ballistics personnel started analyzing pre-breakup shed debris in video, thus JSC-DM generated a generic debris swath.

Initially, the Debris Footprint Team only considered very low ballistic coefficient objects, as the team believed that only low- $\beta$  objects could have fallen off of the orbiter without significant flight control activity onboard the vehicle, and without the crew noticing. The first pre-breakup debris analyzed in video (Debris 6) misled the team into assuming this was a very high ballistic coefficient object, perhaps only slightly lower than the approximately 100 psf ballistic coefficient of the orbiter at the Debris 6 time. Thus, the team also looked at very high ballistic coefficient debris to bound the region where debris could have fallen. Later, the video-based relative motion work showed that nothing higher than about 5 psf fell off of the orbiter, indicating that the team could ignore the higher ballistic coefficient swath. However, the team decided to continue analyzing high ballistic coefficient debris for several reasons. First, several videotaped debris awaited analysis. Second, not all of the trajectory has videotape coverage. Finally, it is still important to consider higher ballistic coefficients because if such objects exist, then they would tend to stray farther from the orbiter's groundtrack due to their momentum carrying them "straight" relative to the banking trajectory of the orbiter. This would expand the range of possible impact locations, as the upcoming figures will show.

The simulations assumed a 0.5 psf and a 220 psf piece shed once every minute, starting at Entry Interface, 400 kft altitude. Again, the team chose 220 psf as that was the maximum observed ballistic coefficient in the debris field. Low- $\beta$  object assumptions: minimum  $\beta$  of 0.5 psf; lifting, L/D varied uniformly from 0 - 0.15; bank from 0 deg - 360 deg. High- $\beta$  object assumptions: maximum  $\beta$  of 220 psf; no lift. The resulting "swath" results from merging all resulting debris footprints.

Figure 4-43 shows the "low-  $\beta$ " debris swath. Figures 4-44 and 45 show this swath laying over the "high-  $\beta$ " debris swath. Lifting and non-lifting footprints appear. The "without lift" footprints indicate where debris is more likely to land. The "with lift" footprints indicate the total area of expected impact (99% probability with 95% confidence). The footprints shown are the ground impact areas. The Debris Footprint Team also generated footprints for 80,000 ft altitude for use by the Radar Analysis Team as described in Section 5.

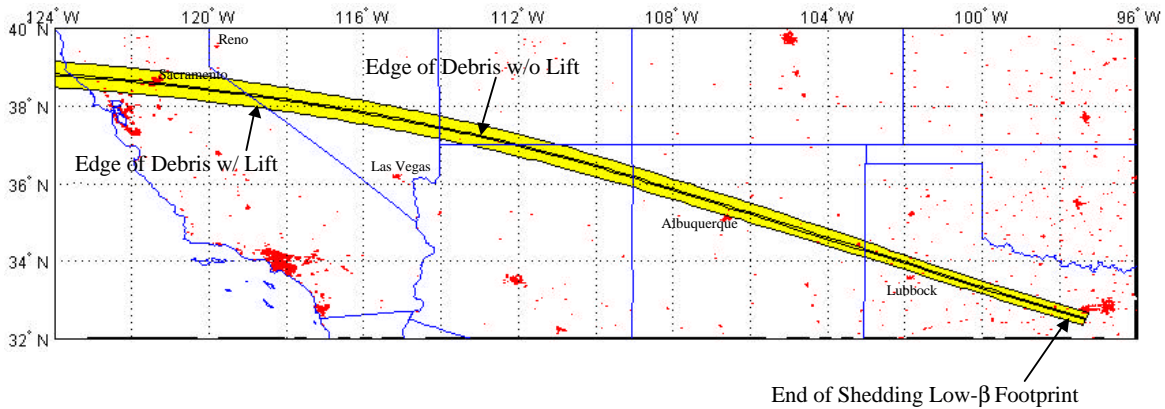


Figure 4-43: Probable Ground Impact Area for Shedding Low- $\beta$  Debris  
Ballistic Coefficient of 0.5 psf, 0-0.15 zL/D,  $C_d$  1.0

Figure 4-44 shows the western half of the resulting ground impact debris swath that would capture any 0.5 psf debris shed pre-breakup, overlaid on the resulting ground impact debris swath that would capture any higher ballistic coefficient (up to 220 psf) debris shed pre-breakup. It is interesting to note that the 220 psf simulated debris footprint is not centered about the groundtrack, but tends to extend quite a bit to the north in this figure. This is due to the momentum of the higher- $\beta$  objects carrying them “straight” while the orbiter is banking toward the south.

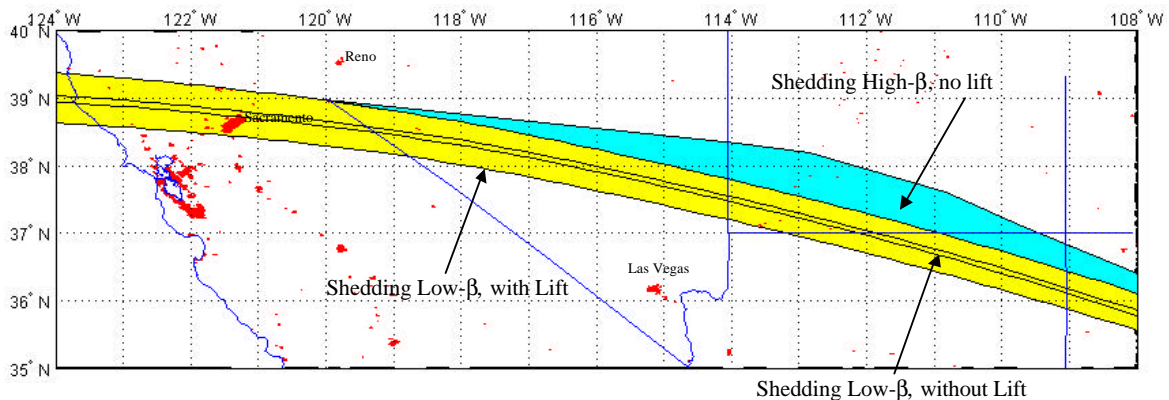


Figure 4-44: Probable Ground Impact Area for Shedding Debris  
Ballistic Coefficient of 0.5 psf, 0-0.15 L/D & 220 psf, 0 L/D,  $C_d$  1.0

Figure 4-45 shows the eastern half of the resulting ground impact debris swath that would capture any 0.5 psf debris shed pre-breakup, overlaid on the resulting ground impact debris swath that would capture any higher ballistic coefficient (up to 220 psf) debris shed pre-breakup. Here, note that the 220 psf simulated debris footprint is again not centered about the groundtrack, and begins to shift its extension from north of the groundtrack towards the south on this figure. This is due to the momentum of the higher- $\beta$  objects carrying them “straight”. While the Orbiter is banking toward the south initially, and thus high- $\beta$  objects tend to land north of the

groundtrack, that effect shifts as the Orbiter does a roll-reversal and begins banking toward the north, thus the high- $\beta$  objects then tend to land south of the groundtrack. Because of this, if any high- $\beta$  objects found south of the primary debris footprint's southern boundary would be a suspect for falling off the orbiter prior to the catastrophic breakup.

Although not shown here, it is possible that debris that fell off the Orbiter prior to catastrophic breakup could have landed within the primary debris footprint boundary. If such debris is found, the more west it is found, the more likely it is debris that came off pre-breakup.

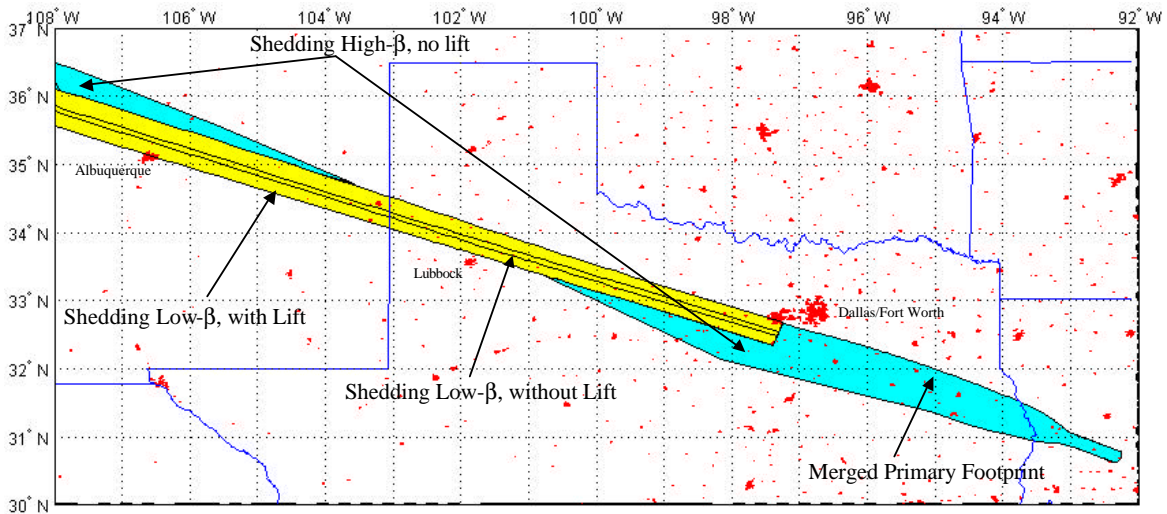


Figure 4-45: Probable Ground Impact Area for Shedding Debris  
Ballistic Coefficient of 0.5 psf, 0-0.15 L/D & 220 psf, 0 L/D,  $C_d$  1.0

The next three figures are the low- $\beta$  debris swaths with ground impact areas and times of impact for various assumed separation times for debris with an assumed ballistic coefficient of 0.5 psf. These were used to estimate the footprints for low- $\beta$  debris shed from any time in the trajectory and were a starting point for trajectory analysis of the debris shedding observed in public video. These results were delivered to the Kennedy Space Center Weather Office, who forwarded them to the Coast Guard and Navy for use with ocean current models to predict beaching locations of any debris that may have landed in the ocean and floated to a beach. The JSC Radar Analysis Team made use of the resulting times over land.

Here is an example of how to read these plots. If one was interested in when a 0.5 psf piece of debris falling off of the orbiter at 13:44:09 GMT would hit the ocean, locate the box with that initial condition (IC) time, and one would see a minimum time and maximum time in the impact time range (in this case 14:27:58.6 - 14:33:17.6 GMT). If one then traces the line from the box down to the "T," then follows left to the dot, and down to the swath, one finds the heel, or western-most line that the debris could have landed. If, instead of left, one traces from the "T" to the right and to the dot, and down again to the swath, one finds the toe, or eastern-most line that the debris could have landed.



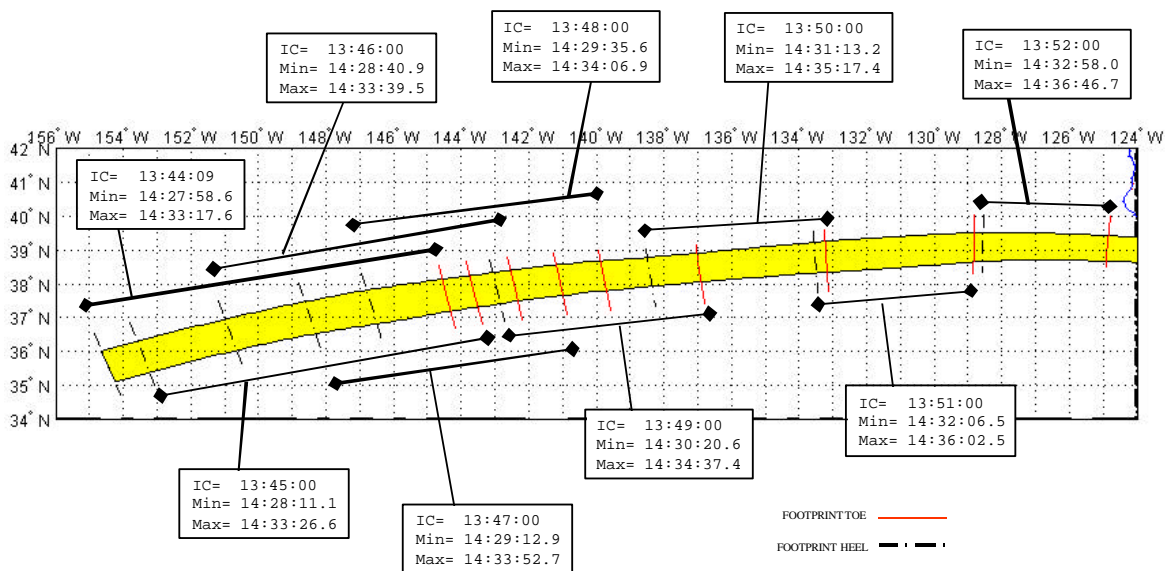


Figure 4-46: Probable Ground Impact Area\* for Shedding Low- $\beta$  Debris  
Off Shore Approaching California  
Ballistic Coefficient of 0.5 psf, 0-0.15 L/D,  $C_d$  1.0

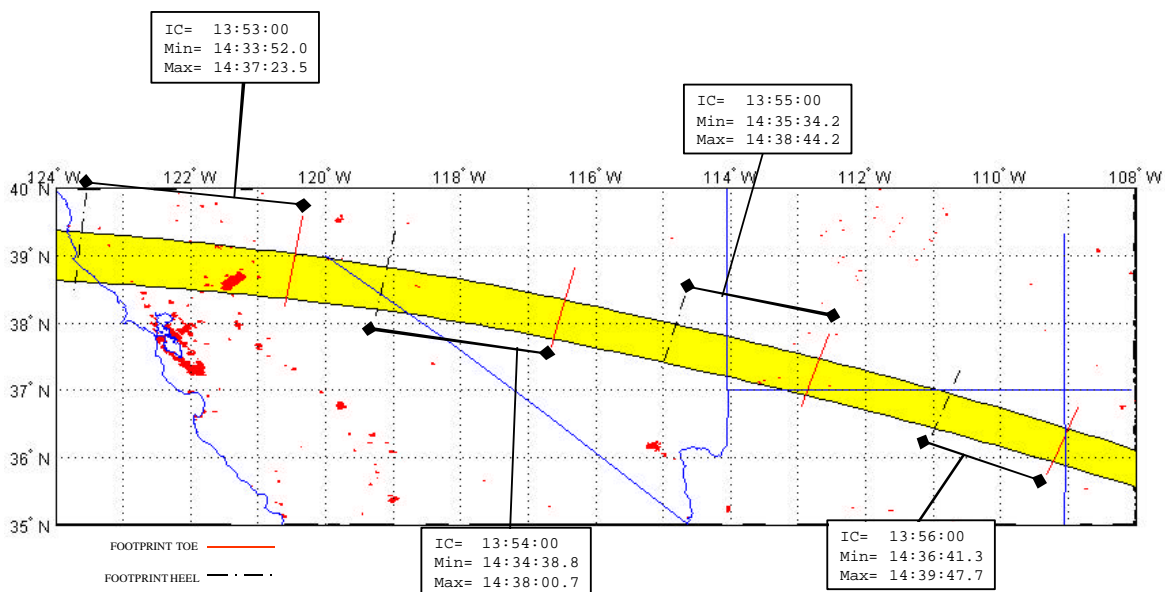


Figure 4-47: Probable Ground Impact Area\* for Shedding Low- $\beta$  Debris  
California through New Mexico  
Ballistic Coefficient of 0.5 psf, 0-0.15 L/D,  $C_d$  1.0

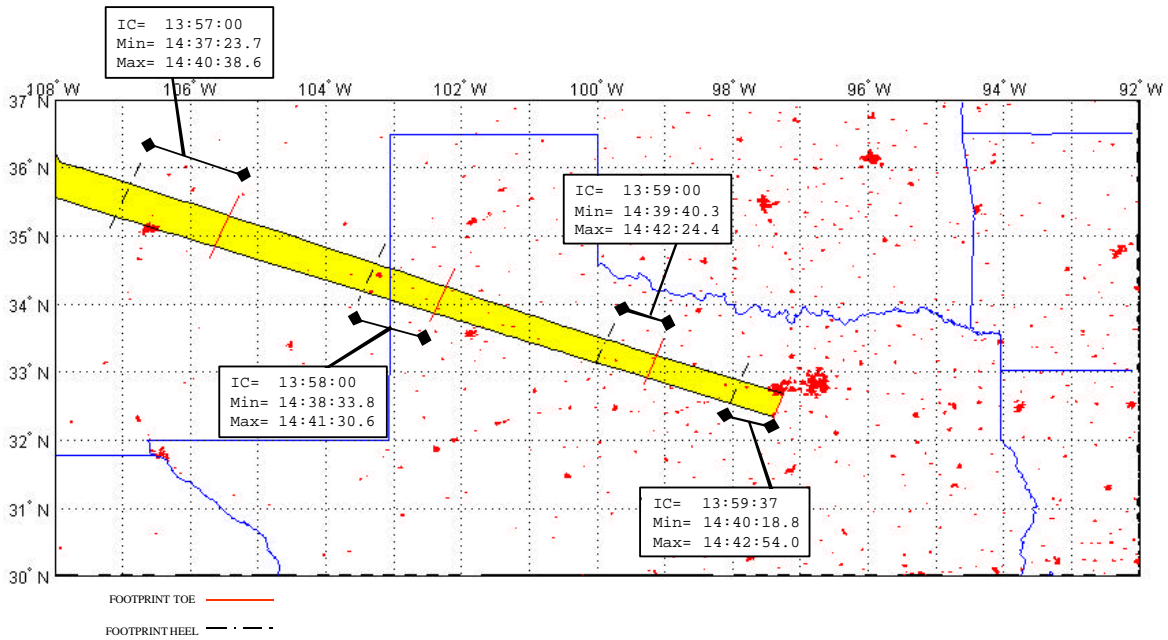


Figure 4-48: Probable Ground Impact Area\* for Shedding Low-β Debris  
New Mexico through Texas  
Ballistic Coefficient of 0.5 psf, 0-0.15 L/D, C<sub>d</sub> 1.0

Based on both the primary debris footprint and the generic swath work, Table 4-6 shows a list of counties across the United States that pre-breakup debris may have landed in as a result of the Columbia entry on February 01, 2003. Some counties are more likely candidates than others, and in some cases only a portion of that county is within any of the debris footprint boundaries.

California Counties	Nevada Counties	Utah Counties	Arizona Counties	New Mexico Counties	Texas Counties			Louisiana Counties
Alpine (a) Amador (b) Calaveras (c) Colusa (b) El Dorado (a) Lake (b) Mendocino (b) Mono (c) Napa (b) Nevada (c) Placer (c) Sacramento (b) Solano (c) Sonoma (b) Sutter (b) Tuolumne (c) Yolo (a) Yuba (c)	Churchill (c) Douglas (b) Esmeralda (c) Lincoln (b) Lyon (b) Mineral (b) Nye (b)	Beaver (c) Garfield (b) Iron (a) Kane (a) Piute (c) San Juan (c) Washington (c)	Apache (b) Coconino (c) Mohave (c) Navajo (c)	Bernalillo (c) Curry (b) De Baca (c) Guadalupe (b) Los Alamos (a) McKinley (b) Quay (c) Rio Arriba (c) Roosevelt (c) San Juan (b) San Miguel (c) Sandoval (a) Santa Fe (b) Torrance (c)	Anderson (b*) Angelina (b*) Bailey (b) Bosque (c) Castro (c) Cherokee (b*) Crosby (b) Dallas (c*) Dickens (b) Eastland (c) Ellis (b*) Erath (b) Floyd (c) Freestone (b*) Hale (b) Haskell (b) Henderson (b*)	Hill (b*) Hockley (c) Hood (a) Houston (c*) Jasper (c*) Johnson (b*) Kaufman (c) Kent (c) King (b) Knox (c) Lamb (b) Leon (c) Limestone (c) Lubbock (c) McLennan (c) Motley (c) Nacogdoches (a*)	Navarro (a*) Newton (c*) Palo Pinto (b) Parker (b*) Parmer (c) Rusk (c*) Sabine (b*) San Augustine (a*) Shackelford (c) Shelby (c*) Somervell (a) Stephens (b) Stonewall (b) Tarrant (c*) Throckmorton (b) Trinity (c*) Young (b)	Allen (c*) Beauregard (c*) Evangeline (c*) Rapides (c*) Sabine (c*) Vernon (b*)
<p>Changes from last list: <u>California</u>: added none; removed Contra Costa, Madera, Marin, Mariposa, San Joaquin, and Stanislaus. <u>Nevada</u>: added none; removed Carson, Eureka, Lander, and White Pine. <u>Utah</u>: added none; removed Wayne. <u>Arizona</u>: added none; removed none. <u>New Mexico</u>: added Los Alamos; removed Cibola, Mora, and Valencia. <u>Texas</u>: added many as list now includes primary debris footprints including Anderson, Angelina, Bosque, Cherokee, Dallas, Ellis, Freestone, Henderson, Hill, Hood, Houston, Jasper, Johnson, Kaufman, Leon, Limestone, McLennan, Nacogdoches, Navarro, Newton, Parker, Rusk, Sabine, San Augustine, Shelby, Somervell, Tarrant, and Trinity; removed Archer, Baylor, Briscoe, Callahan, Cochran, Cottle, Fisher, Foard, Garza, Jack, Jones, Smith, and Swisher. <u>Louisiana</u>: added all counties listed as list now includes primary debris footprints; removed none.</p>								
<p><b>KEY:</b></p> <p>(a) The entire area of this county is under the general debris swath (no *), or is within the primary debris footprint boundaries (*).</p> <p>(b) Most of this county (&lt; 100% but greater &gt;50% of this county's area) is under the general debris swath (no*), or is within the primary debris footprint boundaries (*).</p> <p>(c) This county is partially under the general debris swath (less than 50% of the county's area) (no *), or is within the primary debris footprint boundaries (*).</p>								

Table 4-6: List of Counties Which May Have Columbia Debris

#### 4.3.4. Pre-Breakup Shedding Debris Footprints

NASA has identified nineteen videos that recorded debris falling off of Columbia prior to its catastrophic breakup. Members of the public videotaped twenty distinct debris shedding events and three plasma envelope flashes or flares. In some cases, many of these events appear in multiple videos, and in one case as many as seven videos recorded the same event. NASA carefully screened the videos against previous shuttle entry videos to ensure that debris events were indeed not something that has been seen in previous shuttle entries. [22]

An assessment by the JSC Orbital Debris Program Office predicted that a tile with a ballistic coefficient on the order found in the relative motion results (3.1 psf) would survive to ground impact [51]. Thus, predicting impact points was given a high priority with a goal of locating and recovering pre-breakup debris.

The relative motion and ballistics experts established the initial time of shedding and ballistic coefficient based on videotape analysis. The simulation initializes at the orbiter's state vector at the beginning and end of the computed separation time range. The Debris Footprint Team scaled each derived ballistic coefficient to account for the difference in density used by the relative motion team (the measured value at the orbiter's position at the separation time), and the DAO (rev D) density at this same initial condition in the simulation. The density used by the relative motion and ballistics experts affects the resulting estimate of ballistic coefficient. In all cases, these experts used density values derived from onboard measurements. However, to simulate debris falling below the orbiter trajectory, atmosphere data was needed from the orbiter altitude to the ground along the entire groundtrack. DAO provided this data. When the Debris Footprint Team simulates these debris items with the DAO data, the density at the simulation initial condition never exactly matches these derived density values, because the DAO density is based on meteorological estimates. Thus, a scale factor is used to adjust the ballistic coefficients. This is done via: simulated  $\beta$  = derived  $\beta$  \* (simulated density / derived density).

Five hundred Monte Carlo simulations bound the footprint with the simulation initialized at the orbiter's state vector and the computed separation time. The simulation included day-of-entry density, and wind speed, and wind direction (DAO rev D), with GRAM-99 uncertainties (rpscale = 1.0,  $3\sigma$ ). JSC-DM generated lifting and non-lifting debris footprint boundaries. The non-lifting results show the highest likelihood area to find the object. The lifting simulations vary L/D uniformly from 0 - 0.15, and bank angle uniformly from 0 - 360 deg.

As described earlier, the methodology assumes a constant ballistic coefficient for the pre-breakup shedding debris. The mass, area, and material properties of the debris are unknown, so the methodology cannot model ablation, or drag changes with Mach number, even if no ablation were taking place. Also, the methodology assumes the object remains as a single, intact piece with ballistic properties as measured from video.

There is no evidence in video that any imparted velocity was involved in the debris motion. However, during the time the object was within the orbiter brightness envelope, until the time that the distance was sufficient for the object to be discernable as a separate object, it is possible

that something could have happened to impart some delta-V. Then again, once the object is no longer visible because it has dimmed out or it has left the camera's field of view, it is possible that an energy release event could have occurred. Regardless, the methodology cannot model this type of event with no information about it, or even that it existed.

JSC-DM did not "shape" these footprints as was done for the primary debris footprint, but retained a rectangular shape. This is reasonable because any errors in the estimates of ballistic coefficient and/or separation time would manifest themselves as range errors. In accounting for these errors, a shaped footprint would stretch in range, and would approach a rectangular shape around the locations of the footprints presented here.

Unfortunately, the rectangular shaping can give artificially wide footprints, primarily for the ballistic (non-lifting) footprints. Due to varying crosswinds in some cases, the scatter of simulated impact points may bend relative to the groundtrack (it is not entirely parallel to the groundtrack). However, the plotting routine always bounds the impact points with a rectangle, and assumes that the sides of the rectangle are parallel to the groundtrack (the sides of the rectangle cannot bend with the impact points); thus the rectangle ends up showing an area that is too wide in these cases, although two of the opposing points of the rectangle will always correspond to the extreme simulated impact points.

Figure 4-49 shows how rectangular footprint shapes are applied to simulated debris, rather than "form-fitting" shapes, and how the rectangular shapes can be artificially wide whenever the simulated debris centerline is not parallel to the groundtrack, as just described. In this figure, the red points are the simulated ballistic (non-lifting) ground impact points for Debris 3.

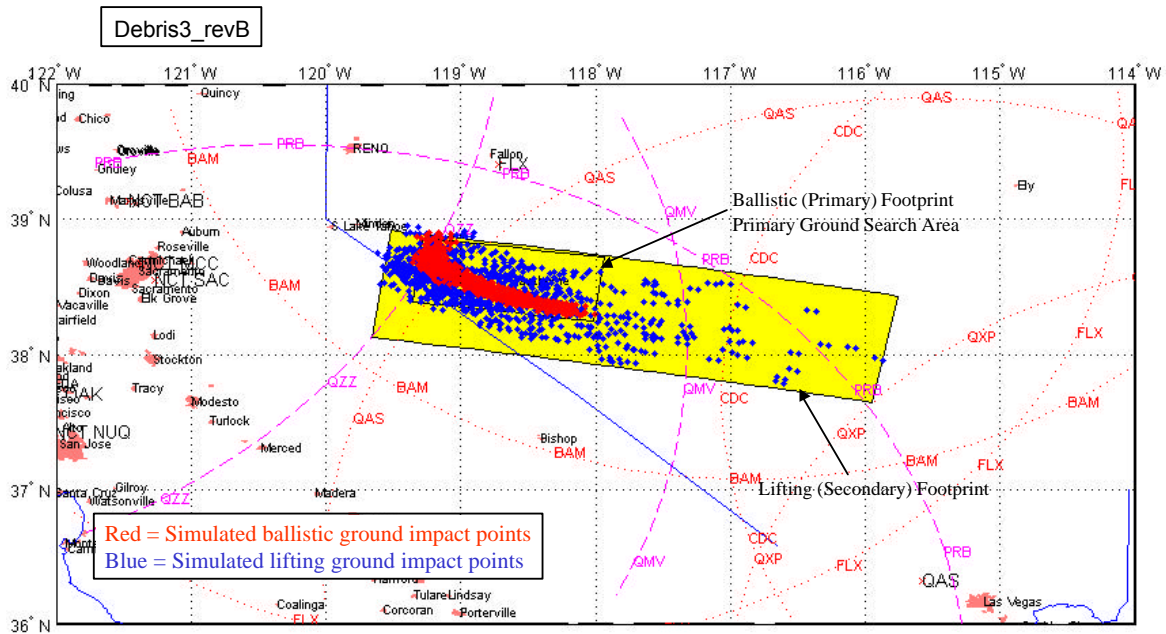


Figure 4-49: Probable Ground Impact Area for Debris 3  
and Simulated Impact Points for Observed Debris  
Separation Time 13:53:55.6 - 13:53:56.6Z  
Constant Ballistic Coefficients between 0.1 to 1.0 psf, 0-0.15 L/D,  $C_d$  1.0

JSC-DM defined Search and Recovery Zones by extending the resulting non-lifting (ballistic) footprint boundaries to the boundaries of the lifting footprint, thus subdividing each entire area into nine different zones, and gave these nine zones likelihood-of-impact values ranging from 1 to 4.

- Zone 1 is the most likely area in which this debris would be found, and is the non-lifting debris footprint.
- Zones 2 are the next most likely areas (errors in separation time and/or ballistic coefficient manifest themselves in range error).
- Zones 3 are the next most likely areas and include lift.
- Zones 4 are the least likely areas, and combine the errors from Zone 2 and lifting.

As with the generic analysis, footprints for each debris shedding event observed in video were generated for 80,000 ft, 35,000 ft and ground impact. Only ground impact footprints are shown in this report. A summary of the observed separation times and ballistic properties are shown in Section 4-2, Table 4-3. The following data are provided in Appendix 10.6 for each of the pre-breakup shedding debris to assist the Radar Analysis Team in locating possible debris tracks:

- latitude/longitude of corner points for all footprints,
- area of all footprints,
- minimum/maximum GMT to altitude,
- airspeed (relative speed) at altitude,

- flight path angle (FPA) (relative topocentric) at altitude,
- groundspeed at altitude,
- Air Traffic Control radar sites which are in range of all lifting debris footprints.

Figure 4-50 shows overlapping debris footprint boundaries for all released debris footprints based on relative motion and ballistics analysis, as well as footprints based on assumed ballistics for Flare 1 and Flare 2, in yellow. This figure shows these results overlaid on results if one assumes a 0.5 - 5.0 psf ballistic coefficient range on videotaped debris whose relative motion and ballistic coefficients are still unknown, in green. Thus, the portion of green that is visible shows potential impact locations for debris 11 and 12 that are outside the released footprints. Note that based on videotaped debris alone, nearly all land under the entire groundtrack is a candidate for potentially finding Columbia debris.

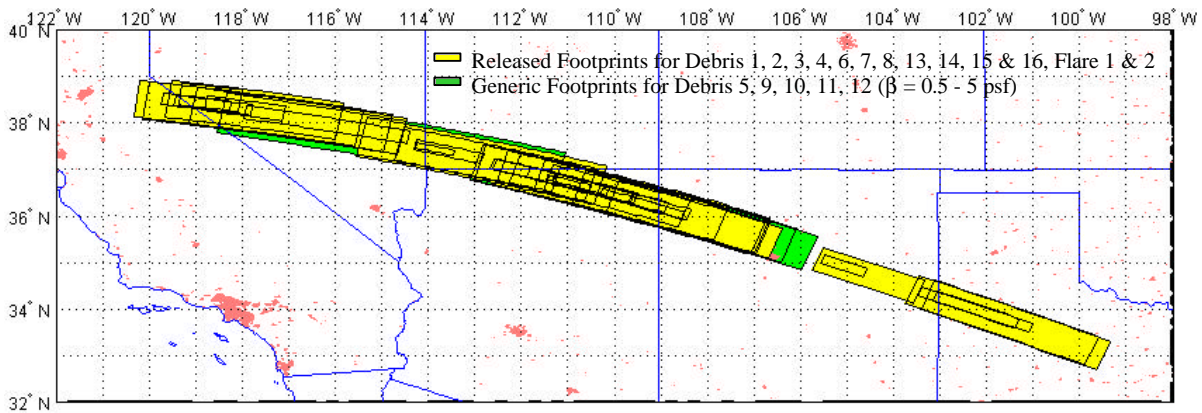


Figure 4-50: Combined Probable Ground Impact Areas  
Observed Debris Events 1, 2, 3, 4, 6, 7, 8, 13, 14, 15 & 16 and Assumed Debris at Flare 1 & 2  
Constant Ballistic Coefficients, 0-0.15 L/D,  $C_d$  1.0

Figure 4-51 below depicts the amount of overlap among the released (yellow) debris footprints with an emphasis on the non-lifting areas. As more non-lifting areas overlap, the shading becomes darker. The darkest regions in the plot were given higher priority when all areas were prioritized as shown in Table 2-1. Prioritizing these areas and the radar search boxes is described in more detail in Section 5.

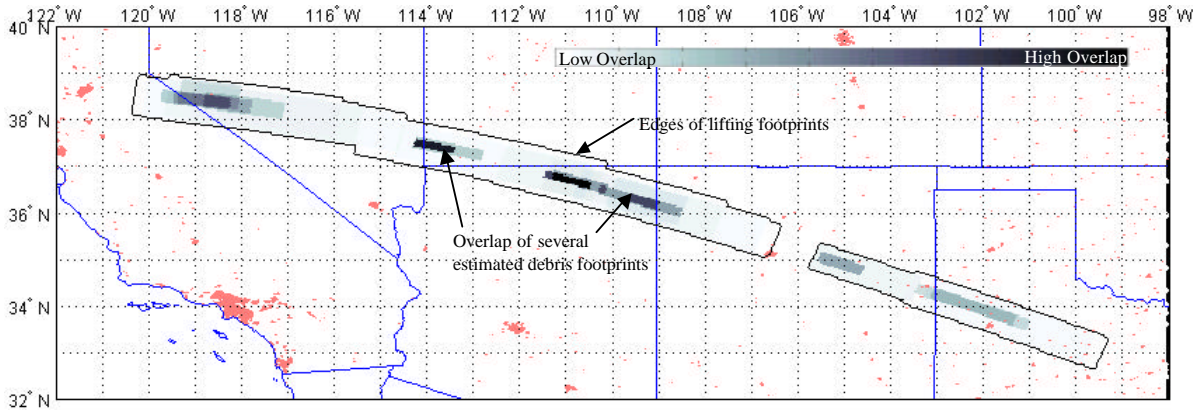


Figure 4-51: Overlapping Non-Lifting Probable Ground Impact Areas  
Observed Debris Events 1, 2, 3, 4, 6, 7, 8, 13, 14, 15 & 16 and Assumed Debris at Flare 1 & 2  
Constant Ballistic Coefficients, 0-0.15 L/D,  $C_d$  1.0



The following footprints were calculated using the DAO rev D mean atmosphere with GRAM-99 uncertainties (rpscale = 1.0, or 3-sigma) and day-of-entry density at event altitude.

### Debris 1

The Aerospace Corporation independently validated the JSC ballistic coefficient, separation time, and both the ballistic (non-lifting) and lifting footprint boundaries, with similar, but slightly different methods for relative motion, ballistic coefficient estimation, and debris footprint estimation [30]. Aerospace calculated an Orbiter/Debris separation time of 13:53:45.4Z compared to a JSC estimate of 13:53:44.2 - 13:53:45.4Z. [23] [30] Likewise, the Aerospace ballistic coefficient was 0.5 - 1.5 psf [30] compared to a JSC estimate of 0.6 - 1.6 psf [23], both derived using day-of-entry density at event altitude.

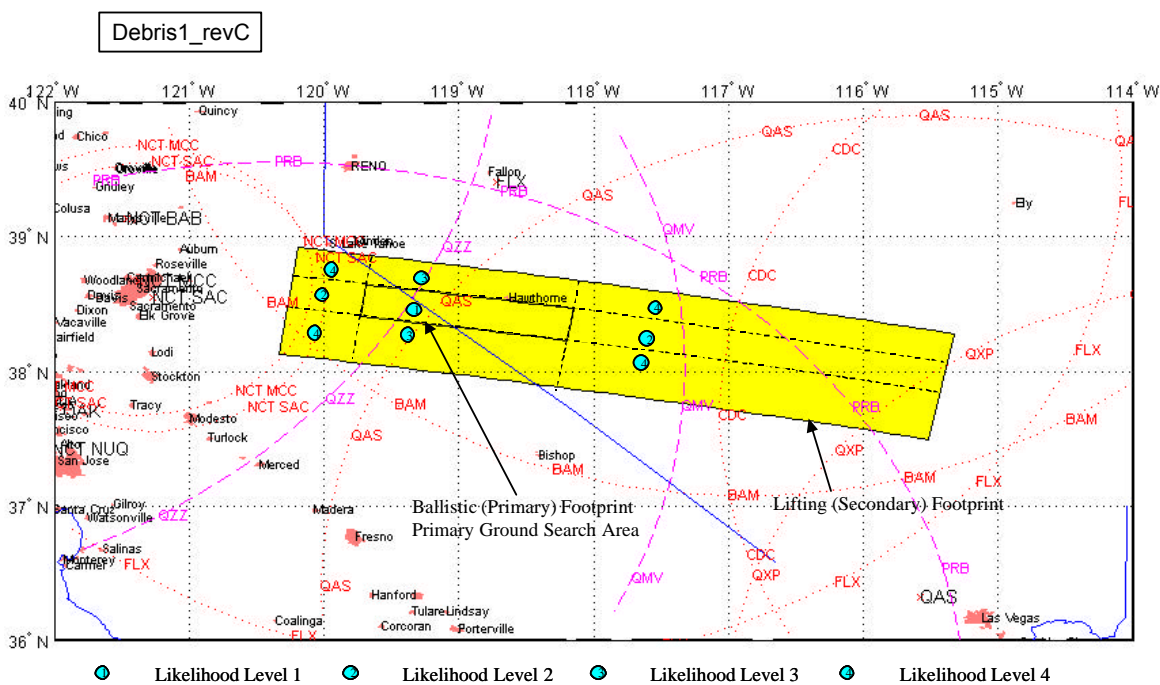


Figure 4-52: Probable Ground Impact Area for Debris 1  
Separation Time 13:53:44.2-13:53:45.4Z  
Constant Ballistic Coefficients between 0.6 to 1.6 psf, 0-0.15 L/D,  $C_d$  1.0

Debris 2

The Aerospace Corporation independently validated the JSC ballistic coefficient, separation time, and both the ballistic (non-lifting) and lifting footprint boundaries, with similar, but slightly different methods for relative motion, ballistic coefficient estimation, and debris footprint estimation [30]. Aerospace calculated an Orbiter/Debris separation time of 13:53:46.8 compared to a JSC estimate of 13:53:45.9 - 13:53:47.1. [23] [30] Likewise, the Aerospace ballistic coefficient was 1.0 - 2.0 psf [30] compared to a JSC estimate of 0.7 to 1.9 psf [23], both derived using day-of-entry density at event altitude.

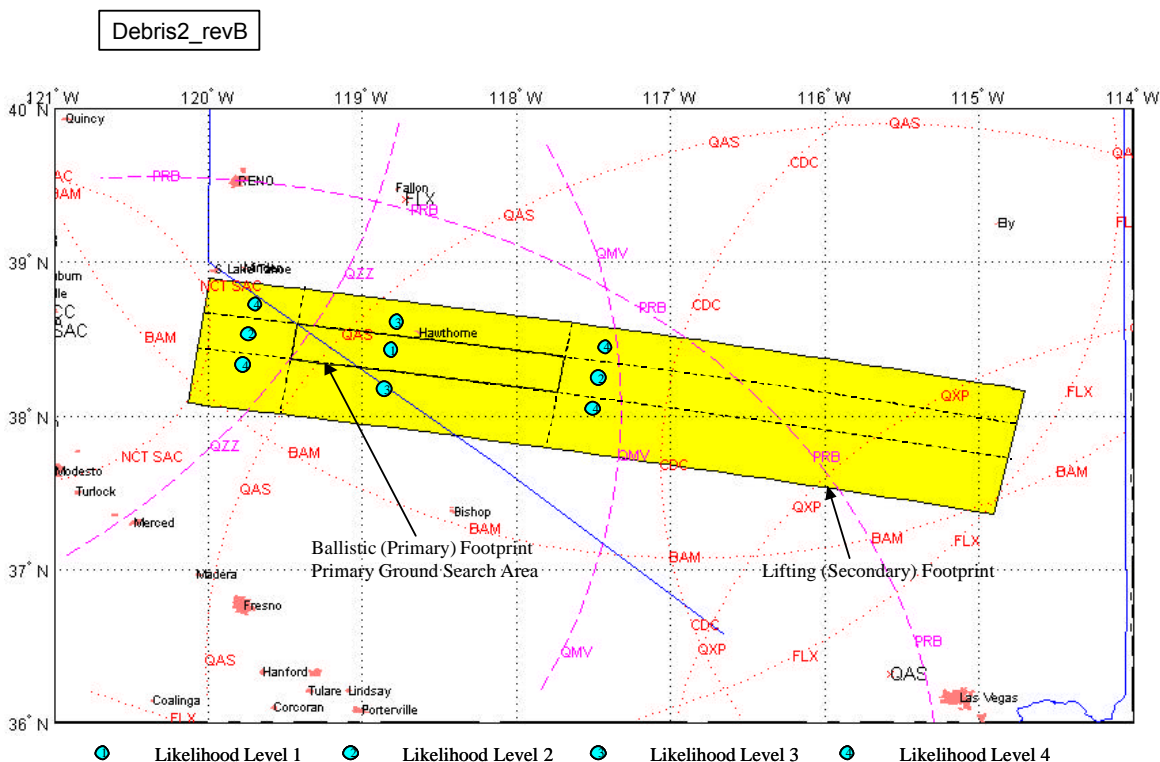


Figure 4-53: Probable Ground Impact Area for Debris 2  
Separation Time 13:53:45.9 - 13:53:47.1Z  
Constant Ballistic Coefficients between 0.7 to 1.9 psf, 0-0.15 L/D,  $C_d$  1.0

Debris 3

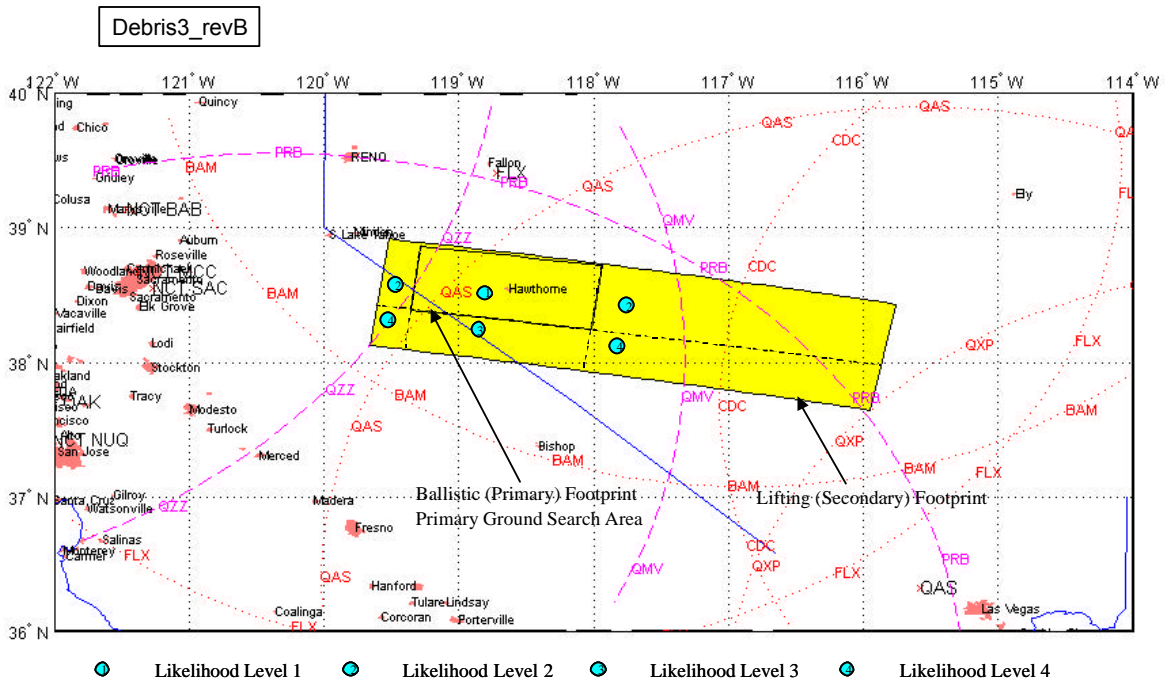


Figure 4-54: Probable Ground Impact Area for Debris 3  
Separation Time 13:53:55.6-13:53:56.6Z  
Constant Ballistic Coefficients between 0.1 to 1.0 psf, 0-0.15 L/D,  $C_d$  1.0

Debris 4

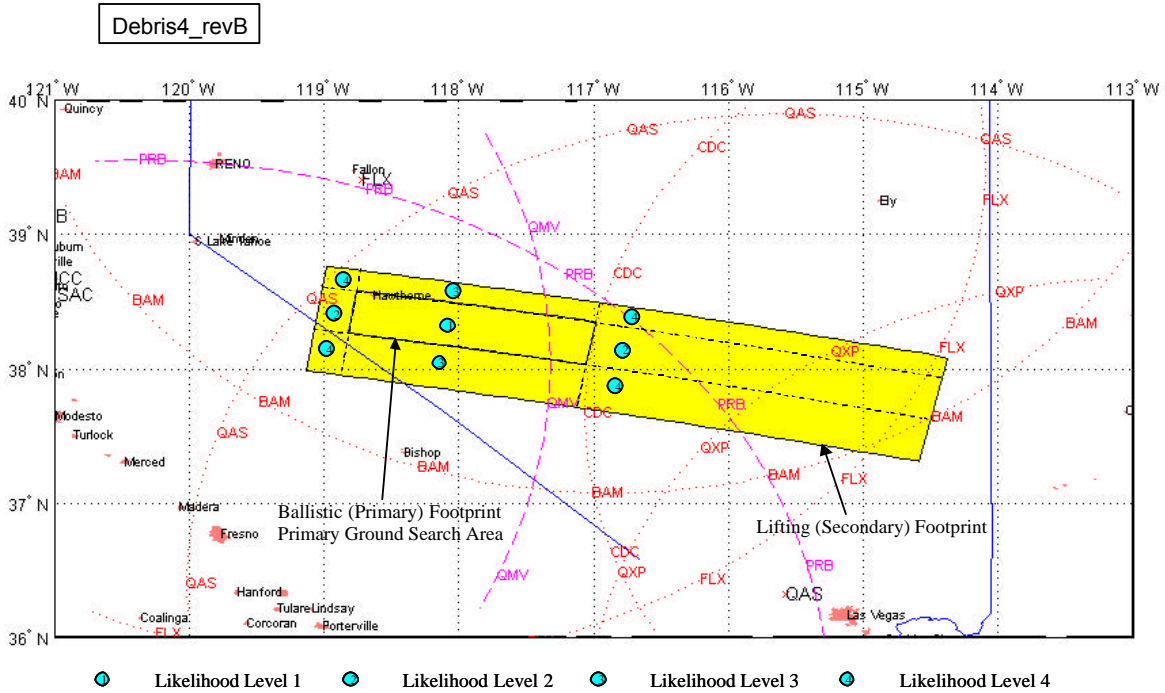


Figure 4-55: Probable Ground Impact Area for Debris 4  
Separation Time 13:54:02.3-13:54:03.5Z  
Constant Ballistic Coefficients between 0.3 to 1.5 psf, 0-0.15 L/D,  $C_d$  1.0

Debris 6

Video for this object was analyzed first due to the Orbiter and debris crossing of Venus, allowing accurate time estimation

The Aerospace Corporation independently validated the JSC ballistic coefficient, separation time, and both the ballistic (non-lifting) and lifting footprint boundaries, with similar, but slightly different methods for relative motion, ballistic coefficient estimation, and debris footprint estimation [30]. Aerospace calculated an Orbiter/Debris separation time of 13:54:33.72 compared to a JSC estimate of 13:54:33.7-13:54:34.7. [23] [30] The Aerospace ballistic coefficient matched the JSC range of 3.0 - 4.0 psf [30] [23], both derived using day-of-entry density at event altitude.

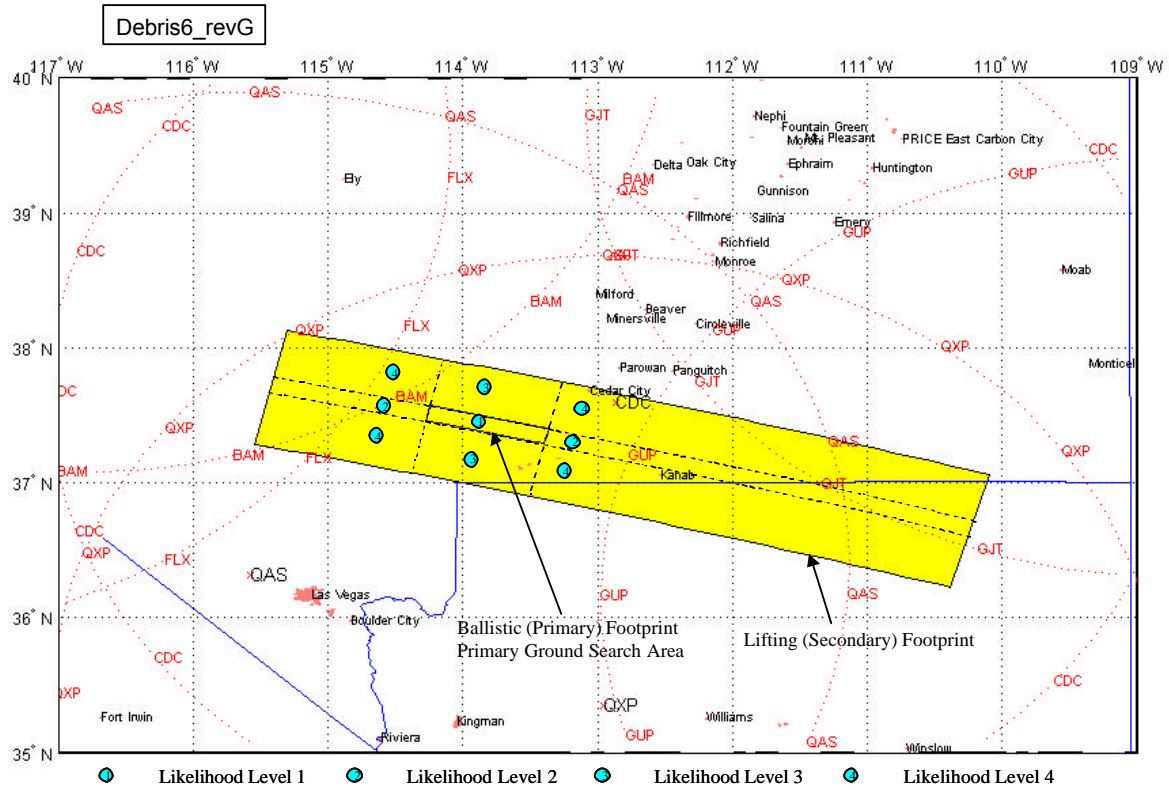


Figure 4-56: Probable Ground Impact Area for Debris 6  
Separation Time 13:54:33.7-13:54:34.7Z  
Constant Ballistic Coefficients between 3.0 to 4.0 psf, 0-0.15 L/D,  $C_d$  1.0

Debris 7

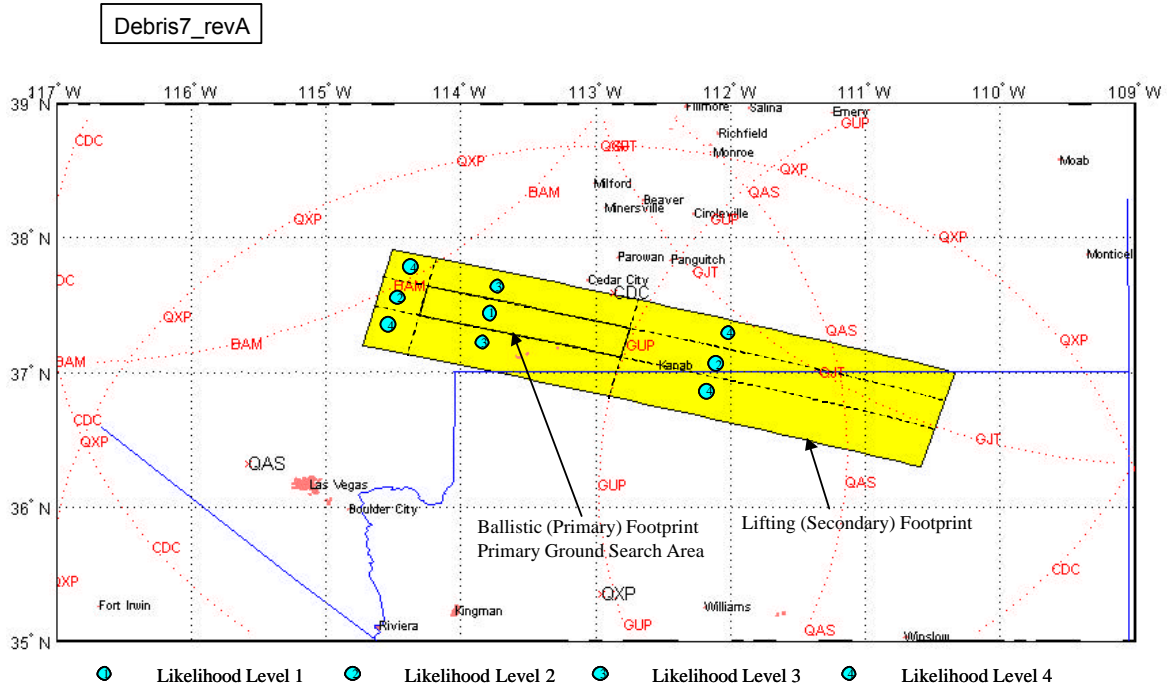


Figure 4-57: Probable Ground Impact Area for Debris 7  
Separation Time 13:55:03.6-13:55:04.6Z  
Constant Ballistic Coefficients between 0.5 to 1.7 psf, 0-0.15 L/D,  $C_d$  1.0

Debris 8

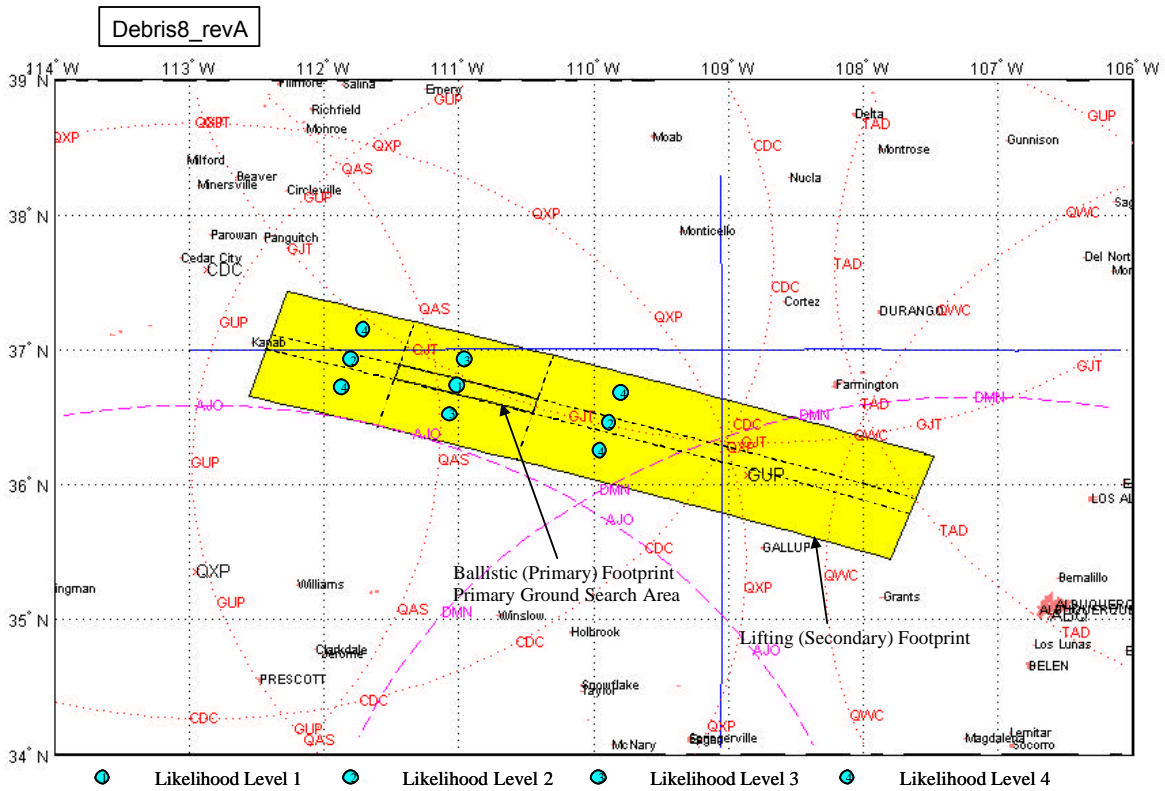


Figure 4-58: Probable Ground Impact Area for Debris 8  
Separation Time 13:55:20.2-13:55:21.4Z  
Constant Ballistic Coefficients between 2.6 to 4.0 psf, 0-0.15 L/D,  $C_d$  1.0

Debris 13

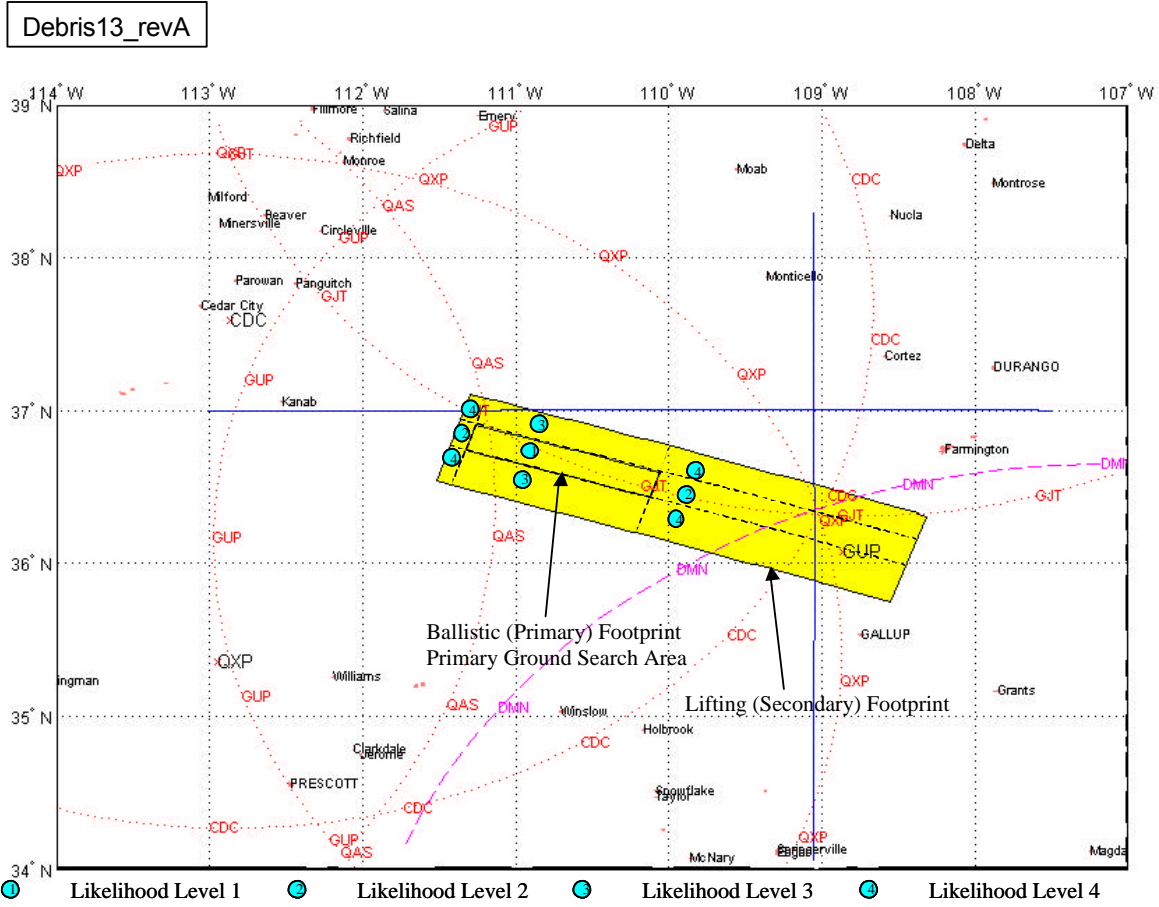


Figure 4-59: Probable Ground Impact Area for Debris 13  
Separation Time 13:55:53.3-13:55:54.3Z  
Constant Ballistic Coefficients between 0.2 to 1.1 psf, 0-0.15 L/D,  $C_d$  1.0



Debris 14

The Aerospace Corporation independently validated the JSC ballistic coefficient and both the ballistic (non-lifting) and lifting footprint boundaries, with similar, but slightly different methods for relative motion, ballistic coefficient estimation, and debris footprint estimation [30]. Aerospace calculated a ballistic coefficient of 1.0 - 2.0 psf [30] compared to a JSC estimate of 1.0 - 2.4 psf [23], both derived using day-of-entry density at event altitude.

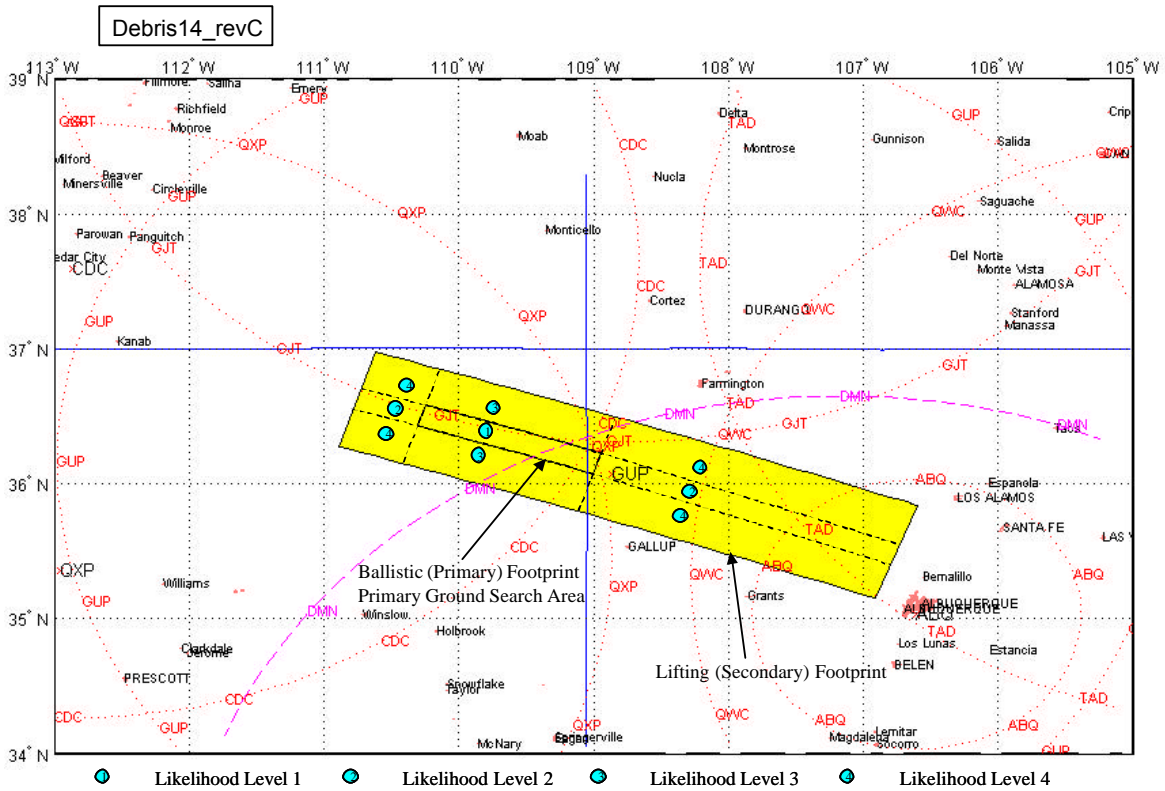


Figure 4-60: Probable Ground Impact Area for Debris 14  
Separation Time 13:55:56.2-13:55:57.2Z  
Constant Ballistic Coefficients between 1.0 & 2.4 psf, 0-0.15 L/D,  $C_d$  1.0

Debris 15

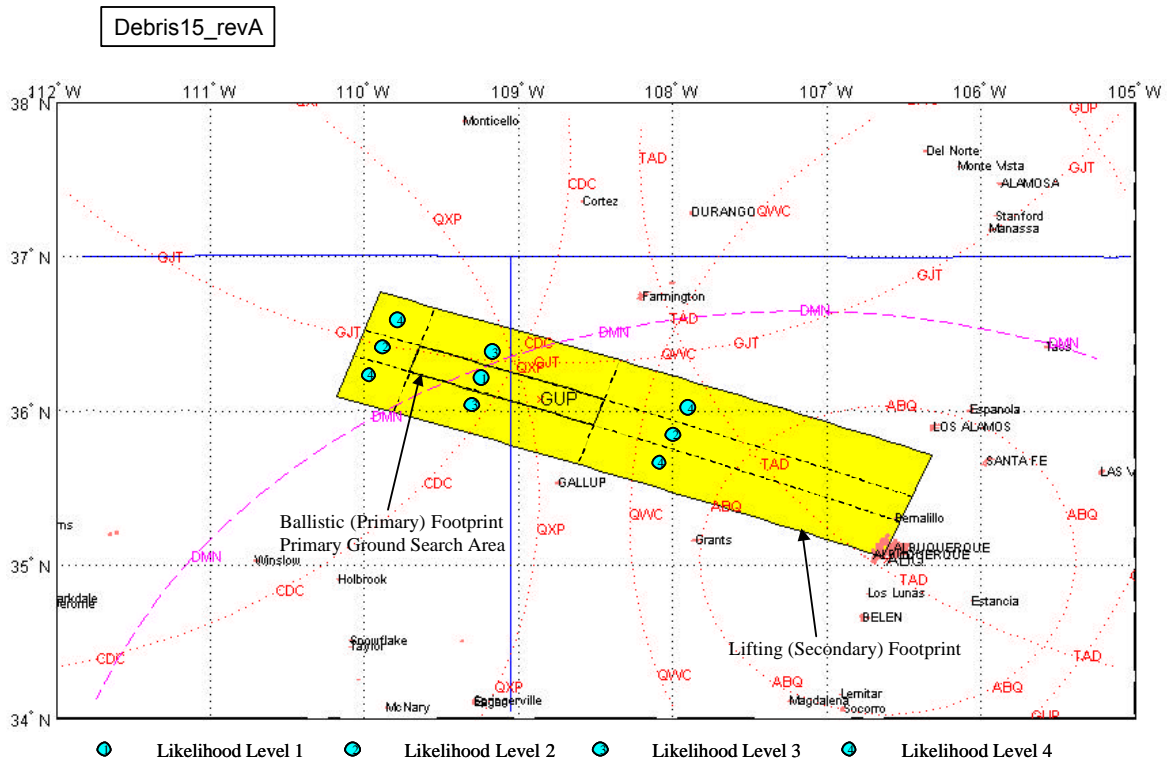


Figure 4-61: Probable Ground Impact Area for Debris 15  
Separation Time 13:56:09.0-13:56:10.0Z  
Constant Ballistic Coefficients between 0.8 to 2.0 psf, 0-0.15 L/D,  $C_d$  1.0

Debris 16

Debris16\_revB

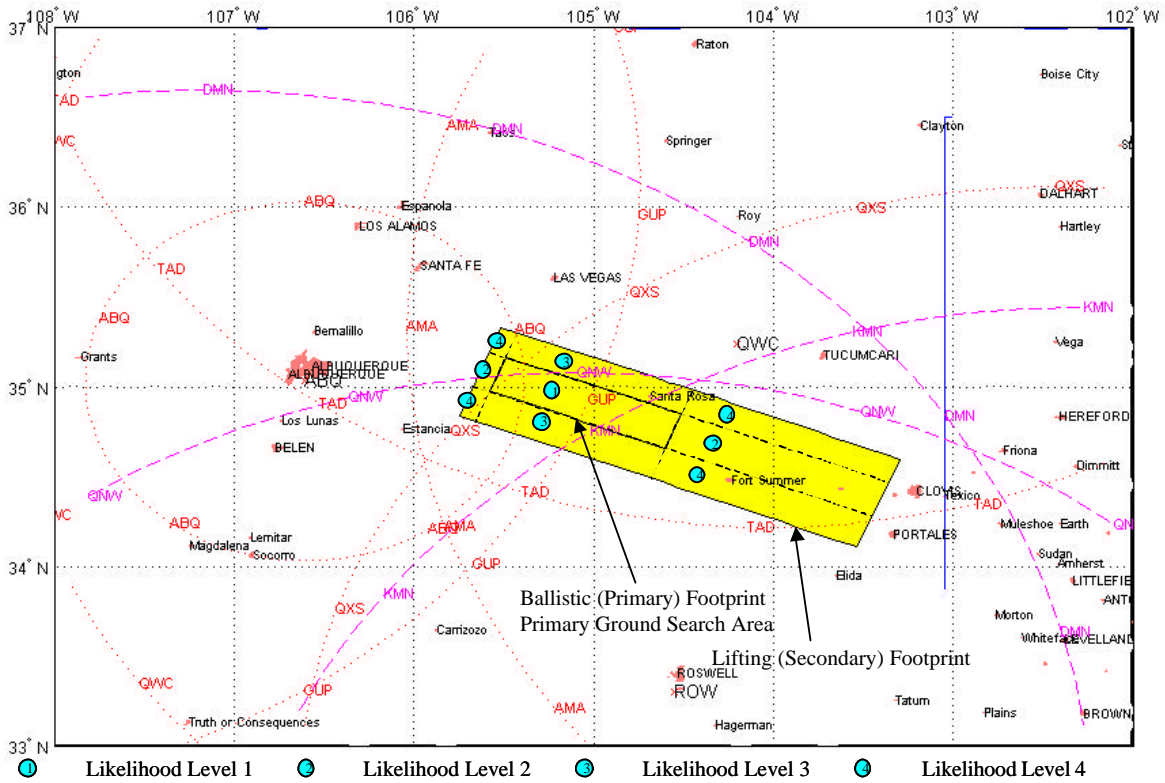


Figure 4-62: Probable Ground Impact Area for Debris 16  
Separation Time 13:57:23.2-13:57:24.2Z  
Constant Ballistic Coefficients between 0.1 to 1.0 psf, 0-0.15 L/D, C<sub>d</sub> 1.0

Flare 1 and 2

Two flares are visible in video coverage [22]. No debris is visible in the video at or near the flare times; debris may be there but may not be visible due to: small size; lighting (in daylight now); and/or short time of observation (Orbiter leaves camera field-of-view immediately). It is possible that debris fell off the Orbiter at these two flare times. The simulation uses the assumed ballistic coefficient range of 0.5 - 5.0 psf since this range approximately bounds ballistic coefficients derived from video of other debris thus far.

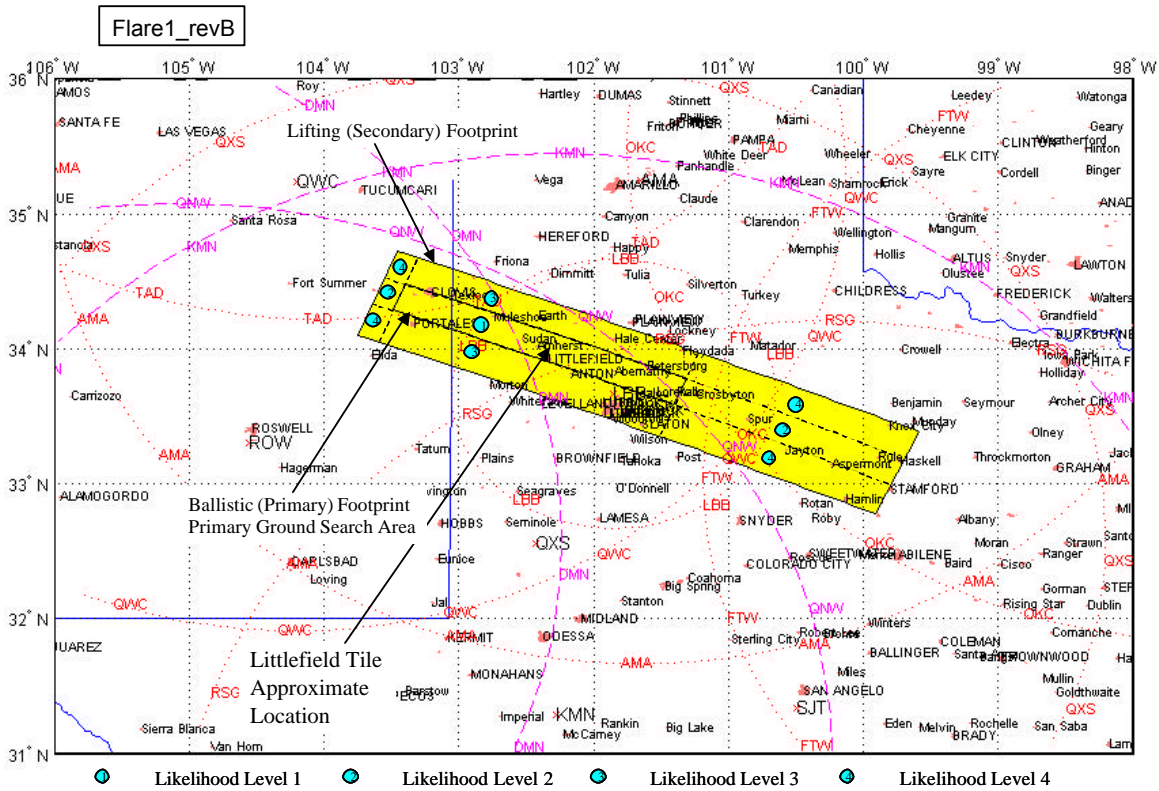


Figure 4-63: Probable Ground Impact Area for Assumed Debris Associated with Flare 1  
Observed Flare at 13:57:54.7Z  
Constant Ballistic Coefficients between 0.5 to 5.0 psf, 0-0.15 L/D,  $C_d$  1.0

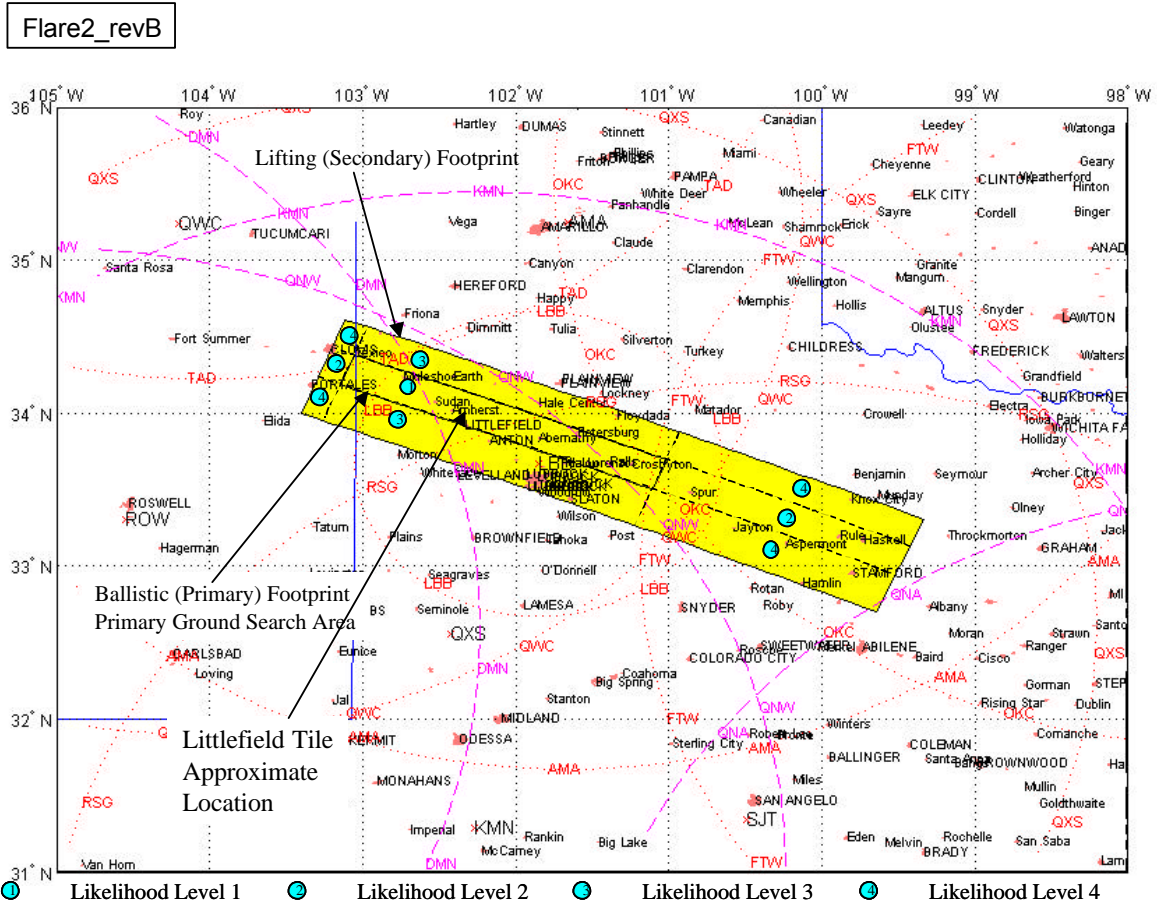


Figure 4-64: Probable Ground Impact Area for Assumed Debris Associated with Flare 2  
Observed Flare at 13:58:00.5Z  
Constant Ballistic Coefficients between 0.5 to 5.0 psf, 0-0.15 L/D,  $C_d$  1.0

#### 4.3.5. Estimated Separation Time for Littlefield Tile

A tile fragment, KSC Database object number 14768, was found in Littlefield, Texas at 33.97083N, 102.3158W. It weighs 16 grams and is 3.2" x 2.8" x 0.561". Shown below in Figure 4-65, the Littlefield Tile is the only confirmed pre-breakup debris found -- i.e., it was found outside of the primary debris footprint boundary and shown analytically to have fallen off prior to loss-of-signal.



Figure 4-65: Littlefield Tile

Assuming this tile fragment separated and fell to the ground intact in the shape and size it was discovered, it is possible to estimate the separation time. The Debris Footprint Team first computed the debris' ballistic coefficient. A series of footprints was then generated based on assumed debris shedding times. These times were iterated on to find the earliest time that results in a footprint boundary with the actual impact location on the edge of the toe, and also to find the latest time that results in a footprint boundary with the actual impact location on the edge of the heel.

Using this method, based on the impact location and ballistic coefficient range of 0.5 - 0.9 psf, the Littlefield Tile is estimated to have been shed between 13:57:49 - 13:58:20Z. This time range encompasses the observed times for Flare 1 and Flare 2. It is possible that if debris fell off the orbiter at Flare 1 or Flare 2, that the Littlefield Tile may be this debris or a portion of this debris. This is shown above in Figures 4-63 and 4-64.

#### 4.4. Debris Trajectory Analysis Lessons Learned

- 1) Observer provided information on location, camera specifications, zoom settings, and time synchronization are invaluable as the debris analysis progressed.
- 2) The combination of automation and parallel processes for calculating a relative range for each time step in video ensured both a quick and accurate answer and is highly recommended to anyone performing a similar analysis in the future.
- 3) The Debris Footprint Team generated the method to shape a debris footprint between the heel and toe specifically for this accident to aid the Search and Recovery Team in avoiding unnecessary search areas, and will be used in all future debris footprint predictions.
- 4) In this incident, the first debris footprint predictions were not available until 4 hours after the accident. To improve the possibility of crew rescue, either:
  - a “running” debris footprint should be designed for future STS missions such that as soon as telemetry is lost, a debris footprint and estimated crew module impact point are available, or
  - a footprint prediction team should be available during entry.
- 5) An upper bound on ballistic coefficient was not known for an Orbiter on entry; the Debris Footprint Team now has a maximum ballistic coefficient to use in any future Orbiter-only debris field analysis, based on the Columbia observed value of 220 psf.

## 5. Radar Search Areas

Unless otherwise footnoted, Section 5 is referenced to [25], Hartman, S.; JSC-DM; JSC Radar Assessment Team Final Report; May 23, 2003. This is included in its entirety in Appendix 10.7.

### 5.1. Radar Analysis Team Summary

The Radar Analysis Team was chartered to look for debris west of Fort Worth, TX (pre-breakup). The team was composed of personnel from NASA JSC, National Transportation Safety Board (NTSB), Federal Aviation Administration (FAA), and USAF 84th Radar Evaluation Squadron (RADES). The NTSB and FAA teams brought recorded FAA air traffic control radar data and analytical software to JSC and trained the JSC personnel to search for radar threads.

For over 3 months, the Radar Analysis Team searched through more than 2 million individual radar returns generated between 1330 and 1500Z on February 1, 2003. From these, the team developed nine search reports based on radar tracks. Of these, a tile fragment was found approximately 1000 feet north of Search Box 1, a tile was found 3.5 miles east of Search Box 1, and another was found inside Search Box 1. The western-most debris found was a tile in Littlefield, TX.

The team was also the primary liaison for the radar cross-section testing conducted by the Air Force Research Laboratory (AFRL) at Wright-Patterson Air Force Base. These tests were performed on materials and components inside the payload bay and on the exterior of the Orbiter in order to fully characterize the radar cross-sections. These were tested for comparison with data from the C-band radars which tracked during ascent, UHF radars which tracked during orbit operations, and the L-band and S-band air traffic control radars which tracked during entry. The tests quantified material-specific radar return properties, resulting in estimated detection ranges. Results show that the various Orbiter external materials have low maximum detection ranges for the air traffic control radars, reducing confidence in the ability to detect the most probable Columbia pre-breakup debris in radar.

AFRL radar testing results are summarized in Section 6. C, L, and S-band data annexes were fully reported to the Columbia Accident Investigation Board (CAIB) and NASA by Air Force Research Laboratory Sensors Directorate on April 24, 2003.



## 5.2. Radar Database and Search Method

The term radar *thread* or *track* refers to a sequential series of radar returns, over a span of time, which displays geographical movement of a potential object of interest. A radar *blob* refers to a sequential series of radar returns, over a span of time, which does not display much geographical movement (i.e., multiple radar returns in the same geographic location, one possible explanation of which would be a vertically falling object). Radar *anomaly* is a general term referring to false radar echoes. These can be the result of many different things, including atmospheric phenomena, radar interference, or unknown reflective objects in the path of the radar.

The specific radars of interest to the Radar Analysis Team were:

- L Band - ARSR and FPS air traffic control radars used for long range aircraft tracking, with a maximum range of approximately 250 nm and a radar sweep every 10-12 seconds. The radars operate approximately between 1220 and 1380 MHz. The ARSR-4 is the only type of these radars that produces data in 3 dimensions (i.e., includes altitude information).
- S Band - ASR-9 air traffic control radars used for terminal area control around airports, with a maximum range of approximately 55 nm and a radar sweep every 4-5 seconds. The radars operate approximately between 2400 to 2600 MHz.
- C Band - NASA ascent/entry tracking radars, used for long range shuttle tracking, generally track the shuttle out to approximately 500 nm during ascent. The radars operate at approximately 5.7 GHz.

Archived radar data was collected by NTSB and FAA and brought to JSC on February 10. Data was collected from 72 two-dimensional radars (no altitude data) and 38 three-dimensional radars (altitude data included). Of these, approximately 10 three-dimensional radars and 25 two-dimensional radars were located within proximity of the shuttle groundtrack and generic debris swath.

FAA and USAF radars record and archive radar data for 15 days and 120 days respectively. Consequently, FAA radar data for ascent was lost since it had exceeded the expiration date by the time of Columbia's entry. NTSB collected data from radar sites in any region of the country that had the potential to observe debris.

The NTSB/FAA team brought a number of software tools to aid in the analysis of the radar data. NTSB analysts develop their own tools and are free to use whatever they are most comfortable with individually. The tools they brought were considered by them to be easiest to train on and use. The existing tools were not designed to detect radar threads for objects at Columbia's altitudes and speed, but NTSB personnel were confident the tools would work.

NTSB/FAA tools include: RS3 (developed by 84th RADES) to display raw radar data, RAPTOR to display raw Terminal Control Radar data, TRACKS, FINDTRACK, BALLISTICS, and WINLATS to manipulate the radar data in order to more easily discover radar tracks.

Some of these tools, while useful, needed to be altered in order to be used to search for pre-breakup Columbia debris. The JSC Team developed a number of software tools to aid in the display/analysis of the radar data.

Enhanced Display Tool:

JSC Radar Analysis Tool (JRAT) - Derived by JSC’s Flight Design and Dynamics Division from the NTSB “TRACKS” tool. JRAT graphically displays radar returns in both 2-D and 3-D formats to allow the user to better view the data, in order to facilitate the search for any potential tracks.

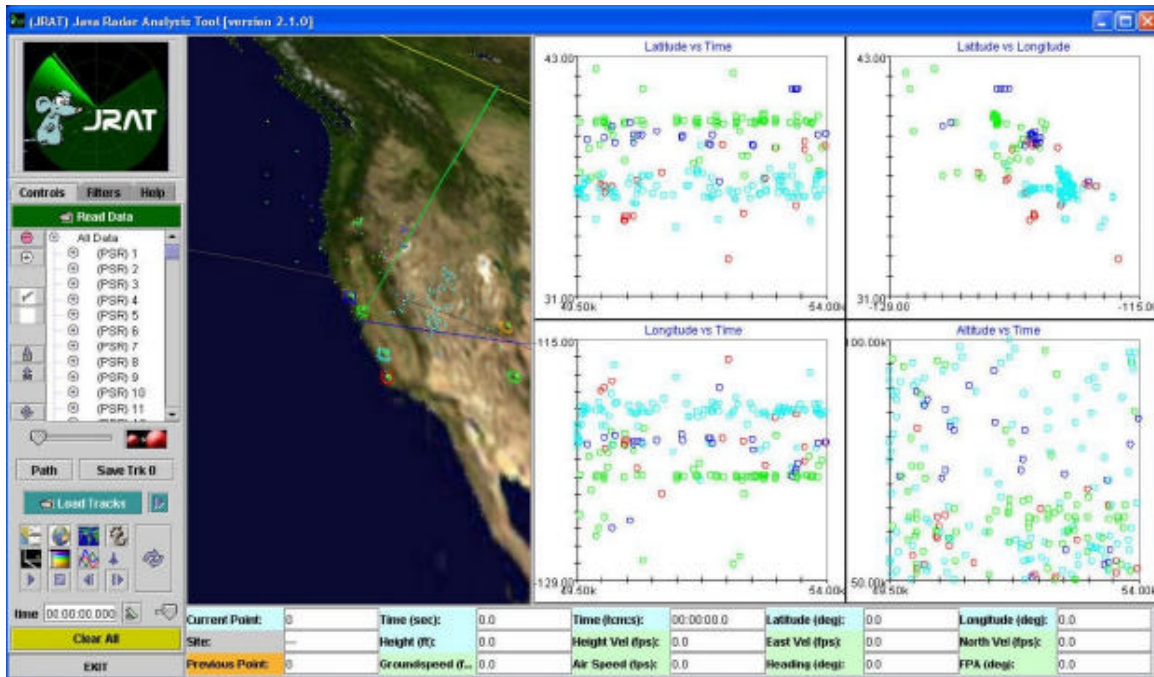


Figure 5-1: JRAT Screenshot

Data Integration Tools:

JSC’s Flight Design and Dynamics Division attempted to build a triangulation tool to estimate the altitude of any tracks that were observed by two radars (neither of which was an altitude-finding radar). However, this was not achievable due to the uncertainties inherent in the radar tracks. It was determined that altitude errors would have been on the order of 5000 to 10,000 ft, or greater. Therefore, this tool development was abandoned.

The Concept Exploration Lab (CEL), led by Joe Hamilton, developed: Convert.exe, Vfilter.tcl, Scrub.tcl, Grid.tcl. These tools were used in conjunction with previously available software to attempt to filter the radar database and “automate” the search for potential tracks.

Tools to aid in automating the search for radar tracks:

Convert.exe - Converts 2D radar text files with azimuth and range information from a given sensor location into a comma delimited file for use in multiple plotting and visualization tools. Latitude and longitude of each radar point is calculated based upon a specified assumed altitude. Output files can be filtered by time, range, and azimuth.

Vfilter.tcl - Accepts output from Convert.exe and RS3 to search the data for correlated tracks and calculates an estimated course and speed for each track. Search parameters are selectable to focus on tracks of interest. This has been extremely successful at finding airline tracks. However, attempts to correlate tracks at shuttle entry velocities resulted in numerous false tracks unless the search parameters were kept very tight. Tracks in the RS3 data, of potentially falling objects, were identified but most of them did not match likely ballistic profiles. A version of vfilter.tcl was created to remove airline tracks from the source data. This was mostly successful, but left some points associated with the airlines in the data.

Scrub.tcl - Accepts output from a specially designed session of the 3D visualization tool PRISMS. The PRISMS session was used to visually scrub points out of the data, such as all remaining points associated with airline tracks. Scrub.tcl deletes points that were visually identified in PRISMS from the original source file.

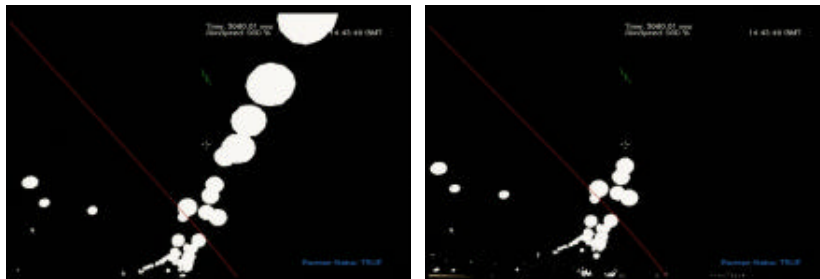


Figure 5-2: PRISMS Screenshots, Before and After Running Scrub.tcl

Grid.tcl - Counts the number of radar returns within specified grids over a time period to create density plots of the radar data. The result is similar to weather radar visualization techniques.

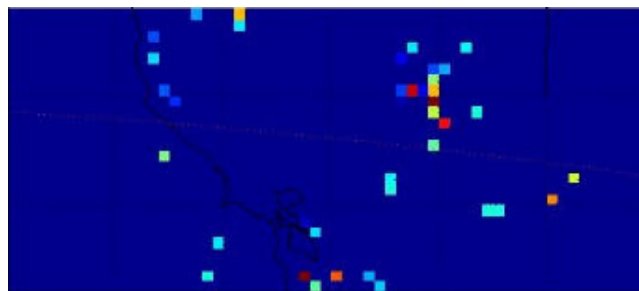


Figure 5-3: Grid.tcl Screenshot

Radar object class information was added to the Global Visualization Process (GVP) trajectory software. This provided the capability to view tens of thousands of radar points simultaneously with color gradients according to time stamp. (Lake Charles radar data and 07Feb03 footprint shown below.)

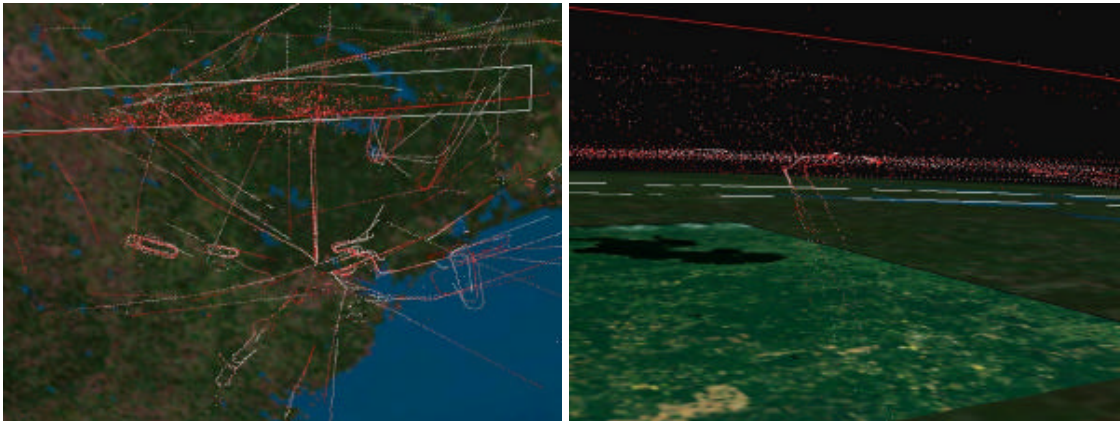


Figure 5-4: Global Visualization Process Screenshots

The NTSB/FAA/JSC team worked together to search for radar tracks. All tracks were reviewed by the full team.

The NTSB set up a password-protected web site that was used as both a repository for data (winds, master radar data file, search reports, etc.) as well as a place to file potential radar track data (accepted, rejected, under review).

The team was split into two sub-teams: groundtrack search and California Fence search.

The Groundtrack Team started by looking for radar tracks near the generic debris swath described in Section 4.3.3. They then focused on areas that reported potential Columbia debris in Albuquerque, New Mexico; Lubbock, Texas; and Littlefield, Texas, as well as the individual ballistic footprints described in Section 4.3.4. Eventually the Groundtrack Team divided the shuttle entry groundtrack into 13 generic search boxes, and completed a systematic search of all radars along the entire groundtrack (three people per box). In addition, the team searched areas near credible eye (and ear)-witness reports. The initial search focused on long radar threads, but migrated more to a “blob” search, looking for objects falling more vertically as the analysis went on. The team tried briefly (mostly unsuccessfully) to automate the search, by trying to look for semi-linear tracks with radar returns having similar velocity, flight path angle, and heading. Analysts attempted to confirm tracks found with RS3, by finding the same (and potentially additional points) using RAPTOR (Terminal Control Radar Data) without much success.

The California Fence Team searched the composite radar picture of four California ARSR-4 radars (Mill Valley, Rainbow Ridge, Paso Robles, Vandenberg). All of these radars have height finding capability, and were combined together in order to best be able to see early debris (potential to be tracked by multiple radars). The California Fence Team also began by searching

the composite radar picture for semi-linear tracks, with similar velocity, flight path angle, and heading. Several software tools were developed to aid in this search; however, the majority of the tracks that they identified were commercial aircraft. This team then transitioned to more of a “Blob” analysis. Specifically, the team attempted to define the density function of the radar returns, and use tools to filter out the background “noise” and identify possible shuttle debris. Thirteen tracks were found that were not identified as commercial aircraft; however, all were dismissed as not being shuttle debris.

Search areas were established which were 2.5 degrees long in longitude, 40 nm wide centered on the ground track as shown below in Figure 5-5. These were intentionally overlapped by 0.5 degrees from the toe of one into the heel of the next. An area search was considered complete when three team members had independently searched each box. Short range radars were not used for these initial searches but were used to confirm a potential radar thread found on a long range radar.

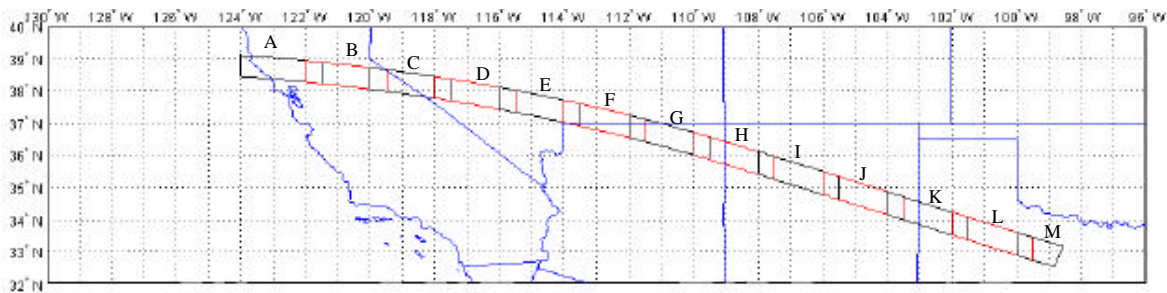


Figure 5-5: Radar Team Search Areas

Area searches of all long range radar were completed from 0 to 20 nm of the CONUS ground track. All areas were searched at least once within 60 nm of the CONUS ground track, but redundant coverage was as low as 79 percent beyond 20 nm from the ground track.

Members of the team searched the radars in one of two different ways: 1) Searching by boxes (defined by the latitude and longitude of their corners), where a team member searches all radars with coverage in that box. 2) Searching by radars, where one radar’s returns were looked at for specific azimuths and within 60 nm of the ground track.

Typically, the NASA team kept track of searching by boxes (such as the generic search boxes or specific footprints.) When a NASA team member reported an area complete, it meant they had searched all the radars with coverage in the box. Because defining an area as “complete” was not a precise measurement, NASA team members were also given the option of calling an area “partially” searched or “fully” searched. If an area was partially searched, the formula only counted that area as 50% searched by one person, or if the area was fully searched, it was counted as 100% searched by one person.

The NTSB/FAA radar team members searched by radar, looking at only one radar’s returns at specific azimuths and only to a range within 60 nm of the ground track. However, for most areas of the sky near the ground track, anywhere from two to six radars had coverage. The percentage

of the area searched per person was the percentage of radars looked at divided by the total number radars with coverage. For example, if one NTSB member looked at radar ABC, but there were two other radars with coverage in the same area that he didn't search, it was reported as 33% searched by one person.

The long range radar search progress is depicted in Figure 5-6. Arrows point to locations along the ground track where certain "boxes" received even greater scrutiny than the rest of the area. Early revisions of the Debris 1, 6 & 14 footprints received a good amount of scrutiny because they were particularly noteworthy video debris events, and the footprints were generated earlier in the process than when the generic boxes were assigned. This kind of system was not used for distances further out, so those search areas were dependent on different kind of searches (such as NTSB-type single radar searches and looking at specific footprints), resulting in not quite 100% completion.

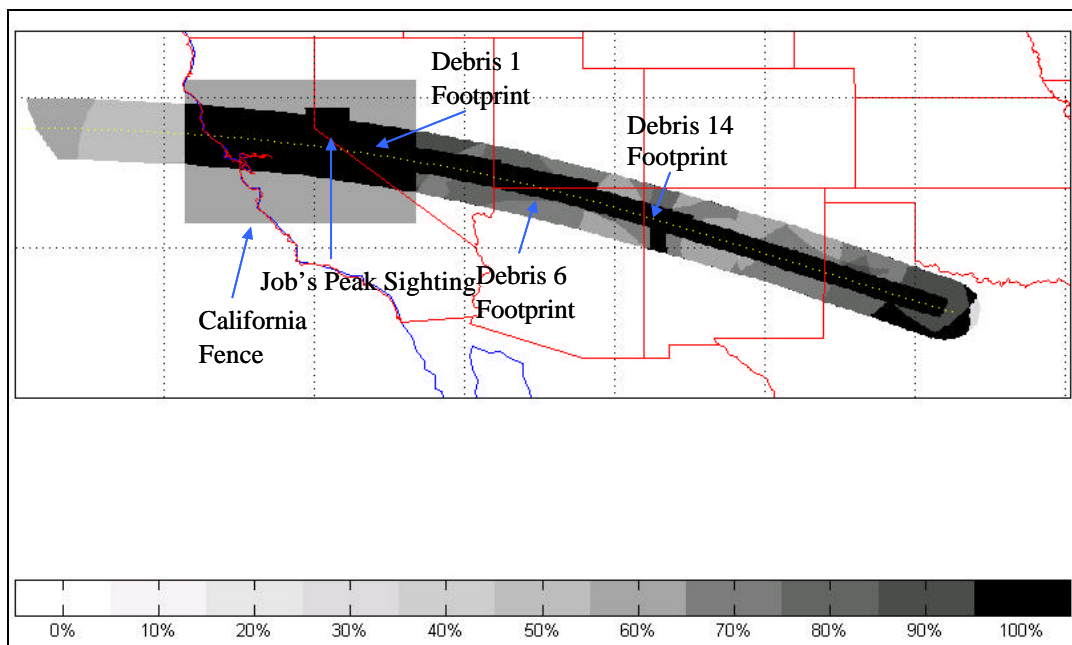


Figure 5-6: NASA/NTSB Team Total Progress (as of May 13, 2003)

Each radar thread was evaluated by the team for the following conditions/characteristics:

- The thread appears at the appropriate time in relation to the shuttle telemetry data - and no radar returns appear before or long after.
- Location of track in relation to the lifting footprint, considered to be the approximate northerly and southerly extent of possible debris.
- Typical behavior of sensor (e.g., noisy data with many spurious returns).
- The behavior of the track is not consistent with an aircraft.
- The location of the track is not consistent with aircraft operations, such as near an airport or an airway.

To be considered, the behavior of the track must be consistent with a valid trajectory of debris in terms of heading, speed, time aloft, known wind conditions, distance from the shuttle groundtrack, and expected range of ballistic coefficient considering the time and location of the track and a range of possible separation times/locations. The track must not be consistent with terrain (peaks or ridges), ground vehicles (located near roadways), or stationary objects such as towers. If a radar thread was determined to be valid, then a search box was generated.

Tracks identified by the Radar Assessment Team were examined for their likelihood of being associated with debris from the space shuttle. Two initial steps were performed to check the validity of the track being associated with a piece of shuttle debris. First, a computer program written by NTSB/Safety Board staff compared the track's location and timing with respect to the Orbiter's known re-entry trajectory. This program iteratively calculates the ballistic coefficient required for the track to be a piece that has departed from the Orbiter and match the radar track's location and timing. For tracks with no associated altitudes, altitude ranges were estimated based on local terrain for the lower bound. The upper bound was based on the upper limit of the range of detection of the respective radar system. This produced a range of calculated required ballistic coefficients for tracks without associated altitudes. The calculated ballistic coefficient was then compared to expected debris in that region, such as tiles or RCC panels, and those ranges of coefficients predicted by the debris footprint team. If the calculated ballistic coefficient for that track was either too large or too small, the track was rejected.

The next validity step performed two functions, as a second validity check and a first step in search box generation. A non-lifting trajectory was calculated using the required ballistic coefficient calculated in the first validity check, the associated (or estimated) altitude of the first return in the track, and the local winds. Tracks that moved in directions close to or in the general direction of the calculated trajectory were considered viable. Factors in this decision included proximity of the track to the local wind measuring point and the local terrain that could change the wind profile.

The calculated trajectory, using the required ballistic coefficient and local winds, was used to calculate the projected ground impact point when the trajectory from the initial point matched subsequent points in the track. If the track differed substantially from the calculated trajectory, then the ground impact trajectory was calculated from the last point in the track. The entire search box area was then defined by running trajectories from the last radar return to the ground and making estimations for: (1) ranges of possible ballistic coefficient, (2) changes in local winds due to terrain, (3) errors in radar return location due to ranging and height estimation errors. All these factors were included in several non-lifting trajectory calculations to define the limits of the search box areas.

### 5.3. California Fence Search

The California Fence search used California ARSR-4 radar sites (all with altitude data -PSR, RBR, VAN, MIL) in an effort to build a composite radar picture. Data shows 110,751 total radar hits from 1330Z to 1500Z. The data was separated based on time into three groups as shown in Figures 5-7 through 5-9 (Note: STS-107 crossed California coast at approximately 13:53:20.):

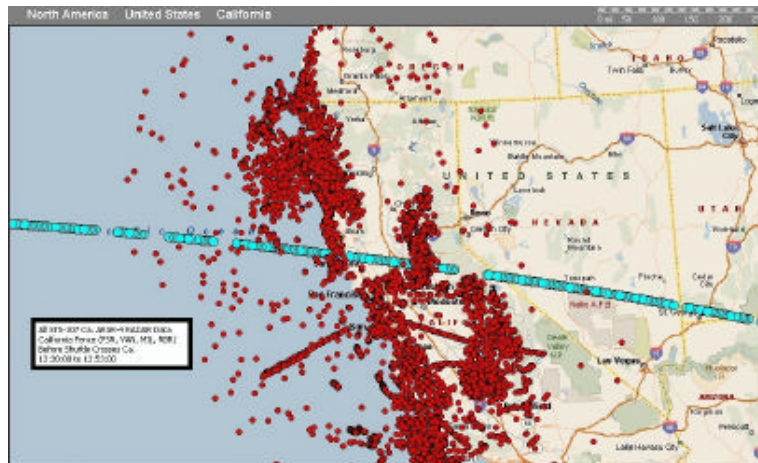


Figure 5-7: California Fence Data, Baseline, 13:30:00 to 13:53:00

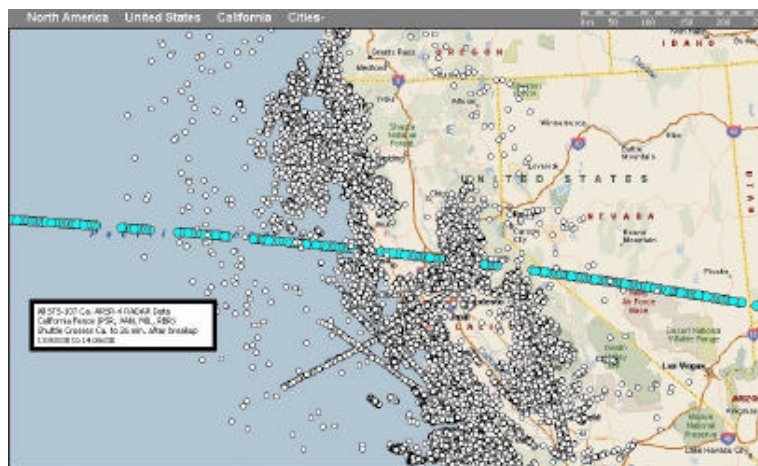


Figure 5-8: California Fence Data, Early, 13:53:00 to 14:26:00



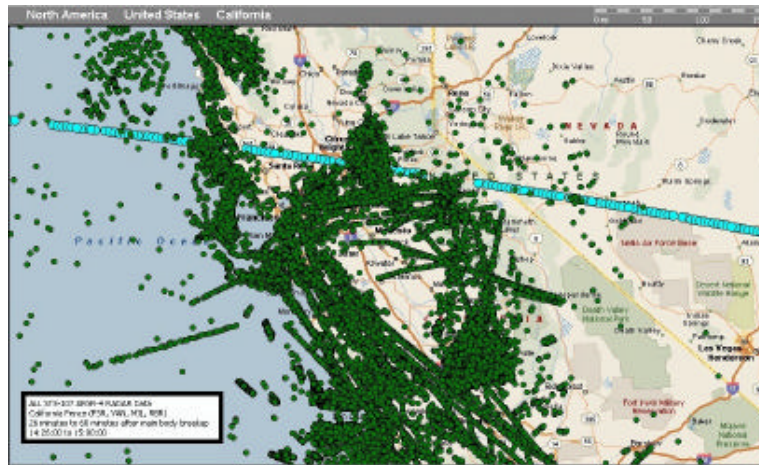


Figure 5-9: California Fence Data, Late, 14:26:00 to 15:00:00

This data was initially searched by analyzing individual tracks. It was postulated that ARSR-4 radar data would generate hits that could be correlated into semi-linear “tracks” with similar velocity, flight path angle, and heading. The team developed several new software packages to correlate data hits and try to automate the search for radar tracks. This resulted in the 13 potential tracks shown in Figure 5-10, but all candidates were rejected as potential shuttle debris.

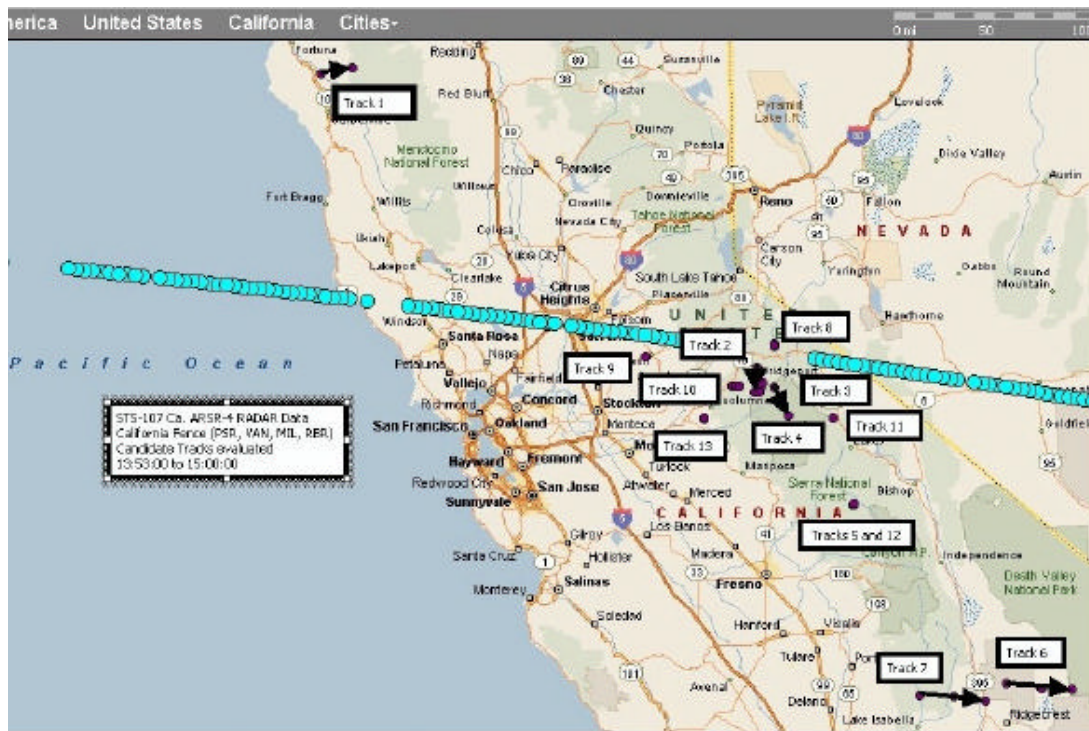


Figure 5-10: Initial “Track” Results: 13 candidates

The second approach used for the California Fence was blob analysis. It was postulated that ARSR-4 radar data would generate hits that could be correlated into groups with corresponding times in a limited latitude and longitude region. This density-approach was intended to identify single particles or “families” of debris falling in non-linear trajectories. The team first scrubbed the database of easily identified “airline” tracks for an approximately 20% reduction in data. They developed new software to count density of data hits within a grid near the groundtrack. This software calculated the number of hits/unit time/unit area before crossing, after crossing, and the change. It then mapped the change in density for easier analysis as illustrated below in Figure 5-11. No footprints have been generated yet from “Blob” analysis.

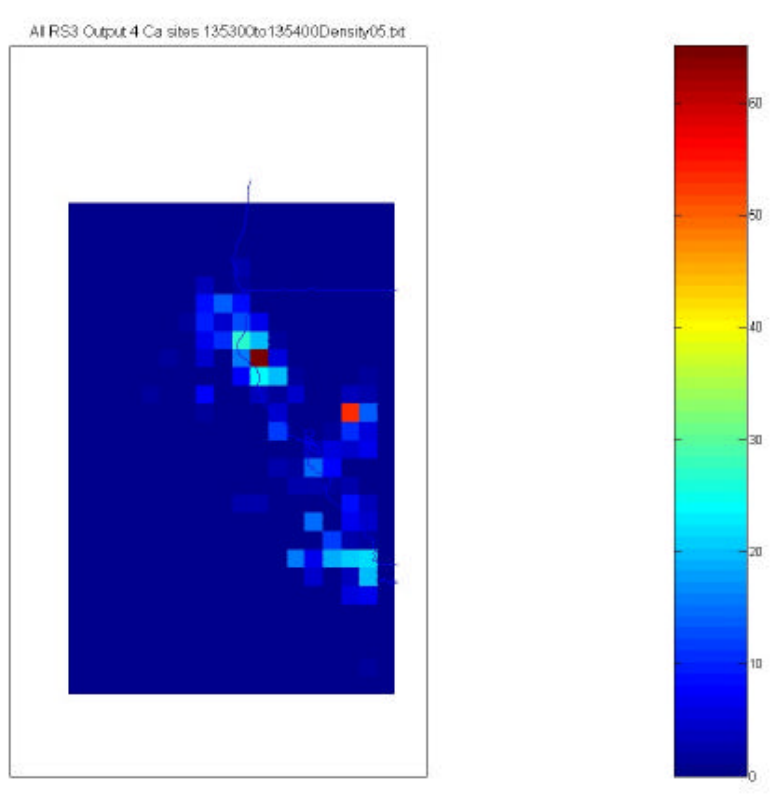


Figure 5-11: Example of Density Map “Blob” Analysis

### 5.4. Radar Based Search Boxes

The Radar Analysis Team searched through more than 2 million individual radar returns generated between 1330 and 1500Z on February 1, 2003. From these, the team developed nine search reports based on radar tracks. These are summarized in priority order in Tables 5-1 and 5-2. The details for each search box are given after the tables, from west to east. The rationale for the relative priorities is described in Section 5.5.

JSC/NTSB Priority	Box	Location Description	# radar hits	# radar antennas	Box Area Sq. NM / Acres (size of Non-lifting areas reflects ONLY the PRIMARY NL areas)	Inside any Lifting or Non Lifting (Ballistic) Footprint? Y/N (see separate Lookup Table)	Thread ID	Comment
1	8	west of Elgin, NV	11	1 (QAS)	1.68 / 1424	Y (Lifting 01 thru 06)	QAS-11-114.77	Delamar Lake, NV witness
2	7-1	Near Pioche, and Caliente, NV	75	1 (CDC)	4.25 / 3602	Y (Non lifting 02 thru 04, and Lifting 01,05,06)	CDC-075-114.4689	Well outside non-lifting, but in Debris-6 lifting foot print.
3	3	Near Floydada, TX	10	2 (QXS,LBB - ASR)	169.02 / 143251	Y(Lifting 16, non-lifting for Flare 1 and Flare2)	LBB-ASR-18-101.3186	Tile found 40 NM west of box
4	7-2	Near Pioche, and Caliente, NV	75	1(CDC)	11.03 / 9384	Y (Lifting 01 thru 06)	CDC-075-114.4690	Well outside non-lifting, but in Debris-6 lifting foot print.
5	6-south	Dixie Natl Forest - Zion Natl Park, UT	18	2 (QXP, CDC)	1.42 / 1203	Y (Lifting 02 thru 07)	QXP-18-113.1506	In/near Debris-6 dense overlap
6	6-north	Dixie Natl Forest - Zion Natl Park, UT	18	2 (QXP, CDC)	1.58 / 1339	Y (Lifting 02 thru 07)	QXP-18-113.1505	In/near Debris-6 dense overlap
7	Dense overlap non-lifting debris 04 thru 06	Near St. George Utah	N/A	N/A	Approx 300 Sq. NM	N/A	N/A	Best relmo cues and ballistics. Considered 1 of 2 most significant events in video. Most dense overlap area.
8	Dense Overlap non-lifting 07 thru 14	NE Arizona, Navajo Indian Reservation	N/A	N/A	approx 1162 Sq. NM	N/A	N/A	Measured relmo, but not as good as Debris-6. Considered 2 of 2 most significant events in video. 2nd most dense overlap area.
9	7-3	Near Pioche, and Caliente, NV	75	1 (CDC)	9.19 / 7789	Y (Lifting 01 thru 06)	CDC-075-114.4691	Outside non-lifting, but in Debris-6 lifting foot print.
10	Dense overlap - non lifting Debris 01 thru 04	CA/NV Border	N/A	N/A	approx 775 Sq. NM	N/A	N/A	Measured relmo, but not as good as Debris-14. 3rd most dense overlap area.

Table 5-1: High Confidence Western Search Box Priorities

JSC/NTSB Priority	Box	Location Description	# radar hits	# radar antennas	Box Area Sq. NM / Acres (size of Non-lifting areas reflects ONLY the PRIMARY NL areas)	Inside any Lifting or Non Lifting (Ballistic) Footprint? Y/N (see separate Lookup Table)	Thread ID	Comment
11	7	Near Pioche, and Caliente, NV	75	1 (CDC)	8.91 / 7551	Y (Lifting 01 thru 06)	CDC-075-114.4688	Well outside non-lifting, but in Debris-6 lifting foot print.
12	9-1	Modena, UT	7	1 (CDC)	1.36 / 1153	Y (Lifting 01 thru 04)	CDC-007-114.0324	
13	2	Near Weinert, TX	4	1 (KNM)	33.2 / 28138	Y (Lifting for Flare 1 and Flare 2)	KMN-4-99.8039	
14	5	Albuquerque, NM	54	2 - (QAS and ABQ-ASR)	7.14 / 6051	Y (lifting 8 thru 13 and 15)	QSA-ABQ-054-106.36	<b>about 17 miles from Probability "2" area of Debris 14 footprint</b>
15	Remaining Non-lifting Debris Footprint 06	Southern Utah/Nevada border	N/A	N/A	NL 06 is 296 Sq. NM but net is 0 - covered by Dense overlap 04 - 06	N/A	N/A	Best relmo cues and ballistics. Considered 1 of 2 most significant events in video.
16	Remaining Non-lifting Debris Footprint 14	Northern Arizona /New Mexico border	N/A	N/A	(1255 Total NL 14 - 1162 Dense overlap 07-14) = 93 Sq. NM	N/A	N/A	Measured relmo, but not as good as Debris-6. Considered 2 of 2 most significant events in video.
17	Remaining Non-lifting Debris Footprint 01	Sacramento, CA to Tonopah, NV	N/A	N/A	(1670 total NL 01 - 775 Dense overlap 01-04) = 895 Sq NM	N/A	N/A	Measured relmo, but not as good as Debris-14.
18	4	Brad, TX Possum Kingdom Lake	16 (2 tracks)	2 - FTW, DFWs (ASR)	73.2 / 62039	Y (Lifting -Flare 2)	FTW-7-098.5959	
19	Remaining Lifting Debris Footprint 01	Sacramento, CA to Tonopah, NV	N/A	N/A	16096 Total - 1670 NL = 14426 Sq. NM	N/A	N/A	Measured relmo, but not as good as Debris-14. Lifting considered very improbable by JSC.
20	Remaining Lifting Debris Footprint 06	Southern Utah/Nevada border	N/A	N/A	(12,026 Total- 296 NL) = 11730 Sq. NM	N/A	N/A	Best relmo cues and ballistics. Considered 1 of 2 most significant events in video. Lifting considered very improbable by JSC.
21	Remaining Lifting Debris Footprint 14	Northern Arizona /New Mexico border	N/A	N/A	(10121 Total - 1255 NL) = 8866 Sq. NM	N/A	N/A	Measured relmo, but not as good as Debris-6. Considered 2 of 2 most significant events in video. Lifting considered very improbable by JSC.

Table 5-2: Lower Confidence Western Search Box Priorities

Search Box 8 Near Elgin, NV

Number of sensors tracking: 1  
 Number of tracks: 1  
 Total number of returns: 11  
 Time span: 1 minute, 48 seconds  
 Ballistic footprints in proximity: Lifting 01 thru 06

A witness (EOC #2-1-1297) reported sighting objects falling ~1.5 statute miles north of the last radar hit in this search box. This report is described in more detail in Section 6. An expanded search area was created using the witness's recommendations.

The topographical map includes:

- Thin, red line = search box
- Yellow dots = radar hits

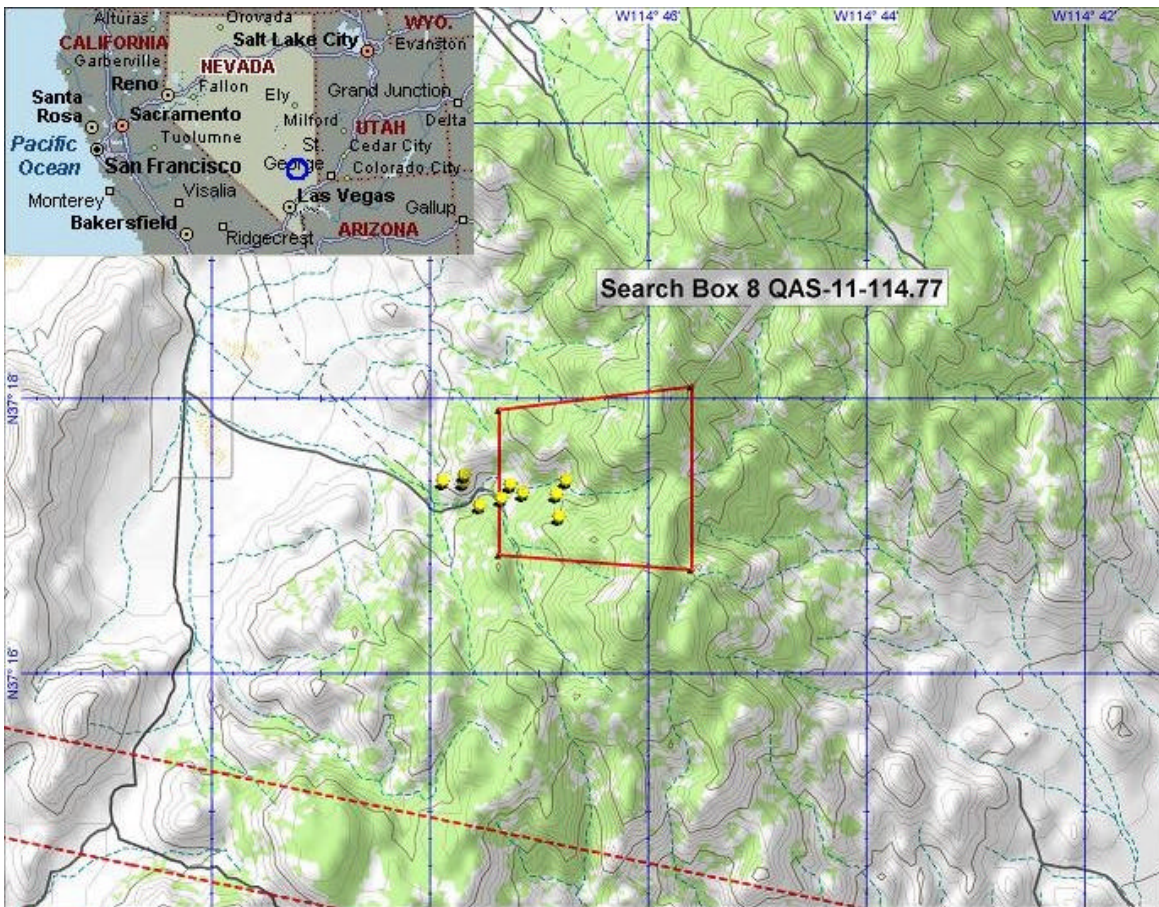


Figure 5-12: Search Box 8 Near Elgin, NV

Search Boxes 7, 7-1, 7-2, 7-3 Near Pioche, NV

Number of sensors tracking: 1

Number of tracks: 1, but may have split into 4 separate pieces

Total number of returns: 75

Time span: 39 minutes, 6 seconds

Ballistic footprints in proximity: 7-1: Non lifting 02 thru 04, and Lifting 01,05,06  
7, 7-2 and 7-3: Lifting 01 thru 06

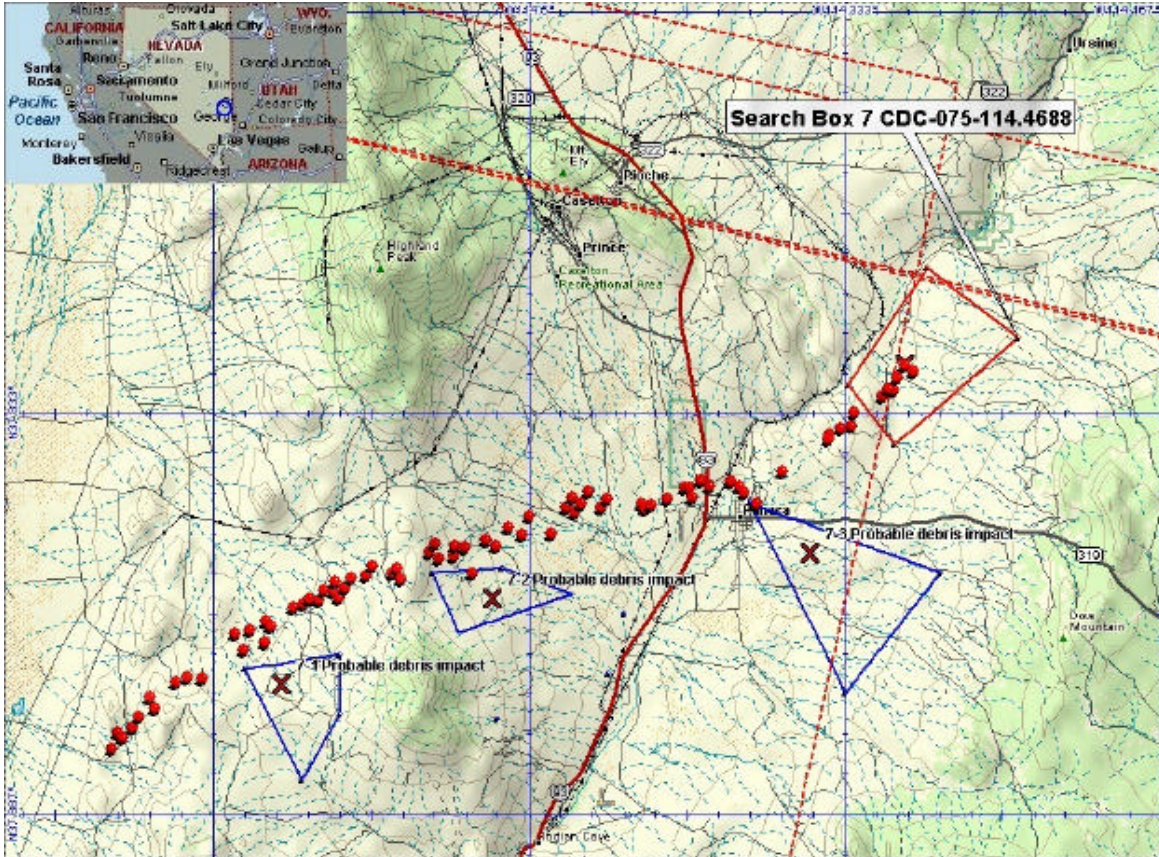


Figure 5-13: Search Boxes 7, 7-1, 7-2, 7-3 Near Pioche, NV

Search Box 9-1 Near Modena, UT

Number of sensors tracking: 1

Number of tracks: 1

Total number of returns: 7

Time span: 3 minutes, 12 seconds

Ballistic footprints in proximity: Lifting 01 thru 04

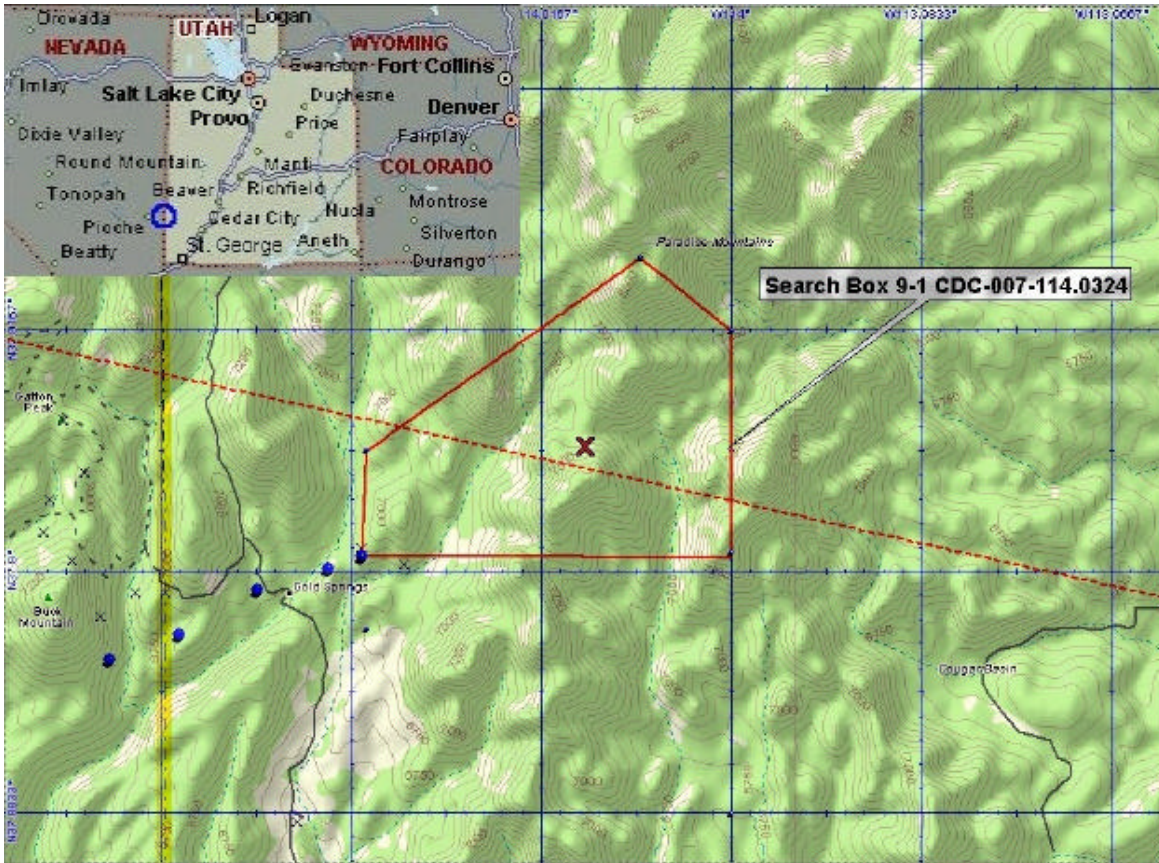


Figure 5-14: Search Box 9-1 Near Modena, UT

Search Box 6 Near Zion National Park, UT

Number of sensors tracking: 2

Number of tracks: 1, but may have split into 2 separate pieces – 2 adjoining search areas were defined

Total number of returns: 18

Time span: 7 minutes, 52 seconds

Ballistic footprints in proximity: Lifting 02 thru 07

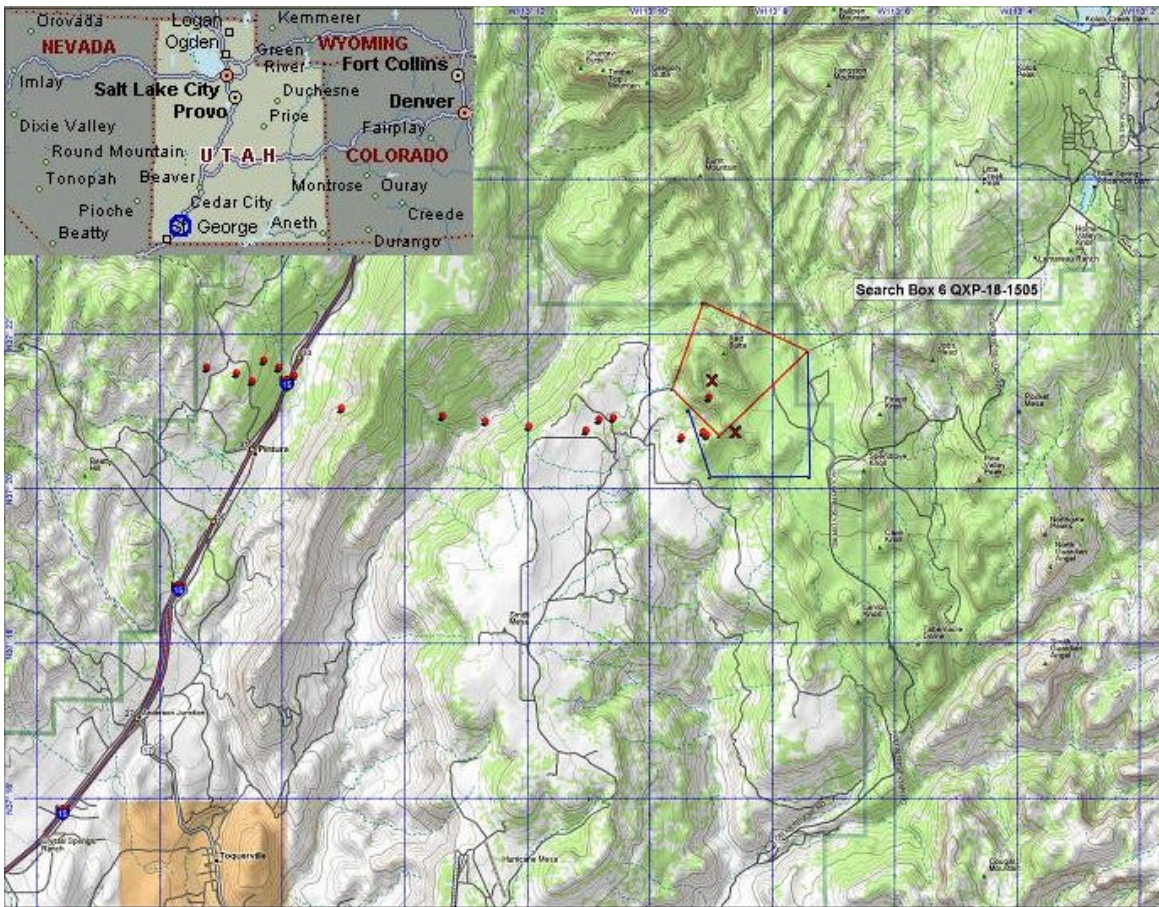


Figure 5-15: Search Box 6 Near Zion National Park, UT



Search Box 5 Near Albuquerque, NM

Number of sensors tracking: 2, 1 of these is a high rate (4.5 second sweeps) sensor

Number of tracks: 1, but may have split into 2 separate pieces – 2 adjoining search areas were defined

Total number of returns: 69

Time span: 11 minutes, 37 seconds

Ballistic footprints in proximity: Lifting 8 thru 13 and 15

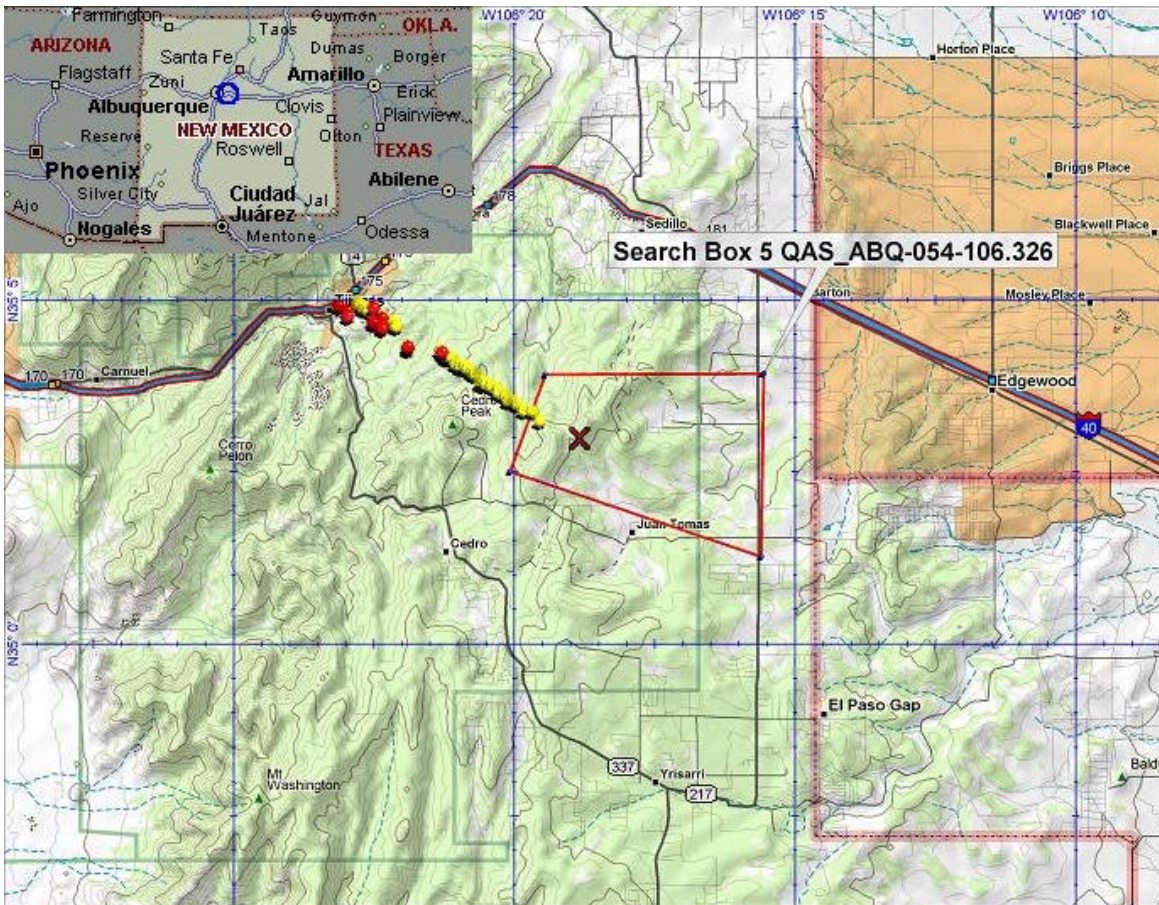


Figure 5-16: Search Box 5 Near Albuquerque, NM

Search Box 2 Near Weinert, TX

Number of sensors tracking: 1

Number of tracks: 1

Total number of returns: 4

Time span: 12 minutes, 16 seconds

Ballistic footprints in proximity: Lifting Flare 1 and Flare 2

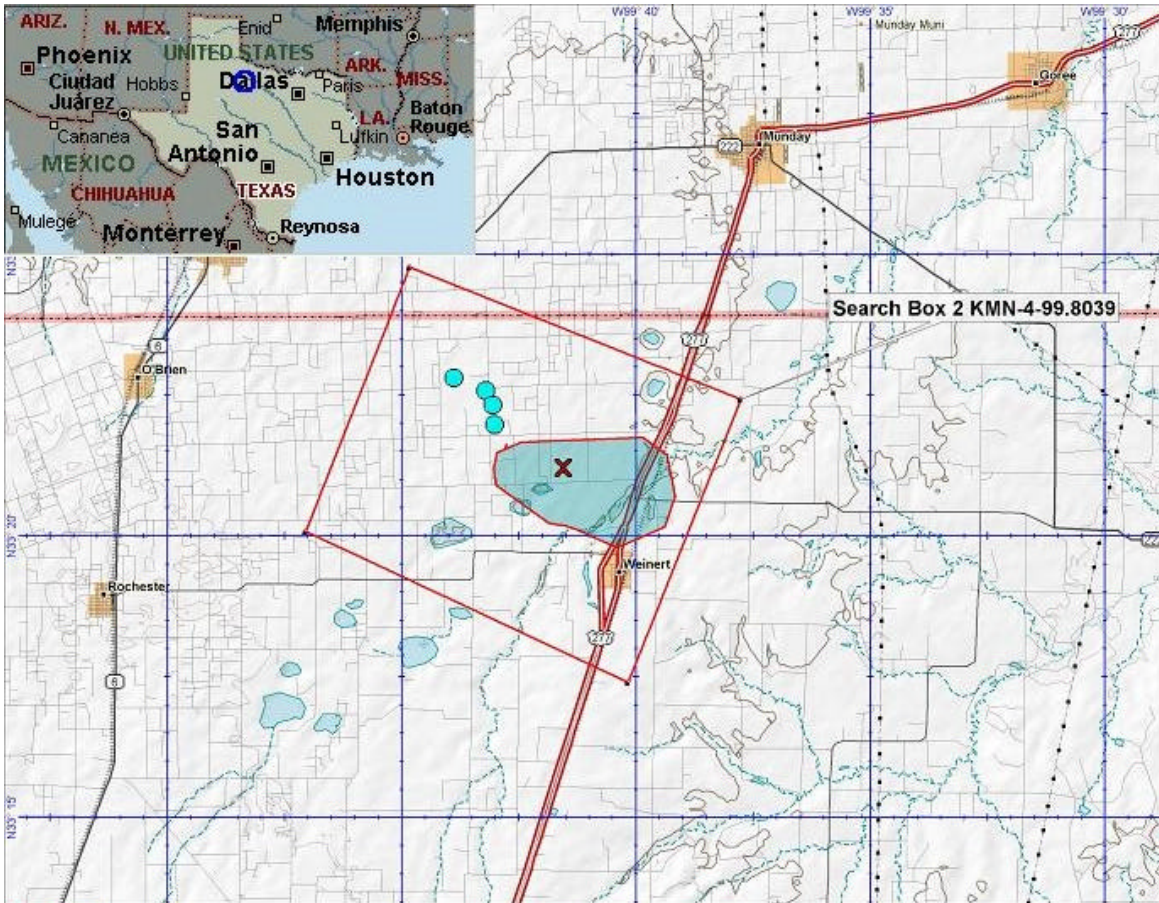


Figure 5-17: Search Box 2 Near Weinert, TX

Search Box 3 Near Floydada, TX

Number of sensors tracking: 2, 1 of these is a high rate (4.5 second sweeps) sensor

Number of tracks: 2

Total number of returns: 28

Time span: 8 minutes, 37 seconds (LBB-ASR-18-101.31) and 6 minutes, 4 seconds (QXS-10-101.433)

Ballistic footprints in proximity: Lifting 16, Non-lifting Flare 1 and Flare 2

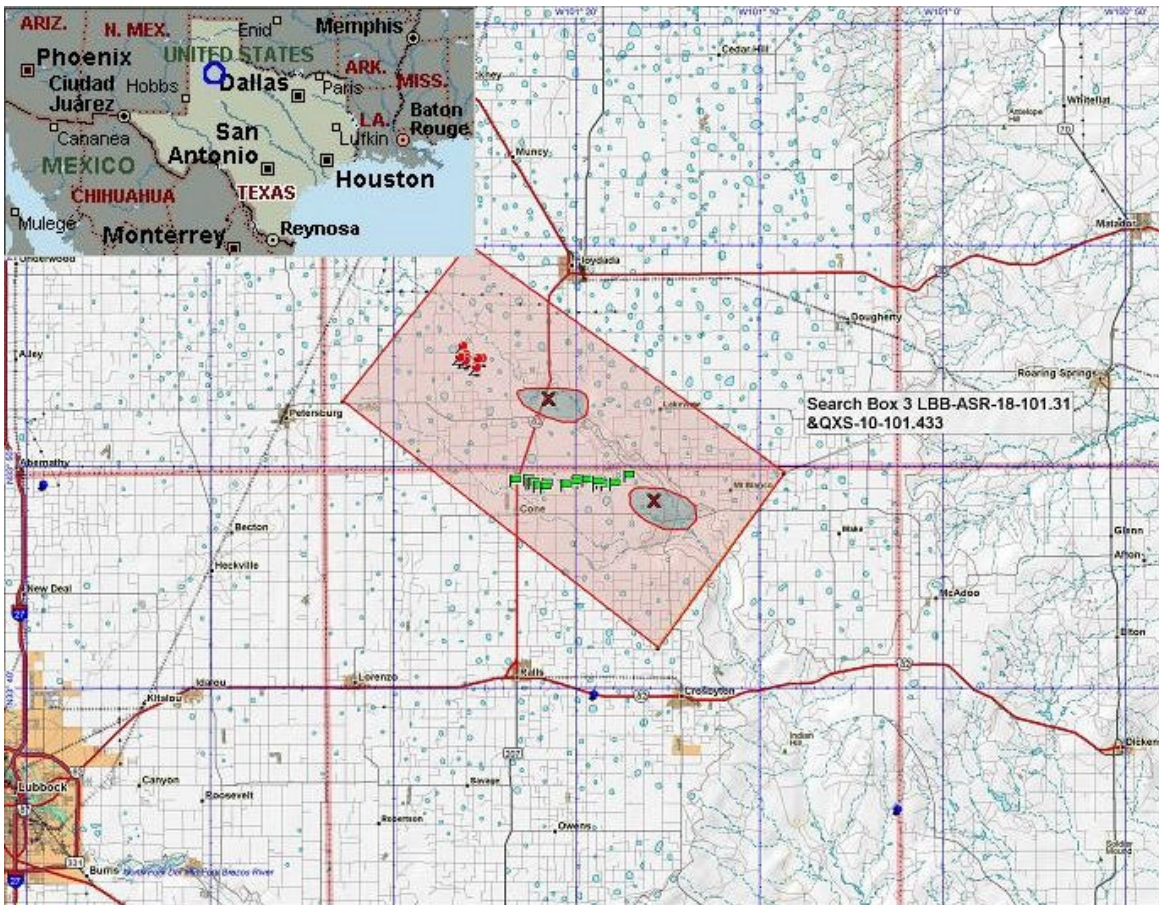


Figure 5-18: Search Box 3 Near Floydada, TX

Search Box 4 Near Brad, TX and Possum Kingdom Lake

Number of sensors tracking: 2, 1 of these is a high rate (4.5 second sweeps) sensor

Number of tracks: 2

Total number of returns: 16

Time span: 3 minutes, 53 seconds (FTW-7-098.595) and 7 minutes, 25 seconds (FTW-9-098.4887)

Ballistic footprints in proximity: Lifting - Flare 2

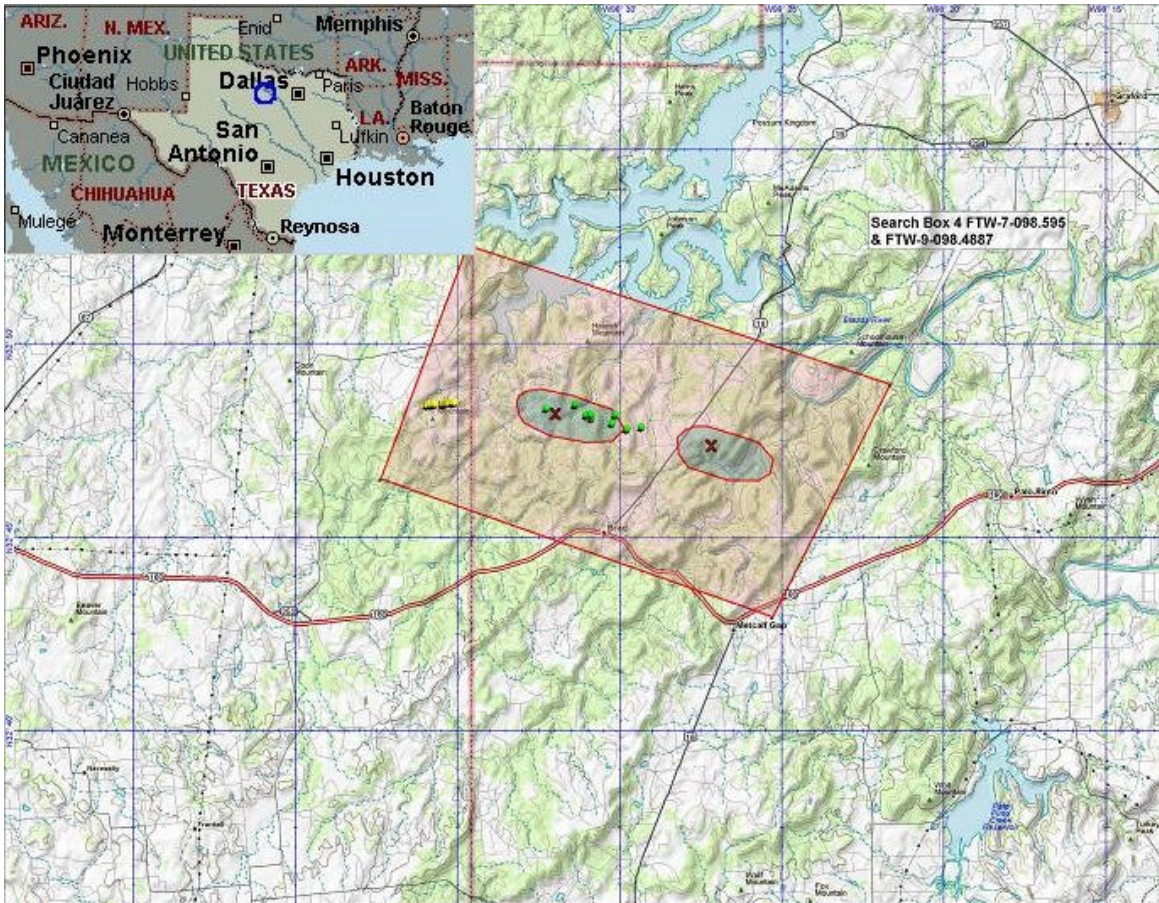


Figure 5-19: Search Box 4 Near Brad, TX and Possum Kingdom Lake

Search Box 1 Near Granbury, TX

Number of sensors tracking: 2  
 Number of tracks: 2  
 Total number of returns: 34  
 Time span: 5 minutes, 36.5 seconds

Tile piece found ~1000 feet north of Search Box 1 on Feb 13.  
 Full tile found 3.5 statute miles east of Search Box 1 on Mar 12.  
 Full tile found inside Search Box 1 on Apr 22.

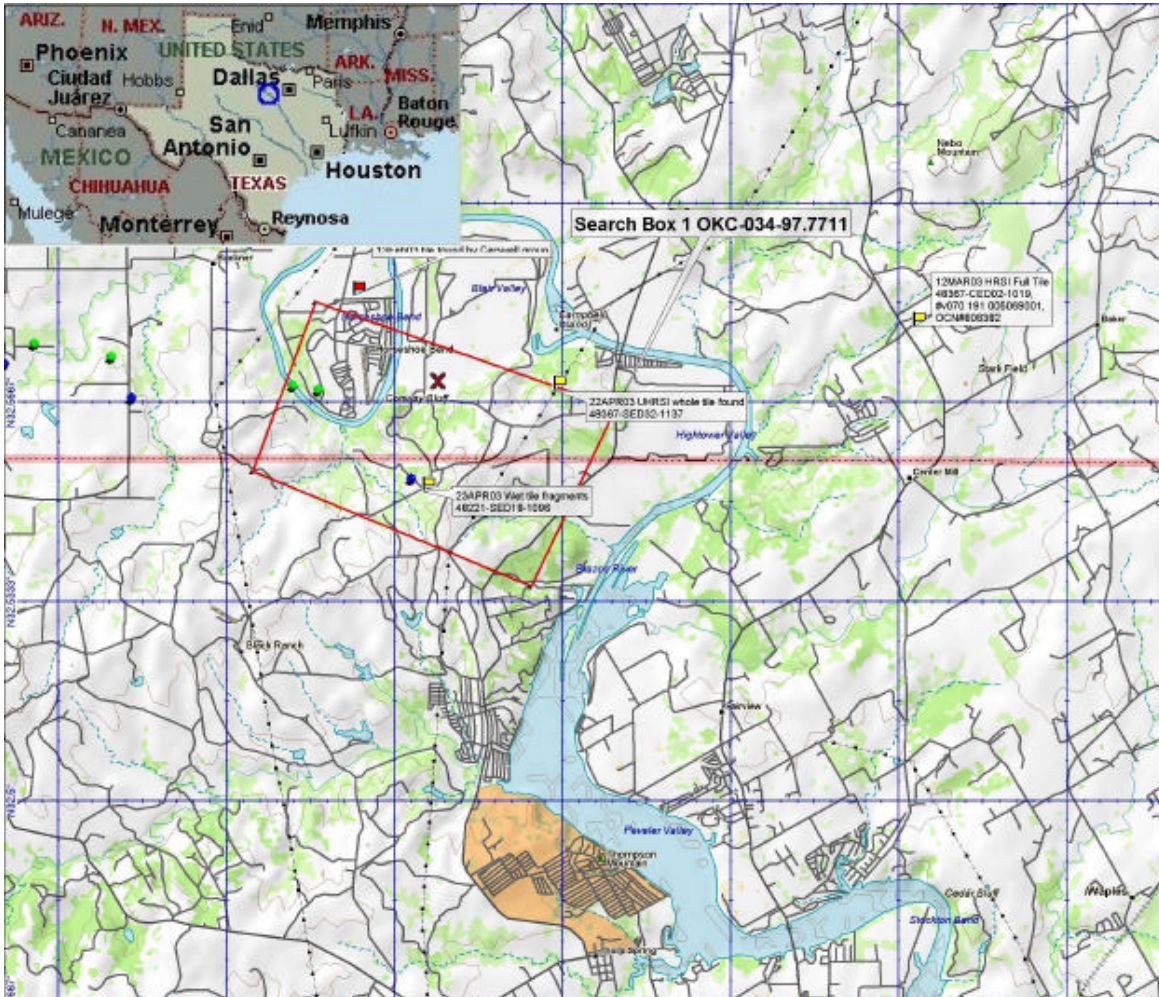


Figure 5-20: Search Box 1 Near Granbury, TX

## 5.5. Implication of Radar Tests for Radar Based Search Boxes

The Air Force Research Laboratory (AFRL) at Wright-Patterson AFB, OH tested various Orbiter external materials for L-band and S-band radar cross sections. These were used to calculate maximum detection ranges for each material and all air traffic control radars near the STS-107 ground track and generic debris swath. AFRL radar testing in support of the ESAT is described in detail in Section 6.4.

While all of these materials are detectable in the air traffic control radars, the various tile, FRSI and AFRSI materials show very low detection ranges, 23 - 35 nm [15], compared to the leading edge components, 105 - 195 nm [16]. The next series of figures shows the detection ranges for all long range radars which could have tracked Columbia, plotted over the groundtrack and the generic debris swath which was described in Section 4.3.3. From these figures, it can be determined which radars have a high probability of tracking the various Orbiter materials.

Figures 5-21 through 5-23 show the detection ranges for all long range radars. Although many of the long range radars could have tracked leading edge components with a high probability of detection, only three have a high probability of detecting the various tile, FRSI and AFRSI.

Similarly, Figures 5-24 and 5-25 show the detection ranges for all short range radars. Again, although many could have tracked leading edge components with a high probability of detection, only four have a high probability of detecting the various tile, FRSI and AFRSI.

Although the larger leading edge components have much higher radar detection ranges as described in Section 4, ballistic analysis and telemetry analysis suggest the long stream of debris observed in video is comprised of smaller objects, not a series of large, near intact, leading edge components. Thus, confidence was reduced that the radar threads used as the basis for search boxes are Columbia debris.

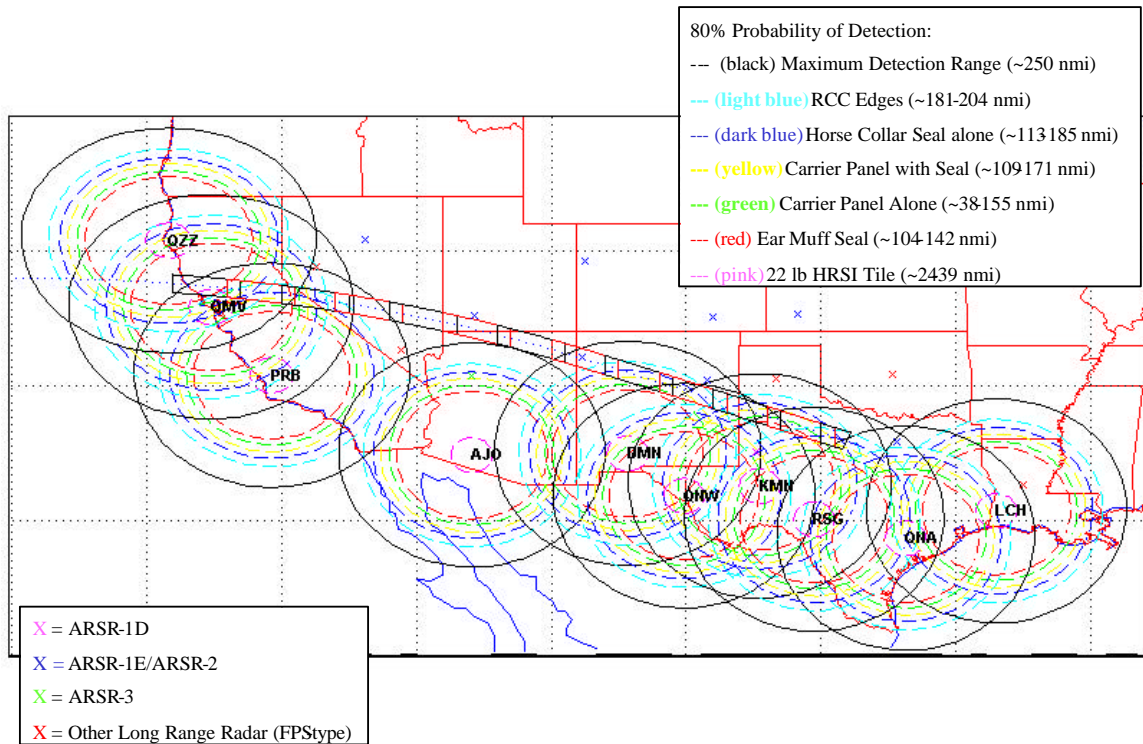


Figure 5-21: Long Range Radar (ARSR-4) Detection Ranges for Orbiter External Materials

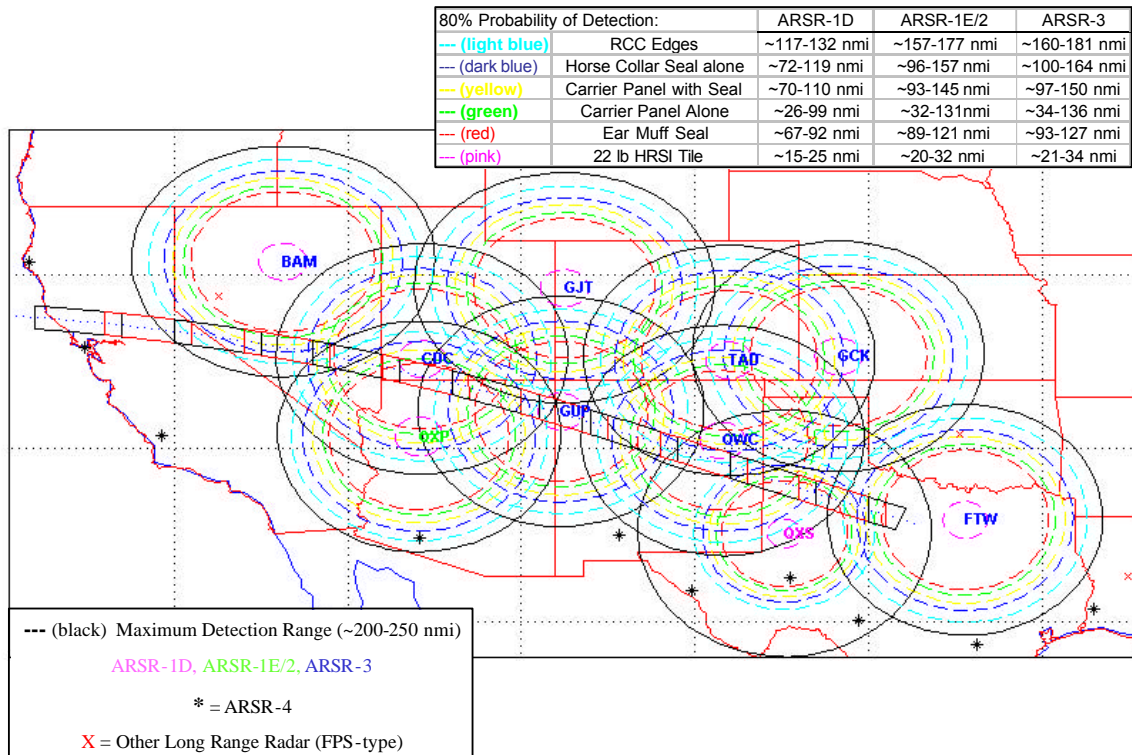


Figure 5-22: Long Range Radar (ARSR-1D, 1E, 2 & 3)  
Detection Ranges for Orbiter External Materials



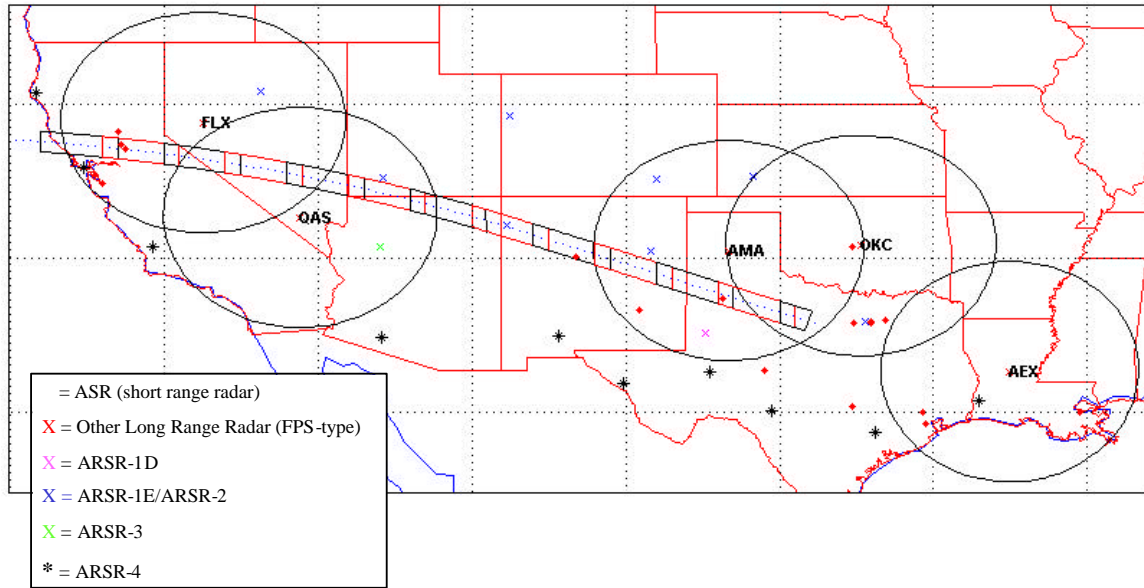


Figure 5-23: Long Range Radar (FPS, similar to the ARSR-1D, 1E, 2 & 3)  
Detection Ranges for Orbiter External Materials

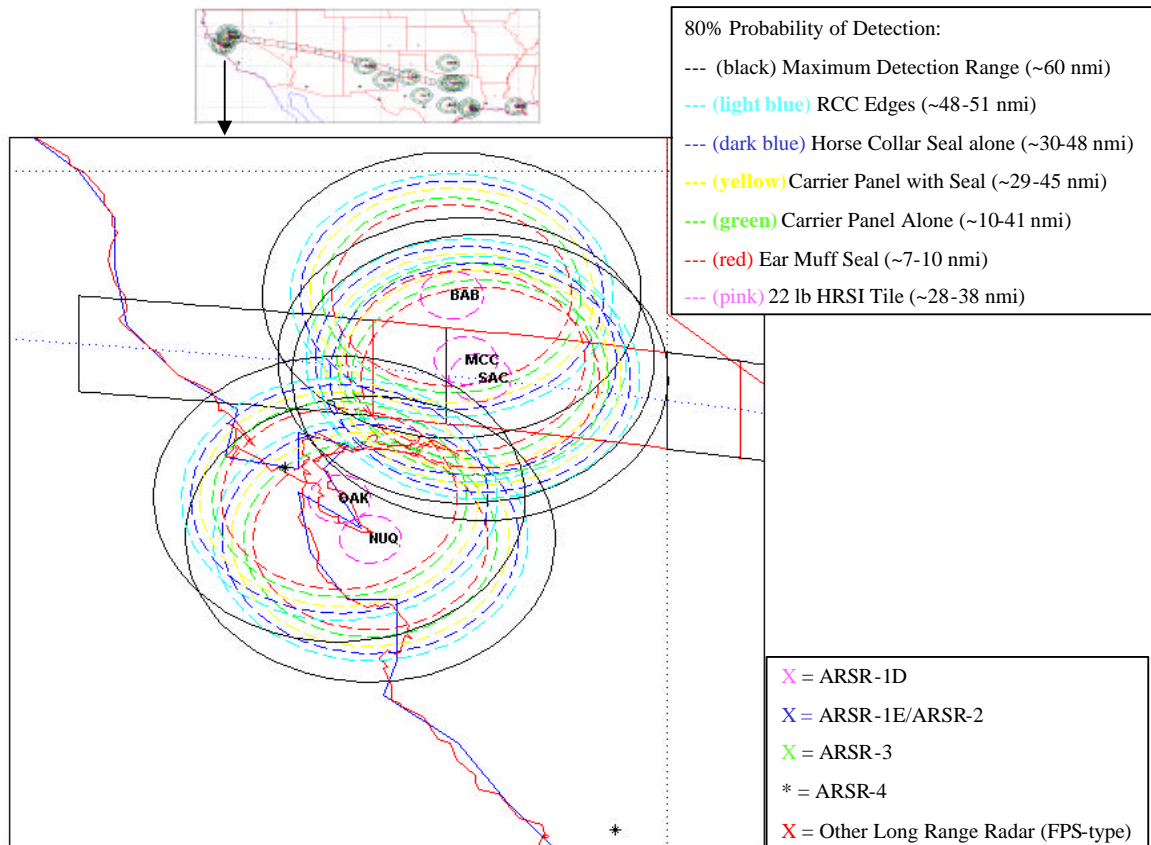


Figure 5-24: West Coast Short Range Radar (ASR-9)  
Detection Ranges for Orbiter External Materials

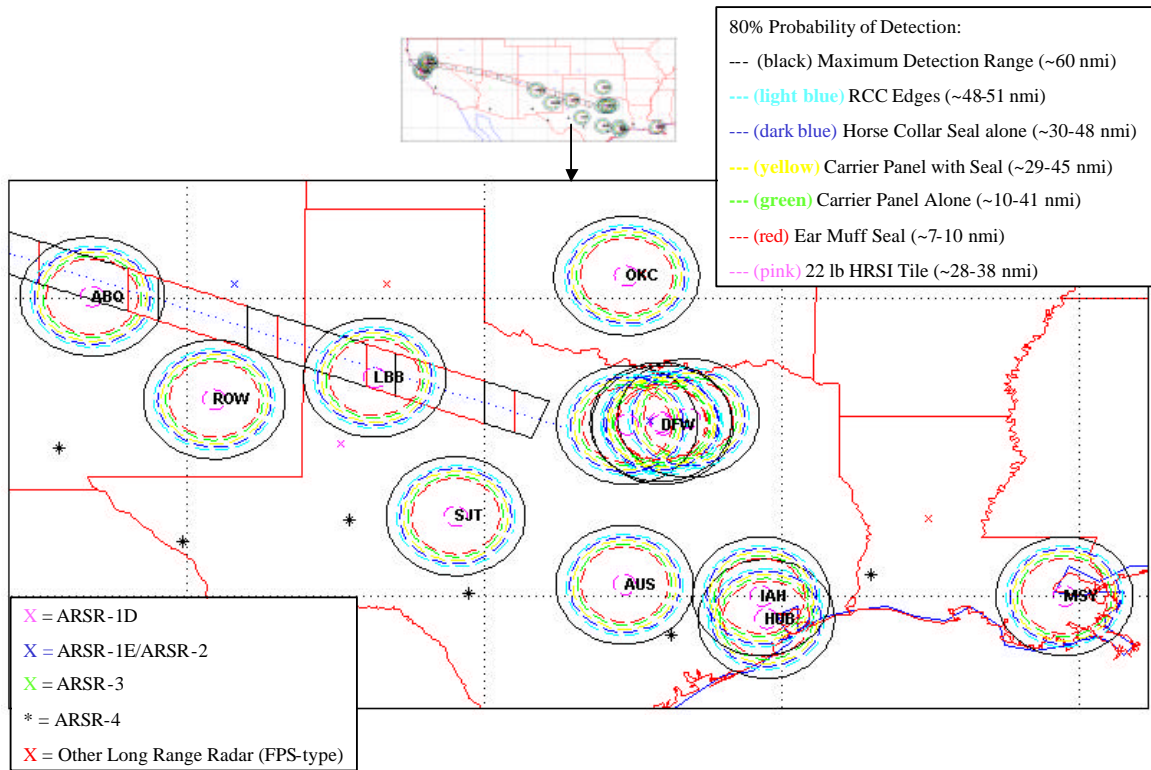


Figure 5-25: New Mexico and Texas Short Range Radar (ASR-9) Detection Ranges for Orbiter External Materials

This leaves the much larger trajectory based footprints as the most reliable predictions for pre-breakup debris ground impact, although they are too large to effectively search for debris. Radar tracks could not be ruled out altogether as returns from Columbia debris, but the associated search areas were prioritized based on their proximity to the non-lifting and lifting footprints for each debris shedding event.

Figure 5-26 shows the combined footprints for all debris shedding captured in public video. The upper plot shows the footprints, and the lower plot highlights the areas where the non-lifting footprints overlap. Of the ballistic footprints, these overlap areas are considered the highest probability areas in which to find pre-breakup Columbia debris.

Figures 5-27 through 5-29 show several of the radar based search boxes mapped with the higher probability overlap areas. Each of the radar search boxes was further prioritized based on the proximity to these overlap areas. As already described, this was then combined with witness reports and probability of detecting Orbiter materials on the given radar, resulting in the prioritized lists in Tables 5-1 and 5-2.

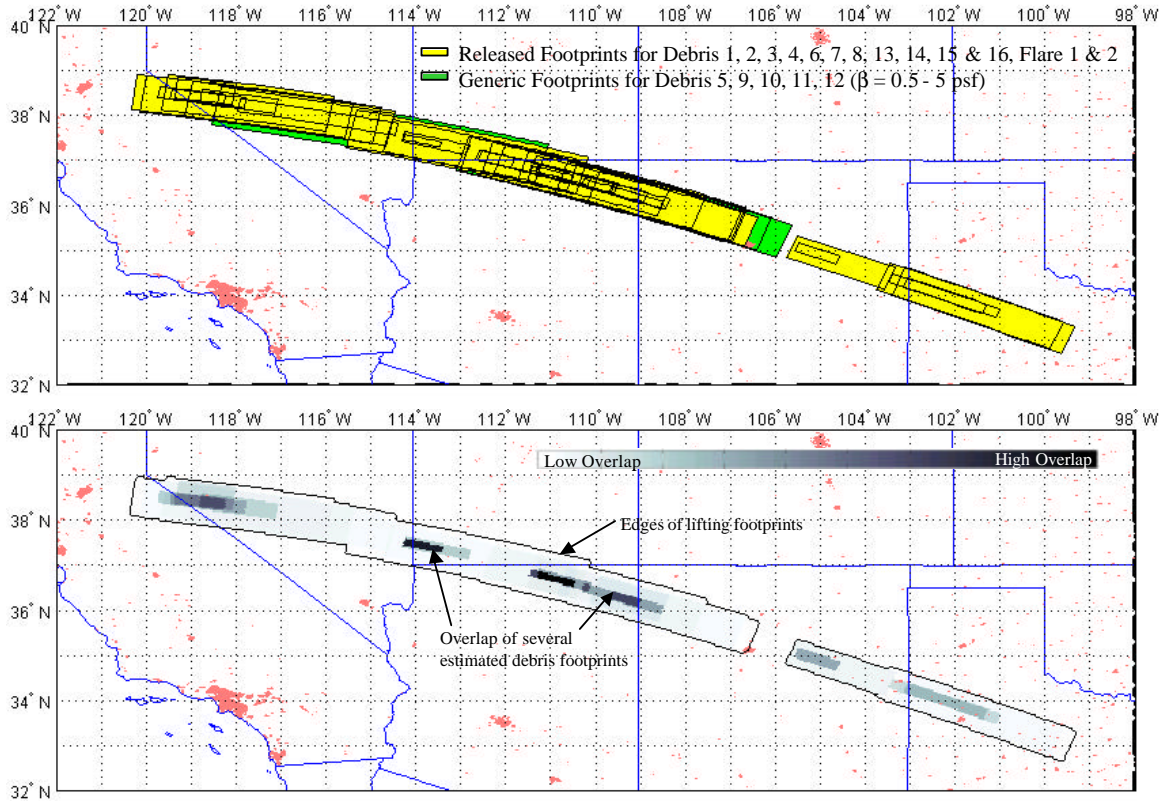


Figure 5-26: Combined Overlapping Ground Impact Footprints of Observed Debris 1 through 16

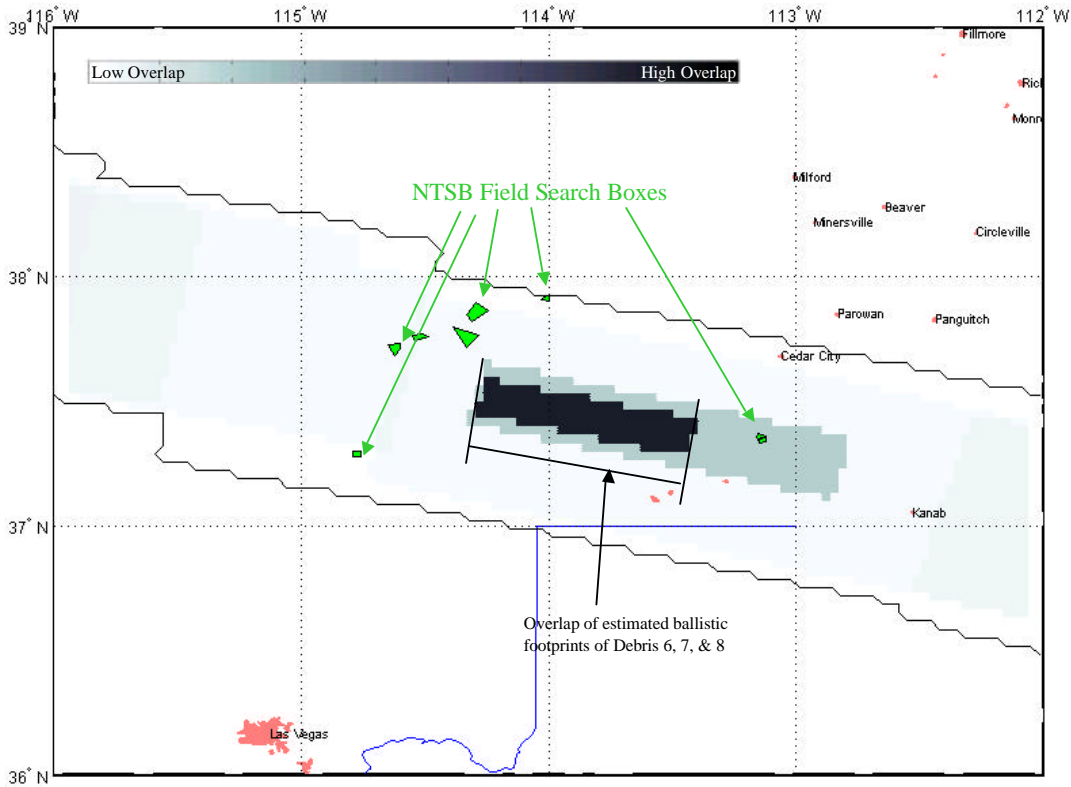


Figure 5-27: Overlap of estimated ballistic footprints of Debris 6, 7, and 8

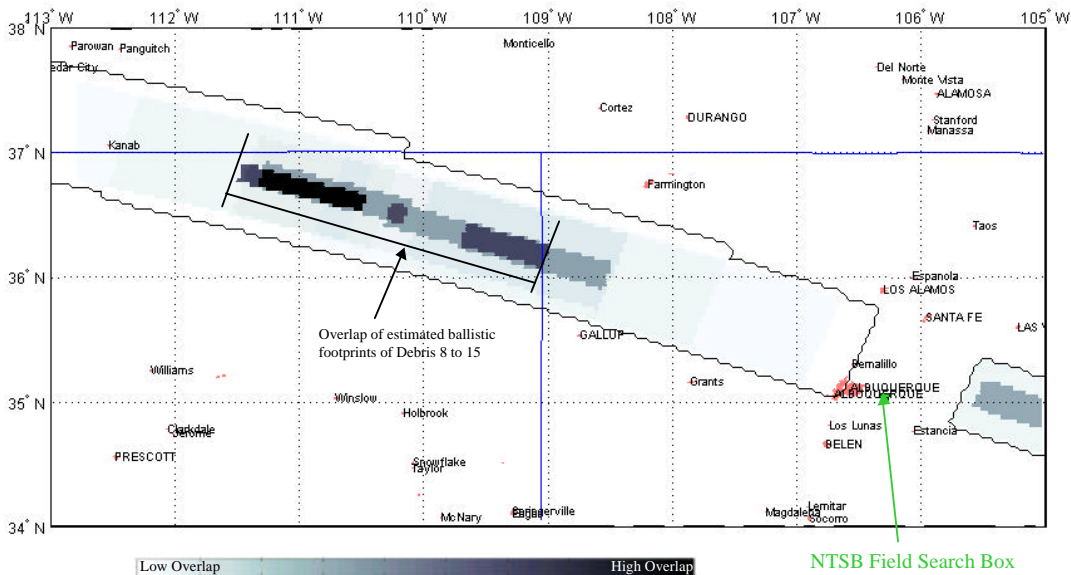


Figure 5-28: Overlap of estimated ballistic footprints of Debris 8 through 15

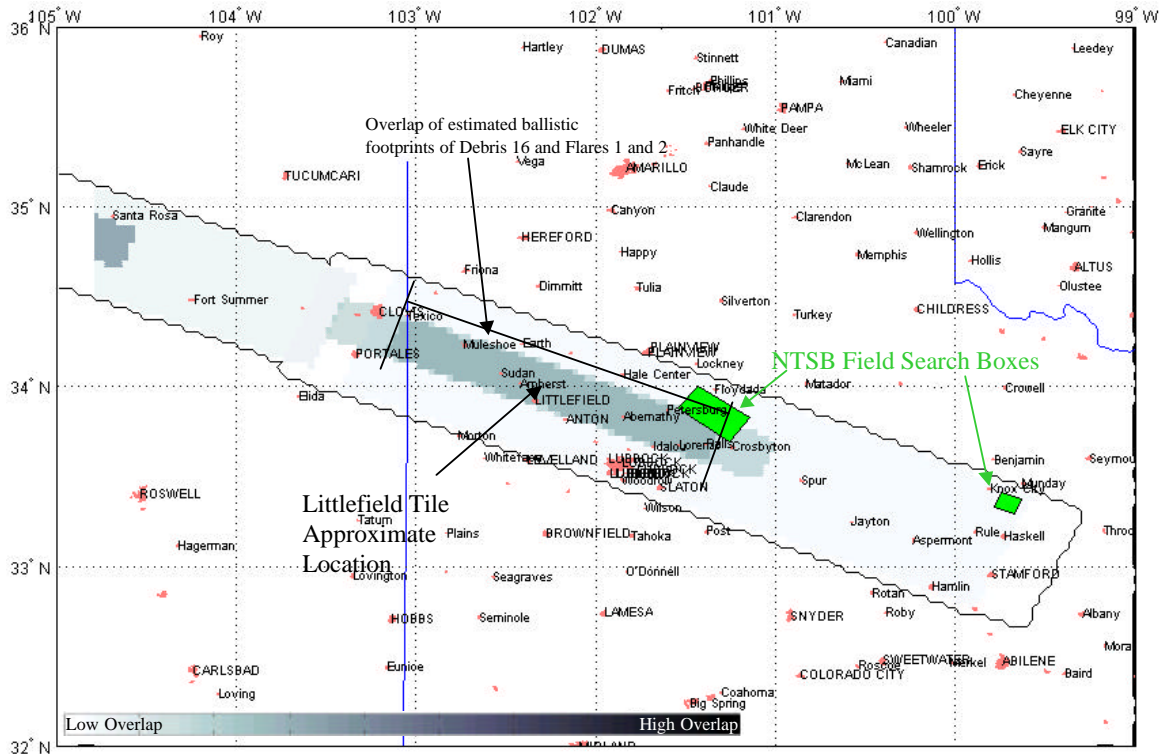


Figure 5-29: Overlap of estimated ballistic footprints of Debris 16, Flares 1 and 2

The ESAT and MIT discussed dropping candidate external Orbiter materials from balloons or aircraft in order to measure radar cross section (RCS) in actual air traffic control radar. Several options were pursued at the conceptual level through AFRL, but ultimately the results still would not have been directly comparable to debris behavior during entry. Initial velocities could not have duplicated the velocities at the altitude of debris that was shed at greater than 12,000 mph, still traveling over 200 mph at 80,000 feet. Ultimately, it was concluded that the AFRL radar test results sufficed.

As described in Section 6.4, AFRL also tested external Orbiter materials for the C-band radars which track during ascent. The C-band radar tests were added to investigate the ability to track debris during ascent, with a primary goal of quantifying the likelihood of discriminating Shuttle debris in the ascent plume and the ability to track the most likely Shuttle debris with the C-bands in general. These tests resulted in detection ranges similar to those shown above for the air traffic control radars.

The C-band data is separated into time slices that correspond with operator initiated changes to the radar characteristics. During launch, the C-band radars are manually adjusted (power/sensitivity/etc.) to optimize tracking performance. These different radar configurations

result in changes to the detection threshold. An example for each C-band radar is shown below, but the full data set is not shown in this report since they are not used for early debris sightings.

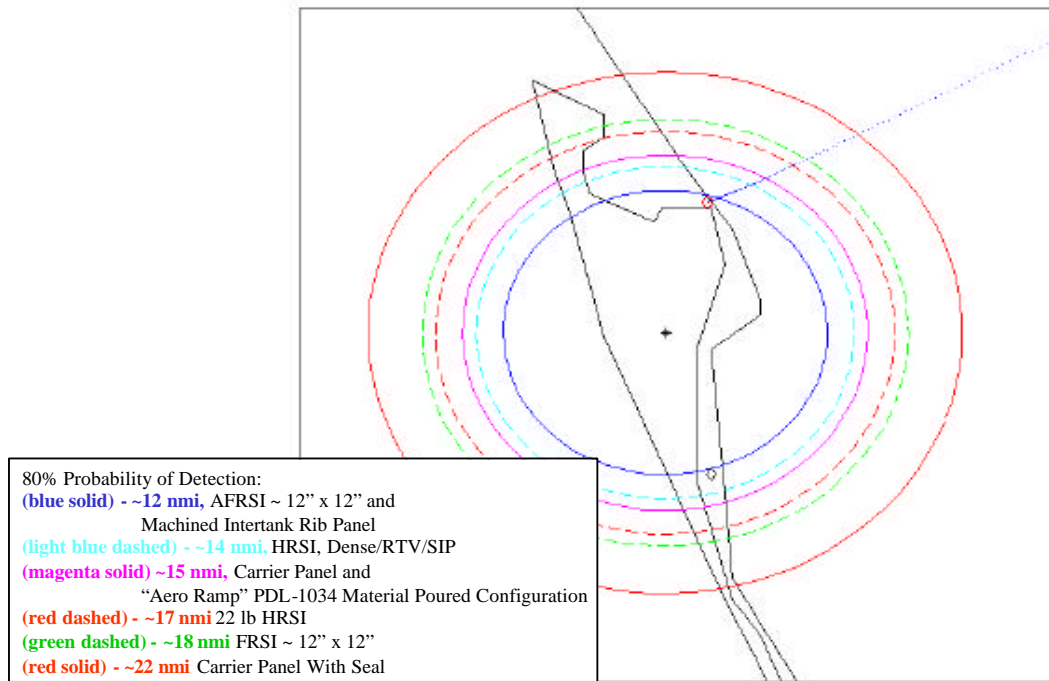


Figure 5-30: Patrick C-Band Radar 19.14, T +20 – 85 sec

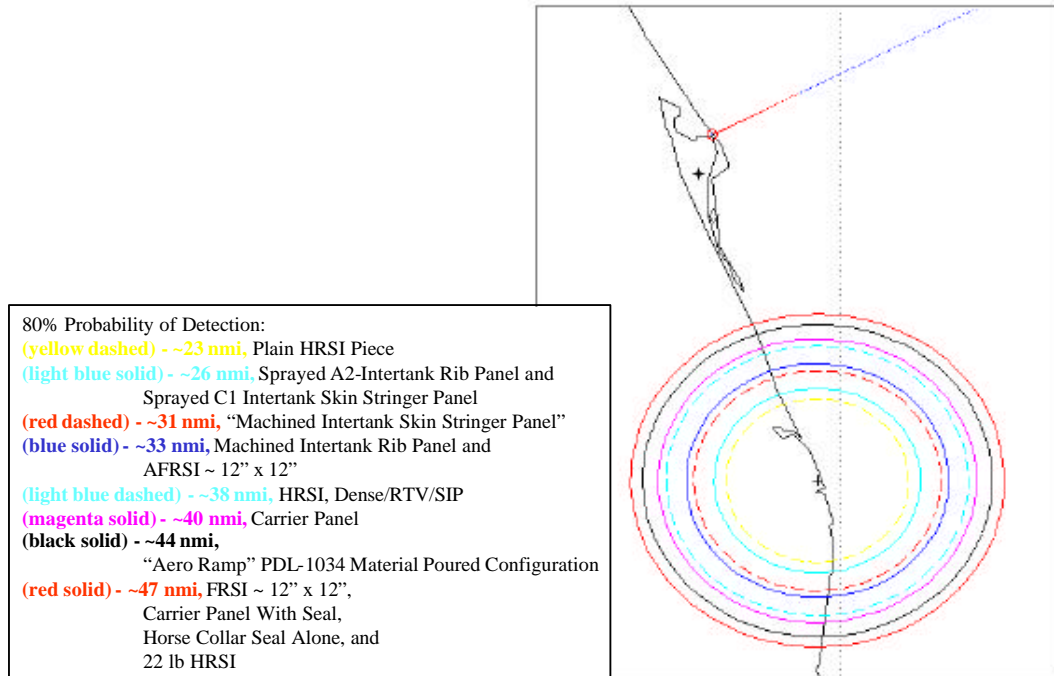


Figure 5-31: Patrick C-Band Radar 0.14, T +31– 120 sec



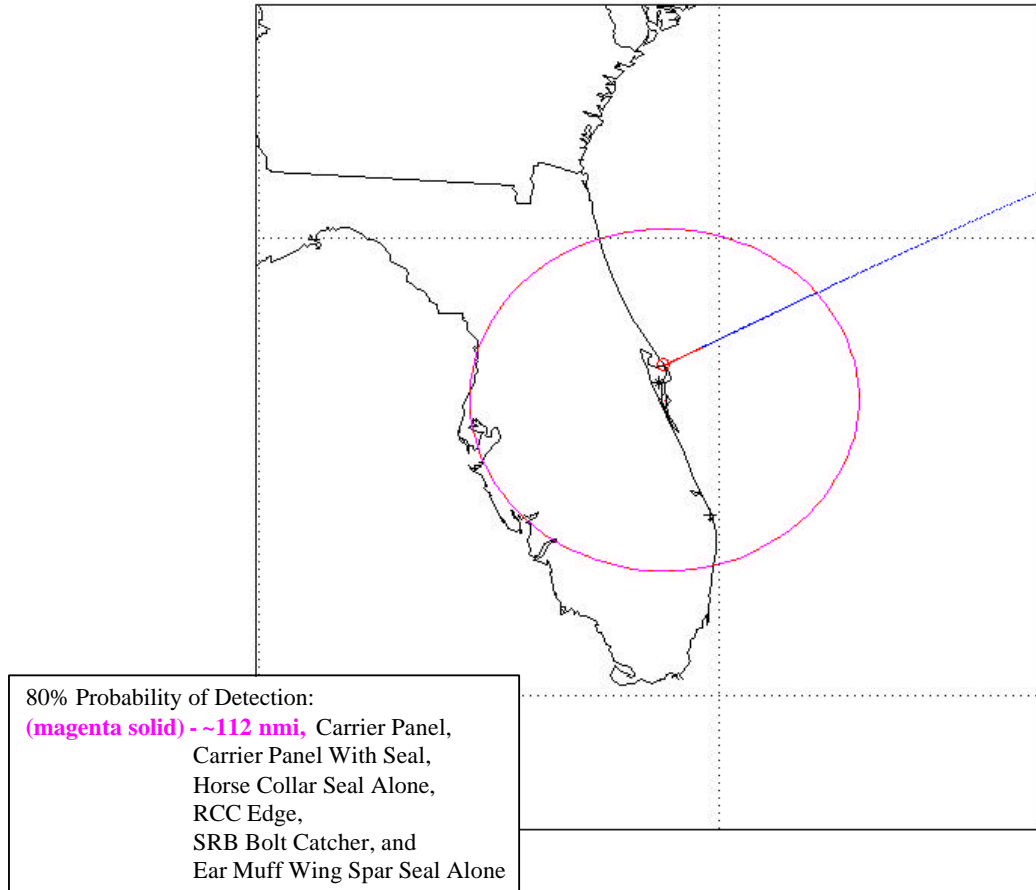


Figure 5-32: Patrick C-Band Radar 28.14, T+0 – 121 sec

### **5.6. Radar Search Areas Lessons Learned**

- 1) Focus energy looking for localized “blob” tracks vice linear radar tracks.
- 2) Focus the search for tracks closer to the groundtrack within the non-lifting footprint.
- 3) Integrate eye-witness reports into radar search as early as possible.
- 4) Station NASA Radar Assessment Team representative at the field operations center for debris searches to help coordinate search box data and act as primary liaison between the RAT and MIT/Search Coordinators.
- 5) Conduct daily telecons with NTSB/FAA/RADES to discuss radar tracks, search boxes, etc.

## 6. Witness Reports

Unless otherwise footnoted, Section 6 is referenced to [53] Schafer, Craig P.; SAIC; Results of Search for Observed Debris Landing Events, and EOC Hotline and Database Lessons Learned for STS-107 Accident Investigation; May 16, 2003. This is included in its entirety in Appendix 10.8.

### 6.1. Witness Report Summary

Eyewitness reports received by the various investigation teams were routed to the ESAT for assessment and prioritization for follow up. Almost 2,000 eyewitness reports were searched for cases where objects were seen falling to earth. This collection of eyewitness reports was searched for citations of observations of objects landing within the generic debris swath that was generated by ballistics analysis.

A hand search was conducted on the ESAT's paper collection of eyewitness reports, and a keyword search of the JSC EOC and Shuttle Interagency Debris Database (SIDDB) electronic databases was performed. These searches focused on eyewitness reports of debris falling to the ground in California, Nevada, Utah, Arizona, New Mexico, and Texas (west of Dallas). Because the SIDDB had over 61,000 entries, an exhaustive search was not possible. However, keywords like "falling," "saw," "ground," and "earth" were used to attempt to identify pertinent reports. The resulting sightings were evaluated and put into three major confidence categories with the following criteria:

- **HIGH:** Eyewitness saw object(s) fall to earth. Event time and place were reasonable relative to Columbia overpass.
- **MED:** Eyewitness saw object(s) fall to earth. The time of the observation was fairly long after Columbia overpass, but not unreasonably so (on the order of an hour).
- **LOW:** Eyewitness observed debris falling in the sky but did not see any landings. Length of time (over an hour) after Columbia overpass or distance from groundtrack was considerable, but the event is not completely ruled out.
- **NONE:** The report was not relevant to this search (ex. sound reports), or the sighting was extremely unlikely to be related to the accident (ex. observing something the day before or after in the sky).

The search yielded two reports of enough confidence to search for radar contact correlations and, in one case, warrant a ground search. The Delamar Lake, NV and Glencoe, CA reports were rated the highest degrees of confidence. These two sightings were coordinated with the Radar Analysis Team to compare with radar contacts. In the Delamar Lake, NV case, the correlation with radar data was strong enough to warrant the dispatch of search teams.

## 6.2. Credible Sightings

### High Confidence Sightings

2-1-1297 (Delamar Lake, NV)

The witness was camping by Delamar Lake, Nevada (about 70 miles north of Las Vegas) on the morning of the accident when he witnessed Columbia pass overhead. At some point during the overpass, he saw a bright flash from the contrail. He heard a boom about two minutes after the overpass. Between two and 10 minutes later, he observed two “twinkles” descend (“drifting down”) into a mountain range between two peaks, and then wink out below the skyline. He thought the objects fell about 10 miles away east or slightly north of east of his campsite, but he did not have a compass or GPS receiver at the time to verify those directions. The sun was still below the horizon at the time of the sighting.

The witness spent two days searching the area he believed the objects fell, but did not find anything. He was confident he could show a NASA search team the exact area he saw the objects fall into. He looked up his campsite location on a map on 2/24/03 and gave the following coordinates: (N 37 deg 19 min 30 sec, W 114 deg 58 min).

His sighting was well within the preliminary lifting footprints of both Debris 1 and Debris 6 as shown in Figures 6-1 and 6-2.

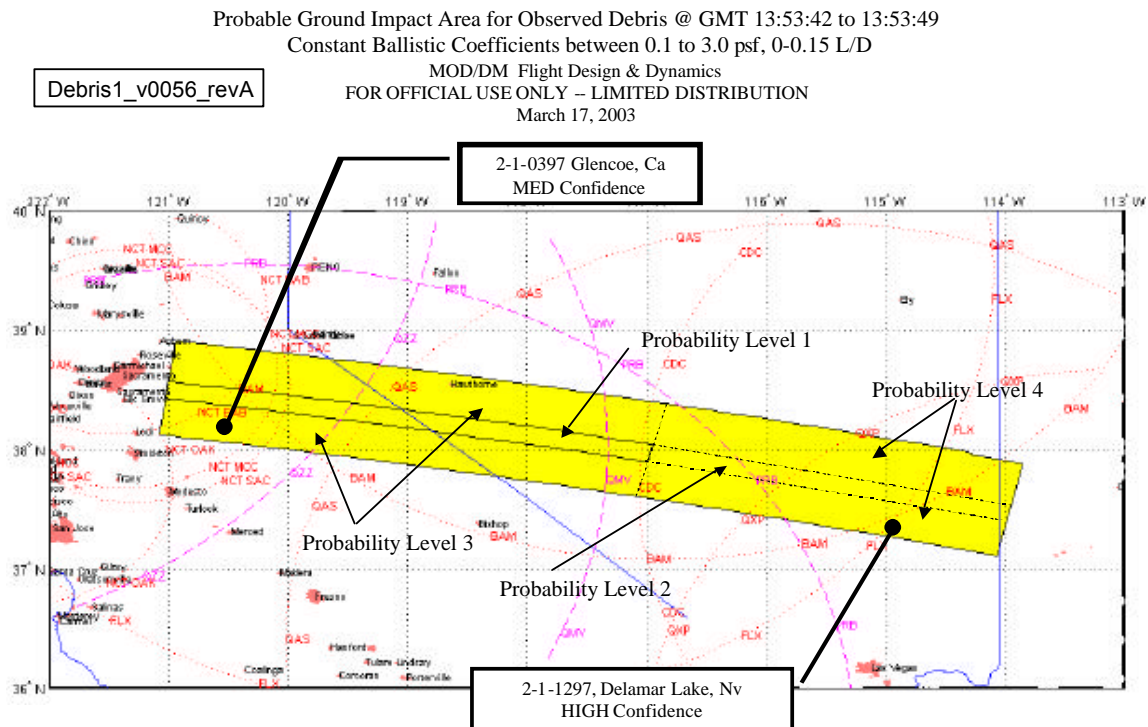


Figure 6-1: Eyewitness Correlations with a Preliminary Debris 1 Footprint

Probable Ground Impact Area for Observed Debris @ GMT 13:54:33.4 to 13:54:34.4  
Constant Ballistic Coefficients between 3.7 to 4.7 psf, 0-0.15 L/D  
MOD/DM Flight Design & Dynamics  
FOR OFFICIAL USE ONLY -- LIMITED DISTRIBUTION  
March 17, 2003

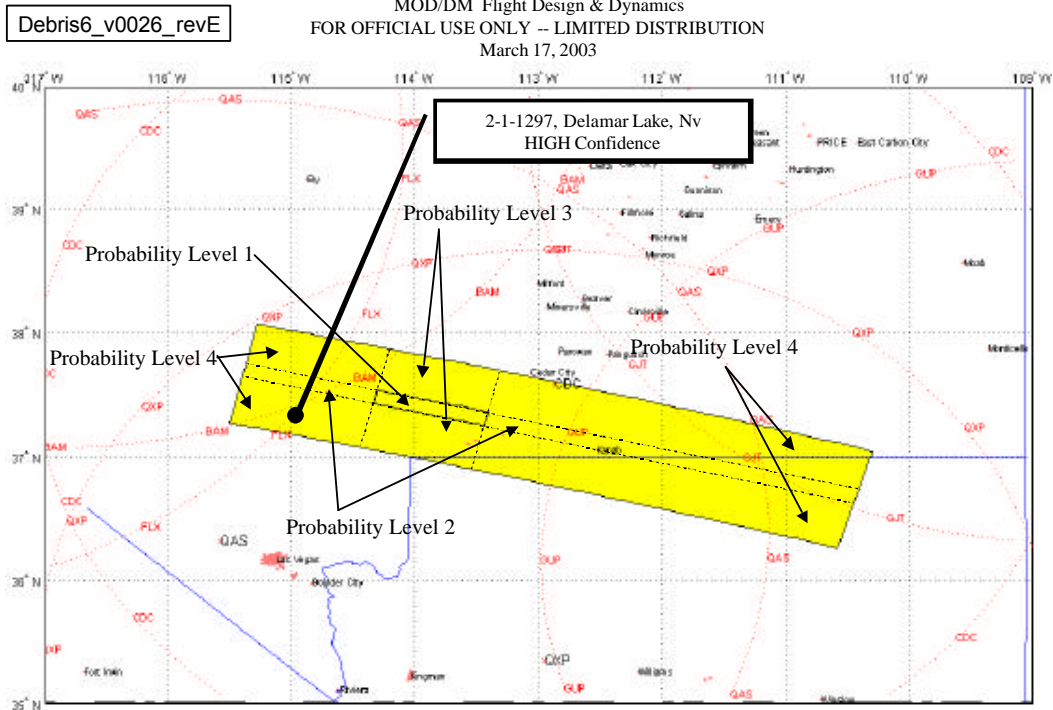


Figure 6-2: Eyewitness Correlations with a Preliminary Debris 6 Footprint

The Delamar Lake sighting is close to the dense overlap area of the ballistic footprints of Debris 6, 7, and 8. This is explained in more detail in Section 5.5, and is shown below in Figure 6-3.

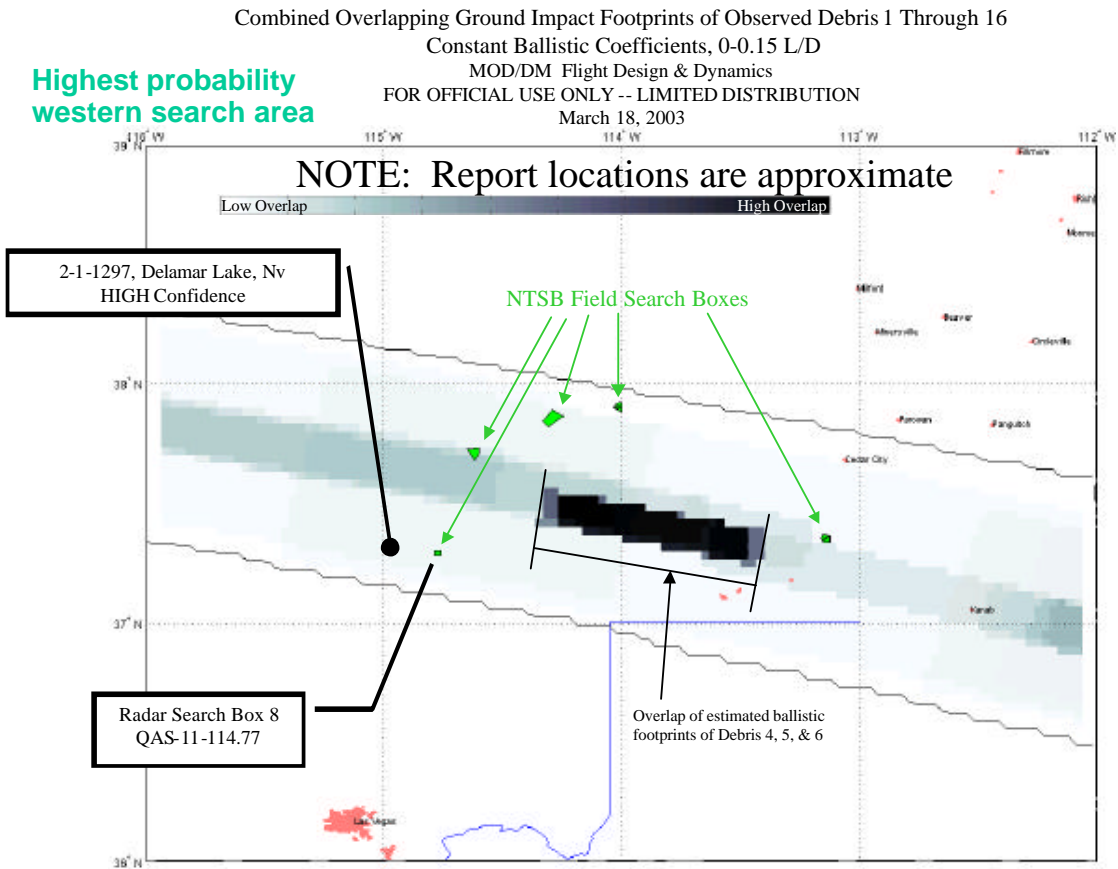


Figure 6-3: Locations of Delamar Lake, NV Campsite, Radar Based Search Box 8 and an Early Version of the Overlap of Estimated Ballistic Footprints of Debris 6, 7, and 8

This sighting is also close to the radar contacts in radar search box 8 as shown in Figure 6-4. Search box 8's location was about 10 miles E-SE of the witness' campsite and within a mile south of where he thought the objects landed.

The Figure 6-4 inset shows a comparison of the area the witness thought the objects fell into (Primary area: blue border, no shading, Secondary area: red border, no shading), and Search Box 8 (red border, yellow shading). Note the black-bordered area is an additional area of interest added by the Debris Recovery Team.

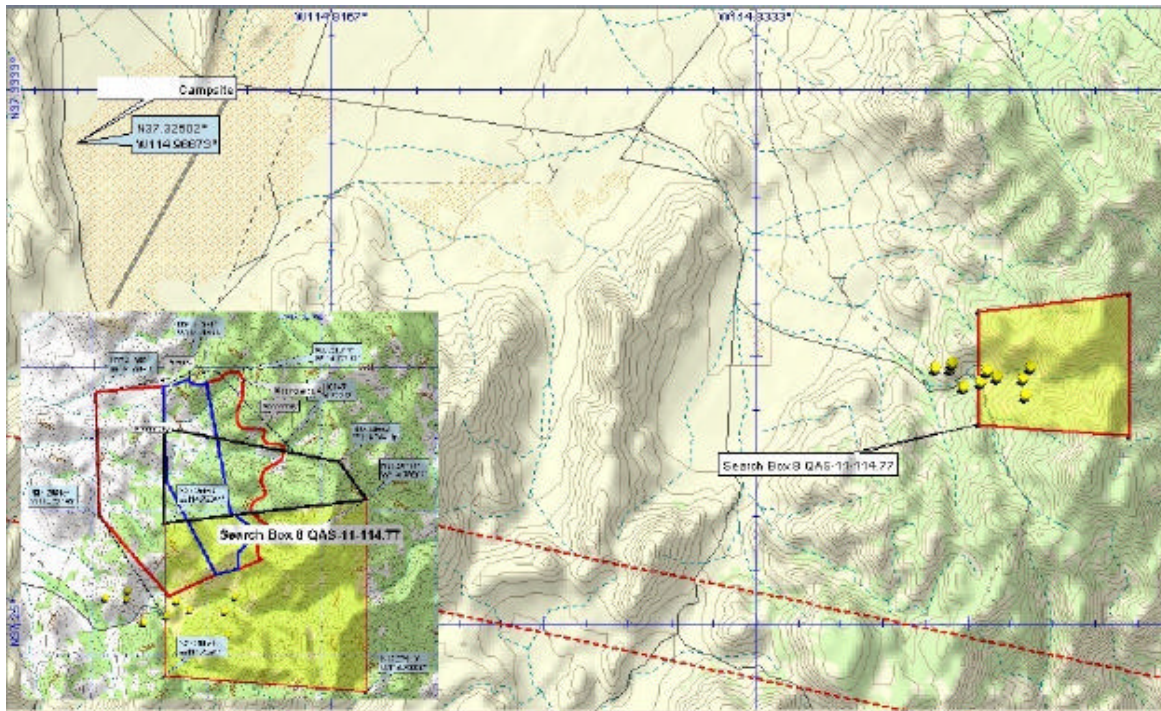


Figure 6-4: Locations of Delamar Lake, NV Campsite and Radar Based Search Box 8  
Inset: Comparison of NTSB Search Box 8 and Search Area Outlined by Eyewitness

The times of the radar contacts in Search Box 8 were found to be at about the same time as the Delamar Lake sighting. It was therefore concluded that there was a strong spatial and temporal correlation between the radar contacts in Search Box 8 and the witness' sighting. A summary report was written on the case and passed on to the California/Nevada/Utah Debris Recovery Team, which made arrangements to search the area.

### MED Confidence Sightings

2-1-0397 (Glencoe, CA)

The witness reported seeing a glowing object falling very quickly down into the Calaveras River canyon area, south of his home on the morning of Columbia's entry. Upon describing the plasma trail, he said that was not what he saw, but rather the object looked like a "shooting star" descending quickly into the canyon area. The map he drew showed the object falling about two miles south from his home, which was still well within the southern lifting footprint of Debris 1. Figure 6-1 plots the witness' approximate location relative to the preliminary Debris 1 footprint.

There were two groups of radar contacts near the area. One single contact was within a mile of where the witness may have seen an object fall, and a cluster farther to the south.

Significant doubt is cast on this report being related to Columbia because the witness' observation was about an hour after Columbia's overpass, and there are about 36 minutes between the approximate time of his observation and the time of the radar contact. The Radar DA8/P. S. Hill

Analysis Team is continuing to investigate the disagreement between the observation and the radar contact and search through radar data, so this incident remains categorized as MED confidence.

#### LOW Confidence Reports

There were numerous reports between California and Western Texas from people seeing debris shedding from the main plasma trail and falling away, or seeing objects falling in the sky. Reports that indicated seeing objects falling but not landing were considered LOW Confidence. Some telephone interviews were conducted to collect additional information on these sightings. In the end, these reports did not add any new information other than confirming debris shedding from Columbia. There is a single report that should be noted because it was particularly unusual. Its details are below.

#### 2-1-2414 (Roswell, NM)

The witness became aware of Columbia's fate about two hours after main breakup. He went outside to see if he could see anything. Looking east, he observed an object slowly 'tumbling' down at an unknown but far distance away. The object would flash then grow dark, which gave him the idea it was tumbling much the way, as he put it, a metal sheet would tumble from high in the sky. He thought it must have been something sizeable to be able to see the tumbling effect. He went inside to get his binoculars to get a closer look. By the time he was outside again, the object had fallen into the sun disc, making observation with the binoculars impossible. He thought the object traveled eastward and downward during his observation. No correlating radar contacts have been found.

This report was interesting because the object was described as a large sheet tumbling out of the sky, which is an unusual occurrence at any time. However, the time between this sighting and Columbia's overpass is quite long, and the object could have been 30 miles or more south of the generic, lifting footprint. Thus, confidence is low that the object is related to Columbia.

#### NONE Reports (No Confidence)

There were also a large number of reports of hearing one or more 'booms' and seeing the plasma trail. These reports were of some use in the early days of the investigation to determine Columbia was seen and heard as far back as northern California, but no more technical information was gained from them. Once it was clear that public imagery was available with near continuous coverage, these reports were of anecdotal use only. People also reported seeing fast moving and/or falling objects days before and after the accident, which could not be reasonably attributed to Columbia's reentry.



### **6.3. Witness Reports Lessons Learned**

NASA should consider developing a method of educating the public on how best to record future reentries so that, if such a mishap ever occurs again, the video would more easily facilitate post-flight analysis. This would include all important imagery characteristics and supporting data which are key to the analysis.

## 7. DOD Data

The DOD Columbia Investigation Support Team (DCIST) was formed to provide a single point of contact to NASA for all DOD sensor support. Through the DCIST, the DOD collected and analyzed all remote sensor data related to STS-107 which included deep space tracking radar, early warning radar, air traffic control radar, telescopes and infrasound. The DCIST impounded all sensor site data immediately to preserve the ability to reprocess and analyze all data.

NASA requested DOD data per the following priorities, in order from highest to lowest [7]:

- 1) Process all data from 1340Z -1400Z for high-energy events (include any luminosity and spectral analysis which may indicate size, mass and constituents). Key events to focus on:
  - Discrete debris shedding times.
  - Times associated with off-nominal telemetry signatures.
  - Times indicated as off nominal in infrasonic data (infrasonic data collection in work separately).
  - Bolide detonation reported from Oceanside, CA 1300-1410Z.
- 2) Process all data from Beale Pave Paws.
- 3) Confirm any and all imagery from 1 Feb 1340-1400Z has been identified, processed and received.
- 4) All data from de-orbit burn through break-up.
- 5) Process the object that has been correlated back to Columbia approx 24 hrs after launch (Flight Day 2 Object).
- 6) Provide trajectory data to all other national agency/organizations so they can check for related data.
- 7) Confirm any and all imagery from Ascent-2 Feb, 1340Z has been identified, processed and received.
- 8) Any “unexpected events” DoD might identify throughout duration of mission via own analysis.

### 7.1. Remote Sensors During Entry

In the first two weeks of the investigation, there were preliminary indications in various unclassified and classified sensors of some anomalous events during entry. In all cases, the data required considerable post-processing for analysis, and in many cases required detailed comparison to previous flight data to confirm the specific phenomena was anomalous and had not been observed during other flights. The early reports are summarized by a generic statement authorized for release by Air Force Space Command on February 24 for all such data:

Department of Defense systems received indications of unusual Columbia mission activity at [DTG]. These indicators imply possible [debris shedding/structural flaw/object impact/increased heating/anomalous flight condition] at that time. [8]

By April 8, all preliminary indications by remote sensors during entry were either attributable to some known and nominal Orbiter entry related event or were considered indistinguishable from the background indications for the given sensor. [10] The following table lists the significant remote sensor events which were considered for the STS-107 Entry Timeline.

<b>Date/Time</b>	<b>Historical or Unique?</b>	<b>Cause Known / Unknown?</b>	<b>Comments</b>
16 Jan 15:56:22-16:01:10	Historical	Unknown	
1 Feb 13:52:19-14:10:08	Historical	Unknown	Location: 13:51:20 Initially labeled as remote sensor event 1
1 Feb 13:52:30	Historical	Known	
1 Feb 13:56:32-14:05:34	Historical	Unknown	Location: 13:55:30 Initially labeled as remote sensor event 2
1 Feb 13:56:28	Historical	Known	
1 Feb 13:56:53	Historical	Known	

Table 7-1: DOD Remote Sensor Indications during STS-107 Entry [9]

In fact, several interim versions of the timeline included “remote sensor events 1 and 2” at 13:52:30 and 13:55:30Z respectively based on initially high confidence by the sensor experts. However, as explained above, these too were better understood after more lengthy analysis and later determined to be explainable or inconclusive. In the final assessment, there are no reliable indications of debris shedding or other anomalous pre-break up phenomena in any DOD remote sensor data. [10]

## 7.2. Imagery: AMOS, Kirtland AFB

Columbia was imaged during 3 days of STS-107 orbit operations by the Air Force Maui Optical & Supercomputing (AMOS) Site. Columbia was also imaged during entry by employees of the Starfire Optical Range at Kirtland AFB, NM, although these images were not through the DOD optics.

These AMOS and Kirtland images are the only DOD images taken of Columbia during STS-107 from any source, unclassified or classified.

AMOS captured visible images on January 17, 22, and 28, and infrared images on January 28. These are predominantly of the upper surfaces with payload bay doors open, obscuring a significant portion of the wings. A few of the visible and infrared frames are from the front of the vehicle, but the quality or lighting is insufficient to show detail. Examples of the visible image and infrared images are shown below in Figures 6-1 and 6-2. [3][4]

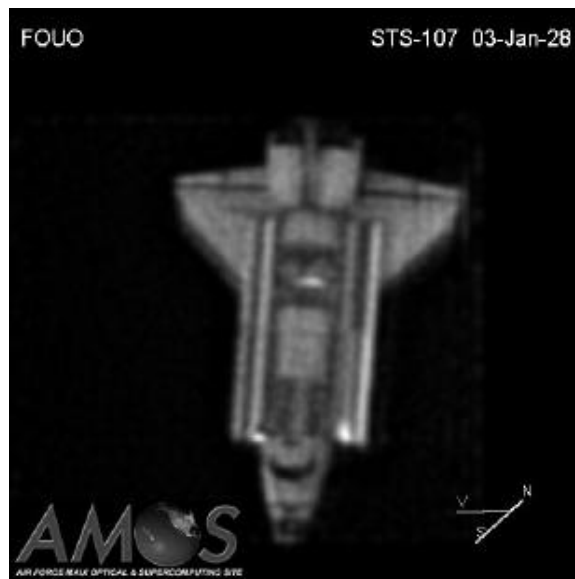


Figure 7-1: Example AMOS Visible Images of Columbia during STS-107 [4]

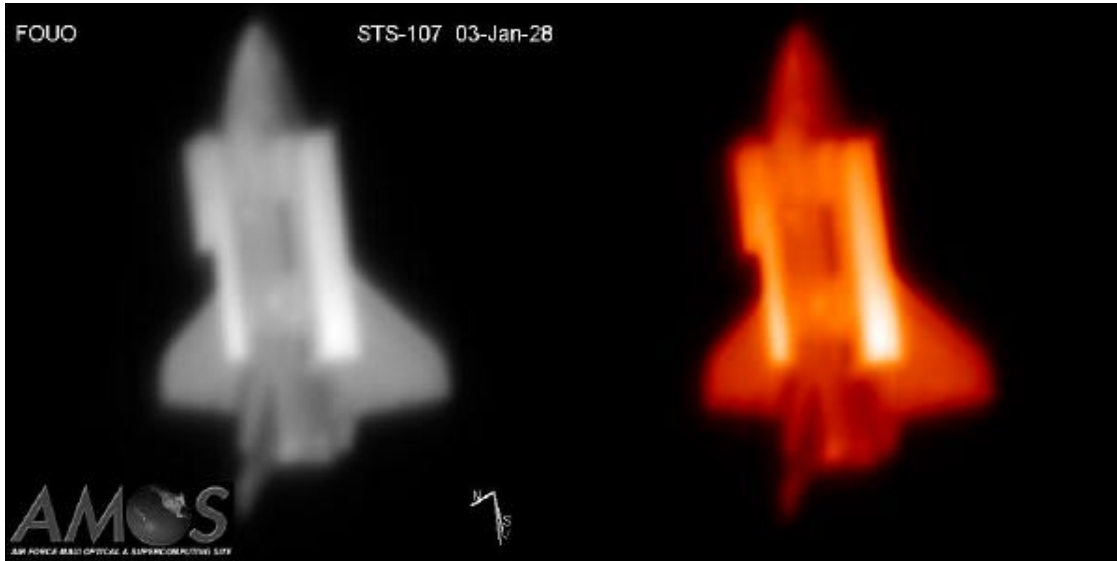


Figure 7-2: Example AMOS IR Images of Columbia during STS-107 [3]

While these images taken from the ground of a manned spacecraft in orbit are fascinating, particularly when individual frames are strung together as a video, they show no discernible damage. The post-processed infrared images and the corresponding thermal mapping shown in Figure 7-3 below suggest that this capability may be valuable on future flights for detecting significant external damage, and this is under study by NASA JSC. To facilitate use of this capability for damage detection on future flights, the Air Force Research Lab (AFRL) has requested detailed material maps of the Orbiters.

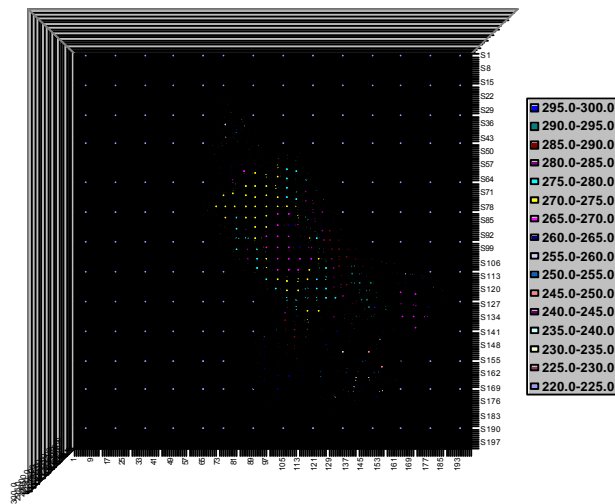


Figure 7-3: Example Thermal Mapping of Columbia Based on AMOS IR Image during STS-107 [3]

A separate NASA tiger team was established under the Orbiter Vehicle Engineering (OVE) Working Group to study the Kirtland images for any data useful to the investigation. All

detailed descriptions and conclusions are therefore deferred to that team. This report includes only representative images and ESAT support to this study.

The images below in Figures 7-4 and 7-5 are representative of three stills and four videos taken by employees of the Starfire Optical Range at Kirtland AFB, New Mexico during STS-107 entry. They are not official DOD images and were taken through personal equipment, not the Starfire optics. Figure 7-4 is the image released to the press that sparked considerable early speculation regarding left wing leading edge damage and asymmetric wake.

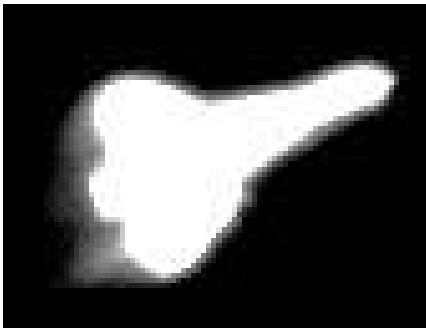


Figure 7-4: Example Raw Still Taken by Starfire Optical Range Employees during STS-107 Entry [5]

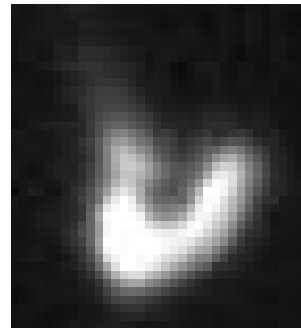


Figure 7-5: Example Frame from Raw Video Taken by Starfire Optical Range Employees during STS-107 Entry [5]

In support of this team's analysis, the ESAT provided Orbiter state vectors, a series of wire frame images of the Orbiter as viewed from Kirtland AFB throughout the pass and coordinated a series of solid model images. These Orbiter images were superimposed over the Kirtland images to help evaluate them for anomalies. Examples are shown in Figure 7-6.

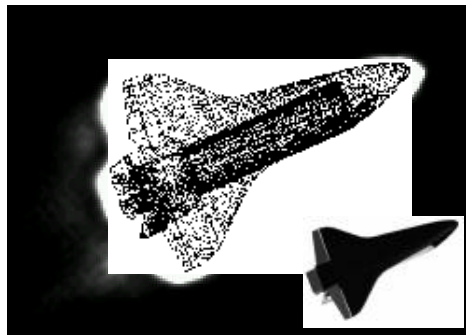


Figure 7-6: Example Orbiter Wire Frame Superimposed over Raw Still Image Taken by Starfire Optical Range Employees during STS-107 Entry and the Associated Solid Model [5]

### 7.3. FD2 Radar Data

A separate NASA tiger team was established under the OVE Working Group to study the Flight Day 2 object for any data useful to the investigation. All detailed descriptions and conclusions are therefore deferred to that team. This report includes only a summary of the radar data and ESAT support to this study.

During a post-flight search, Air Force Space Command discovered anomalies associated with STS-107. Uncorrelated observations from radar data were found in the same orbit as Columbia. Additional observation data was then obtained from four sensors from January 17, 18 and 19. The additional data allowed trajectory reconstruction that indicates an object separated from the Orbiter on January 17, between 1500-1615Z, Flight Day 2 of the STS-107 mission. Preliminary analysis was provided to NASA on February 9. [1]

The DCIST confirmed no other objects were tracked within 5 km of Columbia throughout STS-107.

Several passes of radar cross section versus time data were obtained by a combination of the Cape Cod and Beale UHF phased array radars and the Kwajalein VHF/UHF radar. Data from the Cape Cod passes is shown in Figures 7-7, 8 and 9. Early interpretation of this data suggested a small plate-like, spinning or tumbling object. Orbital behavior indicated a relatively lightweight object which decayed after approximately 60 hours in orbit. [2] It was also pointed out that, “had the SSN been tasked, it could have supplied additional data.” [1] This will be included in a follow on activity to generically review DOD tracking capability for possible changes to routine and contingency tasking on all future Shuttle flights.

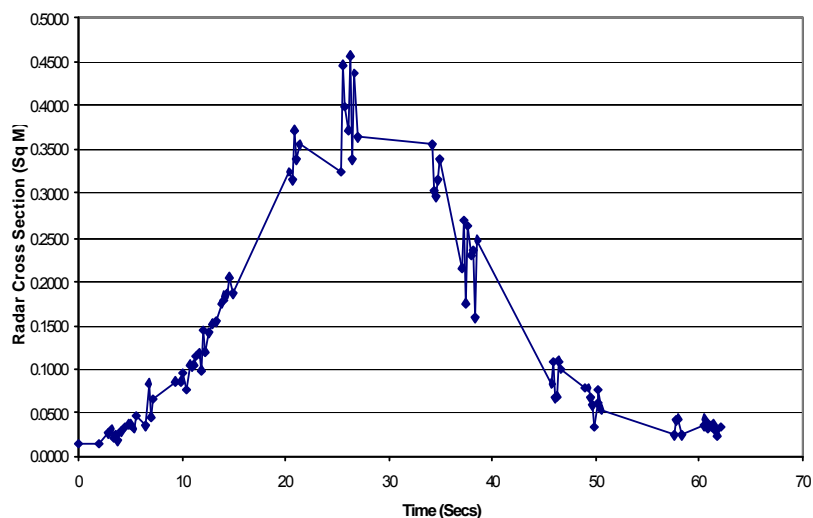


Figure 7-7: Cape Cod Track on January 17, 1857Z [2]

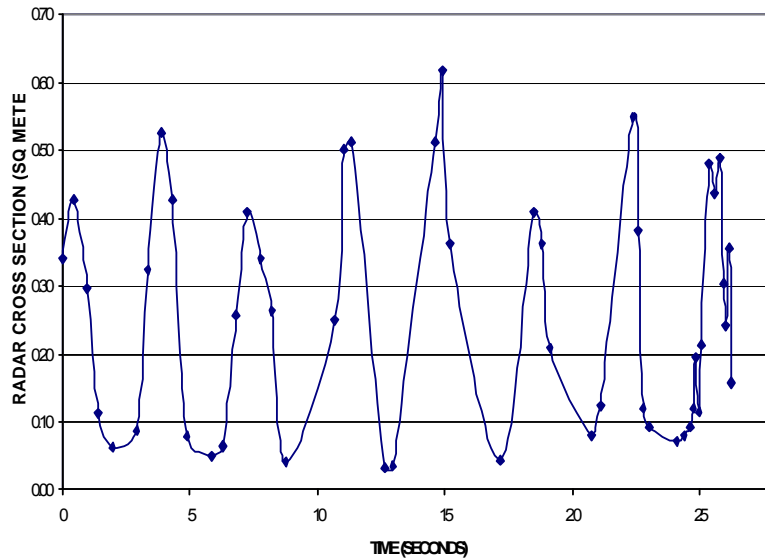


Figure 7-8: Cape Cod Track on January 18, 2029Z [2]

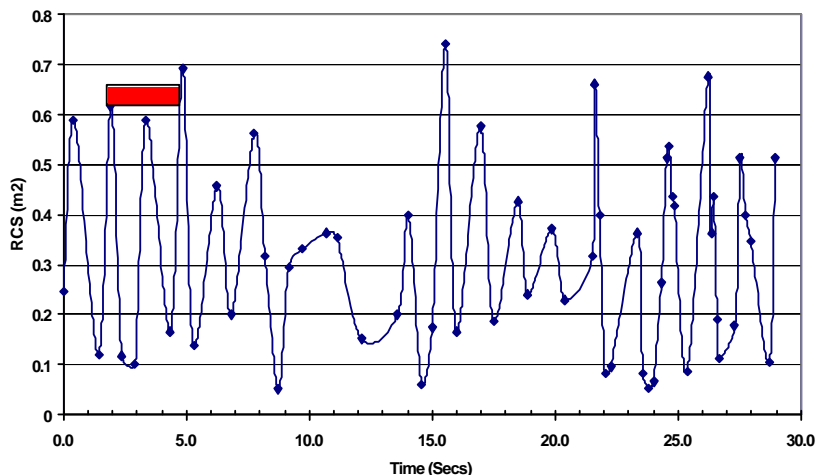


Figure 7-9: Cape Cod Track on January 19, 1539Z [2]

The radar cross section of the object in orbit varied from approximately 0.1 - 0.7 m<sup>2</sup>. The ballistic coefficient of the object in orbit was estimated to be 0.102 m<sup>2</sup>/kg by Air Force Space Command [2] with good agreement by JSC Engineering at 0.09 - 0.11 m<sup>2</sup>/kg. [23]

JSC assembled a list of materials and components from the inside the payload bay and on the exterior of the Orbiter. By February 14, JSC Engineering had sent properties of these materials for correlation to the radar data. The ESAT and DCIST initiated planning for radar tests of these materials by the Air Force Research Lab at Wright-Patterson AFB, OH. This material list included all candidates for an object originating from Columbia during STS-107. (Refer to Section 7.4 Radar Tests for a complete description.)



The goal was to measure radar cross section for each of these materials in various orientations and compare the test data to the radar observation data recorded by Air Force Space Command during the mission. After radar cross sections were compared, Air Force Space Command and JSC compared ballistic coefficients for the test objects and the observed object. The overall goal was to isolate the most likely candidates for this object based on both radar cross section and ballistics.

## 7.4. Radar Tests

C, L, and S-band data annexes were reported to the CAIB and NASA by Air Force Research Laboratory Sensors Directorate on April 24, 2003.

Uncertainty in evaluating the deep space tracking radar data from the Flight Day 2 object led to a series of radar tests at Wright-Patterson AFB, OH for materials and components inside the payload bay and on the exterior of the Orbiter. These tests were tuned to the specific radars that recorded observations of this object with a goal to compare the test data to the radar observation data recorded by Air Force Space Command during the mission.

On March 7, these tests were expanded for the external materials and components to include the C-band radars which track during ascent and the air traffic control radars which are flown over during entry. The C-band radar tests were added to investigate the ability to track debris during ascent, with a primary goal of quantifying the likelihood of discriminating Shuttle debris in the ascent plume and the ability to track the most likely Shuttle debris with the C-bands in general. L-band and S-band air traffic control radars were added to quantify the ability to for these radars to have detected the most likely Orbiter debris during entry over the CONUS.

The goal was to measure radar cross section (RCS) for each of these materials and components in various orientations and compare the test data to the radar observation data during the mission. Ideally, this would reduce the candidate list for the Flight Day 2 object and provide a reasonableness check for the entry debris radar searches described in Section 5.

Items from the exterior of the Orbiter included: thermal blankets (FRSI, AFRSI) and heat tiles (HRSI). Items from the Orbiter wing leading edge included: Reinforced Carbon-Carbon (RCC) panel, ear muff, carrier panel with horse collar seal and an RCC T-seal. Items from inside the payload bay included: thermal blankets (beta cloth), thermal blankets (aluminized), and beta cloth logo panels. These are shown in Figures 7-10, 11, 12 and 13. [11]

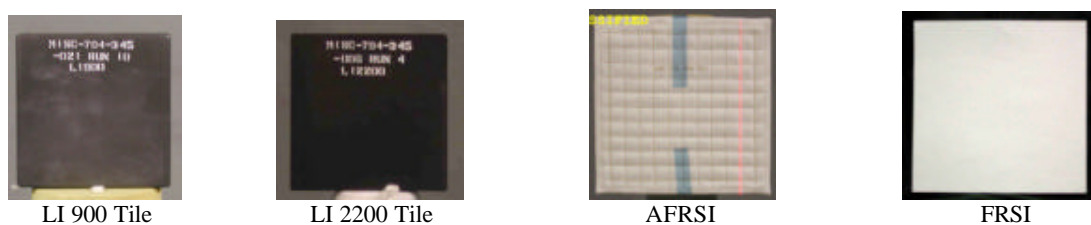


Figure 7-10: External Thermal Protection System Constituent Materials [11]



Carrier Panel Segment



Carrier Panel Segment with Horse Collar



Horse Collar



3 and 4 Tile Carrier Panels with Horse Collar



Figure 7-11: Carrier Panel Combinations [11]



RCC Leading Edge Panel



RCC T-Seal



Incoflex "Ear Muff"

Figure 7-12: Wing Leading Edge Components [11]

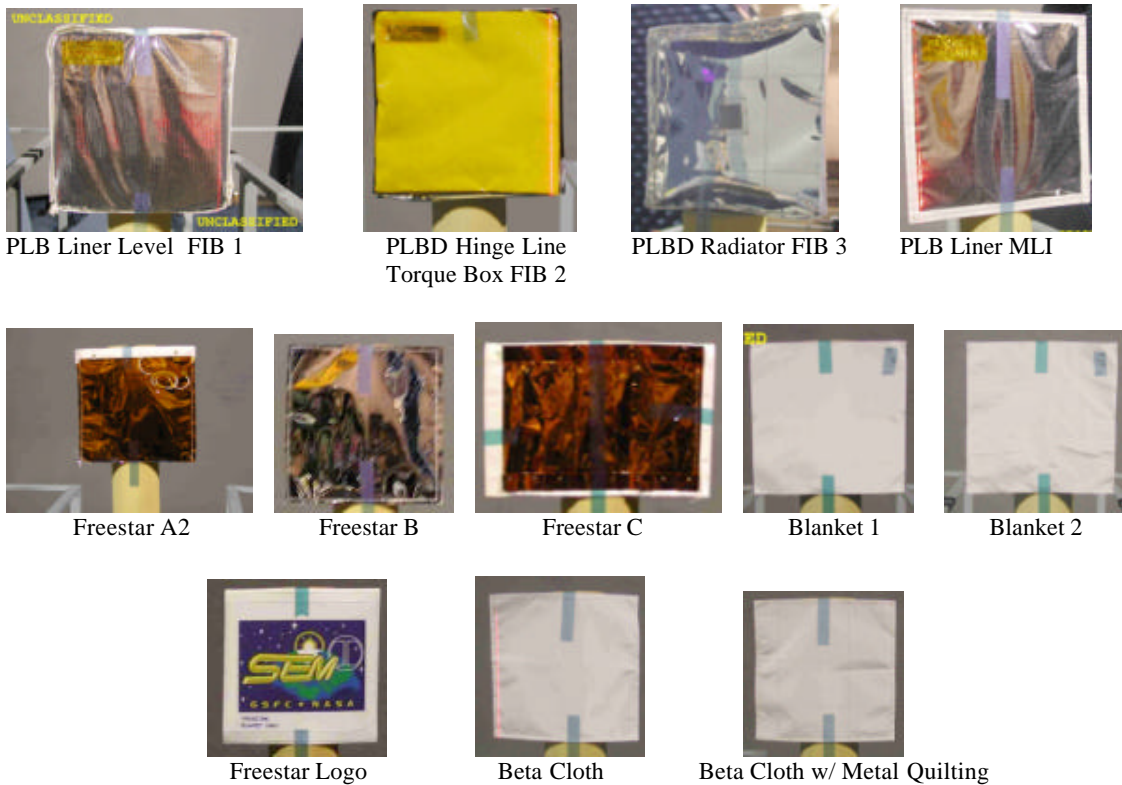


Figure 7-13: Payload Bay and Payload Insulation Materials [11]

Similar items were identified informally as generic ascent debris candidates from the Shuttle External Tank (ET) and Solid Rocket Boosters (SRB). These components were also tested by AFRL for C-band radar frequencies. For the ET, these include: Aero Ramp PDL-1034; Intertank Skin Stringer Panel; Intertank Rib Panel; Intertank/LH2 Flange Divot simulator; A2-Intertank Rib Panel; C1 Intertank Skin Stringer Panel. For the SRB, these include: Solid Rocket Motor Booster Bolt Catcher; and Solid Rocket Motor Booster Bolt Catcher insulation.

Ultimately, AFRL tested thirty-eight different materials and combinations of wing leading edge components. [12] Table 7-2 summarizes the materials, combinations of leading edge components and the radar frequencies tested.

AFRL Part #	NASA Part Description	RCS Test Data Acquired						RCS Test Data Reported					
		VV		HH		Ascent		VV		HH		Ascent	
		On-Orbit	On-Orbit	Descent	Descent	Ascent	Wideband	On-Orbit	On-Orbit	Descent	Descent	Ascent	Wideband
		UHF	UHF	L	S	C	1-6 GHz	UHF	UHF	L	S	C	1-6 GHz
		433 MHz	433 MHz	1.2-1.4 GHz	2.7-2.9 GHz	5.68-5.7 GHz		433 MHz	433 MHz	1.2-1.4 GHz	2.7-2.9 GHz	5.68-5.7 GHz	1-6 GHz
1	AFRSI(Fibrous) 12" x 12	Y	Y	Y	Y	Y	Y	Y	Y	Y	Y	Y	Y
2	FRSI 12" x 12"	Y	Y	Y	Y	Y	Y	Y	Y	Y	Y	Y	Y
3	HRSI (No Backing)	Y	Y	Y	Y	Y	Y	Y	Y	Y	Y	Y	Y
4	HRSI (Dense/RTV/SIP)	Y	Y	Y	Y	Y	Y	Y	Y	Y	Y	Y	Y
5	"Fibrous 001"	Y	Y	N/A	N/A	N/A	N/A	Y	Y	N/A	N/A	N/A	N/A
6	"Fibrous 002"	Y	Y	N/A	N/A	N/A	N/A	Y	Y	N/A	N/A	N/A	N/A
7	"Fibrous 003"	Y	Y	N/A	N/A	N/A	N/A	Y	Y	N/A	N/A	N/A	N/A
8	Beta Cloth (No Conductive Quilt Thread)	Y	Y	N/A	N/A	N/A	N/A	Y	Y	N/A	N/A	N/A	N/A
9	Beta Cloth (Conductive Quilt Thread)	Y	Y	N/A	N/A	N/A	N/A	Y	Y	N/A	N/A	N/A	N/A
10	MLI 004 13" x 13" Piece	Y	Y	N/A	N/A	N/A	N/A	Y	Y	N/A	N/A	N/A	N/A
11	"Freestar panel a2"	Y	Y	N/A	N/A	N/A	N/A	Y	Y	N/A	N/A	N/A	N/A
12	"Freestar panel b"	Y	Y	N/A	N/A	N/A	N/A	Y	Y	N/A	N/A	N/A	N/A
13	"Freestar panel c"	Y	Y	N/A	N/A	N/A	N/A	Y	Y	N/A	N/A	N/A	N/A
14	"Freestar panel logo piece"	Y	Y	N/A	N/A	N/A	N/A	Y	Y	N/A	N/A	N/A	N/A
15	"Insulation Blanket Sample 1"	Y	Y	N/A	N/A	N/A	N/A	Y	Y	N/A	N/A	N/A	N/A
16	"Insulation Blanket Sample 2"	Y	Y	N/A	N/A	N/A	N/A	Y	Y	N/A	N/A	N/A	N/A
17	Aero Ramp" PDL-1034	N/A	N/A	N/A	N/A	Y	N/A	N/A	N/A	N/A	N/A	Y	N/A
18	Intertank Skin Stringer Panel"	N/A	N/A	N/A	N/A	Y	N/A	N/A	N/A	N/A	N/A	Y	N/A
19	"Intertank Rib Panel"	N/A	N/A	N/A	N/A	Y	N/A	N/A	N/A	N/A	N/A	Y	N/A
20	"Intertank/LH2 Flange Divot Simulation"	N/A	N/A	N/A	N/A	Y	N/A	N/A	N/A	N/A	N/A	Y	N/A
21	"A2-Intertank Rib Panel"	N/A	N/A	N/A	N/A	Y	N/A	N/A	N/A	N/A	N/A	Y	N/A
22	"C1 Intertank Skin Stringer Panel",	N/A	N/A	N/A	N/A	Y	N/A	N/A	N/A	N/A	N/A	Y	N/A
23	"Carrier Panel" section by itself - Rcvd 3/17/03	Y	Y	Y	Y	Y	Y	Y	Y	Y	Y	Y	Y
24	"Carrier Panel" with "Horse-shoe" seal installed	Y	Y	Y	Y	Y	Y	Y	Y	Y	Y	Y	AT
25	"Horse Shoe Seal"	Y	Y	Y	Y	Y	Y	Y	Y	Y	Y	Y	AT
26	RCC Edge Flight Spare from Columbia	Y	Y	Y	Y	Y	Y	Y	Y	Y	Y	Y	Y
27	Recovered STS-107 RCC Component	N/A	N/A	N/A	N/A	N/A	N/A	N/A	N/A	N/A	N/A	N/A	N/A
28	Highly Densified Shuttle tile 6"x6"x1.5"	Y	Y	Y	Y	Y	Y	Y	Y	AT	AT	AT	AT
29	Solid Rocket Motor Booster Bolt Catcher	N/A	N/A	N/A	N/A	Y	N/A	N/A	N/A	N/A	N/A	AT	N/A
30	"Ear Muff" Wing Spar Insulation	Y	Y	Y	Y	Y	Y	Y	Y	Y	Y	Y	AT
31	Highly Densified Shuttle tile 6"x6"x2"	Y	Y	Y	Y	Y	Y	Y	Y	Y	Y	Y	AT
32	Solid Rocket Motor Booster Bolt Catcher insulation	N/A	N/A	N/A	N/A	TBD	N/A	N/A	N/A	N/A	N/A	TBD	N/A
33	Carrier Panel w/yoke LH 14, SN AF7843	Y	Y	N/A	N/A	N/A	N/A	Y	Y	N/A	N/A	N/A	N/A
34	Carrier Panel w/yoke LH 4, SN ANG391	Y	Y	N/A	N/A	N/A	N/A	Y	Y	N/A	N/A	N/A	N/A
35	Tee Seal (3 orientations) - From panel 21	Y	Y	N/A	N/A	N/A	N/A	Y	Y	N/A	N/A	N/A	N/A
36	51311 (8" x 13" RCC Fragment with lip)	Y	Y	N/A	N/A	N/A	N/A	N	N	N/A	N/A	N/A	N/A
37	37736 (Compound Curve RCC Fragment)	Y	Y	N/A	N/A	N/A	N/A	N	N	N/A	N/A	N/A	N/A
38	2018 (RCC Flat acrage ~8" x 11")	Y	Y	N/A	N/A	N/A	N/A	N	N	N/A	N/A	N/A	N/A
39	51313 (Upper half RS RCC Tee Seal 9/10)	Y	Y	N/A	N/A	N/A	N/A	N	N	N/A	N/A	N/A	N/A
40	Upper Carrier Panel 9/10	N	N	N/A	N/A	N/A	N/A	N	N	N/A	N/A	N/A	N/A

**Notes**  
 AT = Awaiting RCS Testing or Test Results  
 In Process = RCS Test Done, data being reduced  
 N = no or not completed  
 N/A = Not Applicable or data not required  
 TBD - To be determined by NASA and CAIB  
 BAS = Boxed and Awaiting Shipment Paperwork

Table 7-2: AFRL Advanced Compact Range Shuttle Parts Test Status as of April 25, 2003 [12]

The final evaluation of the test data versus the radar observations from the Flight Day 2 object are shown in Table 7-3. Detailed test results are included on the ESAT data CD. As mentioned above, detailed discussion of the RCS and ballistic comparisons to the Flight Day 2 object are deferred to the tiger team formed under the OVE WG.

Test Article	RCS Result	Other Considerations	Comments
AFRSI 12" x 12"	Excluded		RCS was orders of magnitude too low
FRSI 12" x 12"	Excluded		RCS was orders of magnitude too low
HRSI LI 900	Excluded		RCS was orders of magnitude too low
HRSI LI 900 (Densified Layer/RTV/SIP)	Excluded		RCS was orders of magnitude too low
"Fibrous 001" - Bulk Insulation Blanket, Cargo Bay Liner Level	NOT Excluded		Cd*A/M was off by >factor of 7
"Fibrous 002" - PLBD Hinge Line Torque Box	NOT Excluded		Cd*A/M was off by >factor of 7
"Fibrous 003" - Beneath Radiator	NOT Excluded		Cd*A/M was off by >factor of 7
Beta Cloth (without Conductive Quilt Thread)	Excluded		Cd*A/M was off by >factor of 7
Beta Cloth (with Conductive Quilt Thread)	Unlikely		Cd*A/M was off by >factor of 7
Cargo Bay Liner MLI 004 13" x 13" Piece	NOT Excluded		Cd*A/M was off by >factor of 7
Freestar Panel A2	NOT Excluded		
Freestar Panel B	NOT Excluded		
Freestar Panel C	NOT Excluded		
Freestar Logo	Excluded		
Insulation Blanket Sample 1	NOT Excluded		
Insulation Blanket Sample 2	NOT Excluded		
Carrier Panel SEGMENT	Excluded	Excluded if debris is positively identified AND is in region of interest	Object is unlikely from an RCS perspective unless Cape Cod radar was off by -5 dB
Carrier Panel SEGMENT with "Horse-Collar"	Excluded	Excluded if debris is positively identified AND is in region of interest	Object is unlikely from an RCS perspective unless Cape Cod radar was off by -5 dB
"Horse Collar" Seal	Excluded	Excluded if debris is positively identified AND is in region of interest	Object is unlikely from an RCS perspective unless Cape Cod radar was off by -5 dB
RCC Leading Edge Panel with Attachment Hardware (Flight Hardware Spare)	Excluded		Object was too large in each characteristic dimension.
HRSI LI 2200 Tile	Excluded		
"Ear Muff" Wing Spar Insulation	NOT Excluded	Excluded because Incoflex has no path to depart Shuttle UNLESS RCC panel assumed missing while on orbit	
4 Tile Carrier Panel with Horse Collar (Flight Hardware)	Excluded	Excluded because Incoflex has no path to depart Shuttle UNLESS RCC panel assumed missing while on orbit	
3 Tile Carrier Panel with Horse Collar (Flight Hardware)	Excluded	Excluded because Incoflex has no path to depart Shuttle UNLESS RCC panel assumed missing while on orbit	
Reinforced Carbon-Carbon T-Seal	NOT Excluded		
RCC Panel "Acreage"	In Work		

Table 7-3: Summary of UHF RCS Test Results [14]

L-band and S-band radar testing provided maximum detection ranges with an 80 percent probability of detection. While all of these materials are detectable in the air traffic control radars, the various tile, FRSI and AFRSI materials show very low detection ranges, 23 - 35 nm [15], compared to the leading edge components, 105 - 195 nm [16]. This is shown in Figure 7-14 for the standard ARSR-4 L-band radar. Figure 7-15 shows the ROC curves for all ARSR-4 variants, all of which have similar detection ranges. The ARSR-9 S-band radar detection ranges are lower than the L-band radars as shown in Figure 7-16. The implications of these relatively low detection ranges are discussed in Section 5.

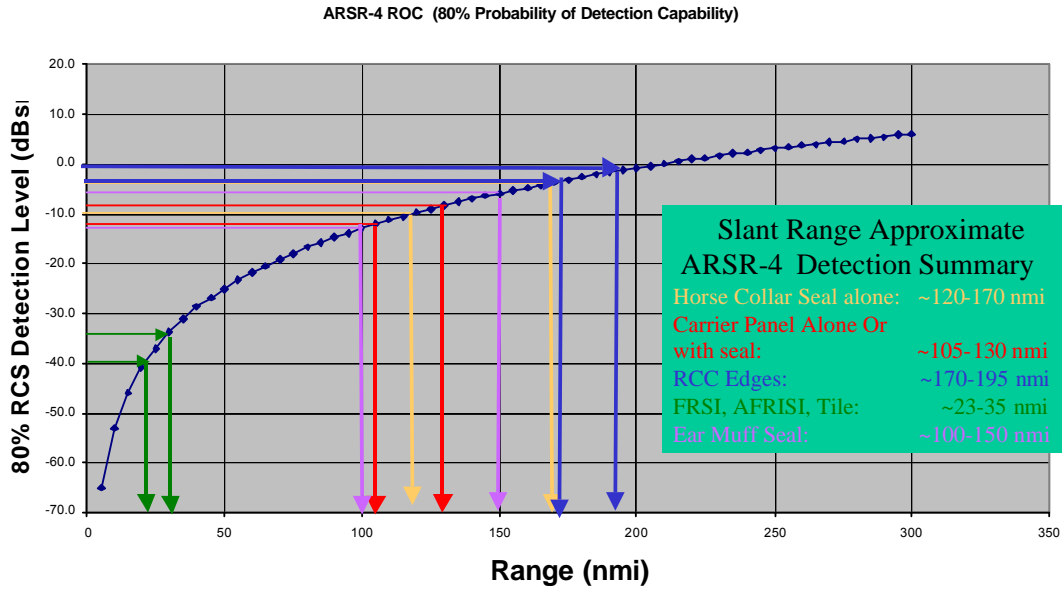


Figure 7-14: ARSR-4 L-Band ROC Curve (slant range, line of sight, perfect weather) [15][16]

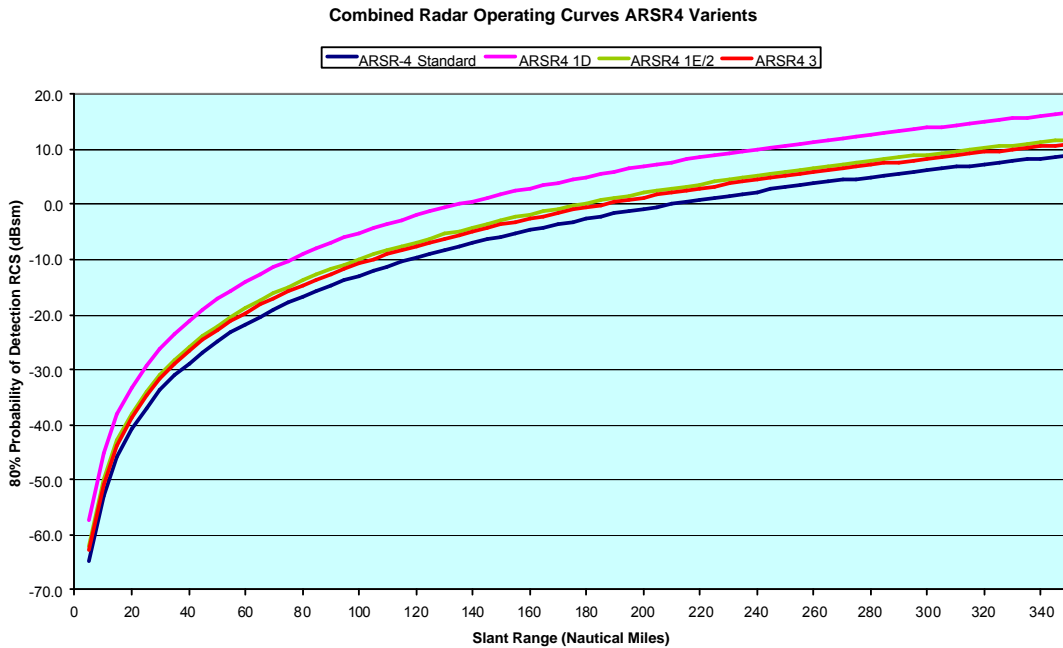


Figure 7-15: All ARSR-4 Variant L-Band ROC Curves (slant range, line of sight, perfect weather) [59]

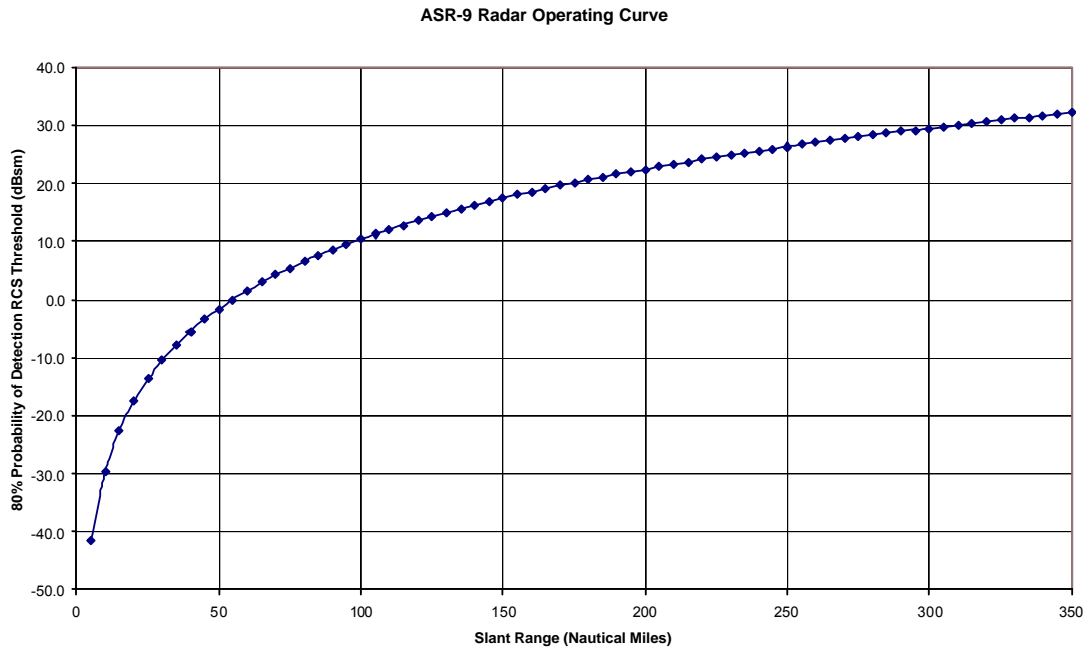


Figure 7-16: ARSR-9 S-Band ROC Curve (slant range, line of sight, perfect weather) [59]



Similar data were produced for the C-band radar and are plotted in Figures 7-17 through 7-19. A series of ROC curves is shown for each C-band radar since these radars' parameters are changed during ascent to optimize tracking as the Orbiter travels down range. Examples of the corresponding coverage for one set of data from each radar is shown in Section 6. Detailed analyses of this data and any implications for detecting debris during ascent are not included in this report.

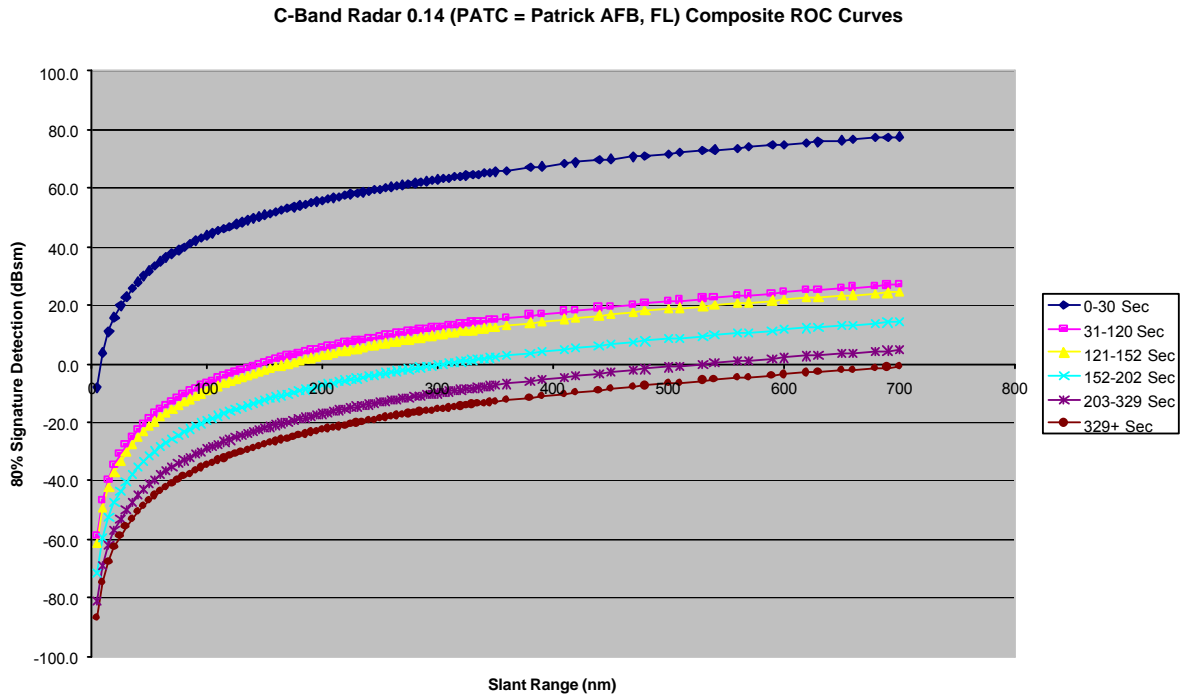


Figure 7-17: C-Band 0.14 Radar ROC Curves (slant range, line of sight, perfect weather) [58]

C-Band Radar 19.14 (MLAC = Merritt Island, FL) Composite ROC Curves

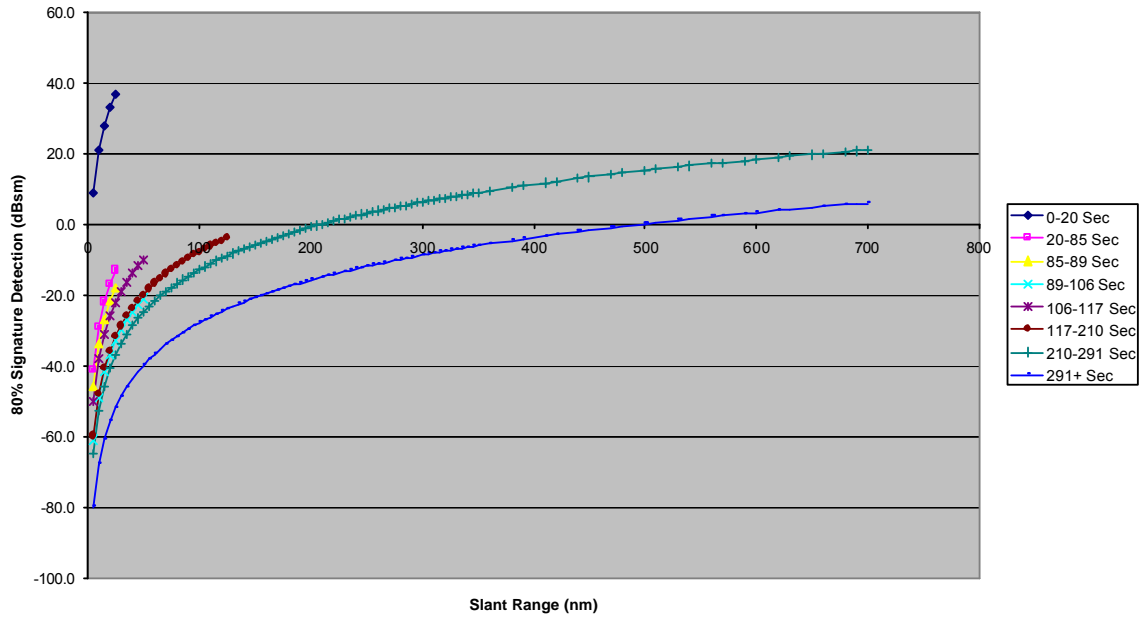


Figure 7-18: C-Band 19.14 Radar ROC Curve (slant range, line of sight, perfect weather) [58]

C-Band Radar 28.14 (JDIC = Jonathan Dickson, FL) Composite ROC Curves

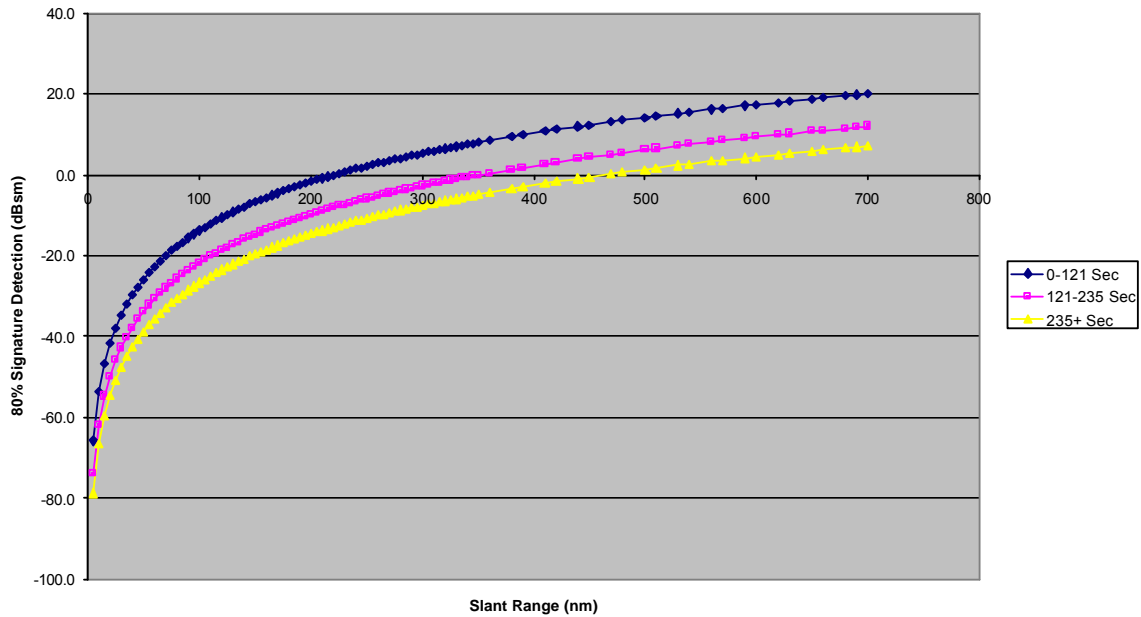


Figure 7-19: C-Band 28.14 Radar ROC Curve (slant range, line of sight, perfect weather) [58]

## **7.5. Miscellaneous Other DOD Data**

### **7.5.1. 16 Jan, 15:56:22-16:01:10**

Post-flight analysis of remote sensor data suggested anomalous signatures after ascent. Similar to the remote sensor data during entry, this required considerable post-processing and detailed comparison to previous flight data. In the final assessment, this signature also was concluded to have been seen on multiple previous missions and was not studied further.

### **7.5.2. Ascent Radar**

STS-107 was tracked during ascent by Eastern Test Range C-band radar. This data was analyzed and reported by the 45th Space Wing, Patrick AFB, Florida. None of the radars detected debris prior to SRB separation. From T+150 to T+230 seconds, radar 0.14 detected 21 objects and radar 28.14 detected 6 objects. The radar return signal strengths were not adequate to determine debris properties, but the data were considered to be consistent with observations from previous Shuttle missions. [54]

### **7.5.3. Other Entry Radar**

No ship based or AWAC's radar tracked Columbia during entry. [55]

The UHF radar at Beale AFS, CA recorded two observations of Columbia during entry. No debris was detected. [56]

The Naval Space Surveillance System recorded 5 distinct radar detections during Columbia's entry over the CONUS. Although several of the cases showed anomalous characteristics, there is no conclusive evidence of pre-break up debris detected in any of this data. [57]

All DOD air traffic control radar during STS-107 entry was recorded by the 84th RADES. This data was included in the radar searches as described in detail in Section 5.

### **7.5.4. Infrasound**

Infrasound signals were recorded by DOD stations during STS-107 entry. Analysis to date provides no data that can be positively identified as off-nominal. This analysis is summarized in Section 8.1, and a complete discussion can be found in Appendix 10.9 of this report.

## 7.6. DOD Data Lessons Learned

- 1) A single DOD POC, located at the NASA center conducting the investigation is essential to effectively exchanging data and requesting additional support.
- 2) Generic DOD tracking capability and the resulting routine taskings on Shuttle flights should be reviewed and updated as required for all phases of flight.
- 3) Generic DOD imaging/sensor capability and the resulting routine and contingency taskings on Shuttle flights should be reviewed and updated as required for all phases of flight.
- 4) NASA and the USAF should study the use of Orbiter-specific material maps to facilitate AMOS' thermal mapping of all Orbiters during Orbit operations.

## 8. Other Sensor Data

### 8.1. Infrasonic

Dr Henry Bass, Director of the National Center for Physical Acoustics, University of Mississippi, led a collection of DOD and other infrasound researchers from several institutions in the United States. This team analyzed data recorded on infrasound monitoring stations across the United States to assist the Columbia accident investigation. This was a collaborative effort with support from DOD, DOE and NOAA.

Infrasound signals were recorded by ten stations during STS-107 entry. These stations recorded clear signals from several previous missions as well. These infrasound arrays can determine the direction of the signal, and it was hypothesized that analyzing the signals would yield data on Columbia debris shedding or some other high energy events during entry over the CONUS. Analysis to date, however, does not provide any data that can be positively identified as off-nominal. A complete discussion can be found in Appendix 10.9 of this report.

The Orbiter was first detected as it crossed the California coast and was observed all the way to break-up over Texas. All stations observed multiple signals associated with sound generated during the entry. These signals may be explained by various atmospheric multi-pathing phenomena, but it is possible that some come from debris. When combining the data with the entry trajectory, it was concluded that there do not appear to be other sources of infrasound in the vicinity of the Orbiter. [18]

Infrasonic Arrivals from Columbia



Figure 8-1: Projected track, altitude, time GMT, and infrasonic detections for the Columbia reentry based on using PMCC with time windows greater than 30 s. (The red lines indicate the observed azimuth of the first arrival, and the blue lines the azimuth of any secondary arrivals.) [18]

Dr. Al Bedard at the NOAA Environmental Technology Laboratory in Boulder, Colorado has routinely detected both Orbiter entries and naturally occurring bolides and meteorites. The infrasonic data from past entries show very consistent and identifiable patterns. His observations

DA8/P. S. Hill 157 of 186 13 June 2003

have shown that specific Orbiters can be discerned from infrasonics. [20] Dr. Bass' team compared signals from STS-107 to STS-77, STS-78, and STS-90 which had similar entry trajectories but fewer infrasound stations on line.

The state of knowledge of infrasonics makes interpreting signal differences problematic. Both Dr. Bass and Dr. Bedard note the sonic boom waveforms from each mission were different in detail. Dr. Bass concludes these were essentially the same in major features, with noticeable differences in the STS-107 signals, especially a long acoustic signal following the sonic boom coming from the West. [18] Dr. Bedard concludes there are distinct energy bursts which can be traced to specific points in the trajectory. He also notes overall frequency shift of the signal is inconsistent with past data. The frequency shift was consistent with the data observed for meteorites. [20]

As described above, there is insufficient data from previous missions to determine such waveform changes are expected. [18] Analysis to date has not correlated any infrasonic data to debris shedding events.

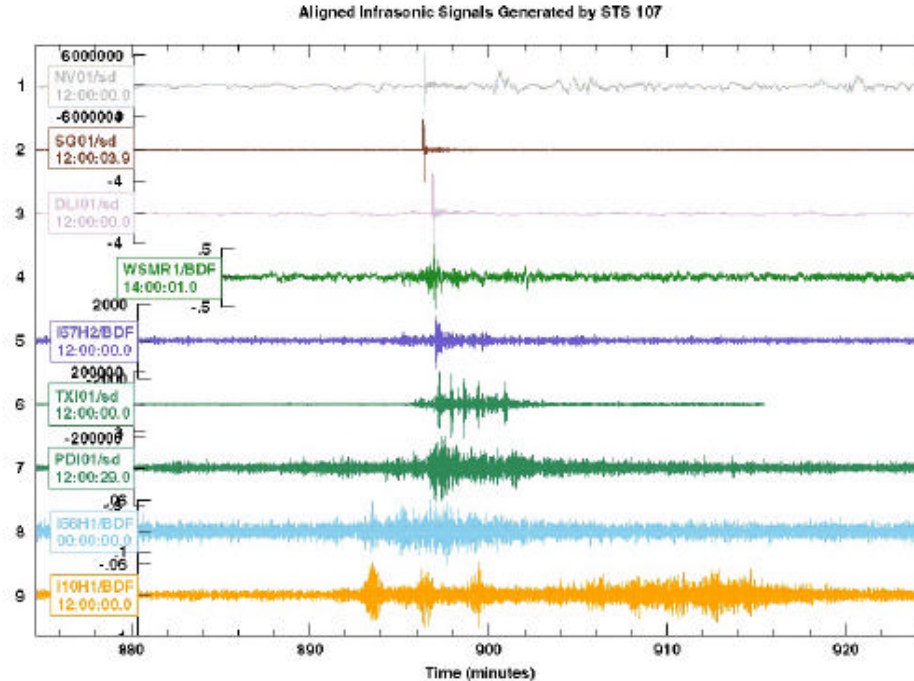


Figure 8-2: Single-channel traces from each of the infrasound arrays whose data were analyzed. [18]

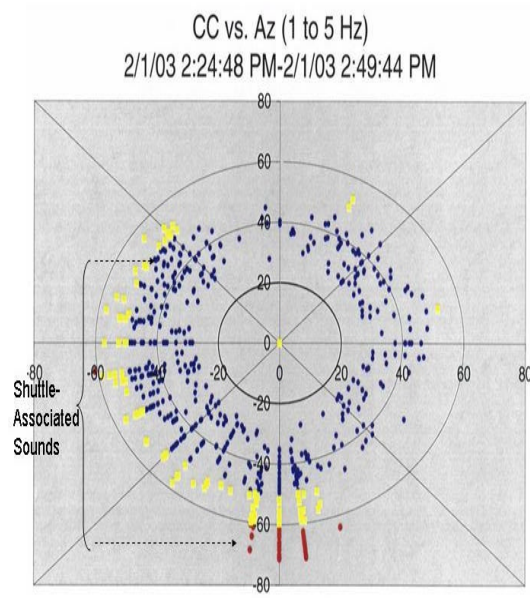


Figure 8-3. Polar plot direction of arrival plot covering the interval 1412 to 1452 UTC on 1 February 2003. The angle indicates the direction from which the acoustic signal is arriving. The radial distance from the origin is a measure of signal quality. The red data points indicate excellent signals, the yellow good signals and the blue data points weak signals or noise. [20]

## 8.2. Seismic

The STS-107 entry was observed by a number of seismograph stations distributed throughout the southwest CONUS with a significant concentration in southern California. The majority of the stations are members of the Princeton Earth Physics Program or the Public Seismic Network. Dr. David Oppenheimer of the United States Geological Survey, Northern California Seismic Network Office compiled the data. Like the infrasonic data analysis, it was hypothesized that analyzing the seismic recordings would yield data on Columbia debris shedding or some other high energy events during entry over the CONUS. Again, however, analysis to date, does not provide any data that can be positively identified as off-nominal. A complete discussion can be found in Appendix 10.10 of this report.

Several stations recorded the bow shock wave as well as some secondary signals associated with the Orbiter flyby. In order to assess unique features of this entry, NASA provided the STS 107 trajectory and four past missions that over flew the southwestern United States. Unfortunately the seismic stations do not routinely record non-earthquake data. Thus, very limited comparisons could be made to previous entries. However, this entry appeared consistent with others that have been observed in the past, and no distinctive features were seen in the STS-107 data. No specific conclusions could be made with regard to the secondary signals, and no obvious signals were present that indicated any debris impacts along the flight path. [19]

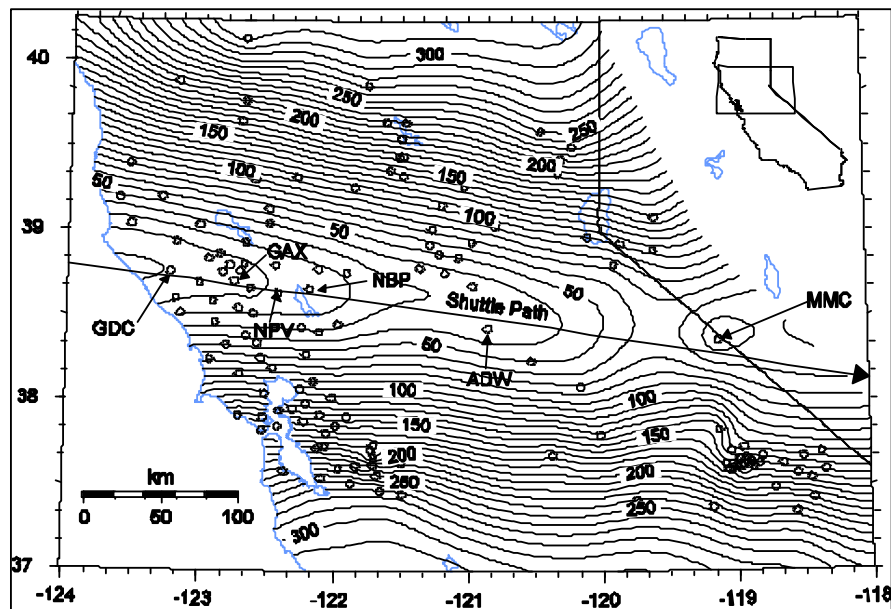


Figure 8-4. Contour map of observed arrival times of sonic boom from Space Shuttle Columbia. Contour interval is 10 s. Open circles depict locations of seismic stations recording the sonic boom. Shuttle path is shown as a straight arrow. [19]



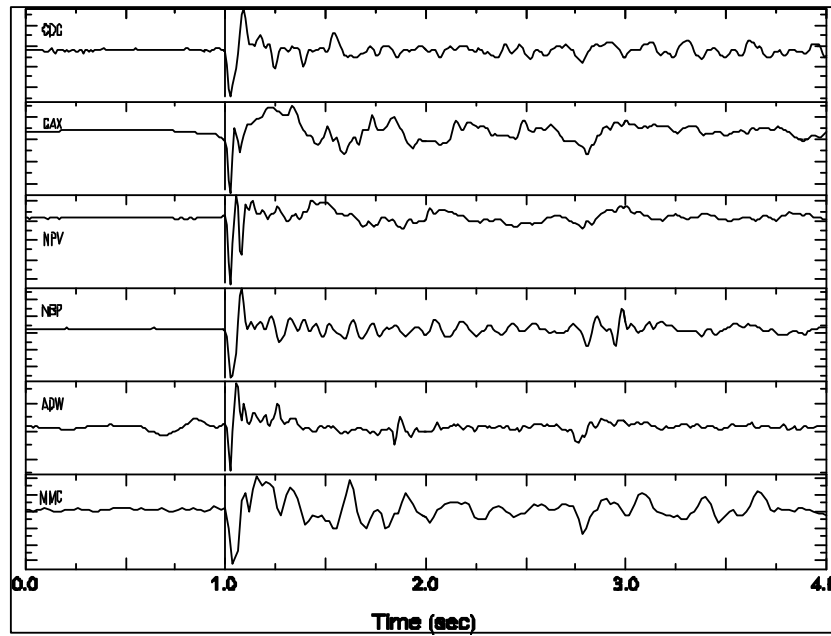


Figure 8-5. Examples of sonic boom N-waves from 6 stations along the shuttle path (see Figure 8-4 for station locations). All seismograms were recorded on a vertical 1-Hz geophone using analog telemetry and sampled at 100sps. Seismograms are shifted in time to align on arrival time. Amplitudes are normalized. [19]

### 8.3. Other Sensor Data Lessons Learned

- 1) The state of the art for infrasonic and seismic data does not support their use for monitoring Orbiter entry.
- 2) The state of the art for infrasonic and seismic data does not provide significant engineering value for Columbia's post-incident investigation.

## 9. References

- [1] Visel, Lt Col Cyndie; Information Paper on Object Associated with STS-107; March 13, 2003.
- [2] HQ AFSPC/XPY; FD2 Piece Characterization (RCS and Area/Mass Ratio) Preliminary Results; April 18, 2003.
- [3] Witte, Dave and Lt Col Jeff McCann; AMOS, AFRL/DE; Quick-look Surface Temperature Mapping of STS-107 Using Long-Wave Infrared Imagery Collected on 28 Jan 03 from the Air Force Maui Optical & Supercomputing (AMOS) Site; March 4, 2003.
- [4] Air Force Maui Optical & Supercomputing (AMOS) Detachment; Data CD: AMOS STS1-107; EOC #2-4-0124; February 2003.
- [5] Jarvis, Kandy; JSC/SX; STS-107 Investigation Kirtland Photo Tiger Team; April 21, 2003.
- [6] Roeh, William; JSC/JA171; Report Tallies e-mail; April 30, 2003.
- [7] Hill, Paul S.; JSC/DA8; NASA-DOD Data Exchange; February 28, 2003.
- [8] Shelton, William L., BGen; HQ AFSPC/XO, Peterson AFB, CO; AFSPC Data Classification Guidance; February 24, 2003.
- [9] Anthony, Jack, Col; AFSPC/DP, Peterson AFB, CO; Remote Sensor Summary; April 17, 2003.
- [10] Summary of classified and unclassified phone conversations and meetings at JSC in March and April 2003.
- [11] Rickman, Steven L.; JSC/ES3; Summary of Radar Cross Section (RCS) Testing and Ballistic Analysis of the STS 107 Flight Day 2 Object; 22 April 2003.
- [12] Kent, Brian, Dr.; AFRL, Wright-Patterson AFB, OH; AFRL Advanced Compact Range Shuttle Parts Testing/Reporting Status; April 25, 2003.
- [23] Broome, Joey and Carlos H. Westhelle; JSC/EG; STS-107 Flight Day 2 Debris Trajectory Analysis Ballistic Number Range Definition; April 24, 2003
- [14] Rickman, Steve; JSC/ES3; Summary of UHF RCS and Ballistic Results REV A; April 17, 2003.
- [15] Kent, Brian, Dr.; AFRL, Wright-Patterson AFB, OH; RCS Assessment of STS-107 Debris Candidates; March 14, 2003

- [16] Kent, Brian, Dr.; AFRL, Wright-Patterson AFB, OH; RCS Assessment of STS-107 Debris Candidates, L-Band Measurements of Carrier Panel, RCC Edge, High Density Tile; March 28, 2003.
- [17] Spencer, James. R.; JSC/DM; Debris Hot list; May 13, 2003.
- [18] Bass, H., Editor, National Center of Physical Acoustics, University of Mississippi; Interim Report to the Department of Defense on Infrasonic Re-Entry Signals from the Space Shuttle Columbia (STS-107) (Revision 3.0); March 31, 2003.
- [19] Oppenheimer, David; U.S. Geological Survey; Analysis of Sonic Booms from the Reentry of the Space Shuttle Columbia over California and Nevada; May 8, 2003.
- [20] Bedard, A.J; Infrasonics Group Leader, NOAA Environmental Technology Laboratory Microwave Systems Development Division; Boulder, Colorado; Infrasound Originating from the 1 February 2003 Reentry of the Space Shuttle Columbia (STS-107), A Summary of Sub-Audible Sound Bursts Detected Near Boulder, Colorado for use by NASA and Others Studying this Accident, Draft V1.2; May 7, 2003.
- [21] Byrne, Greg; JSC-SX; Image Analysis Team - Rev 5 Entry Debris Timeline; April 12, 2003.
- [22] Spencer, J.R.; JSC-DM; STS-107 Early Entry Debris Sighting Timeline; May 2003.
- [23] Abadie, M.; JSC-DM; STS-107 ESAT Final Report Relative Motion and Ballistics Analysis; May 20, 2003.
- [24] Mrozinski, R.B; JSC-DM; STS-107 Columbia Accident Debris Footprint Boundary Estimates; June 3, 2003.
- [25] Hartman, S.; JSC-DM; JSC Radar Assessment Team Final Report; May 23, 2003.
- [26] Mrozinski, R. B., "CRV Deorbit Opportunities, v1.0h," internal memorandum, NASA Johnson Space Center, Houston, Texas, January 24, 2000.
- [27] Mrozinski, R. B., "NASA Pre-Event Debris Footprint Estimates for the Deorbit of Space Station Mir," Proceedings of the International Workshop Mir Deorbit, European Space Operations Center, Darmstadt, Germany, May 14, 2001, pgs. 45 - 55.
- [28] Mrozinski, R. B., "Entry Debris Field Estimation Methods and Application to Compton Gamma Ray Observatory Disposal," proceedings 2001 Flight Mechanics Symposium, NASA Goddard Space Flight Center, Greenbelt, Maryland, June, 2001, pp. 455 - 469.
- [29] Berning, M. J., Sagis, K. D., "User's Guide for the Simulation and Optimization of Rocket Trajectories (SORT) Program, Version 7," NAS9-17900, Lockheed Engineering & Sciences Company, Houston, Texas, October, 1992.

- [30] Hallman, W. P., Moody, D. M., Patera, R. P., Stern, R., "Analyses of Videos of the STS-107 Reentry," Aerospace ATR, The Aerospace Corporation, Los Angeles, California, May 27, 2003.
- [31] Scheffe, H., Tukey, J. W., "A Formula for Sample Sizes for Population Tolerance Limits," Annals of Mathematical Statistics, Vol. 15, p. 217, 1944.
- [32] Oram, T. D., "Final Atmosphere Update," e-mail communication, NASA Johnson Space Center, Houston, Texas, April 11, 2003.
- [33] Jones, R. S., conversation, NASA Johnson Space Center, Houston, Texas, February 03, 2003.
- [34] Oram, T. D. "RE: Weather Uncertainties," e-mail communication, NASA Johnson Space Center, Houston, Texas, April 25, 2003.
- [35] Rao, P. P., Woeste, M. A., "Monte Carlo Analysis of Satellite Debris Footprint Dispersion," AIAA 79-1628, 1979.
- [36] Herdrich, R. J., Nguyen, P. D., "Super Lightweight Tank (SLWT) Footprint Analysis: Technical Report," JSC-27712, NASA Johnson Space Center, Houston, Texas, March 01, 1997.
- [37] Cerimele, C. J., conversation, NASA Johnson Space Center, Houston, Texas, May 03, 2000.
- [38] Jones, R. S., "Checkout Monitor 1," screen printout, NASA Johnson Space Center, Houston, Texas, February 01, 2003.
- [39] Nagle, S. M., telephone conversation, United Space Alliance, NASA Johnson Space Center, Houston, Texas, February 01, 2003.
- [40] Carman, G. L., "FW: TRAJ\_GPS.txt," e-mail communication, NASA Johnson Space Center, Houston, Texas, February 05, 2003.
- [41] Silvestri, R. T., "FW: Inertial V, gamma, azimuth," e-mail communication, NASA Johnson Space Center, Houston, Texas, February 10, 2003.
- [42] Oram, T. D., "RE: Weather Uncertainties," e-mail communication, NASA Johnson Space Center, Houston, Texas, March 26, 2003.
- [43] Carman, G. L., "FW: 10HZ\_BET.txt," e-mail communication, NASA Johnson Space Center, Houston, Texas, March 20, 2003.
- [44] Nuss, R. W., "STS107 GPS post-LOS data," e-mail communication, NASA Johnson Space Center, Houston, Texas, March 19, 2003.

- [45] Feustel, A. J., "FW: Ballistic 100," e-mail communication, NASA Johnson Space Center, Houston, Texas, March 14, 2003.
- [46] Mendoza, A. C., "Updated SRIL," e-mail communication, NASA Kennedy Space Center, Kennedy Space Center, Florida, May 29, 2003.
- [47] <http://usaflwas1.ksc.nasa.gov/fl/debris/index.cfm?fuseaction=reports.roReport&CFID=36890&CFTOKEN=19948634&fakey=64394>, NASA Kennedy Space Center, Kennedy Space Center, Florida.
- [48] <http://usaflwas1.ksc.nasa.gov/fl/debris/index.cfm?fuseaction=reports.roReport&CFID=36890&CFTOKEN=19948634&fakey=66424>, NASA Kennedy Space Center, Kennedy Space Center, Florida.
- [49] <http://usaflwas1.ksc.nasa.gov/fl/debris/index.cfm?fuseaction=reports.roReport&CFID=36890&CFTOKEN=19948634&fakey=38885>, NASA Kennedy Space Center, Kennedy Space Center, Florida.
- [50] "STS-107 Radar Database, Long Range Radar Returns (2/1/03, 13:30Z to 15:00Z)," National Transportation Safety Board and Federal Aviation Administration, Washington, D. C., February 10, 2003.
- [51] Rochelle, W. C., Smith, R. N., Dobarco-Otero, J., "ORSAT Results of STS-107 (Columbia) Early and Late Break-Up Debris Analysis," presentation, NASA Johnson Space Center, Houston, Texas, March 07, 2003.
- [52] <http://usaflwas1.ksc.nasa.gov/fl/debris/index.cfm?fuseaction=reports.roReport&fakey=14768&goback=2&CFID=36890&CFTOKEN=19948634>, NASA Kennedy Space Center, Kennedy Space Center, Florida.
- [53] Schafer, Craig P.; SAIC; Results of Search for Observed Debris Landing Events, and EOC Hotline and Database Lessons Learned for STS-107 Accident Investigation; May 16, 2003.
- [54] 45 RMS/RMSS; PAFB, FL; Shuttle STS-107 Debris Analysis - Instrumentation Systems Analysis Special Report, CDR A205; February 14, 2003.
- [55] Roberts, Katherine E., Col;USSTRATWEST/J3V; e-mail communication; February 21, 2003.
- [56] Roberts, Katherine E., Col;USSTRATWEST/J3V; e-mail communication; March 26, 2003.
- [57] Brad, J., Lydick, E.D., Schumacher Jr., P.W.; Naval Network and Space Operations Command; Dahlgren VA; Analysis of Fence Observations of STS-107 Reentry - NNSOC Technical Report 03-001; February 28, 2003.

- [58] Kent, Brian, Dr.; AFRL, Wright-Patterson AFB, OH; e-mail communication; May 21, 2003.
- [59] Kent, Brian, Dr.; AFRL, Wright-Patterson AFB, OH; e-mail communication; May 14, 2003.